

Water-Soluble Polymers

Publication Date: May 5, 1986 | doi: 10.1021/ba-1986-0213.fw001

ADVANCES IN CHEMISTRY SERIES **213**

Water-Soluble Polymers

Beauty with Performance

J. E. Glass, EDITOR
North Dakota State University

Developed from a symposium sponsored by
the Division of Polymeric Materials Science and Engineering
at the 188th Meeting
of the American Chemical Society,
Philadelphia, Pennsylvania,
August 26–31, 1984



American Chemical Society, Washington, DC 1986



Library of Congress Cataloging-in-Publication Data

Water-soluble polymers.

(Advances in chemistry series, ISSN 0065-2393; 213)

"Developed from a symposium sponsored by the Division of Polymeric Materials Science and Engineering at the 188th Meeting of the American Chemical Society, Philadelphia, Pennsylvania, August 26-31, 1984."

Includes bibliographies and indexes.

I. Water-soluble polymers—Congresses.

I. Glass, J. E. (J. Edward), 1937- . II. American Chemical Society. Division of Polymeric Materials: Science and Engineering. III. American Chemical Society. Meeting (188th: 1984: Philadelphia, Pa.) IV. Series.

QD1.A355 no. 213 [QD382.W3]
540 s [668.9] 86-3534
ISBN 0-8412-0931-6

Copyright © 1986

American Chemical Society

All Rights Reserved. The appearance of the code at the bottom of the first page of each chapter in this volume indicates the copyright owner's consent that reprographic copies of the chapter may be made for personal or internal use or for the personal or internal use of specific clients. This consent is given on the condition, however, that the copier pay the stated per copy fee through the Copyright Clearance Center, Inc., 27 Congress Street, Salem, MA 01970, for copying beyond that permitted by Sections 107 or 108 of the U.S. Copyright Law. This consent does not extend to copying or transmission by any means—graphic or electronic—for any other purpose, such as for general distribution, for advertising or promotional purposes, for creating a new collective work, for resale, or for information storage and retrieval systems. The copying fee for each chapter is indicated in the code at the bottom of the first page of the chapter.

The citation of trade names and/or names of manufacturers in this publication is not to be construed as an endorsement or as approval by ACS of the commercial products or services referenced herein; nor should the mere reference herein to any drawing, specification, chemical process, or other data be regarded as a license or as a conveyance of any right or permission, to the holder, reader, or any other person or corporation, to manufacture, reproduce, use, or sell any patented invention or copyrighted work that may in any way be related thereto. Registered names, trademarks, etc., used in this publication, even without specific indication thereof, are not to be considered unprotected by law.

PRINTED IN THE UNITED STATES OF AMERICA

American Chemical Society
Library
1155 16th St., N.W.
Washington, D.C. 20036

Advances in Chemistry; American Chemical Society: Washington, DC, 1986.

Advances in Chemistry Series

M. Joan Comstock, *Series Editor*

Advisory Board

Harvey W. Blanch
University of California—Berkeley

Alan Elzerman
Clemson University

John W. Finley
Nabisco Brands, Inc.

Marye Anne Fox
The University of Texas—Austin

Martin L. Gorbaty
Exxon Research and Engineering Co.

Roland F. Hirsch
U.S. Department of Energy

Rudolph J. Marcus
Consultant, Computers &
Chemistry Research

Vincent D. McGinniss
Battelle Columbus Laboratories

Donald E. Moreland
USDA, Agricultural Research Service

W. H. Norton
J. T. Baker Chemical Company

James C. Randall
Exxon Chemical Company

W. D. Shults
Oak Ridge National Laboratory

Geoffrey K. Smith
Rohm & Haas Co.

Charles S. Tuesday
General Motors Research Laboratory

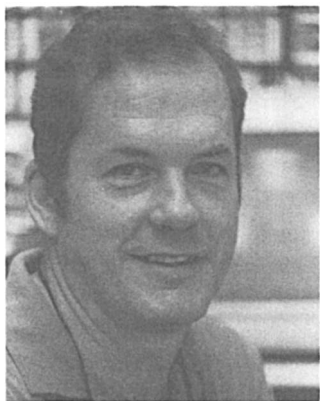
Douglas B. Walters
National Institute of
Environmental Health

C. Grant Willson
IBM Research Department

FOREWORD

The **ADVANCES IN CHEMISTRY SERIES** was founded in 1949 by the American Chemical Society as an outlet for symposia and collections of data in special areas of topical interest that could not be accommodated in the Society's journals. It provides a medium for symposia that would otherwise be fragmented because their papers would be distributed among several journals or not published at all. Papers are reviewed critically according to ACS editorial standards and receive the careful attention and processing characteristic of ACS publications. Volumes in the **ADVANCES IN CHEMISTRY SERIES** maintain the integrity of the symposia on which they are based; however, verbatim reproductions of previously published papers are not accepted. Papers may include reports of research as well as reviews, because symposia may embrace both types of presentation.

ABOUT THE EDITOR



J. E. GLASS is Professor of Polymers and Coatings at North Dakota State University. He received a B.S. degree in Chemistry from Louisiana State University in 1959 and a Ph.D. degree from Purdue University in 1964. From 1963 to 1980, he was employed by the Union Carbide Corporation at its South Charleston Research and Development Center.

His research interests have included nearly all aspects of water-soluble polymers: kinetics and synthesis by free-radical processes, controlled substituent placement in the derivatization of carbohydrate polymers, solution and interfacial adsorption and viscosity behavior of both polymer types, and meaningful extrapolation of such fundamental data to the performance of water-soluble polymers in application formulations. He has published more than fifty technical papers and received several patents in these areas of study.

PREFACE

THE STATE OF THE ART for water-soluble polymers was the topic of a workshop and symposium conducted in 1984, the first since a similar symposium was organized for the 164th National Meeting of the American Chemical Society in New York in 1972 by N. M. Bikales.

The symposium upon which this book is based included sessions on polymer synthesis and characterization and on the performance of water-soluble polymers in applications areas. The applied areas included water treatment, petroleum, coatings, detergency, textiles, and the use of water-soluble polymers as protective colloids in the emulsion synthesis of acrylic and vinyl acetate latices and in the production of poly(vinyl chloride) by suspension processes. Due to space limitations, many of the presentations in both the workshop and the symposium are omitted from this book. A detailed symposium on the synthesis and characterization of water-soluble polymers is planned for the 194th National Meeting of the American Chemical Society in New Orleans in August 1987.

In applications, cost-effectiveness defines the polymers of choice. A detailed description of the polymers complementing evolution in mechanical techniques in water-treatment processes is given in this book. The solution properties of importance in the use of water-soluble polymers both in petroleum recovery processes and in coatings applications are solution rheology, adsorption, and stability. The relative importance of these parameters in their use in a variety of petroleum processes, which include drilling and fracturing, and in coatings applications is discussed in this volume. The aqueous solution characteristics of poly(2-ethyl-2-oxazolines), a product that may contribute significantly to adhesive technology in the next decade, are also described.

The most significant advance in water-soluble polymers during the past decade has been their modification with hydrophobic moieties. Publications on polymeric surfactants, or water-soluble polymers, with a moderate percentage of hydrophobic groups that significantly lower the surface tension of water are abundant. None of the materials described in this "prior art" relate to the technology being developed with water-soluble polymers that contain surfactant-type hydrophobes that are "appropriately placed". This type of water-soluble polymer was developed for use in lubricating fluid formulations where they are accepted commercial materials. The use of hydrophobically modified, water-

soluble polymers in the petroleum recovery areas has been explored, but has not yet achieved acceptance. Products structurally different from the polymers being used in lubrication fluids are achieving commercial acceptance in cosmetic and coatings applications. Their solution characteristics in the presence of conventional, low molecular weight surfactants appropriate to their use in the cosmetic area are given in this book. Their value from a consumer's viewpoint and their mechanistic differences with conventional water-soluble polymers used in coatings applications are also discussed. Hydrophobically modified, water-soluble polymers of the type discussed in this volume will receive significant attention during the next decade.

I express my appreciation to those who participated in the symposium from which this book was developed.

J. E. GLASS
Department of Polymers and Coatings
North Dakota State University
Fargo, ND 58105-5516

December 1985

Structural Features Promoting Water Solubility in Carbohydrate Polymers

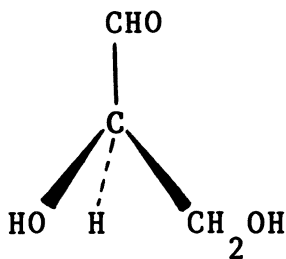
J. E. Glass

Department of Polymers and Coatings, North Dakota State University, Fargo, ND 58105

Although a large variety of carbohydrate polymers have a multitude of industrial uses, most carbohydrate polymers have limited applicability across a wide spectrum of applications. The structural features affecting water solubility in carbohydrate polymers are discussed. Methods of derivatizing the world's most abundant polymer, cellulose, are presented, and derivatization processes are compared with the complexities of synthesizing polymers by fermentation processes. On the basis of three criteria, (1) the parameters promoting solubility, (2) the known limitations of commercially available products, and (3) the solubility trends observed in a limited number of thoroughly investigated carbohydrate polymers, projections of what might be achieved with a structurally designed carbohydrate polymer, obtained from variations in the repeating unit and anomeric and positional bonding patterns, are postulated.

THE CHEMISTRY OF CARBOHYDRATE POLYMERS is an infrequent subject in college curricula. These macromolecules can be appropriately introduced with the chemistry (1, 2) of the simple three-carbon molecule, glyceraldehyde, which is the monomeric prototype for polysaccharides. The middle carbon is asymmetric (i.e., four different groups are bonded to the center carbon); the two optical isomers (distinguished by the direction in which they rotate plane-polarized light) that result are illustrated in structure I. In the dextrorotatory compound, designated by a D prefix, the hydroxyl group is placed to the right of the asymmetric carbon (C*) with the aldehyde group positioned above. In the levorotatory compound (L prefix), the hydroxyl function is placed to the left of the asymmetric carbon atom. As additional carbons (with their hydroxyl functions) are added to this three-carbon molecule, the number of isomers increases by 2^n , where n is the number of asymmetric carbons. The D or L classification continues to apply to the

0065-2393/86/0213-0003\$07.25/0
© 1986 American Chemical Society



I

second to last carbon in the structural formula, regardless of the number of carbons in the molecule. The saccharides are polyhydroxylic compounds with a pendant carbonyl group and can be represented by the formula $(\text{CH}_2\text{O})_n$. Pentoses ($n = 5$) and hexoses ($n = 6$) are the most abundant; the six-carbon molecules are the most important industrial class. The large number of asymmetric carbon atoms gives rise to 16 possible hexose isomers (half are of the D configuration, Chart I, and the remainder are of the L configuration).

Sugars exist as cyclic structures in which six-membered pyranose rings are favored over five-membered furanose rings. Open-chain, free sugars have not been isolated, but some sugars have been detected in trace amounts in solution equilibrium with their closed, ring forms. The closed, ring-form sugars arise by internal condensation of a hydroxyl

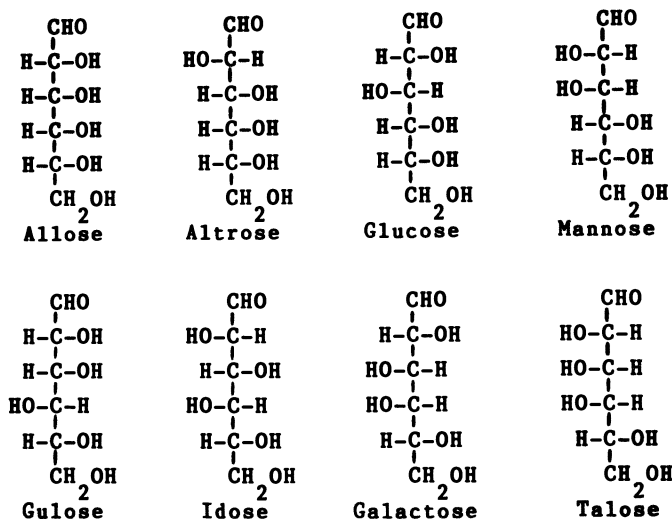
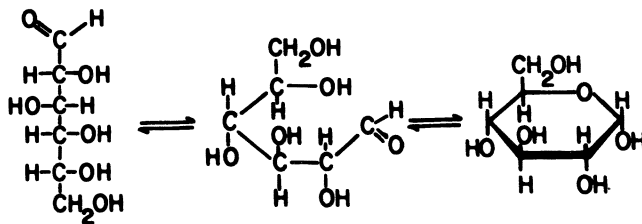


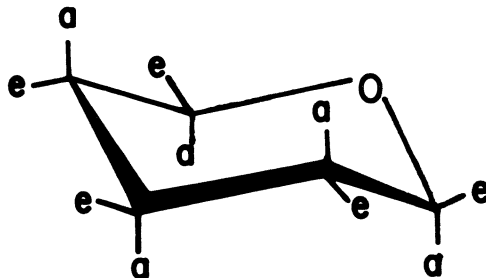
Chart I. D isomers of hexose.



Scheme I. Equilibrium between D-glucose and α -D-glucopyranose (ring form; shown in the Haworth projection).

group with the carbonyl moiety to form an acetal group. Cyclization creates an additional asymmetric center at the reactive carbon position, now designated the anomeric carbon. Thus, D-glucose cyclizes preferentially by reaction of the hydroxyl group on carbon 5 (numbered sequentially down the open-chain structure from the aldehyde carbon) with the aldehyde carbonyl to form a six-membered ring (Scheme I). The newly created hydroxyl group on carbon 1 can position above or below the plane of the ring. With the pyranose ring drawn according to the Haworth convention as in Scheme I, the pendant hydroxymethyl group of D sugars lies above the ring plane while the corresponding group in the L series lies below. Within either series, the isomer with the anomeric hydroxyl group below the ring is called the α anomer; the corresponding hydroxyl lies above the plane in the β anomer. The connection of rings through two different anomeric bonds is an important feature in carbohydrate polymers.

When linear hydrocarbons are structured in rings, the bond angles between contiguous carbon atoms in a six-carbon ring prohibit planar projections. The rings buckle and assume various conformations. Six-carbon rings are known to exist most frequently in a chair form [structure II (a = axial and e = equatorial)] in which substituent bonds to ring carbons, hydrogen, or hydroxyl functions are axial or equatorial. Axial



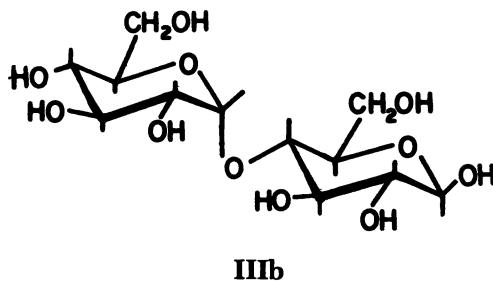
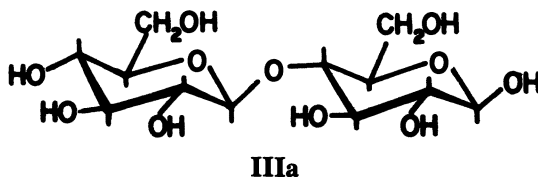
II

bonds are those parallel with the ring's general axis of symmetry. Equatorial bonds lie in the approximate plane of the ring (with its greater continuum of electron density) and generally have different reactivities than axial bonds. Of the conformations possible for the pyranose ring, the one that minimizes steric repulsions among axially disposed hydroxyls and the hydroxymethyl group is favored. Accordingly, the conformation depicted in structure II is preferred by both anomers of D-glucose because it positions the bulky hydroxymethyl and hydroxyl groups on carbons 2, 3, and 4 in equatorial positions.

The difference between α and β linkages is illustrated by using the glucopyranosyl unit in the construction of two disaccharides (structure IIIa and b). If two glucopyranosyl molecules are joined through equatorial bonds, the linkage is referred to as β and the product is cellobiose. If glucopyranosyl units are joined through an axial linkage of one unit, an α linkage is formed, and the product is maltose. Cellobiose is the basic unit of cellulose (structure IIIa) and maltose is the basic unit of starch (structure IIIb)—two of the world's most abundant polymers.

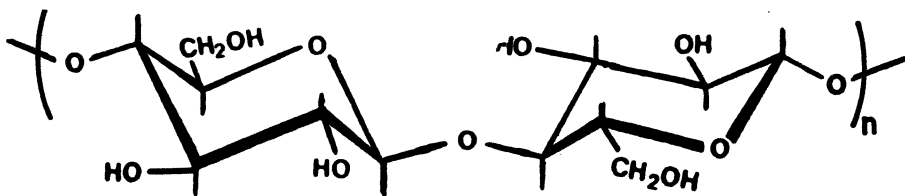
Classification of Polysaccharides by Natural Function: Storage, Structural, and Extracellular

In general, the simple distinction of α versus β linkages between monomer units determines the function of polysaccharides in plant cells. Storage polysaccharides provide an energy supply for plant or animal cells. Generally, storage polysaccharides possess an axial-equatorial bond (i.e., an α linkage) between the 1- and 4-positions of adjacent glucose units. In plant cells, this energy source is starch, either amylose (linear macromolecules of maltose units) or amylopectin (a branched maltose macro-

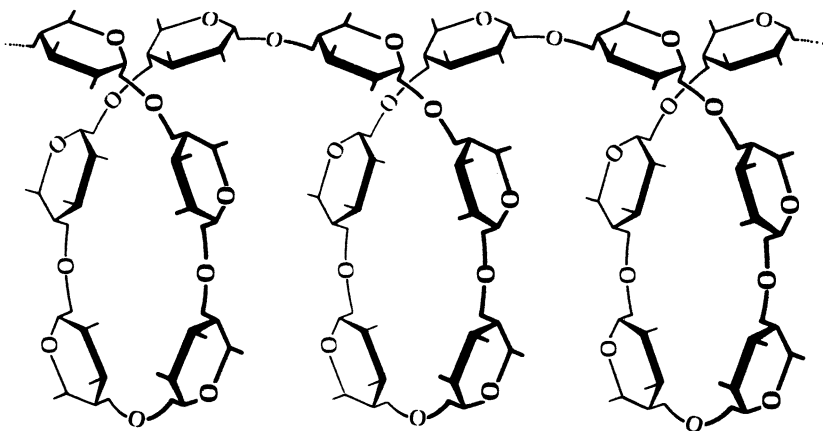


molecule). In animal cells, the energy source is a highly branched arrangement of maltose units, glycogen.

Structural polysaccharides provide the rigidity and elasticity needed to protect cells. Generally, structural polysaccharides are characterized by equatorial-equatorial bonds (i.e., β linkages) between glucopyranosyl units and, like storage polysaccharides, their macromolecular structure varies with variation in life form. Unmodified cellulose is the primary structural polysaccharide of plants. The β linkage produces a nearly linear, extended macromolecular conformation (structure IV), which permits close packing of polymer chains; this close packing in turn encourages intermolecular hydrogen bonding (and crystallinity) between adjacent chains with minimum entropy loss to produce the rigidity required in a structural material. The α linkage of storage polysaccharides imparts a helical conformation to the glucopyranosyl chain (structure V). The helix inhibits extensive interchain associations; therefore, the helix is unfit as a structural entity but excellent as an energy source because rapid degradation for energy release is not hampered by the necessity of first breaking strong intermolecular attractions.

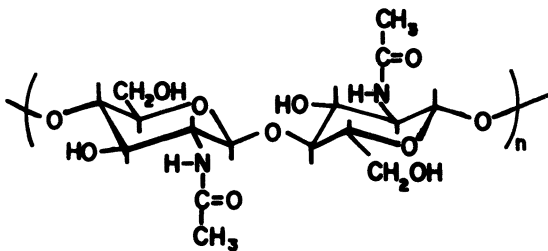


IV



V

In the lower animal forms (insects, spiders, and crabs), the C-2 hydroxyl group in cellulose is replaced with an *N*-acetylamino group (structure VI) to produce chitin (3-5). In many life forms, this polymer functions as the adhesive in a predominantly calcium carbonate matrix. In higher life forms, amino acids are attached to the C-3 hydroxyl.



VI

Certain monosaccharides occur more frequently than others in industrially important carbohydrate polymers. The monomeric units are glucose, mannose, and galactose. In the glucopyranosyl ring, the hydroxyl groups are equatorially positioned in the favored conformation. Mannopyranose is the C-2 epimer of glucose (i.e., the hydroxyl is axial not equatorial); galactopyranose is a C-4 epimer of glucopyranose.

Intricate structural variations will affect solubility and occasion solution properties not observed in the structures discussed previously; these characteristics are found in polysaccharides produced by microorganisms through fermentation synthesis. These extracellular polymers are secreted by microorganisms either as (1) a capsule layer of polysaccharide that clings to the outside of the cell wall or as (2) a slime composed of polysaccharide that accumulates near the cell but eventually diffuses into the aqueous medium. The slime has greater commercial potential because of the ease of recovery. Fermentation polysaccharides can be divided into two classes: (1) the simple polysaccharide homopolymers produced by the action of a single enzyme in the presence of the microorganism to produce a water-soluble polymer; and (2) the structurally complex heteropolysaccharides requiring the sequential actions of a group of enzymes produced by the microorganism.

The synthesis of carbohydrate polymers by fermentation processes represents a more complex commercial process than those used in obtaining water-soluble polymers by a slurry process (e.g., in the derivatization of cellulose or guaran discussed below) because of the generation of highly viscous solutions. The viscosity arises both from the conversion of monomer (e.g., glucose) to polymer and from an increase in the number of microorganism bodies. The increase in viscosity, particularly the pseudoplasticity of the solutions, imposes mixing problems beyond the general capability of standard production equipment to ensure the

necessary transport of oxygen and other ingredients to the microorganism. The reader is referred to other treatises (6, 7) for these and other complexities in fermentation processes.

The solution properties of fermentation polymers that form helical aggregates in aqueous solutions are unique with respect to the viscosity retention at higher temperatures and to mechanical (discussed in Chapter 11), thermal-oxidative and acid-catalyzed degradation, and fermentation polymers have therefore found cost-effective use in many areas of application.

In the remaining sections of this chapter, derivatization techniques and factors affecting the position of adduct substitution in the modification of cellulose and the structural features that affect water solubility in underivatized carbohydrate polymers are discussed.

Solubilization through Derivatization

As noted previously, cellulose is insoluble in aqueous solutions because of intra- and intermolecular hydrogen bonding. Disruption of the polar bonding sequences can be achieved through esterification or etherification (of the anhydrides) to cellulose. Nonuniform addition occurs until the backbone is highly substituted. To achieve water solubility, the fully substituted cellulose ester must be partially hydrolyzed. The commercially important esters are used in plastics and other applications, not as water-soluble polymers.

Water-soluble cellulose ethers are commercially important. Their production involves the base-catalyzed addition of one or a combination of two of the following four adducts: methyl chloride (CH_3Cl), the sodium salt of α -chloroacetic acid ($\alpha\text{-ClCH}_2\text{CO}_2^-\text{Na}^+$), ethylene oxide, and propylene oxide. As in the commercially important esters, mixed ether adducts are produced to meet specific application requirements.

Two of the adducts, CH_3Cl and $\alpha\text{-ClCH}_2\text{CO}_2^-\text{Na}^+$, are added under mole equivalent caustic conditions to produce methylcellulose and (carboxymethyl)cellulose (CMC). The degree of substitution (DS; *see* Chapter 4 for NMR analysis) required to achieve water solubility is lower with the anionic grouping (1.3 versus 0.6). The degree of substitution achieved in the caustic-catalyzed addition of ethylene or propylene oxide is difficult to determine experimentally because the generation of new reaction sites with the addition of each adduct. The molar substitution (MS) of adduct per glucopyranose group can be quantified experimentally (8) and the amount of substitution in oxide derivatives is reported as an MS value.

The relative reactivities (8) of three of these adducts with the three carbon-containing hydroxyl positions (C-2, C-3, and C-6) available on each repeating unit under high caustic conditions are as follows [substituent, relative reactivity ($k_2:k_3:k_6:k_x$, where k_x is the relative reactivity of

positions generated by the addition of ethylene oxide to any of the pyranose hydroxyls]: methyl chloride, 5:1:2; sodium chloroacetate, 2.0:1.0:2.5; and ethylene oxide, 5:1:8:12.

The addition of CH_3Cl and $\alpha\text{-ClCH}_2\text{CO}_2^-\text{Na}^+$ requires equivalent amounts of caustic, generating 1 mol of NaCl per mol of adduct reacted. The addition of ethylene or propylene oxide is catalytic and exothermic. This characteristic with the explosive potential of oxides, and the generation of a new, more reactive anion with each oxide added (the new, more reactive anion promotes chaining and nonuniformity of substitution), has resulted in the use of a slurry process for the addition of oxide units to cellulose products. For achievement of uniform substitution in oxide derivatizations, a moderate concentration of caustic is required. The moderate caustic concentration (e.g., an alkali-to-cellulose ratio of 0.37 or 6.8 M) complemented by the presence of a suitable water concentration (discussed later) disrupts the hydrogen bonding present in cellulose and promotes the availability of all hydroxyl functions for substitution. The similarity in reactivity ratios between high molecular weight (hydroxyethyl)cellulose prepared via the slurry process (9) and that observed from low molecular weight, water-soluble, regenerated cellulose (10) supports this hypothesis.

Variation in ethylene oxide reactivity with the three pyranose hydroxyls with caustic concentration was also demonstrated in the latter studies. The water solubility ensured the availability of all hydroxyl groups, which is not true in some commercial derivatization processes. The relative reactivities as a function of sodium hydroxide concentration observed in this study are as follows [sodium hydroxide concentration (M), reactivity ratio ($k_2:k_3:k_6:k_x$)]: 0.75 M, 3.0:1.0:3.0:1.5; 2.50 M, 4.0:1.0:5.5:4.0; and 4.50 M, 4.7:1.0:8.5:12.0.

At the moderately high caustic concentration (4.50 M), a decided preference for the addition of ethylene oxide to the primary hydroxyl position (i.e., C-6 and the oxyanions generated on oxide addition) is observed; as the caustic level is decreased, little selectivity in addition occurs. A combination of two mechanisms was offered for this variance: (1) a decrease in reactivity of the C-6 hydroxyl with decreasing base (10, 11) due to a sheath of water around the primary hydroxyl and (2) a decrease in reactivity with increasing caustic of the secondary hydroxyls due to adduct formation between the base and the vicinal diols of the 2- and 3-carbon positions (10, 12). Additional complexities due to a neighboring group effects have also been indicated (13). A third mechanism has been recently (14) suggested for this variance. A decreasing contribution of intramolecular hydrogen bonding of the C-3 hydroxyl to the C-2 oxyanion is proposed with increasing caustic. This results in high acidity of the C-2 hydroxyl at low caustic and a low acidity at high caustic.

The caustic sensitivity of ethylene oxide placement noted in the above glucopyranose oligomer study has been used in controlling the placement of ethylene oxide in derivatizing high molecular weight cellulose via a slurry process (9) (the dispersant is generally an alcohol or ketone). The slurry process is used to maintain viscosity control. In the catalyzed ethoxylation of cellulose, 6.8 M NaOH is employed. A water concentration between 9 and 13 wt % containing 6.8 M caustic is effective in disrupting crystallinity and intra- and intermolecular hydrogen bonding to facilitate the availability of all hydroxyl groups. If this combination is used in the slurry addition of ethylene oxide to cellulose and the adduct is added to an MS of 1.0, the caustic concentration can then be decreased to 0.1 M and the ethoxylation continued to achieve a water-soluble (hydroxyethyl)cellulose. Direct ethoxylation of cellulose in a slurry process using a 0.1 M caustic concentration throughout results in nonuniform addition and a water-insoluble (hydroxyethyl)cellulose even if highly substituted. Partial neutralization at an intermediate MS of a standard 6.8 M slurry facilitates the availability of all glucopyranose hydroxyls if the intermediate molar substitution product is not dried. Continued ethoxylation under lower caustic concentrations facilitates equal substitution among the three available positions. This approach permits greater substitution at the C-2 position, and thereby, greater stability to enzymatic degradation (9, 15, 16). The importance of the amount of water added to the slurry is evident in the substitution patterns (9) reflected in the percentage of unsubstituted vicinal diol and of unsubstituted anhydroglucose units as a function of the molar substitution of ethylene oxide. There is a dramatic difference in the unsubstitution patterns between 4 and 7 to 10 wt % water levels or between the 7 to 10 and 13 wt % concentrations (Figure 1). The former transition reflects the amount of water required (17) to complement caustic in affecting the availability of all of the glucopyranosyl hydroxyls; the latter transition is believed to be related to a change in the reactivity ratios by a lower caustic concentration in the cellulose-water matrix of the dispersed slurry at the higher water level.

The importance of water in changing the distribution pattern of oxyethylene placement suggests that the relative placement of CH_3Cl and $\alpha\text{-ClCH}_2\text{CO}_2^-\text{Na}^+$ substituents would follow similar selectivity for the C-6 hydroxyls if these adducts were added at a caustic level. This selectivity has been observed (14).

When an anion is added to propylene oxide, only 2-4% of the oxyanion generated is primary; the predominant species is secondary (Scheme II). Due to steric and inductive effects, the secondary oxyanion should be less reactive; more uniform substitution in cellulose derivatization results. This uniform substitution is reflected in the reactivity profile (Figure 2). The results are in part reflective of the greater selectivity in

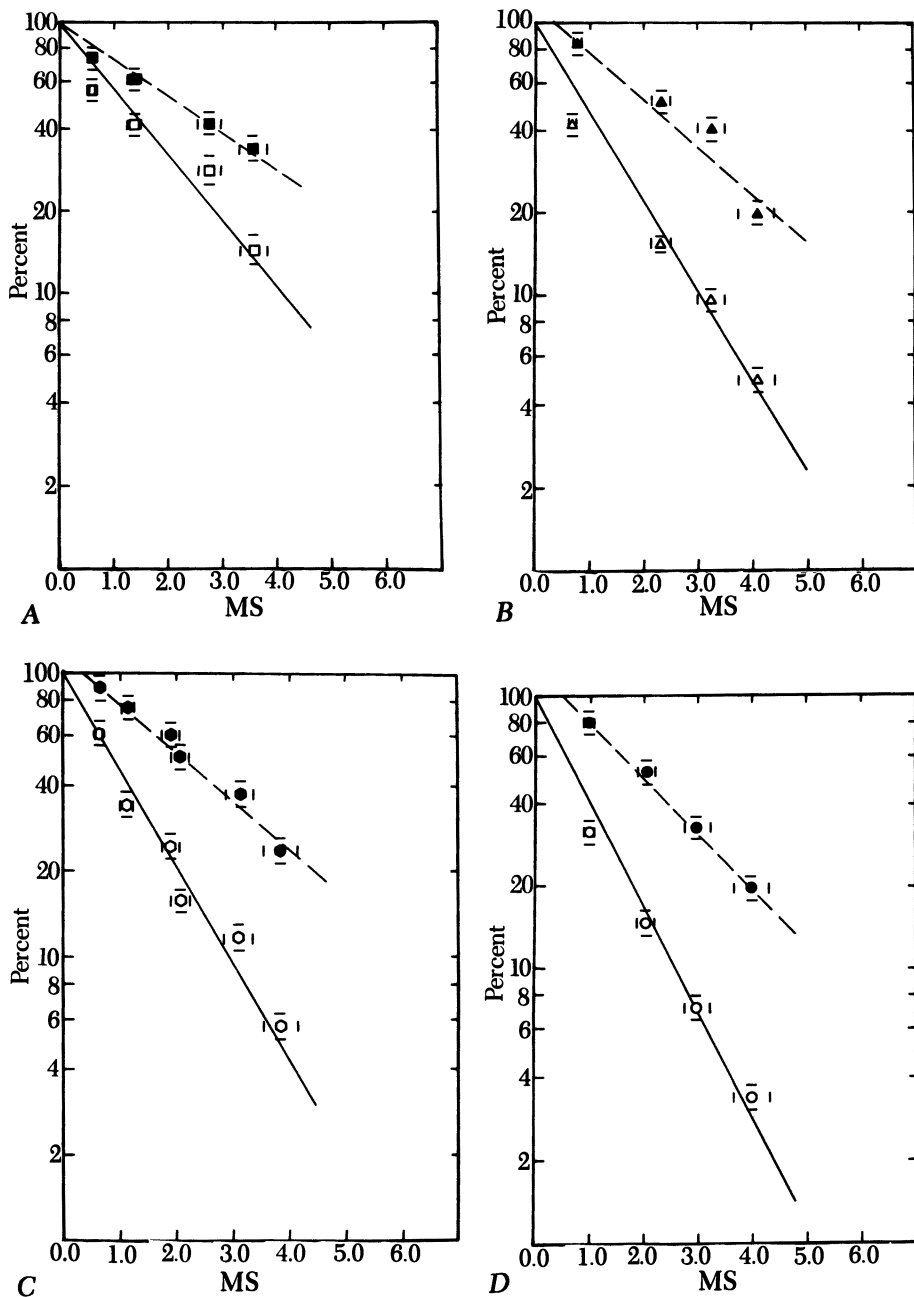
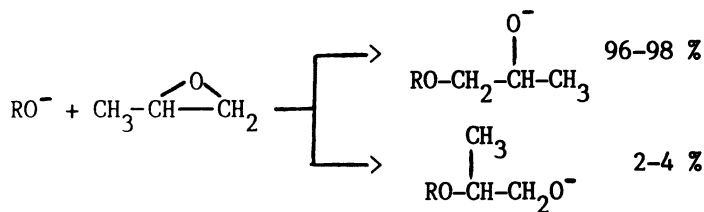


Figure 1. Reaction profile (percent unsubstituted diol, closed symbols; percent unsubstituted glucopyranose units, open symbols; as a function of molar substitution) for (hydroxyethyl)cellulose in slurries containing (A) 4, (B) 7, (C) 10, and (D) 13 wt % water. The alkali-to-cellulose ratio was 0.37.



Scheme II. S_N2 reaction intermediate of propylene oxide.

oxyanion reactivity of propylene oxide relative to that of ethylene oxide. This difference is illustrated in the selective reaction (14) of propylene oxide with the oxyethylene end groups of an intermediate molar substitution (hydroxyethyl)cellulose (MS = 1.0).

Both amylose and guaran are derivatized to low molar substitution levels. High degrees of substitution except in limited application areas are not necessary; the precursors are water soluble, and low levels of substitution will improve their temperature solubility or facilitate additional purification of the precursors. Two primary polymer classes that

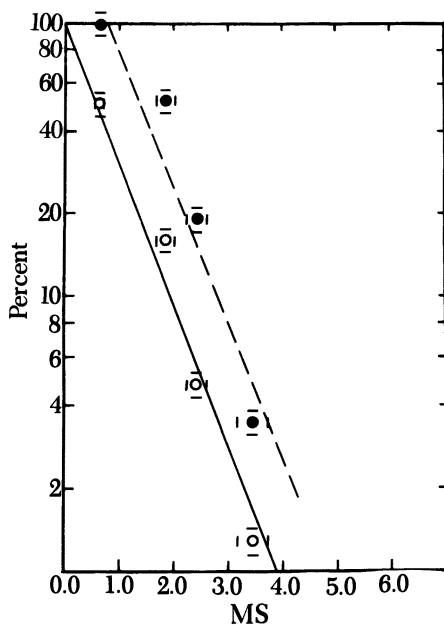


Figure 2. Reaction profile (percent unsubstituted diol, closed symbols; percent unsubstituted glucopyranose units, open symbols; as a function of molar substitution) for (hydroxypropyl)cellulose in slurries containing 13 wt % water. The alkali to cellulose ratio was 0.37.

are derivatized for such purposes are starch and the galactomannans. Direct derivatization of such polymers in their high molecular weight form would result in significant viscosity due to their solubility. In guar gum (guaran, discussed in a later section) derivatizations, borate ions (at a 100-ppm concentration) complex with the 2,3-cis diols (i.e., axial-equatorial stereochemistry) on both the manno- and galactopyranose units present in guaran to minimize solubility. This reactivity of the vicinal diol structure, particularly with borates and titanates, represents a situation where a molecule's stereochemistry is closely related with its utilization. This relation is used in applications where viscous gels under high temperature and pressure conditions are required, for example, in fracturing of petroleum and gas wells for increased productivity. This application is discussed in Chapter 13.

Structural Features That Affect Water Solubility in Underivatized Carbohydrate Polymers

Four structural features impart aqueous solubility to carbohydrate polymers.

The first is branching. Branches on the macromolecular chain will disrupt intermolecular associations and thereby promote solvation.

The second is ionizing groups. Ionizing groups such as carboxylate, sulfonate, or sulfate anions are readily solvated by water, and such groups inhibit intermolecular associations through electrostatic repulsions.

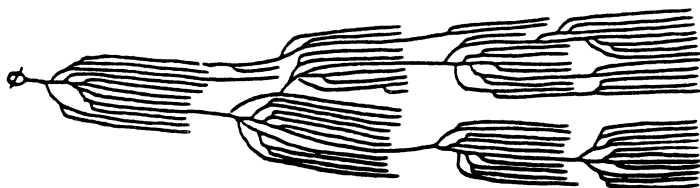
The third is interunit positional bonding. The most abundant polysaccharides are formed by condensation through the 1- and 4-carbon units (designated 1-4). This bonding provides a highly symmetrical structure and facilitates intermolecular association between units of different chains (i.e., if the connecting bond is a β linkage). Bonding through the 1- and 3-carbon units (1-3) imparts less symmetry and produces slightly better solubilization (e.g., solubility in aqueous-caustic media). Too few examples of 1-2 bonding exist to make a generalization concerning solubility characteristics. Linkage through the 1- and 6-carbon positions dramatically improves aqueous solubility. The 5-6 carbon-carbon bond is external to the pyranosyl ring and provides an entropic contribution to solubilization through increased rotational freedom in the solubilized state. The linkage external to the pyranosyl ring also provides a greater distance between rings.

The fourth is nonuniformity in the repeating structure. Nonuniformity can be obtained by (1) alternation of the type of monosaccharide units linked (i.e., to produce a heteropolysaccharide), (2) variation of the linkage position (e.g., 1-4 alternating with 1-3, 1-2, and 1-6), and (3) variation in the anomer linkage (i.e., alternating α with β).

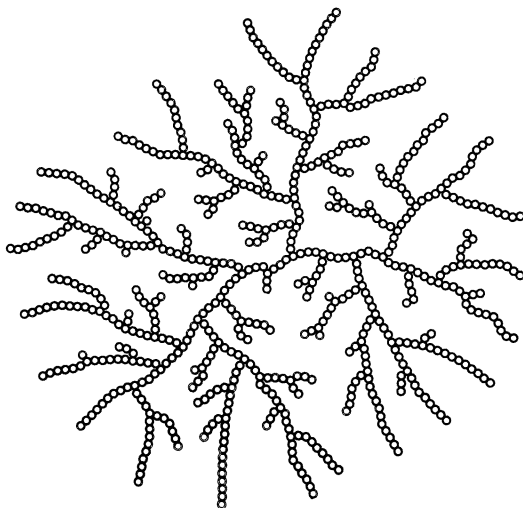
The first three solubilization concepts are supported with specific examples.

Branching. $\alpha(1\rightarrow4)$ -GLUCOPYRANOSE. Storage polysaccharides offer the best example of the effectiveness of branching in providing solubilization. The α linkage of glucose units does not confer true solubility to amylose (the minor component of most starches) but does create an improvement of several orders of magnitude over β -linked units. Amylopectin (structure VII), glycogen (structure VIII), and amylose (structure V) all contain a backbone composed of $\alpha(1\rightarrow4)$ linkages; amylopectin and glycogen differ only by the frequency of branched chains from the 6-carbon hydroxyl, and true solubility is achieved in these polymers (18).

When a macromolecular chain is highly branched as in amylopectin or glycogen, the thickening power of the polymer is compromised. The effective sweep volume for a given molecular weight is lower than that of the linear macromolecule. The problem of inadequate thickening by



VII

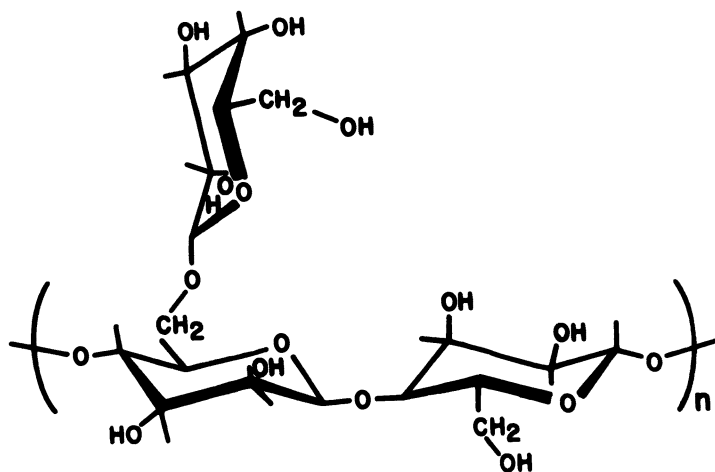


VIII

starch is in part economic. Starch is abundant and can be isolated with a molecular weight of 1 million, but commercial starches have low molecular weights, since low-cost rectification procedures result in molecular weight degradation. Many commercial starches have very low molecular weights because of intentional degradation (e.g., oxidation) to achieve effects other than thickening.

$\beta(1-4)$ -MANNOPYRANOSE. If the branching consists of short segments, spaced randomly, solubility can be achieved without compromising the macromolecule's ability to thicken. Locust bean and guar gums are examples of this type of carbohydrate polymer; the backbone structure is a repeating mannopyranosyl unit. The unbranched 2-carbon epimer of cellulose, ivory nut mannan, unlike cellulose is not easily swollen by caustic and water. The placement of one-unit galactopyranosyl branches from the 6-carbon of the repeating mannopyranosyl units (in locust bean and guar gums) causes solubilization without compromising the rheological properties of the macromolecule.

Locust bean gum is obtained from carob trees and contains an average of six mannopyranosyl units for every galactopyranosyl branch. The polymer achieved commercial acceptance in a wide variety of applications, but the limited growth potential of carob trees restricted its availability. When it was realized that the polysaccharide in guar gum seeds was structurally similar to that in locust bean gum, and that the potential availability of guaran was significantly greater, the utilization of locust bean gum diminished. The mannose-to-galactose ratio (2:1) in guaran is lower than that in locust bean gum (6:1). Originally, the galactose branches in guaran were thought to be alternating (as illustrated in structure IX). Research over the past decade (19-22)—



IX

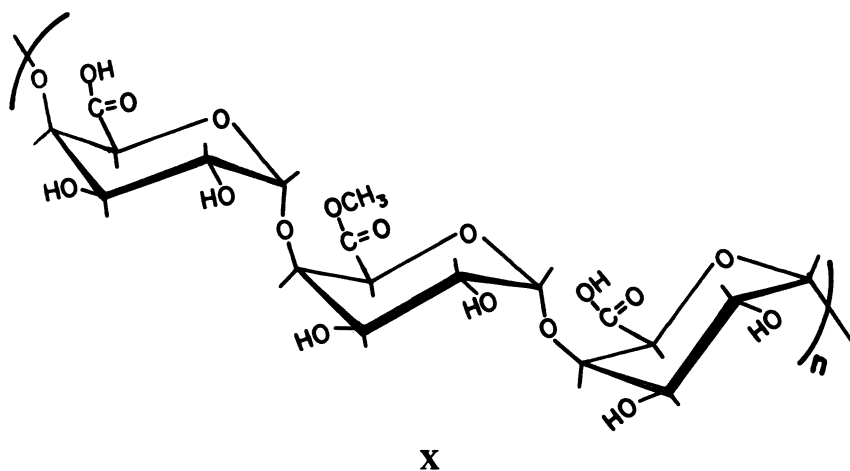
combining periodate oxidations with statistical analysis and detailed chromatographic separation of enzymatically degraded polymer residues (23)—has shown that the galactose branches are randomly placed; sequence runs with no branch attachments and sections where the branches occur in contiguous sequences exist. However the galactopyranosyl residues are spaced, the units are effective in disrupting inter-chain associations and thereby promoting solubilization without compromising the inherent overall thickening potential of the main chain.

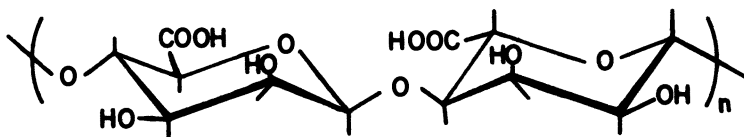
$\beta(1-3)$ -GLUCOPYRANOSE. Short-chain branching in this family of carbohydrate polymers affects solubility with dramatic viscifying properties. For organizational purposes, this class will be discussed under Interunit Positional Bonding.

Ionizing Groups. Carboxylate, sulfonate, and sulfate groups are the most frequently found ionic substituents in polysaccharides, with the former the more abundant.

Carboxylate groups ($-\text{CO}_2\text{H}$) are weak acids; their salt forms are readily solvated by water and the charges inhibit intermolecular associations between chains. One of the most widely used commercial polymers, carboxymethylcellulose (CMC), relies on such solubilizing groups. The technology associated with the derivatization of cellulose to form CMC is discussed under Solubilization through Derivatization. Two naturally occurring structural analogues, pectinic and alginic acids, are illustrated in structures X and XI, respectively.

Pectinic and alginic acids, like CMC, have a backbone comprised of 1-4 positional linkages between monosaccharide units (24, 25). Unlike CMC, the carboxylate function is the C-6 carbon and the acid function is not linked to the 6-, 3-, or 2-carbons as in CMC. When the acid function-





XI

ality is attached to the 5-carbon, the structure is designated as a uronic acid.

Pectinic acid is isolated from citrus fruits. Two types of products are available commercially. As a thickener and gelling agent, pectinic acid is commercially available in low- and high-methoxyl grades. In the high-methoxyl product, at least 50% of the C-5 appendage exists as methyl esters units. The high-methoxyl grades are gelled through hydrophobic bonding. Thickening is obtained in an acid medium, which lowers the free carboxyl ion content; the lower free carboxyl ion content permits greater interchain association, which is potentiated by dehydrating agents (sucrose, glycerine, etc). The dilute aqueous solution properties of pectins are discussed in Chapter 3.

A second example of a naturally occurring carboxylated polymer is alginic acid, isolated from giant kelp, found in the Pacific Ocean off southern California and Australia. Alginic acid can be produced by a number of different algae; the best known is *Macrocystis pyrifera*. Like starch, alginic acid can be isolated in high molecular weight, if care is taken in its rectification. Alginic acid contains unique block arrangements of β -D-mannopyranosyluronic acid and α -L-gulopyranosyluronic acid monomer units (structure XI). The structure of glucose is given in Chart I. This unusual copolymer arrangement was produced by nature millenniums before the uniqueness of block copolymers was recognized by synthetic polymer chemists.

Alginic acid, like pectinic acid, can be used as a gelling agent through either the presence of divalent cations or the use of an acidic medium. In general, a maximum viscosity is realized at a pH of 3.0-3.5. Alginic acid polymers differ in structure with different types of algae, which cause variations in the ratio of mannuronic to guluronic acid units.

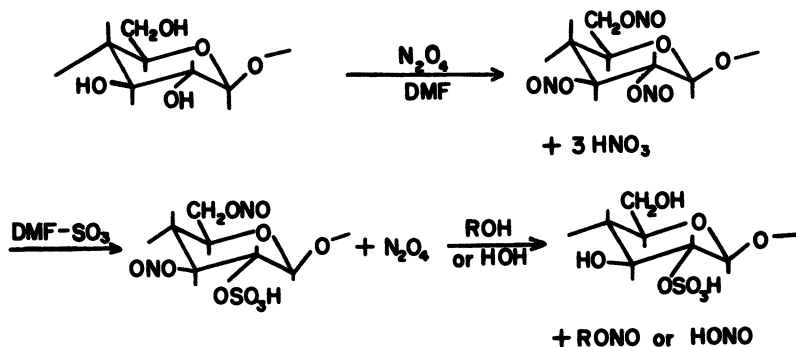
Both the mannose and gulose monomer units of alginic acid have the 2-carbon hydroxyl group in axial placement; in a Haworth convention of the pyranosyl ring, the 2,3-vicinal hydroxyl groups are in a cis position (i.e., both above the plane of the ring). This position is in contrast to the trans arrangement of the vicinal hydroxyl groups in the glucose- and galactose-based polysaccharides discussed previously, where the 2-carbon hydroxyl is equatorially positioned. The cis vicinal hydroxyl arrangement also is observed in guaran polymers; the cis

arrangement is very reactive to multivalent ions (e.g., calcium, borates, and titanates).

Carboxylate anions are the salts of weak acids and are therefore susceptible to significant charge shielding in saline solutions. Without high charge densities between repeating units that maintain the extended polyion rod conformation through charge repulsions, the polymer collapses (in highly saline solutions) and the viscosity of the solution decreases. If the anion is the salt of a strong acid (e.g., a sulfonate or sulfate group), saline solutions are less effective in decreasing viscosities, increasing adsorption, etc. Such carbohydrate polymers are known (e.g., the carrageenans) and are discussed under Nonuniformity in Repeating Structure. A modified cellulosic (cellulose sulfate ester) of this type has been reported (26, 27). Uniform substitution can be achieved on cellulose by first nitrating and then exchanging the substituents with sulfate groups. The reaction sequence is illustrated in Scheme III. The economics of production for a commercial synthesis of this type will be less favorable than those encountered with CMC. Some superior characteristics for cellulose sulfate ester solutions have been observed and are discussed in Chapter 11.

Interunit Positional Bonding. A third factor important to achieving water solubility is variation in the interunit bonding position. The symmetrical $\beta(1\rightarrow4)$ bonding found in cellulose and ivory nut mannan promotes an extended, near-planar macromolecular conformation that facilitates inter- and intramolecular hydrogen bonding, crystallite formation, and insolubility. Derivatization to obtain aqueous solution solubility of cellulose was discussed in the preceding section.

When the interunit bonding is $\beta(1\rightarrow3)$ as noted in the fermentation polymer curdlan, solubility is apparent in hydrogen-bond breaking and alkaline solutions. A $\beta(1\rightarrow3)$ bonding arrangement promotes helical



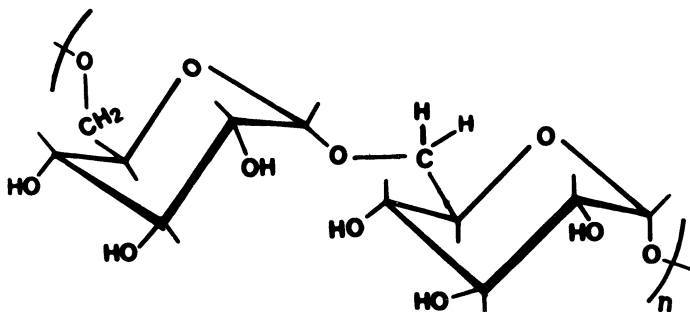
Scheme III. Synthesis of cellulose sulfate ester.

structures as was noted in the $\alpha(1-4)$ -glucopyranosyl polymer (amylose). An $\alpha(1-6)$ bonding unit permits greater rotational freedom than bonding through a ring hydroxyl, and the C-6 position also increases the distance between glucopyranosyl units; both factors favor water solubility.

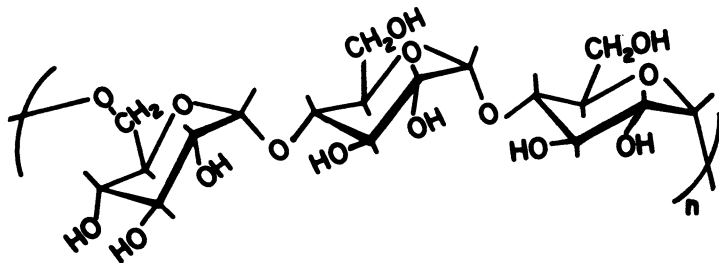
Two polysaccharides made by single-enzyme action and demonstrating the importance of positional substitution patterns in promoting aqueous solubility are the dextrans (3-5) and 1-6-bonded maltotriose polymer (3-5).

Dextran is a polysaccharide that exhibits 1-6 unit bonding; dextran is produced from sucrose by the action of glucosyltransferase, an enzyme from the bacterium *Leuconostoc dextranum*, which transfers the glucose unit to the growing dextran polymer. The most common dextran consists of glucose monomers, 95% of which are linked by $\alpha(1-6)$ bonds (structure XII); the remaining 5% are generally linked by 1-4 bonds, producing a branched structure. Approximately 80% of the side branches are only one glucose unit; the remaining 20% are chains of variable length when produced from B-511 enzyme (U.S. Department of Agriculture laboratory code system). The specific enzyme systems of different bacteria produce the structural variations described. Complexing abilities of dextran are determined primarily by the position of the branched units and are of importance in biomedical applications where dextran is used as a plasma extender, a drug carrier, and as a solubilized salt complexer.

Another example of 1-6 interunit bonding is illustrated by poly [$\alpha(1-6)$ -D-maltotriose] (structure XIII) produced from starch by the yeast *Pullularia pullulans*. The $\alpha(1-4)$ linkages of starch are retained in the three-unit segments; the three-unit sequence constitutes about 94% of the macromolecule. Approximately 6% of the segments are four units in length (not illustrated). The ambient temperature solubility not realized on a long-term basis in amylose and realized only with a cost-thickening



XII

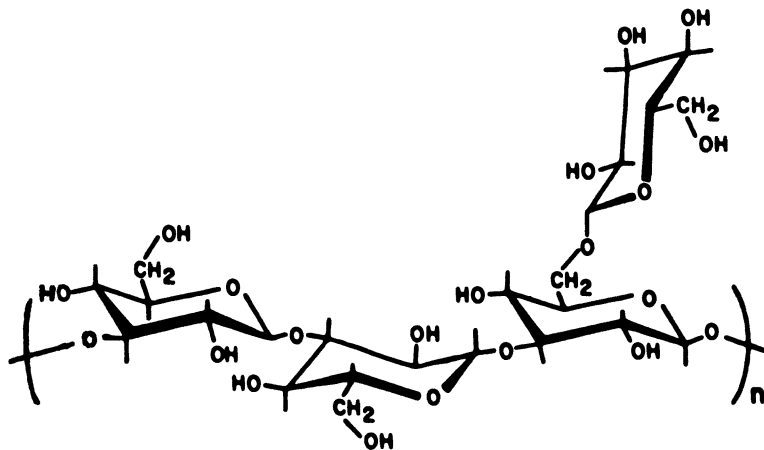


XIII

penalty in amylopectin is obtained through the 1-6 position bonding which occurs after every three or four 1-4 bonding units.

As noted under Branching, poly- β (1-3)-glucopyranose is soluble in alkaline solutions, but cellulose [i.e., poly- β (1-4)-glucopyranose] is not soluble. Solubility in neutral or acidic solutions in the poly- β (1-3)-glucopyranose family can be achieved if branching is introduced. Such a polysaccharide is synthesized by the enzymes of the yeast *Sclerotium glaucium* (SGPS) (28). The structural formula is illustrated in structure XIV; a glucopyranosyl branch occurs on every third main-chain unit. The associations in SGPS leading to helical aggregates are sufficient to promote three-dimensional structures that are not soluble in saline or low-temperature solutions (<10 °C). If the branching occurs at a greater or lesser frequency, aqueous solubility is decreased (29).

At moderate molecular weights (500,000 g/mol), SGPS is a very effective thickener because of its rodlike behavior in aqueous solutions; helices composed of three macromolecular chains are formed as well as



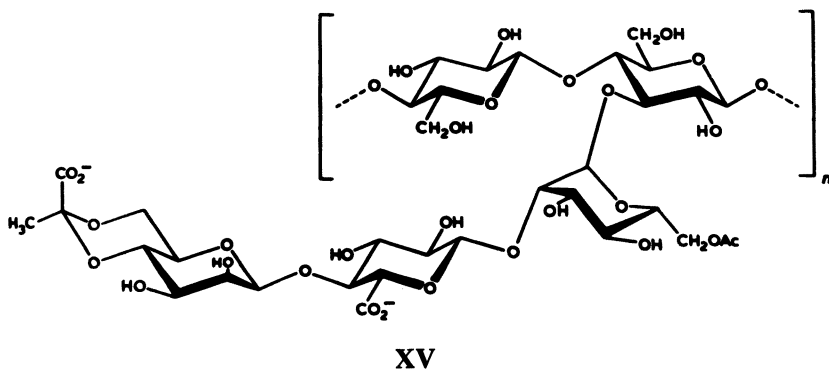
XIV

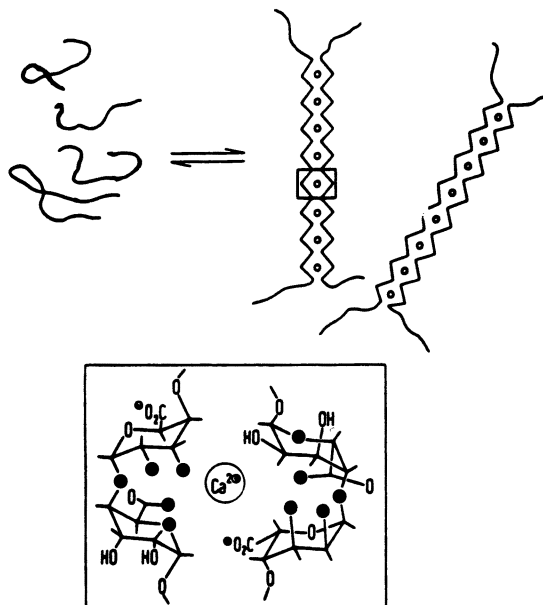
three-dimensional networks (30, 31). The associations inducing the helical structures can be disrupted by the addition of dimethyl sulfoxide to the aqueous solution (32).

Helical structures also can be formed from the $\beta(1\rightarrow4)$ repeating structure (i.e., the insoluble cellulose macromolecular chain). This fermentation polysaccharide, known as xanthan gum, is elaborated by the bacterium *Xanthomonas campestris* (XCPS). The structure (33, 34) of XCPS is given in structure XV. The helical structures of both SGPS and XCPS provide a unique solution behavior that is compared with other less-structured carbohydrate polymers in Chapter 11.

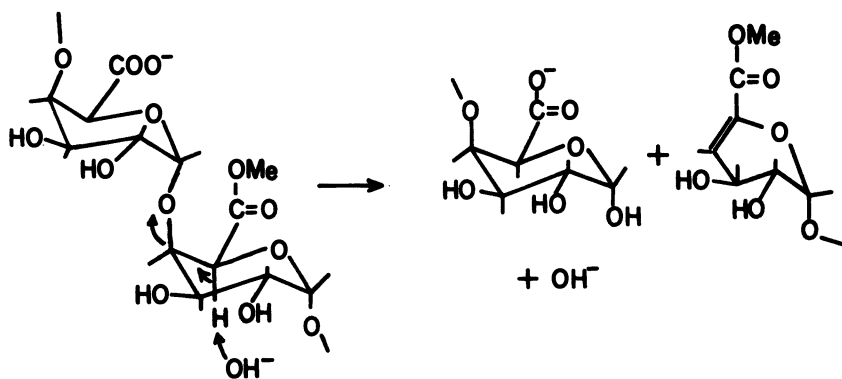
Even when optimized, none of the three solubility factors, even in some rather unique arrangements provided in fermentation products, yield water-soluble polymers with the solution characteristics necessary for adequate performance in many applications. The carboxylated polymers (CMC, XCPS, and pectinic and alginic acids) are sensitive to the presence of divalent cations; alginic and pectinic acids precipitate via "egg-crate" complexes (35, 36) (Scheme IV) in the presence of low concentrations of calcium ion. The carboxylated fermentation polymer XCPS is sensitive to precipitation by divalent ions at a solution pH above 8-9 and in neutral divalent ion solutions at higher temperatures ($>50^\circ\text{C}$). In addition, XCPS is sensitive to borate ion cross-linking, as is alginic acid, due to the presence of cis vicinal diols in the branched units. The uronic acid polymers, pectinic and alginic acids, are unstable in alkaline solutions. The C-6 carbonyl group activates the proton attached to the C-5 carbon, and a β -elimination of the C-4-bonded residue (Scheme V).

Cellulose sulfate ester is not as sensitive to divalent ions. This ester's rigidity in fresh water solutions provides many solution properties associated with the helical fermentation polymers, but the ester group in cellulose sulfate ester is not hydrolytically stable.





Scheme IV. Schematic of egg-crate complex formation of alginic or pectinic acid.



Scheme V. Instability of uronic acid structure.

Despite these limitations the structural versatility available in carbohydrate polymers appears to offer the possibility of obtaining water-soluble polymers capable of meeting the performance demands in many applications. With this thought, the fourth alternative to achieving water solubility in carbohydrate polymers is considered.

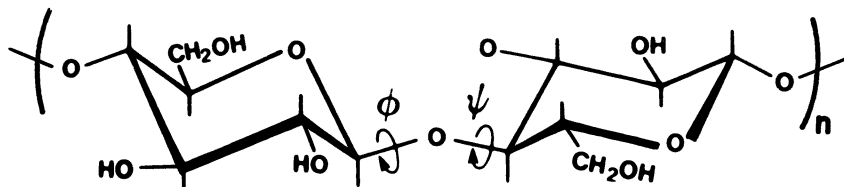
Nonuniformity in Repeating Structure. Variation in the repeating unit (i.e., heteropolysaccharide rather than homopolysaccharide) and

alternation in the interunit bonding pattern (combining both anomeric and positional changes) should in concept provide the means to obtain aqueous solution solubility without

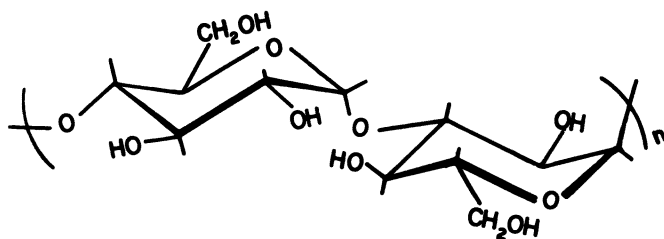
1. losing viscosifying power as noted in the $\alpha(1\rightarrow6)$ or the highly branched $\alpha(1\rightarrow4)$ structures;
2. the salt sensitivity in helical structures noted in the $\beta(1\rightarrow4)$ polyelectrolytes (i.e., XCPS); and
3. the multiplicity of problems cited in 1 and 2 with the helical $\beta(1\rightarrow3)$ class of carbohydrate polymers.

Realizing an optimum in aqueous solution properties through multiple bonding patterns with variable pyranosyl units appears reasonable, but providing specific examples in support of the concept is an elusive task. Theoretical efforts (37-40) that consider conformational energy, primarily estimating the configurational entropy per residue and estimating the degree of rotational freedom of torsional angles (structure XVI), could offer insight if the methods were quantitative tools. Unfortunately, the state of the art in such efforts is unrefined.

A limited example of the irregularity in structure thought to overcome the limitations discussed is found in nigeran (structure XVII). This carbohydrate polymer contains variation in the interunit positional bonding pattern, but the repeating monomer and anomeric linkage are constant. Studies of this polymer have been limited primarily to the solid state (41, 42). The carrageenans, extracted from seaweed and harvested on the coasts of Maine and Massachusetts, are other examples. Although the repeating unit is constant (galactopyranose), the anomeric linkage



XVI



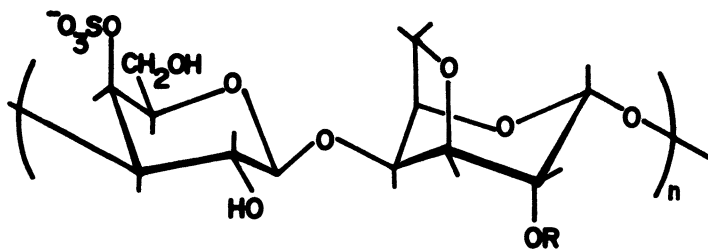
XVII

varies with the interunit bonding patterns; the anomeric and positional patterns alternate as $\beta(1\rightarrow3)$ and $\alpha(1\rightarrow4)$ linkages. This class, however, is also not entirely suitable in that the main chain (structure XVIII: κ -carrageenan, R = H; ι -carrageenan, R = SO_3^-) contains sulfate ester groups. From the general solubility concepts discussed, it might be expected that the carrageenans would be readily soluble in aqueous solutions and saline insensitive. This class of polymer, however, readily gels with salts of monovalent ions (e.g., K^+ or NH_4^+). Gelation is related to helix formation and subsequent desolvation.

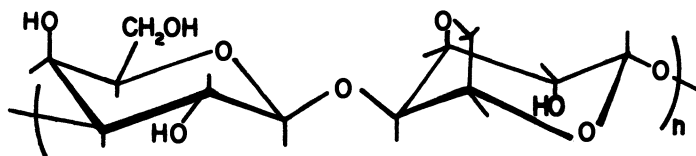
Agarose (structure XIX) is weakly anionic and is structurally similar to the carrageenans. The polymer is soluble in hot ($100\text{ }^\circ\text{C}$) aqueous solutions but gels at ambient temperatures from moderately concentrated solutions. Agarose contains residues of 3,6-anhydro- α -L-galactose that are considered in the carrageenans to promote gelation (36). Thus, agarose is not a suitable example of what might be conceptually possible in aqueous solubility and solution properties.

Conclusions

The primary problem in projecting structural relationships for water solubility in carbohydrate polymers is exemplified in the behavior of poly- $\beta(1\rightarrow6)$ -glucopyranose. This problem relates to residual crystallinity. The water solubility of the anomeric $\alpha(1\rightarrow6)$ isomer (i.e., dextran) is justified on its positional substitution pattern. That the difference in anomeric bonding would not affect insolubility is expected; however, this polymer appears to have an optimum gel formation temperature in the $5\text{--}25\text{ }^\circ\text{C}$



XVIII



XIX

range. Stipanovic proposed (43) that the gelation mechanism involves crystalline regions that act as cross-links or junction zones to establish a three-dimensionally stabilized network structure. The naturally occurring β isomer contains approximately 10% acetylation and does not gel. The low degree of glucopyranose branching might also be a factor in inhibiting gelation in the anomeric (α) polymer (i.e., dextran).

Long usage of carbohydrate polymers has not to date provided sufficient fundamental insights to project what might be achieved with structural variations in carbohydrate polymers. Controlled synthetic products to delineate structure-aqueous solution properties would provide direction and advance our understanding sufficiently for theoretical projections to be of value. The type of insights possible with current instrumental techniques [beautifully demonstrated in the $\beta(1-6)$ -glucopyranose study (43)] offers the possibility of adding significantly to what has been inherited over the milleniums in this family of macromolecules. The reader who desires greater detail on each class of carbohydrate polymer discussed in this brief chapter is referred to the recent series on *The Polysaccharides*, by Aspinnall (44).

Literature Cited

1. Lehninger, A. L. *Biochemistry*; Worth Publishers: New York, 1975, 2nd ed., p 250.
2. Morrison, R. T.; Boyd, R. N. *Organic Chemistry*; Allyn and Bacon: Boston, 1983; 4th ed., Chapter 28.
3. Whistler, R. L. *Industrial Gums*; Whistler, R. L., Ed.; Academic: New York, 1973; 2nd ed., Chapter 1.
4. Bolker, H. I. *Natural and Synthetic Polymers*; Dekker: New York, 1974.
5. Elias, H-G. *Macromolecules*; Plenum: New York, 1977; Vol. II, Chapter 31.
6. *Purification of Fermentation Products*; LeRoth, D.; Shiloach, J.; Leahy, T. J., Eds.; ACS Symposium Series 271: American Chemical Society: Washington, DC, 1984.
7. Saeir, H. H. *Mechanisms and Regulation of Carbohydrate Transport in Bacteria*; Academic: Orlando, FL; 1985.
8. Croon, I. *Sven. Papperstin.* 1960, 63, 247.
9. Glass, J. E.; Buettner, A. M.; Lowther, R. G.; Young, C. S.; Cosby, L. A.; *Carbohydr. Res.* 1980, 84, 245.
10. Ramnas, O.; Samuelson, O. *Sven Papperstin.* 1968, 71, 829.
11. Rowland, S. P.; Roberts, E. J.; Wade, C. P. *Text. Res. J.* 1969, 39, 530.
12. Roberts, E. J.; Wade, C. P.; Rowland, S. P. *Carbohydr. Res.* 1971, 17, 393.
13. Roberts, E. J.; Wade, C. P.; Rowland, S. P.; *Carbohydr. Res.* 1972, 21, 357.
14. Seneker, S. D. Ph.D. Thesis, North Dakota State University, 1986.
15. Klug, E. D.; Winquist, D. P.; Lewis, C. A.; In *Water Soluble Polymers*; Bikalis, N. M, Ed.; Plenum: New York, 1973; p 401.
16. Klop, W.; Kooiman, P. *Biochim. Biophys. Acta* 1965, 99, 102.
17. Seneker, S. D.; Glass, J. E. *Proc. Am. Chem. Soc. Div. Polym. Mater.: Sci. Eng.* 1984, 51, 248.

18. French, D. *Chemistry and Biochemistry of Starch*; Whelan, W. J., Ed.; *Biochemistry of Carbohydrates, Biochem. Series I*; Butterworths: New York, 1979; Vol. V.
19. Gonzales, J. J.; Hemmer, P. C. *J. Chem. Phys.* **1977**, *67*, 2496-2526.
20. Gonzales, J. J.; Kehr, K. W. *Macromolecules* **1978**, *11*, 996-1000.
21. Gonzales, J. J. *Macromolecules* **1978**, *11*, 1074-1085.
22. Painter, T. J.; Gonzales, J. J.; Hemmer, P. C. *Carbohydr. Res.* **1979**, *69*, 217-226.
23. McCleary, B. V. *Carbohydr. Res.* **1979**, *71*, 205-230.
24. McNully, W. H.; Pettitt, D. J. *Industrial Gums*; Whistler, R. L., Ed.; Academic: New York, 1973; 2nd ed., Chapter 4.
25. Cottrell, I. W.; Kovacs, P. *Food Colloids*; Graham, J. D., Ed.; Avir Publishing: Westport, CT, 1977; Chapter 11.
26. Schweiger, R. G. *J. Org. Chem.* **1976**, *41*, 90.
27. *Carbohydrate Sulfates*; Schweiger, R. G. ACS Symposium Series 77, American Chemical Society: Washington, DC 1978; p 163.
28. Rodgers, N. E. *Industrial Gums*; Whistler, R. L., Ed.; Academic: New York, 1973; 2nd ed., Chapter 12.
29. Norisuye, T. Presented at the XI International Carbohydrate Symposium; August, 1982, Vancouver, BC; Vol. 5, p 2.
30. Norisuye, T.; Takashi, T. *J. Polym. Sci., Polym. Lett. Ed.* **1980**, *18*, 547-558.
31. Kashiwagi, Y.; *Macromolecules* **1981**, *14*, 1220-1225.
32. Misaki, A.; Kakuta, M. Presented at the XI International Carbohydrate Symposium, August, 1982, Vol. 5, p 17.
33. Janson, P.-E.; Kenne, L.; Lindberg, B. *Carbohydr. Res.* **1975**, *45*, 275-282.
34. Melton, L. D.; Mindt, L.; Rees, D. A. *Carbohydr. Res.* **1976**, *46*, 245-257.
35. Thom, D.; Grant, G. T.; Morris, E. R.; Rees, D. A. *Carbohydr. Res.* **1982**, *100*, 29-42.
36. Rees, D. A.; Walsh, E. J. *Angew. Chem., (Int. Ed. Engl.)* **1977**, *16*, 214.
37. Abe, A.; Mark, J. E. *J. Am. Chem. Soc.* **1976**, *98*, 6468-6476.
38. Allinger, M. L.; Chung, D. Y. *J. Am. Chem. Soc.* **1976**, *98*, 6798-6803.
39. Twaroska, I.; Bleha, T. *Biopolymers* **1979**, *18*, 2537-2547.
40. Burton, B. A.; Brandt, D. A. *Biopolymers* **1983**, *22*, 1769-1792.
41. Marchessault, R. H.; Revol, J. F.; Bobbitt, T. F.; Norbin, J. H. *Biopolymers* **1980**, *19*, 1069-1080.
42. Barker, S. A.; Bourne, E. J.; O'Mant, D. M.; Stacey, M. *J. Chem. Soc.* **1957**, 2448-2454.
43. Stipanovic, A. J.; Giammatteo, P.; Robie, S. B.; Easter, S. A. *Proc. Am. Chem. Soc. Div. Polym. Mater.: Sci. Eng.* **1985**, *52*, 34.
44. Aspinall, G. O., *The Polysaccharides*; Academic: New York, Vols. 1-3, 1982, 1983, and 1984.

RECEIVED for review March 5, 1985. ACCEPTED August 23, 1985.

Characterization of Water-Soluble Polymers Using Size-Exclusion Chromatography

Howard G. Barth

Research Center, Hercules, Inc., Wilmington, DE 19894

The determination of molecular weight distributions of nonionic water-soluble polymers and polyelectrolytes by aqueous size-exclusion chromatography (SEC) can be difficult because of non-size-exclusion effects. These effects include electrostatic interactions between polymer and packing (ion exchange, ion exclusion, and ion inclusion), intramolecular electrostatic interactions, and adsorption. Furthermore, other non-size-exclusion chromatographic effects, such as viscous fingering and macromolecular crowding, may lead to erroneous SEC results. Guidelines for identifying and eliminating these effects are given. Furthermore, the potential of polymer shear degradation in SEC is discussed. Various methods of column calibration are reviewed with emphasis on the use of absolute molecular weight detectors. A description of high-performance packings for aqueous SEC is given. Finally, future trends regarding SEC and alternative techniques of characterizing polymers are considered.

WATER-SOLUBLE POLYMERS represent a major class of polymers comprising biopolymers as well as synthetic macromolecules. Biopolymers consist of nucleic acids, proteins, and polysaccharides. Synthetic water-soluble polymers comprise a large group of commercially useful products such as modified celluloses, poly(ethylene glycol), poly(vinyl alcohol), poly(acrylic acid), poly(acrylamide), and a host of other polymers. Inorganic polymers, such as polyphosphates, also fall into this category. Most applications of synthetic water-soluble polymers depend mainly on their viscosifying, rheological, and surface-activity properties. As a result, water-soluble polymers find uses in many areas ranging from food additives to flocculating agents.

To be water soluble, these polymers must contain hydrophilic or ionic groups either as part of the backbone or as pendent groups.

0065-2393/86/0213-0031\$07.25/0
© 1986 American Chemical Society

Because synthetic polymers may contain rather hydrophobic regions, a correct balance between hydrophobic and hydrophilic-ionic groups must be met to impart water solubility. In the case of polysaccharides, glycosidic linkages and high hydroxyl content render them water soluble. For proteins, the presence of amide and hydrophilic-ionic pendent groups leads to water solubility. In addition to chemical structure, branching, polymer stereoregularity, and configuration, as in the case of polysaccharides, also play a major role in controlling solubility.

Molecular weight distribution and average molecular weights are highly useful parameters in predicting end-use properties of these polymers. Size-exclusion chromatography (SEC), also referred to as gel permeation chromatography (GPC), is the premier characterization technique used to measure these physical properties. However, because of the presence of hydrophilic, ionic, and hydrophobic groups in water-soluble polymers, a number of non-size-exclusion effects can lead to erroneous results. The object of this chapter is to review the causes and to present guidelines for eliminating these effects. Furthermore, state-of-the-art developments in SEC are described in the areas of new high-performance packings and detector systems. Chromatographic approaches that can be used to estimate the chemical heterogeneity of polymers will be explored. Finally, a brief discussion of alternative chromatographic techniques to determine molecular weight distributions will be considered. A comprehensive review of all aspects of SEC is beyond the scope of this chapter; therefore, readers should refer to references 1-3 for past reviews of aqueous SEC and references 4-10 for recent books on SEC.

Principles of SEC

The separation mechanism of SEC is based on the differential extent of permeation of polymers into and out of porous particles packed into a chromatographic column. Large molecules, which cannot penetrate the pores of the packing, elute first followed by lower molecular weight components that are able to enter the pores. The pore volume available to a polymer is thus a function of the hydrodynamic volume and, to some extent, the shape of the macromolecule.

Figure 1 represents a typical calibration curve obtained from SEC in which the log (molecular weight or hydrodynamic volume) is plotted versus elution volume, V_e . The elution volume of a polymer is

$$V_e = V_o + K_D V_i \quad (1)$$

where V_o is the interstitial volume of the packed bed, V_i is the pore volume of the packed bed, and K_D is the chromatographic distribution coefficient defined as the ratio of the polymer concentration within the pores of the packing (V_i) and the polymer concentration in the intersti-

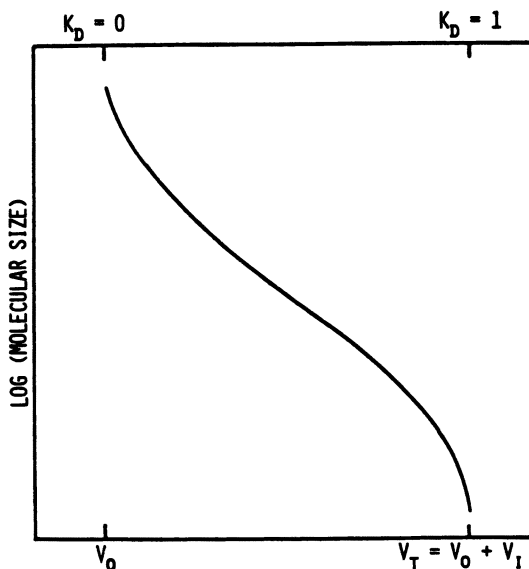


Figure 1. Typical SEC calibration curve. K_D is the SEC distribution coefficient, V_e is the polymer elution volume, V_0 is the interstitial or exclusion volume, V_i is the packing pore volume, and V_T is the total permeation volume. Reproduced with permission from reference 11. Copyright 1984 Astor Publishing Corp.

tial volume, V_0 , $K_D = C_i/C_o$, where C_i and C_o are the solute concentrations in the pore and interstitial volumes, respectively. Thus, K_D ranges from zero for excluded polymer, $V_e = V_0$, to unity for a polymer that can freely diffuse into the packing, $V_e = V_T = V_0 + V_i$, where V_T is the total permeation volume of the column.

From a thermodynamic consideration (5, 11), K_D can also be defined as

$$K_D = \exp(\Delta S/R) \quad (2)$$

where R is the gas constant and ΔS is the entropy change generated when the polymer diffuses from the mobile phase into the pores of the packing. In SEC, the separation is governed strictly by entropic rather than enthalpic contributions in contrast to other chromatographic techniques. Because of this fact, the separation depends only on molecular size.

An important objective in developing SEC methods, which will be treated in the next section, is to ensure that enthalpic interactions between the polymer and chromatographic packing are absent. Elution

of the polymer after V_T is indicative of non-size-exclusion effects. However, as will be discussed, even if $K_D < 1$, there is no guarantee that the separation is based on size exclusion. This point is especially true for polyelectrolytes.

Mobile-Phase Selection for Aqueous SEC

Mobile-phase composition must be selected to prevent enthalpic interactions between polymer and packing. In the case of polyelectrolytes, polymer-packing interactions can be caused by electrostatic as well as hydrophobic forces, whereas for nonionic, water-soluble polymers, hydrophobic forces as well as hydrogen bonding can lead to adsorption. Electrostatic interactions can be classified as ion exchange, ion exclusion, and ion inclusion. Intramolecular electrostatic interactions, which occur with polyelectrolytes, also contribute to non-size-exclusion effects.

Ion Exchange. Most chromatographic packings have anionic groups that can act as cation exchange sites. For example, in the case of silica-based packings, residual silanol groups are responsible for ion exchange of cationic polymers. Packings may also contain carboxyl functional groups that can also behave as weak exchange sites depending on the mobile-phase pH. In the presence of ion-exchange sites, cationic polyelectrolytes may show severe tailing extending beyond the total permeation volume. Depending on the extent of this type of adsorption, K_D may be quite large and the polymer may be irreversibly adsorbed and not elute.

One possible method of eliminating this effect is to reduce the pH of the mobile phase to below 4 to prevent dissociation of silanol or carboxyl groups on the packing. An increase of mobile-phase ionic strength will also aid in the prevention of ion exchange. Depending on the nature of the packing and the charge density and molecular weight of the polymer, an ionic strength between 0.05 and 0.6 M may be required. If these approaches are unsuccessful, a cationic compound, such as a low molecular weight quaternary ammonium compound, may be added to the mobile phase to compete with the sample for active sites (12). Alternatively, small amounts of sample added to the mobile phase may also be employed to deactivate adsorptive sites.

Because of ion-exchange and other electrostatic interactions, bare silica packings should never be used in SEC of polyelectrolytes. Surface-modified silica packings should always be used to reduce the amount of surface silanol groups. Most commercially available high-performance silica packings for aqueous SEC consist of a chemically bonded stationary phase containing diol functional groups. Another way of overcoming cation exchange is to employ packings derivatized with anion-exchange groups (13). This approach produces a cationic charged surface; thus, adsorption of similarly charged polymers is eliminated. A commercial

packing, CATSEC (SynChrom, Inc., Linden, IN), is available, which consists of polyethylenimine-coated silica. This packing is useful for the SEC analysis of cationic polyelectrolytes (14). Obviously, the packing cannot be used for anionic polymers and, as discussed later, the ionic strength of the mobile phase must be adjusted to eliminate ion exclusion (*see* references 15-18 for papers dealing with SEC of cationic polyelectrolytes).

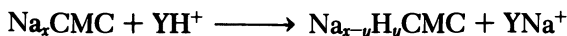
Ion Exclusion. When an anionic polyelectrolyte approaches the surface of packing containing anionic groups, the polymer cannot readily diffuse into the pores of the packing because of electrostatic repulsive forces. This effect, first reported by Neddermeyer and Rogers (19), is termed ion exclusion. As a result, peaks elute earlier than expected and can lead to severe overestimation of molecular weights. Also, the elution volume of the polymer varies with injected concentration accompanied by peak fronting. Interestingly, SEC of chemically heterogeneous anionic polymers can cause rather unusual appearing multimodal molecular weight distributions if ion exclusion is not eliminated (20).

So that ion exclusion can be eliminated, the pH of the mobile phase should be decreased ($\text{pH} < 4$) and the ionic strength increased. Depending on the nature of the polyelectrolyte and packing, an ionic strength between 0.01 and 0.2 M should be sufficient to eliminate this effect.

Ion Inclusion. Ion inclusion is a rather unusual non-size-exclusion effect that is a result of the establishment of Donnan membrane equilibrium between ionic solutes in the interstitial volume (V_o) and those within the pores of the packing (V_i) (21). The interface between V_o and V_i can be considered as a semipermeable membrane. In the presence of polyelectrolyte molecules, which have $K_D < 1$, associated counterions that have $K_D = 1$ (i.e., counterions that can freely diffuse into and out of pores) act as a driving force to pull more polyelectrolyte into V_i to equalize the chemical potential between V_i and V_o (22). This effect leads to an increase in K_D or underestimation of the molecular weight of the polyelectrolyte. The magnitude of this effect is related to the charge density of the polyelectrolyte (23, 24). The effect that permeable counterions have on the elution behavior of polyelectrolytes can be negated or overcome by the addition of low concentrations of electrolyte to the mobile phase (21). However, this addition gives rise to a totally permeated "salt peak" eluting at V_T that may interfere with molecular weight distribution measurements. So that this type of interference can be eliminated, the addition of a low pore-size column (~ 60 - 100 Å) helps to separate the salt peak from the polymer envelope (25, 26).

In addition to salt peaks arising from ion inclusion, another source of error can come from ion exchange between counterions associated with the polymer and ions from the mobile-phase electrolyte. For exam-

ple, in the case of sodium (carboxymethyl)cellulose (CMC) chromatographed in an acidic mobile phase (25)



excess sodium ions from the injected sample will appear at V_T . Also, mobile-phase mismatch during sample preparation is an important cause of salt peaks, especially if fairly high ionic strength mobile phases are employed.

Adsorption. Adsorption is an all-encompassing term in which $V_e > V_T$; it takes into account a variety of enthalpic interactions that can occur between polymer and packing. As previously discussed, ion exchange can be eliminated by increasing the ionic strength or decreasing the pH of the mobile phase (27). Hydrogen bonding, which can occur especially with polysaccharides, can be eliminated by the addition of guanidine hydrochloride (28) or urea (29) to the mobile phase. Hydrophobic interactions, which can occur with polyelectrolytes as well as nonionic water-soluble polymers, may be reduced or eliminated by either decreasing the ionic strength or polarity of the mobile phase or by adding an ionic surfactant. Furthermore, the stationary phase should be fairly hydrophilic and should have relatively few hydrophobic sites.

In addition to aqueous mobile phases, water-methanol solvents were used to analyze water-soluble cellulosics (20). Nonaqueous mobile phases such as dimethylformamide (30-33) and dimethyl sulfoxide (34), which are excellent solvents for polar and ionic polymers, were also employed with and without added electrolytes. These mobile phases not only reduce hydrophobic interactions between polymer and packing but also help to prevent polymer aggregate formation.

Figure 2 illustrates these various types of interactions using low molecular weight test solutes (35). In these experiments, the K_D values are measured as a function of mobile-phase ionic strength by using a high-performance packing material consisting of a glycerylpropylsilyl stationary phase bonded onto porous silica particles (100-Å pore size). Because of the low molecular weights of these solutes, the K_D values should be close to unity if size exclusion were the mechanism of separation. In the case of benzyl alcohol, K_D increases from 1.4 to 1.9 as the ionic strength is increased to 2.4 M. This result is indicative of hydrophobic interaction. With arginine, a basic amino acid, K_D decreases from 1.35 when water is used as the mobile phase to unity when the ionic strength is increased to 0.1 M. Adsorption, in this example, is caused by ion exchange with residual silanol groups of the packing. Glycyltyrosine, a hydrophilic dipeptide, shows no evidence of adsorption, and its elution behavior is independent of ionic strength. At low ionic strengths, citrate ions are ion-excluded from the pores of the packing because of electro-

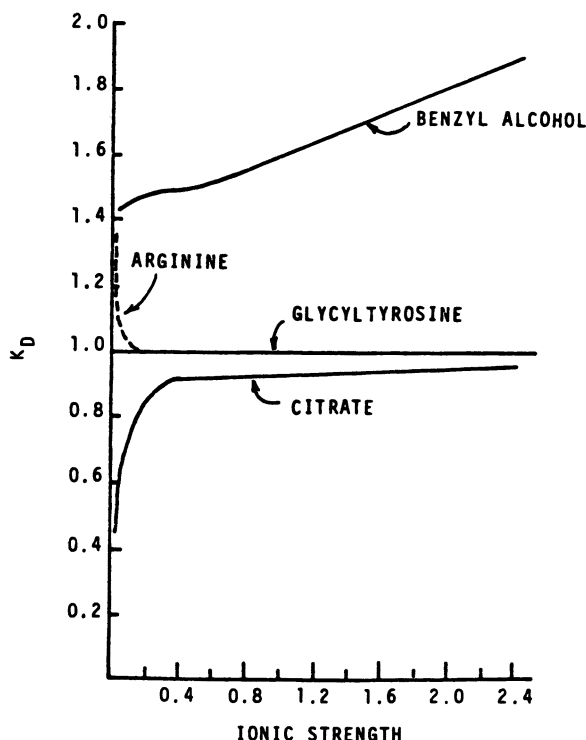


Figure 2. Dependence of the distribution coefficient, K_D , of test solutes on mobile-phase ionic strength. Adapted from reference 35 and used with permission. Copyright 1980 Preston Publishing Co.

static repulsive forces between solute and packing. This effect is reduced by increasing the ionic strength to about 0.4 M.

Although these and other low molecular weight test solutes (35) serve as useful probes for the characterization of SEC packings, optimum mobile phase compositions established with these solutes may not be applicable to polymers. Because of multiple and cooperative interactions that occur with macromolecules, non-size-exclusion effects are usually much more severe and require further mobile-phase modifications. Furthermore, many water-soluble polymers contain ionic, hydrophilic, and hydrophobic groups so that a correct balance between mobile-phase ionic strength and polarity must be maintained to avoid adsorption.

In addition to measurement of K_D as a function of mobile-phase ionic strength to determine whether or not adsorption is occurring, another approach, which is also applicable to organosoluble polymers, is to measure K_D as a function of temperature. According to equation 2, K_D should be almost independent of temperature if the separation is based

strictly on entropic considerations. The universal calibration method (*see* Column Calibration) can also be tested on well-characterized samples—in the absence of adsorption or other secondary mechanisms, $[\eta]M$ versus V_e plots of chemically dissimilar polymers should fall on the same line.

Summary. For optimization of SEC mobile-phase composition, first a well-deactivated packing, either silica or polymeric based, which has minimal residual silanol or ionic sites must be selected. Furthermore, so that hydrophobic interactions can be avoided, the stationary phase must be fairly hydrophilic and contain as few hydrophobic groups as possible.

High ionic strength, low-pH mobile phases should do well for polyelectrolytes. Under these conditions, ionic interactions between sample and packing are minimized and the polymer is in a contracted state. As a result, small differences in mobile-phase composition will not affect elution volume. In addition, smaller pore size packings can be employed. This effect is important in high-performance SEC in which high-resolution large pore size packings ($>4000 \text{ \AA}$) are not commercially available. Finally, when high ionic strength mobile phases are used, the effect of chemical heterogeneity of ionic groups on molecular size is reduced. However, the major disadvantage, of which one should be aware, is the enhancement of hydrophobic interactions at high ionic strength levels.

Other Non-Size-Exclusion Effects

Intramolecular Electrostatic Effects. Polyelectrolytes have unique solution properties because of the presence of ionic groups along the chain. When dissociated, these groups electrostatically repel one another; this result leads to chain expansion. If an electrolyte is added to the solution, the chain contracts because of electrostatic shielding of these repulsive forces. As a result, K_D is a function of mobile-phase ionic strength (25, 26). This effect can be seen in Figure 3 in which K_D of CMC is plotted versus mobile-phase ionic strength (25). K_D is a strong function of mobile-phase ionic strength up to a molar ionic strength of ~ 0.2 . Beyond this region, K_D appears to level off. This effect is caused by molecular contraction; this fact is demonstrated by a plot of intrinsic viscosity, $[\eta]$, which is a measure of the hydrodynamic volume of a polymer, versus ionic strength. As indicated, $\log [\eta]$ decreases with decreasing ionic strength (25); this result suggests molecular contraction. When mobile phases are developed for the SEC of polyelectrolytes, the effect of ionic strength on $[\eta]$ should be determined; the ionic strength at which a minimum $[\eta]$ is obtained should be employed if possible.

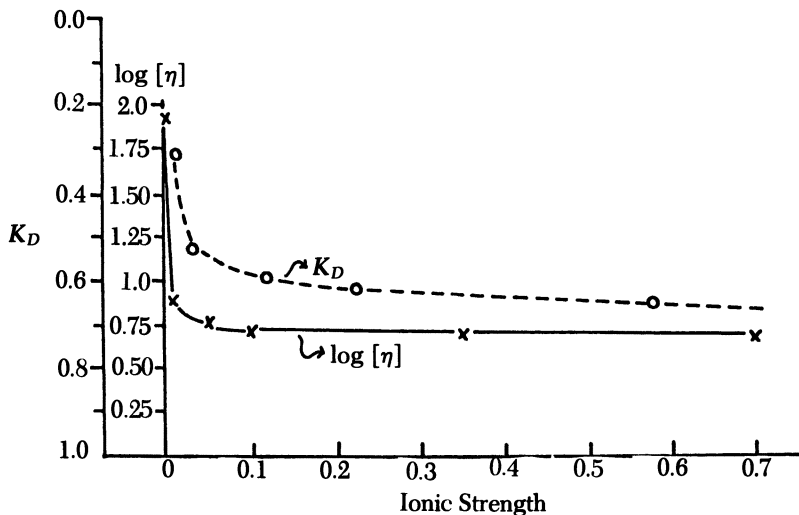


Figure 3. Effect of ionic strength on intrinsic viscosity, $[\eta]$, and distribution coefficient, K_D , of CMC. Key: ○, K_D ; and ×, $\log [\eta]$. Reproduced with permission from reference 25. Copyright 1980 Elsevier Scientific Publishing Co.

Another peculiar property of polyelectrolytes that takes place at low ionic strengths is the expansion of the chain as the polymer concentration is decreased. This phenomenon, called electroviscosity, is caused by the reduction of closely associated counterions surrounding the polyelectrolyte as the polymer concentration is decreased (36). This effect results in decreased electrostatic shielding among ionic sites on the polymer leading to polymer expansion. Because of fixed ionic charges on the polymer, intramolecular osmotic pressure also causes molecular expansion. Thus, if polyelectrolytes are analyzed by using relatively low ionic strength mobile phases, severe peak fronting results (Figure 4) (33). Because the polymer concentration is lower on either side of the peak maximum, the polymer is expanded in these regions and elutes at a higher velocity (has a smaller K_D value) than the peak maximum; a distorted peak profile results. With added electrolyte, the intramolecular electrostatic repulsive and osmotic forces are reduced; thus, this electroviscous behavior is eliminated.

Viscosity Effects. Another important non-size-exclusion effect occurs if the viscosity of the injected solution is higher than that of the mobile phase. This general phenomenon affects organosoluble as well as water-soluble polymers. Two mechanisms have been proposed: macromolecular crowding and viscous fingering (37). In macromolecular

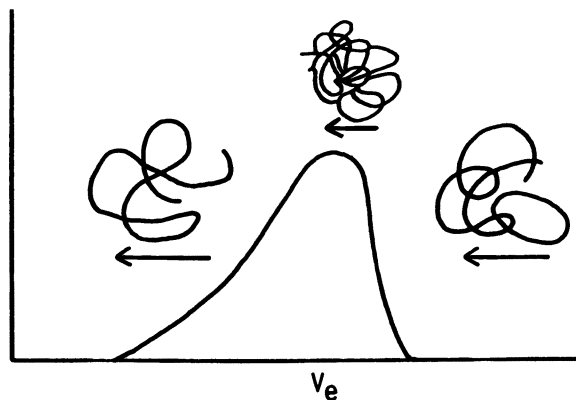


Figure 4. Effect of polyelectrolyte chain expansion during SEC analysis using low ionic strength mobile phases. Adapted from reference 33 and used with permission. Copyright 1979 Elsevier Scientific Publishing Co.

crowding, the conformational entropy of a polymer is reduced as polymer chains begin to overlap. As a result, K_D increases with increased polymer concentration when the critical concentration is reached. The term viscous fingering is used to define a phenomenon, also observed in enhanced oil recovery, in which the less viscous mobile phase breaks (or fingers) through the more viscous injected sample plug; distorted peaks result. Because this type of peak distortion can be reproducible, the appearance of multimodal distributions or shoulders may not be real. In high-performance SEC, macromolecular crowding may occur with samples having relative viscosities ranging from 1.1 to 1.8; viscous fingering has occurred at relative viscosities of 2.1–2.6 (25, 38, 39).

The obvious method of eliminating these effects is to reduce sample concentration. So that sufficient detector response is obtained, the injection volume may have to be increased or a more sensitive detector employed. Depending on the viscosity temperature coefficient of the polymer solution, increasing the column temperature may also help. (This temperature increase also increases column performance.) The mobile phase should also contain enough electrolyte to contract the polyelectrolyte.

Commercially Available High-Performance Packings for Aqueous SEC

In the past 5–6 years, a number of high-performance packings were developed for aqueous SEC (1–3). These packings are divided into silica-based (LiChrospher Diol, EM Laboratories, Elmsford, NY; Synchropak GPC, SynChrom, Inc., Linden, IN; μ Bondagel and Protein

I-Series, Waters Associates, Milford, MA; TSK-SW, Toya Soda, Ltd., Tokyo, Japan; and Shodex AQpak, Showa Denko K.K., Tokyo, Japan) and polymeric-based (TSK-PW, Toya Soda, Ltd., Tokyo, Japan; Spheron, Lachema, Brno, Czechoslovakia; Shodex OHpak and Shodex Ionpak, Showa Denko K.K., Tokyo, Japan; and Plaquagel, Polymer Laboratories, Inc., Shropshire, England) packings. Because of the fairly intense electrostatic interactions caused by silanol groups, unmodified silica packings are not considered because of their limited usefulness in aqueous SEC. (See references 1 and 2 for a complete description of molecular weight separation ranges of high-performance and conventional packings.) For the most part, silica-based packings for aqueous SEC consist of glycerylpropylsilane [$\text{Si}(\text{CH}_2)_3\text{OCH}_2\text{CHOHCH}_2\text{OH}$] and related diol stationary phases. An exception is μ Bondagel, which contains a polyether-bonded phase (40). CATSEC is a polyethylenimine-coated silica, where the amino groups impart a positive charge on the packing; therefore, these groups are suitable for the analysis of cationic polyelectrolytes (14). Because of the stability and inertness of silica-based packings, these packings can also be used with nonaqueous mobile phases as well.

Hydrophilic polymer packings are becoming more popular, and a number of these packings are now commercially available. The TSK PW series contain $-\text{CH}_2\text{CHOHCH}_2\text{O}-$ groups (41) and can be obtained in a wide range of pore sizes (42). Spheron, a poly(hydroxyethyl methacrylate) packing, is available in a variety of particle sizes, the smallest being 25–40 μm . Shodex OHpak is a macroporous methacrylate–glycerol copolymer (43). A rather interesting packing is Shodex Ionpak, which is a sulfonated poly(styrene–divinylbenzene) gel. Finally, a cross-linked poly(acrylamide) packing, Plaquagel, was recently introduced.

In general, large pore size, high-performance silica packings are difficult to produce and use because of the lack of mechanical stability. In addition, some of those packings that are available ($>1000 \text{ \AA}$) have rather broad pore-size distributions (44, 45). Because of the rigid, inert structure of silica, these packings can be used in a wide variety of mobile phases without loss of column performance caused by swelling or shrinkage as is the case with polymeric packings. Polymeric packings generally exhibit higher resolution for low molecular weight samples (oligomers); these packings are available in larger pore sizes and are more pH stable than silica packings. However, these packings are usually more hydrophobic because of the vinyl backbone and nonpolar cross-links.

Pfannkoch et al. (35) reported on the characterization of packings by measuring the K_D of low molecular weight test probes as a function of mobile-phase ionic strength. Results of their study using citrate, arginine, and phenylethanol to measure ion-exclusion, ion-exchange, and hydrophobic interactions, respectively, are shown in Tables I–III. The

Table I. K_D of Citrate as a Function of Mobile-Phase Ionic Strength

Column	Mobile-Phase Ionic Strength ^a			
	0.026	0.12	0.24	2.40
Shodex OHPak B-804	0.83	0.88	0.91	0.94
TSK SW 3000	0.66	0.89	0.92	0.94
LiChrosorb Diol	0.54	0.81	0.95	0.99
Synchropak GPC 100	0.46	0.76	0.89	0.91
TSK SW 2000	0.43	0.75	0.84	0.88
Waters I-125	0.39	0.72	0.79	0.88
Waters μ Bondagel	0.39	0.73	0.80	0.88

SOURCE: Reproduced with permission from reference 35. Copyright 1980. Preston Publishing Co.

^aThe mobile phase consisted of pH 7.05 phosphate buffer of the ionic strengths indicated.

electrostatic interactions could be eliminated by the use of 0.1–0.2 M ionic strength mobile phases. However, rather severe adsorption was encountered, especially for μ Bondagel and Shodex OHPak, when tested for hydrophobicity (Table III).

Polymer Shear Degradation

Only recently was the topic of polymer shear degradation during SEC addressed (46–49). Mechanical degradation of polymers is a complicated phenomenon and depends on a number of parameters including wall shear rate, elongational strain rate, polymer concentration, the nature of the solvent, and the chemical structure of the polymer.

Table II. K_D of Arginine as a Function of Mobile-Phase Ionic Strength

Column	Mobile-Phase Ionic Strength ^a					
	0.026	0.12	0.24	0.60	1.20	2.40
TSK SW 3000	1.30	1.05	1.02	1.00	—	0.98
Synchropak GPC 100	1.35	1.06	1.01	—	—	0.98
LiChrosorb Diol	1.53	1.15	1.05	0.99	—	1.07
TSK SW 2000	1.57	1.06	1.02	0.99	—	0.98
Waters I-125	1.70	1.23	1.16	1.08	—	1.05
Waters μ Bondagel	1.75	1.11	1.06	1.02	—	1.00
Shodex OHPak B-804	2.06	1.16	1.07	1.02	1.02	—

SOURCE: Reproduced with permission from reference 35. Copyright 1980 Preston Publishing Co.

^aThe mobile phase consisted of pH 7.05 phosphate buffer of the ionic strengths indicated.

Table III. K_D of Phenylethanol as a Function of Mobile-Phase Ionic Strength

Column	Mobile-Phase Ionic Strength ^a					
	0.026	0.12	0.24	0.60	1.20	2.40
Synchropak GPC 100	1.44	1.49	1.53	1.63	1.81	2.33
TSK SW 3000	1.47	1.50	1.53	1.61	1.81	2.35
Waters I-125	1.83	1.88	1.88	2.03	2.29	3.03
TSK SW 2000	1.95	2.02	2.10	2.30	2.71	4.01
LiChrosorb Diol	2.49	2.56	2.64	2.93	3.52	5.31
Waters μ Bondagel	5.32	5.19	5.37	5.97	7.44	11.47
Shodex OHpak B-804	6.36	6.65	6.96	8.47	10.96	—

SOURCE: Reproduced with permission from reference 35. Copyright 1980 Preston Publishing Co.

^aThe mobile phase consisted of pH 7.05 phosphate buffer of the ionic strengths indicated.

Although each of these parameters was reviewed in detail (45), apparently elongational strain rate and polymer concentration are highly critical factors.

Elongational strain rate is caused by the converging-diverging flow behavior of the mobile phase as it passes through a packed bed. As a result, the polymer experiences extensional forces that, if high enough, could lead to chain rupture (50). If entangled polymers are present, caused by the overlapping of chains, elongational forces are concentrated at polymer junction regions; this effect enhances chain cleavage (49).

So that the occurrence of polymer shear degradation is reduced, relatively low linear velocities (flow rates) should be employed and dilute polymer solutions injected. Furthermore, for reduction of shear and elongational strain rates, small packing particle sizes ($<10 \mu\text{m}$) should be avoided especially when analyzing fairly high molecular weight polymers ($>500,000$).

The complex hydrodynamics involved in an SEC system make it difficult to give more detailed guidelines. Obviously, a considerable amount of work is needed in this field to define the influence of SEC operational parameters on polymer shear degradation.

Column Calibration

Although qualitatively comparing normalized SEC peak profiles to a control and examining peak shapes to discern molecular weight differences among samples are very useful approaches, the determination of average molecular weights and molecular weight distributions is usually more informative. This determination requires that either the SEC sys-

tem must be calibrated or a molecular weight detector must be employed. The best method uses primary, monodisperse polymer standards chemically and structurally similar to the sample; secondary standards, which are chemically dissimilar to the sample, give apparent molecular weights and should be used with caution; the method using broad molecular weight distribution standards requires extensive data processing and is useful only if the calibration curve is linear; the universal calibration method is good for characterizing chemically heterogeneous or branched polymers, but Mark-Houwink constants or a viscometric detector is needed and non-size-exclusion effects must be absent; absolute molecular weight detectors, i.e., low-angle laser light scattering and viscometry, are becoming increasingly more popular. This section presents an overview of each of these procedures; however, for a more detailed account, *see* references 6 and 7.

In SEC, the size of a polymer governs the separation process. The logarithm of a molecular size parameter, that is, molecular weight or hydrodynamic volume, for a series of monodisperse polymer standards is plotted versus elution volume or K_D to construct a calibration curve. As long as the polymer standards used to construct the calibration curve and the sample that is being analyzed are chemically similar, average molecular weights and the molecular weight distribution of the sample can be easily determined from

$$\bar{M}_x = \Sigma N_i M_i^{x+1} / \Sigma N_i M_i^x \quad (3)$$

where N_i is the number of moles and M_i is the molecular weight at a given incremental elution volume; if $x = 0$, $\bar{M}_x = \bar{M}_n$ (number-average molecular weight), if $x = 1$, $\bar{M}_x = \bar{M}_w$ (weight-average molecular weight), if $x = 2$, $\bar{M}_x = \bar{M}_z$ (z-average molecular weight), and if $x = 3$, $\bar{M}_x = \bar{M}_{z+1}$ ($z + 1$ average molecular weight).

Unfortunately, relatively few commercially available water-soluble polymer standards that are well characterized exist. Nonionic standards include dextrans (Pharmacia Fine Chemicals, Piscataway, NJ, and Research Plus, Inc., Bayonne and Denville, NJ), pullulan (Showa Denko K.K., Tokyo, and Polymer Laboratories, Shropshire, England), oligosaccharides (V-Labs, Covington, LA), poly(ethylene oxide), and poly(ethylene glycol) (Toyo Soda and Polymer Laboratories). Sulfonated polystyrene, an anionic standard, can be obtained from Polymer Laboratories or Pressure Chemical Co. (Pittsburgh, PA). The cationic standard poly(2-vinylpyridine) can be obtained from Pressure Chemical. Peptides and Proteins can be used for ampholytic standards. Ampholytic standards, proteins, are supplied by Research Plus. If standards are not available that are chemically similar to the sample, apparent molecular weight data can still be obtained from a "secondary" standard (1). However, the chemical composition and molecular conformation of the stan-

dard should be fairly close to that of the sample for meaningful results. Nevertheless, this calibration approach is easy and useful for determining only the relative molecular weight differences among samples as in the case of process or quality control. (In the analysis of organosoluble polymers, polystyrene is a commonly used secondary standard.)

If the sample can be fractionated and one (or two) well-characterized fractions of known number and weight-average molecular weights obtained, a broad molecular weight distribution approach can be employed to calibrate the column. In this method, an iterative procedure is used to construct a calibration curve from \bar{M}_n and \bar{M}_w values. However, this approach requires appropriate computer software and, more importantly, can only be used with confidence to define the linear portion of a calibration curve.

When primary calibrants are not available or if the sample consists of branched or chemically heterogeneous polymers, then the calibration curve should be based directly on molecular size to obtain correct molecular weight data. This calibration can be done conveniently by the use of the universal calibration method first proposed by Benoit et al. (51). The theory is based on the fact that each elution volume increment will contain polymers of equivalent hydrodynamic volume. For a given chromatographic system, a plot of hydrodynamic volume, $M[\eta]$, versus V_e for all types of polymer should fall on the same line. For a given elution volume increment

$$[\eta]_1 M_1 = [\eta]_2 M_2 \quad (4)$$

where the subscripts represent different polymers.

In practice, a calibration curve consisting of $[\eta]_1 M_1$ plotted versus V_e is constructed with a series of polymers of known molecular weight. The corresponding molecular weight of the unknown (M_2) at each elution volume can be obtained through the Mark-Houwink equation

$$[\eta] = KM^a \quad (5)$$

where K and a are constants for a given polymer-solvent system at a specified temperature. By combining equations 4 and 5, we obtain

$$\log M_2 = (a_1 + 1)/(a_2 + 1) \log M_1 + 1/(a_2 + 1) \log (K_1/K_2) \quad (6)$$

Thus, Mark-Houwink constants of the sample must be known or a viscometry detector employed to use the universal calibration approach.

Because of the availability of well-characterized, highly monodisperse polystyrene standards, which cover a broad molecular weight range, silica-based packings for aqueous SEC may be calibrated with these standards by using an organic mobile phase, for example, toluene, chloroform, or tetrahydrofuran. After calibration, an aqueous mobile

phase is then employed for the analysis of the water-soluble polymer samples. By means of the universal calibration procedure, average molecular weights may be calculated. For this method to work, non-size-exclusion effects must be absent. The column, of course, must be eluted with mobile phases of intermediate polarity to convert from an organic to an aqueous mobile phase.

Absolute Molecular Weight Detectors

The ideal SEC detection system is capable of determining absolute molecular weights of polymers. Assuming that the resolution of an SEC column is sufficiently high such that each elution volume increment contains monodisperse polymer, that is, $\overline{M}_n = \overline{M}_w$, then detection systems based on any classical molecular weight measurement can, in principle, be used as an absolute molecular weight detector. Because of incomplete separation caused by peak dispersion and limited column resolution, absolute \overline{M}_n and \overline{M}_w values are not possible unless rigorous band-broadening corrections are employed (52). Although methods based on \overline{M}_n measurements have been reported such as end-group analysis (53) and vapor pressure osmometry (54), these detectors are limited to the determination of low molecular weight components.

By far, the most popular absolute molecular weight detectors are low-angle laser light-scattering photometry (LALLS) and viscometry, both of which are commercially available. Chromatix (LDC/Milton-Roy, Sunnyvale, CA) manufactures two models: KMX6, which is a more versatile instrument, and CMX 100, a lower cost unit designed specifically as an SEC detector. Toyo Soda Manufacturing Co., Ltd. (Tokyo, Japan) has introduced an online LALLS unit, Model LS8, which is available in the United States only through special order. Wyatt Technology Corp. (Santa Barbara, CA) has just recently come out with a multiangular, flow-through detector (Model Dawn F) that can be used to determine not only \overline{M}_w but also the radius of gyration of polymers, a useful measurement for characterizing polymer branching. In addition to a number of laboratory-designed viscometric detectors reported in the literature (55-58), a commercial flow-through unit designed for online measurements is available from Viscotek Corp. (Porter, TX) (59).

As discussed in the next sections, polymer concentration must be known at each elution volume increment to calculate molecular weights or intrinsic viscosities. In view of this, a concentration-sensitive detector, such as a differential refractometer, must be present in line with the absolute molecular weight detector. The time delay between both detectors must be known for proper indexing of detector responses.

Low-Angle Laser Light Scattering. In Rayleigh light scattering, incident light, I_0 , interacts with a macromolecule; a temporary dipole

moment that oscillates in phase with I_o is induced. The macromolecule then acts as a radiation source and emits light in all directions. The intensity of scattering is a function of the scattering angle and proportional to molecular weight and polymer concentration. Because we are interested in the scattering caused by the polymer, a term called the excess Rayleigh factor, \overline{R}_θ , is used that is simply the scattering intensity of the solution, $i_{\theta(\text{soln})}$, minus the scattering intensity of the solvent, $i_{\theta(\text{solv})}$, normalized with respect to I_o and the scattering volume, V :

$$\overline{R}_\theta = \frac{i_{\theta(\text{soln})} - i_{\theta(\text{solv})}}{I_o V} \quad (7)$$

\overline{R}_θ is a function of the scattering angle, which in turn depends on the mass and radius of gyration of the macromolecule; however, if measurements are made at fairly low angles with respect to the incident beam, molecular weights can be obtained by using

$$Kc/\overline{R}_\theta = 1/\overline{M}_w + 2A_2c \quad (8)$$

where c is the polymer concentration, A_2 is the second virial coefficient, and K is an optical constant defined as

$$K = \frac{2\pi^2 n^2}{\lambda^4 N} \left(\frac{dn}{dc} \right)^2 (1 + \cos^2 \theta) \quad (9)$$

where n is the refractive index of the solvent, λ is the wavelength of the incident beam, N is Avogadro's number, and dn/dc is the specific refractive index increment of the polymer solution.

Assuming that perfect resolution can be obtained in an SEC system, then each volume increment that passes through the detector is monodisperse, or \overline{M}_w in equation 8 is equal to M_i in equation 3. Thus, with an SEC-LALLS system, average molecular weights, molecular weight distribution, cumulative distribution, and polydispersities can be directly computed. In addition, branching parameters (52, 60-62) can be estimated. Because of LALLS's high sensitivity toward high molecular weight polymers, SEC-LALLS can also be used to detect the presence of trace amounts of high molecular weight components in samples.

A number of limitations are present with LALLS. The accuracy of the measurements depend on the degree to which dn/dc and A_2 are known. Because these parameters depend on chemical composition and molecular weight, appropriate corrections should be made when dealing with chemically heterogeneous or highly polydisperse samples. As previously mentioned, calculated \overline{M}_n values will be somewhat higher than true values because of imperfect resolution. This overestimation will lead to an underestimation of polydispersity.

American Chemical Society
Library

1155 16th St. N.W.

In Water-Soluble Polymers, Glass, J.;
Advances in Chemistry; American Chemical Society, Washington, DC, 1986.

One of the most serious errors arises from the fact that the LALLS sensitivity decreases with decreasing molecular weight. Depending on the polydispersity and molecular weight range of the sample, the low molecular weight region may be truncated; an overestimation of \overline{M}_n results. If relatively small amounts of high molecular weight material are present, higher average molecular weights may be underestimated because of poor response from the concentration detector. However, a number of possible approaches to correct these effects such as increasing the amount of injected solution and curve fitting exist. These limitations will be covered in detail in a forthcoming review (63). Finally, LALLS photometers are expensive, in excess of \$20,000, and require data acquisition and processing capabilities.

Viscometry. The principle of operation of the viscometric detector is based on measuring the pressure drop, ΔP , across a capillary tube (8, 60):

$$\Delta P = k\eta \quad (10)$$

where η is viscosity and k is a constant that depends on flow rate and the dimensions of the capillary tube. When the pressure drop, ΔP_0 , in a reference capillary is measured, the relative viscosity of the SEC effluent can be easily determined:

$$\eta_{\text{rel}} = \Delta P / \Delta P_0 \quad (11)$$

Because

$$[\eta] = \left(\frac{\eta_{\text{rel}} - 1}{c} \right)_{c=0} = \left(\frac{\ln \eta_{\text{rel}}}{c} \right)_{c=0} \quad (12)$$

then

$$[\eta] = \left(\frac{\ln (\Delta P / \Delta P_0)}{c} \right)_{c=0} \quad (13)$$

The polymer concentration, c , is measured by a concentration detector in series with the viscosity detector and is assumed to be close to zero for all practical purposes.

With known Mark-Houwink constants, the molecular weight of the polymer at each elution volume increment can be determined by using equation 5. If these constants are not known, the universal calibration procedure can be employed, that is,

$$M_2 = [\eta]_1 M_1 / [\eta]_2 \quad (14)$$

where subscript 2 is for the unknown polymer. Furthermore, since both $[\eta]$ and molecular weight are known, branching parameters can be easily determined.

Recently, a commercial differential viscometer has been made available by Viscotek Corp. (59). The unit can be used both offline as well as coupled to an SEC system. This instrument is based on a fluid analogue of a Wheatstone bridge network. Limitations of this instrument are similar to those of LALLS with the added constraints that temperature and flow rates must be well controlled, although with the balanced bridge design tight temperature control may not be necessary (59). Because shear rate through the capillary ranges from 1×10^3 to 5×10^3 s^{-1} , the potential of shear degradation of high molecular weight samples and the flow behavior of non-Newtonian polymers need further study. Nevertheless, the detector offers many interesting features and should prove to be a highly useful SEC detector.

Chemical Heterogeneity

Chemical heterogeneity in synthetic water-soluble polymers results from differences in reactivity ratios among the monomers used in the synthesis. In naturally occurring or modified water-soluble polymers, such as polysaccharides, heterogeneity may be induced during biosynthesis, isolation, or modification. For example, during demethylation of pectin, nonuniform regions of polygalacturonic acid may occur depending on reaction conditions. In the case of CMC, in which alkali cellulose is reacted with monochloroacetic acid, substitution can take place on C₂, C₃, and C₆ hydroxyls of the anhydroglucose group. Although reaction kinetics of each vary (64), eight possible combinations of (carboxymethyl)glucoses are present in CMC: (tricarboxymethyl)glucose; three (dicarboxymethyl)glucoses (C₂ and C₃, C₂ and C₆, and C₃ and C₆), three (monocarboxymethyl)glucoses (C₂, C₃, and C₆), and unsubstituted anhydroglucose.

The variation of chemical composition with molecular weight is termed chemical heterogeneity of the first kind as illustrated in Figure 5. If the chemical composition varies for macromolecules of equivalent chain length (degree of polymerization) (Figure 6), this is called chemical heterogeneity of the second kind.

By use of concentration and specific detectors in series (Figure 7), polymer chemical heterogeneity can be determined. Concentration detectors based on measurements involving spectrophotometry, differential refractometry, dielectric constants, flame ionization (moving belt type), and nephelometry (mass detector) can be used. The response of these detectors may depend to some extent on molecular weight, chemical composition, and sample concentration. For accurate measurements, calibration curves or response factors are required. The most commonly used specific detectors are UV and IR spectrophotometers although others, even including pyrolysis GC (65), have been reported.

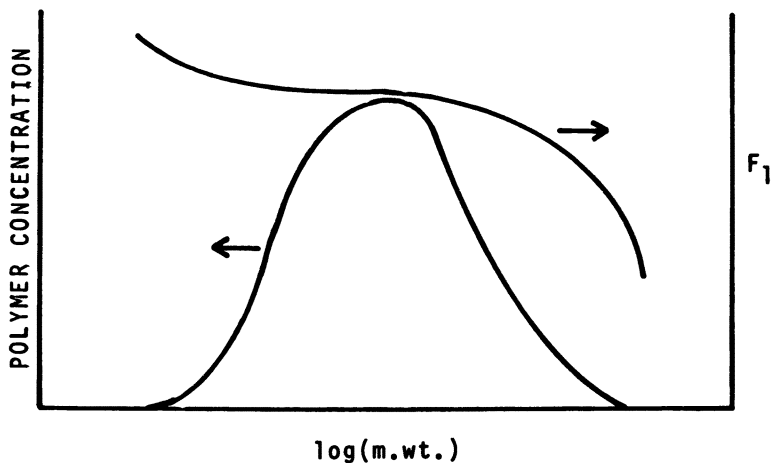


Figure 5. Chemical heterogeneity of the first kind where F_1 , the fraction of monomer in a copolymer, varies as a function of molecular weight.

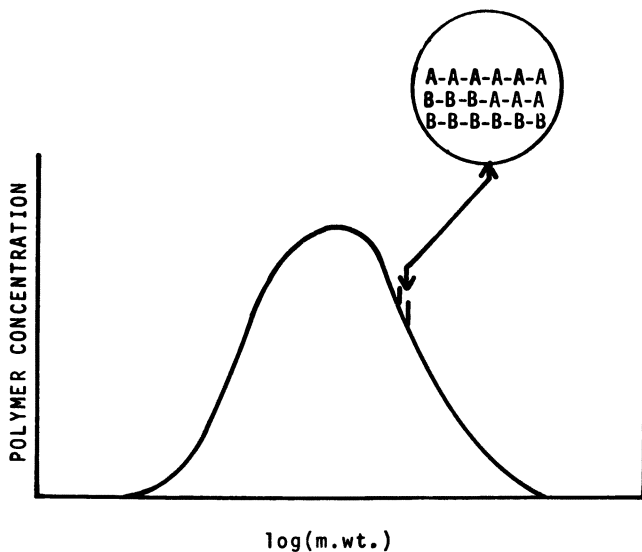


Figure 6. Chemical heterogeneity of the second kind in which polymers of different composition may have the same molecular size.

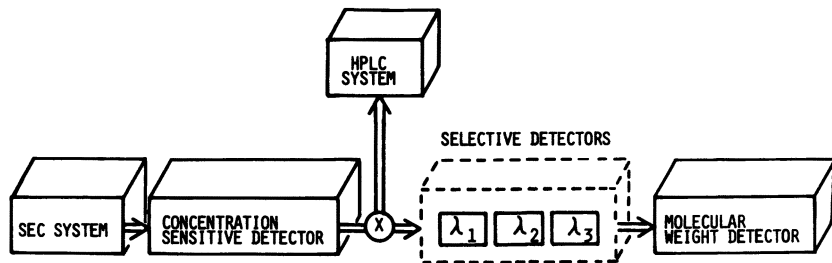


Figure 7. An idealized chromatographic arrangement for the determination of chemical heterogeneity of the first and second kinds of complex polymers.

Multidetector requirements to determine the chemical heterogeneity of polymers are as follows: for refractometer and $n - 1$ wavelength measurements

$$R = \sum_{i=1}^n K_i c_i$$

$$A = a_1 c_1$$

.

.

.

$$A_{n-1} = a_{n-1} c_{n-1}$$

and for n wavelength measurements

$$A = a_1 c_1$$

.

.

.

$$A_n = a_n c_n$$

R is refractive index (RI) response, K is RI response factor, A is absorbance, a is absorptivity, and c is concentration. For a polymer containing n different monomers, then either a concentration-sensitive detector and $n - 1$ wavelengths must be monitored or n wavelengths must be used assuming, of course, that the monomers have distinct absorbance regions.

The simplest way of treating the data from dual detectors is to ratio the peak heights of the specific detector to the concentration-sensitive detector at a given elution volume across the peak profile. These measurements should be corrected for nonlinear detector response behavior.

The resulting ratios are then superimposed on the molecular weight distribution. Positive or negative deviations in these plots signify regions of chemical nonuniformity. Another, more quantitative approach is to normalize the specific detector response at each elution increment with respect to the integrated signal intensity of the selective detector. With appropriate response factors, monomer mole or weight fractions can be computed.

Although this technique works well for copolymers, more complex polymers may require several injections each monitored at different wavelengths. With the introduction of high-performance liquid chromatographic diode-array and rapid-scan detectors with computer capability, this type of analysis is greatly simplified (66). In addition, Fourier transform IR also holds great promise for compositional analysis of complex polymers.

For determination of chemical heterogeneity of the second kind, cross fractionation is required (67). One possible approach is to collect fractions of equivalent hydrodynamic volume and separate them on a second column. The second system may consist of a reversed-phase, ion-exchange, or liquid-solid chromatographic column. This approach has been termed orthogonal chromatography by Balke (66-68), and the reader should refer to his excellent reviews (66, 69) for a complete discussion. Although this technique has been used to characterize organosoluble polymers, no literature regarding water-soluble polymer characterization exists.

Future Trends

SEC is the premier polymer characterization technique for determining molecular weight distribution. However, the analysis of water-soluble polymers, especially polyelectrolytes, requires careful choice of mobile-phase composition and column packing. Although packing pore-size selection and band-broadening corrections were not discussed in this chapter, these topics should also be addressed for optimizing SEC analysis to obtain meaningful data. The use of new HPLC detectors such as LALLS, viscometry, diode-array and rapid-scan spectrophotometers, and Fourier transform IR, which are now commercially available, will greatly extend the capability and usefulness of SEC especially for the analysis of branched and chemically heterogeneous polymers. Other online detection systems, such as dynamic light scattering and flow-through NMR spectrometers, are on the horizon.

With the introduction of high-performance packings, viscosity effects and the potential of polymer shear degradation have placed severe constraints on the applicability of SEC for the analysis of high molecular weight polymers. In view of this, alternative separation tech-

niques, such as field flow fractionation, have great promise for the analysis of ultrahigh molecular weight polymers. Although rather time consuming and experimentally difficult to use, ultracentrifugation, practiced for many years, has been underutilized for the characterization of synthetic polymers. Considering that ultracentrifugation is an absolute method of determining molecular weight distributions and can also be used to estimate chemical heterogeneity, the use of this method unfortunately has decreased over the years.

Column liquid chromatographic techniques, such as liquid-solid, normal-phase, ion-exchange, and reversed-phase chromatography, appear to hold great promise for characterizing polymers especially when mobile-phase gradients are used. Because these separations are usually a function of several mechanisms, that is, SEC and adsorption, polymers are separated on the basis of both molecular weight and chemical composition. Nevertheless, considering the high peak capacity and resolution of HPLC, a great deal of information can be obtained about the nature of a sample.

Literature Cited

1. Barth, H. G. *J. Chromatogr. Sci.* **1980**, *18*, 409.
2. Dubin, P. L. *Sep. Purif. Methods* **1981**, *10*, 287.
3. Dubin, P. L. *Amer. Lab. Fairfield, CT* **1983**, *15(1)*, 62.
4. *Size Exclusion Chromatography* (GPC); Provder, T., Ed.; ACS Symposium Series 138; American Chemical Society: Washington, DC, 1980.
5. *Size Exclusion Chromatography: Methodology and Characterization of Polymers and Related Materials*; Provder, T., Ed.; ACS Symposium Series 245, American Chemical Society: Washington, DC, 1984.
6. Yau, W. W.; Kirkland, J. J.; Bly, D. D. *Modern Size Exclusion Chromatography*; Wiley: New York, 1979.
7. *Steric Exclusion Liquid Chromatography of Polymers*; Janca, J., Ed.; Chromatographic Series Vol. 25; Dekker: New York, 1984.
8. Blenkii, B. G.; Vilenchik, L. Z. *Modern Liquid Chromatography of Macromolecules*; Journal of Chromatography Library Vol. 25; Elsevier: Amsterdam, 1983.
9. Cazes, J.; De La Marre, X. *Liquid Chromatography of Polymers and Related Materials, II*; Chromatographic Science Series Vol. 13; Dekker: New York, 1980.
10. Cazes, J. *Liquid Chromatography of Polymers and Related Materials III*; Chromatographic Science Series Vol. 19; Dekker: New York, 1981.
11. Barth, H. G. *Liq. Chromatogr. Mag.* **1984**, *2*, 24.
12. Buytenhuys, F. A.; van der Maeden, F. P. B. *J. Chromatogr.* **1978**, *149*, 489.
13. Talley, C. P.; Bowman, L. M. *Anal. Chem.* **1979**, *51*, 2239.
14. Gooding, D. L.; Schumuck, M. N.; Gooding, K. M. *J. Liq. Chromatogr.* **1982**, *5*, 2259.
15. Dubin, P. L.; Levy, I. J. *J. Chromatogr.* **1982**, *235*, 377.
16. Levy, I. J.; Dubin, P. L. *Ind. Eng. Chem., Prod. Res. Dev.* **1982**, *21*, 59.
17. Kato, Y.; Hashimoto, T. *J. Chromatogr.* **1982**, *235*, 539.
18. Guise, G. B.; Smith, G. C. *J. Chromatogr.* **1982**, *235*, 365.
19. Neddermeyer, P. A.; Rogers, L. B. *Anal. Chem.* **1968**, *40*, 755.

20. Barth, H. G., unpublished results.
21. Stenlund, B., *Adv. Chromatogr.* **1976**, *14*, 37.
22. Tanford, C. *Physical Chemistry of Macromolecules*; Wiley: New York, 1961.
23. Rochas, C.; Domard, A.; Rinaudo, M. *Eur. Polym. J.* **1980**, *16*, 135.
24. Domard, A.; Rinaudo, M.; Rochas, C. *J. Polym. Sci., Polym. Phys. Ed.* **1979**, *17*, 673.
25. Barth, H. G.; Regnier, F. E. *J. Chromatogr.* **1980**, *192*, 275.
26. Barth, H. G. *J. Liq. Chromatogr.* **1980**, *3*, 1481.
27. Barth, H. G. *Anal. Biochem.* **1982**, *124*, 191.
28. Radhakrishnamurthy, B.; Jeanson, N.; Berenson, G. S. *J. Chromatogr.* **1983**, *256*, 341.
29. Barth, H. G.; Smith, D. A. *J. Chromatogr.* **1981**, *206*, 410.
30. Siebourg, W.; Lundberg, R. D.; Lenz, R. W. *Macromolecules* **1980**, *13*, 1013.
31. Hahn, N. J. *Polym. Sci., Polym. Chem. Ed.* **1977**, *15*, 1331.
32. Dubin, P. L. *J. Liq. Chromatogr.* **1980**, *3*, 623.
33. Nefedov, P. P.; Lazareva, M. A.; Belenskii, B. G.; Frenkel, S. Ya.; Morton, M. M. *J. Chromatogr.* **1979**, *170*, 11.
34. Chuang, J.-Y. *8th Int. Symp. Column Liq. Chromatogr. Mtg.* **1984**, Abstract 2a-19.
35. Pfannkoch, E.; Lu, K. C.; Regnier, F. E.; Barth, H. G. *J. Chromatogr. Sci.* **1980**, *18*, 430.
36. Flory, P. J. *Principles of Polymer Chemistry*; Cornell University: Ithaca, 1953.
37. Tung, L. H., Moore, J. C. In *Fractionation of Synthetic Polymers*; Tung, L. H., Ed.; Dekker: New York, 1977; p 619.
38. Samay, G.; Kubin, M. J. *Appl. Polym. Sci.* **1979**, *23*, 1879.
39. Janca, J. *J. Chromatogr.* **1980**, *187*, 21.
40. Vivilecchia, R. V.; Lightbody, B. G.; Thimot, N. Z. *J. Chromatogr. Sci.* **1977**, *15*, 424.
41. Hashimoto, T.; Sasaki, H.; Aiura, M.; Kato, Y. *J. Polym. Sci., Polym. Phys. Ed.* **1978**, *16*, 1789.
42. Alfredson, T. V.; Wehr, C. T.; Tallman, L.; Klink, F. J. *J. Liq. Chromatogr.* **1982**, *5*, 489.
43. Regnier, F. E.; Gooding, K. M. *Anal. Biochem.* **1980**, *103*, 1.
44. Yau, W. W.; Kirkland, J. J.; Bly, D. D.; Stoklosa, H. J. *J. Chromatogr.* **1976**, *125*, 219.
45. Barth, H. G.; Regnier, F. E. In *Size Exclusion Chromatography: Methodology and Characterization of Polymers and Related Materials*; Provder, T., Ed.; ACS Symposium Series 245, American Chemical Society: Washington, DC, 1984; p 207.
46. Barth, H. G.; Carlin, F. J. *J. Liq. Chromatogr.* **1984**, *7*, 1717.
47. Rooney, J. G.; Verstrate, G. In *Liquid Chromatography of Polymers and Related Materials III*; Chromatographic Science Series Vol. 19; Dekker: New York, 1981, p 207.
48. Giddings, J. C. *Adv. Chromatogr.* **1982**, *20*, 217.
49. McIntyre, D.; Shih, A. L.; Savoca, J.; Seeger, R.; MacArthur, A. In *Size Exclusion Chromatography: Methodology and Characterization of Polymers and Related Materials*; Provder, T., Ed.; ACS Symposium Series 245, American Chemical Society: Washington, DC, 1984; p 227.
50. Hoagland, D. A.; Larson, K. A.; Prud'homme, R. K. In *Modern Methods of Particle Size Analysis*; Barth, H. G., Ed.; Wiley: New York, 1984; Chapter 9.
51. Benoit, H.; Grubisic, Z.; Rempp, P.; Decker, D.; Zilliox, J. B. *J. Chem. Phys.* **1966**, *53*, 1507.

52. Hamielec, A. E. In *Steric Exclusion Liquid Chromatography of Polymers*; Janca, J., Ed.; Dekker: New York, 1984; Chapter 3.
53. Kremmer, T.; Boross, L. *Gel Chromatography*; Wiley: Chichester, 1979.
54. San-Ei Chem. Ind., Ltd. Japanese Patent 82-72060 A2 (5772060); *Chem. Abstr.* 98, 114234h.
55. Ouano, A. C. *J. Polym. Sci., Part A1* 1972, 10, 2169.
56. Ouano, A. C.; Horne, D. L.; Gregger, A. R. *J. Polym. Sci., Polym. Phys. Ed.* 1974, 12, 307.
57. Letot, L.; Lesec, J.; Quivoron, C. *J. Liq. Chromatogr.* 1980, 3, 427.
58. Malihi, F. B.; Kuo, C.; Koehler, M. E.; Provder, T.; Kah, A. F. In *Size Exclusion Chromatography: Methodology and Characterization of Polymers and Related Materials*; Provder, T., Ed.; ACS Symposium Series 245, American Chemical Society: Washington, DC, 1984; p 281.
59. Haney, M. A. *Polym. Prepr. Am. Chem. Soc.* 1983, 24 (2), 455.
60. Quivoron, C. In *Steric Exclusion Liquid Chromatography of Polymers*; Janca, J., Ed.; Dekker: New York, 1984; Chapter 5.
61. Jordan, R. C.; McConnell, M. L. In *Size Exclusion Chromatography (GPC)*; Provder, T., Ed.; ACS Symposium Series 138, American Chemical Society: Washington, DC, 1980, p 107.
62. Foster, G. N.; Hamielec, A. E.; MacRury, T. B. In *Size Exclusion Chromatography (GPC)*; Provder, T., Ed.; ACS Symposium Series 138, American Chemical Society: Washington, DC, 1980; p 131.
63. Barth, H. G.; Huang, S.S. In *Modern Methods of Polymer Characterization*; Barth, H. G., Ed.; Wiley: New York; in press.
64. Reuben, J.; Conner, H. T. *Carbohydr. Res.* 1983, 115, 1.
65. Mori, S.; Suzuki, T. *J. Liq. Chromatogr.* 1981, 4, 1685.
66. Balke, S. T. *Sep. Purif. Methods* 1982, 11, 1.
67. Balke, S. T.; Patel, R. D. In *Size Exclusion Chromatography (GPC)*; Provder, T., Ed.; ACS Symposium Series 138, American Chemical Society: Washington, DC, 1980; p 149.
68. Balke, S. T.; Patel, R. D. *J. Polym. Sci., Polym. Lett. Ed.* 1980, 18, 453.
69. *Modern Methods of Polymer Characterization*; Barth, H. G., Ed.; Wiley: New York, in press.

RECEIVED for review September 24, 1984. ACCEPTED August 14, 1985.

Dilute Solution Properties of Pectin

Marshall L. Fishman, Leonard Pepper, and Philip E. Pfeffer

Eastern Regional Research Center, Agricultural Research Service,
U.S. Department of Agriculture, Philadelphia, PA 19118

The colligative properties of various pectins in the fully protonated and neutralized forms were studied by membrane osmometry. Because van't Hoff plots passed through a minimum, apparently pectins behave as nonideal, dissociating macromolecules in solution. In approaching the $\lim_{c \rightarrow 0} \pi/c$, where c is concentration, number-average molecular weights (\overline{M}_n) from osmometry approached the \overline{M}_n determined from end-group titrations. Second virial coefficients of pectin aggregates in 0.05 M NaCl revealed their ratio of length to width was from 120 to 200. Counterion binding decreased with pectin dissociation and increasing percentage of ester groups in the neutralized form.

PECTIN, predominantly a copolymer of $\alpha(1-4)$ -galacturonate and its methyl esters with about 20% neutral sugars, is important because it is a major structural polysaccharide in plants (1), a ubiquitous gel former and thickening agent in foods (2), and a nutritionally important food fiber (3). The inter- and intramolecular forces within the pectin structure are important in understanding how pectin functions in these systems. Thus, the colligative properties as ascertained by membrane osmometry (O) of various pectins were studied to better understand these forces.

Interestingly, pectic substances were among the first macromolecules studied by membrane osmometry (4). Previously, Owens et al. (5) found the number-average molecular weight, \overline{M}_n , in the range $(1.8-3.9) \times 10^4$ for protonated citrus pectins, whereas Pals and Hermans (6) found \overline{M}_n to be 4.6×10^4 for the sodium salt of citrus pectin. More recently, Jordan and Brant (7) reported an \overline{M}_n of 4.9×10^4 for protonated pectin. In all cases pectin appeared to follow the van't Hoff limiting law.

Measurements by gel chromatography (8, 9), light scattering (7, 10), and electron microscopy (11) indicated that pectins aggregate in solution. Aggregation is further supported by a preliminary observation that \overline{M}_n values determined by end-group titration for pectins were significantly lower than those obtained by membrane osmometry (12). Recent advances in the design of high-speed membrane osmometers, with

This chapter not subject to U.S. copyright.
Published 1986, American Chemical Society

increased sensitivity and reliability, together with a better theoretical understanding of aggregating systems (13), have prompted us to reexamine the osmotic properties of pectins to reconcile these various observations.

Theory

A plot of reduced osmotic pressure, π/c , against concentration, c , according to the van't Hoff limiting law (14) yields

$$\pi/c = RT(1/\bar{M}_n + Bc) \quad (1)$$

for a polydisperse system, \bar{M}_n from the intercept of a straight line. (R is the gas constant and T is the absolute temperature.) For a polyelectrolyte, the second virial coefficient, B , obtained from the slope of a van't Hoff plot contains three contributions

$$B = B_I + B_{II} - B_{III} \quad (2)$$

B_I and B_{II} are positive contributions arising from the Donnan effect and polymer-polymer interactions, respectively, whereas B_{III} is a negative contribution due to preferential solvation effects (13).

So that structural information from equation 1 can be obtained, separation of the various contributions to B is necessary. Thus, protonated and neutralized pectins were measured in 0.05 M NaCl. Under these conditions, we assumed for the protonated form, which is a weak carboxylic acid

$$B_{I,H} \sim B_{III,H} \approx 0 \quad (3)$$

Thus, from equation 2

$$B_H \cong B_{II,H} \quad (4)$$

Here the subscript H refers to the protonated form of pectin.

Previously (8), we showed that the root mean square radii of gyration (R_g) of pectins measured over the pH range 3.7-7.3 are the same within experimental error. Thus

$$B_{II,Na} \approx B_{II,H} \quad (5)$$

Here, the subscript Na refers to the neutralized form. If we further assume

$$B_{III,Na} \approx 0 \quad (6)$$

Then

$$B_{I,Na} \cong B_{Na} - B_H \quad (7)$$

Given the above approximations, the axial ratio (L/d) of pectin can be obtained from solutions of protonated pectin by (14)

$$L/d = B_H \overline{M}_n / 1000 V_1 V_2 \quad (8)$$

Here V_1 and V_2 are partial specific volumes of solvent and polymer, respectively, and L/d is the ratio of macromolecular length to diameter.

Furthermore, the effective charge (Z_{eff}) on neutralized pectins can be obtained from second virial measurements on protonated and neutralized pectins by (14)

$$Z_{\text{eff}} = [4(B_{\text{Na}} - B_H) \overline{M}_n^2 m_3 / 1000 V_1]^{1/2} \quad (9)$$

Here m_3 is the molality of added salt, in this case NaCl.

Moreover, the fraction of dissociated counter ions, α , can be calculated from equations 10 and 11:

$$\alpha = Z_{\text{eff}} / Z_s \quad (10)$$

and

$$Z_s = \overline{DP}_n (1 - \epsilon) X_G \quad (11)$$

where Z_s is the stoichiometric charge on neutralized pectin, \overline{DP}_n is the number-average degree of polymerization, ϵ is the mole fraction of galacturonate residues containing methyl esters, and X_G is the mole fraction of galacturonate residues in pectin.

Experimental Section

Materials. Commercial citrus pectins with degrees of methyl esterification (DM) 35, 58–60, and 70 were gifts from Bulmers Ltd., Hereford, England. Two other pectin samples, DM-37 and 73, were manufactured by Bulmers but were gifts from Drs. E. R. Morris and M. J. Gidley at Unilever. The DM-57 pectin was a gift from Sunkist Growers, Corona, CA. Poly(galacturonic acid) was from Sigma Chemical Co. Characterization and preparation of samples were reported previously (8) with minor modification. Samples to be neutralized with NaOH were dissolved in 0.01 M phosphate buffer (pH 6.1) containing 0.1 M ethylenediaminetetraacetic acid, titrated to pH 7 with 0.1 M NaOH, dialyzed against four changes of water for 48 h, centrifuged for 1 h at 30,000g to remove insoluble matter, and then lyophilized. Dialysis bags were Spectrapor with a molecular weight cutoff of 12,000.

Membrane Osmometry. Osmotic pressures were measured in a Knauer-type 1.00 membrane osmometer equipped with a thermostated cell (Utopia Instrument Co., Joliet, IL). The solvent was 0.05 M NaCl. Semipermeable membranes (Schleicher & Schuell, AC 62) were cellulose acetate with pore-size diameters between 50 and 100 Å. The osmometer cell was maintained at 35 ±

0.1 °C. The output from the electronic pressure transducer in the osmometric cell was monitored continuously by a potentiometric recorder. Recorder traces of π against time, which were flat and parallel to the base line, indicated no tendency for pectin to permeate the membrane. Flat and parallel traces of π were obtained 5–10 min after the third cell rinse with the polymer solution. Samples were measured in increasing order of concentration.

Initially pectins were dissolved at room temperature to a concentration of 1 g/dL in 0.05 M NaCl. The stock solutions were diluted serially and measured within 24 h of initial solvation. Measurements of π at $c < 0.1$ g/dL were scattered. Thus, experiments were conducted to obtain reliable values of π/c when $c \leq 0.1$ g/dL.

On the assumption that a slow approach to equilibrium produced scattered π/c values for $c < 0.1$ g/dL, the approach to equilibrium was followed by measuring π for 0.6 g/dL pectin solutions as a function of time. The solvent was 0.047 M NaCl and 0.003 M sodium azide; samples were contained in capped bottles. These bottles were immersed in boiling water for 10 min at the start of the experiment and then kept in a water bath at 35 ± 1 °C prior to measuring π . The apparent number-average molecular weight, \bar{M}_n^{app} , was obtained from equation 1 with $B = 0$. On the final day of the experiments (days 8–15), the samples were diluted serially to obtain \bar{M}_n and B .

Lastly, pectin solutions (1 g/dL) were heated for 10 min in boiling water as before and allowed to stand for 3 days at 35 °C. In the case of protonated pectin with a DM of 35 or 37, the data were too scattered to obtain \bar{M}_n or B .

End-Group Titration. The \bar{M}_n of pectins was determined also by the reaction of sodium chlorite with aldehyde end groups. This method was first developed for polysaccharides by Launer and Tomimatsu (15, 16) and later applied specifically to pectins by Albersheim et al. (17). Galacturonic acid and rhamnose standards gave the same results within experimental error, provided the chlorite reaction was allowed to proceed for a minimum of 16 h. Within the precision of our measurements, \bar{M}_n was the same for the protonated or neutralized pectins, although neutralized forms dissolved more readily. In several cases, the neutralized forms were heated to 100 °C for 10 min before allowing the chlorite reaction to proceed with refluxing. The results showed no significant change in \bar{M}_n .

Results and Discussion

Unheated Pectins. As indicated in Table I, \bar{DP}_n by membrane osmometry for the unheated pectins was found to be significantly higher than values by end-group titration. The \bar{M}_n values for the high-methoxy pectins (DM-70 and DM-72-73) in both acid and neutralized forms ranged between 3.5×10^4 and 4×10^4 . These values are comparable to those found by Owens et al. (5) but somewhat lower than the values obtained by Jordan and Brant (7) or Pals and Hermans (6). The van't Hoff plots are shown in Figures 1 and 2. Correlation coefficients from linear least squares were ≥ 0.97 . If pectin aggregates as indicated by a value of $\overline{AGR}_n > 1$ (\overline{AGR}_n is $\bar{M}_{n,0}:\bar{M}_{n,\text{EGT}}$, where EGT is end-group titration; see Table I), then at $c \leq 0.1$ g/dL, π/c must decrease with increasing concentration until a minimum is reached. Initial studies at $c \leq 0.1$ g/dL gave scattered values of π/c . Studies were initiated to see if scattered π/c values were caused by a slow approach to equilibrium.

Table I. \overline{DP}_n and \overline{AGR}_n for Unheated Pectins

DM	\overline{DP}_n				
	End-Group Analysis	Osmometry ^a		\overline{AGR}_n^b	
		Na	H	Na	H
0	29.7 ± 4.0	39 ± 1	—	1.3 ± 0.2	—
35	50.7 ± 9.0	183 ± 11	—	3.6 ± 0.9	—
37	32.8 ± 3.5	89 ± 1	—	2.7 ± 0.3	—
57	65.9 ± 1.2	213 ± 1	219 ± 4	3.2 ± 0.6	3.3 ± 0.1
58-60	66.0 ± 8.6	252 ± 34	201 ± 10	3.8 ± 1.1	3.0 ± 0.5
70	67.6 ± 10.9	218 ± 10	200 ± 4	3.2 ± 0.7	3.0 ± 0.5
72-73	60.0 ± 1.2	219 ± 6	213 ± 3	3.7 ± 0.2	3.6 ± 0.1

^aThe values were determined within 24 h of solution preparation.

^b $\overline{AGR}_n = \overline{M}_{n,0} : \overline{M}_{n,ECT}$ (EGT is end-group titration).

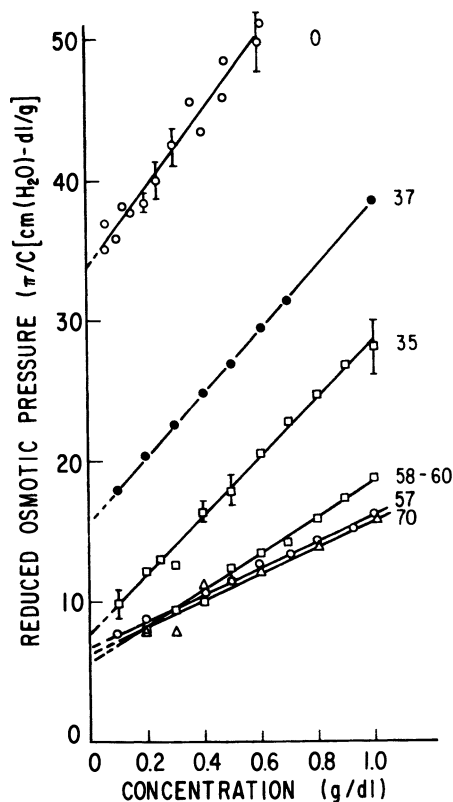


Figure 1. van't Hoff plots for sodium salts of unheated pectins. Key: \circ , DM = 0; \bullet , DM = 37; \square , DM = 35; \square , DM = 58-60; \circ , DM = 57; \triangle , DM = 70.

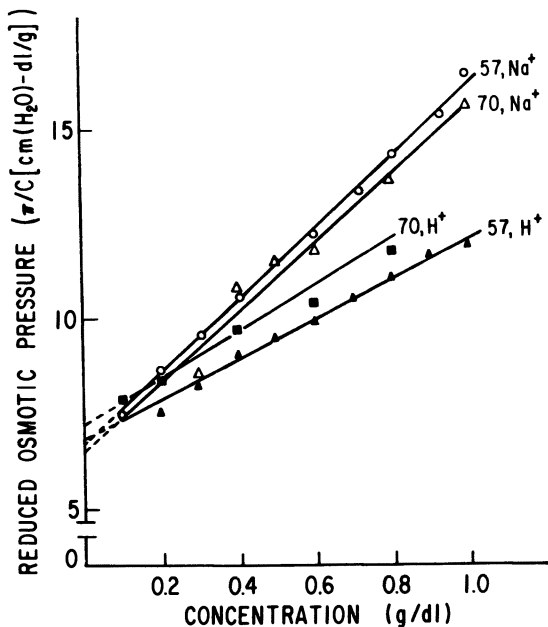


Figure 2. van't Hoff plots for protonated and sodium salts of unheated pectins. Key: \circ , DM = 57, Na^+ ; \triangle , DM = 70, Na^+ ; \blacksquare , DM = 70, H^+ ; and \blacktriangle , DM = 57, H^+ .

Dissociation of Heated Pectins. With one exception, \bar{M}_n^{app} for $c = 0.6$ g/dL, as calculated from equation 1 with $B = 0$, decreased slowly with time. We concluded that such was probable by fitting \bar{M}_n^{app} against time by the linear least-squares procedure. Correlation coefficients (Table II) were moderately to highly negative, except for the low-methoxy protonated pectins. Examination of the data in Figure 3 reveals that the high- (DM-70 and 72-73) and medium- (DM-57 and 58-60) methoxy pectins in the protonated form and the low-methoxy pectins (DM-35 and 37) in the sodium form required several days of incubation before a decrease in \bar{M}_n^{app} was observed. Thus, for these cases, data were not fitted to a linear least-squares equation in view of the lag time between incubation and an observed decrease in \bar{M}_n^{app} . In the case of low- and medium-methoxy pectins in the sodium form, \bar{M}_n^{app} appeared to decrease linearly with time, whereas the low-methoxy pectin in the protonated form remained unchanged. These trends are shown more clearly in Figure 4, in which the data were normalized for molecular weight by the ratio $(\bar{M}_{n,t}^{\text{app}}/\bar{M}_{n,0}^{\text{app}})$ (i.e., \bar{M}_n^{app} at time t divided by the apparent value extrapolated to $t = 0$). The overall rate ($d\bar{M}_n^{\text{app}}/dt$) in order of DM is medium $>$ high $>$ low. Furthermore, at constant DM, the rate is more rapid for the sodium salt than the protonated form.

Table II. Decrease of \overline{M}_n^{app} as a Function of Time (Days) in 0.047 M NaCl and 0.003 M NaN_2 for Pectins

DM	H			Na		
	$-k^a \times 10^{-2}$	$b^b \times 10^{-3}$	Corr Coeff	$-k \times 10^{-2}$	$b \times 10^{-3}$	Corr Coeff
35	-1.7	30.4 ± 0.4	+0.68	0.5	16.3	-0.998
37	0.5 ± 1.0	27.0 ± 0.7	-0.31	0.9 ± 0.4	15.3 ± 0.3	-0.840
57	2.7 ± 0.3	32.5 ± 0.2	-0.98	2.5 ± 0.3	27.6 ± 0.3	-0.980
58-60	3.8 ± 0.7	31.4 ± 0.4	-0.97	—	—	—
70	3.0 ± 0.4	39.1 ± 0.6	-0.89	1.8 ± 0.5	26.7 ± 0.4	-0.980
72-73	1.7 ± 1.0	35.7 ± 0.5	-0.79	1.4 ± 0.2	25.5 ± 0.1	-0.998

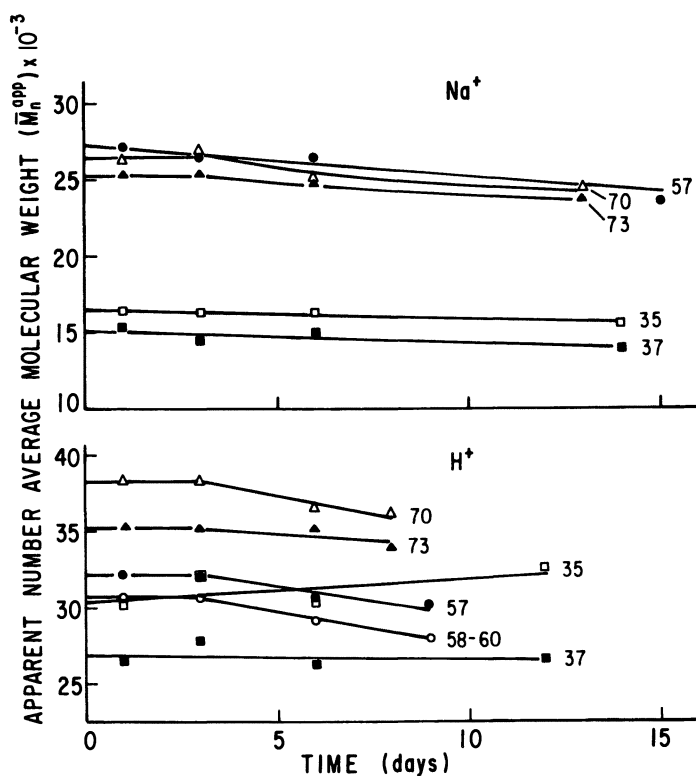
^ak is the slope.^bb is the intercept.

Figure 3. \overline{M}_n^{app} as a function of time for protonated and sodium salts of pectin. The concentration was 0.6 g/dL. Top (for Na^+): ●, DM = 57; △, DM = 70; ▲, DM = 73; □, DM = 35; and ■, DM = 37. Bottom (for H^+): △, DM = 70; ▲, DM = 73; □, DM = 35; ●, DM = 57; ○, DM = 58-60; and ■, DM = 37.

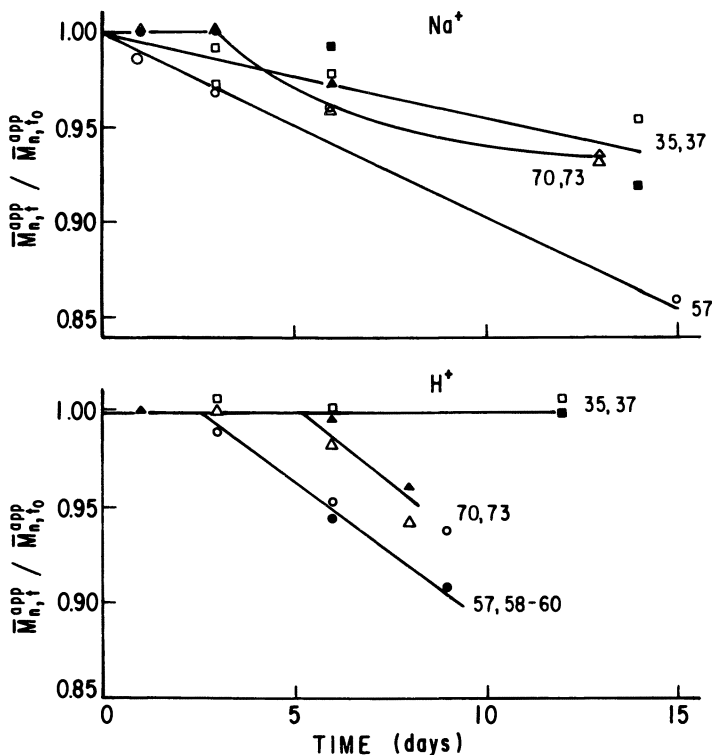


Figure 4. $\bar{M}_{n,t}^{app} / \bar{M}_{n,0}^{app}$ as a function of time for protonated and sodium salts of pectin. The concentration was 0.6 g/dL. Top (for Na^+): \square and \blacksquare , DM = 35 and 37; \triangle and \blacktriangle , DM = 70 and 73; and \circ and \bullet , DM = 57. Bottom (for H^+): \square and \blacksquare , DM = 35 and 37; \triangle and \blacktriangle , DM = 70 and 73; and \circ and \bullet , DM = 57 and 58-60.

Comparison of \overline{DP}_n for Unheated and Heated Pectins. A decrease in \bar{M}_n^{app} could be caused by changes in molecular weight, second virial coefficient, or a combination of the two. Thus, after following the decrease in \bar{M}_n^{app} for 8-15 days, samples were diluted on the final day and van't Hoff plots obtained (Figure 5). In one case, the sodium salt with DM-58-60, the van't Hoff plot was obtained after treating the sample according to the procedure under End-Group Titration. A comparison of the data in Table III with that in Table I revealed that \overline{AGR}_n for the heated and equilibrated pectins was lower than for the unheated pectins. A comparison of second virial coefficients (B in Table IV) revealed these coefficients were greater for the heated pectins. Generally, for comparable samples and conditions, the percentage change in \bar{M}_n^{app} is less than the percentage change in \bar{M}_n . For example, \bar{M}_n^{app} for the medium-methoxy, protonated pectins dropped by about 8% (Figure

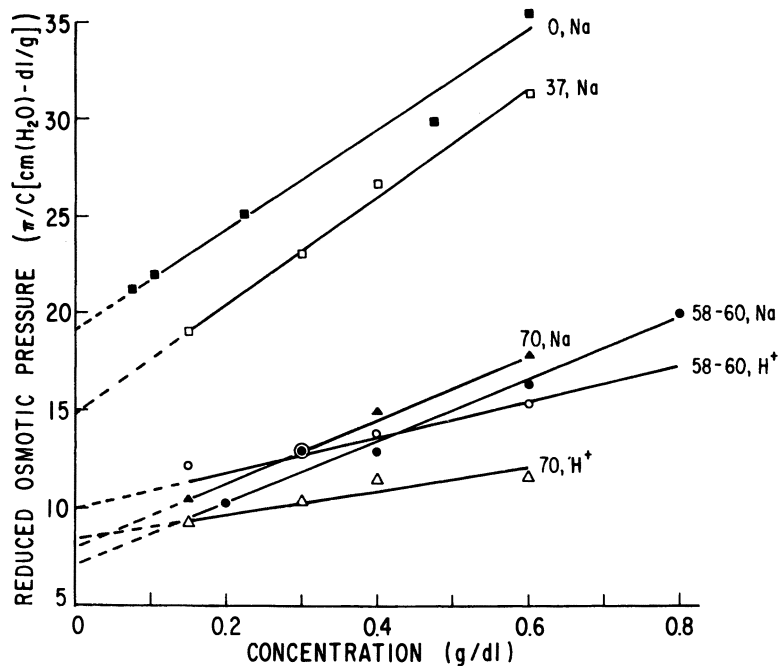


Figure 5. Typical van't Hoff plots for heated and equilibrated pectins after 8-15 days. Key: ■, DM = 0, Na⁺; □, DM = 37, Na⁺; ▲, DM = 70, Na⁺; ●, DM = 58-60, Na⁺; ○, DM = 58-60, H⁺; and △, DM = 70, H⁺.

Table III. \overline{DP}_n and \overline{AGR}_n for Heated Pectins

DM	End-Group Analysis	\overline{DP}_n			
		Osmometry		\overline{AGR}_n^a	
		Na	H	Na	H
0	29.7 ± 4.0	51 ± 1	—	1.7 ± 0.3	—
35	50.7 ± 9.0	126 ± 1	—	2.5 ± 0.5	—
37	32.8 ± 3.5	94 ± 3	—	2.9 ± 0.4	—
57	65.9 ± 1.2	186 ± 2	155 ± 3	2.8 ± 0.5	2.4 ± 0.5
58-60	66.0 ± 8.6	196 ± 13	146 ± 4	3.0 ± 0.6	2.2 ± 0.3
70	67.6 ± 10.9	178 ± 7	170 ± 7	2.6 ± 0.5	2.6 ± 0.5
72-73	60.0 ± 1.2	206 ± 11	171 ± 10	3.4 ± 0.2	2.9 ± 0.2

$$^a \overline{AGR}_n = \overline{M}_{n,0} / \overline{M}_{n,ECT}$$

4) in 8 days, whereas \bar{M}_n decreased by about 30% (cf. Tables I and III). Interestingly, for comparable samples, the percentage drop in \bar{M}_n of the protonated form is either equal to or greater than the percentage change in \bar{M}_n for the sodium form. For high- and medium-methoxy pectins, a comparison of sodium and protonated forms also revealed no significant difference in \overline{ACR}_n for the unheated pectins (Table I).

Comparison of Axial Ratios (L/d) and Counterion Binding for Heated and Unheated Pectins. When L/d was calculated by using equation 8, a value of 0.62 was taken for V_2 of the pectins and 0.56 for poly(galacturonic acid) (18). V_1 was taken as that of water. For the medium-methoxy protonated pectins, L/d appears to have increased somewhat with heating and equilibration, whereas heating and equilibration appeared to have no effect on the axial ratio of high-methoxy pectin (Table IV).

The low-methoxy protonated pectin gave scattered data when van't Hoff plots were attempted. The solubility of poly(galacturonic acid) was too limited to obtain van't Hoff plots. Nevertheless, L/d and B_H were calculated by the following procedure. PG was assumed to be a rod (19) with a virtual bond length of 5 Å (i.e., the length of a monomer unit along the x axis) (20). Thus, the overall length (L) was calculated from the product of the virtual bond length and the \overline{DP}_n . Furthermore, when the diameter (d) was estimated to be 10 Å, an approximate value of L/d could be obtained and an approximate B_H calculated from equation 8 (Table IV).

Unlike the protonated pectins, van't Hoff plots were obtained for all the neutralized pectins, so that values of $1 - \alpha$ (fraction of bound counterions) were obtained from equations 9–11. A value of 0.78 was used for X_G in equation 11 (8). Counterion binding decreased for the heated and equilibrated pectins compared to the unheated (Table IV). Furthermore, for either heated or unheated pectins, $1 - \alpha$ increased with decreasing DM due to decreasing charge density. Decreasing the fraction of esterified carboxyl groups (ϵ) is analogous to the progressive neutralization of a poly(acrylic acid) (21) (Figure 6) or increasing the percentage of charged residues in a copolymer containing a mixture of charged and uncharged comonomers (22).

Concentration-Dependent Dissociation. In light of the findings that pectin dissociation required activation and that, in four of six cases, several days of lag time ensued between activation and an observed decrease in \bar{M}_n^{app} , a series of critical experiments were performed to test the hypothesis that pectins undergo a concentration-dependent dissociation. The experiments are described under End-Group Titration. Remarkably, the minima in the van't Hoff plots of Figure 7 are evidence that neutralized pectins with a DM between 73 and 35 and protonated

Table IV. Structural Information from Second Virial Coefficient (B)

DM	Unheated				Heated			
	H		Na		H		Na	
	$B \times 10^4$ (mL/g ² -mol)	L/d ($\times 10^{-2}$)	$B \times 10^4$ (mL/g ² -mol)	$I - \alpha$	$B \times 10^4$ (mL/g ² -mol)	L/d ($\times 10^{-2}$)	$B \times 10^4$ (mL/g ² -mol)	$I - \alpha$
0	14 ^a	0.2 ^a	106±6	0.74	11 ^a	0.3 ^a	99±7	0.65
35	—	—	80±1	—	—	—	106±1	—
37	—	—	86±4	—	—	—	105±5	—
57	20±1	1.2	36±1	0.69	31±2	1.7	69±1	0.53
58-60	26±5	1.5	49±4	0.61	35±3	2.0	61±7	0.56
70	20±1	1.2	35±4	0.50	23±4	1.2	63±6	0.32
72-73	26±1	1.6	47±3	0.44	29±7	1.8	73±6	0.17

^aThe value was calculated by assuming a rod with residue virtual bond length of 5 Å and a diameter of 10 Å.

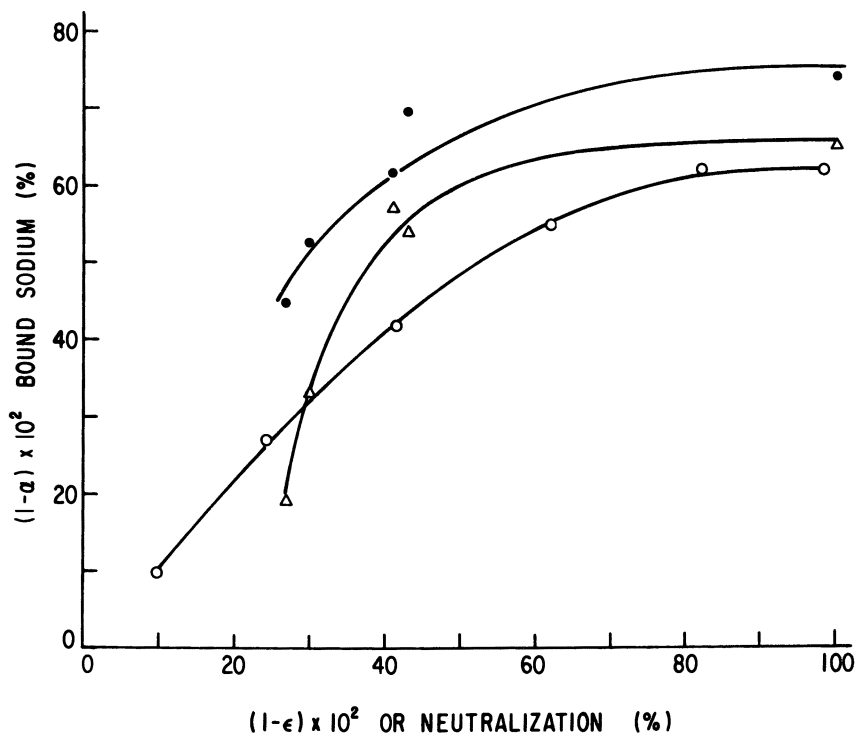


Figure 6. Counterion binding as a function of degree of esterification $[(1 - \epsilon) \times 10^2]$ for heated and unheated pectin. Data for 0.015 N poly(acrylic acid) were taken from reference 21. Key: ●, unheated pectin; Δ, heated pectin; and ○, 0.0151 N poly(acrylic acid).

pectin with DM-72-73 undergo concentration-dependent dissociation in the concentration range below 0.1 g/dL. Although not shown, the DM-70, 57, and 58-60 pectins behave similarly. Values of π/c at the intercept were calculated from \bar{M}_n values obtained by end-group titration.

We note that in the absence of activation and the observance of a lag time, our results were consistent with the osmotic pressure results of previous investigators (5-7). Only after activation and observance of a lag time were we able to obtain π/c values sufficiently free of scatter in the <0.1-g/dL range to observe reproducible minima in van't Hoff plots. Thus, we were able to recognize the concentration-dependent dissociation of pectin, whereas others failed.

In cases where dissociation is accompanied by large free-energy changes, the concentration range of nonlinearity should be rather narrow. Thus, the van't Hoff plots in Figure 7 could arise from dissociating

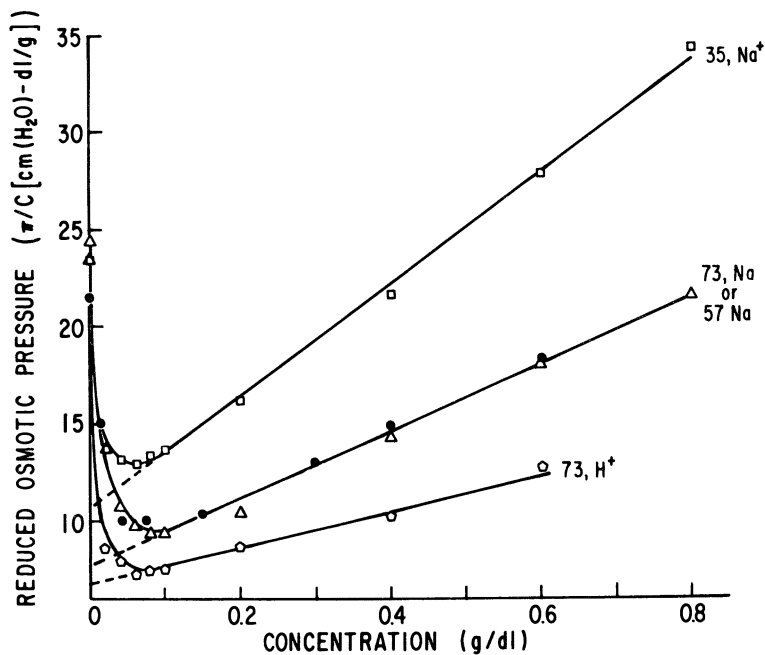


Figure 7. van't Hoff plots demonstrating concentration-dependent dissociation of pectin. Values at the intercept were calculated from end-group titrations. Key: \square , DM = 35, Na^+ ; \bullet and \triangle , DM = 73 or 57, Na^+ ; and \circ , DM = 73, H^+ .

systems that form nonideal aggregates (13) under the influence of relatively large free-energy changes.

Acknowledgment

Reference to brand or firm names does not constitute endorsement by the U.S. Department of Agriculture over others of a similar nature not mentioned.

Literature Cited

1. Olson, A. C.; Evans, J. J.; Frederic, D. P.; Jensen, E. F. *Plant Physiol.* **1969**, *44*, 1594.
2. Towle, G. A.; Christensen, O. In *Industrial Gums*; 2nd ed.; Whittler, R. L.; Be Miller, J. N., Eds.; Academic: New York, 1973; Chapter 19.
3. Story, J. A.; Kritchevsky, D. A. In *Nutrition and the Adult, Macronutrients*; Alfin-Slater, R. B.; Kritchevsky, D. A., Eds.; Plenum: New York, 1980; Chapter 10.
4. Kertesz, Z. I. In *The Pectic Substances*; Interscience: New York, 1951; p 180.
5. Owens, H. S.; Lotzkar, H.; Schultz, T. H.; Maclay, W. D. *J. Am. Chem. Soc.* **1946**, *68*, 1628.

6. Pals, D. T.; Hermans, J. J. *Recl. Trav. Chem. Pays-Bas* **1952**, *71*, 458.
7. Jordan, R. C.; Brant, D. A. *Biopolymers* **1978**, *17*, 2885.
8. Fishman, M. L.; Pfeffer, P. E.; Barford, R. A.; Doner, L. W. *J. Agri. Food Chem.* **1984**, *32*, 372.
9. Davis, M. A. F.; Gidley, M. J.; Norris, E. R.; Powell, D. A.; Rees, D. A. *Int. J. Biol. Macromol.* **1980**, *2*, 330.
10. Sorochan, V. D.; Dzizinko, A. K.; Boden, N. S.; Ovodov, Y. S. *Carbohydr. Res.* **1971**, *20*, 243.
11. Hanke, D. E.; Northcote, D. H. *Biopolymers* **1975**, *14*, 1.
12. Fishman, M. L.; Pepper, L.; Pfeffer, P. E.; Barford, R. A. *Abstracts of Papers*, 186th National Meeting of the American Chemical Society: Washington, DC; 1983.
13. Tombs, M. P.; Peacocke, A. R. In *The Osmotic Pressure of Biological Macromolecules*; Clarendon: Oxford, 1974; Chapters 3 and 4.
14. Tanford, C. In *Physical Chemistry of Macromolecules*; Wiley: New York, 1961; Chapter 4.
15. Launer, H. F.; Tomimatsu, Y. *Anal. Chem.* **1951**, *26*, 382.
16. Launer, H. F.; Tomimatsu, Y. *Anal. Chem.* **1959**, *31*, 1596.
17. Albersheim, P.; Neukom, H.; Deuel, H. *Arch. Biochem. Biophys.* **1960**, *90*, 46.
18. Saverborn, V. K. *Zeitschrift* **1940**, *90*, 41.
19. Fishman, M. L.; Pepper, L.; Barford, R. A. *J. Poly. Sci. Phys. Ed.* **1984**, *22*, 899.
20. Rees, D. A. In *Polysaccharide Shapes*; Halsted: New York, 1977; p 43.
21. Huizenga, J. R.; Grieger, R. F.; Wall, F. T. *J. Phys. Chem.* **1950**, *72*, 4228.
22. Nagasawa, M.; Rice, S. A. *J. Phys. Chem.* **1960**, *82*, 5070.

RECEIVED for review September 28, 1984. ACCEPTED December 6, 1985.

^{13}C -NMR Characterization of Structures of Water-Soluble Polymers

Morris F. Tchir and Alfred Rudin

Department of Chemistry, University of Waterloo, Waterloo, Ontario, Canada N2L 3G1

Structural features of water-soluble polymers can be characterized using ^{13}C -NMR spectroscopy. The techniques are similar to those used for nonaqueous polymer solutions. The state of the art of characterization of the structure by NMR is presented along with the application of the technique to several specific polymers.

POLYMERS MAY DIFFER in molecular weight, composition, sequence distributions of comonomers, stereoregularity, branching, regularity of head-to-tail placements of vinyl monomer residues, and other features. Many of these characteristics are not reflected by current quality-control tests. Variations in some of these properties have important influences on practical uses of certain water-soluble polymers. For example, blockiness of residual vinyl acetate residues is believed to affect surface activity, dispersing power, solubility, and aqueous solution viscosity of partially hydrolyzed poly(vinyl alcohol) (1, 2). Various techniques are used to infer mean block lengths of vinyl alcohol-acetate copolymers and other polymers (3-5). None of these methods can measure sequence lengths directly, however. An absolute analytical technique for detection of mean sequence distribution, branching, and other structural features has appeared only recently, in the form of ^{13}C NMR spectroscopy.

This chapter summarizes the state of the art of the characterization of the structure of water-soluble polymers by ^{13}C -NMR. Examples are given of the application of these techniques to several important polymers. Most practical developments are so recent that very few reports

0065-2393/86/0213-0071\$06.00/0
© 1986 American Chemical Society

link performance to variations in sequence distribution, substituent placement, branching, and so on. Therefore, this important topic is left to future reviews.

¹³C Analytical Techniques

Introduction. The application of ¹³C-NMR spectroscopy to problems in polymer science is now well established. Continued advances in theory, coupled with instrument improvements, make the technique more useful in obtaining precise and detailed information about polymers. The application of NMR to aqueous systems offers some interesting possibilities and some unique problems.

The great advantage of ¹³C NMR over ¹H NMR is the larger chemical shift range (200 ppm for carbon versus 10 ppm for protons). Relatively small structural variations can result in distinct spectral differences in ¹³C NMR. Under normal conditions of spectral determination, each carbon appears as a single line without the complexity of spin-spin coupling found in ¹H NMR. Thus, under proper conditions, a great deal of information can be obtained.

Instrumentation. Because the present concern is with polymers in solution, a high resolution spectrometer is used. (The instrumentation required for solids is somewhat different.) Further, because the nucleus under observation is carbon, the discussion is restricted to pulsed Fourier transform spectrometers. (Possibly, future developments will eliminate the use of the Fourier transform techniques, but this usage is the current mode.) Normally, the accuracy of the interpretation will depend on the degree of dispersion, the resolution, and the signal-to-noise level (*S:N*). The challenge is to obtain a spectrum with good signal and well-resolved (separated) and narrow peaks in the shortest possible time.

Most commercial spectrometers are marketed with some number attached to the name. This number normally refers to the proton frequency for that particular magnet. Thus, numbers such as 100, 200, 500, and so on mean that these spectrometers operate at 100, 200, and 500 MHz for protons. The corresponding carbon frequency is about one-quarter (factor of 0.251) of the proton frequency; for example, a 400-MHz spectrometer measures ¹³C NMR at 100.6 MHz. [Occasional lapses occur in this general practice, particularly in continuous wave (CW) spectrometers. For example, the Perkin-Elmer R-12 and R-24 instruments both operated at 60 MHz, while the R-32 is a 90-MHz spectrometer. The Varian 360 is a CW permanent magnet 60-MHz spectrometer and should not be confused with a Nicolet 360, which operates at 360 MHz. The Varian CFT-20 is really an 80-MHz spectrometer that is "dedicated" to carbon.]

In NMR spectroscopy, the chemical shift range and chemical shift in parts per million (ppm) are independent of field strength. On the other hand, the frequency range is directly proportional to field strength. So that the 200-ppm range on a 100-MHz spectrometer (25 MHz for carbon) is covered, a 5000-Hz region must be scanned. The range would be 10,000 Hz (10 kHz) on a 200 instrument and 20 kHz at 400 MHz. If line width, defined as the width at half the maximum height of a resonance peak, does not change, then the chances of overlap will decrease greatly as field strength increases. This relationship leads to a general rule: use the highest field magnet that can be found.

In pulsed experiments, *S:N* is roughly proportional to the square root of the number of scans. So that *S:N* is increased by a factor of 2, four times as many scans must be run, with four times as much machine time. However, other ways to improve sensitivity exist.

The signal in NMR spectroscopy is approximately proportional to the field strength. Thus, changing from an 80-MHz spectrometer to a 250-MHz machine should result in a signal enhancement by a factor of more than 3 with a time reduction of a factor of at least 9.

Improvements in electronics, particularly in probe design, also serve to increase the signal. For example, a new 250-MHz instrument may actually be better than an old 400-MHz unit and is probably a factor of 5 better than an old 80-MHz spectrometer. This consideration leads to another general rule: all other things being equal, use the newest spectrometer available.

Most new spectrometers are designed for multinuclear use and are supplied with broad-banded tunable probes. Although these probes are more versatile, they usually will not have the sensitivity of a fixed-frequency probe. Thus, a specific carbon probe will give better results than a multinuclear probe that can be tuned to carbon.

The size of the sample can also be important in determining the resolution and *S:N*. (*S:N* can be doubled by doubling the amount of sample.) Proton spectra are normally run in 5-mm tubes although the usual size for carbon spectra is 10 or 15 mm (double the radius and four times the sample). The resolution may not be as good in a 10-mm sample, but this factor is not usually important with polymers because the lines are naturally wide. However, a fixed-frequency 5-mm probe may give better results than a 10-mm tunable probe. The correct sample size may well be dictated by the spectrometer hardware.

Multiple scan accumulation requires a field lock system, particularly with iron core magnets. This system is provided by locking on a deuterium signal that is normally provided by the solvent. In the case of aqueous samples, this signal can be provided by the addition of a small quantity of D₂O. (Some spectrometers can be equipped with an external

lock system.) However, spectrometers equipped with superconducting solenoids (supercon magnets) can often operate without a lock; the field in these spectrometers may be so stable, over the time required to get a good spectrum, that the need for a deuterium lock is obviated and, in the present case, ordinary water can be used. Small amounts of drift may cause some line broadening, but this problem is not important so long as this broadening is less than the natural line width and does not result in an unacceptable loss of resolution.

Finally, the spectrometer should be equipped with variable-temperature capability and with computer capability (software and hardware) to carry out special experiments.

Advances in technology are such that it is now possible to obtain a spectrum in 1 h on a 5-mm sample that would have taken 24 h on a 10-mm sample 5 years ago. Probably, the 1 h will be reduced to minutes in the near future. This rate of advance has always been true in the history of NMR: possibly, a spectrometer that is state-of-the-art when ordered is obsolete by the time it is delivered.

Sample Preparation and Resolution. The care required in preparing a sample of a polymer for ^{13}C NMR is often less critical than for small molecules, but some important points need to be considered.

In NMR spectroscopy, resolution is usually defined in terms of line width (width at half-height). Line width can be influenced by both the sample and the spectrometer: the narrower the line, the closer two lines can be to one another and still be resolved. Any nucleus can have a natural line width, which is a characteristic of the nucleus and of the chemical surroundings. This line width is determined by the relaxation rate and becomes narrower as the lifetime of the excited state becomes longer. For ^{13}C NMR of small molecules in dilute solution, this natural line width is usually less than 1 Hz. However, as the molecular weight increases, or as the viscosity increases, the overall molecular motion is slowed and dipolar relaxation (T_2) increases; the result is that the line width increases. For this reason, the line widths found in the ^{13}C NMR spectra of polymers are inherently larger than those for small molecules.

Some aspects of resolution are at the control of the spectroscopist. The magnetic field homogeneity must be maximized and lines must have the proper Lorentzian shape; that is, the magnet must be properly shimmed. The sample solution must properly fill the coils in the probehead and be free of both solids and paramagnetic impurities; for example, a trace of metallic nickel or iron can cause severe line broadening. Sample tubes should have a very uniform wall thickness, be very straight, and be concentric. These requirements usually imply that the quality of the tube increases with the price. The sample is normally rotated (spun) on its long axis at a rate of 20–30 Hz to average out field

inhomogeneities over the entire sample. This rotation can introduce spinning side bands that may interfere with the spectrum, but spinning is required for really high resolution work. Finally, the magnetic field must be kept constant during multiple scan accumulations, and keeping the magnetic field constant is normally done by locking as mentioned earlier.

As noted previously, line widths in the ¹³C NMR of polymers tend to be broad, and some of this broadness is related to relaxation times. However, a broad line may also be due to the unresolved near superposition of a series of narrow lines; that is, particular carbons within a polymer molecule may each have a narrow line but a range of chemical shifts that is slightly greater than the line width. The net result will be an apparently broad line that is really the summation of a distribution of much narrower lines. In this case, an increase in magnetic field could result in peak structure developing as the lines are pulled farther apart.

For these reasons, the initial studies on any polymer should be done at low solution viscosities (low concentrations), in good-quality tubes, with spinning and with an internal lock, and at as high a field as possible. If, at this point, the lines are wide (>5 Hz), then simplifications can be made. Increased concentration will improve S:N and shorten run times. Spinning of the sample may not be necessary, and spinning side bands can then be eliminated. A lock signal need not be used, and the sample would not require addition of D₂O.

Line widths are adversely affected by high viscosity, and viscosity should be kept as low as possible. One approach is to increase the sample temperature, and in this respect, water (or D₂O) is a good solvent because it has a relatively high (100 °C) maximum temperature. (We have used water up to 130 °C in sealed tubes.) However, increased temperatures can cause other problems. First, a temperature increase causes a decrease in the population difference between spin states (smaller magnetization) with the result that S:N decreases. Second, the relaxation time increases and a longer delay must be allowed between pulses, particularly in quantitative work. Third, the polymer may degrade at elevated temperatures over the time of the run. Finally, some polymers, such as poly(vinyl alcohol), have a negative solubility coefficient in water and may precipitate as the temperature is increased.

High molecular weight polymers may give very viscous solutions even at low concentrations. A somewhat novel approach to viscosity reduction is the use of mechanical shearing to modify a polymer. This shearing is accomplished by exposing the solution in an ultrasonic cleaner bath. However, demonstration that the polymer is unchanged may be necessary, at least in terms of its NMR spectrum.

The standard practice is to remove all solids from an NMR sample by filtration. The usual line broadening caused by solids may not be

important in ^{13}C NMR, and a very viscous solution may be difficult to filter. For this reason, sometimes polymer and solvent can be added to the tube and dissolution allowed to occur in the NMR tube. Any solid particles do not contribute to the NMR signal (very broad lines), but a polymer that is not completely soluble may yield anomalous results if the soluble material is not representative of the whole polymer.

Finally, NMR spectra have to be referenced to some internal standard. Tetramethylsilane $[(\text{CH}_3)_4\text{Si}]$, the usual ^{13}C standard, cannot be used in aqueous solution, and water does not contribute any peaks that can be used for calibration. The aqueous standard $(\text{CH}_3)_3\text{SiCD}_2\text{CO}_2\text{Na}$ contributes the three extra lines to the spectrum (split further by deuterium), and its ionic (soaplike) nature could adversely affect solution characteristics. Probably the best standards are small water-soluble organics that give one or two sharp lines in the spectrum; for example, both methanol and *p*-dioxane give single lines and *tert*-butyl alcohol gives one strong and one weak peak. The material chosen should not have a peak in the polymer absorption region and should, in a separate experiment, be referenced to a more usual silylated standard in the aqueous polymer medium. (Chemical shifts are somewhat solution dependent.) Obviously, the standard chosen should not cause the polymer to precipitate.

The Spectrum. NMR spectroscopy has both qualitative and quantitative aspects. For ^1H NMR this differentiation is immaterial, but for ^{13}C NMR the two aspects should be considered separately.

QUALITATIVE ANALYSES. The standard conditions for ^{13}C NMR on a particular spectrometer should be well-defined. Broad-band decoupling (removal of all C-H couplings) will normally be used. Probably, two-level decoupling should be used to prevent overheating; a low level of decoupling power sufficient to maintain the nuclear Overhauser effect (NOE) is applied during waiting periods and a high level of power is applied during the acquisition. Most new systems operate with decoupling programs such as a Mlev or Waltz, and these programs should be used if available.

The importance of magnetic relaxation is more apparent under Quantitative Analyses, but some relaxation delay should be allowed between pulses. This delay is particularly important if a small number of quaternary carbons are present; rapid pulsing can cause their bands to disappear.

At this stage, the digital resolution and S:N should be such that absolutely all peaks are visible; that is, a small peak should be detectable if it has 5% of the intensity of the strongest peak.

The peaks obtained must be assigned to polymer structural features. This assignment might be straightforward (an ester peak at 175 ppm) or

not (e.g., a small peak at 62 ppm). The spectrum could be run again in the off-resonance decoupling mode in which case methyl groups show up as quartets, -CH₂- as triplets, -CH as doublets, and quaternary carbons as singlets. However, for a polymer, this situation can become very messy, and a pulse sequence that modulates the spectrum according to the C-H couplings [*J* modulated (6), Dept (7), etc.] is much better to use. These spectra usually require about the same amount of time as broad-band decoupling and can probably be run instead.

The application of two-dimensional (2-D) spectra to polymer work is not common, probably because these spectra are easiest to do in the proton-proton sense (8). However, carbon-proton correlations should prove to be useful (for example, a quaternary carbon will not correlate with any Hs), and the potential for carbon-carbon correlations, at the natural abundance level, is even greater.

The assignment of functionality at this level may be easy or difficult, but the next level of assignment can be more critical and is certainly more difficult. As mentioned previously, small structural variations can cause observable spectral differences. The structural variations can include any or all of the following: tacticity (diad, triad, etc., level), propagation anomalies (head-to-head versus head-to-tail placements), and sequence distribution variations in copolymers. Determining which of these variations, or which combination of these variations, is responsible for a set of peaks may not be easy, and each polymer may have to be treated differently. For example, if the sample is a homopolymer, sequence distribution variations are ruled out and propagation anomalies can cause large shifts that could possibly be calculated by using empirical correlations. Tacticity considerations can be greatly simplified if a method exists that allows for the synthesis of a stereoregular version of the polymer.

Finally, if all else fails, synthesis of compounds that correspond to oligomers of the polymer of interest might be necessary. Unambiguous syntheses such as these can be extremely challenging in both an intellectual and technical sense.

QUANTITATIVE ANALYSES. One of the very useful features of ¹H NMR on a CW spectrometer (single slow sweep) is that peak area is directly proportional to the number of Hs producing that peak. Therefore, hydrogens can be counted by NMR. This feature carries over into proton spectra obtained with an FT spectrometer. Carbon, on the other hand, is more difficult to determine quantitatively. Broad-band decoupling of hydrogen introduces an NOE; NOE is a dipolar effect that operates through space. A theoretical maximum enhancement of nearly 2 is often observed for all carbons, including quaternary, in polymers. For quantification of ¹³C spectra, the data must really be accumulated in a decoupled mode but with no NOE. This accumulation is normally done

by running a sequence in which the decoupler is transmitting only during the time of the acquisition. The C-H coupling disappears very rapidly (microseconds) after the power is turned on and the NOE grows in at the same rate as T_1 . This form of decoupling is known as inverse gated and should eliminate the NOE. [This feature is true only if the acquisition time (a system-defined parameter) is much shorter than the relaxation time and this relationship is not always true of polymers.]

Some feel for "rotating frame" and "angle of magnetization" is required to understand the next phenomenon. A discussion of these concepts is found in any NMR textbook (9). The maximum signal is obtained for a 90° pulse angle. (The 90° pulse angle must be constant across the entire sweep range.) For the second accumulation to be identical with the first, the magnetization must be allowed to return to its initial value. The recovery of the magnetization is a first-order process with a rate constant equal to $1/T_1$. Recovery to exactly the same value would obviously require a time approaching infinity; as a compromise, a time equivalent to 5 times the longest T_1 is usually suggested. Carbon relaxation times in polymers are typically less than a few seconds. However, T_1 values of 5–10 s were observed, and these values dictate delays of 30 s–1 min. The T_1 values may need to be measured experimentally. This measurement is relatively easy to do by a number of techniques, but the measurement does require further experimentation. (This should be compared to a nonquantitative spectrum that would be obtained with full NOE at a repetition rate of 5–50 pulses/min.) Thus, the requirement for quantitative data greatly increases the amount of machine time required.

The use of elevated temperatures to improve resolution has already been mentioned. However, a higher temperature lowers the inherent sensitivity (more scans required) and increases T_1 values (more time between scans) by increasing molecular motion. A compromise has to be achieved between the amount of machine time available and quality of data required. This compromise may not be based on purely scientific considerations.

One further parameter needs to be considered in association with quantitative work—the size of computer memory required. The spectrum produced by an FT spectrometer is an analogue plot of digitized data (the algorithm joins the data), and how many data points are required to accurately reproduce a peak must be considered. A rough guide is to have at least five points per peak. For a wide peak, this number might be easy, but care must be taken with narrow peaks. The number of points per frequency unit can be increased by decreasing the frequency width observed (this action increases acquisition time) or by increasing the data size (this action increases acquisition time and processing time). A sweep width and memory size suitable for a qualitative analysis may not be correct for a quantitative spectrum.

Under some circumstances some of these warnings can be ignored. For example, consider a polymer that contains acid and ester functionalities and that has the two sets of carbonyl signals separated. That all the acid carbonyl carbons are more or less equivalent in terms of their NOEs and their relaxation rates can then be assumed, and thus internal relative areas are correct regardless of the acquisition parameters. The same should also be true between the ester carbonyls. However, the approximation would be stretched to compare acid and ester carbonyls and would collapse when comparing to a quaternary aromatic carbon.

The actual measurement of peak areas can be done by using the integration routine within the NMR program. Noise level, base-line roll, overlapping peaks, and other effects may cause errors, however, and better accuracy normally results from use of a planimeter or even from cutting and weighing techniques.

In summary, quantitative ¹³C NMR is not easy and requires some extra experimentation to get the correct conditions. Even with every precaution possible, the areas may still have an inherent error of up to $\pm 5\%$.

The Future. This discussion has been concerned almost exclusively with ¹³C NMR. ¹H NMR has not found much use in polymers (because of spectral overlap), but the application of new two-dimensional (or even three-dimensional) methods may allow for a separation that is not possible in a one-dimensional spectrum. Continued improvements in instrument technology may make other nuclei accessible. Deuterium spectra are usually run on specially prepared deuterated compounds; however, some recent work on deuterium at natural abundance has occurred (a good modern spectrometer can detect deuterium in tap water in a single pulse). Similarly, ¹⁵N ($I = \frac{1}{2}$, natural abundance of 0.365%) could become practical (but difficult).

Further, advances in magnet technology, probe electronics, computer capabilities, and pulse sequences will continue with the net result that ¹³C NMR will continue to become easier and more useful.

Applications

Cellulosics. Reuben (10) reviews the results of ¹³C NMR analyses of the structures of cellulose ethers. Particular emphasis is given to the use of such data to estimate relative rate constants for substitution at the different hydroxyls in starting anhydroglucose units.

Because these polymers are used as thickeners for water, spectra with better S:N ratios are obtained from solutions of degraded polymers. Lee and Perlin (11) used appropriate degradation schemes to study the distribution of hydroxypropyl residues in (hydroxypropyl)cellulose as well as to estimate the characteristics of poly(propylene oxide) side chains. Partial depolymerization by the action of acid or cellulase was also found to be a necessary first step in the characterization of

methyl-, (carboxymethyl)- and (hydroxyethyl)cellulose samples (12). The reactivities of the hydroxyl groups of cellulose were found to be in the order OH-2 > OH-6 > OH-3. The same order of reactivity was found by other workers from proton-NMR analyses of substituted glucoses obtained by hydrolysis of (carboxymethyl)cellulose in aqueous H₂SO₄ (13).

DeMember et al. (14) reported the use of ¹³C-NMR analyses of (hydroxyethyl)cellulose to determine the average chain length of poly-(ethylene oxide) sequences, the degree of substitution of ethylene oxide, and the average relative degree of derivatization of the anhydroglucose hydroxyls.

The properties of cellulose ethers are believed to depend in part on the number of moles of combined derivatizing agent per anhydroglucose unit (MS) and on the number of hydroxyl groups that are substituted per anhydroglucose unit (DS). MS can be measured by classical chemical techniques, but reliable DS analyses are provided primarily by NMR methods (15).

Cellulose acetate may become water soluble when the DS is moderately low (16). The solubility does not depend solely on the DS, however; solubility may also reflect the relative DS at the three different types of hydroxyl groups and the distribution of substituents along the cellulose molecule (17).

Miyamoto et al. (18) showed that the relative DS at individual hydroxyl groups can be determined from the ¹³C-NMR spectra of ring and O-acetyl carbonyl carbons. Examination of water-soluble and insoluble cellulose acetate samples shows that solubility can be achieved by acetylating the C-2, C-3, and C-6 hydroxyl groups to about the same extent (19). This result presumably reflects a more effective disruption of the crystalline character of the cellulose than is achieved by selective acetylation of the more reactive C-6 primary hydroxyl.

Acrylamide Polymers. Polymers and copolymers of acrylamide are used extensively as thickeners and flocculents. The efficiency of these products in this application militates against the use of solutions with sufficiently high concentrations for good analyses. Ultrasonic treatment decreases the solution viscosity to manageable levels (20, 21). Another expedient to achieve satisfactory resolution is, of course, to use lower molecular weight versions of the polymer at elevated sample temperatures (22).

¹³C NMR at 100.6 MHz was used to investigate the stereoregularity of a polyacrylamide specimen prepared by free radical polymerization at 70 °C with chain transfer, to reduce the molecular weight (22a). The methine resonance was analyzed for triad and pentad placements. Bernoulli statistics (22b) resulted in a meso triad placement probability of 0.43.

This is similar to observations with other vinyl polymers and indicates a slight preference for syndiotactic placements.

Copolymers of acrylamide and acrylic acid can be prepared by free radical copolymerization or by hydrolysis of polyacrylamide. In the latter case, the hydrolysis conditions are expected to influence the sequence distribution of residual acrylamide units and, therefore, the behavior of the copolymer as a flocculent or thickener. A careful recent ¹³C-NMR study by Halvorson et al. (23) showed that mild alkaline hydrolysis produces a wide spacing of carboxyl groups along the macromolecule. The distribution provided by acid hydrolysis, by contrast, tends to blocks of carboxyl groups.

Sequential hydrolysis procedures were developed in which an initial low level alkaline hydrolysis step preceded a buffered acid hydrolysis. The resulting products contained acrylic acid blocks of controlled length and distribution (20). Significant differences were seen between these products. For example, calcium titration resulted in much more extensive precipitation of blocky than random copolymers.

Poly(vinyl alcohol). Copolymer composition, tacticity, branching frequency, and mean vinyl acetate-vinyl alcohol sequence lengths were measured from high-resolution ¹³C-NMR spectra (24). Spectra were obtained in D₂O solutions at 100.6 MHz. Use of a high magnetic field instrument is recommended; much of the information that can be derived from the data is lost in a 20.1-MHz ¹³C-NMR spectrum. Peak assignments were made by comparison with those of related polymers and empirical additivity rules.

Mean sequence lengths in partially hydrolyzed poly(vinyl alcohol) are preferably measured from methylene carbon resonances of vinyl alcohol and vinyl acetate residues (24, 25). Carbonyl carbon resonances can also be used if these bands are corrected for configurational differences (26). The methylene carbon region of the ¹³C spectrum generally consists of three well-resolved lines that can be assigned to the alcohol-alcohol, alcohol-acetate and acetate-acetate dyads. Assuming that the NOE is essentially the same among main-chain carbons (27), the integrated intensities of these carbon resonances can be used to measure chemical composition and mean sequence distribution. The reliability of the technique can be assessed by comparing NMR analyses of acetate content with those from chemical or infrared analyses.

The stereochemical configuration of poly(vinyl alcohol) can be assessed from the methine carbon resonances. This information is normally not of great interest because poly(vinyl alcohol) derived from radical-polymerized poly(vinyl acetate) appears to be atactic (24, 28, 29).

Branching is another matter, however. Dunn and Naravane suggested (30) that most branches in poly(vinyl alcohol) will be nonhydrolyzable and short, a result of intramolecular chain transfer to methine carbons on the polymer backbone. The ^{13}C -NMR area of the quaternary branch point is not likely to provide an accurate measure of the number of carbon atoms contributing to it because this carbon will have a very long relaxation time. However, transformation of methine to quaternary carbons will decrease the methine:methylene ratio from the unit value expected for unbranched polymers. This ratio has been used to measure total branching in poly(vinyl alcohol) (24).

A comparison of the branch content from ^{13}C NMR with long chain branching frequency from size-exclusion chromatography shows that some 95% or more of the branches in the samples examined were indeed short (31). Long branches are not defined exactly in this context. By analogy with polyethylene, however, these branches are assumed to comprise more than six carbons (32).

Short branches (six carbons or less) can presumably be characterized by careful ^{13}C -NMR analyses, but such data have not been reported yet. Lacking also are measurements of poly(vinyl alcohols) derived from vinyl acetate-1-olefin copolymers.

The Future. Although not without their share of problems and tedium, ^{13}C -NMR characterizations of water-soluble polymers can evidently provide information that is not directly available from any other current method. The next step in the sequence of understanding requires the establishment of the correspondence between product performance and the structural characteristics that have been thus revealed. Because this link may have considerable commercial value, publication of this information may be slower than development of the basic analytical techniques.

Acknowledgment

We thank F. Halvorson and H. P. Panzer for their helpful review.

Literature Cited

1. Shiraishi, M.; Toyoshima, K. *Br. Polym. J.* **1973**, *5*, 419.
2. Noro, K. *Br. Polym. J.* **1970**, *2*, 128.
3. Nagai, E.; Sagane, S. *Kobunshi Kagaku* **1955**, *12*, 195.
4. Hayashi, S.; Nakano, C.; Moyotama, T. *Kobunshi Kagaku* **1963**, *20*, 1303.
5. Scholtens, B. J. R.; Bijsterbosch, B. H. *J. Polym. Sci. Polym. Phys. Ed.* **1979**, *17*, 1771.
6. Brown, D. W.; Nakashima, T. T.; Rabenstein, D. L. *J. Magn. Reson.* **1981**, *45*, 302.
7. Pegg, D. T.; Doddrell, D. M.; Bendall, M. R. *J. Chem. Phys.* **1982**, *77*, 2745.
8. Lippert, G.; Brown, L. R. *Polymer Bull.* **1984**, *11*, 585.

9. Martin, M. L.; Martin, G. J.; Delpuech, J-J *Practical NMR Spectroscopy*; Heyden: Philadelphia, 1980.
10. Reuben, J. *ACS PMSE Division Preprints* 1983, 51, 763.
11. Lee, D. S.; Perlin, A. S. *Carbohydrate Res.* 1982, 106, 1.
12. Parfondry, A.; Perlin, A. S. *Carbohydrate Res.* 1977, 57, 139.
13. Ho, F. F.-L.; Klosiewicz, D. W. *Anal. Chem.* 1980, 52, 913.
14. DeMember, J. R.; Taylor, L. D.; Trummer, S.; Rubin, L. E.; Chiklis, C. K. *J. Appl. Polym. Sci.* 1977, 21, 621.
15. Ho, F. F.-L.; Kohler, R. R.; Ward, G. A. *Anal. Chem.* 1972, 44, 178.
16. Malm, C. T.; Barkey, K. T.; Salo, M.; May, D. C. *Ind. Eng. Chem.* 1957, 49, 79.
17. Gelman, R. A. *J. Appl. Polym. Sci.* 1982, 27, 2957.
18. Miyamoto, T.; Sato, Y.; Shibata, T.; Inagaki, H.; Tanahashi, M. *J. Polym. Sci. Polym. Chem. Ed.* 1984, 22, 2363.
19. Miyamoto, T.; Sato, Y.; Shibata, T.; Tanahashi, M.; Inagaki, H. *J. Polym. Sci. Polym. Chem. Ed.* 1985, 23, 1373.
20. Panzer, H. P.; Halvorson, F.; Lancaster, J. E. *ACS PMSE Division Preprints* 1984, 51, 268.
21. Halvorson, F.; Lancaster, J. E.; O'Connor, M. unpublished data, 1984.
- 22a. Lancaster, J. E.; O'Connor, M. N. *Polym. J. Sci. Polym. Lett.* 1982, 20, 547.
- 22b. Bovey, F. A. *Chain Structure and Conformation of Macromolecules*; Academic: New York, 1982; p 51.
23. Halvorson, F.; Lancaster, J. E.; O'Connor, M.N. *Macromolecules* 1985, 18, 1139.
24. Bugada, D. C.; Rudin, A. *Polymer (London)* 1985, 25, 1759.
25. Moritani, T.; Fujiwara, E. U. *Macromolecules* 1971, 10, 532.
26. Toppet, S.; Lemstra, P. J.; van der Velden, G. *Polymer (London)* 1983, 24, 507.
27. Schaefer, J.; Natusch, D. F. S. *Macromolecules* 1972, 5, 416.
28. Wu, T. K.; Ovenall, D. W. *Macromolecules* 1973, 6, 582.
29. Wu, T. K.; Sheer, M. L. *Macromolecules* 1977, 10, 529.
30. Dunn, A. R.; Naravane, S. R. *Br. Polymer J.* 1980, 12, 75.
31. Bugada, D. C.; Rudin, A. *J. Appl. Polym. Sci.*, 1985, 30, 4137.
32. Rudin, A.; Grinshpun, V.; O'Driscoll, K. F. *J. Liq. Chromat.* 1984, 7, 1809.

RECEIVED for review February 8, 1985. ACCEPTED November 14, 1985.

Adsorption and Its Influence on Application Properties

J. E. Glass

Department of Polymers and Coatings, North Dakota State University,
Fargo, ND 58105

General concepts in the adsorption of water-soluble polymers are presented and discussed in relation to their use in the applications developed in the latter part of this chapter and this book. In most applications, flocculents are present or induced when the water-soluble polymer is added. In coating applications, the importance of adsorption is further complicated by the variable surface energies and surface areas of the dispersed components and the presence of preadded stabilizers to minimize flocculation. In petroleum applications, adsorption per se does not ensure shale stabilization or protect against fluid loss to the reservoir, but adsorption is necessary if a drilling fluid is to function effectively. These problems and those associated with protective colloid usages are discussed.

General Concepts Governing Adsorption

The adsorption of water-soluble polymers at various types of interfaces is important in many applications. Several pertinent reviews (1-7) address the nature of the conformation of the polymer in its adsorbed state and emphasize the results of studies from dilute solutions. These data are seldom translatable to the performance of water-soluble polymers in commercial applications. In the following discussion, fundamental aspects will be highlighted but not detailed. The data are discussed in relation to the problems associated with adsorption in latter sections of this chapter.

For adsorption to occur, the change in the free energy of the system must be negative. A favorable entropic contribution from the loss of conformational freedom by the adsorbed polymer and concomitant gain by the liberated water molecules should be realized. Examples clearly delineating the relative influence of the entropic contribution are few. The energies of interaction between water and both the substrate and the polymer and between the water-soluble polymer and the substrate

0065-2393/86/0213-0085\$06.00/0
© 1986 American Chemical Society

must be favorable to provide an enthalpic contribution. Examples (1-7) illustrating the importance of enthalpic contributions, except for the substrate-water interactions, are numerous. Given a specific chemical composition, the thermodynamic functions favor adsorption of higher molecular weight species. This property applies to adsorption from solutions of moderately low concentrations and to unflocculated substrates. Numerous examples of the molecular weight dependence are provided in the reviews (1-7).

Entropic Contributions

Entropic contribution to the adsorption process is illustrated by the underivatized carbohydrate polymers discussed in Chapter 1 [*Sclerotium glaucanicum* polysaccharide (SGPS), guaran, and dextran]. All of the carbohydrate polymers contain very hydrophilic repeating segments and do not lower the surface tension of water. The first, SGPS, is noted for its helical and network structure in aqueous solutions (8); of the polymers considered, SGPS would have the least entropic gain on dissolution. Guarant possesses a random conformation in water and would gain a greater degree of entropic freedom on dissolution. Dextran with one of its interunit repeating bonds exo to the pyranosyl ring would experience the greatest conformational freedom on dissolution. Their conformational entropic losses on adsorption would be inversely proportional to the gain on dissolution. The amounts adsorbed on peptized montmorillonite are in agreement (Figure 1) with the expected results. These observations are complemented by the adsorption of amylose on montmorillonite. The retrogradation of amylose (i.e., the formation of a double helix) at ambient temperature would predict greater adsorption at lower temperatures (abnormal behavior for a water-soluble polymer), which is observed.

Enthalpic Contributions

Enthalpic contributions to the free energy of adsorption involve three primary interactions (9): polymer-water, polymer-substrate, and water-substrate. Straightforward examples (1-7) of the importance of the first two types of interaction exist. The nature of the substrate-water interaction has not been quantified, primarily due to an obsession, for the past two decades, with adsorbing polymers only on monodispersed polystyrene latices. Particulate systems offer a high surface area, which makes surface concentration measurements feasible via solution concentration measurements. The recent disclosure (10) of a synthetic technique for preparing methacrylate and methacrylate-acrylate copolymer monodispersed latices may permit quantification of the importance of the substrate-water contribution in the near future. This possibility is dis-

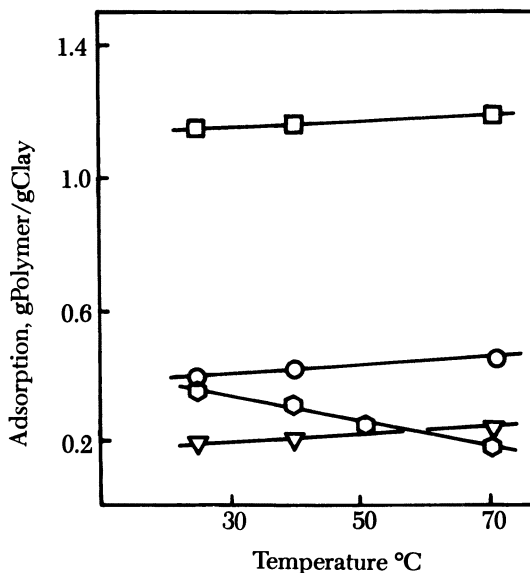


Figure 1. Temperature dependence of adsorption. Substrate: peptized montmorillonite. Polysaccharides; □, SGPS; ○, guaran; ⬡, amylose; and ▽, dextran.

cussed in context with application parameters in a latter section. The nature of polymer–water and polymer–substrate interactions on adsorption are highlighted in the following paragraphs, after a discussion of time- and concentration-dependent phenomena in the adsorption process.

Polymer adsorption at an air, liquid, or solid interface exhibits the general characteristics (11a) illustrated in Figure 2. At a very low concentration, the process is diffusion-controlled. The amount adsorbed, reflected for a homopolymer by the surface pressure (i.e., the difference between the surface tension of water and that of the aqueous polymer solution), increases slowly. At a moderately low concentration, an equilibrium surface pressure is reached within minutes; at concentrations greater than 1000 ppm, common in most applications, the time dependence is essentially undetectable.

The concentration dependence at equilibrium is illustrated in Figure 3. At low concentration the polymer adsorbs as an isolated chain, with a high proportion of its segments in the interface (designated as trains) and only a small percentage of its segments in the continuous phase (loops). As the concentration is increased, the location of the segments is reversed. Fewer segments are located in the interface [ca. 30% on average, based on nonaqueous polymer adsorption studies (11b)]; most

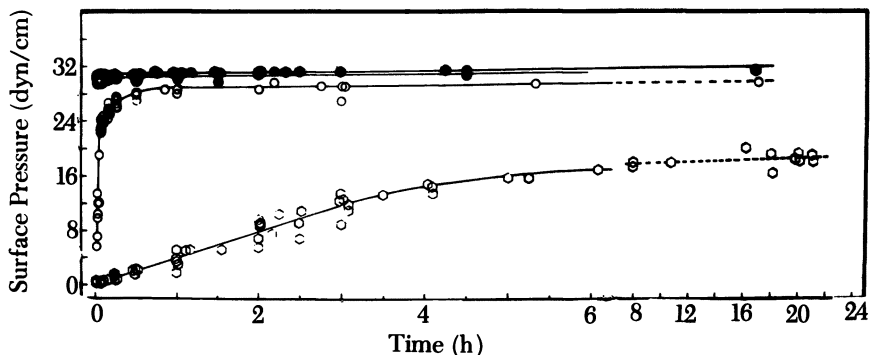


Figure 2. Surface pressure (mN/m) dependence on time (h) of poly(vinyl methyl ether), viscosity-average molecular weight (M_v) = 5×10^5 ; \circ , 1 ppm; \circ , 10 ppm; \bullet , 1000 ppm; and \bullet , 5000 ppm.

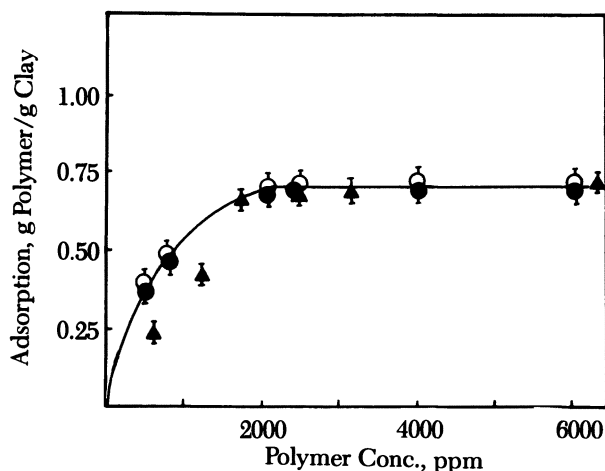


Figure 3. Adsorption (g/g) dependence on water-soluble polymer concentration (ppm). Substrate: peptized sodium montmorillonite. Open symbols: adsorbed from freshwater solutions. Closed symbols: from 0.54 N NaCl solutions. Water-soluble polymers (W-SP): \circ and \bullet , (hydroxyethyl)cellulose (HEC) ($MS = 2.0$); \blacktriangle , HEC ($MS = 2.0$) containing (2-hydroxypropyl)trimethylammonium chloride ($MS = 0.4$) ($HECN^+Me_3Cl^-$; polymer was extracted and gave pH 6.7 in clay slurry).

segments are extended normal to the interface as loops and as tail fragments. An early model (9) representing an interfacial conformation is illustrated in Figure 4.

If the segments of the macromolecule vary in hydrophobicity, adsorption will exhibit a significant time dependence even at high concentrations. An example of the phenomenon is illustrated in Figures 5

and 6 for water-soluble biopolymers. The time dependence is attributed to two phenomena: diffusion to the interface and interfacial reorientation. The mechanism is clearly detailed (12) in a study employing radio-tracer (delineating the short time period involved in adsorption at moderately low concentrations) and surface tension measurements (delineating the rearrangement of the adsorbed chains to permit repositioning of the more hydrophobic segments in the interface). If the segments are not significantly different in hydrophobicity, adsorption from concen-

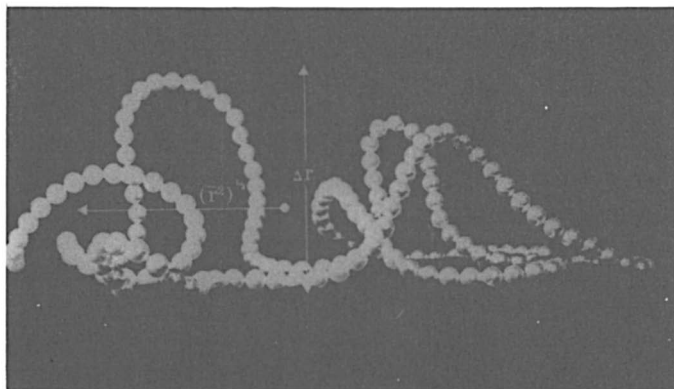


Figure 4. Generalized conformation for adsorbed polymers.

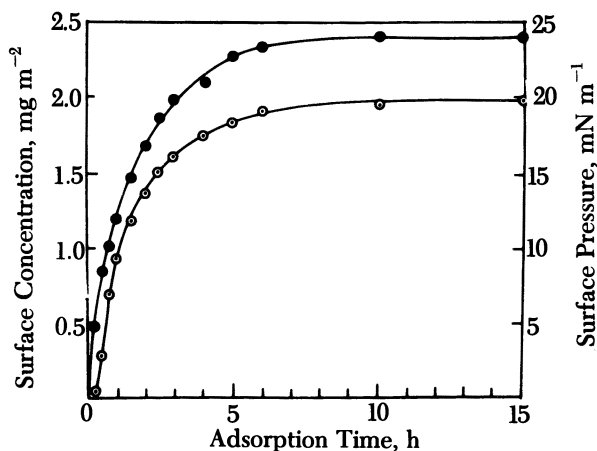


Figure 5. Variation of surface pressure (⊙) and surface concentration (●) with time during the adsorption of β -casein at the air-water interface. The substrate was phosphate buffer (pH 7; $I = 0.1$) at 20 °C and the initial protein concentration was 7.3×10^{-5} wt %. Reproduced with permission from reference 12. Copyright 1979 Academic.

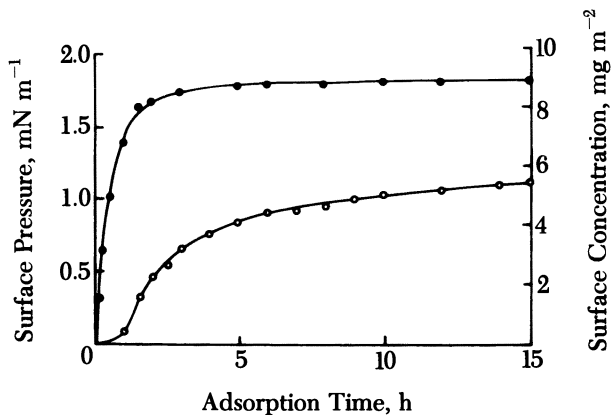


Figure 6. Variation of surface pressure (○) and surface concentration (●) with time during the adsorption of lysozyme at the air-water interface. The initial protein concentration was 7.6×10^{-5} wt %, and the remaining conditions are as described in Figure 4. Reproduced with permission from reference 12. Copyright 1979 Academic.

trated solutions will restrict rearrangement within the time frame important in most application processes.

Polymer-Water Interactions. The importance of the polymer-water interaction on the amount adsorbed at an air- or organic-aqueous interface is illustrated by the time dependence observed in the adsorption of vinyl acetate-vinyl alcohol copolymers (13) of variable acetate content or in cellulose ethers (11) with ether linkages of variable hydrophilicities. The dependencies are comprehensible via the dual mechanism noted previously: diffusion to and reorientation in the interfacial region. The cellulose ether data are given in Figure 7 to illustrate, later, the importance of different types of interaction in determining the amount of adsorption.

Water-soluble polymers with increasing hydrophobicity exhibit lower solubility with increasing temperature, and the effect of polymer-water interactions also can be observed in adsorption dependence as a function of temperature. Examples of the temperature relationship are noted in the adsorption of vinyl alcohol-vinyl acetate copolymers on monodispersed polystyrene latices (14) and for (hydroxyethyl)- and (hydroxypropyl)cellulose on silica particles (15). The latter data are illustrated in Figure 8; (hydroxypropyl)cellulose of molar substitution (MS) of 4.0 precipitates at 45 °C, where a notable increase in its adsorption is observed. The importance of adsorbent-water interaction in adsorption phenomena also is observed with both anionic (16) and nonionic (17) surfactants. These observations will be significant in the performance of

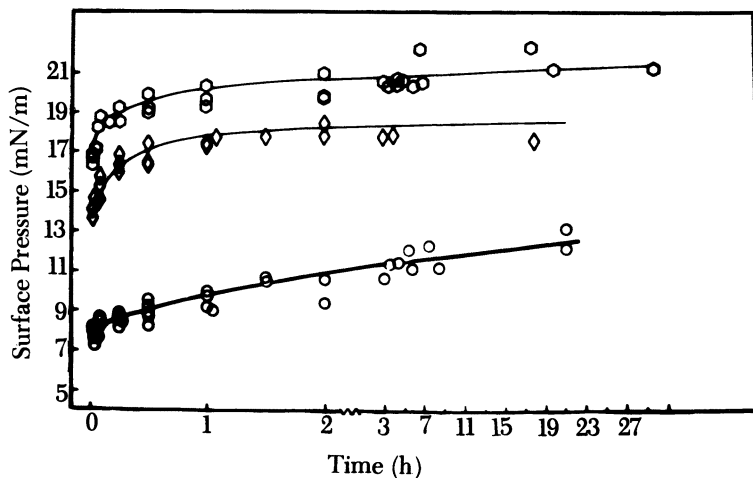


Figure 7. Surface pressure (mN/m) dependence (air-water interface) on time (h) for (hydroxyethyl)- (HE) and (hydroxypropyl)- (HP) cellulose (1000 ppm): \circ , MS = 2.40 (HE) and 0.13 (HP); \diamond , MS = 1.52 (HE) and 0.62 (HP); and \circ , MS = 1.19 (HE) and 1.03 (HP).

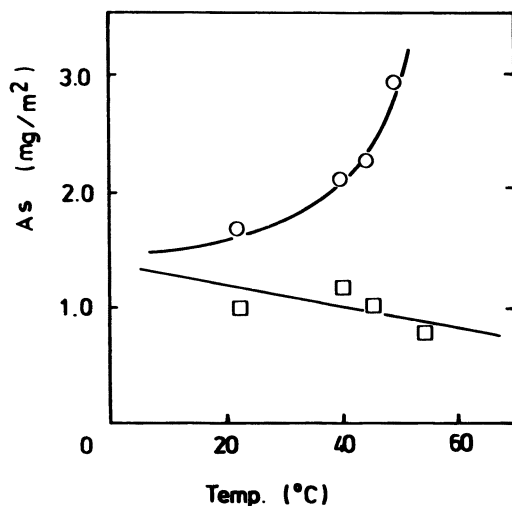


Figure 8. Temperature dependence of saturated adsorption (A_s) of moderate molecular weight (hydroxypropyl) cellulose (\circ) and high molecular weight (hydroxyethyl) cellulose (\square) onto silica particles.

hydrophobically modified, water-soluble polymers in coatings applications (Chapters 19–21).

Polymer–Substrate Interactions. When the substrate is montmorillonite, a significant difference in adsorption relative to that at the air–aqueous interface is observed. The difference is affected by an ion–dipole interaction between the ether oxygens on the polymer and the cations on the surface and in the interlayer of the clay (18). For example, the cellulose ethers illustrated in Figure 7 adsorb on peptized montmorillonite (Table I) in proportion to the amount of oxyethylene or oxypropylene pendent to cellulose or guaran (polymers discussed in Chapter 1), not in relation to the hydrophobicity of the pendent ether linkages.

The dramatic nature of this interaction is evident with variation in the cation. For example, sodium montmorillonite is extensively hydrated in aqueous solution, and water-soluble polymers such as (hydroxyethyl)cellulose are entrapped in the interlayer on recovery of the clay. Expansion of the interlayer does not occur significantly when the cation is calcium and cellulose ethers are not entrained in the interlayer. A notable exception, highlighting the importance of the ion–dipole interaction, is the ability of even high molecular weight (10^6) poly(oxyethylene) to penetrate the interlayer of calcium montmorillonite. Its “reptation” (to borrow a term from the rheology area) into the narrow interlayer channel produces greater structuring (observed in higher order X-ray diffraction patterns) than observed in untreated montmorillonite. The inability of cellulose ethers to penetrate the interlayer of calcium montmorillonite is relatable to their segmental rigidity (note discussion in Chapter 11).

Substrate–Water Affinity. For adsorption to occur, Rhebinder (19) proposed in 1927 that the polarity of the third component should be intermediate to the polarities of the two boundary layers. In the following

Table I. Effect of Cellulose Ethers on the Adsorption and d_{001} Expansion of Montmorillonite with Interlayer Cations Na^+ and Ca^{2+}

W-SP	MS	Ads (g/g)	Interlayer Spacing (nm)	
			Na^+	Ca^{2+}
HEC	4.3	0.98	—	—
HEC	2.5	0.70	—	—
HEC	2.0	0.69	2.4	1.53
HPC	4.0	0.40	1.9	1.90

NOTE: Abbreviations are as follows: W-SP, water-soluble polymer; Ads, adsorption; HEC, (hydroxyethyl)cellulose; and HPC, (hydroxypropyl)cellulose.

decades, investigations of limited scope examined the extent of adsorption of different compounds at various interfaces; in 1941, four different alcohols with increasing hydrophobicity were adsorbed (20) from aqueous solutions at air, *n*-heptane, benzene, and *n*-2-hexanone interfaces. The interfacial tensions of these phases with water varied significantly; the study revealed the interfacial free energy as a major determinant in the amount of low molecular weight alcohol adsorbed. Within each individual low molecular weight alcohol adsorption study, the importance of mutual phase affinities (i.e., of the organic-aqueous interface) on the adsorption of a third component was addressed. A similar series of experiments (21) utilizing poly(vinyl alcohol) (Figure 9) provides parallel results; the higher the interfacial energy (i.e., the lower the mutual affinity of the two continuous phases), the greater the amount of the third component adsorbed.

Coatings Applications. Differences in interfacial energies are realized in the emulsion polymerization of acrylic monomers with ester groups containing variable methylene units. Less surfactant is adsorbed (16) on short-chain acrylate ester latex interfaces (Table II). Vinyl acetate, like methyl acrylate, latices are very hydrophilic. The amount of

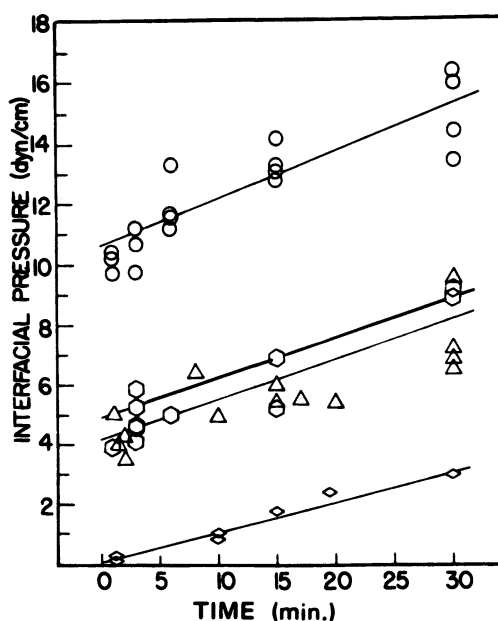


Figure 9. Pendant drop studies (25 °C): 0.1 wt %, $1.2 \times 10^5 M_w$, 99.3% hydrolyzed poly(vinyl alcohol)-aqueous solution interface with hexane (O), benzene (◐), air (Δ), and ethyl acetate (◊). Reproduced with permission from reference 21. Copyright 1971 Wiley.

Table II. Adsorption and Kinetic Characteristics of Polymerization Systems Based on Alkyl Acrylates, Styrene, and Various Alkyl Sulfates

<i>Monomer</i>	<i>Emulsifier</i>	E_{ads} (kJ/mol)	A_{slim} (nm ²)
MA	C ₁₂ H ₂₅ SO ₄ Na	20.0	1.51
EA	C ₁₂ H ₂₅ SO ₄ Na	22.1	0.92
EA	C ₁₄ H ₂₉ SO ₄ Na	23.3	0.82
EA	C ₁₆ H ₃₁ SO ₄ Na	24.6	0.74
BA	C ₁₂ H ₂₅ SO ₄ Na	25.6	0.67
HA	C ₁₂ H ₂₅ SO ₄ Na	—	0.52
Sty	C ₁₂ H ₂₅ SO ₄ Na	—	0.48

NOTE: Abbreviations are as follows: E_{ads} , free energy of adsorption; A_{slim} , adsorption area of surfactant molecule at saturation of the adsorption layer; MA, methyl acrylate; EA, ethyl acrylate; BA, butyl acrylate; HA, hexyl acrylate; and Sty, styrene.

sodium lauryl sulfate adsorbed (22) at a vinyl acetate- or methyl acrylate-aqueous interface is low relative to that of other acrylic latices (Figure 10; the amount adsorbed is inversely proportional to the limiting area). Recently, a model (23) was developed for relating the amount adsorbed to the polarity of the latex. The importance of the amount adsorbed to the stability of the dispersed phase was not addressed, because of the broad particle-size distribution noted with the more polar latices. This result is related in part to the monomer's greater participation in a homonuclear mechanism during an emulsion polymerization. Conceivably, less stabilizer concentration is required to stabilize a vinyl acetate

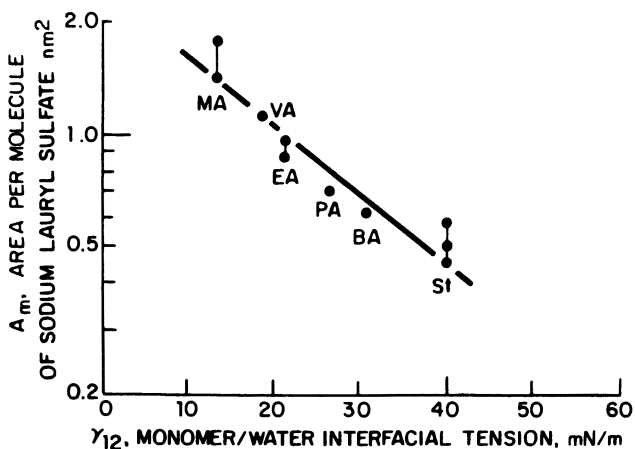


Figure 10. Plot of logarithm of area per molecule of sodium lauryl sulfate against monomer-water interfacial tension. Reproduced with permission from reference 22. Copyright 1980 Plenum.

latex than a higher energy acrylic or styrene latex, because of the vinyl acetate latex's affinity for water.

The cohesive interactions among surfactants at fluid interfaces were examined in relatively ideal cases. In commercial latices, several stabilizing entities significantly increase the complexity of the interfacial region. Chemically attached carboxylate (24) or (hydroxyethyl)cellulose (discussed in Chapter 18) fragments are present at most commercial latex-aqueous interfaces; such groups improve the freeze-thaw and/or mechanical stability of the latex. The carboxylate surface functions provide a steric stabilization component as well as enhancing electrostatic repulsions. The latices of variable median size discussed in Chapter 20 contain 1% of a carboxylate monomer in a methyl methacrylate-butyl acrylate composition.

Even with acid-stabilizing segments, small particle size latices are flocculated in the presence of water-soluble polymers. A general mechanism recently accepted for this behavior is volume-restricted flocculation (VRF) of the latex by the nonadsorbing polymer. References to the early history of this concept are given in Chapter 21. Use of the concept in relation to coatings was recently reported (25-27). The VRF mechanism involves a contribution to the attractive force between colloid particles suspended in a solution of macromolecules when the effective diameter of the macromolecular coils exceeds the distance between particles. The volume-restricted contribution to the net attractive forces between particles is approximately equal to the osmotic pressure of the macromolecular solution. Flocculation of the latex leads to elastic behavior at low deformation rates and poor coatings flowout. Inhibition of the flocculation mechanism by adsorption of hydrophobically modified, water-soluble polymers (Chapters 19-21) can effect osmotic stabilization of the dispersed phases and improve rheology.

In the fully formulated coatings, titanium dioxide and extender pigments are present in addition to the latex. Preadded stabilizers along with a nonionic surfactant (as a wetting agent) are added to the pigments before the formulation is thickened with a water-soluble polymer. If the higher energy pigments are not properly stabilized, the thickener molecules will preferentially adsorb or react with these entities. Statistically, even in a coatings formulation containing high pigmentation, the hydrophobes are favored to react with the greater surface area offered by a small particle size latex. The competitive adsorption of the various components in a coatings formulation provides a complex matrix, and apparently the hydrophobically modified, water-soluble polymers discussed in Chapters 19-21 do not associate with any of the dispersed components in a fully formulated coating. For example, hydrophobically modified, water-soluble polymers adsorb on the surfaces of latex particles with insufficient surface coverage but are displaced when

appropriate amounts of sodium lauryl sulfate are added (Chapter 20). The observations in these detailed but limited studies are certain to vary with changes in the structure of the stabilizing surfactant(s). The comparative efficiencies and rheological variations cited in Chapter 21 strongly suggest that such hydrophobically modified, water-soluble polymers in formulations containing both latex and titanium dioxide preferentially react with the latex.

Petroleum Applications. Adsorption per se does not ensure shale stabilization, protect against fluid loss to the reservoir in high salinity environments, or avoid excessive viscosity buildup at high temperature in the drilling of a well bore (Chapters 10–12), but adsorption is necessary if a drilling fluid is to function effectively. The primary challenge in ensuring shale stability is to inhibit migration of the interlayer cation into the lower salinity drilling fluid. Potassium chloride is added to the fluid to increase its cation content; however, in field testing (Chapter 10), a polymer is also added to ensure integrity of the shale. In static laboratory tests, many water-soluble polymers are observed to be effective but fail as shale stabilizers in dynamic field tests. A critique of static test results is given in Chapter 10. The inconsistency between laboratory and field tests is further highlighted by the changing nature of shale compositions with location. With a lack of detailed understanding of the adsorption behavior of water-soluble polymers (28) on different clay surfaces and an insistence that any test “out of hole” is not a valid test, an understanding of shale stabilization is not immediately on the horizon. If the technique associated with a recent rheological examination (29) of clays were combined with a detailed knowledge of the shale’s composition and the adsorption behavior of the water-soluble polymers on the individual clays of a specific shale in a detailed study, an understanding allowing predictability in this area could be realized. From the data to date, it is apparent that a cohesive or polar interaction is needed after adsorption of the polymer to form a condensed monolayer that facilitates an impermeable membrane.

Bentonite provides the shear-thinning rheology necessary for drilling and surfacing of solids from a well bore, but removal of such drill solids from bentonite is difficult when the mud is surfaced. This lack of solids control and the high elasticity of a clay-thickened fluid (Chapters 9 and 11) necessitated the use of straight polymer-thickened aqueous fluids or polymer-modified, aqueous bentonite slurries. In addition to increases in drill solids, the viscosity is sensitive to loss of the continuous phase to the formation. Viscosity is particularly difficult to control in environments with increasing salinity.

Anionic water-soluble polymers do not readily adsorb from aqueous solutions but adsorb in proportion to the solution’s salinity [theoretically

to the 0.5 power of the electrolyte normality (30)]. The adsorption of (carboxymethyl)cellulose (CMC) and poly(acrylic acid) (PAA) on barium sulfate from basic sodium chloride solutions (31) is illustrated in Figure 11. Both polymers are used in montmorillonite drilling fluids to control fluid loss to the reservoir. Although the adsorption behavior of the two polymers on BaSO_4 is compared, their structural differences are not discussed. The carboxylate groups in (carboxymethyl)cellulose, under the commercial process conditions used to prepare the derivatized carbohydrate polymer, have a preference to group on a given pyranosyl repeating unit (discussed in Chapter 1); this grouping tendency does not occur in poly(acrylic acid). The gross adsorption behavior of (carboxymethyl)cellulose and poly(acrylic acid) on BaSO_4 is similar. When adsorbed from basic saline solutions, the polymers are contracted and the number of adsorbed segments decreases ($p = 0.70$) relative to freshwater solutions ($p = \sim 1.0$). Therefore, an increased number of the adsorbed polymer's segments are extended from the substrate surface. This situation should provide stability by both steric and enhanced electrostatic repulsions to a dispersed phase. A parallel study of the adsorption of 29 carbohydrate and synthetic polymers on montmorillonite is described in Chapter 11. Among the polymers studied to elucidate the mechanism of filtration control in saline environments were rigid-rod and hydrophobically modified water-soluble polymers.

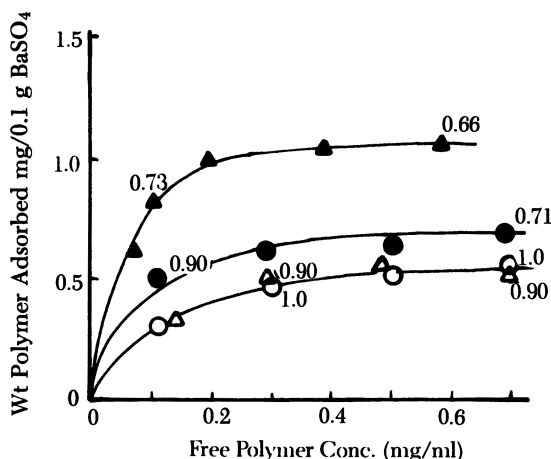


Figure 11. Adsorption isotherm of sodium (carboxymethyl)cellulose (SCMC), $M_v = 1 \times 10^5$, and poly(acrylic acid) (PAA), $M_v = 8 \times 10^4$, onto BaSO_4 at pH 9: Δ , SCMC in H_2O ; \blacktriangle , SCMC in $0.1 \text{ mol dm}^{-3} \text{ NaCl}$; \circ , PAA in H_2O ; and \bullet , PAA in $0.1 \text{ mol}^{-3} \text{ NaCl}$. Numbers correspond to fraction of segments in trains. Reproduced with permission from reference 31. Copyright 1982 Academic.

Volume-restricted flocculation and interparticle bridging, the mechanisms that have been proposed in thickened latex performance, are not viable in explaining the effectiveness of polymers in the filtration control of modified bentonite muds. One of the 29 polymers examined (Chapter 11) was a hydrophobically modified, water-soluble polymer (styrene-maleic acid terpolymer (SMAT); described in Chapter 21). This polymer produced an unusually smooth bentonite slurry but not a slurry effective in maintaining filtration control with increasing salinity. Increasing salinity compresses the electrical double layer surrounding the bentonite particle. Increasing salinity also collapses the conformation of the polyelectrolyte in solution and effects polymer adsorption on the dispersed components. The adsorption of a contracted polyelectrolyte conformation enhances both steric and electrical double-layer repulsions; these repulsions inhibit flocculation and affect filtration control in saline solutions.

In extremely high temperature reservoirs, flocculation and higher viscosities are observed (Chapter 12). Designed, low molecular weight stabilizers are used to inhibit increases in slurry viscosities. Other low molecular weight polymers of this type (e.g., partially sulfonated styrene maleic acid terpolymers) also are used. Both polymers contain sulfonate groups, which are less sensitive to divalent ions than carboxylate groups; generally, sulfonate anions inhibit precipitation of the polymer. Likely, part of the polymer is adsorbed (perhaps in a specific manner related to the molecular design described in Chapter 12) and the sulfonate anion simply inhibits flocculation of the substrate.

Other Applications. With a transition of supplier base and competitiveness in the water treatment area, an open, broad-base coverage of polymers in water-treatment applications is difficult to obtain. Adsorption is important, but its influence is complex because a wide variety of components and possible interactions. A discussion of adsorption related to this area is therefore omitted.

An equally competitive area is the suspension polymerization of commodity monomers vinyl chloride and styrene. Water-soluble polymers are used as suspending agents to complement agitation in inhibiting particle (50–300- μm diameters) flocculation. The ability of the water-soluble polymer to minimize autoclave fouling and decrease the median particle size of the plastic particles produced is related to the water-soluble polymer's interfacial activity and molecular weight. All of the observations to date indicate that the interfacial viscosity of the adsorbed polymer is the parameter of importance in determining application performance. The importance of interfacial viscosities as reflected in coating problems is discussed in Chapter 16.

A recent theoretical treatment (4) predicts the preferential adsorption of low molecular weight polymers [based on previous experiments

from moderately concentrated solutions (32a)]. The preferential adsorption of low molecular weight fractions, when they are present in small amounts in an intentional or accidental production blend, can dramatically increase particle-size distributions and autoclave fouling in the production of commodity plastics. A preferred polymer molecular weight was not delineated (32b) because the interfacial viscosity is dependent on both molecular weight and the amount in the interfacial region. Complementary to the stabilizer in promoting particle stability are the mixing patterns offered by various baffle and impeller designs. The latter approach has prevailed, and dimensional analysis, commonly used in scaling up recipes, was used in predicting (33) particle-size distribution effects. The latter approach is not useful in designing an optimum particle geometry, necessary for ensuring plasticizer acceptance and monomer removal from the particle while maintaining reasonable particle density.

Literature Cited

1. *Polymer Adsorption and Dispersion Stability*; Goddard, E. D.; Vincent, B.; Eds.; ACS Symposium Series 240; American Chemical Society: Washington DC, 1984.
2. Takahashi, A.; Kawaguchi, M. *Adv. Polym. Sci.* **1982**, *46*, 1.
3. Vincent, B.; Whittington, S. In *Surface and Colloid Science*; Matijevic, E., Ed.; Plenum: New York, 1981; Vol. 12.
4. Scheutjens, J. M. H. N.; Fleer, G. J. *J. Chem. Phys.* **1980**, *84*, 178.
5. Vincent, B. *Adv. Colloid Interface Sci.* **1974**, *4*, 193.
6. Fontana, B. J. In *The Chemistry of Biosurfaces*; Hair, M. L., Ed.; Dekker: New York, 1971; Chapter 3.
7. Stromberg, R. R. In *Treatise on Adhesion and Adhesives*; Patrick, R. L., Ed.; Dekker: New York, 1967; Vol. 1.
8. Kashiwagi, Y.; Norisuye, T.; Fujita, H. *Macromolecules* **1981**, *14*, 1220.
9. Roland, F. W.; Eirich, F. J. *Polym. Sci.* **1966**, *A4*, 2401.
10. Donners, W. A. B.; Peeters, L. G. *Macromol. Chem., Suppl.* **1985**, *10/11*, 297.
- 11a. Glass, J. E. In *Polymer Adsorption and Dispersion Stability*; Goddard, E. D.; Vincent, B.; Eds.; ACS Symposium Series 240; American Chemical Society: Washington, DC, 1984; Chapter 7.
- 11b. Thies, C. J. *Phys. Chem.* **1966**, *70*, 3783.
12. Graham, D. E.; Phillips, M. C. J. *Colloid Interface Sci.* **1979**, *70*, 403.
13. Lankveld, J. M. G.; Lyklema, J. J. *Colloid Interface Sci.* **1972**, *41*, 454.
14. Garvey, M. J.; Tadros, Th. F.; Vincent, B. J. *Colloid Interface Sci.* **1974**, *49*, 57.
15. Furusawa, K.; Kimura, Y.; Tagawa, T. In *Polymer Adsorption and Dispersion Stability*; Goddard, E. D.; Vincent, B., Eds.; ACS Symposium Series 240; American Chemical Society: Washington, DC, 1984; Chapter 9.
16. Yeliseyeva, V. I. In *Emulsion Polymerization*; Piirma, I., Ed.; Academic: New York, 1982; Chapter 7.
17. Kronberg, B. J. *Disp. Sci. Technol.* **1981**, *2*(2 and 3), 215.
18. Ahmed, H.; Glass, J. E.; McCarthy, G. J. *Society Petroleum Engin. Publ. No. 10101*, 1981, Richardson, Texas.

19. Rhebinder, P. A. *Z. Phys. Chem.* **1927**, *129*, 161.
20. Bartell, F. E.; Davis, J. K. *J. Phys. Chem.* **1941**, *45*, 1321.
21. Glass, J. E. *J. Polym. Sci.: Part C* **1971**, *34*, 141.
22. Vijayendran, B. R. In *Polymer Colloids II*; Fitch, R. M., Ed.; Plenum: 1980, p 209.
23. Kronberg, B.; Stenius, P. *J. Colloid Interface Sci.* **1986**, *102*(2), 410.
24. Hoy, K. L. *J. Coat. Technol.* **1979**, *51*(651), 27.
25. Sperry, P. R.; Hopfenberg, H. B.; Thomas, N. L. *J. Colloid Interface Sci.* **1981**, *82*(1), 62.
26. Sperry, P. R. *J. Colloid Interface Sci.* **1982**, *87*(2), 375.
27. Sperry, P. R. *J. Colloid Interface Sci.* **1984**, *99*(1), 97.
28. Theng, B. K. G. *Formation and Properties of Clay-Polymer Complexes*; Development in Soil Science 9; Elsevier, 1979.
29. Lu, C-F. Society Petroleum Engin. Publ. No. 14249, 1985, Richardson, Texas.
30. Hesslink, F. Th. *J. Colloid Interface Sci.* **1977**, *60*(3), 448.
31. Robb, I. D.; Cafe, M. C. *J. Colloid Interface Sci.* **1982**, 86.
- 32a. Cohen, M. A.; Schentjens, J. M. H. M.; Fleeer, G. J. *J. Polym. Sci. Phys. Ed.* **1980**, *18*, 559.
- 32b. Glass, J. E.; Fields, J. W. Proceedings National AICHE Meeting, 1983, Houston, Texas.
33. Hopff, H.; Luessi, H.; Hammer, E. *Makromol. Chem.* **1964**, *84*, 274.

RECEIVED for review May 20, 1985. ACCEPTED December 9, 1985.

Viscosity Studies of Hydrophobically Modified (Hydroxyethyl)cellulose

Robert A. Gelman and Howard G. Barth

Hercules, Inc., Research Center, Wilmington, DE 19894

Complete dissolution of hydrophobically modified water-soluble polymers is sometimes difficult owing to intermolecular interactions mediated by the hydrophobic substituent groups. Studies on hydrophobically modified (hydroxyethyl)cellulose demonstrated that the hydrophobic interactions must be completely disrupted by the solvent to obtain meaningful intrinsic viscosity data. A number of solvent systems containing either methanol or surfactants were considered. The results indicate that several systems are appropriate for use with these macromolecules. Constants for the Mark-Houwink equation for hydrophobically modified (hydroxyethyl)cellulose in 0.1% sodium oleate are reported.

THE CONCEPT OF POLYMERIC SURFACTANTS was first considered in the early 1950s (1, 2). Since that time, a substantial body of literature has developed that deals with surface-active or amphiphilic polymers, particularly as related to the concept of steric stabilization (3). Water-insoluble polymer systems have been reported (3) and are of interest in the stabilization of particles in nonaqueous media. Studies (4, 5) of water-soluble polymeric surfactants were made; these surfactants are usually based upon polyelectrolytes. However, few reports of nonionic water-soluble polymers containing hydrophobic groups exist. Landoll (6) reported work on the addition of long-chain alkyl epoxides to cellulose ethers. The addition of low levels of hydrophobic groups to polymers, such as (hydroxyethyl)cellulose (HEC), results in alterations of the material such that the polymers now possess unusual rheological properties (6). Solutions of hydrophobically modified (hydroxyethyl)cellulose (HM-HEC) exhibit non-Newtonian behavior at low shear rates, whereas solutions of HEC are Newtonian under similar conditions. The concept of associative thickeners, molecules that associate in solution and exhibit a vastly different rheology, led to increased industrial interest in this area.

The unique property of HM-HEC is the enhanced solution viscosity, a result of intermolecular hydrophobic interactions among alkyl groups.

0065-2393/86/0213-0101 \$06.00/0
© 1986 American Chemical Society

For example, HM-HEC containing 1.2% (by weight) cetyl groups has a Brookfield viscosity (2% aqueous solution) of 3×10^4 cPs as compared to 3×10^2 cPs for a HEC sample of similar molecular weight and hydroxyethyl molar substitution.

Although the hydrophobic interactions give HM-HEC its unique solution characteristics, these forces make it rather difficult to determine accurate intrinsic viscosities and molecular weight distributions. Furthermore, the solubility of HM-HEC is highly dependent on both the amount and chain length of the alkyl groups. Small increases in either amount or chain length can lead to partially insoluble products.

Brookfield viscosity measurements are extremely valuable for determining the solution properties of HM-HEC for end-use evaluation. These measurements reflect the extent of hydrophobic intermolecular interactions and, to a slight degree, molecular weight. However, when the solution properties of HM-HEC are characterized, information regarding the molecular size of chains is important. These data can be obtained from intrinsic viscosity determinations. Intramolecular interactions may occur at low concentration, which would result in an underestimation of molecular size. Furthermore, poor solubility of HM-HEC will lead to erroneous results. Thus, the objective of our studies was to determine a suitable solvent system for measuring reliable intrinsic viscosities of HM-HEC samples.

Experimental Section

The HM-HEC samples were prepared as previously reported (6). The chain length and level of the linear alkyl hydrophobic group are listed in Tables I-V. Viscosity data were determined with Brookfield and Ubbelohde viscometers at 25 °C. Intrinsic viscosity was measured by a five-point dilution procedure; no shear-rate corrections were made for these data. Solutions were made by first dissolving the polymer in water, usually overnight, and then adding the appropriate solvent to obtain the desired final solvent and polymer concentrations.

Results and Discussion

Viscosity Studies in Aqueous Solutions. The standard method of determining intrinsic viscosities of HEC is to use water (7) or dilute salt solution (8) as the solvent. Table I lists the result of intrinsic viscosity determinations made by using a series of HM-HEC samples in dilute salt solution; these materials were prepared such that the molecular weight of these samples would be similar. The data indicate, however, that a progressive decrease in the intrinsic viscosity occurs with both the amount and chain length of the substituent hydrophobe. Intramolecular association of hydrophobic groups, which tends to force the polymer into a more compact coil, contributes to the lower viscosity. In addition, the solution clarity of these samples in water varies from clear to hazy. The

Table I. Intrinsic Viscosity of HM-HEC Samples Using 0.02 M KH_2PO_4 as the Solvent

Sample	Hydrophobe		$[\eta]^b$
	Type	Amount ^a	
C1 ^c	— ^c	— ^c	9.28
A	C ₈	1.0	8.75
B	C ₈	2.5	8.28
C	C ₈	3.4	4.12
D	C ₁₆	0.5	7.55
E	C ₁₆	0.6	6.24
F	C ₁₆	0.9	3.78
G	C ₁₆	1.1	3.31

^aThe amount is in units of weight percent of alkyl present.

^b $[\eta]$ is the intrinsic viscosity in 0.02 M KH_2PO_4 , pH 5.5, at 25 °C.

^cThe control was unmodified HEC of the same furnish and preparation conditions as the HM-HEC samples.

solubility characteristics of these samples, as expected, appear to have a pronounced effect on intrinsic viscosity results.

In related work, we found that the addition of either alcohol or surfactant to HM-HEC solutions disrupts association between hydrophobic groups. These components, particularly alcohols, are generally used in liquid chromatography to moderate hydrophobic interactions between solute and the stationary phase. At high concentration, alcohol or surfactant molecules compete effectively for hydrophobic sites on the polymer; this action prevents intra- or intermolecular association.

Viscosity Studies Using Methanol. BROOKFIELD VISCOSITIES. The Brookfield viscosity of HM-HEC in aqueous solutions is predominantly a measure of intermolecular interactions. Because of the moderate shear rates involved in these measurements, the rheological properties of HM-HEC solutions also play a role. Intermolecular interactions increase with polymer concentrations, that is, the higher the concentration of hydrophobes or HM-HEC in solution, the greater the probability of hydrophobe-hydrophobe contacts.

To test this hypothesis the Brookfield viscosity of HEC (control), 0.60% (by weight) C₁₈ HM-HEC, and 0.75% C₁₈ HM-HEC, where C₁₈ is the length of the hydrophobic side chain, was measured as a function of polymer concentration. The two HM-HEC samples were prepared from the control; all three samples, therefore, had the same chain length and hydroxyethyl substitution level. The results are shown in Table II. Brookfield viscosities of both HM-HEC samples, as expected, rapidly approached the viscosity of the control as the concentration was decreased. For these samples, polymer concentrations of

Table II. Effect of HM-HEC Concentration on Brookfield Viscosity Using Water as the Solvent

<i>Concn (%)</i>	<i>HEC (Control)</i>	<i>0.6% C₁₈ HM-HEC</i>	<i>0.75% C₁₈ HM-HEC</i>
2.0	9.3	110.0	246.0
1.0	3.4	7.0	7.1
0.50	1.9	2.1	2.2
0.25	1.4	1.4	1.4
0.125	1.2	1.1	1.1

NOTE: The solvent viscosity was 0.9 cP.

<0.5% were sufficiently low to eliminate polymer association. However, the Brookfield viscosities at these concentrations (<0.5%) are close to the solvent viscosity. Thus, measurements are not very accurate at these polymer concentration levels, and the data must be interpreted with caution.

The Brookfield viscosities of the control and the 0.60% C₁₈ HM-HEC sample were determined in 50% methanol-water, and the results are listed in Table III. As indicated, both the control and HM-HEC had similar viscosities over this concentration range. The higher viscosities exhibited by the control and by the HM-HEC sample at <0.5% polymer as compared to values obtained in water (Table II) reflect the better solvating power of the 50% methanol-water solvent.

INTRINSIC VISCOSITY MEASUREMENTS. As discussed, polymer association of HM-HEC could be eliminated by measuring viscosities at low polymer concentration or by the addition of methanol to the solvent. Because of the relative insensitivity of Brookfield viscosity measurements to small changes in concentration and solution properties, intrinsic viscosity is the measurement of choice. Moreover, intrinsic viscosity data can be related to fundamental molecular parameters that are related to the hydrodynamic volume of a polymer chain.

Table III. Effect of HM-HEC Concentration on Brookfield Viscosity Using 1:1 Methanol-Water as the Solvent

<i>Concn (%)</i>	<i>HEC (Control)</i>	<i>0.6% C₁₈ HM-HEC</i>
2.0	17.1	17.3
1.0	6.1	5.9
0.50	3.4	3.3
0.25	2.4	2.4
0.125	2.0	2.0

NOTE: The solvent viscosity was 1.8 cP.

The intrinsic viscosities of the following three test samples were determined as a function of solvent methanol content: HEC (3.60 MS; control), HM-HEC (3.7 MS; 0.9% C₁₆), and HM-HEC (3.8 MS; 1.0% C₈), where MS is the molar substitution of hydroxyethyl groups. These samples were all produced from the same cellulose starting material and had similar molecular weights. The results are given in Table IV, and reduced viscosity curves are shown in Figures 1-3.

The intrinsic viscosity of the HEC control was found to be independent of methanol content and obeys the Huggins equation:

$$\eta_{sp/c} = [\eta] + k'[\eta]^2c \quad (1)$$

where $\eta_{sp/c}$ is the reduced viscosity at concentration c_1 .

Table IV. Intrinsic Viscosity and Huggins Constant of HM-HEC Samples as a Function of Solvent Composition

Methanol (%)	HEC (Control) (3.6 MS)		1.0% C ₈ HM-HEC (3.8 MS)		0.9% C ₁₆ HM-HEC (3.7 MS)	
	$[\eta]$	k'	$[\eta]$	k'	$[\eta]$	k'
0	8.57	0.49	7.50	0.57	3.52	2.2
20	8.63	0.47	7.60	0.55	4.98	2.6
40	8.81	0.47	7.87	0.46	9.76	0.72
50	—	—	—	—	9.96	0.47
60	8.59	0.42	7.95	0.44	9.51	0.46
70	—	—	—	—	9.83	0.46
80	—	—	—	—	10.10	0.38

NOTE: Intrinsic viscosities were determined from Martin's equation. The Huggins constant was calculated from $k' = [(\eta_{sp/c})_1 - [\eta]]/(c_1[\eta]^2)$ where $\eta_{sp/c}$ is the reduced viscosity at concentration c_1 (typically 0.1 g/dL).

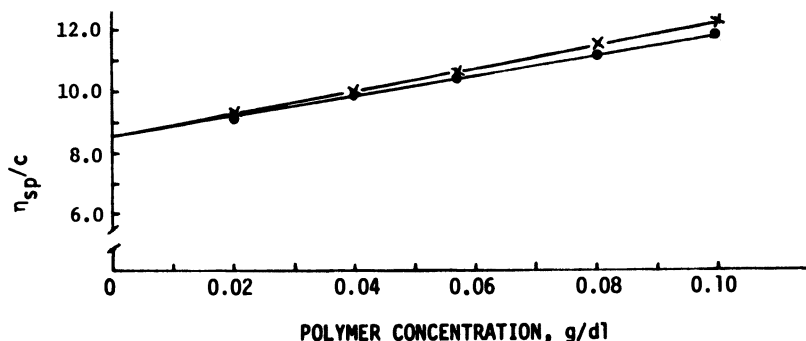


Figure 1. Reduced viscosity as a function of concentration of HEC in water (×) and 60% methanol (●).

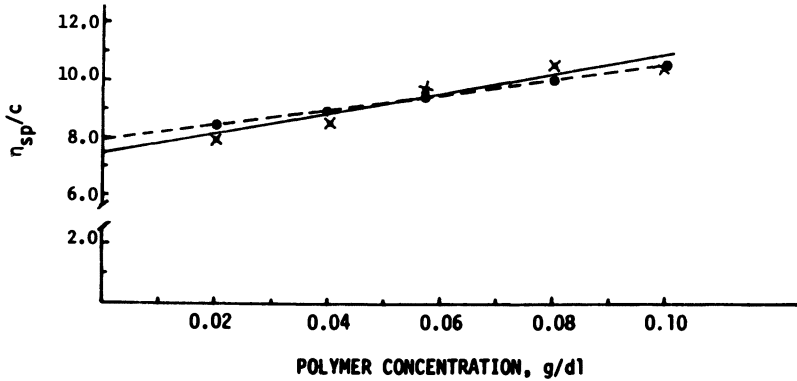


Figure 2. Reduced viscosity as a function of concentration of 1.0% C_8 HM-HEC in water (x) and in 60% methanol (●).

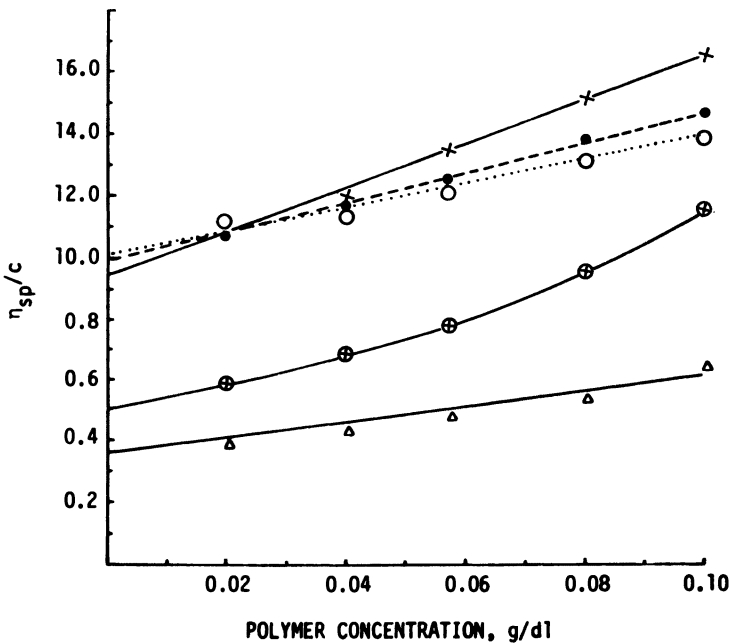


Figure 3. Reduced viscosity as a function of concentration of 0.9% C_{16} HM-HEC in water (Δ) 20% methanol (⊗), 40% methanol (x), 50% methanol (○), and 80% methanol (●).

The Huggins constant, k' , ranged from 0.49 in water to 0.42 in the 60% methanol solvent. Generally, the Huggins constant ranges from about 0.3 for a good solvent to about 0.7 at θ conditions. Larger values are indicative of polymer association (9, 10). These results demonstrate that HEC solvation has increased with increasing methanol content; however, intrinsic viscosities remain at about the same level (Figure 1).

For 1% C_8 HM-HEC, as for HEC, the k' value decreased from 0.57 in water to 0.44 in 60% methanol. A significant increase in intrinsic viscosity was also observed; the data, 7.50 in water to 7.95 in 60% methanol, suggest polymer expansion in the better (methanol-water) solvent (Figure 2). More scatter of data was noted when water was used as the solvent; with the addition of methanol, the scatter was eliminated.

The 0.9% C_{16} HM-HEC sample exhibited rather unusual viscosity behavior (Figure 3). In water and 20% methanol, the Huggins constants are very large, 2.2 and 2.6, respectively. These values imply strong polymer association. On the basis of the low intrinsic viscosities, apparently this material is considered not to be completely soluble. The curvature of the 20% methanol plot signifies that the Huggins equation is not obeyed under these conditions. As the methanol concentration is increased, a corresponding decrease of the Huggins constant from 0.72 for 40% methanol to 0.38 for 80% methanol occurs. The 0.46 value of k' at 60% methanol agrees well with that of the HEC control and 1.0% C_8 HM-HEC. The intrinsic viscosity of the sample appears to reach a constant value of about 40% methanol.

Intrinsic viscosity data as a function of methanol composition are summarized in Figure 4. At methanol concentrations of >40%, constant intrinsic viscosities are obtained. This outcome is a result of complete sample solubility caused by the elimination of hydrophobic intermolecular association. These results are in agreement with the trends observed with k' values. As shown in Figure 5, k' values approach the limiting value of 0.3 for a good solvent. Thus, as the percent of methanol increases, there are less intermolecular hydrophobic interactions and the chains become highly solvated. Intramolecular interactions probably play a role when measuring intrinsic viscosities of HM-HEC using water as the solvent. As shown in Figure 4, the intrinsic viscosity of 1.0% C_8 HM-HEC was slightly smaller in water and the Huggins coefficient was also higher (Figure 5). These effects might have been caused by intramolecular interactions, although these interactions appear to be small.

Viscosity Studies Using Sodium Oleate Solutions. Sodium oleate was chosen as the surfactant for this study. Table V shows intrinsic viscosity and Huggins constant data using 0.05%, 0.10%, and 0.20% sodium oleate solutions. For 0.05% sodium oleate, the Huggins constant is extremely high; this result suggests significant polymer association. This level of surfactant is probably not sufficient to totally disrupt all

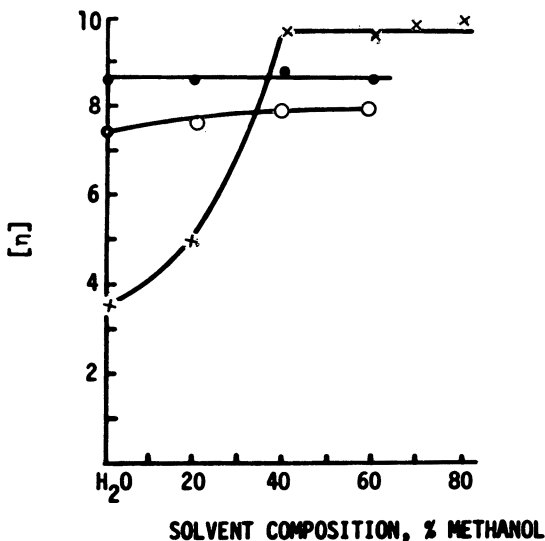


Figure 4. Influence of solvent composition on intrinsic viscosity. Key: ● HEC; ×, 0.9% C₁₆ HM-HEC; and ○, 1.0% C₈ HM-HEC.

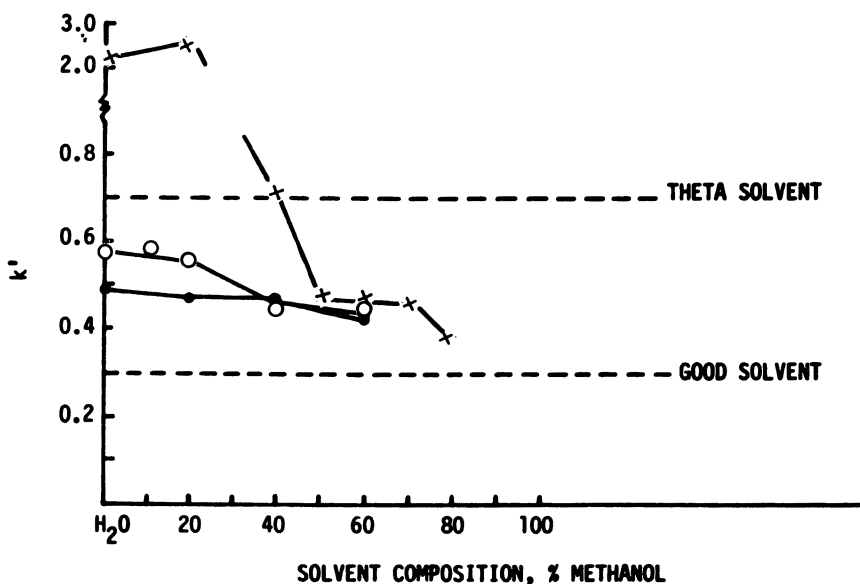


Figure 5. Influence of solvent composition on the Huggins constant (k'). Key: ●, HEC; ×, 0.9% C₁₆ HM-HEC; and ○, 1.0% C₈ HM-HEC. k' is equal to 0.3 for a good solvent and 0.7 for a θ solvent.

Table V. Intrinsic Viscosity of HM-HEC Samples Using Sodium Oleate Solutions

MS ^a	Hydrophobe		0.05% SO ^b		0.10% SO		0.20% SO	
	Type	Amount	[η]	k'	[η]	k'	[η]	k'
3.4	C ₁₆	0.3	7.2	1.6	13.1	0.5	10.1	0.6
3.5	C ₁₆	0.6	5.2	3.0	11.1	0.5	9.2	0.7
3.6	C ₁₆	1.0	7.4	0.9	11.2	0.8	10.3	0.6

^aMS is the molar substitution of hydroxyethyl groups.

^bSO represents sodium oleate.

the intermolecular interactions. At the higher levels of sodium oleate, the Huggins constant decreases to a lower value, which is indicative of negligible intermolecular interactions.

Both sodium oleate and methanol appear to be suitable solvent systems for determining the weight-average degree of polymerization (DP_w) of HM-HEC. Thus, intrinsic viscosities of a series of HEC samples were measured in 0.10% sodium oleate. The DP_w of the HEC samples was previously determined in 0.02 M KH_2PO_4 buffer by using the Mark-Houwink equation (8):

$$[\eta] = (6.7 \times 10^{-3})(DP_w)^{0.92} \quad (2)$$

Figure 6 shows the double logarithmic plot of intrinsic viscosity as a function of DP_w for HEC samples in 0.10% sodium oleate. Least-squares

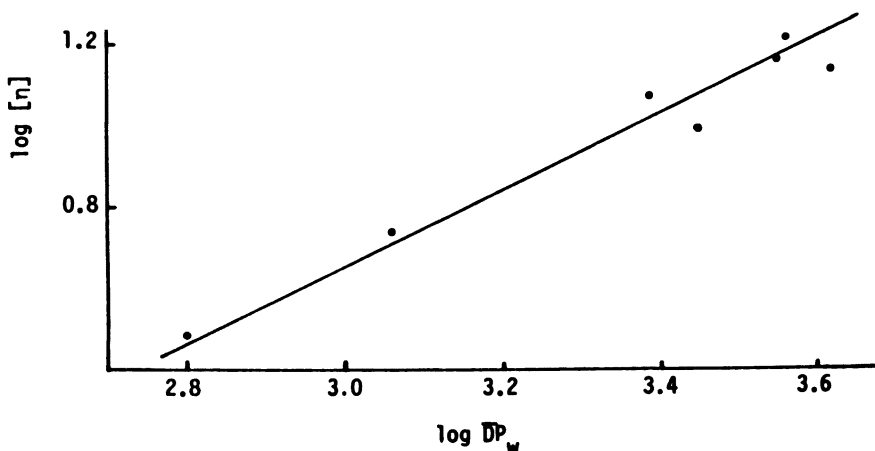


Figure 6. Double-logarithmic plot of intrinsic viscosity as a function of the weight-average degree of polymerization for HEC in 0.10% sodium oleate.

analysis was used to fit the data, and the slope and intercept were the constants for the Mark-Houwink equation:

$$[\eta] = (1.2 \times 10^{-2})(DP_w)^{0.88} \quad (3)$$

This equation was used to determine the DP_w of a number of HM-HEC samples. The values obtained were consistent with those of the control samples.

Conclusions

Intrinsic viscosity measurements of HM-HEC in water can lead to misleading results because of intramolecular association of the polymer and incomplete sample solubility. This effect is a result of hydrophobic interactions of the pendant alkyl groups along the polymer chain. To disrupt this association, we recommend the use of either alcohol or surfactant solution as solvents. In the case of alcohol, studies with methanol indicate that >40% solutions by volume in water were sufficient to essentially eliminate hydrophobic interactions. Sodium oleate gave reliable intrinsic viscosity measurements at concentrations of >0.10% by weight. In view of this, Mark-Houwink constants were established for 0.10% sodium oleate as the solvent to determine the DP_w of HM-HEC samples.

Acknowledgments

We gratefully acknowledge the support and assistance of Albert R. Reid, Richard D. Royce, and Kenneth E. Steller of Hercules, Inc.

Literature Cited

1. Strauss, U. P.; Jackson, E. G. *J. Polym. Sci.* **1951**, *6*, 649.
2. Assony, S. J.; Layton, L. H. *J. Polym. Sci.* **1952**, *9*, 509.
3. Wingrave, J. A. In *Stabilization of Colloidal Dispersions by Polymer Adsorption*; Sato, T.; Rach, R. Eds.; Dekker: New York, 1980.
4. Salamone, J. C.; Israel, S. C.; Taylor, P.; Snider, B. *J. Polym. Sci., Polym. Symp.* **1974**, *45*, 65.
5. White, W. W.; Jung, H. *J. Polym. Sci., Polym. Symp.* **1974**, *45*, 197.
6. Landoll, L. M. *J. Polym. Sci., Polym. Chem. Ed.* **1982**, *20*, 443.
7. Wirick, M. G.; Elliott, J. H. *J. Appl. Polym. Sci.* **1973**, *17*, 2867.
8. Gelman, R. A. *J. Appl. Polym. Sci.* **1982**, *27*, 2957.
9. Moore, W. R. In *Progress in Polymer Science*; Jenkins, A. D., Ed.; Pergamon: Glasgow, 1967; Vol. 1, p 3.
10. Morawetz, H. *Macromolecules in Solution*; 2nd ed.; Wiley: New York, 1975; p 332.

RECEIVED for review September 11, 1984. ACCEPTED August 15, 1985.

Application and Function of Synthetic Polymeric Flocculents in Wastewater Treatment

P. A. Rey and R. G. Varsanik

Calgon Corporation, Pittsburgh, PA 15230

The performance of a polymeric flocculent in wastewater systems is influenced by several factors that can be grouped into the categories of system variables, polymer-related parameters, and operational factors. System variables encompass factors such as particle charge, particle size, and solids composition. Polymer-related parameters include flocculent chemistries and structural characteristics that can affect polymer performance. Operational factors cover the importance of proper sludge conditioning and polymer makeup procedures. The specific advantages and disadvantages of a polymer's physical form are discussed. Municipal wastewater treatment can be broken into several stages. The purpose of each treatment stage and the reason for the polymer application are discussed. Polymers are used to reduce the suspended solids and biological oxygen demand loadings and are especially effective in operations at or near design capacity.

THE APPLICATION OF SYNTHETIC FLOCCULENTS for solid-liquid separations is now widely practiced; economic and environmental restrictions provide the greatest impetus toward acceptance. In the 1970s, Federal stream discharge standards (1) required municipal wastewater plants to improve their suspended solids and biological oxygen demand (BOD) removals. The most economical method of upgrading was by improving the solid-liquid separation processes with chemicals. Polyelectrolytes, in many cases, are used to replace inorganic coagulants such as lime, alum, and FeCl_3 , but occasionally polyelectrolytes are used as a supplement. A wide range of flocculents tailored to satisfy the unique requirements of each plant exists. Although relatively few monomers that are commercially economical exist, present technology can produce flocculents with a wide range of charge densities and molecular weights, which are available in dry, liquid, or emulsion form.

0065-2393/86/0213-0113\$08.75/0
© 1986 American Chemical Society

Currently, flocculation remains more an art than a science and selection of the most cost-effective polymer for a particular application is determined by laboratory evaluations followed by plant trial.

Factors That Influence Polymer Performance

For examination of the performance of a particular polyelectrolyte, the most important variables must be identified. From the large amount of literature (2-7) available on various aspects of flocculation, the key parameters affecting settling and dewatering can be grouped into the categories of system variables, polymer-related parameters, and operational factors.

System Variables. PARTICLE CHARGE. Particle charge has one of the greatest effects on colloidal stability. Under natural conditions, most colloidal solids found in municipal wastewater carry a negative charge. In water, the particle charge is counterbalanced by an ionic atmosphere that develops around the solid, and this property is known as the electrical double layer (8). The charge associated with a particle can be inferred by the measured ζ potential. Colloidal stability can be attributed to the repulsive forces that arise when two similarly charged particles approach and their double layers interact. Dissolved solids, organics such as humic acids or polysaccharides, and pH have a significant effect on this double layer. Figure 1 (9) illustrates the effect of pH and of two common divalent ions on the ζ potential of clay particles. A high concentration of cations or adsorption of oppositely charged polyelectrolytes causes a compression of the electrical double layer and enhances interparticle contact (10-12). Certain ions, such as Ca^{2+} , are also instrumental in promoting adsorption of polymers (13, 14). The nature and magnitude of the particle charge determine the amount and type of flocculent needed to satisfy the charge demand of the solid.

PARTICLE SIZE. Particle size is often recognized as the most important factor influencing settling and dewatering. Fine particles cause turbidity or can blind filter media when not effectively tied up in the solid-liquid separation process (15). Colloidal solids consume more than their fair share of polymer, based on their weight percent of solids concentration. This feature is due to the increased surface area to mass ratio that accompanies the decrease in particle size. Flocculent consumption is directly related to surface area (16-19). In general, this fact is the reason that digested sludge, which has a smaller mean particle size, has a higher polymer demand than undigested sludge.

SOLIDS CONCENTRATION. Polymer consumption is related to the number of particle solids present. A higher solids concentration improves particle interaction and, in general, results in better performance at a lower polymer dosage on a pound per dry ton basis.

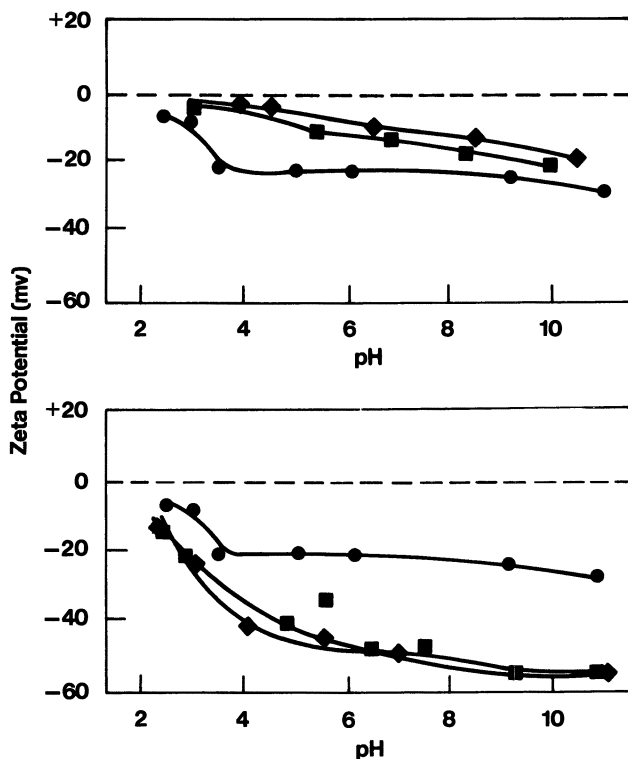


Figure 1. Effect of divalent ions on the surface properties of a clay slurry mixture. Top: Ca^{2+} . Key: ●, none; ■, 150 ppm; and ◆, 400 ppm. Bottom: SO_4^{2-} . Key: ●, none; ■, 1500 ppm; and ◆, 4000 ppm.

COMPOSITION OF SOLIDS. The composition of wastewater will depend on many factors. Contaminants such as proteins, carbohydrates, oils, clays, trace metals, color bodies, and digested matter are common constituents in wastewater. Industrial sources contribute a wide variety of inorganic and synthetic organic compounds to the system. Knowledge of these materials prior to design of the treatment plant can prevent many headaches. For example, copper ions in excess of 100 mg/L are toxic to the biological system in sludge digesters (20). Cyanides and phenols may also be present in industrial wastes. In many cases, pre-treatment at the industrial site is required before the wastes enter the municipal system. Groundwater infiltration and storm sewer runoff can have a pronounced effect on the strength of the sewage. For instance, in a combined sewer system, the strength of the sewage (e.g., BOD and suspended solids) during a storm is generally much lower than normal due to the diluting action of the runoff. Factors such as those mentioned contribute to the uniqueness of the sewage.

Numerous publications (15, 21-23) are available relating sludge characteristics to dewaterability. As a general rule, highly metabolized solids, such as material from the activated sludge process, reduce the dewatering efficiency as illustrated in Figure 2 (24). Most municipal waste treatment plants dewater a blend of primary and waste-activated sludge. Waste-activated sludges generally require treatment with highly charged cationic polymers.

Polymer-Related Parameters. Commercial synthetic polymers are generally defined as either nonionic, cationic, or anionic (*see* Table I). The type of ionogenic group on the polymer is instrumental in determining the effectiveness of a flocculent, which depends on its ability to attach to a particle surface. Adsorption may occur by electrostatic attraction, chemical bonding, hydrogen bonding, hydrophobic association, complex formation, or a number of other means (25-28). The energy of bonding will depend on the magnitude and number of interactions between the charge groups of the polymer and the particle surface. Charged polymers have an extended conformation in solution because of intramolecular repulsion of their functional groups. This extended conformation may be of some advantage for bridging between particles, but electrostatic repulsion may hinder adsorption if the molecule con-

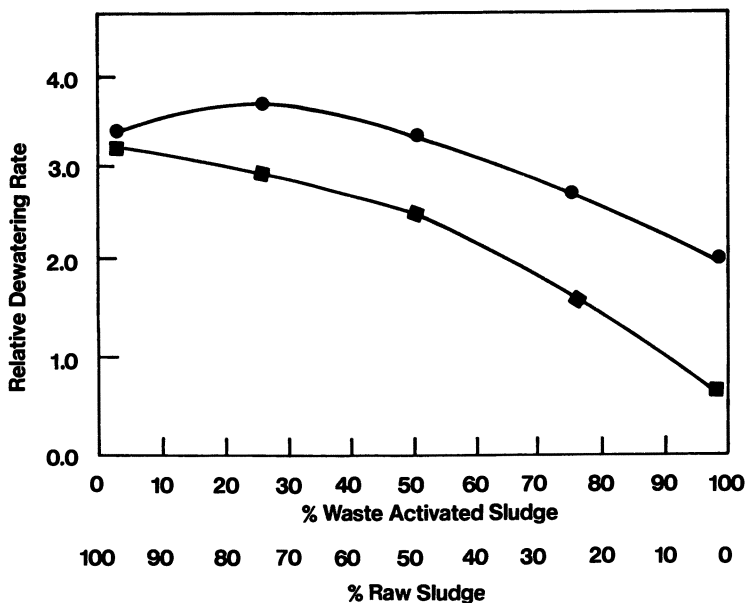


Figure 2. Relationship between dewatering rate and sludge composition [adapted from Morgan *et al.* (24)]. Key: ●, polymer A; and ■, polymer B.

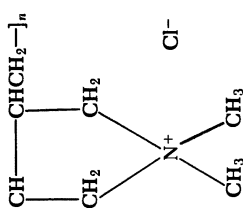
tains too great a number of charge groups similar to those on the solids. Alternately, strong adsorption may cause the polymer to flatten out on the particle surface; the result is very little bridging. Therefore, different flocculent chemistries and structural characteristics can have a significant effect on flocculent performance.

SIGN AND MAGNITUDE OF CHARGE. *Anionic and Nonionic Polymers.* A good many of the synthetic polyelectrolytes used by industry as flocculents are based on poly(acrylamide). Poly(ethylene oxide) has some limited application in the treatment of mining tailings (29). The most common functional group on an anionic polymer is a carboxylate ion ($-\text{COO}^-$). Among polymer flocculents, anionic polymers tend to form the most viscous solutions because of chain extension—the result of intramolecular repulsion of their ionized functional groups. Polymer charges range from nonionic (<3% mol % hydrolysis) to slightly charged (3–10%) to moderately charged (11–25%) to highly charged (26–40%) to very highly charged (+40%). A true nonionic poly(acrylamide) polymer is rare, and a slight charge on some of the polymer molecules is acceptable practice. Differences in structure can exist between carboxylate polymers manufactured by copolymerization and those that are hydrolyzed. The influence of pH on the reactivity of acrylic acid and acrylamide monomer (30, 31) can be expected to affect polymer structure. For hydrolyzed poly(acrylamides), the charge distribution is related to the ionic strength during hydrolysis (32). The uniformity of charge distribution is expected to vary depending on conditions in the reactor during manufacture. For example, nonideal mixing during hydrolysis of a high-viscosity solution polymer would intuitively produce a nonuniform distribution of charged molecules or blocks of charge along the polymer structure. This nonuniform distribution can lead to a difference in performance of polymers with essentially the same building blocks.

Carboxylate polymers are considered a weak polyelectrolyte and are sensitive to pH. As shown in Figure 3, maximum polymer extension occurs at a slightly alkaline pH. The reason is the intramolecular repulsion of the functional groups. The availability of Ca^{2+} ions in the inner electrical double layer of the solids enhances flocculation with hydrolyzed poly(acrylamides) (33). At low pH (e.g., <4), highly charged anionic poly(acrylamide) polymers are relatively ineffective flocculents. At this point, the majority of the carboxyl groups are protonated and are relatively ineffective in adsorbing to the solids. Slightly hydrolyzed and nonionic poly(acrylamides), which have a number of amide groups for hydrogen bonding, are generally selected for these applications.

Cationic Polymers. A variety of cationic polymers exist because of a greater selection in cationic monomers. These polymers are made primarily by incorporating amine and quaternary amine groups into the polymer molecule. The most common cationic homopolymers appear to

Table I. Typical Synthetic Polyelectrolyte Structures Used in Wastewater Treatment

Name	M_r / Monomeric Unit	Structure	Typical Charge Type	M_r Range
Poly(acrylamide)	71	$[-H_2CC(C(=O)NH_2)H-]_n$	nonionic	$(1-15) \times 10^6$
Poly(ethylene oxide)	44	$[-CH_2CH_2O-]$	nonionic	$(1-8) \times 10^6$
Hydrolyzed poly(acrylamide)	—	$[-H_2CC(C(=O)NH_2)HH_2CC(C(=O)O^-M^+)H-]_n$	slightly to highly anionic	$(1-15) \times 10^6$
Poly(DMDAAC)	161.5	$[-H_2CCH-CHCH_2-]_n$ 	very highly cationic	10^4-10^6

Poly(AM-DMDAAC)	—	$\left[-\text{H}_2\text{CCH}-\text{CHCH}_2\text{C}(\text{=O})\text{NH}_2\text{H}- \right]_n$	$10^5-2.5 \times 10^6$	slightly to highly cationic
Polyamine epichlorohydrin quaternary polymer AMPAM	—	$[-\text{N}^+(\text{CH}_3)_2\text{CH}_2\text{C}(\text{OH})\text{HCH}_2-]_n$	10^4-10^6	highly cationic
Poly(AM-MAPTAC)	220.5 ^a	$\left[-\text{H}_2\text{CC}[\text{C}(\text{=O})\text{NH}_2]\text{HH}_2\text{CC}[\text{C}(\text{=O})\text{NH}_2]- \right]_n$ $\left[-\text{H}_2\text{CC}[\text{C}(\text{=O})\text{NHCH}_2\text{N}(\text{CH}_3)_2\text{H}-]_n \right]_n$ $\left[-\text{H}_2\text{CC}(\text{CH}_3)[\text{C}(\text{=O})\text{NH}(\text{CH}_2)_3\text{N}^+(\text{CH}_3)_3\text{Cl}^-]\text{CH}_2\text{C}[\text{C}(\text{=O})\text{NH}_2]\text{H}- \right]_n$	$(1-10) \times 10^6$ $(3-10) \times 10^6$	moderate to highly cationic low to moderately cationic
Poly(AM-METAMS)	283.1 ^b	$[-\text{H}_2\text{CC}(\text{CH}_3)[\text{C}(\text{=O})\text{O}(\text{CH}_2)_2\text{N}^+(\text{CH}_3)_3(\text{CH}_3\text{SO}_4)^-]\text{CH}_2\text{C}[\text{C}(\text{=O})\text{NH}_2]\text{H}-]_n$	$(3-10) \times 10^6$	low to moderately cationic
Poly(AM-METAC)	207.5 ^c	$[-\text{H}_2\text{CC}(\text{CH}_3)[\text{C}(\text{=O})\text{O}(\text{CH}_2)_2\text{N}^+(\text{CH}_3)_3\text{Cl}^-]\text{CH}_2\text{C}[\text{C}(\text{=O})\text{NH}_2]\text{H}-]_n$	$(3-10) \times 10^6$	moderately to highly cationic

^aValue for MAPTAC.^bValue for METAMS.^cValue for METAC.

NOTE: See page 120 for definitions of abbreviated polymer names.

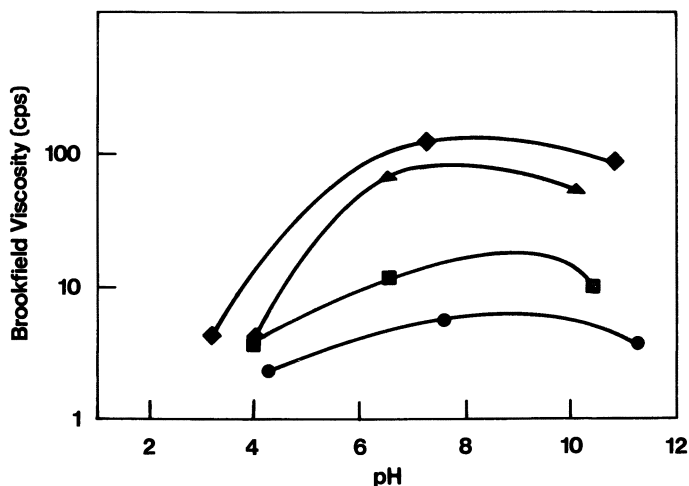


Figure 3. Effect of pH and degree of hydrolysis on 1 g/L of poly(acrylamide) solution viscosity. Key (% HYPAM): \blacklozenge , 35; \blacktriangle , 20; \blacksquare , 5; and \bullet , 0. HYPAM is hydrolyzed high molecular weight poly(acrylamides).

be poly(dimethyldiallylammonium chloride) and condensation polyamines. Unlike polyamines, the charge density of quaternized cationic polymers is not pH dependent. Quaternized polymers are also more resistant to degradation by chlorine (34).

Improvements in molecular weight can be accomplished by copolymerizing cationic monomers with acrylamide but only at the expense of charge density. Aminomethylated poly(acrylamides) (AMPAMS) and aminomethylated cationic copolymers (AM) have been very effective in municipal sludge treatment. Because of the temperature sensitivity of the reversible aminomethylation reaction, these products are available only in liquid form. The following cationic monomers are often used in commercial polymers: dimethyldiallylammonium chloride (DMDAAC), [(methacrylamido)propyl]trimethylammonium chloride (MAPTAC), {[methacryloyl]oxy}ethyl]trimethylammonium methosulfate (METAMS), and {[methacryloyl]oxy}ethyl]trimethylammonium chloride (METAC).

A copolymer product is not composed of identical molecules; rather, a copolymer product is a heterogeneous mixture of polymers whose bulk charge is equivalent to the initial ratio of monomers. For example, a 75:25 DMDAAC-AM copolymer may actually consist of a mixture of DMDAAC homopolymer, acrylamide homopolymer, and slightly charged AM-DMDAAC polymers. Because the reactivity of the monomers has a significant effect on polymer composition, monomer reactivity also will affect flocculent performance. By improved control

over the polymerization process, more homogeneous polymer compositions can be obtained.

Depending upon the desired charge level on the polymer structure, certain monomers are preferred in the manufacture of the trimethyl-amino quaternary derivative of alkyl (acrylic or methacrylic ester)-acrylamide copolymers. As a rule, lower charge density polymers (<20% cationic) were produced with MAPTAC, moderately charged polymers (20–40% cationic) used METAMS, and the higher charge density polymers (>40% cationic) were prepared with METAC. However, raw materials and manufacturing costs are still the principal determinants in selecting the monomer that is most suitable for a given charge range.

Because of the highly competitive nature of the wastewater treatment business, polymer application is determined by the cost-effectiveness of the treatment (35). Polymer manufacturing costs are dependent on the ability to produce or locate a low-cost, high-quality monomer. This problem has been a major obstacle to the application of many synthetic organic polymers. Flock and Rausch (36) and others (37–40) reviewed many of these polymer compositions and their potential application. Hoover (41) compiled a comprehensive literature review on structural types of quaternary polymers.

MOLECULAR WEIGHT AND ASSOCIATED MECHANISMS OF FLOCCULATION. Adsorption of cationic homopolymers occurs primarily through electrostatic attraction (42, 43). Optimum flocculation with this type of polymer is related to the degree of charge neutralization (23, 44). Due to the highly localized charge neutralization upon adsorption, these polymers are generally more effective in promoting agglomeration of particles than simple inorganic electrolytes. Cationic homopolymers can be linear or branched and typically have molecular weights of less than 10^6 . Higher molecular weight homopolymers tend not to be effective on a cost-performance basis. Moderate molecular weight polymers are produced by copolymerizing AM with DMDAAC.

Cationic copolymers have higher molecular weights and also appear to have considerable bridging capabilities, as observed by their much larger floc structure. Typically, AMPAMS, AM-MAPTAC, AM-METAMS and AM-METAC polymers constitute the higher molecular weight cationic polymers. Molecular weights of cationic copolymers generally range from 10^6 to 10^7 . Optimum branching of cationic copolymers is very effective in dewatering of primary and activated sludge (24). Figure 4 illustrates the effect of different levels of branching agent added during polymerization on the filtration rate of a sludge blend using the resultant polymers.

Nonionic and anionic polymers are generally the highest molecular weight polymers available and can attach to solids by hydrogen, hydrophobic, or chemical bonding. Polymer adsorption is generally con-

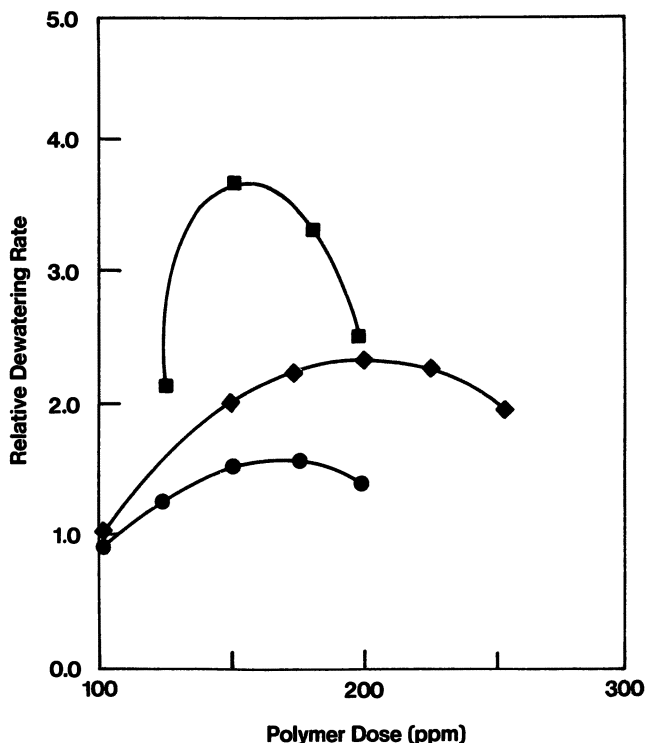


Figure 4. Büchner funnel evaluation of 75:25 DMDAAC-AM copolymers on a 50% raw-50% waste-activated sludge blend [adapted from Morgan *et al.* (24)]. TAMAC is the branching agent, triallylmethylammonium chloride. Key (mol % TAMAC): ●, none; ◆, 0.4; and ■, 0.2.

sidered irreversible because of the multiplicity of bonds on the solid, although any segment of the molecule is a dynamic system that can undergo adsorption and desorption.

Polymer bridging of particles is a primary mechanism for flocculation by high molecular weight polymers (45). This finding implies that linear polymer structures would be the most effective; although, maximum settling rates are obtained with the highest molecular weight polymers (46, 47). In some cases of settling, and particularly in filtration, the most cost-effective polymer may be in the intermediate molecular weight range. In settling, at low polymer dosages, the higher molecular weight polymers may not have enough molecules to effectively flocculate the solids while the intermediate molecular weight polymers will. Once the high molecular weight polymer reaches a threshold dosage, the settling rate increases rapidly, surpassing that of its lower molecular weight counterpart. In filtration, lower molecular weight polymers tend

to have a broad optimum dosage and need less attention from the operator. At dosages above the optimum, rapid dewatering is inhibited by the floc structure. Also, excess polymer may blind the filter media. Unlike cationic polymers, restabilization of particles by overdosing with a nonionic or anionic polymer is highly unlikely. However, the utility of these polymers is mostly limited to primary solids.

Operational Factors. The equipment type and its loading are facts of life for a particular plant and contribute to the uniqueness of the system. To be effective, the polymer must work under these conditions. However, polymeric flocculents are not a cure-all. Polymers work best when equipment is in good operating condition. Proper equipment maintenance has no substitute.

POLYMER APPLICATION. Proper conditioning of the sludge may be the single most important factor for optimum equipment performance. Sludge conditioning is a function of polymer dosage, dilution water, and mixing energy. Certain polymers are known to perform better with significant mixing, while the performance of other polymers is enhanced with less strenuous mixing. However, insufficient conditioning of the sludge can result in unadsorbed polymer and subsequent blinding of the filter media. Figure 5 illustrates lower conditioning energy favoring optimum performance of a medium molecular weight AMPAM, and a high molecular weight AMPAM performing better with additional shear. The medium molecular weight AM-DMDAAC copolymer did not produce a shear-resistant floc with this particular sludge.

The optimum mixing energy required to thoroughly condition a sludge varies with polymer and sludge (48). Proper applications for efficient polymer usage can be summarized as follows: (1) Good flocculation depends on adequate dissipation of polymer throughout the suspension. This dissipation can be accomplished by feeding across the entire process stream at points of local turbulence such as pump intake, pump discharge, and grating across the launder. (2) Flocculation is not strongly affected by the initial concentration of the polymer stock solution as long as sufficient mixing accompanies the polymer addition (49). Generally, where significant mixing exists, increasing the dilution water can be of significant value in improving the polymer transport to the solid. (3) Staged addition of polymer provides improved floc formation by reconditioning any shear-degraded floc. (4) Adsorption of the polymer onto the solid is relatively irreversible and excess shear leads to degradation of the flocs.

A polymer found to be effective under low-shear conditions may not produce good results when subjected to high shear. Testing of flocculents should be performed under optimum mixing conditions to ensure the best evaluation for each polymer. The proper feed system is

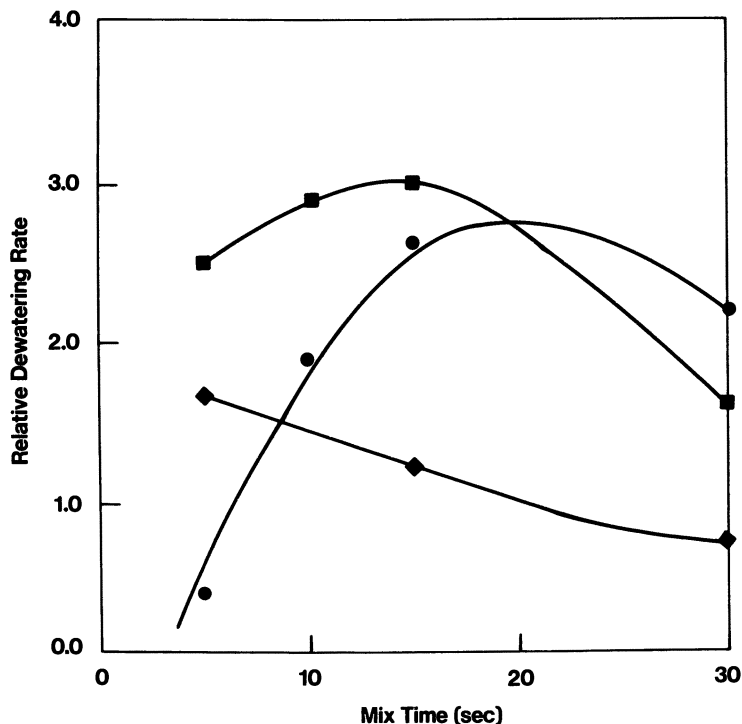


Figure 5. Effect of shear on polymer performance in dewatering of primary sludge. Key: ■, medium molecular weight AMPAM; ●, high molecular weight AMPAM; ◆, 75:25 DMDAAC-AM. Polymer dosage was 5 lb/ton active.

essential to successfully and consistently treat at an effective cost-performance level.

PHYSICAL FORM OF POLYMERS AND THEIR APPLICATION. Polymers are generally supplied in either dry, solution, water-in-oil emulsion, or gel form. Each physical form has its own advantages and disadvantages (see Table II).

Solution Polymers. Liquid polymers are probably the easiest form to apply. Commonly, a water eductor and an in-line static mixer is used to prepare the polymer solution; thus, the need for a mixing tank is eliminated (see Figure 6). Typical products in this form are AMPAM, cationic homo- and copolymers, and low molecular weight hydrolyzed poly(acrylamides). Liquid polymers that contain 10-50% active material are typically lower molecular weight products. Higher molecular weight polymers produce very viscous solutions and, therefore, generally contain less than 10% active product in solution. Cold temperatures increase

Table II. Advantages and Disadvantages of Different Physical Forms of Polymers

<i>Form</i>	<i>Advantages</i>	<i>Disadvantages</i>
Dry	highest active product lower total transportation costs product stability broad product selection	dusting ^a fisheyes ^a on dissolution hygroscopic requires more elaborate feed system longer mixing time (~1 h)
Solution	bulk system easily diluted mix and feed in line homogeneous product several products available only in this form	low percent active short shelf life (<1 year) can freeze viscosity dependent on temperature generally not high M_r can be susceptible to biological attack
Emulsion	bulk system product easily pumped high molecular weight products more highly concentrated than liquids broad product selection automated feed system available	must be inverted before use short shelf life (<6 months) susceptible to freeze-thaw oil may separate with storage; requires mixing prior to use
Gel	higher active product than liquid can be high M_r products no product degradation due to drying available as individual flocs	expensive feed equipment long mixing time (~1 h) equipment can be utilized only for gel makedown

^aFisheyes are gels that have not fully dissolved.

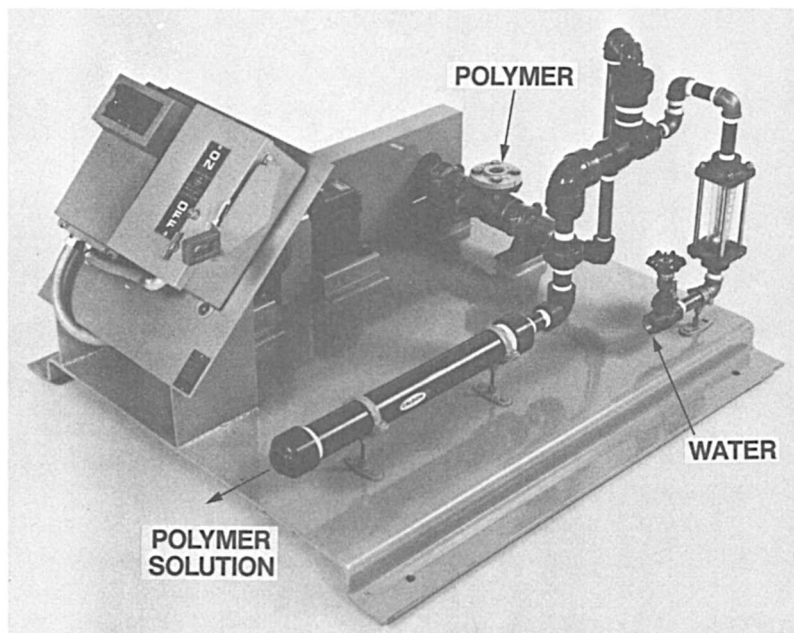


Figure 6. Liquid polymer feed system (courtesy of Calgon Corp.).

the viscosity of solution polymers and may cause some difficulty in handling. However, heat tracing of bulk loads or inside storage minimizes this problem. Some polymers that tend to air oxidize are stored with a nitrogen cap.

Dry Polymers. Dry polymers provide the most active material on an “as product” basis. Dry polymers are available in powder, granular, or bead form. Generally, the finer the particle size, the greater the solubility rate; however, dusting also increases. Polymer vendors offer a variety of automated feed equipment to ensure proper polymer wetting and dissolution (see Figure 7). A hold day tank is often used after the dissolving tank to provide feeding of a consistent solution strength. Feeding of the dry polymer too fast for adequate dispersion is the leading cause of “fisheyes”. Fisheyes are gels of polymer that have not fully dissolved. High-speed mixing (>500 rpm) or excessive mixing times (>1 h) are discouraged because a loss of polymer performance can result. In addition, high levels of dissolved solids and dissolved oxygen can reduce polymer effectiveness. After only 24 h, dilute polymer solutions prepared in deionized water are much more effective than those prepared in hard water. The viscosity of the polymer solution limits the maximum recommended solution strength to 0.5% for anionic polymers and 1.0% for nonionic and cationic polymers. Solutions of dilute polymers should be used within 24 h of preparation to minimize product degradation.

Emulsion Polymers. Self-inverting water-in-oil emulsion polymers containing anywhere between 25% and 60% active product have gained popularity in recent years, especially cationic products that range up to 60% active. High molecular weight anionic and nonionic polymers contain approximately 25–35% active solids. When a proper makedown procedure is followed, a polymer solution can be prepared in less than 30 min. Solution strength is generally limited by solution viscosity; however, as a rule of thumb, a solution of approximately 0.5% active polymer will ensure complete inversion. The rate of inversion of an emulsion is dependent on the polymer type. Nonionic emulsions invert more slowly than the higher charge polymers. Anionic and nonionic emulsions have been successfully prepared down to as low as 0.05% solution on an active polymer basis. The lower limit in single-stage preparation of a dilute emulsion polymer solution is determined by a minimum surfactant level, necessary for proper inversion. Emulsions are most effective when prepared in potable water or soft water. Highly dissolved solids can impair emulsion inversion. The advantages of an emulsion are higher percent active than liquid and faster makedown than the dry product. Often, emulsions are more effective than their dry polymer counterparts on an “active” basis. An automated bulk feed system can be installed to mini-

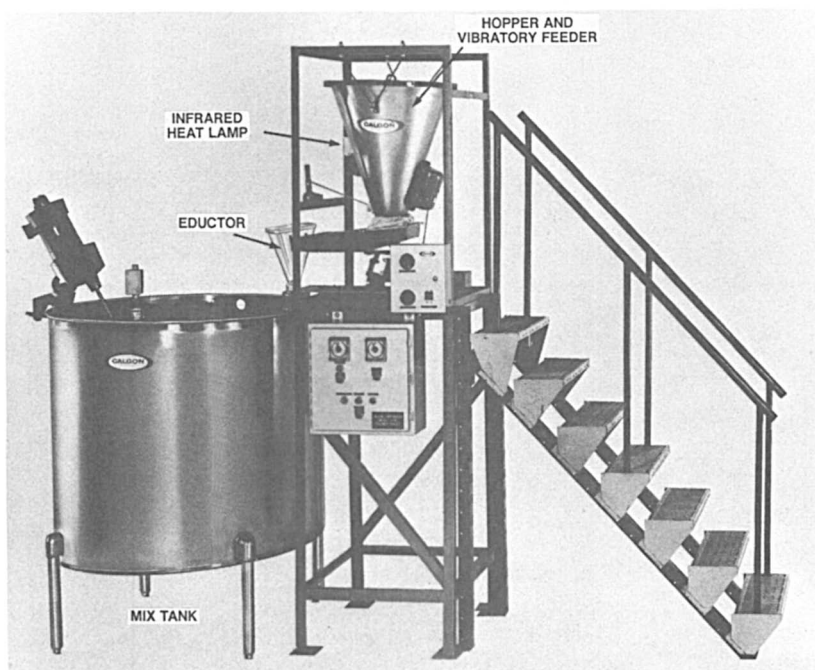


Figure 7. Automatic dry polymer feed system (courtesy of Calgon Corp.).

mize operator supervision. Equipment cleanup is accomplished by running a saturated brine (NaCl) or a dilute bleach solution through the makedown module. Calgon's emulsion makedown system is illustrated in Figure 8.

Gel Polymers. The advantage of a gel product is that a high molecular weight product is provided that, unlike dry polymers, has not undergone any degradation during drying and grinding. Also, gel polymers have found application in areas where no electricity is available. The gel log can be placed in water and allowed to dissolve slowly. Dissolution is related to the water velocity, temperature, and the exposed surface area. Dry polymers can be applied in a similar manner by partially filling a fine mesh bag, such as a nylon stocking, and allowing the polymer to solubilize (50). For other applications, a special unique makedown system is required.

Polymer Applications in Wastewater Treatment

Municipal waste treatment can be broken down into the following stages:

- preliminary
- primary clarification
- secondary treatment
- sludge thickening
- sludge dewatering

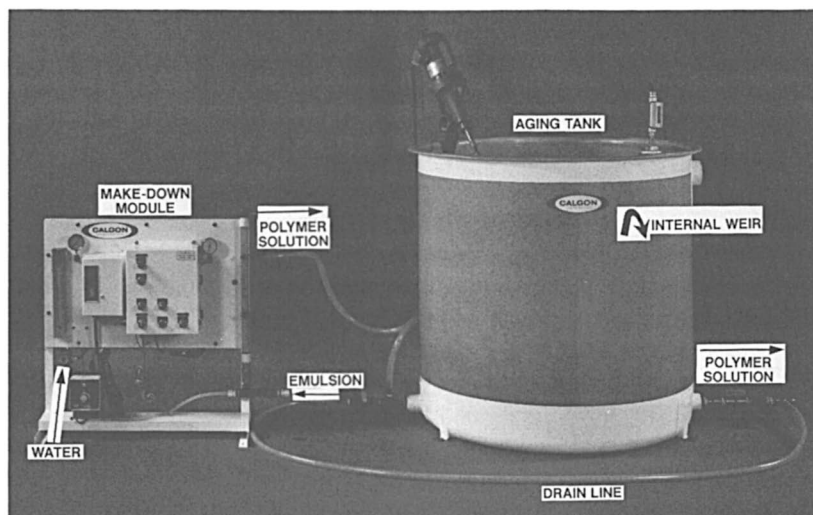


Figure 8. Emulsion feed system (courtesy of Calgon Corp.).

Figure 9 illustrates a flow diagram of a typical sewage treatment plant with secondary treatment. As a rule, higher cationic charge and higher polymer dosage are required with each progressing stage of treatment. Table III provides a general description of various stages of municipal wastewater treatment and the polymer requirements.

Preliminary Treatment. The purpose of preliminary treatment is to remove larger solids, heavy inorganics, abrasive materials, or excess oils and greases that can interfere with further treatment. This removal can be accomplished by use of grit chambers, screens or bar racks, comminutors, aerators, and oil separators. Raw municipal wastewaters typically contain 100–400 mg/L of suspended solids consisting of organic and mineral matter. The most widely used parameter to identify the organic content of wastewater is BOD. BOD is used to estimate the quantity of oxygen needed to biologically stabilize the organic material. Generally, fresh sewage is gray and septic sludges are black in color. Preaeration may be used to improve oxygen levels in septic wastes. Polymers are generally not applied at this stage of municipal wastewater treatment unless to adequately ensure mixing for primary clarification.

Primary Sedimentation–Clarification. The primary stage removes organic and inorganic materials by physical processes and improves suspended solids and BOD removal. This stage removes approximately 30–60% of the suspended solids and 30–40% of the BOD. The resultant sludge averages 2–10% solids, is typically dense and fibrous in nature, and dewateres well. The performance of the primary clarifier affects the extent of secondary treatment and can control overall effluent quality. Polymers are often used in primary sedimentation to increase settling of hydraulically overloaded units. Incorporation of the colloidal-size particles into the floc structure results in significantly higher settling rates; thus, subsequent unit operations are improved. Application of hydrolyzed high molecular weight poly(acrylamides) (HYPAM) is often very effective, while nonionic polymers have found little utility in primary sedimentation. Table IV (36, 51–54) illustrates the effect that anionic polymers have on primary clarification. The coaddition of an inorganic coagulant and polymer is also effective on suspended solids and BOD removal. The five-plant average for removal increased from 45% to 70% for suspended solids and from 38% to 55% for BOD.

In general, conventional primary clarifiers with anionic flocculent additions of <1 mg/L will provide >50% suspended solids removal and >40% BOD removal. Cationic polymers, such as AMPAMS or AM-DMDAAC copolymers, can be used to settle primary solids, although cationic polymers are generally not cost-effective unless a considerable amount of secondary material or digester supernate is recycled.

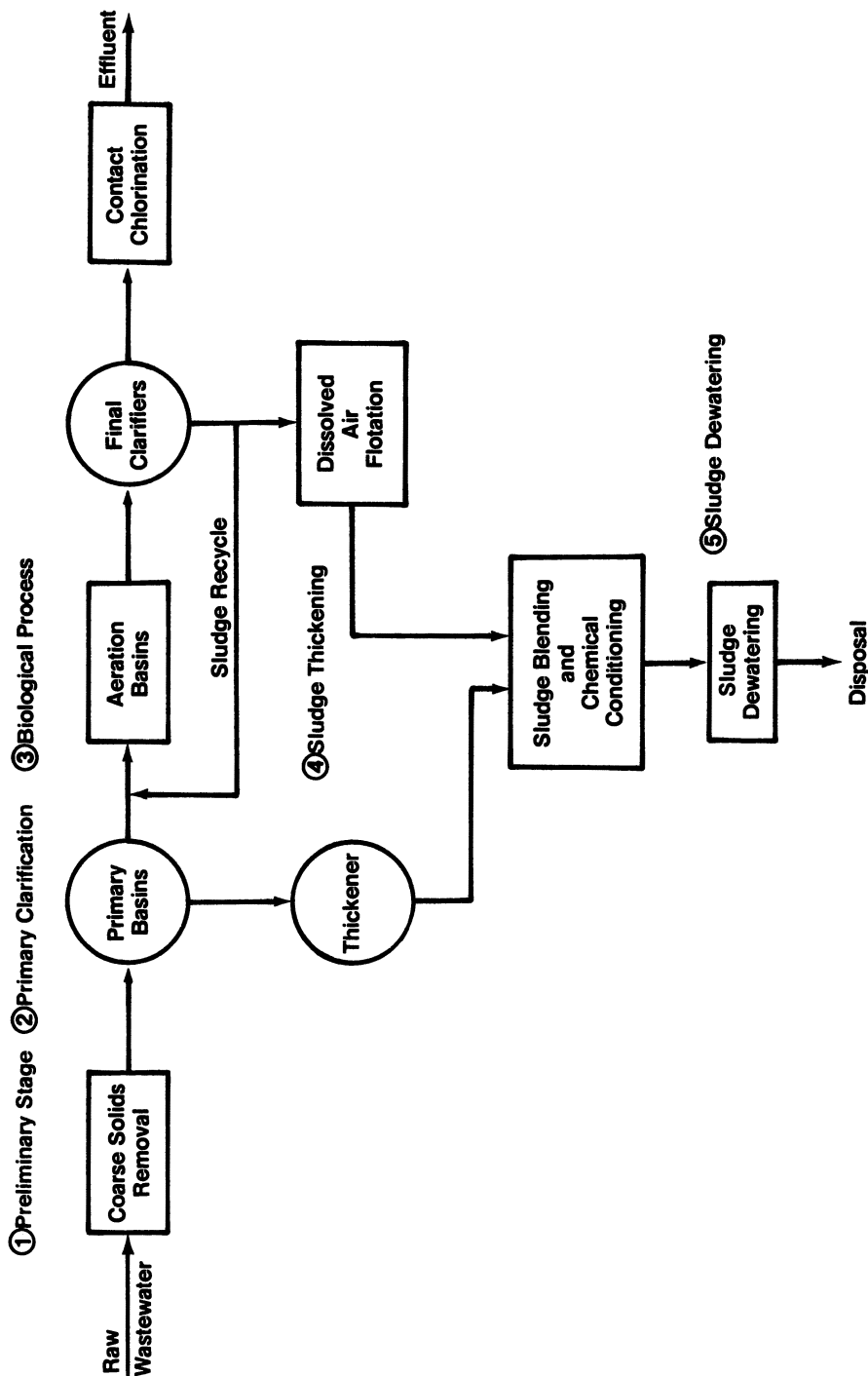


Figure 9. Schematic representation of municipal waste treatment with a secondary sludge process.

Table III. General Application of Polymers in Municipal Wastewater Treatment

Stage	Purpose	Feed Solids	Polymer Character	Dosage Active Polymers	Comments
Preliminary	initial cleanup; removal of large particles; preaeration	125-400 mg/L	none	—	—
Primary	removal of organic and inorganic materials by physical means	100-400 mg/L	moderate to high charge, high M_r HYPAMS used with or without inorganic coagulants; AMPAMS; low to high charge cationic polymers	0.1-3.0 mg/L	cationic polymers are often used when recycle of secondary material
Secondary	further reduction of BOD loading by biological attack	0.1-1.5%	moderate to high charge, moderate to high M_r cationic polymers	0.1-5.0 mg/L	dense enough floc to settle and minimize process upset
Sludge thickening	improvement of dewatering process	0.1-5.0%	high charge, moderate to high M_r cationic polymers	0.1-5.0 lb/ton	—
Sludge dewatering	reduction of moisture content of sludge for disposal	2.0-10.0%	high charge, moderate to high M_r cationic polymers	0.5-15.0 lb/ton	high shear unit operations generally require high M_r cationic polymers

Table IV. Effect of Chemical Treatment on Municipal Primary Sedimentation

Plant	Treatment	Suspended Solids			BOD			Ref
		Influent (mg/L)	Effluent (mg/L)	Removal (%)	Influent (mg/L)	Effluent (mg/L)	Removal (%)	
1	none	111	49	56	117	60	49	51
	74 mg/L of FeCl ₃ + 0.6 mg/L of HYPAM	160	23	86	95	20	79	
2	none	110-280	45-80	56	110-145	42-72	54	52
	150 mg/L of alum + 0.5 mg/L of HYPAM	110-260	14-50	81	116-145	13-29	82	
3	none	—	—	50	—	—	36	53
	1 mg/L of HYPAM	—	—	63	—	—	45	
4	none	201	133	34	147	121	18	36
	0.25 mg/L of HYPAM	172	58	66	158	114	28	
5	none	—	—	31	—	—	31	54
	0.25 mg/L of HYPAM	—	—	51	—	—	46	
5-plant av	none	—	—	45	—	—	38	—
	chemical	—	—	70	—	—	56	—

Secondary Treatment. The purpose of this stage is to further reduce BOD loading through the use of microorganisms metabolizing the organic matter under a controlled environment, which results in a biomass for settling. The unit processes that are most often identified with the stage are

- trickling filters,
- activated sludge process, and
- aerobic and anaerobic digestion.

As the mean cell residence time of the process increases, the surface charge on the organic matter decreases. At the same time, biopolymers are produced by the microorganisms that promote settling (55, 56). The majority of BOD discharge from activated sludge, biological activated sludge, or biological treatment plants is associated with the suspended solids. Cationic polymers of the DMDAAC or AM-DMDAAC class are often applied for final clarification to reduce the suspended solids and, therefore, BOD levels in the effluent. In particular, polymers offset sludge bulking, hindrance of settling caused by cold weather, and minimize operational upset. Goodman and Mikkelsen (57) added a cationic polymer to the aeration tank to improve suspended solids capture in the final clarifiers. Figure 10 shows that the application of 1 mg/L of polymer enabled the reduction of suspended solids in the effluent to <20 mg/L, as compared to 700 mg/L without polymer treatment. Cationic polymers react with the anionic biofloc to neutralize

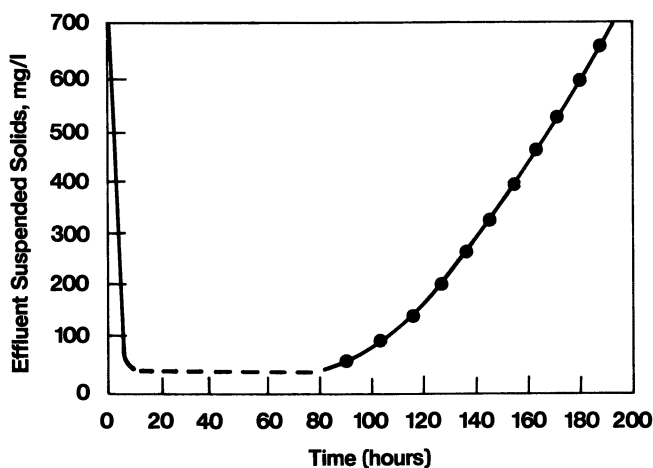


Figure 10. Effect of a cationic polyelectrolyte on secondary sedimentation basin performance. Key: —, 5 mg/L of polymer; ---, 1 mg/L of polymer; and ●, no polymer. Reproduced with permission from reference 57. Copyright 1970 McGraw-Hill.

and bridge the sludge particles. The operating polymer dosage is lower than the initial treatment because of the recirculating nature of the process. Polymers are normally fed across the overflow weir of the aeration basin or the trickling filter effluent. When inorganic coagulants are used, they are generally applied to the activated sludge aeration basin or the trickling filter effluent ahead of the polymer. Polymer requirements increase as the ratio of biological solids increase. Prior to discharge, the wastewater effluent is disinfected, usually by chlorination.

TRICKLING FILTERS. Trickling filters are classified as high rate or low rate, depending on the hydraulic and organic loading. A tank filled with permeable media provides a large surface area under aerobic conditions for biological growth. Trickling filters convert approximately 60-80% of the process BOD into biological slimes. Primary sludge is usually blended to the high-density, low-volume humus for improved dewatering.

ACTIVATED SLUDGE PROCESS. The activated sludge process exists in many versions. In general, this process consists of mixing a portion of the aerated sludge to seed the influent stream of the aeration tank. This procedure increases the amount of microbes for improved oxidation of the organics. The activated sludge process further reduces approximately 70-90% of the BOD in the remaining raw wastewater. Waste-activated sludge tends to have a fragile floc structure.

SLUDGE DIGESTION. Digestion is a means of sludge stabilization that kills noxious organisms while reducing the volume and mass of the sludge prior to dewatering. The biological treatment can be classified by the oxygen dependence of the microorganisms involved.

Aerobic Digestion. Aerobic digestion is an extension of the activated waste process. Continual aeration of the waste sludge encourages endogenous respiration (self-cannibalism) of the biomass; a largely biologically stable end product results (58). The main disadvantage of aerobic digestion is the high energy cost to supply oxygen to the system.

Anaerobic Digestion. Anaerobic digestion is carried out in a closed, heated environment in the absence of oxygen. An inert sludge of fine particle size is produced, particularly in the early stages of digestion (59). The supernate from this process is generally very high in nutrients and organic material. A valuable byproduct of this process is methane. Anaerobic treatment of sludge is slower than the aerobic process and reacts slower to environmental changes.

Sludge Thickening. Prior to final dewatering, the sludge may be further thickened to improve the efficiency of the final process. Often, sludge thickening will result in reduced chemical costs in the dewatering stage. Gravity thickening and dissolved air flotation are the most common unit processes.

GRAVITY THICKENING. A conventional gravity thickener allows solids to settle under the influence of gravity; a high-solids underflow is produced. Typically, a thickener is designed for a surface loading rate of 400–900 gallons per day (gpd)/ft² and can produce a sludge of 5–6% solids. A well-run thickener can achieve 50% reduction in sludge volume with approximately 95% solids recovery. The sludge is continuously stirred to promote channels for water and gases to escape during densification. Polymers are generally applied to gravity thickeners for the following purposes: (1) to increase the hydraulic or solids loading of the unit, (2) to achieve higher density sludge blankets, and (3) to improve the solids capture in the thickener and reduce the recycle load on the plant. Typically, cationic polymer treatment will be about 6–60 lb/dry ton of solids for liquid polymers and 0.5–5.0 lb/dry ton of solids for dry polymers.

DISSOLVED AIR FLOTATION (DAF). DAF, a process used to thicken sludge, can produce a floated sludge of over 5% solids. This process is used primarily with waste-activated sludges and is particularly suited to wastewater containing oil or grease. Performance is heavily influenced by the solids loading. In general, the higher the solids loading, the lower the concentration of thickened sludge and the poorer the solids recovery. Figure 11 (60) illustrates that polymer is very effective in improving the solids recovery of a floated sludge, especially under higher solids loading. Cationic polymers are usually added to the discharge side of the pressurized water just prior to flotation; therefore, good agitation is ensured. Unlike coagulants, polymer addition prior to pressurization reduces the effectiveness of the treatment. A wide range of polymer products has been observed to be effective in the DAF process. AMPAMS or AM-DMDAAC polymers are used primarily on activated sludge, while hydrolyzed poly(acrylamides) are sometimes applied in the thickening of raw sludge.

Sludge Dewatering. Sludge dewatering is the final solid–liquid step before disposal and generally accounts for a large percentage of the total chemical requirement of a plant. Lime, ferric chloride, and polymers are the most common chemicals used at this stage. Chemical dosages can be expected to fall within the following ranges (sludge, pounds of polymer per dry ton of dry solids, pounds of lime per ton of dry solids, and pounds of ferric chloride per ton of dry solids), (61): raw primary and waste activated, 15–20, 110–300, and 40–50; and digested primary and waste activated, 30–40, 160–370, and 80–200, respectively.

The polymer cost to treat blends of sludges can be expected to range from \$2–10/dry ton for primary solids to \$4–30/dry ton for raw plus secondary sludges. Polymer consumption will increase with the percentage of biological solids present.

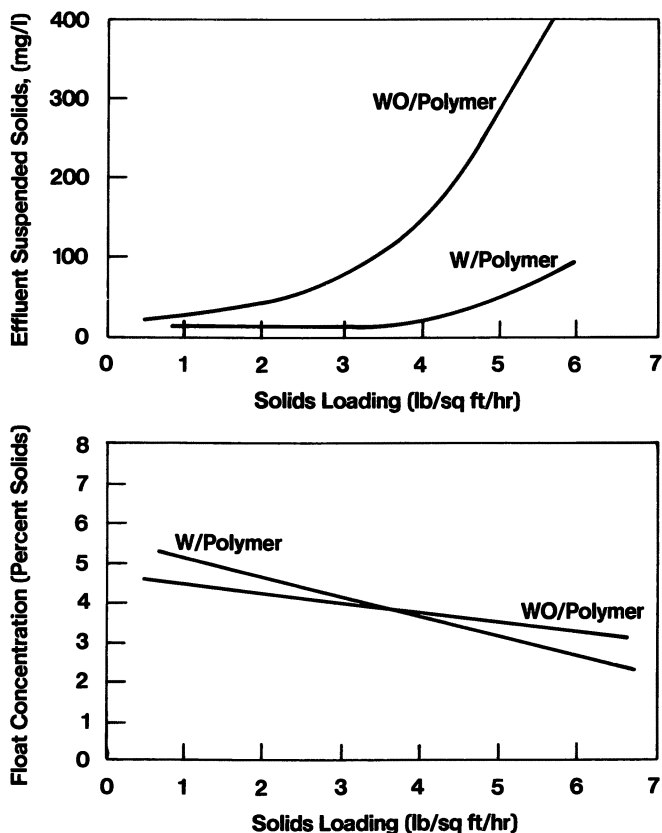


Figure 11. Effect of polymer on float concentration and effluent suspended solids as a function of solids loading [adapted from Noland et al. (60)].

The following unit processes are most widely associated with sludge dewatering:

- vacuum filtration
- centrifugation
- belt-press filtration
- pressurized filtration

Polyelectrolytes have probably had the most profound effect on sludge dewatering of any solid-liquid separation process. Vacuum filters, which were commonly installed up to the mid-1970s, have generally lost favor to belt presses and solid bowl centrifuges. The advent of high molecular weight, high charge density, cationic polymers, which form shear-resistant flocs, can account for much of the shift in emphasis on these mechanical devices.

VACUUM FILTRATION. In vacuum filtration, polymer addition is very important in the formation of a porous filter cake. Porosity of the cake is critical for maximum cake pickup during the cake formation cycle and also provides good air flow through the cake in the dry cycle. As long as cracking of the cake is not severe, residual moisture will tend to migrate with air flow. Feed solids to vacuum filters range between 2.0% and 10.0% solids and result in yields of 2–10 lb/ft⁻² h⁻¹. With polymer treatment, 99% solids recovery can be obtained; therefore, solids recycling is minimized.

Sometimes polymers are used in conjunction with lime or ferric chloride. Typical chemical dosages in vacuum filtration are 4–10 lb/ton for the polymer and 150–300 lb/ton of lime or 50–125 lb/ton of ferric chloride. Generally, application of a polymer will reduce the usage rates of the inorganic coagulant and minimize sludge formation. When a plant is converted from inorganic coagulants to polymers, the filter media must be evaluated. Often the differences in floc characteristics of a flocculated sludge require a different weave to minimize floc penetration into the fabric. Filter operations are generally evaluated on production, solids capture, and cake moisture.

CENTRIFUGES (BASKETS, DISK, AND CONCURRENT SCROLL). Several types of centrifuges are available, but in general, production is influenced by the feed rate and solids loading. Typically, in a continuous-flow centrifuge, sludge is fed axially where high-rate sedimentation takes place because of centrifugal forces. Higher centrifugal acceleration can improve cake dryness, although excessive shear can break apart the floc structure. Proper application of a flocculent is essential to form a coherent, shear-resistant floc. The polymer is primarily used to enhance solids capture. Typically, a high molecular weight cationic polymer such as AMPAMS or AM-METAC copolymers is dictated. Polymer dosage can be expected to range between 1 and 20 lb/ton but, most likely, is 4–10 lb/ton. Polymer performance is generally defined by the cost to meet specifications for cake solids and clarity at a constant production rate.

BELT PRESS. Belt presses are simple and relatively easy to maintain. With polymer treatment, belt presses can be used to dewater problematic secondary biological and petrochemical sludges. Low-solids influent is the bane of dewatering processes such as belt presses. Sludges are first flocculated to a cottage cheese consistency and then dewatered in a gravity drainage section to a nonfluid consistency, followed by incrementally increased pressure dewatering applied by converging belts. Large, shear-stable flocs are essential for proper operation. Cationic polymers such as AMPAMS and AM-METAMS or METAC copolymers are very effective in this application. Occasionally, AM-DMDAAC copolymers or high molecular weight hydrolyzed poly(acryl-

Table V. Polymer Application in Wastewater Treatment

<i>Stage of Treatment</i>	<i>Application</i>	<i>Property</i>	<i>Polymer Type</i>	<i>Charge</i>	<i>M_r</i>
Primary	clarification	evaluate for settling and turbidity	HYPAM HYPAM + inorganic AM-DMDAAC	moderately to very highly anionic	very high
Final	clarification	improved suspended solids removal	DMDAAC AM-DMDAAC	low to highly cationic low to highly cationic	low to medium low to medium low to medium
Biological process	decantation aerobic digester	reduced sludge volume	AMPAM DMDAAC AM-DMDAAC	highly cationic very highly cationic highly cationic	medium to high low to medium medium
Biological process	anaerobic digester	reduced sludge volume	AMPAM AM-DMDAAC AMPAM DMDAAC AM-METAMS	highly cationic highly cationic highly cationic very highly cationic moderately to highly cationic	high medium medium to high low to medium high
Sludge thickening	thickener	produced secondary sludge	AM-DMDAAC; AM-METAMS AMPAM	cationic high moderately cationic	medium high

Sludge thickening	DAF	increased rise rate of waste-activated sludge; improved supernatant clarity	AMPAM ^a AM-DMDAAC	highly cationic moderately to highly cationic	medium to high medium
Dewatering	vacuum filter	produced large floc	DMDAAC AM-METAMS AMPAM; AM-METAMS; AM-METAC	very highly cationic low to moderately cationic moderately to highly cationic	low to medium high medium to high low to high
Dewatering	belt press	produced medium floc	AM-DMDAAC; AMPAM	moderately to highly cationic	low to medium high
Dewatering	centrifuge	produced cottage cheese floc, shear resistant	DMDAAC ^b AM-METAC AM-METAMS AMPAM	very high highly cationic highly cationic highly cationic	low to medium high medium medium high
Dewatering	centrifuge	produced large floc, shear resistant produced medium floc, shear resistant	AM-DMDAAC AMPAM; AM-METAC quaternary AMPAM; AM-METAMS	medium to highly cationic highly cationic moderately cationic	medium high high

^aThis polymer possibly has the best cost performance.

^bPrecondition.

amides) are cost-effective. Typical polymer dosages range from 4 to 20 lb/ton. Figure 12 illustrates the effectiveness of several polymer compositions in laboratory tests for gravity drainage of a primary-secondary sludge blend.

PRESSURE FILTERS AND FILTER PRESSES. Pressurized filtration is used primarily on industrial sludges because of high capital costs and labor intensiveness. High pressures tend to cause blinding of the filter media, and periodic washings are required. Previously, flocs developed with polyelectrolytes were considered too sensitive for pressures encountered during the filter cycle. However, inorganic coagulants, as well as polymers, are used successfully in this application. Cationic polymers such as AMPAMS, AM-DMDAAC, AM-METAC, or AM-METAMS copolymers are used in filter-press applications.

Summary

A summary of polymer application in municipal wastewater treatment is given in Table V. As a rule, higher cationic charge and higher polymer dosage are required with each stage of treatment. Polymeric flocculents are used to improve suspended solids and BOD removal and are particularly effective in improving the hydraulic capacity of the unit processes. Polymers have had the greatest impact on sludge dewatering. A major trend toward belt presses and centrifuges has occurred with the advent

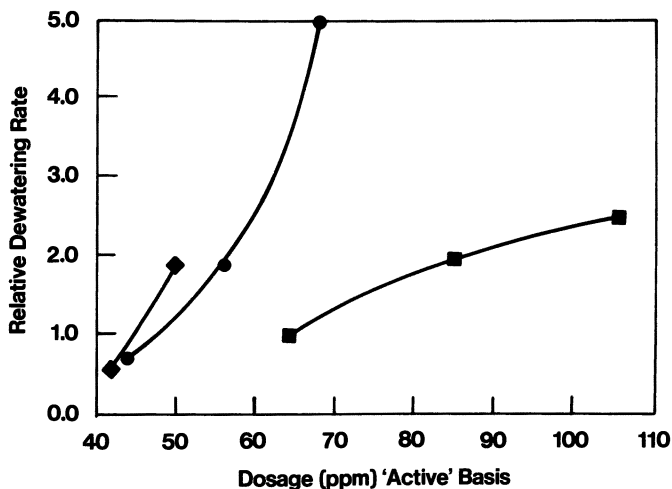


Figure 12. Effect of polymer composition on dewatering rate of a primary-secondary sludge blend. Key: \blacklozenge , high charge, high molecular weight AM-METAC; \bullet , moderate-charge, high molecular weight AMPAM; and \blacksquare , high-charge, moderate molecular weight AM-DMDAAC.

of high molecular weight, highly charged, cationic copolymers that produce strong shear-resistant flocs.

New developments in the area of polymer technology and improved application of these polymers led to more effective treatments. Because of the wide variety in active ingredients and, therefore, pricing on various polymer products, a comparison should always be made on a cost per dry ton of solids basis as opposed to pounds per dry ton of solids. Consideration should also be given to equipment costs required to store and feed the product. Research continues toward development of polymers with improved cost-effectiveness and functional effectiveness. Cationic polymers will still enjoy special attention in sludge dewatering. Currently, research is focused on emulsion technology and structure-performance relationships.

Literature Cited

1. Federal Water Pollution Control Act, *Public Law 92-500*, 816, October 18, 1972.
2. Kitchener, J. A. *Br. Polym. J.* **1972**, *4*, 217.
3. Audsley, A. *Mineral Processing Note No. 5*, Warren Spring Laboratory: Herts, 1965.
4. Omelia, C. R. In *Physicochemical Processes for Water Quality Control*; Weber, J., Jr., Ed; Wiley-Interscience: New York, 1972.
5. Birkner, F. *J. Am. Water Works Assoc.* **1971**, *73*, 99.
6. *Polyelectrolytes for Water and Wastewater Treatment*; Schowyer, W. L. K., Ed.; CRC: Boca Raton, FL, 1981.
7. *Coagulation and Flocculation*, Bratby, J., Ed.; Uplands: Croyden, England, 1980.
8. Adamson, A. W. In *Physical Chemistry of Surfaces*; Adamson, A. W., Ed.; Interscience: New York, 1967; Chapter 4.
9. Rey, P. M.S. Thesis, The Pennsylvania State University, Pennsylvania, 1981.
10. Bleier, A.; Goddard, E. D. *Colloids and Surfaces* **1980**, *1*, 407.
11. Dixon, J. K.; Zietyk, M. W. *Environ. Sci. Technol.* **1969**, *3*, 551.
12. Black, A. P.; Birkner, F. B.; Morgan, J. J. *J. Colloid Interface Sci.* **1966**, *61*, 209.
13. Eriksson, L.; Axberg, C. *Water Res.* **1981**, *15*, 421.
14. Van Lierde, A. *Int. J. Miner. Process.* **1980**, *7*, 235.
15. Karr, P. E.; Keinath, T. M. *J. Water Pollut. Control Fed.* **1978**, *50*, 8.
16. Langelier, W. F.; Ludwig, H. F.; Ash, A. M.; Ludwig, R. G. *Am. Soc. Civil Eng. Proc.* **1952**, *78*, 147.
17. Kane, J. C.; LaMer, V. K.; Lindford, H. B. *J. Phys. Chem.* **1964**, *68*, 3539.
18. Black, A. P.; Vilaret, M. R. *J. Am. Water Works Assoc.* **1969**, *61*, 209.
19. Iler, R. K. *J. Colloid Interface Sci.* **1971**, *37*, 364.
20. *Industrial Water Pollution Control*; Eckenfelder, W. W., Jr., Ed.; New York, 1966.
21. Parker, D. S.; Kaufmann, W. J.; Jenkins, D. *J. Water Pollut. Control Fed.* **1971**, *43*, 9.
22. Randall, C. W.; Turpin, J. K.; King, P. H. *J. Water Pollut. Control Fed.* **1971**, *43*, 1.

23. Novak, J. T.; Becker, H.; Zurow, A. *J. Environ. Eng. Div. Am. Soc. Civ. Eng.* **1977**, *103*, EE5.
24. Morgan, J. E.; Yorke, M. A.; Boothe, J. E. In *Ions in Polymers*; Eisenberg, A., Ed.; Advances in Chemistry Series 187; American Chemical Society: Washington, DC, 1980, p 13.
25. Linke, W. F.; Booth, R. B.; *Trans. Am. Inst. Min. Metal. Pet. Eng.* **1959**, *217*, 364.
26. Sommerauer, A.; Sussman, L.; Stumm, W. *Koll. Polymer* **1968**, *46*, 485.
27. *Physical Chemistry of Surfaces*; Adamson, A. W., Ed.; Interscience: New York, 1967; Chapter 6.
28. Gregory, J. In *Chemistry and Technology of Water-Soluble Polymers*; Finch, C. A., Ed.; Plenum: New York, NY, 1983, p 307.
29. Smelly, A. G.; Feld, I. L. "RI 8349"; *U.S. Bur. Mines*, 1979.
30. Young, L. J. In *Polymer Handbook*; Brandrup, J.; Immergut, E. H., Eds.; Wiley & Sons: New York, 1975; p II-105.
31. Cabanes, W. R.; Lin, T. Y. C.; Parkanyi, I. C. *J. Polym. Sci.* **1971**, *9*, 2155.
32. Halverson, F.; Lancaster, J. E.; O'Connor, M. N. *Macromolecules* **1985**, *18*, 1139.
33. Black, A. P.; Birkner, F. B.; Morgan, J. J. *J. Am. Water Works Assoc.* **1965**, *57*, 1547.
34. Mangravite, F. J. In *Proc. of AWWA Seminar, Use of Organic Polyelectrolytes in Water Treatment*; Am. Water Works Assoc.: Denver, 1983.
35. Varsanik, R. G. *Proc. of ACS, Div. of Colloid and Surface Chemistry*, 1984.
36. Flock, H. G.; Rausch, E. G. In *Water-Soluble Polymers: Proc. ACS, Polymer Science and Technology*; Bikales, N. M., Ed.; Plenum: New York, 1973.
37. Halverson, F.; Panzer, H. P. In *Encyclopedia of Polymer Science and Technology*; Bikales, N. M., Ed.; Interscience: New York, 1980, Vol. 10.
38. Collie, M. J. In *Industrial Water Treatment Chemicals & Processes—Developments Since 1978*; Noyes Data Corp.: Park Ridge, NJ, 1983.
39. Gutcho, S. In *Waste Treatment with Polyelectrolytes and Other Flocculents*; Noyes Data Corp.: Park Ridge, NJ, 1977.
40. Molyneux, P. In *Chemistry and Technology of Water-Soluble Polymers*; Finch, C. A., Ed.; Plenum: Boca Raton, FL, 1983.
41. Hoover, M. F. *J. Macromol. Sci.* **1970**, A4.
42. Gregory, J. *J. Colloid Interface Sci.* **1973**, *42*, 448.
43. Edzwald, J. K.; Lawler, D. F. In *Proc. of AWWA Seminar, Use of Organic Polyelectrolytes in Water Treatment*; 1983, pp 17.
44. Tiranti, G.; Lore, F.; Sornante, G. *Water Res.* **1985**, *19*, 93.
45. Reuhewein, R. A.; Ward, D. W. *Soil Sci.* **1952**, *73*, 485.
46. Wilde, P. F.; Dexter, R. W. *Br. Polymer J.* **1972**, *4*, 239.
47. Walles, W. E. *Colloid and Interface Sci. J.* **1968**, *27*, 797.
48. Baskerville, R. C.; Bruce, A.; Day, M. *Filt. Sep.* **1978**, *15*, 445.
49. Keys, R. O.; Hogg, R. Presented at 71st Annual Meeting AIChE, Miami Beach, Nov. 16, 1978.
50. Private Communication with C. W. Fetrow, Calgon Corp.
51. Bernardin, Jr., F.; Kusnisak, R. Presented at 46th Annual Conf. of Water Poll. Control Fed., October 2, 1973.
52. LoSasso, R. A. *Water and Wastes Eng. J.* **1973**, *10*, 45.
53. Freese, P. V.; Hicks, E.; Bishop, D. F.; Griggs, S. H. Federal Water Quality Admin. Contract No. W.P.E.D. 53-01-67, 1968.
54. Wirts, J. J. *Fed. Water Poll. Control Admin.*, Grant No. W.P.R.D. 102-01-68, May, 1969.
55. Grutsch, J. F. *Environ. Sci. Technol.* **1978**, *12*, 1022.

56. Busch, P. L.; Stumm, W. *Environ. Sci. Technol.* **1968**, *2*, 49.
57. Goodman, B. L.; Mikkelson, K. A. In *Chem. Eng./Deskbook Issue*, 1970, 77, p 75.
58. Rudolfs, W.; Henkelekian, H. *Sewage Works J.* **1934**, *6*, 1073.
59. Mignone, N. A. *Water and Sewage Works* **1976**, *123*, 57.
60. Noland, R. F.; Dickerson, R. B. In *USEPA Technology Transfer Seminar on Sludge Treatment and Disposal*; USEPA-MERL, Technology Transfer: Cincinnati, OH, 1978.
61. Heim, N. E.; Burris, B. E. In EPA Contract No. 68-01-5085; 1979, p 33.

RECEIVED for review August 6, 1984. ACCEPTED December 10, 1985.

Metal-Activated Redox Initiation for the Synthesis of Low Molecular Weight Water-Soluble Polymers

Kathleen Hughes and Graham Swift

Rohm and Haas Research Laboratories, Spring House, PA 19477

Metal-activated redox initiation in aqueous solution, employing aqueous peroxide solutions and water-soluble transition metal salts, provides one interesting industrial route to low molecular weight water-soluble polymers. Synthesis of low molecular weight poly(acrylic acids) (\bar{M}_w 1,000–20,000), using hydrogen peroxide and copper salts as the initiator system, is described. Molecular weight control is dependent upon reaction temperature, hydrogen peroxide level, and hydrogen peroxide to copper salt molar ratios. Reaction temperatures of 80–100 °C and hydrogen peroxide levels of approximately 1–20 wt % (on monomer) are employed. Hydrogen peroxide to copper molar ratios of approximately 50:1 to 100:1 provide the lowest molecular weight poly(acrylic acids) for a given hydrogen peroxide level. Inclusion of low levels (<2 wt %) of tertiary amines with the copper salt tends to yield lower molecular weight products. No mechanistic studies were conducted.

WATER-SOLUBLE POLYMERS OF LOW MOLECULAR WEIGHT (\bar{M}_w <20,000), particularly high acid content polyelectrolytes, such as poly(acrylic acids), find utility in a variety of application areas, including industrial water treatment, trade-sales paints, and detergents. Many approaches to the synthesis of low molecular weight poly(acrylic acids) are reported in the patent literature: these include aqueous polymerization employing mercaptan chain transfer agents (1) and synthesis in isopropyl alcohol followed by solvent exchange to water (2). Recently, we developed aqueous solution metal-activated redox initiation processes (3), which accommodate facile and economic polymerization of water-soluble monomers such as acrylic acid. In these metal-activated redox processes, hydrogen peroxide and copper salts are employed for the synthesis of water-soluble homopolymers and copolymers.

0065-2393/86/0213-0145\$06.00/0
© 1986 American Chemical Society

As first noted by Fenton in 1894 (4), in the presence of certain metal catalysts, hydrogen peroxide exhibits increased oxidizing activity. These Fenton oxidations are believed to proceed through the intermediate formation of hydroxyl free radicals (5):



Our analyses indicate that hydroxyl free radicals initiate our polymer chains; however, the complete mechanism of initiation is not established. In this chapter, we present interesting findings regarding one industrial approach to the synthesis of poly(acrylic acids). Results regarding polymerization using this type of metal-activated initiation as well as the dependence of polymer molecular weight control on hydrogen peroxide to copper salt molar ratios are discussed.

Experimental Section

Synthesis. The poly(acrylic acid) polymers described were all prepared at 55 wt % solids in deionized water by using gradual addition processes at the temperatures indicated under Results and Discussion. Water, the metal salt, and the amine (if included) were charged to a 2-L, four-necked flask equipped with a mechanical stirrer, a condenser, a thermometer, and addition funnels for the gradual additions of the acrylic acid monomer and hydrogen peroxide solutions were completed linearly and separately during 2–3 h. Hydrogen peroxide concentrations of 30 wt % were used. Sulfate salts of the metals were used, and the amount of metal used is expressed as parts per million of metal (not metal salt) on monomer. Amine and hydrogen peroxide charges are expressed as weight percent active ingredient on the monomer throughout the tables. Molar ratios of hydrogen peroxide to metal salt are based on the total charges of each (i.e., not on the molar ratio at each point throughout the gradual addition of hydrogen peroxide).

Characterization. Characterization of the poly(acrylic acid) samples include Brookfield viscosity measurements on samples equilibrated at 25 °C, gas-liquid chromatographic analysis for residual acrylic acid monomer, iodometric titration for residual peroxide, and gel permeation chromatography for molecular weight measurements.

Results and Discussion

Survey of Metal Activators. Table I data illustrate the relative efficiencies of copper, iron, and manganese as metal activators in 98 °C polymerizations of acrylic acid when 5% active hydrogen peroxide was used as the initiator. In each case, the sulfate salt was used, and also in each experiment, 2% (dimethylamino)ethanol was included. On the basis of monomer conversion and use of hydrogen peroxide in this limited survey of metal activators, copper is the preferred metal for these aqueous polymerizations. Although molecular weight measurements on these Table I samples were not done, the viscosity at 50% solids indicates that the copper system yields the lowest molecular weights under the condi-

Table I. Efficiency of Hydrogen Peroxide as an Initiator for Poly(acrylic acid) Synthesis in the Presence of Several Transition Metals

<i>Metal (on Monomer)</i>	<i>AA^a Monomer Conversion (%)</i>	<i>H₂O₂ Residue (%)</i>	<i>25 °C Brookfield Viscosity^b (cP)</i>
380 ppm of Cu ²⁺	100	5	220
380 ppm of Fe ²⁺	95	25	8200
380 ppm of Mn ²⁺	80	50	NA ^c

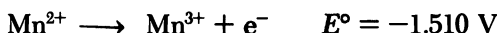
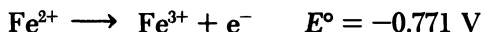
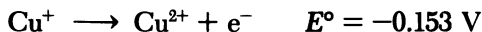
^aAA represents acrylic acid.^bAt 50% solids.^cNA is not available.

tions studied. Hydrogen peroxide initiation of aqueous acrylic acid polymerizations, using the same level of hydrogen peroxide, in the absence of metal activation under similar reaction conditions, yields poor utilization of hydrogen peroxide (>70% residual) and a higher molecular weight product.

On the basis of the monomer conversion and hydrogen peroxide utilization, the copper redox transition is more facile than the iron or manganese electron transitions:



This observed order of metal efficiency is consistent with the oxidation potentials for these metals (6):



Effect of Copper to Hydrogen Peroxide Molar Ratio Variations. Metal-activated redox initiation was then pursued by using copper salt and hydrogen peroxide as the initiating system. The effect of the hydrogen peroxide to copper molar ratio on peroxide utilization, monomer conversion, and molecular weight control in poly(acrylic acid) synthesis was investigated. Two hydrogen peroxide levels were studied (1 and 5 wt % on the monomer); all experiments were run at 95 °C, and 1 wt % triethanolamine was charged to the reactor with the copper salt. Data for these experiments are provided in Tables II and III.

The Table II data illustrate the effect of hydrogen peroxide to copper molar ratios on peroxide utilization, monomer conversion, and molecular weight in the 1% hydrogen peroxide experiments. In terms of monomer conversion, peroxide utilization, and molecular weight, the 60:1 to 120:1 molar ratio range seems optimum for these reaction conditions.

**American Chemical Society
Library**

1155 16th St., N.W.

In Water-Soluble Polymers, Glass 1:
Washington, D.C. 20036
Advances in Chemistry; American Chemical Society, Washington, DC, 1986.

Table II. Effect of Hydrogen Peroxide (1%) to Copper Salt Molar Ratios on Poly(acrylic acid) Synthesis

<i>Cu</i> (ppm)	<i>mol of H₂O₂: mol of Cu</i>	<i>H₂O₂ Residue (%)</i>	<i>AA^a Conversion (%)</i>	<i>Viscosity (cP) at 25 °C</i>	\bar{M}_w	\bar{M}_n
3600	5:1	0	23	NA	NA	NA
1500	12:1	0	54	NA	NA	NA
600	30:1	0	82	NA	NA	NA
300	60:1	0	100	1000	9800	4140
150	120:1	11	100	3000	17350	7800
30	600:1	60	100	72000	49900	13500

^aAA is acrylic acid.

To prepare lower molecular weight poly(acrylic acids), we performed the Table III experiments at the 5% hydrogen peroxide level using the reaction conditions listed in Table III.

In these Table III experiments, the 60:1 to 150:1 hydrogen peroxide to copper molar ratios, as in the 1% hydrogen peroxide experiments, appear to be in an optimum range for these reaction conditions in terms of molecular weight control and peroxide utilization.

Effect of Hydrogen Peroxide Level Variation at Constant Hydrogen Peroxide to Copper Molar Ratio. Table IV data show the effect of hydrogen peroxide level on molecular weight at a constant hydrogen peroxide to copper molar ratio (60:1) under the same reaction conditions as in the Table II and III experiments. These Table IV data demonstrate the dependence of molecular weight on initiator level at a constant H₂O₂ to copper molar ratio. Figure 1, a plot of \bar{M}_n vs. $1/[H_2O_2]^k$, illustrates the Table IV \bar{M}_n data.

Synthesis of the lowest molecular weight products requires high levels of copper as well as hydrogen peroxide. Over the range studied, the presence of copper at even 6000 ppm does not present a solubility or storage stability problem. However, if desirable, copper can be effi-

Table III. Effect of Hydrogen Peroxide (5%) to Copper Salt Molar Ratios on Poly(acrylic acid) Synthesis

<i>Cu</i> (ppm)	<i>mol of H₂O₂: mol of Cu</i>	<i>H₂O₂ Residue (%)</i>	<i>AA Conversion (%)</i>	<i>Viscosity (cP) at 25 °C</i>	\bar{M}_w	\bar{M}_n
1500	60:1	0	100	185	4700	2160
600	150:1	8	99	320	6250	2820
300	300:1	26	98	750	8150	3620
150	600:1	27	99	780	8700	2820
50	1800:1	52	100	3000	13300	5500

Table IV. Varying Hydrogen Peroxide Levels at 60:1 Hydrogen Peroxide to Copper Salt Molar Ratios

H_2O_2 (wt %)	Cu (ppm)	H_2O_2 Residue (%)	AA Conversion (%)	Viscosity (cP) at 25 °C	\overline{M}_w	\overline{M}_n
1	300	0	100	1000	9800	4140
5	1500	0	100	185	4700	2160
10	3000	0	100	110	3520	1600
20	6000	0	100	40	2450	1120

ciently removed postpolymerization by using well-known ion-exchange techniques.

Effect of Amine Level. Another variable examined was the effect of amine inclusion and amine level on these metal-activated redox processes. Data for these experiments are provided in Table V. The Table V experiments were run at 95 °C, the copper level was 600 ppm, the H_2O_2 level was 5% on monomer (hydrogen peroxide to copper molar ratio of 150:1). These Table V data show that inclusion of low levels of a tertiary amine, such as triethanolamine, tends to lower the molecular weight and improve peroxide utilization. The role of the amine in these

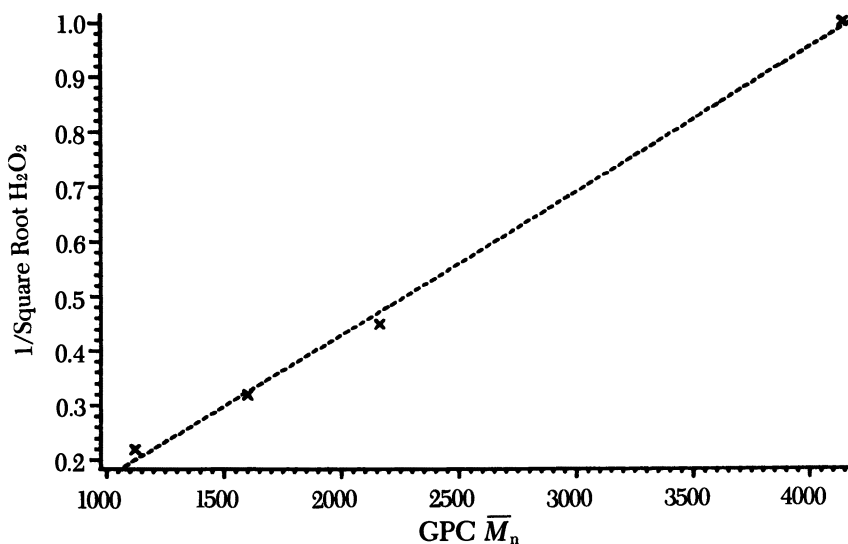


Figure 1. A plot of $1/[H_2O_2]^{1/2}$ is an illustration of the Table IV gel permeation chromatographic data. These data show the dependence of poly(acrylic acid) \overline{M}_n on the hydrogen peroxide level at a constant hydrogen peroxide to copper salt molar ratio.

Table V. Effect of Amine Inclusion on Poly(acrylic acid) Synthesis

TEA ^a (wt %)	H ₂ O ₂ Residue (%)	AA ^b Conversion (%)	Viscosity (cP) at 25 °C	\overline{M}_w	\overline{M}_n
0	33	95	655	7000	3280
1	8	99	325	6250	2820
2	0	99	275	5600	2500

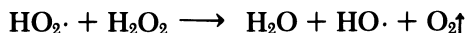
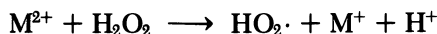
^aTEA represents triethanolamine.

^bAA is acrylic acid.

reactions is not completely understood at this time; however, its function may be that of a chelate.

Effect of Temperature. Temperature also is an important factor in controlling molecular weight, efficiency of peroxide utilization, and monomer conversion. Table VI contains data for experiments done in the 80–95 °C range: higher temperature favors lower molecular weight and more efficient peroxide utilization. In the mechanism proposed (*see* next section), for this initiation, the hydrogen peroxide serves as both the oxidizing and reducing agent for the metal; presumably, the $\text{Cu}^{2+} \rightarrow \text{Cu}^+$ transition requires higher temperatures.

Proposed Mechanism. The complex mechanism of initiation in our processes is not fully understood. Peroxides, including hydrogen peroxide, are commonly used to initiate addition polymerizations of acrylate and vinyl monomers. Hydrogen peroxide probably functions by redox decomposition to the hydroxyl free radical (7). A mechanism for the formation of the hydroxyl free radical that initiates these polymerizations is

**Table VI. Effect of Temperature on Poly(acrylic acid) Synthesis**

Synthesis Temp (°C)	H ₂ O ₂ Residue (%)	AA Conversion (%)	Viscosity (cP) at 25 °C	\overline{M}_w	\overline{M}_n
95	8	99	320	6250	2820
90	10	98	500	7150	3240
80	44	90	1200	11400	4730

HO· is an effective initiating species, and NMR analysis of these poly-(acrylic acid) polymers verifies hydroxyl end groups. Also, monitoring of the reaction atmosphere verifies the presence of oxygen.

Acknowledgments

We thank the Rohm and Haas Company for allowing us to publish this work. We acknowledge the contributions of Steven Edwards and Benjamin Kine in this work and the analytical support of Al Weiss and Betty Ginsberg in the gel permeation chromatographic analysis of our polymers.

Literature Cited

1. Song, D. S.; Duffy, R. J.; Witschonke, C. R.; Schiller, A. M.; Higgins, M. A. U.S. Patent 4 001 161, 1973.
2. Muenster, A.; Rohmann, M. U.S. Patent 4 301 266, 1981.
3. Hughes, K. A.; Kine, B. B.; Swift, G. U.S. Patent 4 314 044, 1982.
4. Fenton, H. J. H. *J. Chem. Soc.* **1894**, 65, 899.
5. Barb, W. G.; Baxendale, J. H.; George, P.; Hargrave, K. R. *Trans. Faraday Soc.* **1951**, 47, 462.
6. *Handbook of Chemistry and Physics*, 44th ed.; CRC Pr: Boca Raton, FL, p 1743.
7. Wallace, J. G. *Hydrogen Peroxide in Organic Chemistry*, E. I. du Pont de Nemours: Wilmington, DE, 1962; p 107.

RECEIVED for review September 28, 1984. ACCEPTED August 14, 1985.

Role of Water-Soluble Polymers in Oil Well Drilling Muds

Jack C. Estes

Amoco Production Company, Tulsa, OK 74102

The uses and problems of water-soluble polymers in oil well drilling muds are discussed in this chapter. Uses include that of a flocculent of the drilled solids, a bentonite clay extender, and a fluid-loss reducer, a viscosifier, and a well-bore stabilizer. Because well-bore stability and drilling costs are related to the drilling rate, a drilling-rate model based on the particle-size distribution of the dispersed clays is discussed. The performance of polymer extenders with the current American Petroleum Institute bentonite is compared to the performance of extenders used 20 years ago. Guidelines concerning desired solids concentrations in a drilling fluid and the effect polymers have on this concentration are presented. Finally, the future of polymers in drilling is discussed.

THE MAJOR GOAL OF DRILLING RESEARCH is to study those variables that influence the rate at which wells are drilled, while well-bore stability is maintained and damage to producing formations is prevented. For this reason, the properties of drilling fluids and the effects of additives such as polymers and electrolytes on the drilling rate and formation stability are studied by the drilling industry. This chapter discusses the use of water-soluble polymers in oil well drilling muds as applied by one major oil company. Standard Oil Co. (Indiana), now Amoco Corp., pioneered the use of mud systems that are called low-solids, nondispersed, polymer-extended (LSND) muds.

Background

The presence of electrical charges on the surfaces of colloidal clay particles in bentonite slurries has been known for a long time (1). Scientific investigations of the effects of inorganic electrolytes in such suspensions were carried out by Standard Oil Co. (Indiana) as early as the late 1930s and continue to the present. Early studies concentrated on the effect of

0065-2393/86/0213-0155\$06.00/0
© 1986 American Chemical Society

particle-size distribution within the suspension on the rheological and fluid-loss properties (described later) of drilling muds (2). More recent work emphasizes the effect of electrolytes on clay minerals in shales being drilled, the effect of fluids on formation evaluation techniques, and the nature and extent of filtrate permeability damage to producing formations.

During the 1950s, attention was turned to a study of the interaction of clays and organic electrolytes such as surface-active anionic detergents and water-soluble polymers. The detergents eventually found a market in mud systems requiring emulsions or improved lubrication for the drill pipe rotating against the side of the well bore. Lubricants are particularly useful in directional wells where the hole bottom horizontally offsets the surface location by several thousand feet (2).

The uses found for the water-soluble polymers were more varied than for the detergents. The first such polymers were natural gums used for viscosity control (3). The first synthetic polymer used in the field was (carboxymethyl)cellulose to lower the 30-min fluid loss of the mud filtrate by using an American Petroleum Institute (API) test cell (4). Later, poly(acrylamide)-carboxylic acid copolymer was used to completely flocculate clay-formation solids to prevent the solids from making a mud (5).

Problems

Sloughing Shale. Flocculation of drilled solids allowed for drilling with a clear fluid, and this approach resulted in much faster drilling rates. Unfortunately, in many areas the clear drilling fluids greatly increased the probability of shale formations sloughing into the well bore; severe hole enlargements are caused, and in some cases, sticking to the drill pipe results. In some areas, sodium chloride brines prevented the shale formations from sloughing into the well bore. However, even sodium chloride would not work in other areas, and potassium or ammonium salts had to be employed along with the polymer flocculents (6).

Work in recent years developed our understanding of this problem. Research indicates that the water activity of the shale is the determining factor in whether brines made up of sodium chloride would stabilize the formation being drilled. Shales that have water activities higher than 0.77 can be stabilized by brines of matching activity. However, because 0.77 is the lowest water activity achieved by NaCl brines, and because the sodium ion is highly hydrated, NaCl brines will destabilize shales that have water activities lower than this. So that the hydration process is slowed, less strongly hydrated cations such as potassium or ammonium must be employed and polymers must be used to coat the shales. This area is currently the subject of intense research within the petroleum industry.

Effect of Solids Content. In wells where drilling with plain water on native mud was not possible or not desired, drilling faster while maintaining well-bore stability was a real problem in the 1950s. Mud solids slowed the drilling rate. Well-bore stability problems were time dependent; i.e., the more time in open hole, the more likely the hole would fall in. In 1960, a field survey was conducted in an attempt to quantify the effect of solids on the drilling rate. Feet per day, number of bits, and number of rig days to reach a depth of 10,000 ft were tabulated, and a least-squares curve fit was performed on the data correlated against solids content. Figure 1 is the result of that survey (7).

Such a correlation from field data would be difficult today because of the wide variety of bits, rig pumps, and mud systems now used. However, in 1960, basically only three types of bits existed: soft, medium, and hard formation. Almost all had steel teeth, nonsealed roller bearings, and no jets. The bit designs severely limited the fluid flow rate range. Too little flow and the teeth plugged up with the drilled rock, and too much flow resulted in severe erosion of the steel teeth of the bit. Most rig pumps were 16- or 18-in. duplexes with cast iron fluid ends that limited the pressure range available. Therefore, any major drilling rate

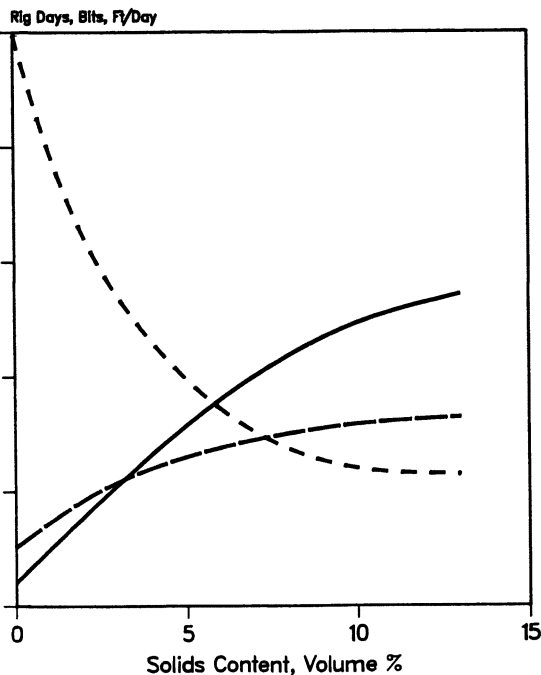


Figure 1. Effect of mud solids. Key: —, bits; - - -, rig days; and - · -, feet per day. Reproduced with permission from reference 7. Copyright 1961 Petroleum Publishing.

change from well to well was most likely due to formation differences or the mud system being used.

Because feet per day, number of bits, and number of rig days were major factors in determining the cost of the well, an analysis of Figure 1 data resulted in the following conclusions: (1) the solids content has a major effect on drilling costs, (2) little sensitivity to cost factors exists above 5% by volume clay solids, and (3) the maximum sensitivity of the variables that affect cost occurred below 5% solids. In other words, the clay solids content of a drilling mud must be kept below 5%, if control of the mud system was to have any impact on the total cost of drilling the well.

If the shale formations had a high value for water activity, i.e., close to 1.0, then no problem occurred in implementing the conclusions of the aforementioned study into field practice. Newly discovered polymer flocculents could be used to drill essentially with water. However, if a colloidal mud was needed because of well-bore stability problems, high-pressure zones, or formation evaluation and coring requirements, a mud of desired properties could not be made and used to drill without exceeding the 5% by volume solids content limit. In fact, most muds, even with the best of attention, were in the 6–8% solids range.

Beneficiation of Bentonite. If some polymer could be found that would increase the viscosity of the clay suspensions without flocculating the clay, then possibly a mud system could be formulated with suitable properties with less than 5% clay content. If the mud was considered as a Bingham plastic (8), suitable properties were defined as a 10–14-lb/bbl polymer-extended clay slurry having the same apparent viscosity, yield point, and filtration properties as a 17–22-lb/bbl high-quality Wyoming bentonite slurry. These values were 15 cP, 10–15 lb/100 ft², and less than 13.5 cm³/30 min in an American Petroleum Institute (API) cell, respectively (9).

The 5% by volume limit for total clay solids dictated this definition, because once a mud circulated during drilling, complete removal of all of the drilled solids was impossible. The ratio of the drilled solids content to the bentonite content (*D:B* ratio) would always be greater than 1:1 and frequently would exceed 3:1, the maximum desired limit for this ratio. For the mud system to have less than the 5% total clay solids, commercial bentonite content had to be in the 10–14-lb/bbl range, the ideal concentration being 10.5 lb/bbl. However, at this concentration bentonite alone would not give acceptable mud properties.

A word concerning units is appropriate here. Volume percent is used in field measurements, because this measurement is derived from a retort but usually is grossly inaccurate. Weight percent is used to make up laboratory concentrations, because this value is a weighed quantity. Bentonite has a specific gravity of about 2.2 and a drilled solids average of

2.65; thus a 1% volume approximately equal to 2.5% by weight. Our limit of 5% volume is approximately 42 lb/bbl of clay solids; thus, 10.5 lb/bbl is the ideal bentonite concentration if a *D:B* ratio of 3:1 is not exceeded. However, few commercially available bentonites are extendable at this low concentration. Therefore, it is more reasonable to expect a polymer extender to be able to extend bentonite slurries made up of 14 lb/bbl, or less.

Extensive laboratory experiments were therefore carried out in a search for polymers that would react at an economic concentration with the bentonite to produce the desired effect. These experiments resulted in the discovery that minute concentrations of some water-soluble polymers extended the bentonite clay by thickening the mud without actually flocculating the solids and causing settling. The mud particles did not settle, and the fluid-loss properties actually improved, by decreasing the amount of filtrate from the API test cell. In larger polymer concentrations, the thickening process was reversed. If the bentonite concentration was below about 14 lb/bbl, the mud was undesirably thinned, so that the viscosity was actually below that of the original untreated slurry.

A patent (10) was issued in 1962 describing a vinyl acetate-maleic anhydride (VAMA) copolymer that would produce the required effect at concentrations of less than 0.05 lb/bbl. Laboratory tests also indicated that the polymer should flocculate low-yield clays found in shales. This finding was correlated to ζ potential measurements on the clays. Bentonites that had ζ potentials in the -40- to -20-mV range were extended; illites and other low-yield clays, which were less negative, flocculated with the polymer addition. Polymers that exhibited this dual behavior in relation to ζ potential were named dual-action polymers.

Field usage confirmed that the dual-action polymers helped in controlling the *D:B* ratio to less than 3:1. Drilling research revealed that the lower solids also made other drilling variables more responsive to change, i.e., bit selection, weight on bit, rotary speed, and hydraulics. This discovery (11) made the practice of optimized drilling a reality.

Polymer Properties. Whether a given class of polymer would act as a fluid loss reducer, a bentonite extender, or a flocculent was considered to be a function of its molecular weight as determined by intrinsic viscosity measurements. Intrinsic viscosity is an indication of a polymer's average molecular weight, but the molecular weight distribution is also an important variable that determines polymer behavior in mud systems. Polymers must therefore be classified more closely than just chemical class and average molecular weight.

Narrow-range, low molecular weight, water-soluble polymers appear to function as fluid-loss reducers in clay systems, whereas high molecular weight, broad-range polymers seem to function as flocculents or viscosifiers in their own right. The performance of polymers of

intermediate weights and ranges is not as easily classified, and an attempt at some sensible classification along these lines is in progress.

Chemical class and structures are also important where degradation of polymers occurs from mechanical or temperature effects. Shear degradation in a mud system appears to be a function of both structure and molecular weight. Indirect evidence indicates that temperature limitations of a polymer in a mud system are not identical with the limitations on the polymer by itself. This observation is of polymer performance in deep, hot holes. In other words, the polymer may function in the mud system at higher temperatures than laboratory thermal degradation tests indicate.

The reason may be that at high well-bore temperatures the polymer in a mud is also subjected to pressures greater than 10,000 psi. The pressure may act to prevent thermal degradation of the polymer or the pressure may force a chemical reaction with other components of the mud system, to form a stable structure. This reaction, of course, is difficult to simulate in most mud laboratories, where a "high-pressure" test means only 1000 psi. If the aforementioned rationale is correct, then further advances in polymer usage in drilling mud systems will be contingent upon research conducted above 250 °F and 10,000 psi.

Discussion of Technical Data

Effect on Drilling Rate. Drilling research by industry was getting under way in the late 1950s to address the causes of the detrimental effect of solids in muds on drilling rates. However, 1958 saw the postwar drilling activity peak out. A precipitous drop in rig count occurred in the following 2 years, and a steady decline occurred for the next 13 years. As a result, most companies curtailed or canceled their drilling research efforts. Standard Oil Co. (Indiana), however, continued the drilling research it had started in 1939 and, in fact, increased its effort substantially by building in 1961 a 1500-hp research drilling rig inside a four-story research building.

Drilling-rate experiments comparing muds with varying solids content with clear water usually produce a response curve similar to that shown in Figure 2 (12). Bit type, rock type, weight on bit, rotary speed, flow rate, borehole pressure, type of clay solids, and chemical treatment influence the severity of the response. In general, anything added to water causes a reduction in the drilling rate.

Different clays will produce a family of curves, so that a homologous series of curves above and below the Figure 2 curve would result. In a given clay concentration (holding all other variables constant), any number of drilling rates may result, depending upon the type of clay and the chemical treatment to which the mud was subjected.

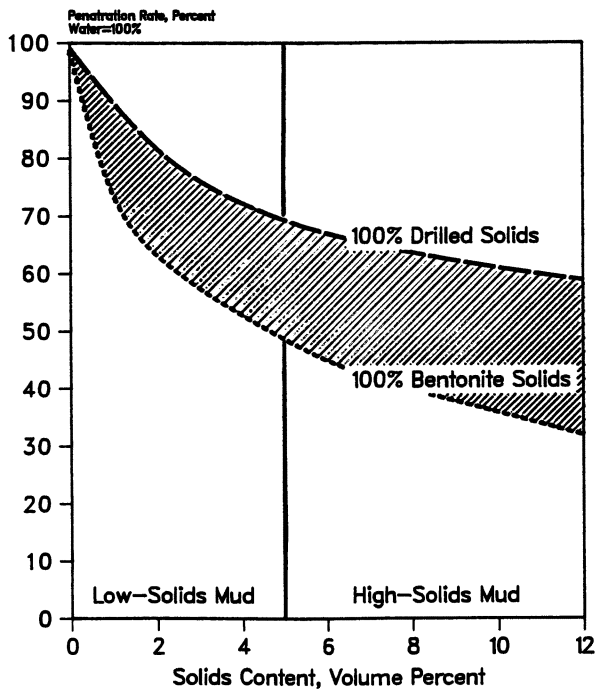


Figure 2. Penetration rate vs. clay-solids content. Key: — —, 100% drilled solids; and ---, 100% bentonite solids. The penetration rate of water was 100%. The left panel is low-solids mud; the right panel is high-solids mud. Reproduced with permission from reference 12. Copyright 1960 American Petroleum Institute.

The observation that led to a viable theory upon which to base a drilling-rate model was that lignosulfonate dispersants (which thinned) cause a decrease in drilling rate, whereas the new polymer extenders (which thickened) produce an increase in drilling rate, compared to an untreated clay slurry. However, increasing viscosity generally resulted in slower drilling rates. Obviously, a drilling-rate model based on viscosity could not be made, because the unusual drilling-rate increases obtained with polymer treatment occurred even when the mud was thickened to the point where it was almost un pumpable.

Because dispersants cause a breakup of clay particles, the polymer extenders were postulated to do the reverse, i.e., tying the clay particles together to shift the particle-size distribution to the higher side (12). Careful particle-size distribution measurements using a time-consuming super-centrifugal procedure confirmed this theory.

Bentonite gel slurries aged by rolling for 3 weeks had a very narrow particle-size range as measured by this technique. Eighty percent of the

particles were less than 3 μm ; however, only 13% were less than 1 μm . If this slurry (6% solids by weight) was dispersed with lignosulfonate and sodium hydroxide and aged by rolling for 3 weeks, 100% of the particles measured were less than 3 μm and 80% were less than 1 μm (1 μm was at the lower limit of our measurement ability with the supercentrifuge).

Polymer treatment produced an opposite effect. The submicron particle concentration actually decreased to 6% less than 1 μm . Particle-size distribution then became the explanation of why different drilling rates existed at the same clay solids concentration with different clays and chemical treatment.

This effect was modeled by comparing the resulting drilling rate of a given clay concentration to the drilling rate of clear water in the form of a ratio, drilling rate of mud to drilling rate of water, DRM:DRW. For water, the ratio is equal to 1.

Because any solids added to water generally lower the drilling rate, for a mud DRM:DRW is some number less than 1. This ratio was related to the particle-size distribution. For convenience, this distribution was divided into *A*, the effect of submicron fine (*F*) particles, which probably had a greater effect, and *B*, the effect of coarser (*C*) particles. The equation then becomes

$$\text{DRM:DRW} = 1 - A(F) - B(C) \quad (1)$$

where (*F*) and (*C*) indicate the pounds per barrel concentration of the fine and coarse particles, respectively, in the mud system.

After drilling with 28 different mud systems and running the particle-size distribution, a regression analysis of the data resulted in a value for *A* of 0.0133, and a value for *B* of 0.00114 (13). This discovery was rather startling because it indicated that the submicron particles were almost 12 times more detrimental to the drilling rate than the coarser particles. This discovery also explained why polymer-extended muds did so much better than just the reduction in solids content alone could explain.

Lack of space does not allow a complete discussion of the complex reasons for the detrimental effects of the submicron particles. The factors involved include an effect of borehole pressure because of filtration properties; the effect of hydraulic-pressure losses dependent upon viscosity properties, which determine the hydraulic horsepower reaching the bit; and the cost of maintenance of solids-control specifications of the mud system (14). In other words, those variables that we could not model directly are indirectly modeled by this particle-size model.

Of course, the centrifugal technique is not practical to use at the rig site, so a methylene blue test (MBT) procedure was developed that allowed estimation of the highly reactive submicron particles (15). The total clay content could be calculated by mud weight or retort values,

and MBT provided an estimate of the bentonite fraction of these. The type of mud system provided the multiplication factor to apply to the MBT-calculated values. For an untreated water gel slurry, the pounds per barrel bentonite concentration from the MBT was multiplied by 0.13 (because 13% is less than 1 μm) and then entered into equation 1 as the concentration for F, and the concentration of fines was subtracted from the total solids content to arrive at the concentration for C. In a dispersed mud, the factor was 0.80, but for a polymer-extended mud, the factor was only 0.06. This model has been used successfully and continuously by Standard Oil Co. (Indiana), now Amoco, since 1967. The procedure obviously could be used to good advantage by polymer salesmen to market water-soluble polymers to the drilling industry.

Polymer Extenders for Bentonite. The original bentonite specifications were written in oil field terms of barrels per ton yield for a 15-cP mud. The conversion to barrels of 15-cP mud per ton of bentonite clay is the concentration, c , in pounds per barrel required to yield a 15-cP mud taken from a viscosity plot and applied in equation 2:

$$\text{barrels/ton} = 2000/c + 2 \quad (2)$$

When the VAMA polymer extender went on the market in 1960, high-grade Wyoming bentonite averaged 105 bbl/ton yield of 15-cP mud. Treatment with VAMA polymer would increase this yield to 150–213 bbl/ton. Thus, half the bentonite usually required could be used, and at last a low-solids mud of excellent properties with less than 5% by volume total low-density solids content, even with a $D:B$ ratio of up to 3:1, could be used to drill.

Typical data for API Wyoming bentonite at various concentrations, taken June 27, 1962, are shown in Table I. (The test procedures are defined in reference 9.) The 6% by weight concentration refers to 21 g of clay in 350 cm^3 of tap water. Later specifications required that deionized water be used and the volume be corrected for the effect of adding the clay solids, so that 6% by weight in recent tests refers to 22.5 g in 350 cm^3

**Table I. API Bentonite, June 27, 1962
(Aged Overnight)**

<i>Concn</i> (wt %)	<i>Plastic</i> <i>Viscosity</i> (cP)	<i>Yield Point</i> (lb/100 ft ²)	<i>Fluid Loss</i> (cm ³ /30 min)
3	2	1	22
4	5	3	10
5	7	9	7
6	11	15	6

of distilled or deionized water. For comparison purposes, all data in this chapter used original procedures with deionized water. Properties for the bentonite alone shown in Table I are after aging overnight. Polymer extender data of Table II were taken after hydrating the clay only 20 min, adding polymer, and mixing only 5 min. This study was done to prove that the polymer also accelerates the yield time considerably, an important consideration in oil well drilling. Apparent viscosity versus concentration of the mud used in Tables I and II is plotted in Figure 3.

Table II. API Bentonite, June 27, 1962 (Not Aged),
Extended with 0.05 lb/bbl of Polymer

Concn (wt %)	Plastic Viscosity (cP)	Yield Point (lb/100 ft ²)	Fluid Loss (cm ³ /30 min)
3	4	6	9
4	10	17	8
5	12	47	7
6	12	126	6

NOTE: bbl is oil field barrel of 42 gal. or 350 lb of water.

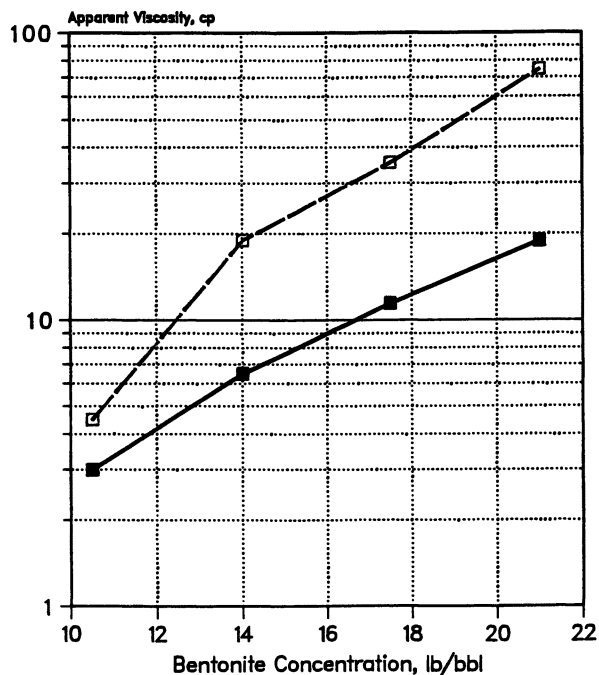


Figure 3. API bentonite, 1962. Key: ■, no extender; and □, polymer extended.

The polymer extends the bentonite (allows the use of less bentonite for the same viscosity), and the extended curve is above and does not cross the base clay line.

Particularly interesting is the 6-cm³ fluid loss of the 1962 API bentonite. The current API specifications call for a 6% weight slurry to have a fluid loss of less than 15 cm³. This value is almost three times higher than that of the material supplied in 1962.

Although this situation is distressing for oil well drilling operators, it is not the worst story as far as clays are concerned. Lower yield clays are now being blended with higher yield clays, and polymer is added at the mills to achieve even these relaxed API specifications. In laboratory checks, at 6% weight concentration the yield point will exceed the plastic viscosity by more than 2:1 if the bentonite has been treated with polymer. Unfortunately, this practice results in a thinning effect at lower bentonite concentrations when polymer extenders are added at the rig site, because of the previous polymer treatment at the mill.

Some API untreated bentonite is available today that gives a 92-bbl/ton yield and can still be extended by the operator at the rig site but not nearly to the extent of the bentonite available in 1962. This result is shown by the curve of apparent viscosity versus concentration of the mud used in Tables III and IV plotted in Figure 4. Again the polymer-extended curve is above and does not cross the original clay curve.

**Table III. API Untreated Bentonite, June 1984
(Aged Overnight)**

<i>Concn</i> (wt %)	<i>Plastic</i> <i>Viscosity</i> (cP)	<i>Yield Point</i> (lb/100 ft ²)	<i>Fluid Loss</i> (cm ³ /30 min)
3	2	1	20
4	4	1	17
5	6	2	13
6	10	3	12

**Table IV. API Untreated Bentonite, June 1984,
Extended with 0.05 lb/bbl of Polymer**

<i>Concn</i> (wt %)	<i>Plastic</i> <i>Viscosity</i> (cP)	<i>Yield Point</i> (lb/100 ft ²)	<i>Fluid Loss</i> (cm ³ /30 min)
3	4	0	18
4	7	1	15
5	10	19	13
6	15	53	12

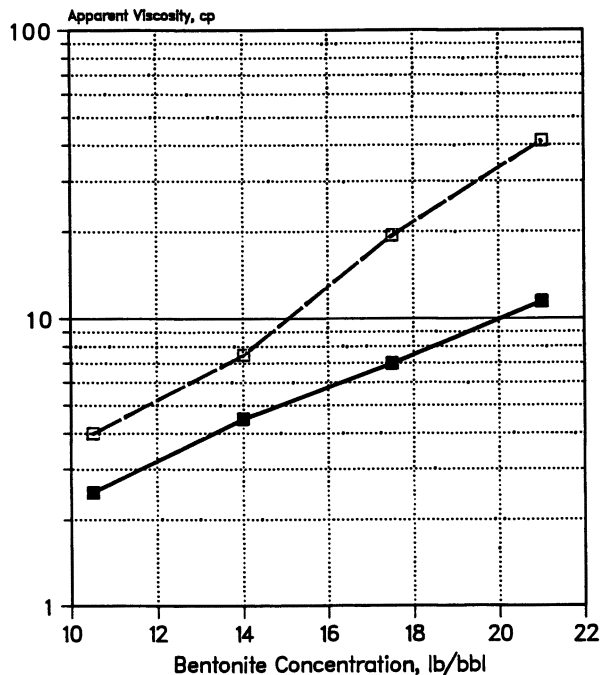


Figure 4. Untreated API bentonite, 1984. Key: ■, no extender; and □, polymer extended.

More typical of currently supplied API bentonite, however, is the highly treated bentonite shown by Table V data. This bentonite cannot be further extended at the lower concentrations (Table VI). Figure 5 is an apparent viscosity plot of this mud. Notice that the polymer-extended curve crosses the original clay curve at 15 lb/bbl. The polymer actually thins the mud at the lower clay concentrations, where thinning is not desired, and thickens at higher clay concentrations. The polymer is, therefore, producing the reverse effect of what is desired.

Therefore, instead of using 10–14 lb/bbl of bentonite and a mud system of less than 5% volume total clay solids, we are right back where

Table V. Example of 1984 API Bentonite (Aged Overnight)

Concn (wt %)	Plastic Viscosity (cP)	Yield Point (lb/100 ft ²)	Fluid Loss (cm ³ /30 min)
3	3	3	31
4	4	8	24
5	5	14	19
6	10	22	16

Table VI. Example of 1984 API Bentonite Extended with 0.05 lb/bbl of Polymer

<i>Concn (wt %)</i>	<i>Plastic Viscosity (cP)</i>	<i>Yield Point (lb/100 ft²)</i>	<i>Fluid Loss (cm³/30 min)</i>
3	3	0	25
4	6	3	22
5	8	16	19
6	10	50	18

we were 25 years ago using 17–25 lb/bbl; difficulties arise in running a low-solids clay-based mud with a *D:B* ratio of 3:1 while staying under the 5% by volume solids limit.

The onset of this situation has not been sudden, and in 1967 Standard Oil Co. (Indiana) introduced a polymer extender based on acrylic acid that would extend lower yield bentonites better than the VAMA copolymer (16). Another improved polymer was introduced in 1971 (17). However, even these polymers may not extend some bentonites already polymer treated by the supplier, as demonstrated by the aforementioned data.

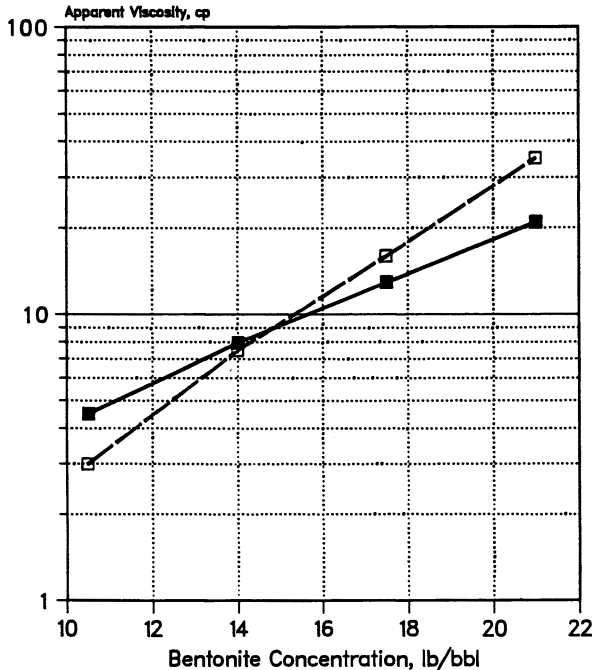


Figure 5. Example API bentonite, 1984. Key: ■, no extender; and □, polymer extended.

Future of Polymers in Drilling

Prediction 1. In the immediate future, more expensive oil-emulsion muds will replace water-base clay muds in expensive drilling areas where slow drilling rates or directional drilling causes hole stability problems. This replacement will accelerate as more environmentally safe oils are introduced and accepted by operators and government regulators alike. The development of synthetic polycrystalline diamond compact bits has made these oil-emulsion muds a viable alternative, as more sophisticated operators realize that lower well costs are achievable if sound engineering is applied when these very expensive bits and mud systems are used.

Prediction 2. In the next decade, as oil and gas reservoirs become more difficult to find, exploration departments will demand that wildcat wells be drilled with water-based muds, to allow for adequate formation evaluation of possible producing horizons. Progressive drilling departments, not wanting to return to slow-drilling, dispersed clay-based muds, will turn to polymers to accomplish these objectives.

However, the polymers will not be extenders, which are used in minuscule quantities anyway. Drillers will want polymer viscosifiers capable of cleaning the well bore of drill cuttings and suspending weight materials such as barite and hematite. Drillers will want filtration control and a valid test procedure for fluid loss (polymer muds go right through API filter paper, but not through most formation rocks). Drillers will want resistance or tolerance to well-bore contaminants frequently encountered such as salt, anhydrite, or calcium and magnesium salts. Drillers will want stability at the high well-bore temperatures (250–450 °F) found at depth.

Prediction 3. Prediction 2 describes what the oil well drilling operators will likely want. Prediction 3 is that the operators will get what they want.

We are already making high temperature stable, water-insoluble polymers that 20 years ago were considered impossible. Some water-insoluble polymers are presently being modified to render them water soluble. I attribute the current thermal limitations of currently available drilling polymers to the test conditions traditionally applied, i.e., 1000 psi at 300–500 °F. The pressure test conditions must be increased some 10-fold if we are to understand how a polymer will likely behave in a deep hot well bore.

I predict that when these changes are made, some polymers that were found unstable at 300 °F and 1000 psi will appear suitable at 400 °F and 10,000 psi.

Prediction 4. Therefore, within the next 5–10 years, with the increased usage of high-temperature polymer muds in exploratory wells, the use of oil-emulsion muds should diminish for development wells; thereby, the polymer market will be greatly expanded. For we are no longer talking about polymer concentrations of 0.05 lb/bbl but 100 times that amount, and instead of 1500-bbl mud systems for the typical well now, we are projecting twice that volume for the deeper wells required in the future.

Conclusion

A number of conclusions can be drawn from the discussion presented in this chapter. One conclusion is that polymers may replace bentonite as the primary viscosifier in drilling mud. The reason is that because bentonite is so detrimental to penetration rate (Figure 2), if the quality continues to deteriorate to a point where low-solids, nondispersed muds cannot be run, more expensive polymers become economical because of high drilling rig operating costs. Even if this situation does not happen, polymers have a bright future in the makeup of drilling fluid systems.

This chapter has suggested that effective polymers must be able to perform one or more of five functions in a drilling mud: (1) a flocculent for drilled solids, (2) an extender for bentonite, (3) a viscosifier, (4) an agent to reduce filtration loss, and (5) a shale stabilizer.

No one polymer is likely to perform equally well at all functions, nor is this necessarily desirable. Polymer drilling fluid systems are therefore formulated with two or three different polymers, each designed to perform specific functions.

The chapter has discussed the limitation of polymer flocculents and extenders. Polymer viscosifiers must exhibit shear thinning behavior, while not being overpowered by the drilled solids making mud and thus allowing the solids content to exceed 5% by volume. Polymer viscosifiers, alone or in combination with other materials, must exhibit gel structure capable of suspending weighting agents, such as barite or hematite.

The chapter has suggested that the current API test procedures are not adequate for research development and evaluation of polymer mud systems. Of particular concern is the performance at high temperatures, which needs to be investigated at higher pressures than the API tests, and the filtration properties, which must be carried out by using porous media rather than API filter paper.

Literature Cited

1. Vold, Margorie J.; Vold, Robert D. *Colloid Chem.*; Reinhold: New York, 1964.
2. Rogers, Walter F. *Composition and Properties of Oil Well Drilling Fluids*; Gulf Publishing: Houston, 1953.

3. Kennedy, H. T.; Teplitz, A. J. U.S. Patent 2 337 296, Issued Dec. 21, 1943.
4. Wagner, C. R., U.S. Patent 2 425 768, 1947.
5. Gallus, J. P.; Lummus, J. L.; Fox, J. E., Jr. *Use of Chemicals to Maintain Clear Water for Drilling*; AIME Petroleum Transactions, American Institute of Mechanical Engineers, Dallas, TX, 1958, Vol. 213.
6. Scott, P. P.; Anderson, D. B.; Park, A. U.S. Patent 3 017 351, 1962.
7. Lummus, J. L.; Fox, J. E., Jr.; Anderson, D. B. *Oil and Gas J.* 1961, Dec. 11, pp 87-91.
8. Metzner, A. B. *Non-Newtonian Technology*, Advances in Chemical Engineering, Academic: New York, 1956; pp 77-153.
9. API Bulletin RP13-B, American Petroleum Institute: Dallas, TX, 1984.
10. Scott, P. P. U.S. Patent 3 070 543, 1962.
11. Lummus, J. L. "Drilling Optimization" *J. Pet. Technol.* Nov. 1970.
12. Park, Arthur; Scott, P. P.; Lummus, J. L. *Chemical and Mechanical Means of Maintaining Low Solids Drilling Fluids*; API Paper 851-34-I, March 31-April 1, 1960, Wichita, Kansas.
13. Estes, J. C. "Techniques of Pilot-Scale Drilling Research"; *Transactions of ASME. J. Pressure Vessel Technol.*, May 1978.
14. Anderson, D. B.; Estes, J. C. "Review of Low Solids Mud Control Gives New Insights"; *World Oil*, April 1981.
15. Jones, F. O., Jr. "New Fast Test Measures Bentonite in Drilling Mud"; *Oil and Gas J.* June 1, 1964.
16. Lummus, J. L. U.S. Patent 3 323 603, 1967.
17. Lummus, J. L. U.S. Patent 3 558 545, 1971.

RECEIVED for publication September 13, 1984. ACCEPTED August 14, 1985.

Applications of Water-Soluble Polymers as Shale Stabilizers in Drilling Fluids

R. K. Clark

Production Operations Research Department, Shell Development Company,
Houston, TX 77001

Water-soluble polymers are often used in oil and gas well drilling fluids as stabilizers for water-sensitive shales encountered in subsurface formations. Polymer chemistry, ionic character, degree of charge, molecular weight, and other factors play a role in determining the effectiveness of a polymer as a shale stabilizer. Some of the more common polymer types that have been used, with varying degrees of success, are natural gums (guar, xanthan, and flaxseed), cellulose derivatives (carboxymethyl and hydroxyethyl), starches, and high molecular weight acrylate-acrylamide copolymers. This chapter reviews laboratory test methods for evaluating polymer performance, presents results from one of the methods described, and discusses possible shale stabilizing mechanisms.

APPPLICATIONS OF WATER-SOLUBLE POLYMERS in oil and gas well drilling fluids include use as viscosity builders, filtration control agents, flocculents, deflocculents, and shale stabilizers. Shale stabilizers may be one of the least understood uses of polymers in drilling fluids. Problems arising from borehole instability resulting from adverse interactions between the drilling fluid and clay-bearing shales are among the more costly difficulties that occur in drilling operations. Maintenance of a stable borehole is one of the many functions that a drilling fluid must fulfill. Selection of the proper polymer for incorporation into the system can often reduce or eliminate shale stability problems, while an improper choice can increase well costs significantly.

Drilling Fluids: Functions and Properties

The most important functions of a drilling fluid are to (1) remove formation cuttings from the bottom of the hole and transport them to the surface, (2) provide sufficient hydrostatic pressure against the formation to prevent influx of formation fluids, (3) stabilize downhole formations and

0065-2393/86/0213-0171\$06.00/0
© 1986 American Chemical Society

prevent hole collapse, (4) prevent loss of fluid to permeable formations, (5) cool and lubricate the bit and drill string, and (6) help suspend the weight of the drill string and casing (1). The fluid is expected to perform these and other functions simultaneously.

Drilling fluids are pumped down the well through a hollow drill string, out the drill bit at the bottom of the hole, and back up to the surface in the annulus formed by the borehole wall and the rotating drill string. The fluid is passed through a series of vibrating screens, hydrocyclones, and centrifuges on the surface to remove formation cuttings, which are discarded. One or more additives are then used to return the system to a desired set of physical and chemical properties, after which the fluid is pumped back down the well to repeat the cycle. The fluid is a dynamic, circulating system that changes from day to day in response to the drilling conditions being experienced. The drilling fluid system may be used for a few days, weeks, or months and in some cases is reconditioned for use on subsequent wells.

Drilling fluids are most frequently formulated with water as the continuous phase (2). Viscosity-building clays or polymers and various organic chemicals are added for controlling the rheological and filtration properties. Water-soluble polymers used for rheological and filtration control include (carboxymethyl)- and (hydroxyethyl)cellulose, xanthan gum, starch, and acrylate-acrylamide copolymers of various compositions and molecular weights. Naturally derived complex polymers such as lignosulfonates, lignites, and plant tannins may be added to modify the rheological and filtration behavior of added clays.

The composition of the water phase ranges from fresh to highly saline solutions that may contain substantial levels of soluble calcium and magnesium ions. Water-based fluids are commonly maintained at an alkaline pH with sodium hydroxide, calcium hydroxide, or potassium hydroxide. The resulting complex aqueous solution constitutes the environment in which commercial clays and polymers must work and be effective.

Powdered, high specific gravity solids such as barite or hematite are added to reach the desired fluid density, which may range from 1 to 2.5 g/cm³. The density requirement is dictated by the formation pressures that are encountered while the well is being drilled and by the earth stresses imposed on the formation. A high-density drilling fluid may contain up to 40 vol % suspended solids (formation solids, commercial clays, and weighting materials). The specific composition of the fluid depends on the downhole conditions being experienced. Temperatures exceeding 205 °C (400 °F) and pressures up to 140 MPa (20,000 psi) are not uncommon in deep wells. Water-in-oil emulsion (oil continuous phase) fluids are often used for borehole stability and deep well drilling but are outside the scope of this chapter.

Shale Composition and Properties

Shales are fine-grained sedimentary rocks that contain various clay minerals, quartz, feldspar, calcite, etc. The interaction between a drilling fluid and a shale is dominated by the response of the clay minerals in the shale to contact by the water phase of the fluid. The most water-sensitive clay minerals are the smectites (traditionally known as montmorillonite) and smectite-illite mixed-layer clays. Shales containing large amounts of illite can also exhibit extreme water sensitivity. Chlorite and kaolinite are commonly found in subsurface shales but are rarely considered detrimental to borehole stability and drilling operations.

The clay minerals are colloidal, high surface area, layered aluminosilicates that frequently occur in nature as assemblages of thin plate-shaped particles stacked face to face like pages in a book (3). The planar surfaces carry a negative charge arising from substitution of lower valent cations in the clay crystal lattice. The edges may be positively or negatively charged depending on the environment: positive at low pH and negative at high pH. Cations associated with the planar surfaces may be loosely held and readily exchanged by other cations or may be tightly held and nonexchangeable. Water can be drawn into the interlayer region of some clays by hydration of the exchange cations and the silicate surface. An osmotic force arising from differences between the activity of the interlayer water and that of the drilling fluid can result in increases in layer separation beyond that of the initial surface hydration.

Surface area and cation-exchange capacity are key properties that determine the response of a clay mineral to water. The same is true of a shale (4). Shales high in smectite or smectite-illite mixed-layer clays are typically young marine shales that swell and may disperse completely in fresh water. These are the "gumbo" shales common along the Gulf Coast that are characterized by high surface area and moisture content, moderate to high cation-exchange capacity, and low mechanical strength. At the other end of the scale are the hard, black illitic shales found from Texas to the Rockies and in many deep wells. These shales are older and much more highly compacted than the soft gumbo shales even though they may be found at or near the surface. Although the total clay mineral content may exceed 50%, the illitic shales are low swelling and nondispersive and are characterized by low surface area, cation-exchange capacity, moisture content, and high mechanical strength. Immersion of a large competent piece of a hard illitic shale in freshwater may result in disaggregation along fracture planes into firm shale splinters.

The box lists the parameters often measured on shale samples for the purpose of characterization and classification. By classifying shales, one may be able to estimate the drilling fluid chemistry required to drill a given shale problem-free (4).

Parameters Measured for Shale Characterization

Geologic age and depositional environment
Mineralogy by X-ray diffraction (clay content and composition)
Bulk and grain density
Cation-exchange capacity
Surface area
Moisture content
Composition of interlayer water
Water absorption-swelling properties
Dispersibility
Mechanical properties (compressive and tensile strength)

Drilling Fluid–Shale Interactions

The water phase of the drilling fluid can dramatically alter the properties of exposed subsurface shales. The effect ranges from swelling and dispersion of soft shales to mechanical spalling of hard shales, all of which can severely reduce drilling efficiency. The composition of the water phase plays an important role in determining the response. Fresh-water has the most pronounced effect: maximum alteration of the shale properties results. Increasing the salinity reduces the hydration and swelling resulting from water absorption by the shale. Because the mechanical strength of the shale is inversely proportional to the moisture content, reducing water absorption will retard degradation of the mechanical properties and promote shale stability.

Sodium chloride, potassium chloride, gypsum, and lime are often used to reduce the rate and magnitude of water absorption by shales. Both laboratory and field experiences indicate a preference for potassium over sodium for shale stability (4, 5). Calcium ions derived primarily from gypsum and lime are also preferred over sodium ions, but are less compatible with the other fluid additives. Typical concentration ranges found for the various cations when used for shale stability are 100–1000 mg/L for calcium, 2000–100,000 mg/L for potassium, and 12,000–125,000 mg/L for sodium.

Polymers for Shale Stability

Added electrolyte may not provide adequate stability, and a polymeric material is often needed. A variety of water-soluble polymers have been touted as shale stabilizers for use in drilling fluids. The polymer may be used with one of the cation stabilizers as mentioned above or it may be

used alone, as it often performs other functions in the fluid as well. Selection of the polymer must be not only on the basis of its shale stabilizing ability, but also on the basis of its compatibility with the other drilling fluid components and with the downhole drilling conditions, particularly temperature.

Polymers used as shale stabilizers in field applications include natural, microbial, and derivatized polysaccharides and synthetic high molecular weight acrylic copolymers. Prominent among the polysaccharides are (carboxymethyl)cellulose (6), (hydroxyethyl)cellulose (7), starch (8), and gums such as xanthan (5), flaxseed (9), and guar. Acrylate-acrylamide copolymers are used in drilling fluids for many purposes including shale stabilizers (10, 11). The specific application depends on the molecular weight and the degree and magnitude of charge on the polymer. These and other polymers not commonly found in the oil field will be discussed in terms of laboratory performance as shale stabilizers in the following sections.

Laboratory Test Methods for Shale Stabilization

A large number of methods have been used to assess the performance of drilling fluid additives as shale stabilizers. Unfortunately, no standard method is widely accepted in the industry. The diversity of test methods is partly due to the inability to accurately simulate the downhole environment in the laboratory. Evaluation of drilling fluids and additives is also complicated by the difficulty in obtaining suitable shale samples in a large enough quantity for testing. Although shale is encountered in virtually every well, the state of the shale cuttings collected at the surface usually renders them unsuitable for testing. Cores are rarely taken in shale except by mistake or occasionally when shale problems are severe. Surface shale outcrops are badly weathered and may not be representative of subsurface formations. In spite of the difficulties, sufficient shale can often be obtained to allow stability tests to be conducted, although some alteration from in situ properties is probable.

Laboratory testing of shale-fluid interactions includes both static and dynamic methods. Static methods include immersion-soaking, water absorption (15), and swelling (linear volumetric) (5, 12, 14) techniques. Static tests assess changes in the physical size or structure of the shale during contact with the test fluid. Swelling tests using strain gauges have been described for low- (5), medium- (12), and high-pressure (13, 14) conditions. Fluid absorption tests can be used to measure the rate and magnitude of water uptake under a variety of conditions (15). Salt and cation effects are readily evaluated in static tests, but stabilizing polymers may have little effect on the swelling properties of shales, particularly when tested under pressure (12).

Dynamic methods include immersion-stirring (16), immersion-tumbling (5), capillary suction time (15), triaxial flow (17), and microbit drilling machine (18) techniques. Agitation (stirring or tumbling) of shale cuttings in a test fluid followed by sieving is used to determine the particle size and integrity of the sample after contact (5, 9). The dispersibility of the shale can be assessed by the capillary suction test (15). The presence of polymers can give misleading results in the capillary suction test as the movement of filtrate through the filter media is influenced by solution viscosity. Wenzel used an apparatus that stirs the test fluid over a fixed shale sample to determine the ability of polymers and salts to prevent softening and cracking of shales (16). Stirring- and tumbling-type tests appear to be useful for determining the performance of polymers as shale stabilizers, although the test conditions do not simulate the downhole environment.

More sophisticated dynamic tests flow drilling fluid through shale specimens with (17) or without (18) the shale under stress. Such tests assess the ability of the fluid chemistry to maintain the integrity of the shale under conditions that more nearly approximate the downhole conditions. Shale samples used in the flow tests are usually formed in the laboratory in a compaction cell as natural samples of sufficient size and integrity are rarely available for machining to the dimensions needed in the test. The triaxial shale tester described by Darley (17) requires a 5-cm-diameter by 2.5-cm-long sample with a 0.64-cm hole in the center through which the test fluid is pumped. The test specimens used by Simpson (18) are even larger. The shale stabilizing ability of polymers is more properly evaluated in flow tests than in the static or tumbling-stirring tests, although questions arise over the effect of reconstituting the shale samples. Flow tests require rather complicated equipment, which is currently of limited availability.

Laboratory Performance of Polymers as Shale Stabilizers

The performance of polymers as shale stabilizers discussed in this section is based on the results of flow tests in the triaxial shale tester described by Darley (17). Many different polymers have been evaluated by using different types of shales and test conditions. Data on only two shales are given here because polymer performance is not influenced greatly by shale composition. Shales chosen for this study are Atoka, a hard, illitic shale from Oklahoma; and Pierre, a relatively soft shale containing high levels of swelling clays. The clay mineral composition of the shales is given in Tables I and II.

Table I lists triaxial test data using Atoka shale and a number of commercial polymers, many in use as drilling fluid additives. Table II gives similar data for Pierre shale. Potassium chloride was used in most

Table I. Triaxial Test Results with Atoka Shale

<i>Polymer</i>	<i>Polymer Concn (g/L)</i>	<i>KCl Concn (g/L)</i>	<i>Time to Failure (min)</i>	<i>Erosion (%)</i>
Polysaccharides				
Potato starch	0.0	30	5	21
	15.0	30	110	9
	50.0	30	1371+	<1
Hydroxypropyl-substituted guar	0.7	30	83	9
	1.5	30	1380+	<1
Xanthan gum	1.5	30	21	11
	2.9	0	34	12
	1.4	30	38	9
(Carboxymethyl)cellulose ^a				
Acrylate-acrylamide copolymers				
0-10% acrylate ^b	1.5	30	100 ^c	12 ^c
30% acrylate ^d	1.5	30	115	11
30% acrylate ^e	0.7	30	1400+	<1
	1.5	0	1440+	—
	1.5	30	1420+	<1
70% acrylate ^f	11.0	0	761	—
AMPS ^g	2.0	30	1488+	2
Other synthetic polymers				
Polyethylene oxide ^h	1.5	30	55	12
Methyl vinyl ether- maleic anhydride				
Low viscosity	4.3	0	100	—
Medium viscosity	4.3	0	321	—
High viscosity	4.3	0	1267	—
	1.5	30	1380+	1
Vinyl acetate- maleic anhydride	1.5	30	1410+	<1
Vinyl ether- vinylpyrrolidone	3.0	30	6	17

NOTE: The test shale used was Atoka (22% illite, 25% kaolinite, and 3% chlorite). The stress level was 3500 psi. + designates no failure at the test time indicated. ^aThe degree of substitution is 1.0. ^bThe molecular weight is $(1-12) \times 10^6$. ^cThis value is an average. ^dThe molecular weight is 1×10^6 . ^eThe molecular weight is 2×10^6 +. ^fThe molecular weight is 5×10^5 . ^gAcrylamide-methylpropanesulfonate. ^hThe molecular weight is 6×10^6 .

of the tests, as the presence of potassium ion is highly beneficial for stabilizing water-sensitive shale. Note that the performance of some polymers improves with the addition of salt although performance diminishes for others. Stress conditions on the test specimens were 24 MPa (3500 psi) on Atoka shale and 17 MPa (2500) on Pierre shale. A flow rate of 4 m/s (800 ft/min) through the 0.64-cm hole was chosen to quickly erode any shale weakened by the test fluid. Radial collapse of the test specimen will occur when it can no longer withstand the applied stress. The test is either terminated by sample failure or after about 1400 min in

Table II. Triaxial Test Results with Pierre Shale

<i>Polymer</i>	<i>Polymer Concn (g/L)</i>	<i>KCl Concn (g/L)</i>	<i>Time to Failure (min)</i>	<i>Erosion (%)</i>
Polysaccharides				
Hydroxypropyl-substituted guar	0.0	30	30	28
	3.0	0	720	23
(Carboxymethyl)cellulose	3.0	0	676	16
	3.0	30	284	16
(Hydroxyethyl)cellulose	3.0	0	720	23
	3.0	30	1319+	6
Xanthan gum	3.0	0	438	19
Flax meal (10% gum)	15.0	30	203	24
	30.0	30	339	21
	45.0	30	1325	13
Acrylate-acrylamide copolymers				
30% acrylate ^a	0.7	30	834	19
	1.5	30	1383+	1

NOTE: The test shale used was Pierre (21% smectite, 11% illite, and 4% chlorite). The stress level was 2500 psi. + designates no failure at the end of the test time indicated. ^aThe molecular weight is $2 \times 10^6+$.

the absence of failure. An effective polymer is one that will result in a long run time without failure and with little sample erosion.

The results given in Tables I and II can be used to identify polymers that appear to be effective in stabilizing shale and those that are ineffective. Table III contains a list of polymers found to be effective in triaxial tests as indicated by the data in Tables I and II and other data not shown. Table IV lists polymers found ineffective in similar testing. The nonionic polysaccharides (hydroxyethyl)cellulose, hydroxypropyl-substi-

Table III. Polymers Found Effective for Stabilizing Shale

<i>Polymer</i>	<i>Molecular Weight</i>	<i>Min Effective Concn (g/L)</i>
Polysaccharides		
(Hydroxyethyl)cellulose	700,000	0.7
Hydroxypropyl-substituted guar	200,000	1.5
Flaxseed gum	—	3.0
Potato starch	—	30.0
Acrylate-acrylamide copolymers		
20-40% acrylate	>2,000,000	0.35
AMPS ^a	—	2.0
Vinyl acetate-maleic anhydride	—	0.7
Methyl vinyl ether- maleic anhydride	high viscosity	0.7

^aAcrylamide-methylpropanesulfonate.

Table IV. Polymers Found Ineffective for Stabilizing Shale

<i>Polymer</i>	<i>Molecular Weight</i>	<i>Max Test Conc'n (g/L)</i>
Polysaccharides		
(Carboxymethyl)cellulose ^a	700,000	3.0
Xanthan gum	5,000,000	3.0
Acrylate-acrylamide copolymers		
0-10% acrylate	1,000,000-12,000,000	3.0
30% acrylate	<1,000,000	1.5
70% acrylate	500,000	10.0
Other synthetic polymers		
Methyl vinyl ether-maleic anhydride	medium and low viscosity	4.3
Vinyl ether-vinylpyrrolidone	—	3.0

^aThe degree of substitution is 1-1.2.

tuted guar, and flaxseed gum (slightly anionic) and a relatively narrow range of acrylate-acrylamide copolymers, more commonly known as partially hydrolyzed polyacrylamides, appear to have the most utility as shale stabilizers. These materials are effective at low concentrations in the drilling fluid and are available at reasonable cost. Potato starch is also effective but only at very high concentrations. The acrylamide-methylpropanesulfonate (AMPS)-type polymers look promising but as yet have found only limited use in drilling applications. The maleic anhydride copolymers perform well but are not currently used in drilling fluids because they are not cost effective compared to other commercial and readily available polymers.

Shale Stabilizing Mechanisms

The specific mechanism by which polymers stabilize shales has not been studied in detail. Test shales and polymers, most of which are commercial materials, are rarely well characterized, and test methods are primarily designed to determine performance. Thus, only limited information on the stabilizing mechanism is available. Descriptions of shale stabilization by water-soluble polymers range from lowering the erosive action of the fluid at the shale surface by friction reduction to encapsulation of the shale by a polymer coating that prevents disintegration. The true mechanism probably lies somewhere in between and may depend on the type of polymer involved.

That polymers can adsorb on shale surfaces to retard degradation and dispersion is well-known (19). Nonionic polymers such as (hydroxyethyl)cellulose can adsorb on shale surfaces regardless of the surface

charge. Anionic polymers such as a partially hydrolyzed polyacrylamide must either adsorb on positive edge sites (which probably do not exist in an alkaline media), associate with multivalent cations, or link to the clay surface through ligand exchange with aluminum at an edge site (20, 21). Adsorption of anionic polymers on clays under alkaline conditions is rather low, but does increase as the ionic strength of the medium increases (22). Provided the polymer has a high molecular weight and is rather flexible, each polymer molecule can attach to several exposed clay platelets; this attachment links them together and retards layer separation.

Shale exposed to the drilling fluid on the borehole face is confined on all but one side. Thus, only one surface must be protected. Stabilizing polymers appear to adsorb rapidly on this exposed surface to provide the integrity required to prevent erosion by the flowing fluid. This action, when combined with a stabilizing salt, particularly a potassium salt, can reduce or prevent swelling and weakening of the shale in contact with the drilling fluid. Polymers are most certainly confined to the borehole surface as their size is large relative to the very small pore openings in the shale. Only water and some dissolved salts can enter the interlayer regions of the shale. Sodium chloride solutions can offset part or all of any osmotic swelling force, but potassium because of its small hydrated ion size can more easily penetrate the interlayer region and become fixed on the clay planar surface and eventually reduce the interlayer distance. Potassium ions have a favorable size for the surface hexagonal sites created by the arrangement of silicate tetrahedrons and so are the preferred monovalent cations for ionically bonding clay layers together. Potassium ion diffusion and fixation in the interlayer region are slow relative to polymer adsorption at the borehole surface. The combination of a fast acting polymer and a slower cation-exchange-fixation process appears to explain many of the laboratory observations reported in the literature.

Field Applications of Stabilizing Polymers

Many of the polymers listed in Table IV have had successful applications in stabilizing problem shales. Difficulties arise in attributing improved borehole stability to the action of the polymer or to some other factor in the drilling process. Thus, claims of stabilization for a particular polymer by one party are disputed by others. The lack of a widely accepted laboratory test procedure undoubtedly adds to the confusion.

The partially hydrolyzed polyacrylamides appear to have found the widest acceptance as shale stabilizers with many applications in both potassium chloride and freshwater systems. Some cationic polyacrylamides are finding application in highly saline fluids even though they are

not compatible with most drilling fluid additives. These polymers are available in a liquid emulsion form, which greatly aids in their addition to the drilling fluid. The cellulose polymers, starches, and xanthan gum are often added for shale stability in addition to the other functions they are expected to fulfill. Shale stabilizing polymers appear to have been most effective in the harder, less dispersive shales. Maintenance of polymer concentration and drilling fluid chemistry in soft, gummy shales is very difficult and can result in excessive treatment costs. Considerable research is still required to determine the specific mechanism by which polymers protect water-sensitive shales and to provide better guidance on polymer selection.

Literature Cited

1. Gray, G. R.; Darley, H. C. H.; Rogers, W. F. *Composition and Properties of Oil Well Drilling Fluids*, 4th ed.; Gulf Publishing: Houston, TX, 1980.
2. Clark, R. K.; Nahm, J. J. *Encyclopedia of Chemical Technology*, 3rd ed.; Wiley: New York, 1982; Vol. 17, p 143.
3. Steiger, R. P. *J. Pet. Technol.* **1982**, *34*, 1661.
4. Van Olphen, H. *An Introduction to Clay Colloid Chemistry*, 2nd ed.; Interscience: New York, 1977.
5. O'Brien, D. E.; Chenevert, M. E. *J. Pet. Technol.* **1973**, *25*, 189.
6. Shell, F. J. *Drilling Nov.* **1969**, 47.
7. Darley, H. C. H. *Pet. Eng. Sept.* **1976**, 49.
8. Kennedy, J. L. *Oil and Gas J.* **May 29 1972**, 41.
9. Anderson, D. B.; Edwards, C. D. *Pet. Eng. Sept.* **1977**, 105.
10. Clark, R. K.; Scheuerman, R. F.; Rath, H.; Van Laar, H. *J. Pet. Technol.* **1976**, *28*, 719.
11. Mickey, V. *Drill Bit Dec.* **1981**, 31.
12. Roehl, E. A.; Hackett, J. L. SPE Paper 11117, Presented at the Society of Petroleum Engineers Annual Meeting, New Orleans, LA, Sept. 1982.
13. Chenevert, M. E. *J. Pet. Technol.* **1970**, *22*, 1141.
14. Bates, T. R.; Bonner, R. B.; Clark, R. K. U.S. Patent 4 359 901, 1982.
15. Wilcox, R.; Fisk, J. *Oil and Gas J.* **Sept. 12 1983**, 106.
16. Wenzel, F. *Erdoel-Erdgaz.-Z.* **1979**, *95*, 345.
17. Darley, H. C. H. *J. Pet. Technol.* **1969**, *21*, 883.
18. Simpson, J. P. *J. Pet. Technol.* **1971**, *23*, 1294.
19. Theng, B. K. G. *Formation and Properties of Clay-Polymer Complexes*; Elsevier: Amsterdam, 1979.
20. Theng, B. K. G. *Clays Clay Miner.* **1982**, *30*, 1.
21. Siffert, B.; Espinasse, P. *Clays Clay Miner.* **1980**, *28*, 381.
22. Espinasse, P.; Siffert, B. *Clays Clay Miner.* **1979**, *27*, 279.

RECEIVED for review January 7, 1985. ACCEPTED August 14, 1985.

Influence of Water-Soluble Polymers on the Filtration Control of Bentonite Muds

S. A. Heinle, S. Shah, and J. E. Glass

Department of Polymers and Coatings, North Dakota State University, Fargo, ND 58105

The adsorption of various polysaccharides on peptized montmorillonite is examined, and the influence of the polysaccharides on the filtration control properties of polymer-modified bentonite drilling muds (at 4.2 wt % or 14.4 lb/bbl) is studied as a function of increasing solution salinity. The studies indicate that adsorption per se is detrimental to filtration control, but adsorption is necessary in saline solutions to inhibit loss of fluid to the formation. The ability of an anionic polymer to effect filtration control with increasing salinity is related to the nature and amount of anionic substituent on the polymer (i.e., the total ionization of the macromolecule).

WATER-BASED DRILLING FLUIDS, in the 1950s, were thickened with bentonite at an approximate concentration of 8.4 wt % (or 28.8 lb/bbl, the units commonly used in oil field operations). At this level, bentonite, an alumina-silicate, smectite clay with platelet geometry, provides thick aqueous slurries that are very shear thinning. The viscosity is low at the drill bit; this low viscosity minimizes the torque necessary for operation, and the viscosity is high in other areas of the well bore where deformation rates are low. The high viscosities are necessary for lifting drill solids to the surface. Yield stress values, currently viewed as a reflection of the magnitude of the viscosity at very low shear rates, are important in inhibiting the sedimentation of dispersed components. This carrying capacity is particularly important if a high-density component such as barium sulfate is added to the bentonite slurry to balance high overburden pressures in the formation.

In the drilling of a well bore, many porous regions are encountered. It is important that the viscosity of the fluid not increase unexpectedly because of partial loss of fluid to the subterranean formation. Bentonite

0065-2398/86/0213-0183\$06.00/0
© 1986 American Chemical Society

clays in freshwater are effective in controlling the amount of fluid loss to the formation; however, filtration control with bentonite slurries is lost when saline connate waters are encountered. The ability of water-soluble polymers to promote filtration control in modified bentonite slurries exposed to increasing salinity and its relationship to polymer adsorption will be the focus of this chapter. The effectiveness of polymer-modified bentonite slurries in relation to straight bentonite slurries and to straight polymer-thickened fluids will be addressed peripherally.

Experimental Section

Polymer-Modified Bentonite Slurries. Water-soluble polymer (W-SP) modified sodium bentonite slurries were studied at a 4.2-wt % (14.4-lb/bbl, aqueous slurry) concentration, a common industry practice. All polymers were employed at 0.5 lb/bbl (0.14 wt %) except in certain studies that are indicated. The viscosities and fluid loss behavior were determined with a Fann 35 viscometer and American Petroleum Institute (API) standard fluid loss control units, both supplied by the Magcobar Division of Dresser Industries. Photographs of the equipment are given in Chapter 12. The W-SPs examined were supplied by commercial producers (1). The polymer-modified bentonite drilling fluids were prepared by dispersing bentonite in aqueous solution under high-shear conditions (Waring Blender). The W-SPs prepared in 1–2-wt % aqueous solutions were added to the dispersed clay slurries. Initial studies were in deionized water. In subsequent evaluations, three salt levels were employed: 3.3, 6.6, and 13.2 wt % (10:1 ratio by weight of sodium chloride to calcium chloride).

Polymer Dissolution. All W-SPs contained adsorbed water (approximately 5 wt %) and inorganic salts; some polymers contained microorganism debris. The ash content of each polysaccharide was determined by method B of ASTM^{*}D 3516-76; the water content was determined by thermal gravimetric analysis. The ash and water contents were taken into account in preparing the polymer solutions. The salts were extracted with an aqueous (25 vol %)-2-methyl-2-propanol (75 vol %) mixture and vacuum-dried. Microorganism debris was removed by filtration through Millipore polyacetate filters. Concentrated W-SP aqueous solutions were prepared by adding the required weight of dried polymer to deionized water under vigorous agitation (blender) for approximately 30 s. The polysaccharide-dispersed slurries were immediately added to 700 cm³ of water and stirred vigorously (but less so than in the blender) by blade impellers until dissolution occurred. The adsorption studies were undertaken at equal viscosities using *Xanthomonas campestris* polysaccharide (XCPS) (2500 ppm) as the standard. Viscosities (1 s⁻¹) were determined with a Cone/Plate Brookfield RVT viscometer (cone angle of 3° and diameter of 4.8 cm). In the salinity studies, concentrated freshwater solutions were diluted with concentrated saline solutions to obtain final polymer-bentonite slurries of variable salinity.

Clay Preparation. Bentonite, a commercial product consisting principally of sodium montmorillonite, was obtained from Dresser Industries, Magcobar Division (Houston, TX). The material was ground and sieved. The clay was identified by using the JCPDS[†] powder diffraction files (2). One percent aqueous

^{*}American Society for Testing and Materials

[†]Joint Committee Powder Diffraction Standards

bentonite suspensions were prepared and kept for 24 h to remove heavier particles such as quartz and iron oxide. The procedure was repeated twice. Homionic sodium- and potassium-saturated clays were prepared by treating 200 mL of a 1% clay suspension with metal chloride solutions (200 mL; 1 M) for 24 h at pH 4 (acetic acid). The procedure, repeated twice, was followed with deionized water washings (four times) to remove residual salt. The final suspension was made under high shear (blender). In the filtration control studies, bentonite was used as received. The peptized sodium montmorillonite in saline solutions containing only sodium chloride was employed in the adsorption studies.

Adsorption on Peptized Montmorillonite Surfaces. In adsorption studies from saline environments, the W-SP and peptized montmorillonite must be prepared in freshwater and each added to the saline solution.

Polyelectrolytes will frequently not "yield" the same viscosity as when they are dissolved in freshwater. Montmorillonite will flocculate in saline solutions. With freshwater mixing of components, reproducible results were obtained in most of the saline studies. The components were mixed in glass ampules. After component mixing, agitation of the slurry was maintained with gentle stirring via micromagnetic polytetrafluoroethylene bars. The clay was separated by centrifugation and the polymer concentration was determined by colorimetric measurement (3). The amount of polysaccharide adsorbed was calculated by using a standard calibration curve for each polysaccharide. The effect of dilution was considered in quantification of polymer loss. Clay suspension concentrations were determined by drying 25 mL of the dispersion for 26 h at 110 °C.

Results and Discussion

General. The relative drilling rates with the three types of thickened fluids discussed in the introduction have been quantified in Chapter 9 and in the patent literature (4) (Table I). Drilling rates are highest when only polymer is used; however, thermal oxidative and mechanical degradation are observed with polymer-thickened aqueous fluids. The slowest drilling rate is observed with a straight bentonite mud. An additional disadvantage of the straight bentonite mud type is the difficulty in removal of drill solids when they are surfaced.

The mechanical degradation of straight polymer-thickened fluids has been related to extensional deformations (5, 6) and to the conforma-

Table I. Average Drilling Fluid Cost and Penetration Rate Through Interval Drilled

<i>Sample No.</i>	<i>Type of Drilling Fluid</i>	<i>Drilling Fluid Cost (\$/ft)</i>	<i>Penetration Rate^a (ft/h)</i>
41	polymer-bentonite	5.12	5.37
42	polymer-bentonite	6.08	5.57
43	polymer-bentonite	6.33	5.77
44	invert emulsion (water in oil)	8.50	4.77
45	low-solids shale control drilling fluid	3.33	6.66

^aFrom reference 4.

tion of the polymer in solution (5-7). When polymers are utilized in various recovery processes, synthetic W-SPs are very mechanically unstable. Carbohydrate polymers are generally used when mechanical stability is desired. Fermentation polymers such as XCPS or *Sclerotium glaucanum* polysaccharide (SGPS) (discussed in Chapter 1) generally have greater stability than other carbohydrate polymers. This property has been related to the greater conformational rigidity (8) and dynamic uniaxial extensional viscosity (DUEV) of fermentation polymers (9). DUEV data for the classical W-SPs are as follows [W-SP, concentration (wt %), and DUEV (Pa·s)]: XCPS, 1.00, and 0.24; HEC, 1.00, and 1.22; and POE, 0.10, and 3.62. The rate of extension for the DUEV data was 100 s^{-1} .

The slower drilling rates observed in straight bentonite formulations are associated with their elasticity. The elasticity of a fluid can be estimated from either first normal stress differences (N_1) or storage modulus (G') response as a function of measurement frequency or time after deformation (10, 11). Variations in N_1 as a function of shear rate among the different types of fluid are illustrated in Figure 1. The straight bentonite mud was weighted with barium sulfate; the polymer-thickened

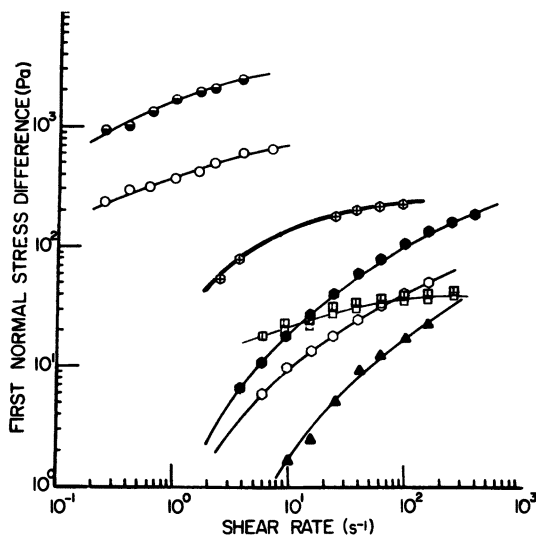


Figure 1. First normal stress difference (Pa) dependence of the shear rate (s^{-1}) of fluids commonly used as drilling fluids. Key: bentonite (8.4 wt %) containing, ●, 4.2 wt % BaSO_4 and, ○, neat; bentonite (4.2 wt %) containing, ⊕, HEC (0.29 wt %; $M_S = 2.0$; $M_r = 10^5$), □, 0.29 wt % XCPS, and, ○, 0.58 wt % XCPS; and clay-free thickened fluids containing HEC ($M_r = 10^6$) at 0.58 wt % containing, ●, 42 wt % CaCl_2 and, ○, neat and at 0.29 wt % containing, ▲, 42 wt % CaCl_2 .

fluid was weighted with soluble calcium chloride. The differences in N_1 values parallel the relative drilling rates. The elastic behavior of clays is also evident in their G' response after deformation (Figure 2); the data illustrated are taken from the response of a clay-thickened coating formulation. The high elastic response immediately after deformation is not observed in water-soluble polymer-thickened coating formulations (discussed in Chapter 21).

A compromise in performance properties intermediate between those of a straight polymer and those of a straight bentonite mud is observed if the amount of bentonite is reduced to half its original concentration and the drop in viscosity is regained by polymer addition. For example, thermal oxidation, mechanical degradation, and drilling rates are intermediate. Less sensitivity in viscosity and filtration control losses with increasing salinity is also observed.

The rheological behavior (Fann viscometer) of a 8.4 wt % (28.8 lb/bbl) straight bentonite drilling fluid is illustrated in Figure 3. The viscosities illustrated are approximate values due to the large distance between concentric cylinders. The data also are plotted as dial readings versus revolutions per minute. In the low revolutions per minute range, the concave curvature reflects the presence of yield stress behavior. In a polymer-modified bentonite drilling fluid, the amount of clay is reduced to 4.2 wt % (14.4 lb/bbl). The rheological profiles at ambient temperature and more meaningful higher temperature (65 °C) data are illus-

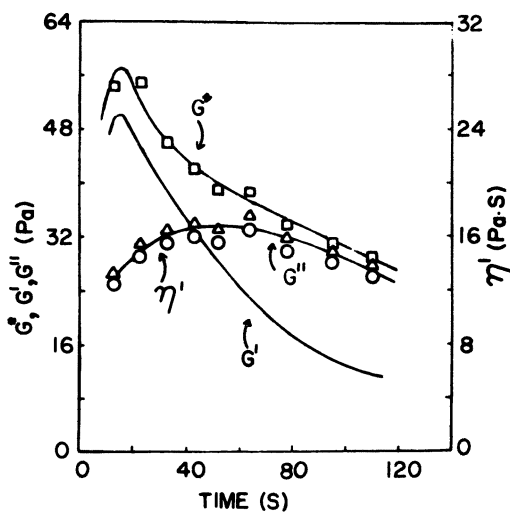


Figure 2. Complex modulus (G^*), storage modulus (G'), and dynamic viscosity (η') dependence on recovery time (s) after deformation for an interior coating thickened with attapulgite clay. Key: □, G^* ; △, G'' ; and ○, η' .

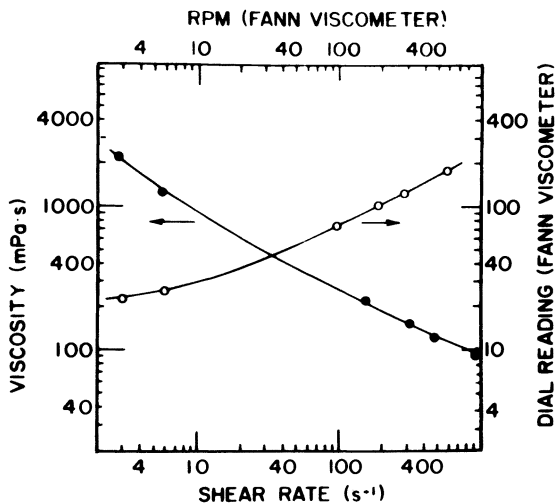


Figure 3. Rheological profile of an 8.4 wt % (28.8 lb/bbl) bentonite slurry obtained by using a Fann 35 viscometer. Key: closed symbols, viscosity ($mPa \cdot s$) dependence on the shear rate (s^{-1}); and open symbols, dial reading dependence on spindle revolutions per minute.

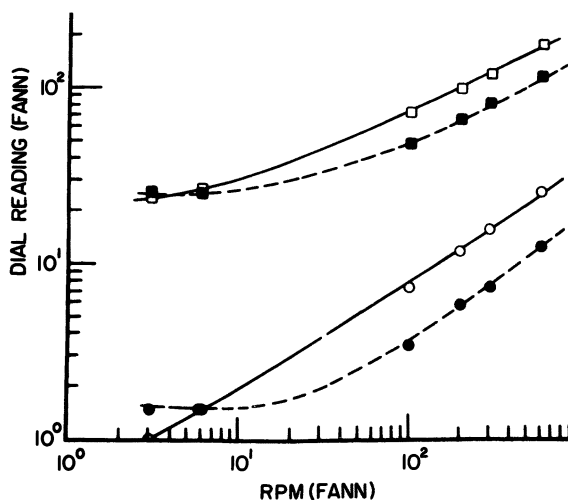


Figure 4. Rheological profiles of bentonite slurries. Key: \square and \blacksquare , 8.4 (28.8 lb/bbl); \circ and \bullet , 4.2 wt % (14.4 lb/bbl); open symbols, 27 °C; and closed symbols, 65 °C.

trated in Figure 4. Reducing the amount of bentonite in the aqueous slurry by half dramatically lowers the viscosity and yield stress characteristics at lower temperatures. The use of different types of W-SPs will increase the viscosity of the lower 4.2 wt % bentonite slurry; however, not all of the W-SPs maintain the advantageous yield stress behavior of the high-concentration bentonite slurry. For example, polymers such as (hydroxyethyl)cellulose (HEC) and partially hydrolyzed poly(acrylamide) increase the viscosity but do not maintain the yield stress behavior (Figure 5). The latter two polymers are generally used for shale stabilization (discussed in Chapter 10). The vinyl acetate-maleic acid-copolymer provides neither shale stabilization nor rheological beneficiation of the bentonite drilling fluid but effects drill solids release from the fluid when it is surfaced at the well bore. The performance requirements of W-SPs in bentonite drilling fluids are many.

Filtration control is facilitated by alignment of bentonite platelets against a porous substrate (simulating the well-bore interface). The influence of two W-SPs as a function of concentration on the amount of fluid loss from a standard API cell (note photographs of equipment in Chapter 12) in freshwater is illustrated in Figure 6. The W-SPs are HEC [molar substitution (MS) = 2.0], a nonionic ether, and sodium (carboxymethyl)cellulose (CMC) [degree of substitution (DS) = 1.46], an anionic ether. At low W-SP concentrations, filtration control of the bentonite slurries is not affected; however, as a 0.5-wt % level of HEC is

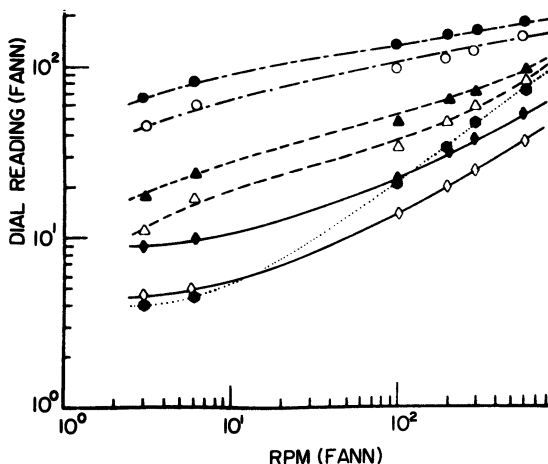


Figure 5. Rheological profiles of 4.2 wt % polymer-modified bentonite muds. Polymers at 0.5 wt %. Key: open symbols, 1.0 wt %; closed symbols, $M_r = 10^6$; ○ and ●, HEC; △ and ▲, hydrolyzed (30 mol %) poly(acrylamide); ◇ and ◆, XCPS; and ●, methyl vinyl ether of maleic acid of low molecular weight.

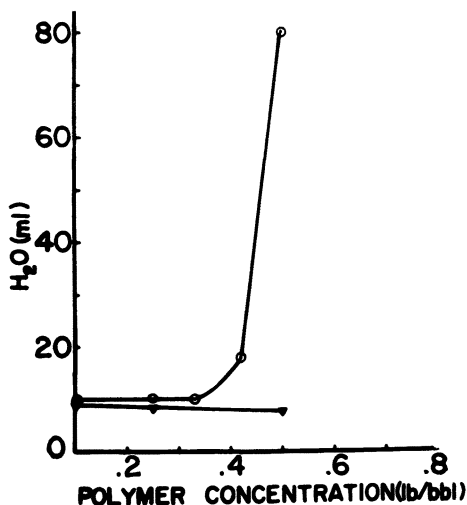


Figure 6. Fluid loss dependence of 4.2 wt % bentonite slurries on polymer [O, HEC; and ▼, CMC (DS = 1.46)], concentration in freshwater.

approached, rapid fluid loss is observed in the modified mud. CMC, an anionic polysaccharide, does not impede bentonite filtration control at high concentrations. HEC adsorbs on bentonite due to ion-dipole interactions (1) and is entrapped in the interlayer of compressed bentonite platelets; neither adsorption nor entrapment occurs with CMC (DS = 1.46). CMC does not adsorb from freshwater solutions because of electrostatic repulsions.

With increasing salinity, CMC adsorbs (Figure 7) inversely to its degree of substitution. The same trend is evident in the adsorption of variable degree of substitution cellulose sulfate ester W-SPs (Figure 8). As the degree of substitution of a cellulose ether decreases, it becomes less soluble in water. Addition of an electrolyte like NaCl reduces electrostatic repulsion between a polyelectrolyte and bentonite, and NaCl reduces the solvent power of water. The net result is higher adsorption with decreasing degrees of substitution. With increasing degree of substitution, CMC is more effective in controlling the fluid loss of the bentonite slurry (Figure 9). A synergistic effect also is noted with increasing concentration with any of the CMCs, but only with the high degree of substitution (1.46) CMC at high concentration is the filtration control of nonmodified bentonite slurries in freshwater approached. Bentonite slurries without CMC do not exhibit good filtration control in saline solutions.

The influence of a wide variety of water-soluble polymers at a concentration of 0.5 wt % on the filtration control in 4.2 wt % bentonite slur-

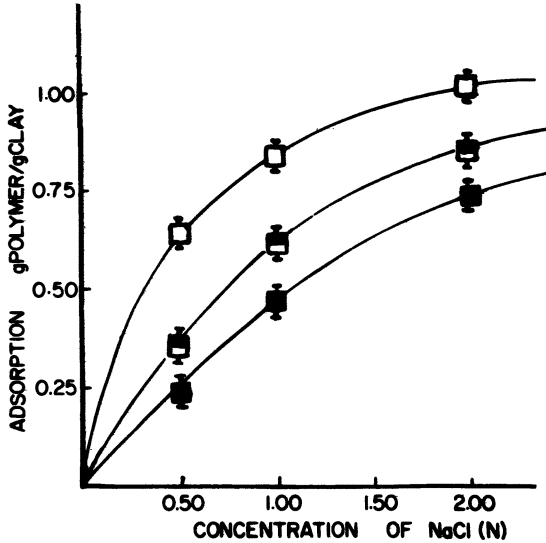


Figure 7. Adsorption (g/g) dependence of variable degree of substitution (\square , 0.99; \blacksquare , 1.19; and \blacksquare , 1.46) CMC at equal viscosities on the salinity of the aqueous solution. Substrate: peptized sodium montmorillonite.

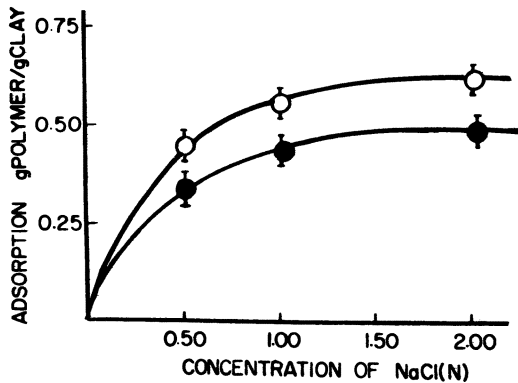


Figure 8. Adsorption (g/g) dependence of variable degree of substitution (\circ , 0.7; and \bullet , 1.0) CSE at equal viscosities on the salinity of the aqueous solution. Substrate: peptized sodium montmorillonite.

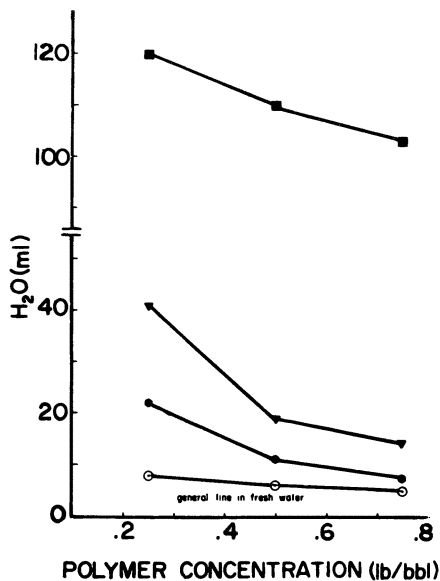


Figure 9. Fluid loss dependence of 4.2 wt % bentonite slurries on variable degree of substitution (■, 0.99; ▼, 1.19; and ●, 1.46) CMC concentration in 3.3% saltwater.

ries was examined. Those W-SPs that passed more than 30% of the water in 100 mL of bentonite slurry under 100 psi of pressure from the API cell were classified as poor filtration-control polymers [HEC, (hydroxyethyl)-methylcellulose, guaran, poly(vinylpyrrolidone), polyethylenimine, and styrene-maleic acid terpolymer]; those W-SPs in which more than 70% of the slurry fluid was retained in the cell within 7.5 min under 100 psi were classified as good filtration-control polymers [CMC (DS = 0.99-1.46), (carboxymethyl)guaran, vinyl acetate-maleic acid copolymer, XCPS, SGPS, pectinic acid, alginic acid, ethyl acrylate-acrylic acid copolymer, and sodium 2-(acrylamido)-2-methylpropanesulfonate]. The W-SPs that decrease the ability of bentonite to inhibit fluid loss in freshwater with two exceptions are nonionic. They have been observed to substantially adsorb both on the surface and, when the cation is monovalent and the polymer contains ether linkages, in the interlayer of montmorillonite. The two exceptions are SGPS and poly(oxyethylene) (POE). SGPS (discussed in Chapter 1) forms helical, three-dimensional networks (12) in aqueous solution that may inhibit flocculation of bentonite platelets; POE exhibits a unique ability to order (1) montmorillonite above that observed in the untreated clay.

As the salinity of the aqueous solution is increased approximately to that of seawater (3.3 wt % in which 0.3% is divalent calcium ion), the

number of W-SPs that effect filtration control in modified bentonite slurries decreases. Those W-SPs with only a small degree of anionic charge become ineffective with increasing salinity. In part, this ineffectiveness could be related to their adsorption with increasing salinity because of depression of diffuse double layers. As noted, adsorption per se cannot be related directly to poor filtration control.

Adsorption from High Salinities. Salinity in the petroleum area involves both monovalent and divalent ions, generally in a 10:1 ratio. As a parallel to the fluid loss studies, HEC (MS = 2 and 2.5), a salt-insensitive polymer, was adsorbed from saline solutions containing both Na^+ and Ca^{2+} ions. The adsorption data were not reproducible. The cation-exchange capacity of montmorillonite differs with different cations (being greater with Ca^{2+} than with Na^+). This complication necessitated that subsequent adsorption studies be conducted from NaCl solutions only; however, in the filtration control test, a 10:1 monovalent to divalent cation ratio was maintained.

In the presence of electrolyte, even if it is only monovalent, montmorillonite will flocculate. If flocculation occurs, macromolecules of lower molecular weight will exhibit greater adsorption due to the greater surface available to smaller hydrodynamic volumes (i.e., lower molecular weight polymers). Higher molecular weight polymers will adsorb less. Using a postcomponent addition to saline solutions, we did not observe an adsorption dependence on molecular weight (Figure 10); therefore, flocculation did not occur.

The adsorption behaviors as a function of salinity of two anionic polymers effective in maintaining filtration control at higher salinities are compared with CMC at the approximate degree of substitution levels in

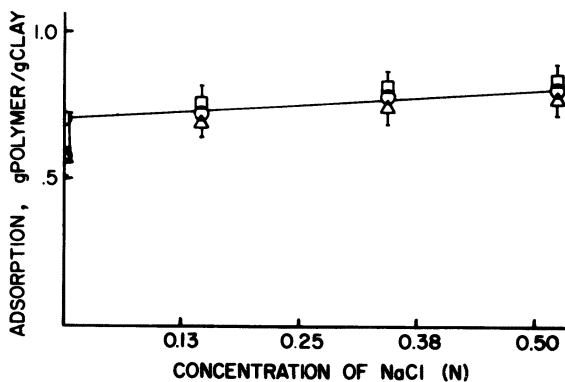


Figure 10. Adsorption (g/g) dependence of HEC (MS = 2.0) of variable molecular weights (\square , 10^4 ; \circ , 10^5 ; and \triangle , 10^6) at 2500 ppm on the salinity of the aqueous solution. Substrate: peptized sodium montmorillonite.

Figure 11. Viscosity reductions of cellulose sulfate ester and XCPS solutions are less sensitive to NaCl than is that of CMC. Carboxylate groups are more susceptible to charge neutralization in NaCl solution than are sulfate ester groups. This feature is reflected in the adsorption behavior; despite a lower degree of substitution, CSE adsorbs much less than CMC. XCPS, a helical, rigid-rod polymer in aqueous solution, also adsorbs less than CMC. The carboxylate groups of XCPS are similar to those of CMC, but the degree of dissociation is higher (13) in XCPS than in CMC with increasing ionic strength, a property probably associated with the difference in conformational structure.

As the salinity of the medium is increased to 6.6 wt % and finally to 13.2 wt %, only 5 (anionic polyelectrolytes with a high charge density) of the 29 W-SPs examined initially in this study effected fluid loss control in 4.2 wt % (14.4 lb/bbl) bentonite slurries. Of the five, two contain anions of a strong acid [cellulose sulfate ester and sodium 2-(acrylamido)-2-methylpropanesulfonate]. Two contain anions of a weak acid, in helix-forming macromolecules [S-130 (14) and XCPS], and one is the high degree of substitution CMC. The effectiveness of the W-SP in promoting fluid loss control of bentonite in saline environments appears to be associated with the nature and amount of the anionic group.

Several proposals for the mechanism by which anionic polymers promote filtration control of bentonite slurries in saline solution can be made. The most frequent is adsorption, bridging, and flocculation of

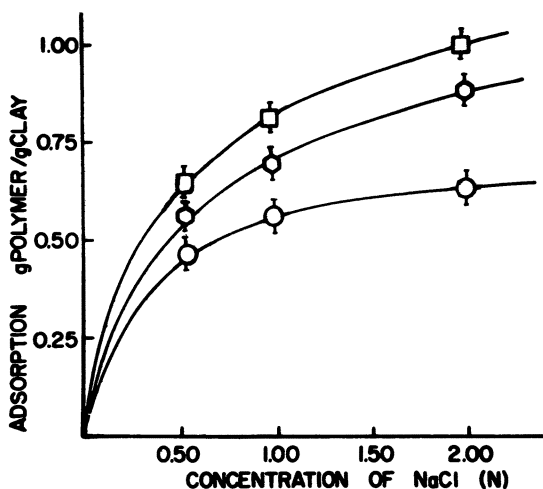


Figure 11. Adsorption (g/g) dependence of various anionic cellulose [\square , CMC (DS = 0.99); \diamond , XCPS (DS = 0.7); and \circ , CSE (DS = 0.7)] polymers [CMC, XCPS, and CSE (discussed in Chapter 1)] at 2500 ppm on the salinity of the aqueous solution. Substrate: peptized sodium montmorillonite.

bentonite particles by the W-SP. This often-cited mechanism is not applicable to the results presented because the five highly anionic polymers effective at high salinities adsorb significantly from such solutions. Flocculation by a volume restriction mechanism, discussed in Chapter 5 and one that is effective in explaining performance differences in waterborne latex coatings (discussed in Chapter 21), would seem inappropriate because polyelectrolytes are more effective in promoting flocculation by this mechanism than nonionic polymers. Bentonite platelets are different from catalyst-stabilized lattices; in acidic media, the surface edges of the platelets bear positive charges. The mechanism that would seem most attractive and has often been invoked is the preferential adsorption of anionic polymers on the positive edges; this adsorption enhances the stability of the platelets against a house-of-cards flocculent structure in highly saline solutions. As discussed in Chapter 10, positive edges are not thought to exist in alkaline media, and the formulations studied were alkaline (pH 9). The simplest mechanism and one that is consistent with all of the data is flocculation of the montmorillonite particles due to decreased electrostatic repulsion. Nonionic polymers adsorb from freshwater solutions and effect a reduction in electrostatic forces and loss in filtration control of bentonite slurries. With increasing salinity, anionic polymers with low charge densities are adsorbed, accompanied by fluid loss. The adsorption of highly charged anionic polymers will result in less charge reduction, particularly if the polymers contain a significant number of neutral segments adsorbed as trains on the surface of the clay and the charged segments are extended from the surface as loops. Enhanced stabilization to flocculation results from both osmotic and electrostatic stabilization (Chapter 5) of the clay particles.

Conclusions

With two exceptions, nonionic polymers inhibit the inherent filtration control of bentonite slurries in freshwater. Untreated bentonite slurries lose their inherent filtration control with increasing salinity; the control can be regained through the use of anionic W-SPs. Highly anionic polymers are required in highly saline solutions. Several mechanisms are considered for the changes in filtration control noted with different polymer types with increasing salinity. The mechanism consistent with the adsorption data on peptized montmorillonite is one of reduction in electrostatic repulsions among clay particles through increasing solution salinity and polymer adsorption. Those polymers with high anionic charge densities adsorb with increasing salinity to provide enhanced stability to the clay particles, due to extended loops of anionically charged segments and the increased hydrophilicity such segments provide.

Literature Cited

1. Ahmed, H.; Glass, J. E.; McCarthy, G. J. *Adsorption of Water-Soluble Polymers on High Surface Area Clays*; Soc. Petroleum Engin.: Dallas, TX, 1981; Publ. No. 10101.
2. McClune, W. F. *User Guide for 2dTS Diffraction Data Telesearch*; Joint Committee Powder Diffraction Standards: Swarthmore, PA, 1975, 30 pp
3. Malone, T. R.; Raines, R. H.; Weintritt, D. J. *Colorimetric Field Test for Determining Hydroxyethyl Cellulose and Other Polysaccharides in Drilling Fluids*; SPE 8741, Presented at the Eastern Regional Mtg. of the Society of Petroleum Engineers, 1979, Charleston, WV.
4. U.S. Patent 3 989 630, issued to Texaco, Inc., November 1976.
5. Keller, A.; Odell, J. A. *Colloid Polym. Sci.* **1985**, *263*, 181.
6. Horn, A. J. Ph.D. Thesis, Massachusetts Institute of Technology, Cambridge, MA, 1985.
7. Zakin, J. L.; Hunston, D. L. *J. Appl. Polym. Sci.* **1978**, *22*, 1763.
8. Glass, J. E.; Soules, D. A.; Ahmed, H.; Eglund-Jongewaard, S. K.; Fernando, R. H. *Viscosity Stability of Aqueous Polysaccharide Solutions*; Soc. Petroleum Engin.: Dallas, TX, 1983; Publ. No. 11691.
9. Soules, D. A.; Fernando, R. H.; Glass, J. E. *Proc. Am. Chem. Soc. Div. Polym. Mater. Sci. and Eng.* **1985**, *53*, 555.
10. Ferry, J. D. *Viscoelastic Properties of Polymers*; 2nd ed.; Wiley: New York, 1970.
11. Dealy, J. M. *Rheometers for Molten Plastics*; Van Nostrand Reinhold: New York, 1982.
12. Norisuye, T.; Yanaki, T.; Fujira, H. *J. Polym. Sci., Polym. Phys. Ed.* **1980**, *18*, 547.
13. Rinaudo, M.; Miles, M. *Biopolymers* **1978**, *17*, 2663.
14. Jansson, P-E; Lindberg, B.; Widmalm, G.; Sandford, P. A. *Carbohydr. Res.* **1985**, *139*, 217.

RECEIVED for review February 8, 1985. ACCEPTED October 24, 1985.

Water-Soluble Polymers for Aqueous Drilling Fluid Additives

Robert Gow-Sheng Chen and Arvind D. Patel

Magcozar Group, Dresser Industries, Inc., Houston, TX 77251

A series of novel sulfonate- and carboxylate-containing, low molecular weight, water-soluble polymers was developed for use as mud thinners and stabilizers in aqueous drilling fluids. The rheology of these polymers in aqueous drilling fluids was evaluated by using the Fann Model 35 VG meter and Fann Model 50C viscometer. Viscosity, yield point, gel strength, and filtrate loss were utilized to characterize these polymer-treated mud samples. Thermal stability was compared with that of existing commercial dispersants. The unique composition and functionality, as well as the inherent chelating capability, of these polymers make them superior dispersants. They significantly reduce viscosity, yield point, gel strength, and filtrate loss over a wide range of temperatures.

AQUEOUS DRILLING FLUIDS HAVE BEEN WIDELY USED to drill subterranean oil and gas wells. These fluids are usually pumped down through the drill stem of the rotary rig, circulated around the drill bit, and returned to the surface through the annular passage between the drill stem and well wall. In most drilling operations, controlling the viscosity, gel strength, yield point, and filtrate loss of the drilling fluids within a given range is vitally important (1). This control is usually achieved with drilling fluid additives, such as dispersants and filtrate loss control agents.

Treatment of aqueous drilling fluids with phosphate-containing materials deflocculates colloidal clays and drilled solids. However, these chemicals are generally unstable at the high temperatures encountered in deep wells and, as a result, lose their effectiveness as colloidal dispersants.

Lignite has been used in aqueous drilling fluids to control thixotropy. The effectiveness of lignite as a dispersant is limited because it is sensitive to commonly encountered contaminants such as gypsum and

0065-2393/86/0213-0197 \$06.00/0
© 1986 American Chemical Society

drilled solids. Also, lignite is less effective as a dispersant in drilling deep wells where elevated temperatures are encountered.

Lignosulfonates complexed with transition metals have been used in the past as dispersants (2). They show good dispersion properties in aqueous drilling fluids at bottom of the hole temperatures below 320 °F.

In recent years, an increasingly large number of synthetic and naturally occurring water-soluble polymers have been investigated and used in the oil field as drilling fluid additives (3). Anionic polymers with carboxylic or sulfonic acid functionalities are of special interest as dispersants or filtrate loss control agents.

Low molecular weight homopolymers of acrylic acid and its alkali metal or ammonium salts have been used as dispersants (4). Acrylic acid-acrylamide random copolymers, partially hydrolyzed polyacrylamides and polyacrylonitriles, which are flocculents at high molecular weight, show different properties and act as deflocculents at low molecular weight (5). Lignosulfonate-*graft*-poly(acrylic acid) is also claimed to be a dispersant (6). These types of polymers, however, are sensitive to divalent ion contaminants and are only marginally effective in drilling fluids that contain relatively high concentrations of clay or drilled solids.

The preparation procedure and viscosity data for sulfonate-containing copolymers have been reported earlier in great detail (7). Sulfonated styrene-maleic anhydride copolymers have been used as thermally stable dispersants (8). High molecular weight copolymers of 2-(acrylamido)-2-methylpropanesulfonic acid are claimed to be effective viscosifiers (8-10), filtrate loss control agents (11), and fracture acidizing gellants (12).

Recently we successfully developed a series of water-soluble polymers for use as aqueous drilling fluid stabilizers and dispersants (13-15). This chapter outlines the preparation and laboratory evaluation of these polymers.

Experimental Section

Materials. Reagent grades of acrylic acid, tetrahydrophthalic anhydride, 2-(acrylamido)-2-methylpropanesulfonic acid, eugenol, maleic anhydride, *N*-vinyl-*N*-methylacetamide, sodium hydroxide, sodium bisulfite, formaldehyde, and potassium persulfate were used as received. Sodium lignosulfonate from Georgia Pacific Corporation had a number-average molecular weight between 1000 and 12,000.

Graft Copolymerization. A series of graft copolymers was prepared by cografting of sodium acrylate, sodium tetrahydrophthalate (THPA), and sodium 2-(acrylamido)-2-methylpropanesulfonate [NaAMPS (Lubrizol Corporation)] onto sodium lignosulfonate. The reactions were conducted in a 250-mL three-necked flask equipped with a mechanical stirrer, a condenser, and a nitrogen line. The feed composition of the product, designated C-141, was 33 g of acrylic acid, 24 g of NaAMPS, 23 g of THPA, and 20 g of sodium lignosulfonate in 180 g of

water. The pH of the reaction medium was adjusted to 9.0 with sodium hydroxide. The reaction medium was then deaerated with nitrogen for 20 min, and 5 g of potassium persulfate was added. After 3 h of reaction at 60 °C, the resulting polymer was precipitated into acetone. The graft copolymer was further purified by dissolution in water followed by precipitation into acetone. The product was vacuum-dried at 60 °C for 24 h. Conversion, determined gravimetrically, was 99.6%. The number-average molecular weight of the product was 6500.

Eugenol–Maleic Anhydride–*N*-Vinyl-*N*-methylacetamide Terpolymer. A series of random terpolymers of eugenol, maleic anhydride, and *N*-vinyl-*N*-methylacetamide (VMA) was prepared in 1,2-dichloroethane by using azobisisobutyronitrile as the initiator. The feed composition of the terpolymer, designated P-127, was 30.7 g of eugenol, 46.2 g of maleic anhydride, and 23 g of VMA. The reaction procedures were similar to those just described for the preparation of graft copolymers. The reaction was carried out at 70 °C for 2 h, and the resulting polymer was vacuum-dried at 45 °C for 24 h. Conversion, determined gravimetrically, was 98.8%.

Sulfomethylation. Terpolymer P-127 was further sulfomethylated as follows: 30 g of polymer and 15 g of sodium bisulfite–formaldehyde adduct were dissolved in 70 g of water, and the pH of the solution was adjusted to 10.0. The reaction mixture was heated at 60 °C for 12 h. The sulfomethylated polymer P-127-B was precipitated into acetone and further purified by dissolution in water followed by precipitation into acetone. The polymer was vacuum-dried at 60 °C for 24 h. The number-average molecular weight of the product was 7000.

Infrared Measurement. Polymer P-127-B was dissolved in distilled water, coated onto a silver chloride minicell window, and vacuum-dried at room temperature for 1 h. The IR spectrum was recorded with a Perkin-Elmer 283 spectrophotometer.

Membrane Osmometry. Number-average molecular weights of the samples were measured with a Knauer membrane osmometer in aqueous 0.2 M NaCl solution at 30 °C. Polymer concentrations ranged from 1.0 to 2.5 g/dL.

Aqueous Drilling Fluid. A 12-lb/gal. aqueous drilling fluid containing 198 g of barite, 18 g of Wyoming bentonite, 20 g of X-act clay (primarily a calcium montmorillonite), and 0.2 g of soda ash in 325 g of tap water was prepared by using a Premier mill dispersator at high speed. The aqueous drilling fluid was then rehydrated for 24 h prior to use.

Rheological Measurements. The drilling fluid was contaminated with 4 g of gypsum/350 mL of drilling fluid and was then treated with 3 g of polymer sample and 6 g of chromium lignosulfonate; the pH of the samples was adjusted to 11.0 with sodium hydroxide. Treated samples were rotated constantly in an oven for 16 h at each temperature in the sequence 200, 300, 400, and 425 °F. Plastic viscosities, yield points, and gel strengths after each aging step were determined by using a Fann Model 35 VG meter.

The viscosity–temperature relationships of the drilling fluids were obtained by using a Fann Model 50C viscometer. Samples were heated at 3.8 °F/min from 80 to 450 °F and were then cooled. The viscosity was recorded throughout the temperature range. The working pressure was kept between 500 and 700 psi.

American Petroleum Institute Filtrate Loss. Filtrate losses of the drilling fluids were measured in Fann filter press cells in accordance with American Petroleum Institute approved procedure RP-13B (16). Filtrate losses over a 30-min period were measured at room temperature at 100 psi.

Rheology and filtrate loss data for the prepared polymers and similar commercial polymers are shown in Table I.

Results and Discussions

Polymer Design. MOLECULAR WEIGHT CONTROL. Controlling the molecular weight is vitally important in preparing polymeric defloculents for aqueous drilling fluids. For example, high molecular weight poly(acrylic acid) is used as a thickener or a flocculent for aqueous drilling fluids, whereas low molecular weight poly(acrylic acid) has been used as a deflocculent. Molecular weight can be controlled by regulating reaction temperature, solvent, initiation system, monomer and initiator concentration, by using scavengers, or by introducing functional monomers with high chain-transfer capability.

Salts of tetrahydrophthalic acid (THPA) (structure I) are extremely useful in preparing low molecular weight water-soluble polymers. Dur-

Table I. Comparative Performance of Commercial and Synthetic Dispersant Polymers

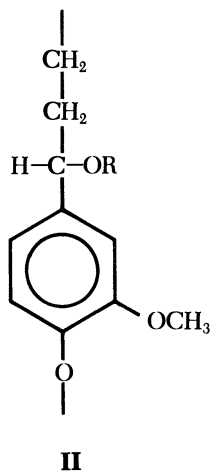
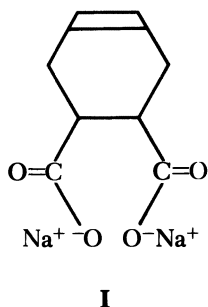
<i>Polymer</i>	<i>Aging Temp (°F)</i>	<i>Plastic Viscosity (cps)</i>	<i>Yield Point (lb/100 ft²)</i>	<i>Initial:10-min Gel (lb/100 ft²)</i>	<i>Filtrate Loss (mL)</i>
Base mud ^a without polymeric dispersant	200	48	9	1:3	—
	300	43	3	1:39	12.2
	425	— ^b	— ^b	— ^b	— ^b
3 g of sample T ^c	200	43	27	1:29	—
	300	28	0	1:1	—
	425	59	6	2:23	11.8
3 g of sample DP ^d	200	37	22	1:13	—
	300	32	0	1:1	—
	425	50	5	1:14	11.9
3 g of C-141	200	33	5	1:1	—
	300	31	0	1:1	—
	425	51	10	2:10	9.5
3 g of P-127-B	200	30	0	2:2	—
	300	29	0	2:2	—
	425	64	10	2:9	9.0

^aThe base mud is a 12-lb/gal. of fresh water mud containing 6 g of chrome lignosulfonate and 4 g of gypsum per 350 mL of mud.

^bThe polymer was too thick for this value to be measured.

^cSample T is the sodium salt of poly(acrylic acid), $M_n = 5000$.

^dSample DP is the sodium salt of the terpolymer of acrylic acid, acrylamide, and AMPS, $M_n = 4700$. The composition is as follows: 78 mol % sodium acrylic acid; 10 mol % acrylamide, and 12 mol % NaAMPS.



ing free-radical polymerization, THPA has a high chain-transfer constant because of its allylic resonance. The molecular weight of THPA-containing polymers is thereby limited.

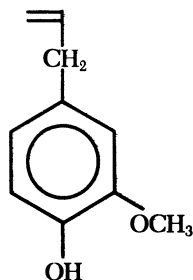
Sodium lignosulfonate is an extremely inexpensive sulfonated material containing hydroxyphenylpropane units (structure **II**: R = H, CH₃, or SO₃⁻Na⁺). These units provide grafting sites where graft copolymerization can proceed in the presence of a free-radical initiator (17, 18). Hydroxyphenylpropane units also regulate the molecular weight of the resulting graft copolymer because of their role in chain transfer. The number-average molecular weight of the graft copolymer prepared by using THPA and sodium lignosulfonate, C-141, was 6500.

An allylic benzene compound, eugenol (structure **III**) was used in preparing the sulfomethylated terpolymer, P-127-B, to regulate molecular weight. The number-average molecular weight of P-127-B was 7000.

CHARGE DENSITY. Charge density is also an important parameter in designing dispersants. Carboxylate units in the polymer backbone increase charge density; thus, the rheological performance in uncontaminated drilling fluids is enhanced. Sodium acrylate and sodium tetrahydrophthalate were used to enhance the charge density of graft copolymers.

Sodium tetrahydrophthalate units also exhibit a chelating ability; this chelating ability makes them excellent divalent cation stabilizers. Additionally, sodium tetrahydrophthalate units enhance the absorption between polymers and clay particles and reduce flow resistance and gel development in aqueous drilling fluids.

NaAMPS is also utilized in preparing graft copolymers. NaAMPS units exhibit an enhanced mono- and divalent ion stability attributable to



their exceptionally high ionization constant and hydrogen-bonding capability.

Compositional analysis of the graft copolymer was not successful, because the structure of sodium lignosulfonate is poorly defined (19).

Sodium maleate was used in preparing polymer P-127 to enhance charge density. In addition to increasing charge density, sodium maleate units also chelate calcium ions encountered in a drilling operation.

Polymer P-127 was further sulfomethylated to introduce sulfonic acid groups and, as a result, to improve dispersability in aqueous drilling fluids. *N*-Methylacetamide functionalities of terpolymer P-127 were hydrolyzed under alkaline conditions to the corresponding *N*-methylamine groups, which were then sulfomethylated by using the formaldehyde-sodium bisulfite adduct. The activated benzene ring and benzyl hydrogen on eugenol units provided additional reaction sites for sulfomethylation. IR spectroscopy (Figure 1) was used to analyze the sulfomethylated polymer, P-127-B, qualitatively. IR absorbances at 1200 and 1043 cm^{-1} can be attributed to S=O stretching, whereas the absorbance at 620 cm^{-1} can be attributed to C-S stretching. These data indicate that polymer P-127-B was sulfomethylated. Quantitative analysis of the sample is in progress.

Performance. The control of apparent viscosity, gel strength, yield point, plastic viscosity, and filtrate loss of the aqueous drilling fluids is extremely important in a drilling operation. Unsatisfactory performance of the drilling fluids may result in serious problems.

A 12-lb/gal. water-base drilling fluid containing 4 lb of gypsum ($\text{CaSO}_4 \cdot 2\text{H}_2\text{O}$) per barrel was used to evaluate the performance of the samples. This test drilling fluid represents the severe conditions of divalent cation contaminations. Monovalent cation contaminants, such as

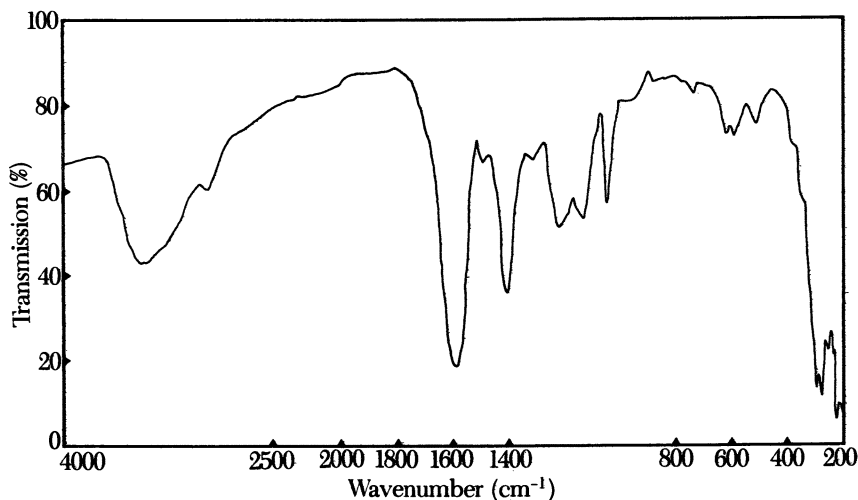


Figure 1. IR spectrum for polymer P-127-B.

sodium, are less detrimental to the drilling fluids than divalent cations such as calcium.

GEL STRENGTH. Gel strength is a measure of the thixotropic properties of a fluid and denotes the force of flocculation under static conditions. Gel strengths of the polymer-treated mud samples were measured by the Fann Model 35 VG meter and are listed in Table I. The difference between the initial gel strength and that taken after a 10-min rest period is used to judge how thick the mud will get during the periods when circulation is stopped, for example, when removing the drilling pipe. Both the gel strengths and the difference between the 10-min gel and initial gel for the C-141- and P-127-B-treated muds remained low throughout the heat aging cycles. Such "fragile" gels require low pump pressure to start or restart circulation and cause fewer problems during drilling operations. The gel strength differences for muds treated with commercial samples T and DP after being heat-aged at 200 °F are 28 and 12 lb/100 ft², respectively. Such "progressive" gels require increased pump pressure to start circulation and may cause more problems. The base mud also exhibits progressive gel structure after such heat-aging.

YIELD POINT AND PLASTIC VISCOSITY. The yield point in drilling fluids terminology is the resistance to initial flow, or the stress required to start fluid movement. This resistance is due to electrical charges on or near the surface of clay particles suspended in the mud. The yield point of muds treated with C-141 and P-127-B are within the desired range

after each heat-aging cycle. However, the yield points of muds treated with samples T and DP increased drastically after heat-aging at 200 °F for 16 h. Such high yield points are usually not desirable in dispersed aqueous drilling fluids.

Aqueous drilling fluids contain solids that contribute to the apparent viscosity. The plastic viscosity is a measure of the internal resistance to fluid flow attributable to the concentration, type, shape, and size of solids present. The base mud shows a higher plastic viscosity after heat-aging; this increase reflects higher friction between clay particles. The plastic viscosities of polymer-treated muds are substantially lower.

VISCOSITY-TEMPERATURE RELATIONSHIPS. The viscosity-temperature relationship of the drilling fluid is very important, because the drilling fluid may be circulated many times while drilling a deep well and may be exposed to different temperature gradients. The viscosity-temperature relationships for drilling fluids containing polymers designated as T, DP, C-141, and P-127-B are demonstrated in Figures 2, 3, 4, and 5, respectively. The temperature and fluid viscosity with respect to time are represented by dotted and solid lines, respectively. Drilling fluids containing polymers T and DP flocculate at 135 and 195 °F, respectively. As the temperature increases further, the fluid viscosities increase drastically. Mud containing C-141 flocculates at 415 °F, and its viscosity profile is relatively unaffected by the heating and cooling cycle from

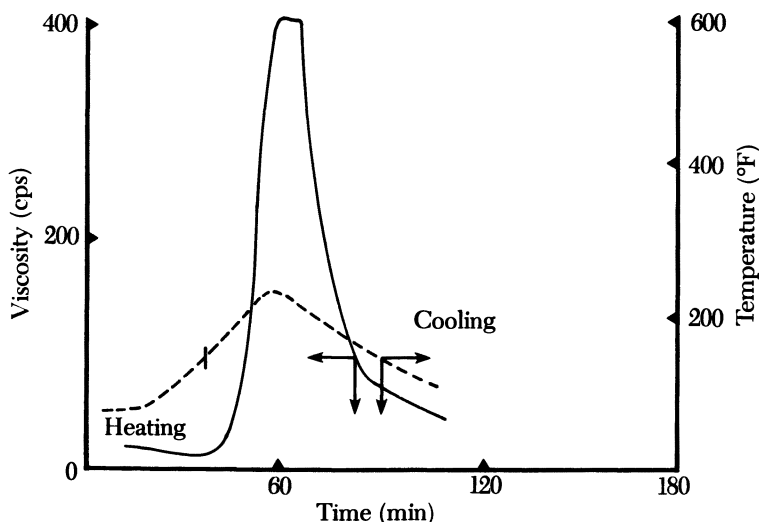


Figure 2. Viscosity-temperature profile for drilling fluid containing polymer T. The temperature of flocculation was 135 °F.

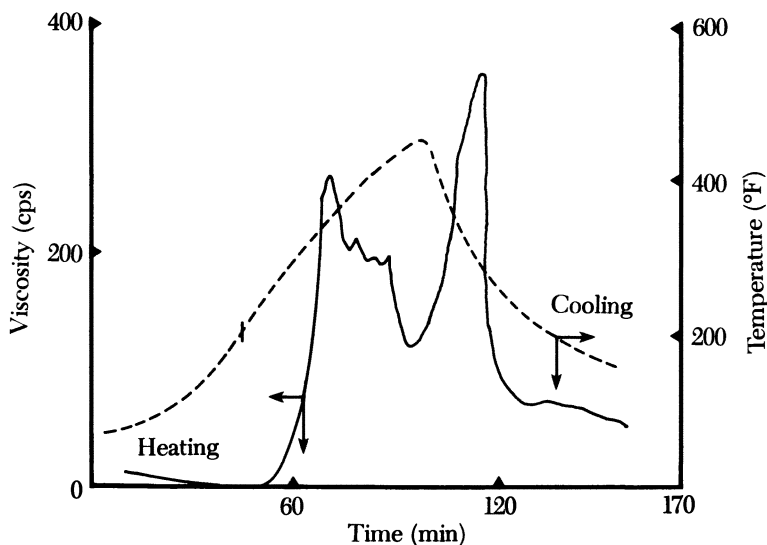


Figure 3. Viscosity-temperature profile for drilling fluid containing polymer DP. The temperature of flocculation was 195 °F.

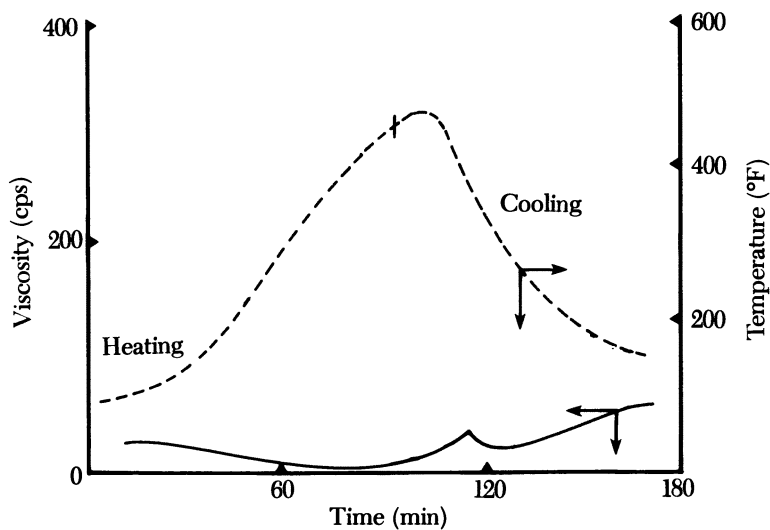


Figure 4. Viscosity-temperature profile for drilling fluid containing C-141. The temperature of flocculation was 415 °F.

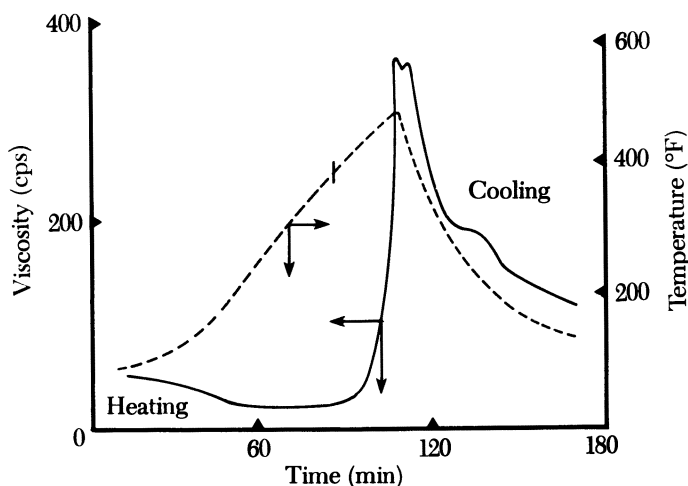


Figure 5. Viscosity-temperature profile for drilling fluid containing P-127-B. The temperature of flocculation was 380 °F.

ambient to 450 °F. The mud containing P-127-B flocculates at 380 °F. Because the drilling fluid may be exposed to such temperatures during a drilling operation, these results indicate that C-141 and P-127-B copolymers are effective in stabilizing the rheology of such a fluid.

Conclusion

The unique composition of the low molecular weight water-soluble polymers described makes them effective dispersants for aqueous drilling fluids.

Acknowledgments

We thank Dresser Industries, Magco-bar Group, for permission to publish this work.

Literature Cited

1. Gray, G. R.; Darley, H. C. H.; Rogers, W. F. *Composition and Properties of Oil Well Drilling Fluids*; 4th ed.; Gulf Publishing: Houston, TX, 1980; pp 1-36.
2. Javora, P. H.; Green, B. Q. U.S. Patent 4 220 585, 1980.
3. Gray, G. R.; Darley, H. C. H.; Rogers, W. F. *Composition and Properties of Oil Well Drilling Fluids*; 4th ed.; Gulf Publishing: Houston, 1980; pp 526-601.
4. Burland, P. D.; Stephenson, J. L.; Stobart, E. H. U.S. Patent 3 764 530, 1973.
5. Siegele, F. H.; Ondera, E. V.; Liberatore, M. A. U.S. Patent 3 434 970, 1969.
6. Felicetta, V. F.; Wenzel, D. E. U.S. Patent 3 985 659, 1976.

7. Chen, R. G.-S. Ph.D. Dissertation, University of Southern Mississippi, Hattiesburg, 1982.
8. Perricone, A. C.; Young, H. F. U.S. Patent 3 730 900, 1973.
9. McCormick, C. L.; Chen, G.-S. *J. Polym. Sci.* **1982**, *20*, 817.
10. Neidlinger, H. H.; Chen, G.-S.; McCormick, C. L. *J. Appl. Polym. Sci.* **1984**, *29*, 713.
11. Uhl, K.; Bannerman, J. K.; Engelhardt, F. J.; Patel, A. D. U.S. Patent 4 471 097, 1984.
12. Deysarkar, A. K.; Dawson, J. C.; Sedillo, L. P.; Davis, S. K. *J. Can. Pet. Technol.* **1984**, *23*, 26.
13. Chen, G.-S.; Patel, A. D.; Sample, T. E., Jr. U.S. Patent 4 521 578, 1985.
14. Patel, A. D. U.S. Patent 4 525 562, 1985.
15. Patel, A. D., Sample, T. E., Jr. U.S. Patent pending.
16. *American Petroleum Institute Recommended Practice Standard Procedures for Testing Drilling Fluids*, API RP 13-B, 9th ed., Dallas, TX, May, 1982.
17. Tirzinya, Y. E.; Zoldners, Y. A.; Surna, Y. A. *Khim Drev.* **1975**, *6*, 98.
18. Chen, R.; Kokta, B. V. In *Graft Copolymerization of Lignocellulosic Fibers*; Hon, D. N.-S., Ed.; ACS Symposium Series 187; American Chemical Society: Washington, DC, 1982; p 285.
19. Pearl, I. A. *The Chemistry of Lignin*; Dekker: New York, 1967; pp 1-6.

RECEIVED for review October 23, 1984. ACCEPTED August 9, 1985.

Use of Gelation Theory To Characterize Metal Cross-Linked Polymer Gels

Juan A. Menjivar¹

Hercules, Inc., Research Center, Wilmington, DE 19894

This chapter presents a novel approach to characterize metal cross-linked polymer gels through the use of gelation theory and rheological concepts and measurements. A simple gelation model that provides the essential features of a liquid-gel phase diagram is used. This model introduces the importance of a critical polymer concentration (C^) for gelation and the gel-liquid transition temperature (T_c). These two properties of a polymer solution or gel determine, to a great extent, the rheological properties of fracturing gels. In this work, C^* and the T_c are determined experimentally by using rheological techniques. Their impact on the rheological properties of fracturing gels is discussed.*

HYDRAULIC FRACTURING IS A WIDELY USED METHOD for stimulating the production of oil and gas formations. Reportedly, about 35–40% of all drilled wells are hydraulically fractured, and about 25% of the total U.S. oil reserves have been made economically producible by this process (1).

Hydraulic fracturing is performed by injecting the subterranean formation with a viscous polymeric fluid containing particulate solids (propping agents) in suspension. Sufficient pressure is applied to the fluid to wedge open fractures in the subterranean formation (Figure 1a). The pressure must be maintained while injecting the fluid into the formation in order to extend the fracture wings. Once the desired network of fractures is developed, the pressure on the fracturing fluid is reduced and the propping agent prevents the complete closure of the fracture (Figure 1b) (2). Eventually, the polymer is broken by enzymes such as cellulases or oxidizing chemicals such as persulfates, which reduce the viscosity of the fluid.

¹Current address: Pillsbury Research and Development Laboratories, Pillsbury Company, Minneapolis, MN 55414. Correspondence should be addressed to Carl A. Lukach, Hercules, Inc., Research Center, Wilmington, DE 19894.

0065-2393/86/0213-0209\$06.00/0
© 1986 American Chemical Society

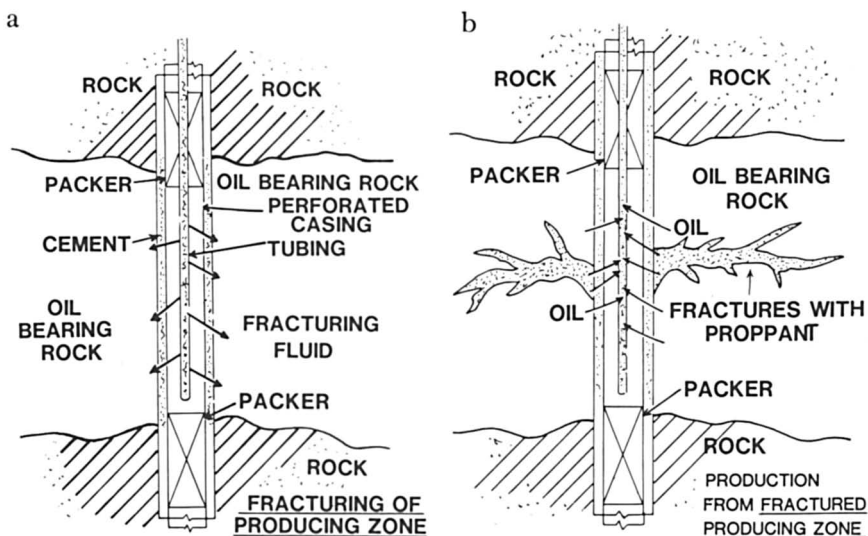


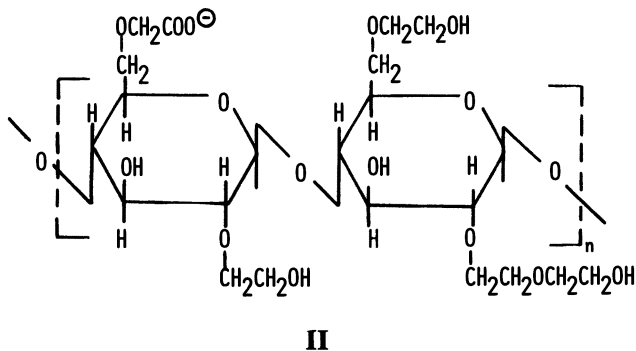
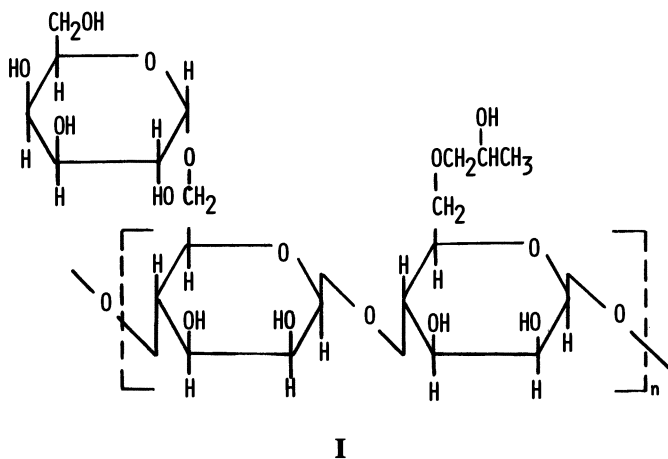
Figure 1. Hydraulic fracturing of producing zone. (a) Injection of fracturing fluid; (b) production from fractured producing zone. Reproduced with permission from reference 16. Copyright 1985 Hemisphere.

Typical fracturing gels contain a variety of additives in addition to thickening and cross-linking agents. These additives are aimed at improving specific functions of the fracturing gels. A partial list is as follows (1, 2): guar gum, HPG, and CMHEC function as viscosifiers (0.25–5.00 wt %); borate, titanium, aluminum, and chromium function as cross-linking agents (0.01–0.10 wt %); potassium chloride functions as a clay stabilizing agent (0.50–2.00 wt %); bentonite, starch, and silica flour function as fluid-loss control agents; thiosulfate salts and methanol function as antioxidants; fluorosurfactants and petroleum sulfonates function as surfactants; enzymes and oxidizers function as degrading agents; and silica sand and sintered bauxite function as proppants.

This chapter mainly discusses the cross-linking, rheological, and thermal stability properties of the polymer thickening agent and its gels. The polymer, which is used for rheology control, plays a central role in a number of the desirable features of a fracturing fluid. Important functions of this role are (1) to provide sufficient viscosity to create the necessary fracture width, (2) to lower the fluid loss to the formation, and (3) to transport and distribute the proppant along the fracture. All of these functions are intimately related to the rheological properties of the polymer solutions and gels, as well as to their thermal stability. Thus, rheological and thermal stability properties of fracturing gels are the key to their performance in hydraulic fracturing treatments (3).

Guar gum, its hydroxypropyl derivative (HPG; I), and cellulose derivatives, particularly (carboxymethyl)(hydroxyethyl)cellulose (CMHEC; II), are the most extensively used polysaccharides in commercial fracturing fluids (4). The repeating units of these polymers are shown in I-III. Metal cross-linked polysaccharide gels are superior to un-cross-linked polysaccharide solutions for at least two reasons: (1) small amounts of metal substantially increase the viscosity of the original polymer solution and the gels maintain this higher viscosity at typical application temperatures (200–400 °F) and (2) the gels have excellent friction reduction properties. As a consequence, polysaccharide gels have the capability of developing wider fractures and have better particle transport properties.

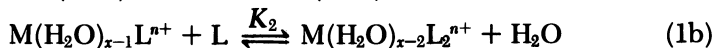
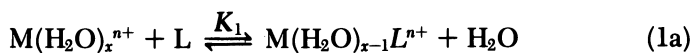
A large number of metals have been reported to successfully cross-link polysaccharide materials (4). However, fracturing fluids in current use are cross-linked with boron, chromium, antimony, aluminum, titanium, or zirconium (4, 5).



The work presented in this chapter deals with HPG and CMHEC polymers cross-linked with titanium compounds. Titanium cross-linked gels were introduced in the oil field primarily because of their enhanced thermal stability over their predecessors (5). Their use is currently widespread throughout the industry. For the purposes of this work, polymer gels cross-linked with titanium are used only as a model system to introduce general factors that affect the design of polymer gels.

Mechanism of Gelation

On a purely intuitive basis, a number of workers (3-5) reported that guar reacts with metals through a metal-ligand complexation type of reaction, as described below by equation 1. A metal complex is formed by association between a metal atom or ion (M^{n+}) and another species, known as the ligand (L), which is either an anion or a polar molecule. When L is an uncharged unidentate ligand, the formation of complexes proceeds in a stepwise manner, with successive replacement of water molecules:

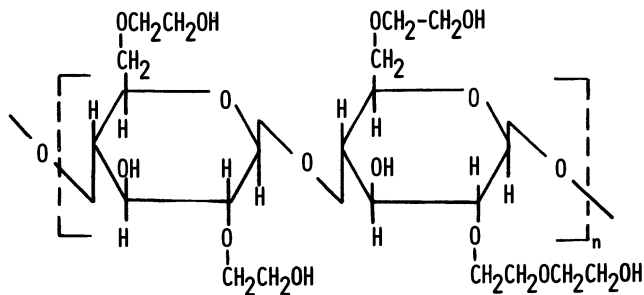


K_1 and K_2 represent the equilibrium constants for the reaction.

Any of the numerous hydroxyl groups of the guar molecule (I) should be able to serve as cross-linking sites. However, because of the proximity and cis orientation of the hydroxyl groups in the 2- and 3-positions of the mannopyranose rings, and the 3- and 4-positions of the galactopyranose rings, the complexation of metals should—on the basis of the chelate effect—be more favorable (6). This effect can be exemplified by comparing the cross-linking characteristics of titanium with HPG to those of (hydroxyethyl)cellulose (HEC; III). Their characteristic cross-linking profiles as a function of solution pH are contrasted in Figure 2. In the case of HEC, all the neighboring hydroxyl groups in the anhydroglucose units have a trans configuration with respect to each other (*see* III). Apparently, this configurational difference between HPG and HEC is enough to cause dramatically different cross-linking profiles (Figure 2).

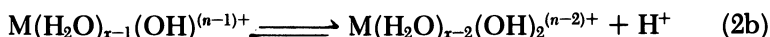
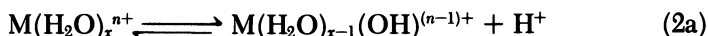
Another interesting comparison can be made between the titanium cross-linking profile of CMHEC and HPG. In the case of CMHEC, the active cross-linking sites are the carboxyl groups (II); Figure 2 shows that this difference between active functional groups in the two polymers, CMHEC and HPG, causes a difference in their pH cross-linking profiles.

The gelation curves shown in Figure 2 suggest the presence of processes competing with the cross-linking reaction of the ligand with the metal. One competing process is the hydrolysis of the metal ion (6). In



III

aqueous solutions, hydrated metal ions behave as acids and thus undergo hydrolysis by releasing one or more protons from coordinated water molecules:



The extent of hydrolysis depends on the polarizing characteristics of the metal ion and the pH of the solution. Figure 3 illustrates the hydrolysis profile of Al^{3+} as an example of the hydrolysis of metals (7).

At low pH conditions, a competing reaction to the cross-linking reaction can be the protonation of the ligand. The formation of hydroxo complexes can be repressed by the addition of acid. This acid addition

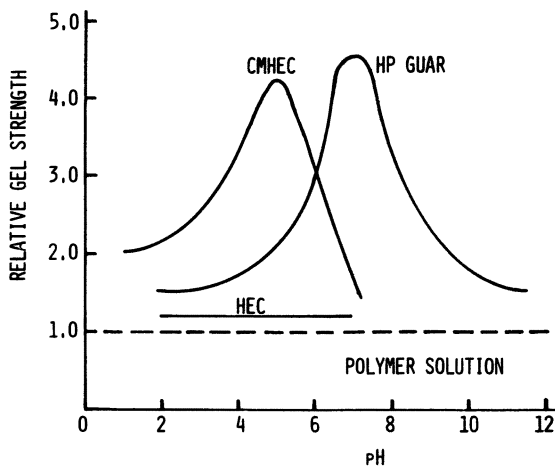


Figure 2. Cross-linking profiles of polysaccharides with titanium acetyl acetate (TiAA). Reproduced with permission from reference 16. Copyright 1985 Hemisphere.

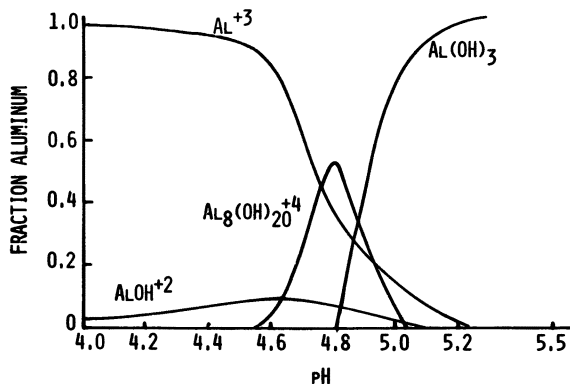


Figure 3. Distribution of aluminum species as a function of pH (ionic strength is $2.5 \times 10^{-4} M$). Reproduced with permission from reference 7. Copyright 1980 T. R. Aranson.

has the effect of maintaining the metal ion predominantly as $M(H_2O)_x^{n+}$. However, the acid also promotes protonation reactions that involve the ligand. For instance, in the case of carboxylic ligands



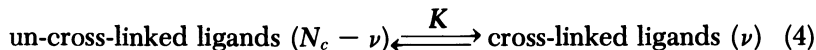
These protonation reactions compete with the complexing action of carboxylic groups toward metal ions, particularly below the pK_a of the carboxylic group.

The end result of the competing processes is the existence of an optimum pH range for the gelation of a polymer with a metal (Figure 2). The gelation profile of a particular polymer-metal pair depends on the acid-base properties of the ligands on the polymer and the hydrolysis characteristics of the metal ion.

Gelation Theory

There is no direct evidence of the detailed reaction mechanism between a polymer like HPG or CMHEC and transition metals. Still, chemical equilibrium concepts can be used to gain insight to the physicochemical properties of metal-polymer gels.

A simplified model that describes the gelation curve of gelatin was proposed by Tanaka et al. (8). This model is based on the chemical equilibrium between unreacted and reacted ligands:



K represents the equilibrium constant, N_c represents the initial number of ligands that can be effectively involved in a cross-linking reaction

between polymers, and ν represents the number of cross-links formed. Then, by definition

$$K = \nu / (N_c - \nu) \quad (5a)$$

or, rearranging

$$\nu = N_c K / (1 + K) \quad (5b)$$

The initial number of effective ligands can be calculated by using the mean-field approximation (8):

$$N_c = V \phi^2 f^2 \quad (6)$$

V represents the total number of lattice sites, ϕ represents the volume fraction of polymer, and f represents the fraction of monomers that contains active cross-linking sites (ligands).

Moreover, Stockmayer's (9) and Flory's (10) criterion that an infinite network appears when the average number of cross-linking bonds per polymer is equal to or larger than 1 can be used to arrive at the expression

$$\phi = 1 / (lf^2)(1 + K^{-1}) \quad (7)$$

l represents the degree of polymerization. The equilibrium constant, K , is related to the standard reaction free energy, ΔG° , by

$$K = \exp(-\Delta G^\circ / RT) \quad (8)$$

R is the universal gas constant and T is the absolute temperature of the system. Also, ΔG° is related to the change in enthalpy (ΔH°) and entropy (ΔS°) associated with the formation of a cross-linked bond by

$$\Delta G^\circ = \Delta H^\circ - T \Delta S^\circ \quad (9)$$

Equation 7 combined with equations 8 and 9 gives rise to the following relationship, which in turn provides the gelation curve shown in Figure 4.

$$T_c = \frac{\Delta H^\circ}{\Delta S^\circ - R \ln [(\phi - \phi^*) / \phi^*]} \quad (10)$$

where $\phi^* = 1 / (lf^2)$. $\phi^* = 1 / (lf^2)$ was obtained from equation 7, when $T = 0$ so that the cross-linking reaction goes to 100% completion (i.e., $K \rightarrow \infty$). Substituting this value for K in equation 7 gives rise to this expression for the minimum volume fraction of polymer for gelation (ϕ^*).

Figure 4 and equation 10 lead to a number of conclusions that are of practical relevance to the design of fracturing gels: (1) A minimum

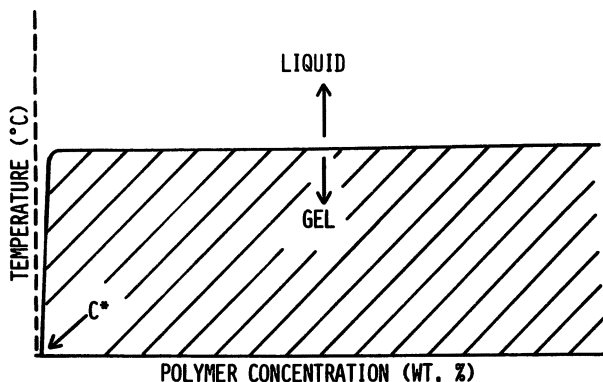


Figure 4. Liquid-gel phase diagram. Reproduced with permission from reference 16. Copyright 1985 Hemisphere.

polymer concentration, ϕ^* , necessary for gelation exists. According to the model shown here, the minimum polymer concentration is inversely related to the polymer molecular weight. (2) The liquid-gel transition temperature, T_c , is primarily a function of the thermodynamic properties associated with the formation of cross-linking bonds (i.e., ΔH° and ΔS°). (3) Beyond the minimum polymer concentration, ϕ^* , T_c is practically independent of polymer concentration and polymer molecular weight.

The applicability of chemical equilibrium and classical gelation concepts has not been generally recognized in the literature as related to metal cross-linked fracturing gels. Our work has been motivated, in part, by the availability of a new and unique instrument, the Rheometrics pressure rheometer (Rheometrics, Inc., Piscataway, NJ), which provides the capability of doing oscillatory shear experiments on water-based gels at temperatures above 100 °C (normal boiling point of water). In this chapter, the use of rheological techniques to determine ϕ^* and T_c is presented for the first time, and the importance of these two properties in the design of fracturing gels is demonstrated.

Experimental Determination of Critical Polymer Concentration (C^*)

Rheological methods were used to estimate C^* required to form a homogeneous gel. In the following discussions, the polymer concentration will be expressed in weight by volume units and referred to as C , rather than ϕ (volume per volume). The rheological data presented were obtained at 25 °C as follows: the intrinsic viscosity was determined with Cannon-Fenske capillary viscometers, low-shear viscosities were obtained with a low-shear 30 Contrares rheometer (Tekmar Co., Cincin-

nati, OH), and the oscillatory shear data were obtained with a Rheometrics pressure rheometer.

The method used is depicted in Figure 5. In essence, the concentration at which the hydrodynamic volume of polymer molecules in solution starts to overlap can be estimated (Figure 6). This estimation is experimentally accomplished by plotting the viscosity (low-shear specific viscosity) against the concentration of polymer in solution. A transition in the solution behavior of the polymer takes place at C^* (Figures 5 and 6). C^* represents the concentration beyond which polymer-polymer entanglements become significant (11). From the polymer gelation

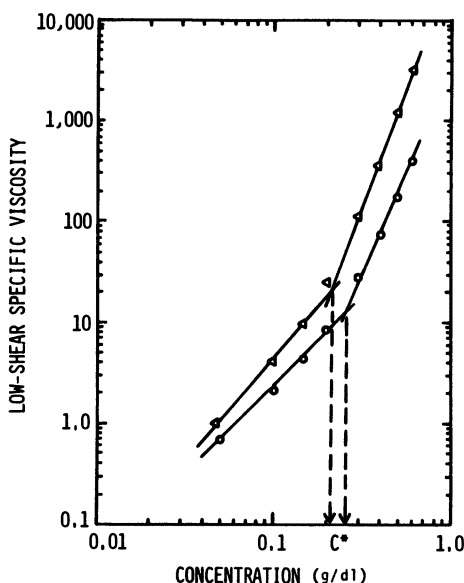


Figure 5. Low-shear specific viscosity-concentration profiles for HP-guar.

Key: Δ , sample B (Table I); and \circ , sample F (Table I).

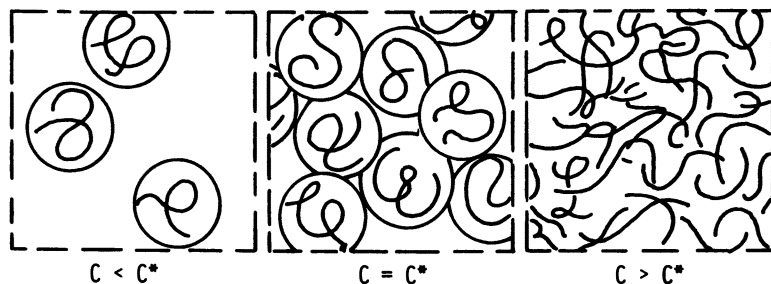


Figure 6. Critical concentration (C^*).

standpoint, C^* is important because it represents the minimum polymer concentration above which an infinite polymer network can be formed. Below C^* , cross-linking the polymer chains eventually leads to polymer segregation. Conceptually, C^* is related to ϕ^* , which therefore must be dependent on polymer molecular weight.

The effect of polymer molecular weight on C^* can be determined experimentally (Figure 7). A single master plot of viscosity (low shear specific viscosity) versus dimensionless concentration (concentration multiplied by intrinsic viscosity, $C[\eta]$) for solutions of polysaccharides can be obtained (12). For the case of HPG solutions in 2% KCl, the plot shown in Figure 7 was experimentally determined. The intersection between the two straight lines depicted in Figure 7 occurs at

$$C^* = 3.4/[\eta] \quad (11)$$

The intrinsic viscosity, $[\eta]$, is dependent on the polymer molecular weight as expressed by the Mark-Houwink equation:

$$[\eta] = KM_w^{a'} \quad (12a)$$

The parameters K and a' depend on the particular polymer-solvent pair. a' is usually related to the stiffness of the polymer. For the particular

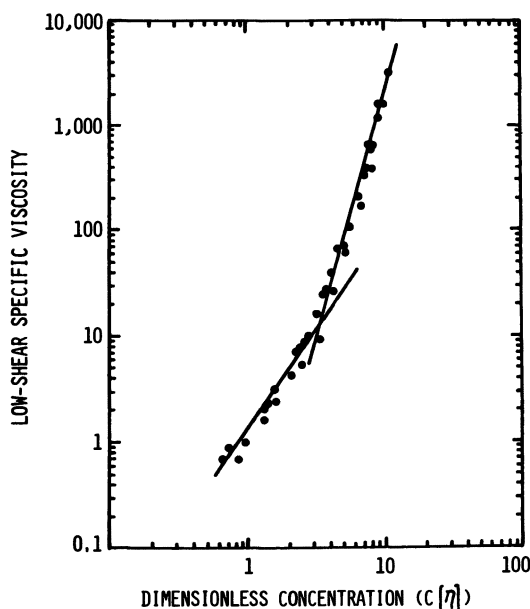


Figure 7. Master curve of low-shear viscosity against concentration for HPG [molar substitution (MS) is 0.5] polymers in 2% KCl.

case of guar in deionized water, Robinson et al. (13) have determined that the intrinsic viscosity obeys the relationship

$$[\eta] = (3.8 \times 10^{-4})M_w^{0.72} \quad (12b)$$

Table I lists the critical concentrations obtained experimentally for a series of HPG samples with different intrinsic viscosities and molecular weights. According to these data, C^* values for these HPG polymers range from 0.19 g/dL for the highest molecular weight sample to 0.27 g/dL for the lowest molecular weight sample.

Figure 8 illustrates the effect of polymer concentration on the elastic properties of HPG cross-linked with titanium acetyl acetate. For the particular HPG sample used (sample C), C^* was experimentally determined to be 0.22 g/dL. The oscillatory shear data shown in Figure 8 indicate that at a polymer concentration of 0.20 g/dL, the storage modulus (G'), a measure of gel strength, remains low regardless of cross-linker concentration. However, as the polymer concentration is gradually increased above 0.20 g/dL, significantly stiffer gels can be made by simply increasing the cross-linker concentration. This rheological behavior suggests that indeed C^* represents a good estimate for the minimum polymer concentration required to form an infinite network. Typical polymer concentrations used in practice range from 0.24 to 0.72 g/dL, which correspond to approximately one to three times higher values than C^*

Effect of C^* or Polymer Molecular Weight on Rheological Properties of Polymer Solutions and Gels

Because apparent molecular weight has a significant effect on C^* (equations 11 and 12), polymer molecular weight is expected also to have a significant impact on the rheology of HPG solutions and gels. Figure 9 shows the steady shear viscosity of 0.5-g/dL solutions of a few of the HPG samples listed in Table I. In this series, the highest molecular

Table I. C^* for Several HPG Samples

<i>HPG sample</i>	$[\eta]$ (dL/g)	C^* (g/dL)	M_w^a ($\times 10^{-6}$)
A	18.1	0.19	3.0
B	16.4	0.21	2.6
C	15.9	0.22	2.5
D	15.4	0.22	2.4
E	13.8	0.25	2.0
F	13.3	0.26	1.9
G	12.5	0.27	1.8

Source: Reproduced with permission from Ref. 16. Copyright 1985 Hemisphere.

^a M_w is the estimated weight-average molecular weight.

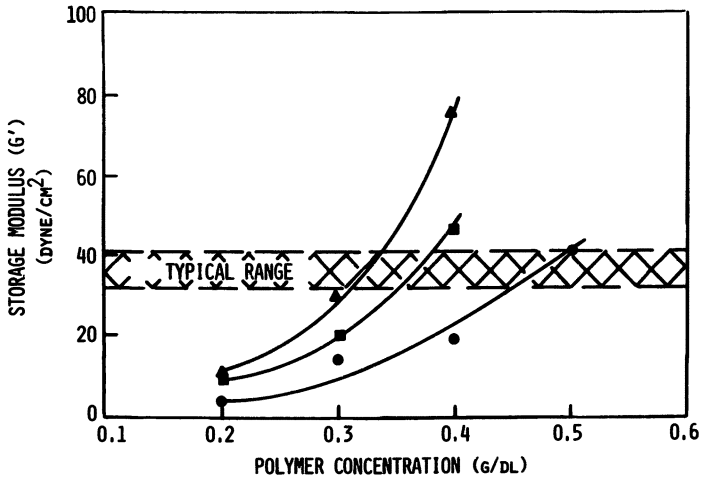


Figure 8. Effect of polymer and cross-linker (TiAA) concentration on viscoelastic properties of HPG ($MS = 0.5$) gels. Key: \blacktriangle , 1200 ppm; \blacksquare , 600 ppm; and \bullet , 300 ppm.

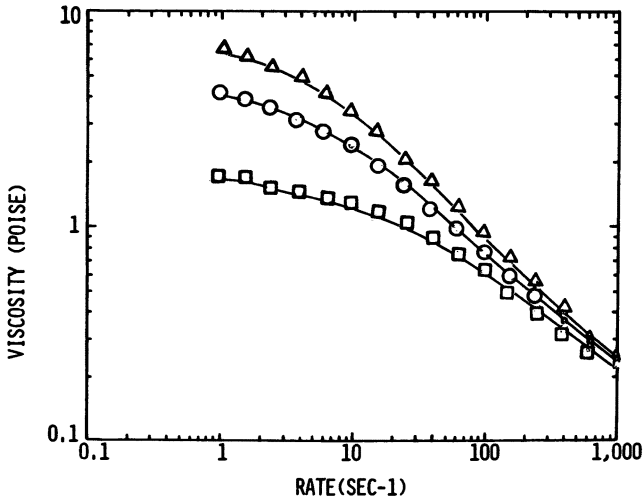


Figure 9. Apparent viscosity profiles of 0.5 wt % HPG solutions in 2% KCl. Key: Δ , sample A; \circ , samples B and C; and \square , sample G.

weight polymer (sample A) exhibits the highest viscosity, and the order ranking of the remaining samples is in accordance with their molecular weights. Furthermore, Figure 10 shows that when 0.5 g/dL HPG solutions are cross-linked with incremental amounts of titanium acetyl acetonate and oscillatory shear experiments are performed on the resultant gels, the same order ranking in accordance with the molecular weight of the starting polymer is obtained. These experimental results are in agreement with the effect of polymer molecular weight on the viscoelastic properties of synthetic polymer melts and solutions (14).

From the fracturing fluids standpoint, the implication of this finding is that the rheological properties of a metal cross-linked polymer gel can be related to the dilute solution properties (i.e., intrinsic viscosity) of the polymer, as well as to the low-shear Newtonian viscosity of the polymer solutions (Figure 7).

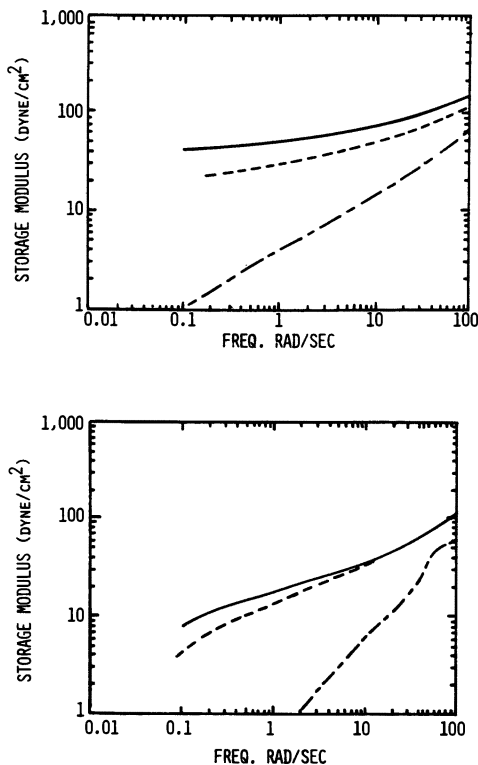


Figure 10. Viscoelastic properties of HPG-TiAA gels. Key: —, sample A; ---, sample C; and —·—, sample G. Top: 300 ppm TiAA. Bottom: 150 ppm TiAA.

Effect of Temperature on the Elastic Properties of Metal Cross-Linked Polymer Hydrogels

In the past, studying the rheological behavior of metal cross-linked polymer hydrogels at high temperatures was difficult. This problem has been due to the difficulty of handling and measuring the viscosity of gels. Conway et al. (4) attempted to study these systems using a concentric cylinder viscometer and reported broad temperature ranges for the stability of HPG and CMHEC gels cross-linked with a variety of metals. However, rotational steady shear viscometers do not accurately determine the rheological properties of viscoelastic gels. In these measurements, experimental artifacts such as sample slippage at the wall of the testing cell and gel fracture are commonplace.

Hercules has since pioneered the use of oscillatory shear measurements to characterize the high-temperature rheology of fracturing gels. Advantages of the oscillatory shear flow technique over steady shear flow measurements are (1) the oscillatory shear flow technique is non-destructive and therefore does not fracture the gel during testing, (2) it allows clear-cut determination of the gel viscous and elastic properties, and (3) it offers higher resolution than steady shear measurements on gels.

Using the Rheometrics pressure rheometer, we have observed for the first time an interesting phenomenon when HPG-metal gels are heated rapidly. This phenomenon is illustrated in Figure 11 for titanium gels. The storage modulus (G') of the gels, determined at a constant oscillation frequency and strain amplitude, remains fairly constant up to a critical temperature, beyond which a catastrophic loss of elasticity takes

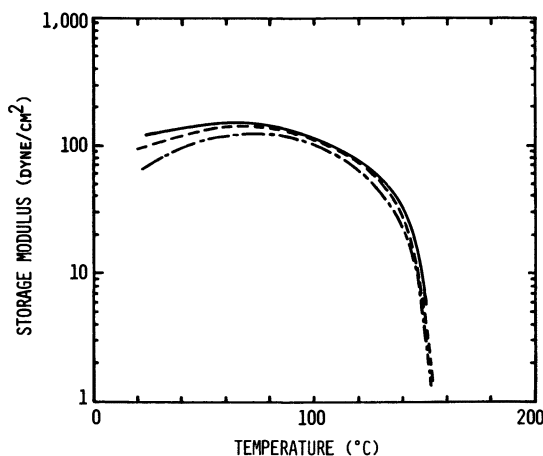


Figure 11. Thermal stability of HPG-TiAA hydrogels. Key: —, 100 rad/s; ---, 50 rad/s; and -·-·-, 10 rad/s.

place. This temperature is termed the thermal breakdown temperature (TBT) and defined as the temperature at which the onset of gel strength loss is detected. Interestingly enough, the TBT appears to be characteristic of the polymer–ligand bond and therefore can be used to characterize the strength of the cross-linking bond. This finding is in accordance with equation 10, which predicts that the T_c is essentially a function of the thermodynamic properties associated with the cross-link bond. From a practical standpoint, the TBT of a given polymer–metal gel defines the upper temperature limit below which the hydrogel can be used in fracturing jobs. TBT has been found to be independent of strain amplitude and oscillation frequency (Figure 11) and, more importantly, of cross-linker and polymer concentration (Figure 12), provided $C > C^*$.

One of the key and most stringent requirements for a fracturing gel is its stability at high temperatures. In general, as oil wells are drilled deeper, the transport of proppant along the fractures has to be done at higher temperatures. Therefore, the capability of determining the TBT of any polymer gel is of great value for determining its suitability for hydraulic fracturing applications.

From the standpoint of designing a gel with the right thermal stability, questions such as the effect of type of metal or functional group of the polymer on the TBT of a gel can be easily addressed by using the oscillatory shear technique. For example, Figure 13 illustrates the thermal stability differences between an HPG–titanium and an HPG–antimony gel. Moreover, if the cross-linking sites on the polymer backbone are carboxyl groups (as is the case for CMHEC, II) instead of the cis diols of HPG (I), a difference in the thermal breakdown temperature

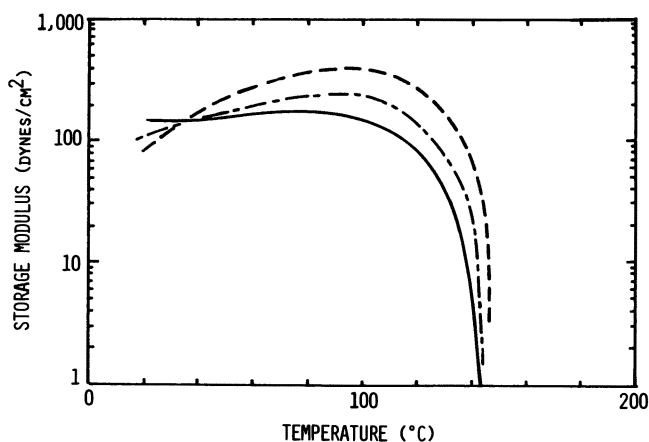


Figure 12. Effect of polymer and cross-linker concentration on thermal stability of HPG–TiAA gels. Key: —, 0.50% HPG–300 ppm TiAA; ---, 0.33% HPG–1200 ppm TiAA; and —·—, 0.38% HPG–600 ppm TiAA.

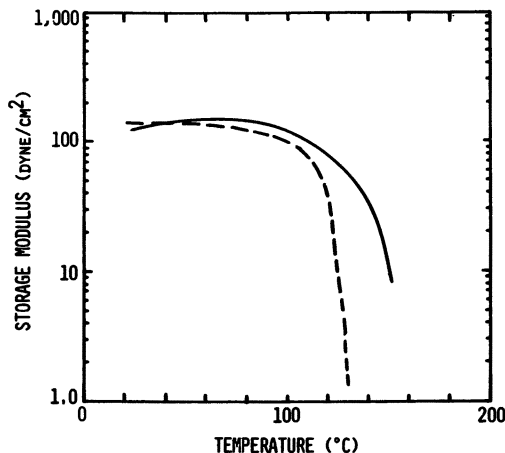


Figure 13. Effect of metal type on thermal stability on HPG gels. Key: —, titanium; and ---, antimony.

of their gels is obtained (Figure 14). These differences in TBTs are presumably due to the particular enthalpy and entropy changes associated with each ligand-metal bond.

Polysaccharides are known to be labile to acid hydrolysis and oxidative depolymerization (15). The results shown here were obtained under experimental conditions that would minimize polymer degradation. Specifically, heating rates of approximately 4 °C/min were used, and the results were independent of the absence or presence of sodium thiosulfate.

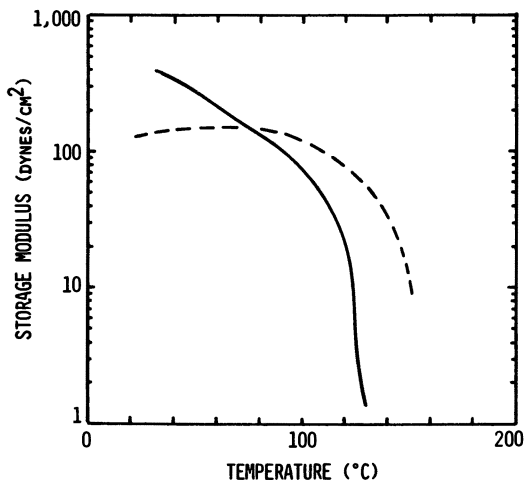


Figure 14. Thermal stability of polysaccharide-metal gels: Effect of ligand. Key: —, CMHEC-Ti; and ---, HPG-Ti. Reproduced with permission from reference 16. Copyright 1985 Hemisphere.

Conclusions and Recommendations

Metal-ligand complexation reactions can explain the gelation behavior of HP-guar and CMHEC as a function of pH. The optimum pH range for cross-linking a particular polymer can be affected by two additional reactions that compete with the cross-linking reaction. These reactions are the hydrolysis of the metal ion and, in the case of ionic polymers, the protonation of the polymer ligands.

In our experimental work, we have studied, for the first time, metal cross-linked fracturing gels from the standpoint of classical gelation theory. On the basis of this analysis, we identified and experimentally determined two properties that are fundamental and key to the performance of fracturing gels. These properties are (1) a critical polymer concentration (C^*) for gelation and (2) a gel-liquid transition temperature (T_c), which characterizes the thermal stability of the gel.

The effect of polymer molecular weight on C^* and the effect of polymer ligands and metal type on T_c were also demonstrated by using novel rheological measurements of polymer solutions and their metal cross-linked gels.

Acknowledgments

I thank a number of people at Hercules Research Center for their contribution to this paper: Shao-Tang Sun for his valuable technical discussions, Sheila Mulrooney for the professional execution of most of the experiments presented here, and Leslie Truono for taking the time to carefully edit the text of this manuscript.

Literature Cited

1. Veatch, R. W., Jr. *J. Pet. Technol.* **1983**, April, 677-687.
2. Howard, G. C.; Fast, C. R. *Hydraulic Fracturing*; Society of Petroleum Engineers Monograph: New York, 1970, Vol. 2.
3. Hsu, C. H.; Conway, M. W. *J. Pet. Technol.* **1981**, November, 2213.
4. Conway, M. W.; Almond, S. W.; Briscoe, J. E.; Harris, L. E. *J. Pet. Technol.* **1983**, February, 315.
5. Ely, J. "Fracturing Fluid Systems: State of the Art," presented at the Southwestern Petroleum Short Course, Texas Tech. University, April 1981.
6. Cotton, F. A.; Wilkinson, G. *Advanced Inorganic Chemistry*; third ed., Interscience: New York; 1972.
7. Arnson, T. R. Ph.D. Thesis, Institute of Paper Chemistry, Lawrence University, 1980.
8. Tanaka, T.; Swislow, G.; Ohmine, I. *Phys. Rev. Lett.* **1979**, *42*, 23, 1556-1559.
9. Stockmayer, W. H. *J. Chem. Phys.* **1943**, *11*, 45.
10. Flory, P. J. *J. Am. Chem. Soc.* **1941**, *63*, 3083, 3091, 3096.
11. Graessley, W. W. *Adv. Polym. Sci.* **1974**, *16*, 1.
12. Morris, E. R.; Cutler, A. N.; Ross-Murphy, S. B.; Rees, D. A.; Price, J. *Carbohydr. Polym.* **1981**, *1*, 5-21.

13. Robinson, G.; Ross-Murphy, S. B.; Morris, E. R. *Carbohydr. Res.* **1982**, *107*, 17-32.
14. Ferry, J. D. *Viscoelastic Properties of Polymers*; third ed., Wiley: New York, 1980.
15. Glass, J. E.; Soules, D. A.; Ahmed, H.; Eglund-Jongewaard, S. K.; Fernando, R. H. Presented at 1983 California Regional Meeting, Ventura, California, March 1983. Society of Plastics Engineers Paper No. 11691.
16. Menjivar, J. A. In *Biotechnology of Marine Polysaccharides*; Colwell, R. R.; Pariser, E. R.; Sinskey, A. J., Eds; Hemisphere: New York; 1985; pp 249-280.

RECEIVED for review November 8, 1984. ACCEPTED December 2, 1985.

Fundamental Criteria in Polymer Flow Through Porous Media And Their Importance in the Performance Differences of Mobility-Control Buffers

G. Chauveteau

Institut Français du Pétrole, Rueil-Malmaison, France

Recent fundamental investigations on the relation between macromolecular properties and flow behavior through porous media of high molecular weight water-soluble polymer solutions used in enhanced oil recovery processes are described. New experimental techniques and analysis methods to characterize molecular weight distribution and rheological behavior in shear and partly elongational flows are given. For porous media flows at low deformation rates, theoretical models for predicting both polymer velocity and effective viscosity of polymer solutions as a function of macromolecular conformation, macromolecule to pore size ratio, and polymer concentration are proposed and compared successfully to experimental results. For high deformation rate flows, both thickening behavior and mechanical degradation are interpreted at a molecular level and shown to depend on stretched molecule to pore size ratios. This new knowledge is used to propose guidelines for designing polymers more suitable for mobility control.

THE USE OF HIGH MOLECULAR WEIGHT WATER-SOLUBLE POLYMERS to control the mobility of the water injected into oil wells has continuously increased in recent years, and a quite recent review (1) reported that a large part of the field tests were estimated to be successful from both technical and economical points of view.

More than 200 papers dealing with the different aspects of the application of polymers in enhanced oil recovery (EOR) processes have been published in the last two decades in the petroleum literature since the pioneer paper by Sandiford (2). However, the complexity of pore shape and structure inside natural porous media, the lack of knowledge

0065-2393/86/0213-0227\$11.25/0
© 1986 American Chemical Society

and methods to characterize polymer solutions used in EOR processes, and some artifacts inherent in the use of industrial polymers often containing microgels have led to insurmountable difficulties in reaching definitive interpretations of the phenomena observed. On the other hand, most of the first fundamental investigations, which were carefully reviewed by Savins (3), were performed in porous media having large pores compared to macromolecular size, so that the effects of the pore size on rheological properties, which are of importance in oil reservoirs, were negligible.

In the last few years, the influence of the macromolecule to pore size ratio was studied both theoretically and experimentally by using well-defined porous media and well-characterized solutions of xanthan gums (XCPS) and hydrolyzed poly(acrylamides) (HPAM), which are currently used for EOR. Thus, the rheological behavior in porous media could be related to macromolecular properties. This chapter, which discusses the synthesis of these new studies, aims to show how to use this new fundamental knowledge for selecting polymers as a function of field conditions and for designing new improved polymers.

HPAMs and XCPSs that have been actually used in oil fields are polyelectrolytes having variable molecular weights [$(2 \times 10^6 < \bar{M}_w < 15 \times 10^6)$ (\bar{M}_w is weight-average molecular weight)]. However, the experiments described were carried out mainly by using two samples, an HPAM and a fully pyruvated XCPS, the main characteristics of which are given. Because the first sample behaves as a flexible coil and the second sample as a rigid rod, the phenomena described are thought to be valid for any polymer that might be developed in the future.

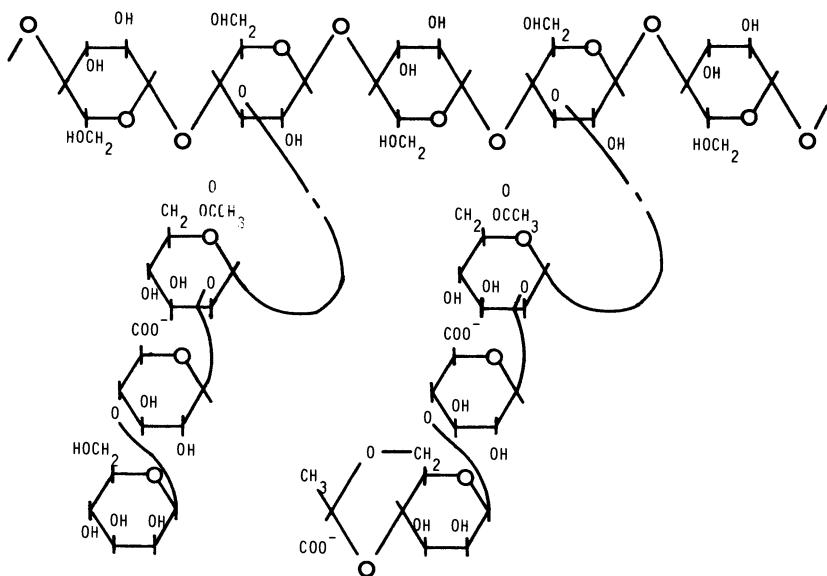
In the first section of this chapter, some basic concepts on physico-chemical behavior of water-soluble polymers having very high molecular weight and more or less standard techniques usable for characterizing such polymers are described. The second section shows how to deduce, from simple rheological experiments in shear and partly elongational flows, some information essential for understanding polymer behavior in porous media. In the third section, new theoretical models able to predict the effects of pore size and polymer concentration on the effective viscosity in nonadsorbent and adsorbent porous media are proposed and compared with experimental results. Then, the main features determining the propagation of polymer slugs through reservoirs are analyzed. In the last section, some additional methods suitable for testing EOR polymers are given.

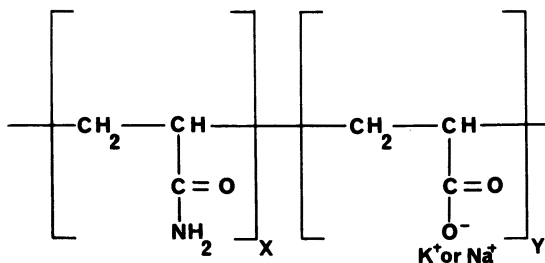
Characterization of Macromolecules in Solution

Chemical Structure. XCPS is an extracellular polysaccharide produced by fermentation of the microorganism *Xanthomonas campestris*. Its primary structure has been clearly established (4, 5) and consists of a

linear 1→4-linked D-glucan chain substituted on every glucose residue by a trisaccharide side chain (I). In the native form, every internal mannose of the side chain is acetylated, whereas the terminal mannose has a variable degree of pyruvate substitution, which is claimed to be possibly dependent on both the bacterial strain and fermentation conditions. After much controversy about the actual conformation of xanthan, particularly on the question of whether the molecule is a single or a double strand in aqueous solution (6–10), recently Lecourtier et al. (11) showed that the native xanthan molecule is a compact double helix that can be extended and sometimes dissociated into two single strands during industrial treatments after the fermentation step. Whatever the conformation, an order–disorder transition corresponding to the breakage of hydrogen bonds between trisaccharide side chains and the backbone is observed at high temperature and low ionic strength (12–14). Because of the intrinsic stiffness of the xanthan molecule in ordered state, its dimensions and thus solution viscosity are weakly affected by the reservoir water's salinity (15).

Partially hydrolyzed poly(acrylamide) can be obtained by hydrolyzing poly(acrylamide) with sodium or potassium hydroxide or by free-radical copolymerization of acrylamide with sodium acrylate. The chemical structure of HPAM is II. The hydrolysis degree, τ , is defined as the ratio of the number of acrylate groups to the total number of acrylamide and acrylate functional groups. The value of τ ranges from 0% to





II

35% for the polymers currently used in EOR. The conformation in solution of these flexible molecules, which has been widely studied (16-18), is very sensitive to the salt content.

Macromolecular Dimensions. In dilute solutions, the parameter commonly used to characterize the effective size of polymer molecules is the radius of gyration, R_G , which is the root mean square distance of the elements of the chain from its center of gravity. The value of R_G can be deduced from variations in the intensity of scattered light with the observation angle.

For flexible coils such as HPAM in salted waters, a viscometric radius of gyration, $R_{G\eta}$, can also be estimated from viscosity measurements by using the Fox-Flory equation (19):

$$R_{G\eta}^2 = ([\eta]_0 M_r \phi'^{-1})^{2/3} \quad (1)$$

$\phi' = 4.2 \times 10^{24}$ cgs is a universal constant, M_r is the molecular weight, and $[\eta]_0$ is the intrinsic viscosity, which is the limiting value at zero polymer concentration and zero shear rate of the reduced specific viscosity:

$$[\eta]_0 = \lim_{\dot{\gamma} \rightarrow 0}^{C \rightarrow 0} (\eta - \eta_s) / \eta_s C \quad (2)$$

η is the polymer solution viscosity, η_s is the solvent viscosity, C is the polymer concentration, and $\dot{\gamma}$ is the shear rate.

For very high molecular weight polymers, particularly when they are dissolved in good solvents, $R_{G\eta}$ is usually slightly smaller than R_G (19).

The root mean square end-to-end distance, $\langle r^2 \rangle$, is related to R_G^2 by

$$\langle r^2 \rangle = n R_G^2 \quad (3)$$

where $n = 6$ for unperturbed coils and $n = 7$ for macromolecules in a good solvent.

For semirigid polymer chains such as XCPS molecules in aqueous solutions over a wide range of salinity or HPAM molecules in water

at very low salinity, the macromolecule dimensions can be calculated by using the wormlike chain model proposed by Ktasky and Porod (20) and Benoit and Doty (21) where R_G^2 and $\langle r^2 \rangle$ are expressed as a function of their persistence length, q , and their contour length, L_c :

$$R_G^2 = (qL_c/3)\{1 - 3/x + (6/x^2)[1 - (1/x)(1 - e^{-x})]\} \quad (4)$$

$$\langle r^2 \rangle = 2qL_c[1 - (1/x)(1 - e^{-x})] \quad (5)$$

where $x = L_c/q$.

The persistence length, which is equal to the half-length of the Kuhn statistical segment (20), characterizes the rigidity of the polymer molecule. For polyelectrolytes, the total persistence length, q , can be considered as the sum of a structural part, q_s , and an electrostatic part, q_e (22). New refinements concerning this theory were proposed recently (23).

No analytical solution is available to calculate the intrinsic viscosity of a wormlike chain from q and L_c , but numerical solutions have been proposed by Yamakawa and Fujii (24). These calculations were recently used (8) to deduce from the $[\eta]$ versus M_r dependence the conformational characteristics of the highly pyruvated xanthan sample we investigated. In this manner, this sample was shown to be a monostranded helix having a persistence length equal to 50 nm under conditions where the structure is ordered (0.1 M NaCl; $\Theta = 30^\circ\text{C}$). The variations of this persistence length with salinity were fully analyzed (15).

For strictly rigid molecules, the relationship between $[\eta]$ and macromolecule dimensions was calculated for ellipsoids (25) and rods (26). For the highest values of the length to diameter ratio, p , the relationship between p and the viscosity factor $V_0 = [\eta]/V_{sp}$, where V_{sp} is the specific volume, can be approximated by power-law functions; very similar results are obtained whichever model is used (27):

$$V_0 = 0.141p^{1.812} \text{ (ellipsoids)} \quad (6)$$

$$V_0 = 0.159p^{1.801} \text{ (rods)} \quad (7)$$

On another hand, the length of the rod, L_c , can be calculated from M_r and $[\eta]$ by the equation (25)

$$L_c^3 = (45/2\pi N)[\eta]M_r(\ln 2p - 0.5) \quad (8)$$

where N is Avogadro's number.

Then, the radius of gyration can be calculated by

$$R_G^2 = L_c^2/12 \quad (9)$$

Dynamic Properties. The relaxation time of macromolecules is a useful parameter for predicting their flow properties. The Rouse model

(29), which describes coiled macromolecules as a succession of beads linked by springs, is generally used to calculate the longest relaxation time, τ_R :

$$\tau_R = (6/\pi^2)\eta_s[\eta]M_r/RT \text{ (at zero concentration)} \quad (10)$$

$$\tau_R = (6/2)\eta_s(\eta - \eta_s)/(\eta_s C)M_r/RT \text{ (for dilute solutions)} \quad (11)$$

R is the constant of ideal gas and T is the absolute temperature.

For rigid rods, the rotational relaxation time, τ_r , can be estimated from the rotational diffusional coefficient, D_r :

$$\tau_r = 1/2D_r \quad (12)$$

The theoretical value of D_r was predicted by Burgers (26):

$$D_r = (3kT/\pi\eta_s L_c^3)(\ln 2p - 0.8) \quad (13)$$

where k is the Boltzmann constant.

The translational diffusion coefficient, D_t , can be deduced from quasi-elastic light-scattering measurements. For high molecular weight polymers, the D_t values of macromolecules are very low ($\approx 10^{-8}$ cm²/s) compared to that generally obtained for small molecules ($\approx 10^{-5}$ cm²/s).

D_t can be related to the hydrodynamic radius of macromolecules, R_H , through the Stokes-Einstein equation:

$$D_t = kT/6\pi\eta_s R_H \quad (14)$$

R_H is the radius of the hard sphere having the same translational diffusion coefficient.

Concentration Regime. The properties of macromolecular solutions are strongly dependent on polymer concentration especially for coiled polymers above the overlap concentration, C^* , which characterizes the limit between dilute and semidilute systems (30, 31). Above C^* , macromolecular dimensions decrease and the physical laws linking viscosity and diffusion coefficients to polymer concentration and molecular weight are entirely different (30).

For coils, simple geometrical arguments suggest that C^* is reciprocally related to the intrinsic viscosity; that is, $C^*[\eta] = 0.7$. However, Graessley (32) reported that, to observe a significant effect on dynamic properties, the concentration must be higher, say, $C^*[\eta] \approx 3-5$.

For rod polymers, the concept of overlap corresponds to the concentration where the number density of rods exceeds $1/L^3$ and the rods can no longer rotate freely (33, 34), but the transition between the dilute and semidilute regime is smoother than with flexible polymers and pertinent values for C^* are still debated.

Salt Sensitivity. As outlined, the HPAM macromolecule has a structural flexibility that makes it very sensitive to the ionic environment. Cations have screening effects on the electrostatic repulsions between charged monomers, which decreases the excluded volume and then macromolecular size. Divalent ions have a stronger effect on viscosity than monovalent ions (35) and can lead to the precipitation of HPAM having a high hydrolysis degree, τ (36–38). Nevertheless, when monovalent ions or an excess of divalent ions is added, polymer redissolution is observed (38). Moreover, for a given τ value, copolymers of acrylamide and acrylic acid, which have a more sequenced microstructure, are less stable in the presence of divalent cations than hydrolyzed polymers (39) and increasing temperature promotes polymer precipitation (40).

The viscosity of semirigid xanthan molecules is much less sensitive to the presence of ions except in very low salinity range, but its solubility also decreases as pH decreases or salinity increases (15).

Macromolecules Near an Interface. In the vicinity of a solid–liquid interface, the properties of a polymer solution are strongly modified compared to the properties exhibited in unbounded solutions.

Near a noninteractive wall such as a nonadsorbent solid surface, macromolecule centers of mass are sterically excluded from the wall vicinity. This phenomenon, which has been theoretically predicted under static conditions for both flexible (41) and rodlike (42) polymers, leads to a depletion layer at the solid interface. In polymer flows through porous media, this depletion layer produces two main effects: (1) The polymer solution viscosity in nonadsorbent porous media is lower than in unbounded solutions (43). (2) The exclusion of macromolecules from the slowest stream lines near the wall induces a mean polymer velocity higher than the solvent velocity; this polymer velocity increases with macromolecular dimensions, and, thus, chromatographic size fractionation occurs (44). The implications of these two effects are analyzed in the next section.

Molecular Weight Distribution. Very few techniques are effective for determining the molecular weight distribution of polymers used for EOR processes. GPC was found to fail (45, 46) when applied to the characterization of very large macromolecules because hydrodynamic forces orient and deform such molecules and thus disturb steric exclusion mechanisms.

Direct observation of macromolecules by electron microscopy (47) or measurement of sedimentation coefficients (48, 49) can give the molecular weight distribution of such polymers, but these methods are mainly analytical and cannot be used to prepare polymer fractions.

A new chromatographic technique, commonly called hydrodynamic chromatography and based on the exclusion of suspended particles from

the slowest stream lines near the pore wall, was developed for protein (50) and latex (51-54) size determination. Prud'homme et al. (55) applied this technique to hydrosoluble polymer fractionation, but the efficiency of the size separation observed was poor because of the too high flow rates used in these experiments. A study of the influence of shear rate and polymer concentration on xanthan fractionation by hydrodynamic chromatography was recently reported (44). Small slugs of xanthan solutions were injected through a porous medium composed of silicium carbide (SiC) particles. The efficiency of the fractionation is displayed at the outlet of the porous medium (Figures 1 and 2) by the strong decrease of the intrinsic viscosity of xanthan fractions as the elution volume increases. The results show that the experimental conditions necessary for obtaining an efficient separation are quite severe: (1) very low shear rates in order to prevent any shear-induced macromolecule orientation (Figure 1) and (2) polymer concentration low enough to minimize viscous fingering at the trailing edge of the injected polymer peak (Figure 2). Under these conditions, the complete molecular weight distributions of two XCPS samples and their polydispersity indexes could be determined (Figure 3).

More recently, an original size fractionation technique (56) based on the flow rate dependent filtration of macromolecules through nonadsorbent calibrated pores having a radius r smaller than their radius of gyration, R_G , was found to be promising in obtaining HPAM fractions.

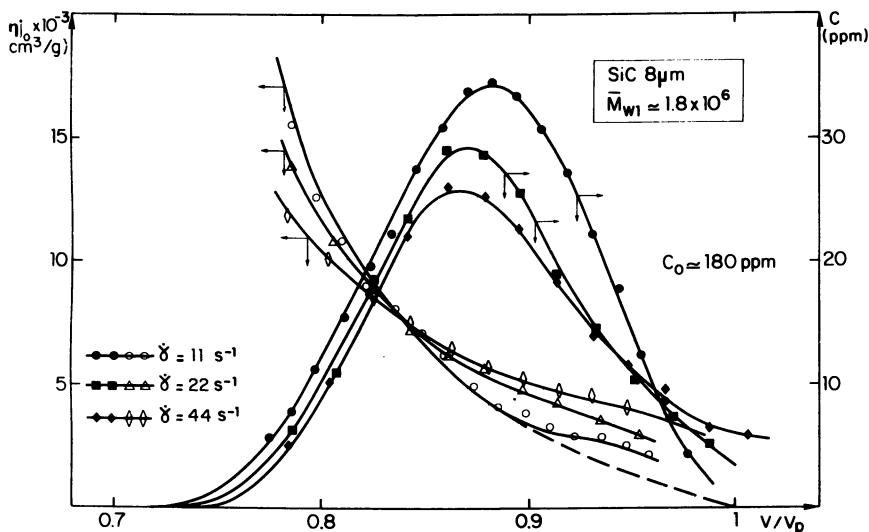


Figure 1. Influence of shear rate on XCPS chromatographic fractionation. Reproduced from reference 44. Copyright 1984 American Chemical Society.

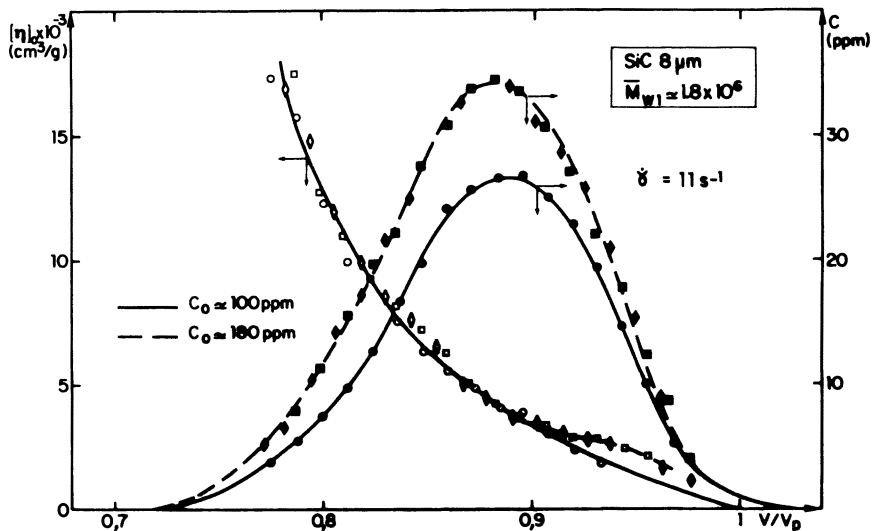


Figure 2. Influence of polymer concentration on XCPS chromatographic fractionation. Reproduced from reference 44. Copyright 1984 American Chemical Society.

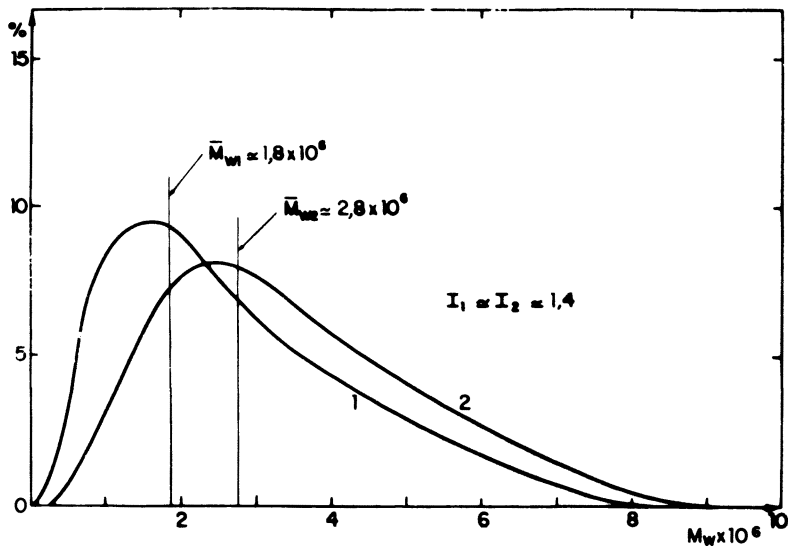


Figure 3. Molecular weight distribution of two XCPS samples. Reproduced from reference 44. Copyright 1984 American Chemical Society.

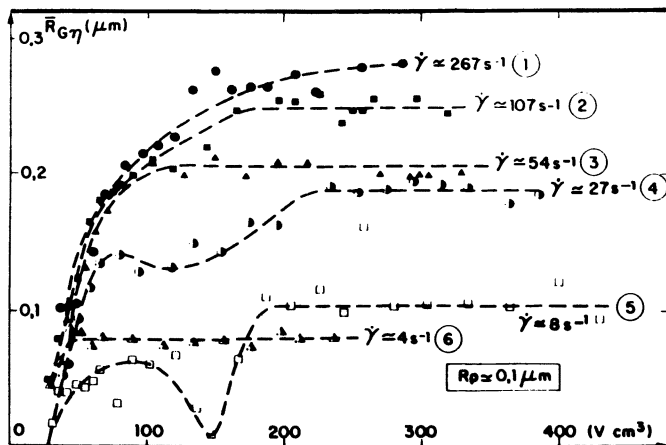


Figure 4. Fractionation of HPAM by flow rate dependent filtration. Reproduced with permission from reference 56. Copyright 1984 Editions Technip.

As an example, the curves in Figure 4 show that the viscometric radius of gyration, $R_{G\eta}$, of the samples collected at the outlet of the porous membrane increases with the shear rate, $\dot{\gamma}$. However, this technique is still time consuming, and technical improvements are in progress to reduce experimental time.

Characteristics of Polymer Samples Used. The two samples used in the experiments were characterized under our standard conditions, that is, $\Theta = 30^\circ\text{C}$, pH 8, and 5 g/L NaCl for XCPS and $\Theta = 30^\circ\text{C}$, pH 8, and 20 g/L NaCl for HPAM. The main characteristics of the polymers are given in Table I.

Rheological Properties

The velocity field inside porous structures is complex even under non-inertial laminar flow conditions, which prevail inside an oil reservoir. Macromolecules are subjected to both shear and extensional stresses.

Table I. Polymer Characteristics

Polymer	\bar{M}_w	I_p	$[\eta]_0$ (cm^3/g)	D_t (cm^2/g)	$R_{G\eta}$ (nm)	R_C (nm)	R_H (nm)
HPAM ^a	7.5×10^6	2.1	3800	1.4×10^{-8}	240	200	150
XCPS ^b	1.8×10^6	1.4	4300	2.4×10^{-8}	170	—	115

^a $\tau \approx 30\%$.

^bThe degree of substitution of pyruvate is 1.

Thus, the rheological characterization of the polymer solutions to be used in EOR processes must include the determination of their viscosity in both shear and extensional flows.

Viscosity in Shear Flows. VISCOSITY VERSUS SHEAR RATE AND POLYMER CONCENTRATION. Shear viscosity can easily be determined by using a coaxial-cylinder viscometer designed for very low shear rate measurements. For better accuracy, mainly for dilute solutions, special capillary viscometers previously described (43) may also be used. Typical curves of relative shear viscosity versus shear rate plotted in log-log coordinates are shown in Figure 5 for the XCPS sample dissolved in salted water under conditions (0.1 M NaCl and $\Theta = 30^\circ\text{C}$) where macromolecules assume an ordered conformation (43). Over the concentration range tested, the curves have a standard shape. As the shear rate increases, the following occur: (1) A Newtonian regime, in which relative viscosity is independent of shear rate, $\dot{\gamma}$, and equal to the zero shear rate relative viscosity, $\eta_{r,0}$, is found. In this shear-rate range, both conformation and orientation of macromolecules are unaffected by shearing forces and entirely governed by Brownian motion. (2) A transition zone, characterized by a critical shear rate equal to the inverse of a rotational relaxation time, τ_r , of the solution (57) is revealed. (3) A shear-thinning regime, in which relative viscosity decreases with shear rate according to a power law whose exponent $2m$ is negative, is determined.

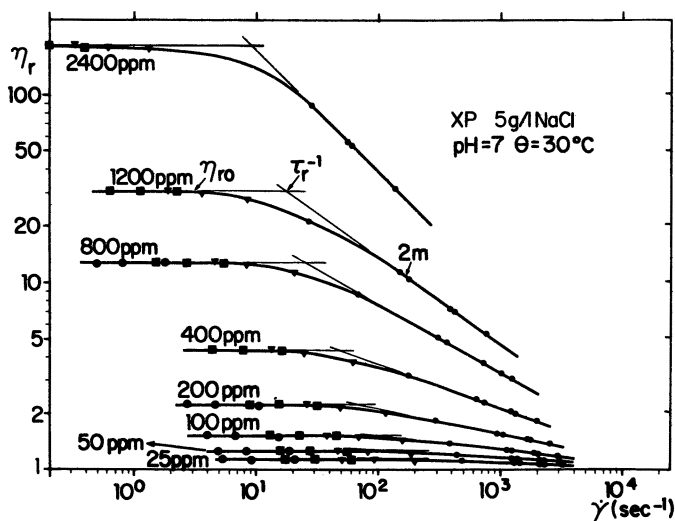


Figure 5. Viscosity vs. shear-rate curve for various polymer rates (XCPS). Reproduced with permission from reference 43. Copyright 1982 Society of Rheology.

Over the shear-rate range tested, the experimental data fit very well in Carreau et al.'s (57) model A.

$$\eta_r = \eta_{r,0} / [1 + (\tau_r \gamma)^2]^m \quad (15)$$

Moreover, the plots of the variations of the three parameters $\eta_{r,0}$, τ_r , and m versus polymer concentrations (*see* reference 43) are used to derive an analytical equation that gives shear viscosity as a function of shear rate for any polymer concentrations up to $C[\eta] \approx 10$.

INTRINSIC VISCOSITY AND MACROMOLECULAR DIMENSIONS. The intrinsic viscosity can be determined at different shear rates by extrapolation, at zero polymer concentration, of the curves of reduced specific viscosity $(\eta_r - 1)/C$ (Figure 6). This extrapolation in the Newtonian system is valid only at low polymer concentrations where the curves of $(\eta_r - 1)/C$ versus C are straight lines, that is, for $C < C^*$. As expected, this linearity is limited to the concentration system where the Simha overlap parameter $C[\eta]_0$ is less than 0.7. As a consequence, sufficiently numerous and accurate experimental points are needed in this concentration range.

The mean macromolecular dimensions of the xanthan sample used were first estimated (43) from the values of the intrinsic viscosity, $[\eta]_0 = 4300 \text{ cm}^3/\text{g}$, and the chain diameter, $d = 20 \text{ \AA}$, by using equations 7 and 8, that is, by assuming the molecule is a rigid rod. The equivalent length, L_{eq} , was found equal to $0.82 \text{ }\mu\text{m}$. More realistic calculations (8) based on the wormlike chain model gave a mean end-to-end distance equal to $0.55 \text{ }\mu\text{m}$ for a contour length of $2 \text{ }\mu\text{m}$.

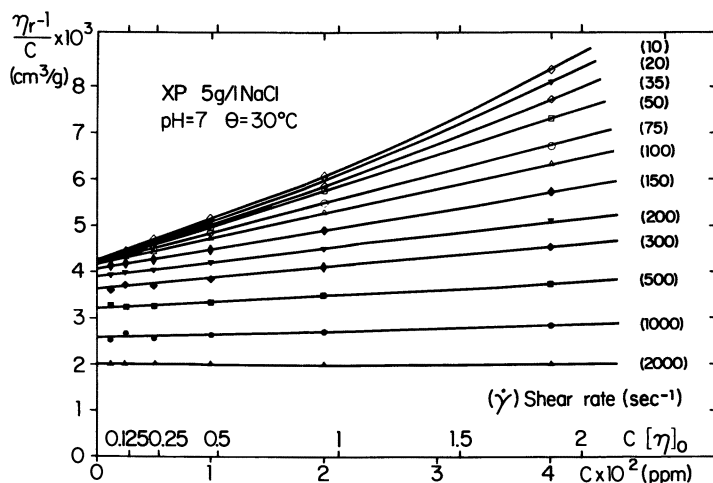


Figure 6. Reduced specific viscosity as a function of shear rate (XCPS). Reproduced with permission from reference 43. Copyright 1982 Society of Rheology.

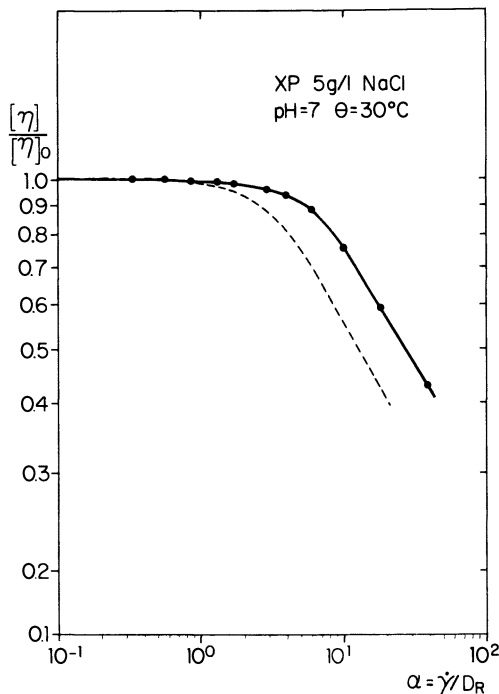


Figure 7. Experimental and theoretical variations of reduced intrinsic viscosity vs. reduced shear rate (XCPS). Key: $\bullet\text{---}\bullet$, experiments; and --- , rod theory. Reproduced with permission from reference 43. Copyright 1982 Society of Rheology.

SHEER-RATE DEPENDENCE OF INTRINSIC VISCOSITY. The shear-rate dependence of intrinsic viscosity is a characteristic of both rigidity and conformation of macromolecules. The results of the numerical calculations (25) based on the Saito model (58) for rigid rods were used to plot (Figure 7, dashed line) the theoretical intrinsic viscosity as a function of dimensionless shear rate $\alpha = \dot{\gamma}/D_r$, where D_r is the rotational diffusion coefficient determined by equation 12. The shear-rate dependence at high shear rates, $2m = -0.44$, is quite close to the theoretical value (25) for rigid rods. The difference observed at the onset of shear-rate dependence can be explained by the overestimation of D_r , calculated by using the rigid-rod model. A more realistic value of D_r , based on the wormlike chain model would give a better agreement between theoretical and experimental curves.

SHEAR-RATE DEPENDENCE OF CONCENTRATION REGIME. Under dilute conditions ($C \ll C^*$), the most usual intermolecular interaction parameter is the Huggins constant, k' , which is defined as the second-

order term coefficient in the equation linking viscosity and concentration:

$$\eta_r = 1 + C[\eta] + k'C^2[\eta]^2 \quad (16)$$

The value of k' can be calculated from the slopes of the curves of $(\eta_r - 1)/C$ versus C . The variation of k' values versus shear rate is plotted in Figure 8. The value obtained in the Newtonian system, $k' = 0.44$, is close to the theoretical value, $k' = 0.4$, expected for polymers without any specific interactions in the free-draining case (59-61). At higher shear rates, hydrodynamic forces induce an orientation of macromolecules along stream lines, and this orientation decreases intermolecular interactions; thus, k' decreases as $\dot{\gamma}$ increases. At $\dot{\gamma} > 2000 \text{ s}^{-1}$, no interactions ($k' \approx 0$) are detected up to 2400 ppm. This extension of the dilute system up to relatively high polymer concentrations is also expected in purely stretching flows, which also induce preferential macromolecule orientation along stream lines.

INFLUENCE OF POLYMER CONFORMATION. Very similar results were obtained recently (62, 63) for an unhydrolyzed poly(acrylamide) ($\bar{M}_w \approx 4.5 \times 10^6$ and $I_p = 2.1$), the chain of which is flexible. The same

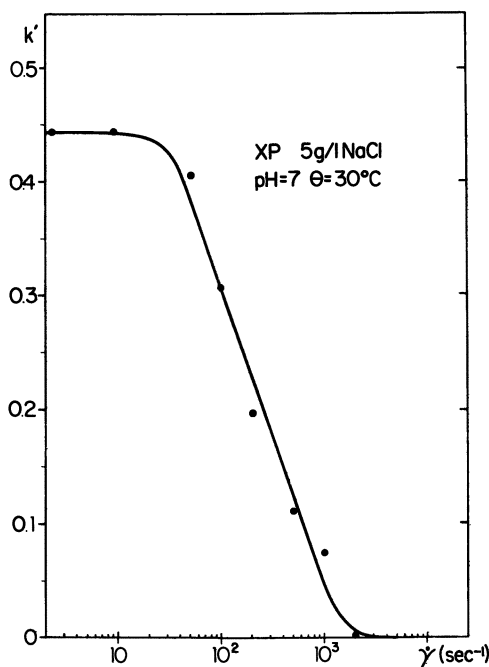


Figure 8. Shear-rate dependence of the Huggins constant (XCPS). Reproduced with permission from reference 43. Copyright 1982 Society of Rheology.

method of analysis was used to calculate the main characteristics of the macromolecule in solution with equations 1 and 10. The intrinsic viscosity was found to decrease much more slowly with shear rate than for rigid rods, and the extension of the dilute system as shear rate increases is not so drastic as with a stiff molecule such as xanthan.

Viscosity in Partly Elongational Flows. Many studies have suggested that the partly elongational nature of flows through porous media was the source of the thickening behavior (i.e., the increase in viscosity as the flow rate increases) observed at high deformation rates. This hypothesis was recently supported by studies both in porous media (64–65), and in capillary systems (66–68) and thus the close relation between the thickening behavior observed in porous media and in more simple models having an elongational character is now well-established. Because experiments in such models are much less time consuming and give results that are more reproducible and easier to interpret than those carried out in porous media, these experiments can be used as a selection method for EOR polymers. Most of the experiments were carried out with HPAM, but a comparison with XCPS was also made.

FLOW-THROUGH CAPILLARIES. A fluid flowing through a cylindrical capillary experiences pure shear stresses inside the capillary but also extensional stresses in both entrance and exit zones. Thus, measuring the apparent relative viscosity, η_r (i.e., the ratio between total pressure drop for polymer and water flow), versus wall shear rate, $\dot{\gamma}$, in capillaries having the same diameter but different lengths is a simple way to study the behavior in elongational flows. The capillary diameter must be small enough to remain in the noninertial regime over the shear range tested in order to obtain data representative of reservoir conditions. The results of such experiments are shown in Figure 9.

At low and medium shear rates below a critical value of $\dot{\gamma}$, termed $\dot{\gamma}^*$, the apparent viscosity is practically equal to relative shear viscosity and independent of capillary length. This finding means that in this shear-rate range the viscosity in the elongational parts of flow, that is, in the inlet and outlet of the capillaries, is nearly equal to the Trouton viscosity; the effect is a negligible contribution to the total end-pressure loss. However, beyond $\dot{\gamma}^*$, high-pressure drops that strongly increase with the flow rate are observed at the ends of capillaries; thus, the apparent viscosities increase as the length-to-diameter ratio of capillary decreases (Figure 9). This behavior has been shown recently (66, 68) to be due to the elongation of macromolecules in the stretching flows in both the entrance and the exit of capillaries.

The coil-stretch transition of a macromolecule in an elongational flow theoretically occurs when the product of the stretch rate, $\dot{\epsilon}$, and its relaxation time, τ_R , reaches a value close to 1 (69, 70). As the molecule

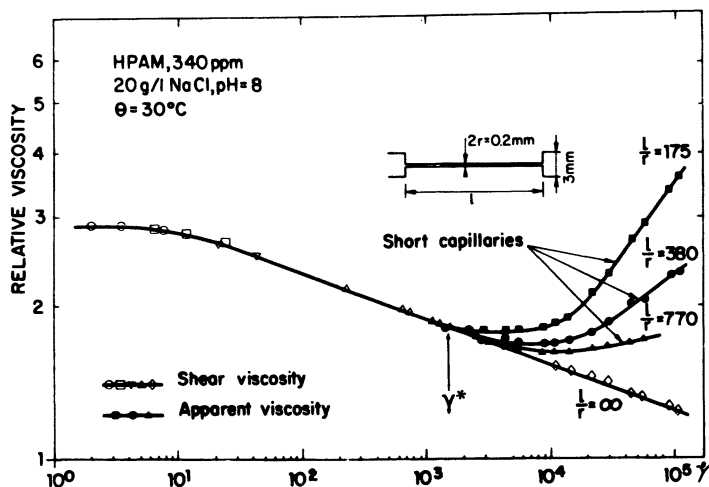


Figure 9. Effective viscosity in capillaries having different lengths (HPAM). Reproduced with permission from reference 67. Copyright 1979 Elsevier.

becomes nearly fully extended in the flow direction, a high extensional viscosity increasing as the square of its length is expected (71). However, a large extension of the macromolecule and consequently a high extensional viscosity are obtained only if the macromolecule is subjected to this high stretch rate, $\dot{\epsilon}$, during a time t sufficiently long to achieve this elongation, $\dot{\epsilon}t > a$, where $a \approx 4$ for high weight-average molecular weights. This second condition was predicted theoretically (70) and studied experimentally in pure elongational flows (72). Both conditions are fulfilled at the entrance of the capillaries at high stretch rates ($\dot{\epsilon}\tau_R > 1$) when the contraction ratio R/r at the entrance is high enough ($\dot{\epsilon}t > a$). For instance, for constant stretch rate flows, the product $\dot{\epsilon}t$ is equal to $2 \ln(R/r)$ (73).

EFFECTS OF GEOMETRIC FACTORS ON THICKENING BEHAVIOR. Because the behavior is thickening only in elongational parts of the flow, the effects of the contraction ratio, R/r , on the length of entrance, L , and on the number of contractions were tested in cylindrical models (Figure 10) having the same low value of the length-to-radius ratio, $l/r = 10$. In Figure 10, the apparent relative viscosity has been plotted as a function of the wall shear rate, $\dot{\gamma}$ calculated by the equation $\dot{\gamma} = 4Q/\pi r^3$, where Q is the flow rate and r is the capillary radius. The curves show the following: (1) the onset of thickening behavior ($\dot{\gamma} \approx 1500 \text{ s}^{-1}$) is the same in the three models and corresponds to the onset observed in capillaries having a greater length-to-diameter ratio (Figure 9) or having a profiled entrance (67). This result is not surprising because the maxi-

mum elongational rate, $\dot{\epsilon}$, which determines macromolecule elongation, is located on the central stream line and thus does not depend on the exact entrance shape. (2) The magnitude of thickening behavior at the highest shear rates increases with the contraction ratio as expected. (3) The existence of successive contractions gives a sharper increase in apparent viscosity just beyond the critical shear rate, $\dot{\gamma}^*$. This phenomenon is due to the fact that, in such a model, the macromolecule partially elongated in the first contraction is not completely relaxed upon arriving in the second contraction. The macromolecule's elongation is further increased in the second contraction; a higher viscous dissipation results. This effect was recently studied in detail (74). A similar effect of succession occurs in porous media flows. (4) The apparent viscosity tends, at the highest deformation rates, toward a constant value that depends on geometric shape. This plateau value probably means that the maximum elongation of the macromolecule for this geometry has been reached.

EFFECTS OF POLYMER CONCENTRATION AND SOLUTION SALINITY. These effects were investigated in the model consisting of 45 successive elements (Figure 10). The effects of polymer concentration are shown in Figure 11: (1) The apparent viscosities are equal to relative shear viscosities below $\dot{\gamma}^*$; this finding confirms the results in Figures 9 and 10. (2) The critical shear rate, $\dot{\gamma}^*$, decreases slightly as the polymer concentration increases, so that the product $\dot{\gamma}^* \tau_R$, where τ_R is the Rouse relaxation time (equation 11), is nearly constant and equal to 10. (3) The

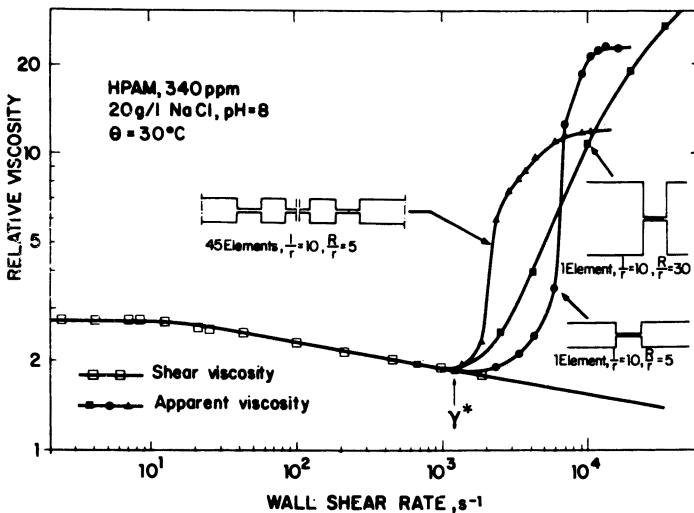


Figure 10. Effects of some geometric factors on thickening behavior in various models (HPAM). Reproduced with permission from reference 65. Copyright 1981 Society of Petroleum Engineers.

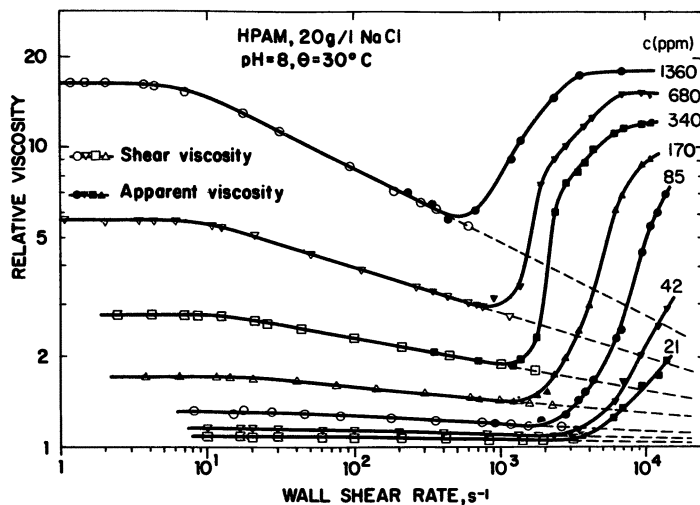


Figure 11. Effects of polymer concentration of thickening behavior in a model including successive constrictions (HPAM). Reproduced with permission from reference 67. Copyright 1979 Elsevier.

apparent viscosity at the highest $\dot{\gamma}$ tends toward stabilized values that increase very slowly with polymer concentration.

The influence of solution salinity, which changes repulsions between charged groups and thus the static conformation of macromolecules, is shown in Figure 12. (1) The critical shear rate, $\dot{\gamma}^*$, decreases as salinity decreases, but the product $\dot{\gamma}^* \tau_R$ is always approximately constant and close to 10. (2) The divergence from shear-thinning behavior beyond $\dot{\gamma}^*$ becomes sharper as salinity increases as expected. Indeed, the coil-stretch transition causes a higher conformational change at high salinity because the coil is then weakly expanded. (3) The apparent viscosities tend toward asymptotic values that depend only slightly on salinity at the highest deformation rates. This observation means that the viscous dissipation on elongated macromolecules does not depend on salinity. Indeed, the end-pressure drops, which are related to extensional viscosity, were deduced from these data and were found to be insensitive to salinity.

EFFECTS OF POLYMER CONFORMATION. The behavior of XCPS solution in the same model including successive contractions (Figure 13) is qualitatively similar to that observed with poly(acrylamides). The apparent viscosity becomes higher than shear viscosity beyond a critical shear rate, but this thickening behavior in the elongational parts of the flow is very slight. Such a result is quite consistent with the interpretation of the thickening behavior by the flow-induced elongation of macromolecules.

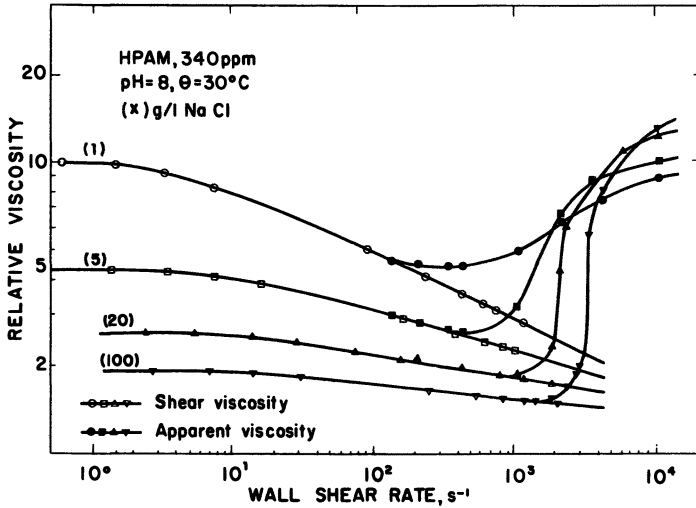


Figure 12. Influence of salinity on thickening behavior in a model including successive constrictions (HPAM). Reproduced with permission from reference 67. Copyright 1979 Elsevier.

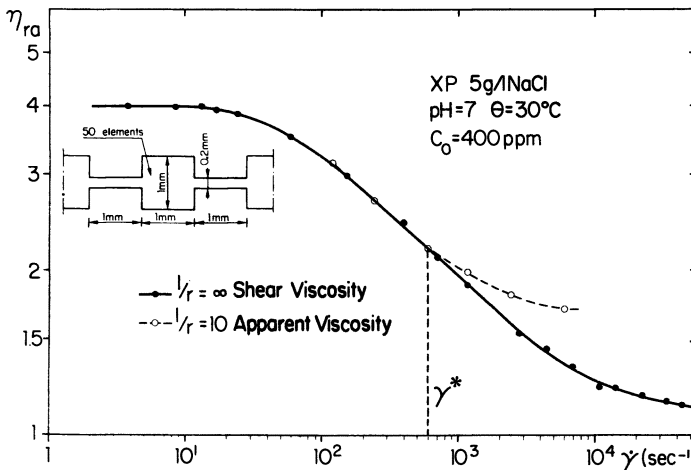


Figure 13. Effective viscosity in a model including successive constrictions (XCPS). Reproduced with permission from reference 43. Copyright 1982 Society of Rheology.

Indeed, the elongational viscosity of a fully extended chain is proportional to the square of the contour length (71), and this contour length is about 10 times smaller for XCPS than for HPAM.

Mechanical Degradation in Elongational Flows. The mechanical degradation of a nonhydrolyzed poly(acrylamide) solution was studied in capillaries of different lengths by using a multipass system (75). The main results of this study were that dilute solutions are not degraded in shear flows and that degradation occurs only in the entrance of capillaries for $\dot{\gamma} > \dot{\gamma}^*$ when the extensional forces exerted on elongated macromolecules by the water surpass the C-C bond strength.

Flow Behavior In Porous Media

The rheological behavior of polymer solutions in porous media is expected to differ from that observed in capillary systems consisting in a series of constrictions and expansions for two main reasons: (1) the geometric shape is much more complex and (2) the dimension of macromolecules can become nonnegligible compared to pore size, mainly in low permeability porous media, which involves an effect of pore wall depletion for nonadsorbent media and modifications of flow due to the adsorbed layer thickness for adsorbent ones. So that any perturbing dimensional effect could be prevented, the influence of geometrical shape of pores was studied in porous media with pores very large compared to molecular size.

Flow-Through Porous Media Having Large Pores. Because of the complexity of the shape of pores and their arrangement, the mean value of wall shear rate, $\dot{\gamma}_{PT}$, in the pore throats of a porous medium that corresponds to the wall shear rate in capillary systems described previously must be experimentally determined by fitting the onset of shear-rate dependence in both capillary viscometers and porous media. For glass bead packs, an experimental equation was established (43):

$$\dot{\gamma}_{PT} = 1.7 \times 4v(8k\varphi^{-1})^{-0.5} \quad (17)$$

v is the frontal velocity, k is the permeability and φ is the porosity. Thus, $\dot{\gamma}_{PT}$ is about 2.45 times higher than the mean value of the shear rate, $\dot{\gamma}_m$, commonly used for glass bead packs:

$$\dot{\gamma}_m = 2v(2Tk\varphi)^{-0.5} = 4v(8kT/\varphi)^{-0.5} \quad (18)$$

v is the Darcy velocity and T is the tortuosity, which is equal to 25:12 for sphere packs.

Before the flow of polymer solutions through stochastic porous media is studied, their behavior in the two glass-bead arrangements with

three and four beads shown in Figure 14 and previously suggested in reference 76 should be described. When the polymer solution flows through the tricuspid triangle formed by the first three beads, the onset of thickening behavior is observed at a critical shear rate, $\dot{\gamma}^* \approx 1500 \text{ s}^{-1}$, equal to that found in the capillary systems; this result confirms the fact that entrance shape is not a determining factor. However, when a fourth bead is added upstream from the three previous beads, the critical shear rate is nearly 150 s^{-1} , that is, about 10 times less. The elongation of macromolecules, which explains the thickening behavior, cannot occur in the entrance of the three upstream openings because the deformation rates are much too low ($\dot{\gamma} \approx 50 \text{ s}^{-1}$). However, the presence of bead 4 creates a flow-induced deformation of macromolecules that is not completely relaxed when the macromolecules arrive in the entrance of the opening 1-2-3. Their relaxation time is thus increased; this effect makes possible a coil-stretch transition in opening 1-2-3 at a much lower deformation rate ($\dot{\gamma} = 150 \text{ s}^{-1}$) with the bead 4 than without bead 4 ($\dot{\gamma} = 1500 \text{ s}^{-1}$).

The same mechanism of predeformation of macromolecules is thought to explain why the thickening behavior is observed in porous media at shear rates (calculated by equation 17) such as $\dot{\epsilon}_{TR} \approx 1$, that is,

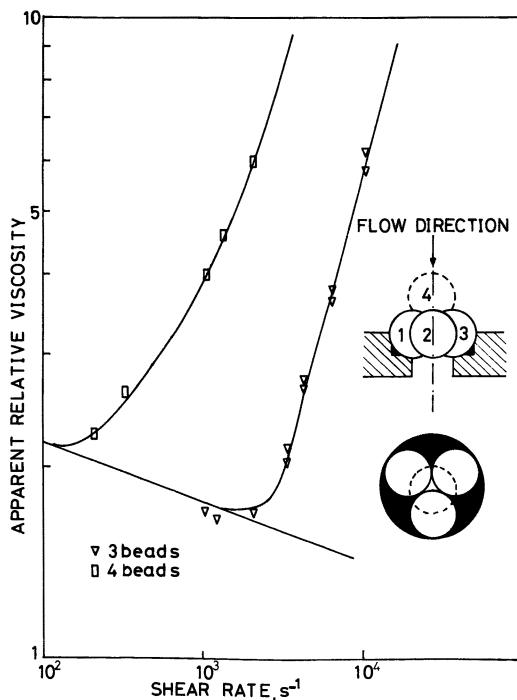


Figure 14. Thickening behavior in two different glass-bead arrangements (HPAM). Copyright 1984 Editions Technip.

American Chemical Society
Library

about 10 times less than in the capillary model with successive constrictions (Figure 15). Indeed, in this model as in the entrance of capillaries, the macromolecules arrive in the converging section without any predeformation.

Thus, the thickening behavior is expected in porous media for values of the product $\dot{\epsilon}\tau_R$ much less than 1. The critical value of $\dot{\epsilon}\tau_R$, which is around 0.1 for glass-bead packs, depends on the pore structure shape, which creates the predeformation of macromolecules.

These experimental results clearly show that the thickening behavior in porous media is due to the elongation of macromolecules and can be predicted from the Rouse relaxation time and the geometrical shape of the porous media.

Flow-Through Nonadsorbent Small Pores. An influence of pore size on the apparent viscosity of polymer solutions flowing through porous media having small pores is expected from the effects of both depleted and adsorbed layers. Small pores refer to situations where the characteristic size of the macromolecule is not negligible with respect to the size of the pores [$R_C \geq 0.02r$].

Getting accurate and representative data on flow through porous media having small pores is a somewhat delicate problem. Precautions must be taken to avoid artifacts such as those caused by the presence of even small amounts of aggregated macromolecules (77). These so-called microgels can partially plug a porous medium and give anomalously high apparent viscosities mainly at low shear rate (compare Selection of

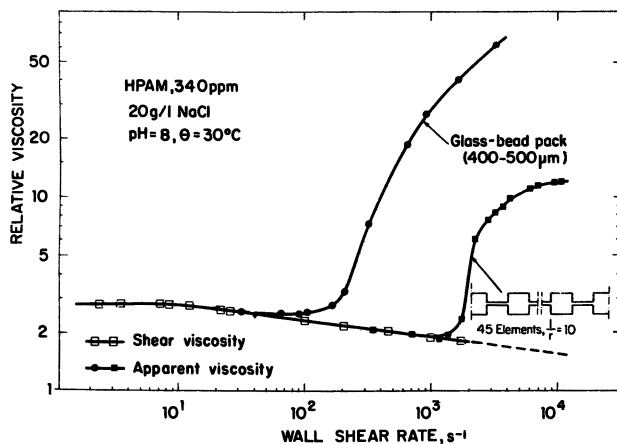


Figure 15. Comparison of rheological behavior in a glass-bead pack and in a model including successive constrictions (HPAM). Reproduced with permission from reference 65. Copyright 1981 Society of Petroleum Engineers.

Polymers for EOR). The microgels can be removed from solutions by a very slow filtration method previously described (78). During the injection of a polymer solution into an oil reservoir, the few microgels contained in the solution are retained by adsorption or mechanical entrapment in a zone located around the injection well; this result decreases the solution's injectivity. Therefore, getting data representative of the behavior of the solution that will actually sweep the oil from the reservoir at large distance from injection wells involves performing experiments with perfectly microgel-free polymer solutions (78).

NEWTONIAN REGIME. The first experiments showing the effects of pore size on the effective viscosity of polymer solutions were carried out with microgel-free solutions of XCPS flowing through polycarbonate Nuclepore membranes, which are nonadsorbent and have a well-defined cylindrical shape (43). The effective viscosities in membranes having different pore sizes are compared in Figure 16 with shear viscosity. In the Newtonian plateau, the effective viscosity is always less than the bulk viscosity and decreases with pore size as expected from the effects of a concentration-depleted layer. Of course, such a result is not found for a membrane having a pore diameter less than the molecular size where macromolecules accumulate upstream from the membrane. Because of the different pore length to pore ratio, l/r , of the membranes used, the values of the effective viscosities beyond the Newtonian plateau are affected differently by the increased viscous dissipation in the entrance (cf. Figure 13) and thus are difficult to compare. However, because the effects of these different l/r on the apparent viscosity are expected to

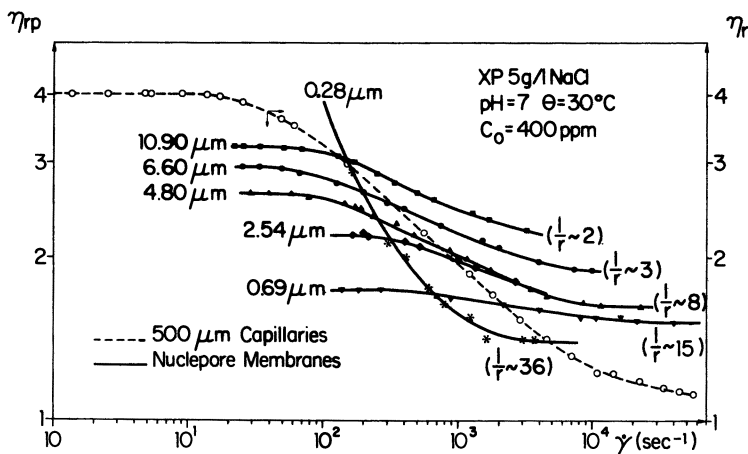


Figure 16. Effective viscosity in polycarbonate membranes (XCPS). Reproduced with permission from reference 43. Copyright 1982 Society of Rheology.

be quite negligible in the Newtonian plateau, an analytical model, fully discussed in reference 43, is proposed to predict the effective viscosity in the pore, η_{rp} , as a function of the pore radius, r , of the depleted layer thickness, δ , and of parameter ρ , which is the ratio of the bulk viscosity, η_{rb} , to the mean viscosity in the depleted layer, η_{rw} :

$$\eta_{rp} = \eta_{rw}[1 - (1/\rho)(1 - \delta/r)^4]^{-1} \quad (19)$$

The values of the effective viscosities in the Newtonian plateau (Figure 16) are predicted quite well by equation 19.

Similar results obtained with an HPAM solution (65) are shown in Figure 17. As expected, equation 19 gives a good fit of the experimental data at low shear rates in the Newtonian plateau.

SHEAR-THINNING REGIME. The effects of pore size on the effective viscosity of XCPS solutions, at shear rates beyond the Newtonian regime, were studied in calibrated glass bead packs in which pore shape is statistically homothetic. Figure 18 shows that the effects of pore size, which are maximum and effectively predicted by equation 19 in the Newtonian plateau, decrease continuously as the shear rate increases and vanish at 3000 s^{-1} . This behavior is due to the shear-induced orientation of macromolecules, which decreases the thickness of the depleted layer up to a quite negligible value at 3000 s^{-1} . The behavior of XCPS solutions in quartzitic sandstones (79), which are nonadsorbent for XCPS in the low salinity range, is quite similar (Figure 19). Moreover, as discussed in references 43 and 79, careful measurements of the effective viscosity versus the shear rate of a well-known polymer in nonadsorbent

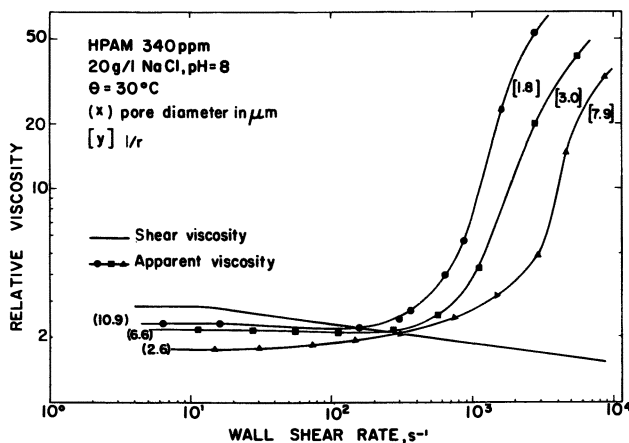


Figure 17. Effective viscosity in polycarbonate membranes (HPAM). Reproduced with permission from reference 65. Copyright 1981 Society of Petroleum Engineers.

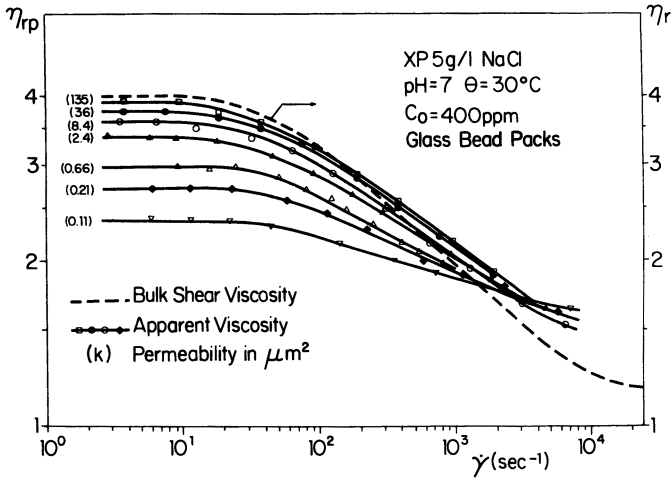


Figure 18. Effective viscosity in glass-bead pack (XCPS). Reproduced with permission from reference 43. Copyright 1982 Society of Rheology.

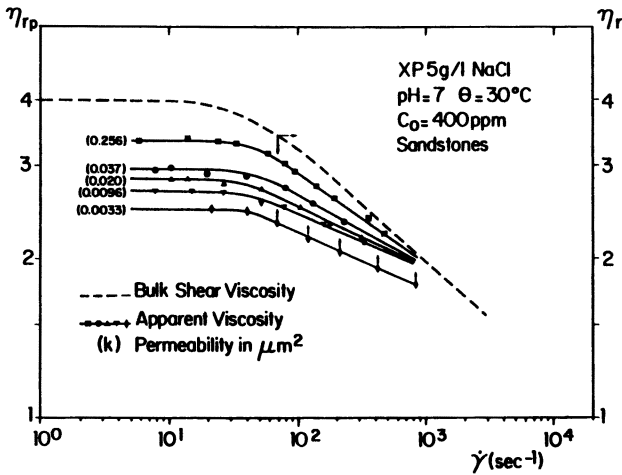


Figure 19. Effective viscosity in sandstones (XCPS). Reproduced with permission from reference 79. Copyright 1981 Elsevier.

porous media can lead to the determination of the effective hydrodynamic diameter of their pore throats (Figure 20) and of the actual wall shear rates in these pore throats.

EFFECTS OF POLYMER CONCENTRATION. The two parameters δ and η_{rw} , which are included in equation 19, were recently (80) related to the dimensions and the conformation of macromolecules and to polymer

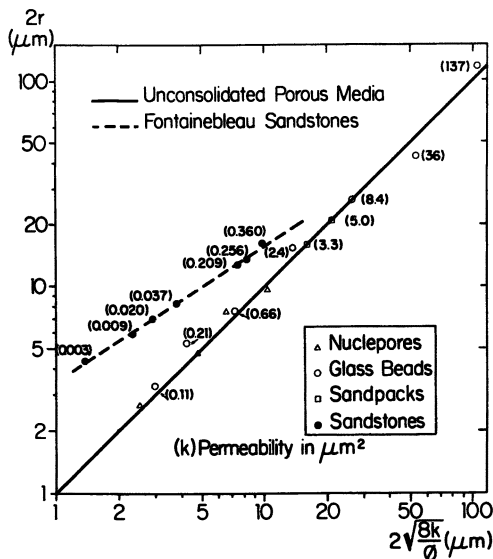


Figure 20. Pore throat diameter determination by polymer flow characteristics. Reproduced with permission from reference 79. Copyright 1981 Elsevier.

concentration far from the pore wall, C_b , by using the variations of polymer concentration versus pore wall distance, which are plotted in Figure 21 according to the predictions of Casassa and co-workers (81-83) for coiled flexible chains and of Auvray (42) for rodlike polymers. For the dilute regime where the coil dimensions are constant ($C[\eta]_0 < 3.5$) and for pore dimensions much larger than polymer size ($\delta/r \ll 1$), the following equation was derived:

$$\eta_{rb}/\eta_{rp} = 1 + 4(1 - \beta)(\delta/r)C_b[\eta]_0 + 6(1 - \beta)(\delta^2/r^2)C_b^2[\eta]_0^2 \quad (20)$$

where $\beta = C_w/C_b$ is the ratio of average concentration in the wall layer to the concentration far from the wall and δ and r are respectively wall layer thickness and pore radius. The values of δ and β , deduced from macromolecular properties, are respectively

$$\beta \approx 0.64 \text{ and } \delta \approx 0.7L_{eq} \text{ (for rigid rods)} \quad (21)$$

$$\beta \approx 0.3 \text{ and } \delta = (6/2)^{1/2}R_C \approx 1.24R_C \text{ (for flexible coils)} \quad (22)$$

As shown in Figures 22 and 23, the experimental results are in agreement with the predictions of equation 20 for both rigid and flexible polymers in various types of nonadsorbent porous media having different pore size.

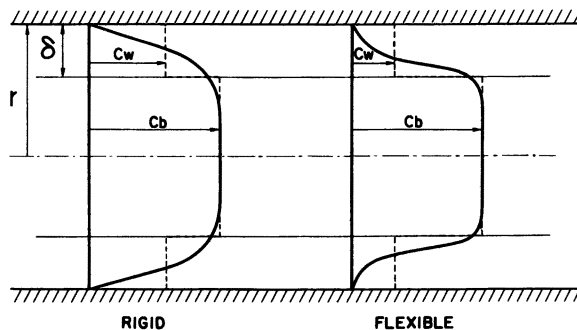


Figure 21. Schematic diagram of concentration profiles in cylindrical pores for rigid and flexible macromolecules. Reproduced with permission from reference 80. Copyright 1984 Academic.

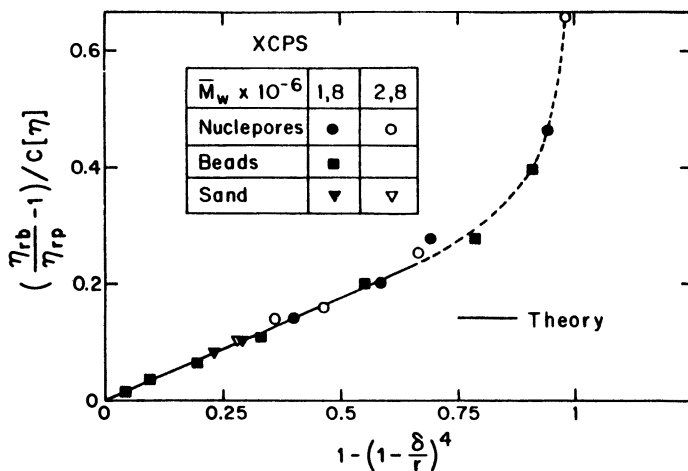


Figure 22. Comparison of bulk and pore relative viscosities vs. relative molecular and pore size (XCPS). Reproduced with permission from reference 80. Copyright 1984 Academic.

The concentration dependence of the effective viscosity is also well predicted by equation 20 in the dilute systems as shown by Figures 24 and 25. The depletion layer thickness, δ , does not change for rigid molecules in the semidilute regime, that is, for $C > C^*$ ($C^*[\eta]_0 \approx 3.5$). However, for flexible polymers, the value of δ is found to decrease as the polymer concentration increases beyond C^* , according to equation 23, which is deduced from recent polymer theories based on scaling laws (30):

$$\delta \approx 1.24R_C(C/C^*)^{-\frac{1}{2}} \quad (23)$$

The agreement between theory and experiment is fairly good, but obviously these experimental data are not yet numerous enough to be taken as a definite test for the scaling exponent $-\frac{3}{4}$. Additional experiments are still in progress.

Flow Through Small Adsorbent Pores. THICKNESS OF ADSORBED LAYER. Attractive walls produce adsorption of macromolecules. If the

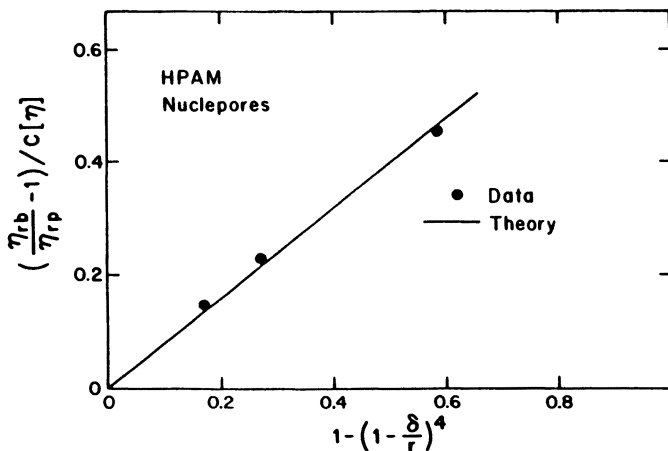


Figure 23. Comparison of bulk and pore relative viscosities vs. relative molecular and pore size (HPAM). Reproduced with permission from reference 80. Copyright 1984 Academic.

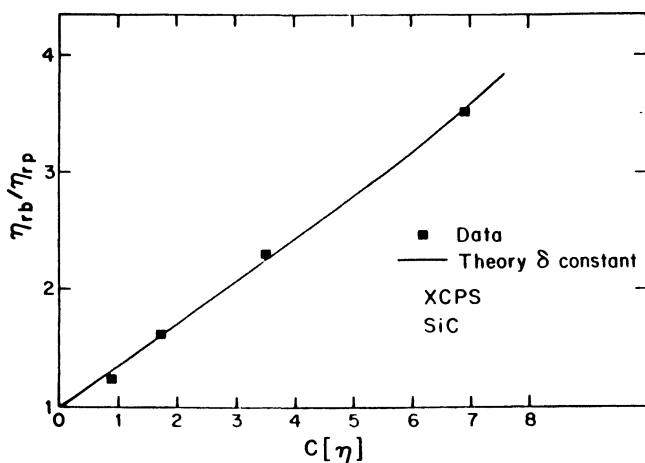


Figure 24. Comparison of bulk and pore relative viscosities vs. concentration in SiC packs (XCPS). Reproduced with permission from reference 80. Copyright 1984 Academic.

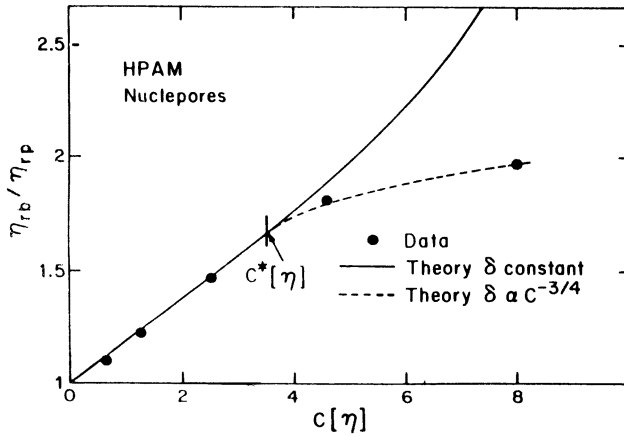


Figure 25. Comparison of bulk and pore relative viscosities vs. concentration in polycarbonate membranes (HPAM). Reproduced with permission from reference 80. Copyright 1984 Academic.

thickness of the layer adsorbed on the wall is large enough, this layer can exert a detectable influence on the apparent rheological characteristics of a fluid flowing in a small pore. This thickness is determined by several factors including molecular weight, degree of saturation of surface sites by the polymer, and strength of binding. The experiments described here, which were carried out with HPAM in a good solvent (standard conditions), concern the weak binding situation where the adsorbed layer thickness is large.

In practice, measurement of the thickness of a layer of adsorbed polymer on the inside of a porous medium is frequently done inferentially by calculating from a capillary model the apparent hydrodynamic radius after adsorption on the pore walls has occurred (65). The permeability reduction, R_k (final to initial permeability ratio), due to a hydrodynamically impermeable adsorbed layer having thickness ϵ_h inside a cylinder (or equivalent cylinder for porous media) having a radius r is

$$R_k = (1 - \epsilon_h/r)^{-4} \quad (24)$$

For both the sand pack and sandstones, the values of R_k , which have been plotted as open symbols in Figure 26, correspond in the Newtonian plateau to an adsorbed layer thickness, $\delta \approx 0.40 \mu\text{m}$, slightly higher than R_C under the conditions of experiments (65). The thickening behavior observed at high flow rates is due to an extension of the adsorbed molecules in the zones that are elongational, such as downstream of the sand grains.

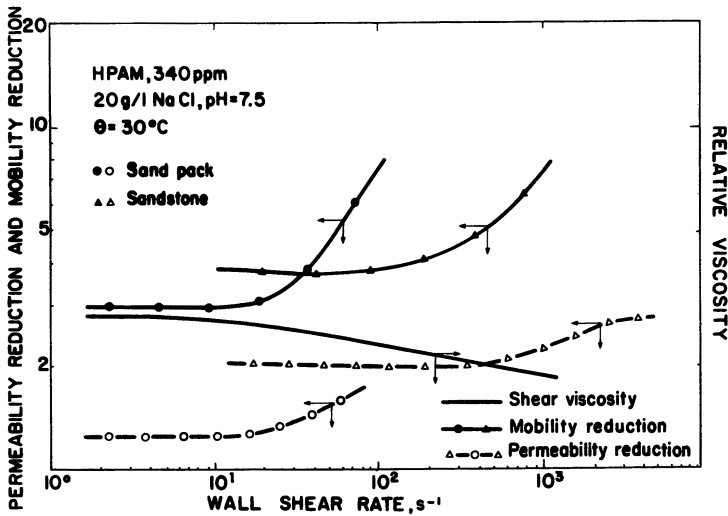


Figure 26. Effective viscosity in porous media with polymer adsorption effects (HPAM). Reproduced with permission from reference 65. Copyright 1981 Society of Petroleum Engineers.

EFFECT OF POLYMER CONCENTRATION. If we assume that the thickness of the adsorbed layer is unaffected by the presence of the polymer flowing through the pores and that the adsorbed layer is impenetrable by this polymer, a depleted layer could exist on top of an adsorbed layer. Under these conditions, an equation similar to equation 20 was proposed to calculate the apparent viscosity as a function of pore size in adsorbent porous media (80):

$$\eta_{rb}/\eta_{rp} = 1 + 4(1 - \beta)(\delta/r)C_b[\eta]_0(1 - 4\epsilon_h/r) \quad (25)$$

This equation effectively predicts the experimental results shown in Figure 26 where the ratio between mobility reduction (which is equal to η_{rp}) and permeability reduction is less than the bulk viscosity and decreases as the pore size decreases.

The variations of $\eta_{rb}R_{k0}/\eta_{rp}$ versus polymer concentration measured in a sand pack are also effectively predicted by equation 25 in the dilute system (Figure 27). The result obtained in the semidilute system suggests a decrease of both δ and ϵ_h in this regime as predicted by scaling laws. However, the existence of such a depleted layer on top of an adsorbed layer is certainly restricted to good solvent situations and cannot be considered as definitively understood. Additional research on adsorption properties is obviously needed.

Pore-Size Dependence of Thickening Behavior and of Mechanical Degradation. The papers (49, 84, 85) published in the last decade on the mechanical degradation induced by flow-through porous media have suggested that this degradation is governed by both the deformation rates and the length of porous media. However, an increased polymer degradation in low-permeability porous media has been reported (86) but was attributed to inaccessible pore volume effects.

A recent study (63) carried out with a microgel-free solution of unhydrolyzed poly(acrylamide) ($\bar{M}_w \approx 4.5 \times 10^6$) flowing through packs of nonadsorbent glass beads of relatively large diameters (150 and 270 μm) showed that both thickening behavior (Figure 28) and mechanical degradation (Figure 29) increase as the pore size decreases. However, the onset of thickening behavior does not depend on pore size (Figure 28). This pore-size dependence can be explained as follows. As long as the molecule assumes a coil conformation, that is, for $\dot{\gamma} < \dot{\gamma}^*$, its dimensions are quite negligible compared to pore dimensions, and thus the onset of thickening behavior does not depend on pore size. However, when elongated in the thickening system, the macromolecules may have lengths close to their contour length, which is not negligible compared to pore size. The macromolecules are thus subjected to a mean stretch rate higher than that existing at their center of mass; the result is higher viscous dissipation and then higher mechanical degradation for a given mean deformation rate.

Such a situation is expected to occur in many field applications, and adsorption will increase this phenomenon. Consequently, the mechanical degradation is a quite severe limitation for the use of HPAM.

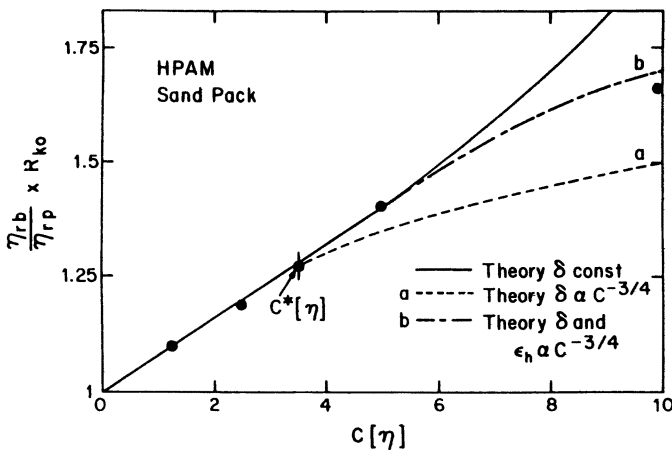


Figure 27. Relative bulk and pore viscosities vs. concentration with adsorption effects (HPAM). Reproduced with permission from reference 65. Copyright 1981 Society of Petroleum Engineers.

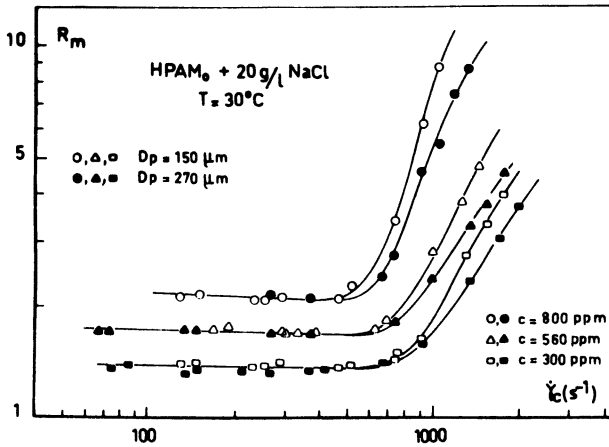


Figure 28. Effect of pore size on thickening behavior (HPAM).

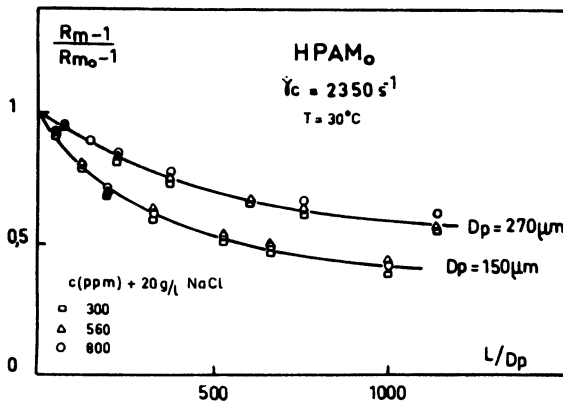


Figure 29. Effect of pore size on mechanical degradation (HPAM).

Propagation of Polymer Slugs in Porous Media

The spreading out of polymer slugs during their propagation through reservoirs is a very detrimental phenomenon because it can lead to a loss in mobility control and thus to a decrease in polymer flooding efficiency. The main mechanisms explaining this spreading out are analyzed in a recent paper (87).

Influence of Inaccessible Pore Volume. Dawson and Lantz (88) observed that polymer molecules move through a porous medium faster than water. They attributed this phenomenon to the existence of a pore volume fraction inaccessible to the polymer because the dimensions of

the macromolecules were too large compared to the size of the pore throats. If we disregard the case of low-permeability natural cores, the pore volume fraction that is strictly inaccessible to the polymer molecule is too small to explain the significant differences in velocity observed between polymer and solvent. However, the pore wall exclusion of macromolecules described previously is expected to increase polymer velocity more strongly than inaccessible pore volume and thus to be more able to explain the experimental observations (87-90).

Effects of Pore-Wall Exclusion on Polymer Velocity. If the porous medium is assumed equal to a bundle of capillaries with radius r , the velocity of a polymer molecule in the Newtonian regime can easily be calculated by using the Poiseuille equation and the concentration profile of rodlike macromolecule centers of mass in the vicinity of a repulsive wall (42). For molecules with length L_c and for $L_c < r$, the value of R_F , which is the ratio of polymer velocity, v_p , to solvent velocity, v_s , can be approximated by (44)

$$R_F \approx 1 + (1/2)L_c/r + (1/6)L_c^2/r^2 \quad (26)$$

In the absence of both hydrodynamic dispersion and viscous fingering, that is, for low polymer concentrations and at very low flow rates, polymer velocity can be predicted by equation 26. The validity of this equation was checked by injecting a small xanthan solution slug in a long column packed with small SiC particles. Figure 30 shows good agreement between experiments and the predictions of equation 26. The experimental values of the lengths of equivalent rigid rods were calculated from intrinsic viscosity measurements by using equation 8.

Propagation of Viscous Polymer Slugs. The main characteristic features of the propagation of a xanthan slug through a nonadsorbent SiC porous medium can be observed in Figure 31. The pore wall exclusion has two main effects: (i) both the leading and the trailing edges of the polymer slug move at a mean velocity higher than that of a slug of small molecules and (ii) a separation in molecular weight is clearly revealed by the decrease in intrinsic viscosity versus volume injected at both the leading and trailing edges of the slug. However, due to the too high viscosity of the polymer slug, a large dissymmetry between the concentration profiles at the leading and trailing edges of the slug is clearly observed.

Because the polymer solution density is practically equal to water density at the polymer concentrations used, no gravity effect occurs and the displacement is always stable at the leading edge of the polymer slug. However, an increase in shear rate reduces the effects of pore-wall exclusion by shear-induced orientation of macromolecules and thus

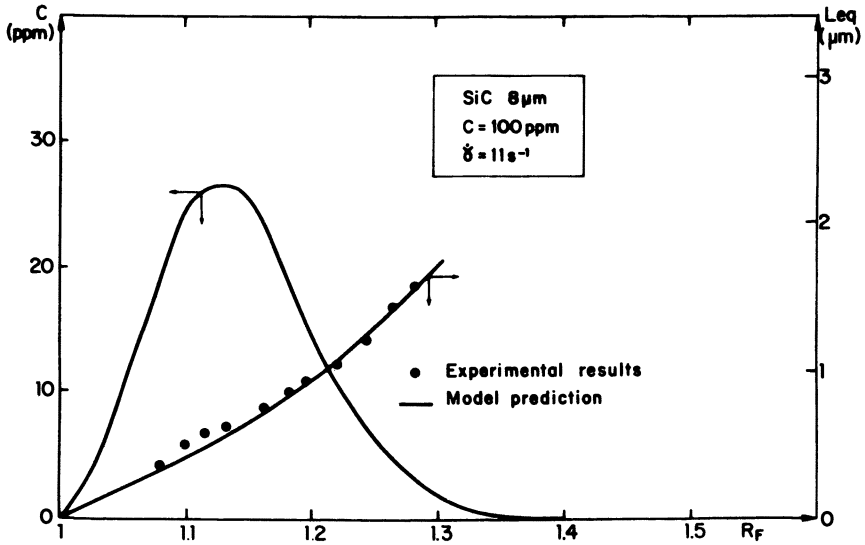


Figure 30. Comparison between theoretical prediction and experimental data for velocity vs. molecular length (XCPS). Reproduced with permission from reference 87. Copyright 1984 Society of Petroleum Engineers.

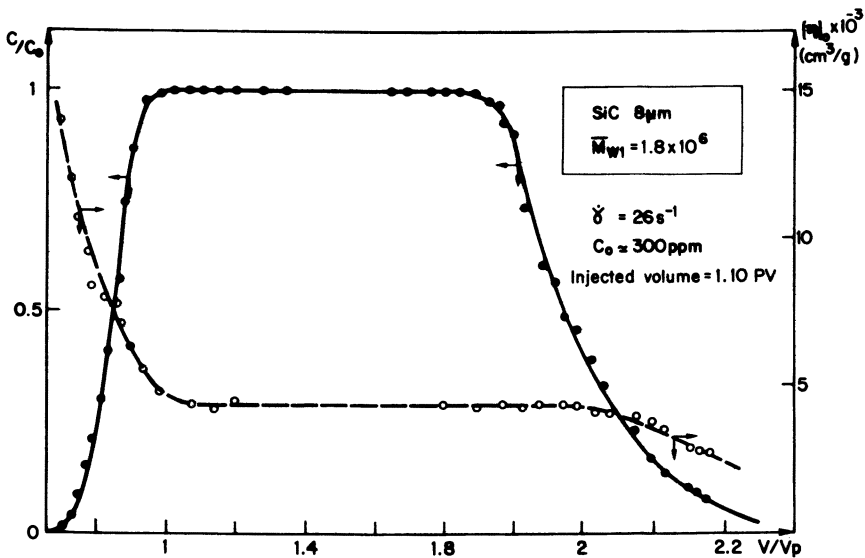


Figure 31. Spreading out of polymer slug during its propagation (XCPS). Reproduced with permission from reference 87. Copyright 1984 Society of Petroleum Engineers.

reduces the difference between polymer and solvent velocities (Figure 31). Increasing polymer concentration increases hydrodynamic interactions between macromolecules. Increased interactions enhance the orientation of the molecule and thus decrease polymer velocity (87).

At the trailing edge, the viscosity ratio is unfavorable, and thus the effects of viscous fingering increase markedly with polymer solution viscosity and consequently with polymer concentration; strong spreading out of the trailing edge results (Figure 32). Moreover, the effects of a flow-rate increase are very significant at the trailing edge of the slug; an increase in the dispersion occurs (Figure 33).

Selection of Polymers for EOR

Some fundamental criteria for selecting polymers to be used as mobility-control buffers in EOR processes can be deduced from the experimental and theoretical results. Very high molecular weight flexible polyelectrolytes such as HPAM are expected (1) to have lower injectivity due to their thickening behavior at high flow rates, (2) to be very sensitive to mechanical degradation mainly in low permeability reservoirs, and (3) to be subjected to conformational changes leading to decreased viscosity and even to precipitation in highly salted or acidic brines. Polymers having a stiff chain because of their chemical structures, such as biopolymers,

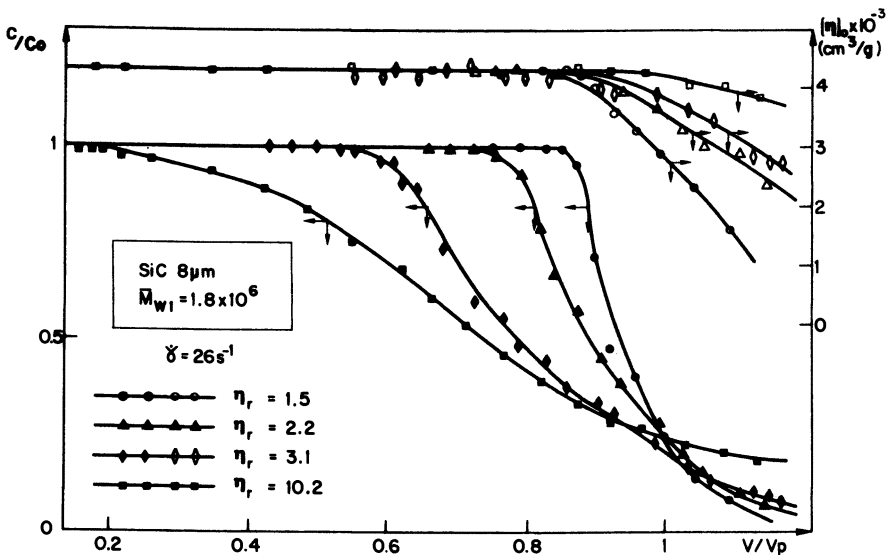


Figure 32. Concentration dependence of polymer spreading out at the trailing edge of the slug (XCPS). Reproduced with permission from reference 87. Copyright 1984 Society of Petroleum Engineers.

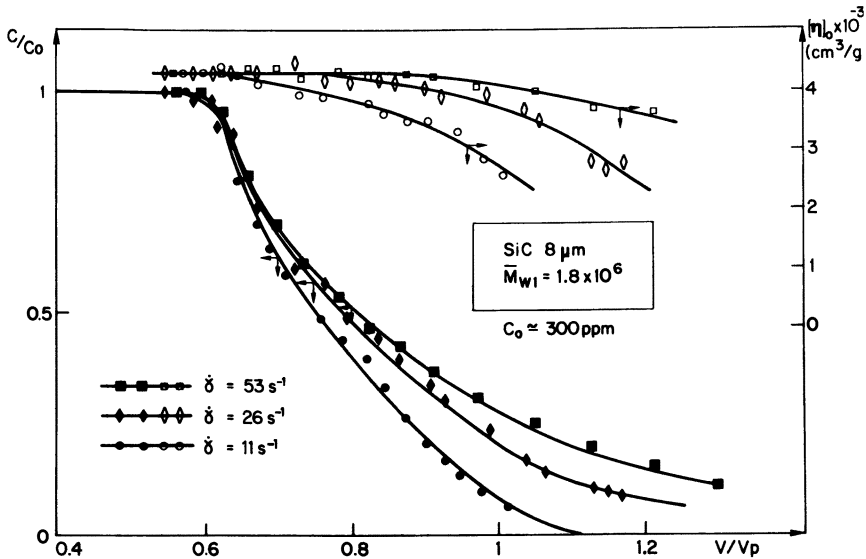


Figure 33. Flow-rate dependence of polymer spreading out at the trailing edge of the slug (XCPS). Reproduced with permission from reference 87. Copyright 1984 Society of Petroleum Engineers.

are more promising in this respect, but they must be protected against bacterial degradation.

A quite important additional criterion for selecting among available commercial polymers is their filterability. Indeed, most industrial polymers contain microgels that cause a progressive plugging of the zone located around injection wells; thus, injectivity is reduced (77, 78). For poly(acrylamides), this partial plugging leads also to higher deformation rates in unplugged pores and thus to increased mechanical degradation at high injection flow rates.

Procedure for Testing Filterability. A new procedure for testing the filterability of polymer solutions was developed (77). This procedure, based on the injection of the polymer solution to be tested at a low injection rate through Millipore filters, gave very selective and reproducible results.

Figure 34 gives an example of the results that can be obtained by using this procedure. The XCPS solution obtained by dissolution of a powder (PP) displays very poor filterability compared to another solution prepared by simple dilution of a fermentation broth (PFB). Such filterability tests can also be performed in natural sandstones (Figure 35), but such experiments, which give the same classification between polymer samples, are much more time consuming.

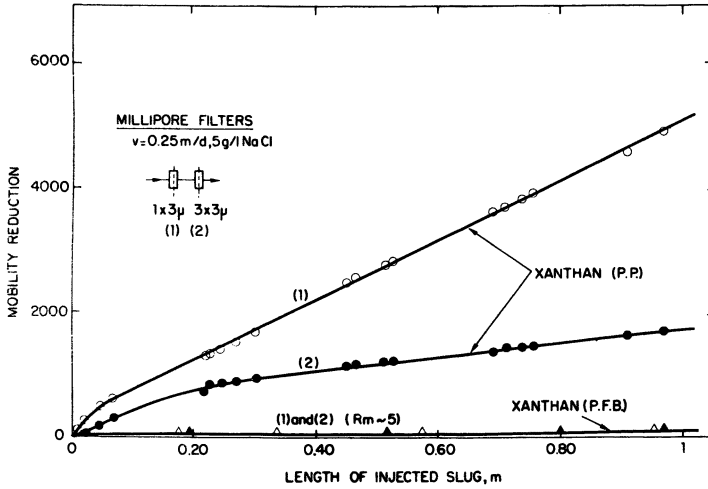


Figure 34. Influence of the drying process on filterability (XCPS). Reproduced with permission from reference 78. Copyright 1984 Society of Petroleum Engineers.

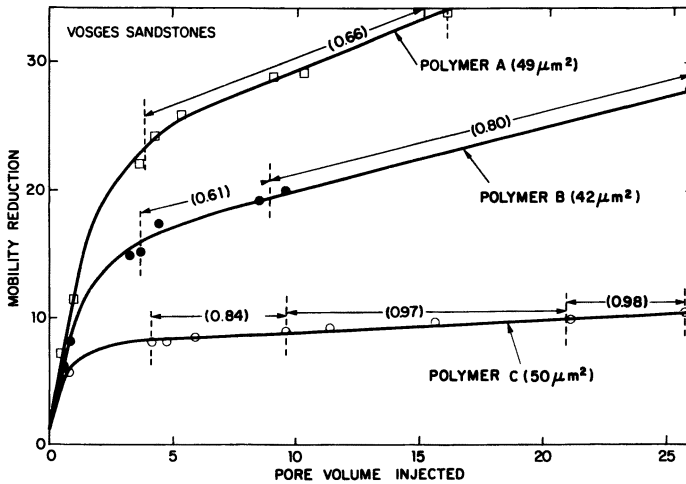


Figure 35. Difference in filterability of XCPS samples through shaly sandstones. Reproduced with permission from reference 78. Copyright 1984 Society of Petroleum Engineers.

Influence of Microgels on the Behavior in Porous Media. The influence of microgels on porous media behavior was systematically studied (78) with xanthan solutions in different types of porous media. Because of their adsorption or mechanical entrapment inside the porous structure, even a few microgels can strongly modify flow behavior in porous media. Their presence in the solution creates a permeability reduction even under conditions where isolated macromolecules are not adsorbed. Therefore, the apparent viscosity is strongly increased, mainly at low shear rates. As expected, their effects are much greater in porous media with low permeabilities (glass-bead packs of $0.125 \mu\text{m}^2$ in Figure 36) than in porous media with high permeabilities (sand pack with a permeability of $5 \mu\text{m}^2$ in Figure 37).

Conclusion

The relationships between the rheological behavior in porous media of aqueous solutions of high molecular weight polymers and their molecular properties that are analyzed in this review give some useful criteria for both selecting the best product among available polymers for EOR applications and designing new improved polymers. However, the adsorption properties of these polymers onto mineral surfaces (91) and their stability under severe salinity and temperature conditions are not completely understood. Because these properties are also important criteria for the use of polymers as mobility-control buffers, further fundamental research work is still needed in these two directions.

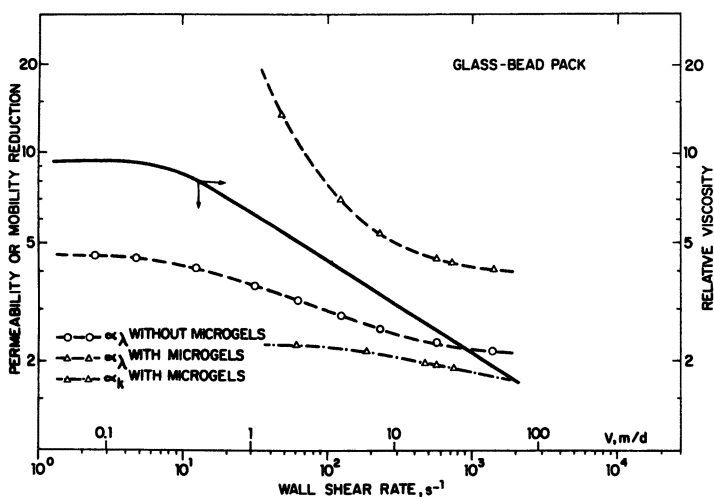


Figure 36. Effects of microgels on flow-through glass-bead packs (XCPS). Reproduced with permission from reference 78. Copyright 1984 Society of Petroleum Engineers.

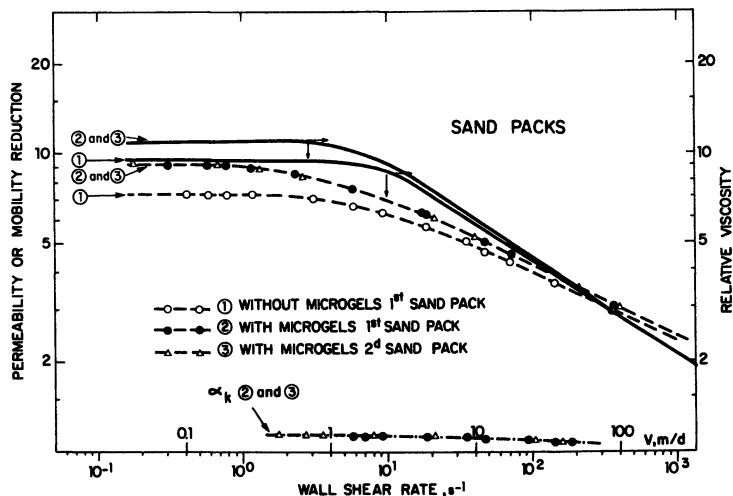


Figure 37. Effects of microgels on flow-through sand packs (XCPS). Reproduced with permission from reference 78. Copyright 1984 Society of Petroleum Engineers.

Literature Cited

1. Leonard, J. *Oil and Gas J.* 1984, 82(4), 83.
2. Sandiford, B. B. J. *Pet. Technol.* 1964, 16(8), 917.
3. Savins, J. G. *Ind. Eng. Chem.* 1969, 61, 10.
4. Jansson, P. E.; Kenne, L.; Lindberg, B. *Carbohydr. Res.* 1975, 45, 275.
5. Melton, L. D.; Mindt, L.; Rees, D. A.; Sanderson, G. R. *Carbohydr. Res.* 1976, 46, 245.
6. Paradossi, G.; Brandt, D. A. *Macromolecules* 1982, 15, 874.
7. Moorhouse, R.; Walkinshaw, M. D.; Winter, W. T.; Arnold, S. In *Cellulose Chemistry and Technology*; Arthur, J. C., Jr., Ed.; ACS Symposium Series No. 48; American Chemical Society: Washington, DC, 1977; p 133.
8. Muller, G.; Lecourtier J.; Chauveteau G.; Allain C. *Makrom. Chem. Rap. Comm.* 1984, 5, 203.
9. Sato, T.; Kajima, S.; Norisuye, T.; Fujita, H. *Polym. J.* 1984, 16(5), 423.
10. Sato, T.; Norisuye, T.; Fujita, H. *Polym. J.* 1984, 16(4), 341.
11. Lecourtier, J.; Chauveteau G.; Muller G. "Salt-Induced Conformational Changes of a Native Double Stranded Xanthan"; presented at the National Meeting of the American Chemical Society, Chicago; 9-13 September 1985; *J. Int. Biol. Macrom* 1986, in press.
12. Holzwarth, G. *Biochem.* 1976, 15, 4333.
13. Rinaudo, M.; Milas, M. *Biopolymers* 1978, 17, 2663.
14. Milas, M.; Rinaudo, M. *Carbohydr. Res.* 1979, 76, 186.
15. Muller, G.; Anhourache, M.; Lecourtier, J.; Chauveteau, G. *J. Int. Biol. Macrom*, 1986.
16. François, J.; Schwartz, T.; Weill, G. *Macromolecules* 1980, 13, 564.
17. Schwartz, T.; François, J.; Weill, G. *Polymer*, 1980, 21, 247.
18. Klein, J.; Westerkamp, A. J. *Polym. Sci., Polym. Chem. Ed.* 1981, 19, 707.
19. Flory, P. J. *Principles of Polymer Chemistry*; Cornell: Ithaca, NY, 1953.
20. Ktrasky, O.; Porod, G. *Rec. Trav. Chem. Pays-Bas* 1948, 68, 1106.

21. Benoit, H.; Doty, P. *J. Phys. Chem.* **1953**, *57*, 958.
22. Odijk, O. *J. Polym. Sci., Polym. Phys. Ed.* **1977**, *15*, 477.
23. Davis, R. M.; Russel, W. B. submitted for publication *J. Polym. Sci., Polym. Phys. Ed.*
24. Yamakawa, H.; Fujii, M. *Macromolecules* **1974**, *7*, 128.
25. Simha, R. *J. Phys. Chem.* **1974**, *44*, 25.
26. Burgers, J. M. *Second Report on Viscosity*; Norman: Washington, 1938; Chapter 3.
27. Layec, Y.; Wolff, C. *Rheol. Acta.* **1974**, *13*, 696.
28. Benoit, M.; Freund, L.; Spach, G. In *Poly- α -amino Acids*; Fasman, G. D., Ed.; Dekker: New York, 1967, pp 105-155.
29. Rouse, P. E. *J. Chem. Phys.* **1953**, *21*, 1972.
30. De Gennes, P. G. *Scaling Concepts in Polymer Physics*; Cornell: Ithaca, NY, 1979.
31. Edwards, S. F. *Proc. Roy. Soc. London* **1965**, *85*, 613.
32. Graessley, W. W. *Polymer* **1980**, *21*, 258.
33. Doi, M.; Edwards, S. F. *J. Chem. Soc. Faraday Trans. 2* **1978**, *74*, 560.
34. Doi, M.; Edwards, S. F. *J. Chem. Soc. Faraday Trans. 2* **1978**, *74*, 918.
35. Ward, J. S.; Martin, F. D. *SPE J.* **1981**, *21(5)*, 623.
36. Muller, G.; Laine, J. P.; Fenyó, J. C. *J. Polym. Sci., Polym. Chem. Ed.* **1979**, *17*, 659.
37. Schwartz, T.; François, J. *Makromol. Chem.* **1981**, *182*, 2775.
38. Zaitoun, A.; Potie, B. *SPE Paper No 11785*, Society of Petroleum Engineers: Dallas, TX 1983.
39. Truong, D. N.; Galin, J. C.; François, J.; Pham, Q. T. *Polymer Commun.* **1984**, *25*, 208.
40. Truong, D. N.; François, J. *Stabilité de solutions de polyacrylamides hydrolysés en présence de sels de métaux divalents*; Colloque sur les interactions solide-liquide; Nancy, France; February 1984.
41. Joanny, J. F.; Leibler, L.; De Gennes, P. G. *J. Polym. Sci.* **1979**, *17*, 1073.
42. Auvray, L. *J. Phys.* **1981**, *42*, 79.
43. Chauveteau, G. *J. Rheol.* **1982**, *26(2)*, 111.
44. Lecourtier, J.; Chauveteau, G. *Macromolecules* **1984**, *17*, 1340.
45. Lambert, F.; Milas, M.; Rinaudo, M. *Polym. Bull.* **1982**, *7*, 185.
46. Shawki, S. M.; Hamielec, A. E. *J. Appl. Polym. Sci.* **1979**, *23*, 3323.
47. Wellington, S. L. *Prep. Div. Polym. Chem. Am. Chem. Soc.* **1981**, *22(2)*, 63.
48. Holzwarth, G. *Carbohydr. Res.* **1978**, *66*, 173.
49. Seright, R. S.; Maerker, J. M. *ACS Polym. Div. Prep.* **1981**, *22(2)*, 30.
50. Pedersen, K. O. *Arch. Biochem. Biophys.* **1962**, *1*, 157.
51. Small, H. *J. Colloid Interface Sci.* **1974**, *48(1)*, 147.
52. Small, H.; Saunders, F. A.; Solo, J. *Adv. Colloid Interface Sci.* **1976**, *6*, 237.
53. Silebi, C. A.; McHugh, A. J. *AIChE J.* **1978**, *24*, 204.
54. Silebi, C. A.; McHugh, A. J. *J. Appl. Polym. Sci.* **1979**, *23*, 1699.
55. Prud'homme, R. F.; Froiman, G.; Hoagland, D. A. *Carbohydr. Res.* **1982**, *106(2)*, 225.
56. Bagassi, M.; Chauveteau, G. *Filtration de solutions de polyacrylamides hydrolysés dans les milieux poreux très fins*; Colloque sur les interactions solide-liquide; Nancy, France; February 1984.
57. Carreau, P. J.; Bui, Q. H.; Leroux, P. *Rheol. Acta.* **1979**, *5*, 18.
58. Saito, N. *J. Phys. Soc. Jpn.* **1951**, *6*, 297.
59. Saito, N. *J. Phys. Soc. Jpn.* **1950**, *5*, 4.
60. Felderhof, B. V. *Physica* **1976**, *82 (A)*, 611.
61. Russel, W. B. *J. Fluid. Mech.* **1967**, *92*, 401.

62. Sengelin, M.; Chauveteau, G. "Rheological Behavior of Dilute Unhydrolyzed Polyacrylamide Solution in Shear and Partly Elongational Flows", unpublished.
63. Sengelin, M.; Chauveteau, G. "Polymer Degradation and Thickening Behavior in Porous Media Flows"; Presented at the National Meeting of the American Chemical Society: Philadelphia, August 25-31, 1984.
64. James, D. F.; McLaren, D. R. *J. Fluid. Mech.* **1975**, *70*, 733.
65. Chauveteau, G. *SPE Paper No 10060*, Society of Petroleum Engineers: San Antonio, TX, 1981.
66. Moan, M.; Chauveteau, G.; Ghoniem, S. *J. Non. Newt. Fluid. Mech.* **1979**, *5*, 463.
67. Hoa, N. T.; Chauveteau, G.; Gaudu, R.; Anne-Archard, D. *C.R. Acad. Sci., Paris* **1982**, *294*, 927.
68. Chauveteau, G.; Moan, M.; Magueur, A. *J. Non Newt. Fluid Mech.* **1984**, *16*, 315.
69. De Gennes, P. G. *J. Chem. Phys.* **1974**, *60*, 5030.
70. Marucci, G. *Polym. Eng. Sci.* **1975**, *15*, 229.
71. Hinch, E. J. *Phys. Fluids* **1977**, *20*, 522.
72. Acierno, D.; Titomanlio, G.; Nicodemo, L. *Rheol. Acta* **1974**, *13*, 532.
73. Daoudi, S. *J. Phys.* **1975**, *36*, 1285.
74. Magueur, A.; Moan, M.; Chauveteau, G. *Chem. Eng. Commun.* **1984**, *36*, 351.
75. Ghoniem, S.; Chauveteau, G.; Moan, M.; Wolff, C. *Can. J. Chem. Eng.* **1981**, *59*, 450.
76. James, D. F.; Saringer, J. H. *J. Non. Newt. Fluid. Mech.* **1982**, *11*, 317.
77. Kohler, N.; Chauveteau, G. *J. Pet. Tech.* **1981**, *34(2)*, 349.
78. Chauveteau, G.; Kohler, N. *Soc. Pet. Eng. J.* **1984**, *24(3)*, 361.
79. Chauveteau, G.; Zaitoun, A.; Europ. Symp. on EOR, Bournemouth, England, Sept. 21-23, 1981, Elsevier.
80. Chauveteau, G.; Tirrell, M.; Omari, M. *J. Colloid Interface Sci.* **1984**, *100*, 41.
81. Casassa, E. F. *J. Polym. Sci. Part B* **1967**, *5*, 273.
82. Casassa, E. F.; Tagami, Y. *Macromolecules* **1969**, *2*, 14.
83. Casassa, E. F. *Macromolecules* **1984**, *17*, 601.
84. Maerker, J. M. *Soc. Pet. Eng. J.* **1976**, *15*, 4.
85. Seright, R. S. *Soc. Pet. Eng. J.* **1983**, *23*, 3.
86. Martin, F. D.; Ward, J. S. *Polym. Prep., Prep. Div. Polym. Chem. ACS* **1981**, *22(2)*, 24.
87. Lecourtier, J.; Chauveteau, G. *SPE Paper No 13034*, Society of Plastics Engineers: Dallas, 1984.
88. Dawson, R.; Lantz, R. B. *SPE Paper No 3522*, Society of Plastics Engineers: New Orleans, 1974.
89. Liauh, W. C.; Duda, J. L.; Klaus, E. E. *AICHE I. Chem. E. Symp. Ser.* **1982**, *78*, 70.
90. Willhite, G. P.; Dominguez, J. G. In *Improved Oil Recovery by Surfactant and Polymer Flooding*; Academic: New York, 1977.
91. Lecourtier, J.; Chauveteau, G., 3rd Europ. Meet. on EOR, Rome, April 16-18, 1985, Agip.

RECEIVED for review August 6, 1984. ACCEPTED November 22, 1985.

Anatomy of a Full-Field Polymer-Augmented Waterflood Project

P. A. Argabright, J. S. Rhudy, and E. M. Trujillo

Marathon Oil Company, Denver Research Center, Littleton, CO 80160

Polymer-augmented waterflooding is the most important and widely used oil recovery process utilizing water-soluble polymers. From the multitude of available products, only two types are extensively used, namely, partially hydrolyzed poly(acrylamides) (PHPA) and xanthan gum (a biopolymer). Both products have the capability of significantly reducing the mobility of water, a necessary feature of any water-based enhanced oil recovery process. The design and ultimate implementation of a PHPA-based polymer-augmented waterflood project are discussed in accordance with the following protocol: (1) polymer selection, (2) coring, (3) performance (laboratory oil recovery), (4) field feasibility tests, (5) modeling, and (6) full-field development.

CERTAIN WATER-SOLUBLE POLYMERS are especially suited for a wide variety of oil field applications. These polymers are routinely employed as drilling fluid additives, diverting agents, fluid loss additives, and drag reducers, to name a few. With recent emphasis on more effectively exploiting our domestic oil reserves, water-soluble polymers now enjoy a major role in a number of enhanced oil recovery processes. Polymer-augmented waterflooding, surfactant-polymer flooding, and caustic-polymer flooding are the most important and widely used enhanced oil recovery processes utilizing water-soluble polymers (1). From the multitude of available water-soluble polymers, only two types are extensively used, namely, partially hydrolyzed poly(acrylamides) and xanthan gum (a biopolymer). Both products have the capability of significantly reducing the mobility of water, a necessary feature of any water-based process designed to obtain additional oil.

The following is a brief review of the course of events following the drilling of a successful oil well. When a productive hydrocarbon formation is tapped, the oil and gas are produced by the natural energy of the reservoir. Thus, the liquid hydrocarbon is forced to the surface via a

0065-2393/86/0213-0269\$11.75/0
© 1986 American Chemical Society

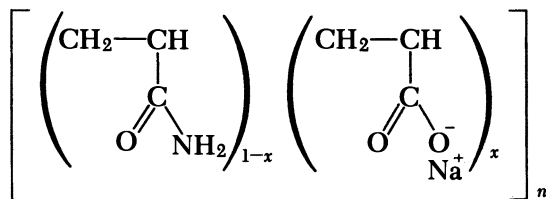
natural pressure drive. Ultimately, this in situ energy source diminishes to the point where pumps are required to lift the oil to the surface. This phase is referred to as *primary* production and typically accounts for approximately 20% of the original oil in the reservoir.

In time, pressure depletion reaches a point where insufficient energy is present to displace oil through the reservoir to the well. At this time, new injection wells are drilled around the original producing well or producing wells are converted to injection of water or gas to restore the original reservoir pressure. This operation constitutes *secondary* recovery whereby the injected fluid continues to force oil from the rock interstices to the producing well. Depending on the nature of the reservoir and the development strategy, an additional 15–30% of oil may be recovered by waterflooding. Waterflooding is continued until the water-to-oil ratio of the produced fluids is so high as to render the operation uneconomical.

A more efficient alternative to waterflooding is polymer-augmented waterflooding. This approach involves the addition of relatively small quantities of polymer to reduce the mobility of water. The resulting increase in overall sweep efficiency of the aqueous phase leads to accelerated oil production.

Although water-soluble polymers play an important role in a number of oil recovery processes, this chapter is restricted to one specific polymer—*partially hydrolyzed poly(acrylamide)* (PHPA)—in one specific application—*polymer-augmented waterflooding*. A stepwise procedure for the development of a full-field polymer-augmented waterflood is presented. The protocol will include the following items:

- PHPA selection,
- coring,
- performance (oil recovery),
- field feasibility tests,
- modeling, and
- full-field development.



PHPA

PHPA Selection

Mechanism. The mechanisms by which polymers increase the efficiency of waterflooding an oil-bearing reservoir are not completely understood. However, the following three phenomena play important roles.

1. **Improved areal sweep efficiency (2):** A natural consequence of waterflooding is the generation of oil-depleted channels having a high permeability to water. Subsequent water injection tends to follow these “watered-out” flow channels. On the other hand, injection of a lower mobility fluid (polymer solution) establishes a resistance for water to flow through these watered-out channels. Thus, the flow of water is redirected to the oil-containing channels heretofore bypassed by water.
2. **Vertical conformance:** Reservoirs for the most part are composed of layered rock intervals of varying permeabilities. Again, injected water tends to flow through the path of least resistance—the more permeable zone. Polymer may redirect water flow from a high permeability strata to a lower permeability strata by a mechanism similar to the pore-to-pore description given in the areal sweep case discussed under 1.
3. **Mobility ratio:** The efficiency of displacing oil by water in porous media is diminished by the unfavorable oil-to-water mobility ratio. Thus, water, having a lower viscosity than the crude oil, fingers into the oil phase, breaks through, and leaves behind a considerable amount of oil. When a polymer is used, the viscosity of water can be increased; this increase leads to a more favorable mobility ratio and more efficient displacement of oil.

Although the relative importance of the above-mentioned factors influencing waterflooding is not completely understood, lowering the mobility of the displacement fluid is important.

Mobility. PHPA reduces the mobility of displacement water in porous media (reservoir rock) by a combination of (1) *increasing* the water's viscosity and (2) *reducing* the permeability of the matrix to water (3). As shown in Figure 1, PHPA is an extremely effective viscosity-building polymer. This characteristic is attributed to its high molecular weight [(3–10) × 10⁶] and its relatively distended configuration. Distension of the polymer chain results from the electrostatic repulsion of the negatively charged carboxylate groups (4) introduced through hydrolysis or copolymerization. The incorporation of negative groups in poly(acrylamide) also reduces adsorption of the polymer on the rock (especially

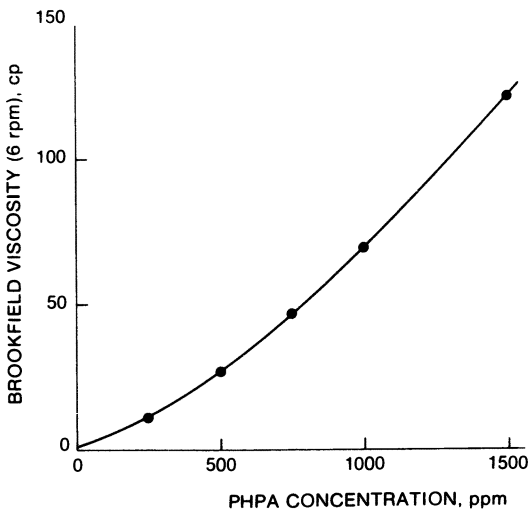


Figure 1. Effect of PHPA concentration on viscosity.

sandstone) surface (5). This result is an important consideration toward the effective propagation of polymer solutions through the reservoir.

The other component of mobility, permeability reduction, is thought to result from selective pore throat plugging in the porous media by the very high molecular weight polymer molecules (6). Controlled permeability reduction is a very efficient way of reducing the mobility of water. To be effective, however, PHPA-induced permeability reduction must be propagated uniformly throughout the reservoir.

Unfortunately, some commercially available PHPAs exhibit face plugging (7). That is, permeability reduction is greater at the point of injection than at more remote distances. Essentially, the reservoir rock acts as a filter to remove ultrahigh molecular weight species or polymer aggregates (microgels). Face plugging must be avoided as it dramatically reduces the permeability near the well bore; this factor reduces the injection rate and thereby prolongs project life.

Comparative Behavior. A very effective technique for evaluating the performance of polymers as mobility-reducing agents is radial disk flooding (8). This method provides information on the mobility of flowing polymer solutions as a function of distance from the point of injection. Experimentally, a disk of Berea sandstone (6 in. \times 2 in.) containing a $\frac{1}{8}$ -in.-diameter center hole is mounted in a watertight, pressure-fitted core holder. The disk holder is equipped with four pressure taps that essentially divide the disk into four concentric domains (Figure 2). The PHPA solution is injected at a constant rate and the pressure (ΔP) response recorded across the appropriate pressure taps. When the Darcy

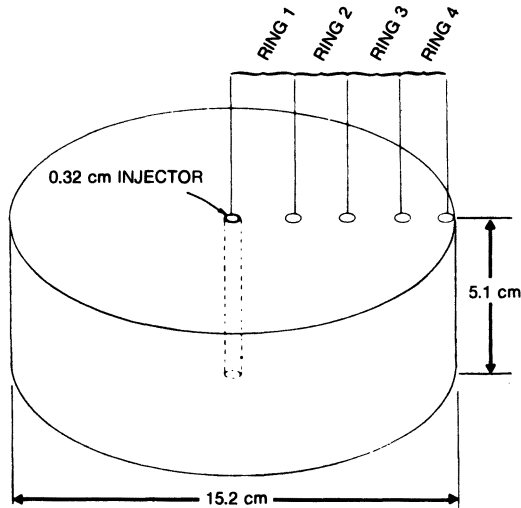


Figure 2. Disk configuration for polymer flooding. Reproduced with permission from reference 21. Copyright 1983 Society of Petroleum Engineers of the American Institute of Mining, Metallurgical and Petroleum Engineers.

equation for radial flow (equation 1) is used, the pressure data can be translated to reciprocal relative mobility (RRM).

$$\text{RRM} = \mu = \frac{0.427kh(\Delta P)}{q \ln(r_o/r_i)} \quad (1)$$

where μ is viscosity (cP), k is permeability (d), h is disk thickness (cm), ΔP is differential pressure (psi), q is injection rate (cm^3/s), r_o is distance to outer tap (cm), and r_i is distance to inner tap (cm). RRM values during polymer and postpolymer flush-water injection are comparable to resistance factor and residual resistance factor terminology also used in the industry.

The mobility behavior (RRM as a function of injection volume) for a custom-manufactured PHPA is shown in Figure 3. The onset of polymer injection results in a sharp increase in RRM for all rings and a subsequent rapid stabilization of the inner rings. The fact that the outermost ring (no. 4) has not reached a constant RRM may be a manifestation of nonequilibrium conditions as regards ion exchange (observed). Importantly, the RRM values for the polymer increase with increasing radial distance. Following the PHPA flood (2.5 pore volumes), the disk was flushed with water. At the end of water injection, RRM was low and equal in all of the rings. This result is good evidence that for this PHPA, the induced permeability reduction was low and, more importantly, uniform throughout the entire disk.

The mobility behavior of a commercial PHPA contrasts markedly from that of the above-mentioned custom-manufactured product (Figure 4). That is, the RRM never stabilized in the near-injector region (ring 1), was the greatest in ring 1, and tended to decrease with increasing radial distance. The fact that the RRM around the injector (ring 1) remained high (compared with rings 2–4) after flushing with water shows that this polymer face plugs. For commercial polymers, laboratory mixing procedures recommended by the supplier were used.

The mobility behaviors of the two polymers are compared in Figure 5. The custom-manufactured PHPA shows RRM to be lowest near the injector and increasing with radial distance. The steady increase in RRM with radial distance is due to the pseudoplastic nature of the polymer solution—viscosity increases with decreasing shear rate (frontal velocity). This behavior allows for high injection rates in the field with excellent mobility control in the bulk of the reservoir. Again, this behavior results from uniform permeability reduction (plugging) and, more importantly, a high effective viscosity that increases with distance.

The commercial PHPA shows a less-than-ideal mobility profile. That is, RRM is greatest around the injector and rapidly diminishes with radial distance. The gradual upturn of the curve at remote distance is a result of low permeability reduction superimposed on a gradually increasing viscosity. This undesirable profile arises from excessive non-uniform plugging around the injector with very low effective viscosity throughout. As injectivity is inversely proportional to the total disk RRM (near-injector dominated), polymers that cause no preferential well-bore

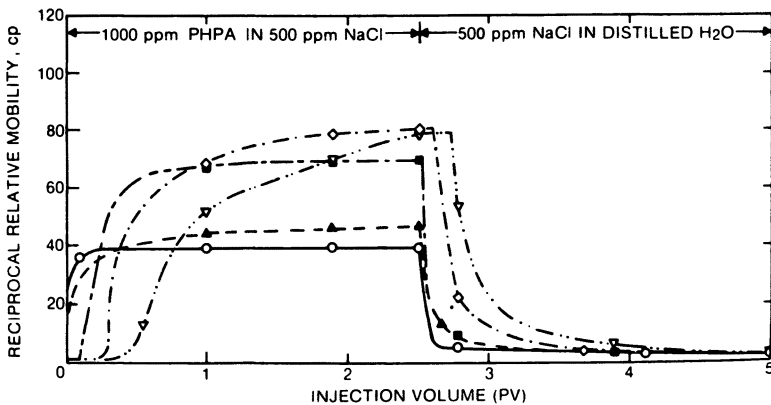


Figure 3. Mobility behavior of custom-manufactured PHPA. Key: \circ —, ring 1; \blacksquare ---, ring 2; \diamond —·—, ring 3; ∇ ·—·—, ring 4; and \blacktriangle —·—, total. Reproduced with permission from reference 7. Copyright 1982 Society of Petroleum Engineers of AIME.

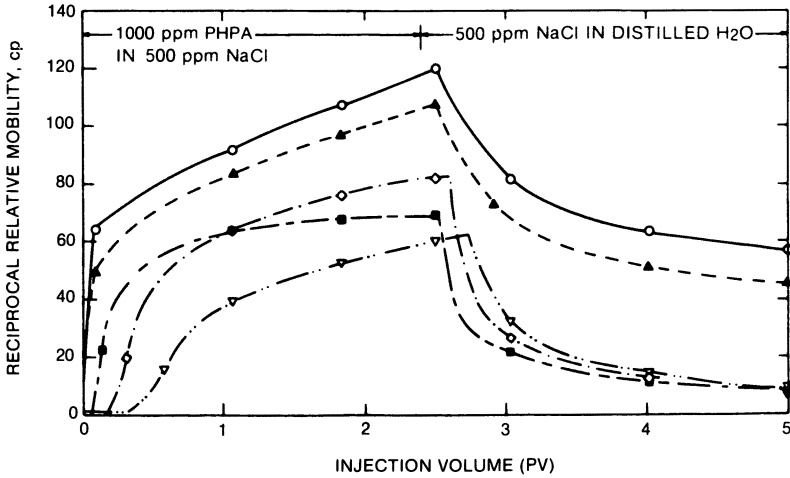


Figure 4. Mobility behavior of a commercial PHPA. Key: \circ —, ring 1; \blacksquare ---, ring 2; \diamond ---, ring 3; ∇ ---, ring 4; and \blacktriangle ---, total. Reproduced with permission from reference 7. Copyright 1982 Society of Petroleum Engineers of AIME.

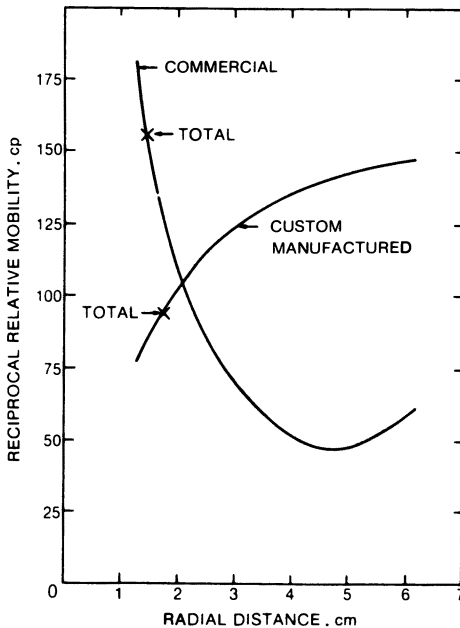


Figure 5. Comparison of mobility profiles. Reproduced with permission from reference 7. Copyright 1982 Society of Petroleum Engineers of AIME.

plugging will give both maximum injectivity and mobility control in depth.

Salinity. An important consideration in the selection of a polymer for a specific polymer-augmented waterflood prospect is the compatibility of the polymer with the injection water. PHPA, being a polyelectrolyte, loses much of its effectiveness in the presence of salts (9), particularly those containing multivalent cations. Most field projects utilizing massive amounts of polymer do not have the luxury of freshwater wells to maximize polymer effectiveness. One alternative—water treatment—can be cost prohibitive. Thus, the effective PHPA concentration usually must be designed to accommodate the available water. As shown in Figure 6, the relative viscosity of PHPA at a fixed shear rate is a power-law function of salinity at lower NaCl concentrations. At some higher salinity, the relative viscosity becomes constant. As anticipated, the salinity tolerance of PHPA increases with the average molecular weight, \bar{M}_v .

The influence of salt on mobility behavior is shown in Figure 7. The matrix (ring 2) behavior of RRM is adversely affected by salt. As in the case of viscosity versus salinity, RRM increases with increasing \bar{M}_v , at a given salt concentration.

Molecular Weight. Molecular weight plays an important role in the performance of PHPA. RRM is a linear function of \bar{M}_v for a homologous series of PHPAs (Figure 8). This information is helpful in screening PHPAs for a given reservoir. Thus, the PHPA of choice should have as high of an \bar{M}_v as the permeability of the reservoir rock will tolerate. That

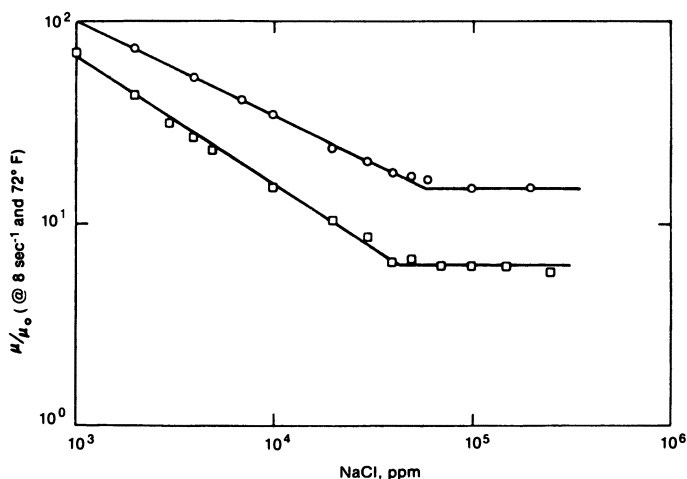


Figure 6. Effect of salinity on the relative viscosity of PHPA. Key: □, $\bar{M}_v = 4.44 \times 10^6$; and ○, $\bar{M}_v = 7.02 \times 10^6$.

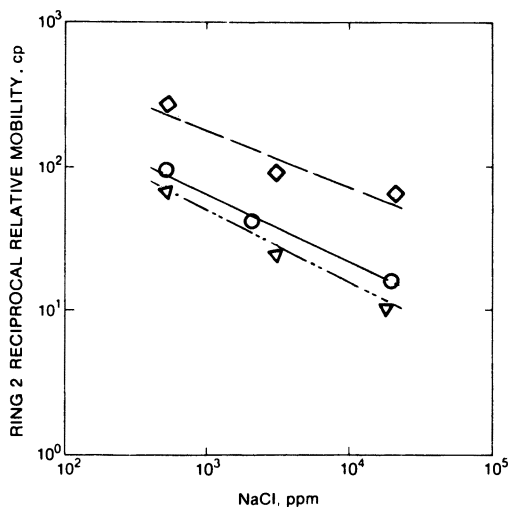


Figure 7. Effect of salinity on matrix RRM for PHPA. Key: ∇ , $\bar{M} = 4.44 \times 10^6$; \circ , $\bar{M} = 6.07 \times 10^6$; and \diamond , $\bar{M} = 7.02 \times 10^6$. Reproduced with permission from reference 7. Copyright 1982 Society of Petroleum Engineers of AIME.

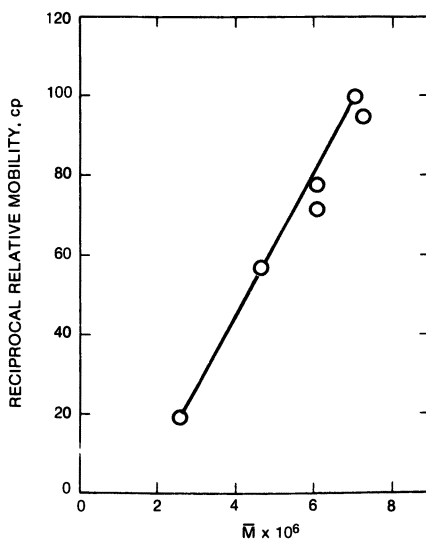


Figure 8. Dependence of RRM on \bar{M}_r . Reproduced with permission from reference 7. Copyright 1982 Society of Petroleum Engineers of AIME.

is, \bar{M}_w , cannot be so high as to give near-well-bore plugging. A judicious trade-off between \bar{M}_w and permeability reduction is the key to an effective polymer-augmented waterflood.

Although a number of methods are claimed for the measurement of \bar{M}_w , ultracentrifugation provides the most useful data (8, 10). Ultracentrifugation can also provide molecular weight distributions (although much more difficult to obtain) as well as \bar{M}_w . Figure 9 compares the molecular weight distribution for two PHPAs having the same \bar{M}_w . The product having the narrower molecular weight distribution (Figure 3) clearly outperforms the PHPA with the broader molecular weight distribution (Figure 4). The enhanced performance of the PHPA with the narrow distribution may be attributed to the absence of the low molecular weight species that contribute little to viscosity and the exclusion of ultrahigh molecular weight molecules responsible for excessive permeability reduction. However, as mentioned earlier, the dominant factor in face plugging is microgel, an artifact in polymerization at high concentration or polymer isolation (especially at elevated temperature).

In summary, in the screening of PHPAs for use in a polymer-augmented waterflood, consideration must be given to near-well-bore plugging as well as overall mobility behavior in the reservoir matrix. These data can be generated by disk flooding.

Coring

One purpose of coring is to provide reservoir material for laboratory studies. The reservoir core is used for disk flooding in evaluating a polymer-augmented waterflood prospect. In addition, core material is also used for other analyses including porosity, permeability, fluid saturations, relative permeability curves, capillary pressure data, and other

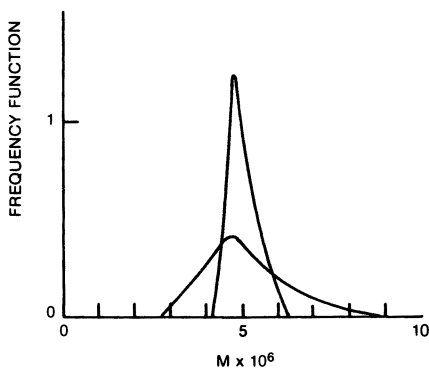


Figure 9. Comparison of molecular weight distribution. Reproduced with permission from reference 7. Copyright 1982 Society of Petroleum Engineers of AIME.

information required for geological and engineering analysis of the reservoir.

For laboratory disk floods, a large-diameter whole core is desirable. Normally, 5¼-in.-diameter cores are obtained. In most cases, the length of the core retrieval barrel is 30 ft.

A water-based drilling mud is usually the recommended coring fluid. Mud additives such as sulfonates, polymers, and caustic should be avoided where possible as they may alter core wettability or change the characteristics of the core.

A geologist should be on site to describe the core immediately after it comes out of the ground. This on-site description using a geologic work-sheet format includes (1) core-depth footages, (2) the lithology, (3) the amount of oil staining, (4) the sedimentary structure, (5) the number and type of fractures, (6) apparent porosity and permeability, and (7) additional remarks to clarify the core description (Figure 10).

After the well has been drilled, the formation of interest is logged. The suite of logs chosen may vary for each particular reservoir. Information that may be obtained from logs includes hole-size variation, lithology, porosity, apparent permeability, and relative saturations.

The well logs and core description are invaluable for selecting representative material for disk flooding and special core analysis. These data are also useful in well-to-well correlations.

Immediately following the geologic description, the core (3-ft sections) is shipped to the laboratory in sealed cylinders. The core sections are immersed under produced reservoir fluids. Again, produced water (or crude) used to cover the core should be free of added chemicals (deemulsifiers, corrosion inhibitors, etc.).

For the purpose of disk flooding, the core is cut into 2-in.-thick disks with a diamond saw. These rough disks are then trimmed to disk holder dimensions, and a ¼-in. hole is drilled in the center to serve as the injector. The core is kept under reservoir fluid until the laboratory flood is completed. This condition is required to minimize alterations of clay minerals or wettability.

Performance

Disk flooding is used to design and optimize conditions for a full-field polymer-augmented waterflood. Because polymer-flood performance is dependent upon reservoir characteristics, actual reservoir rock and fluids *must* be used in these laboratory tests. Complex rock-fluid-polymer interactions are unique for each reservoir. Therefore, only fresh, preserved core material containing reservoir fluids is recommended for use. Use of unpreserved or restored core or refined oils may not reflect existing reservoir conditions and give misleading results.

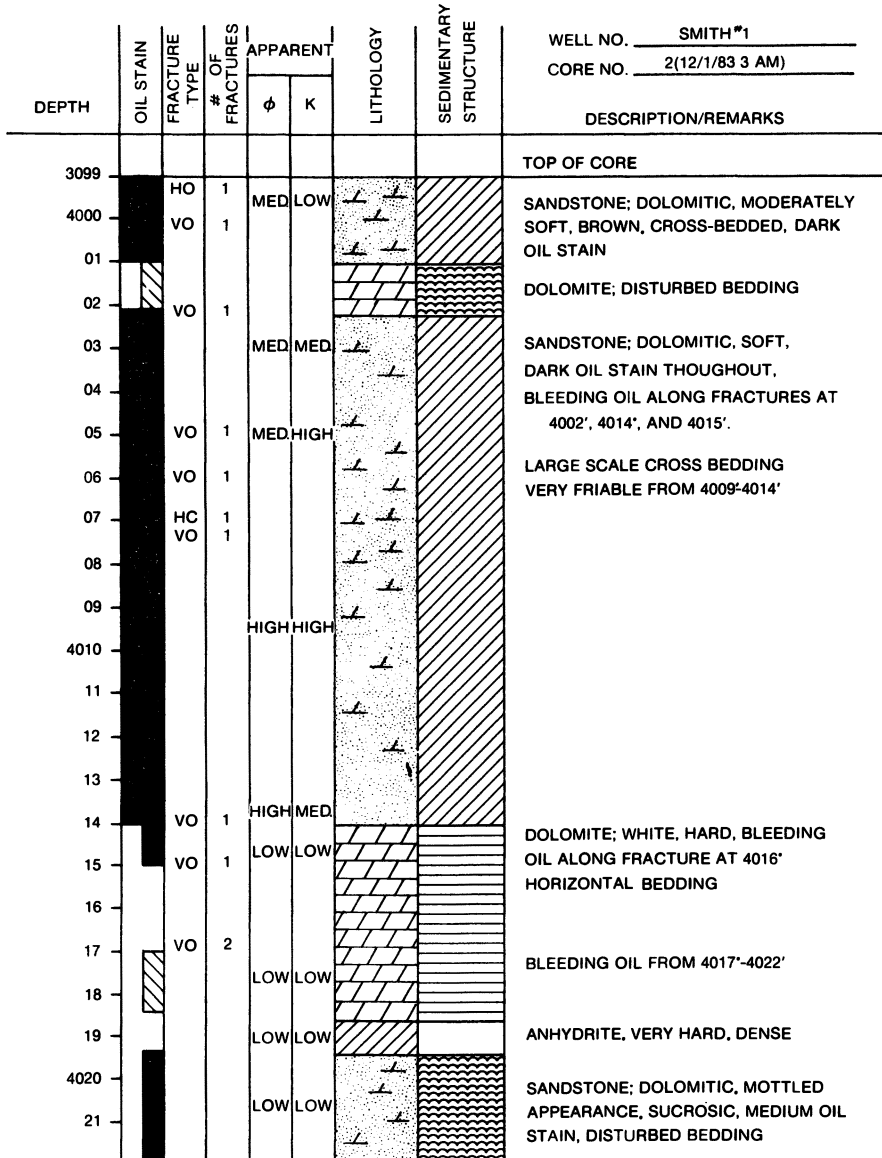


Figure 10. Well site description of a 5¼-in.-diameter core section.

Technique. For the following reasons, disks are preferred over linear cores for polymer flood design.

- The large void volume required for accurate data measurement is more readily obtained with disks.
- As polymer solutions usually exhibit non-Newtonian (rate-dependent) flow behavior, radial floods simulate the non-

linear streamlines present in reservoir patterns much better than linear floods.

- Because of rate effects, laboratory floods need to be conducted at frontal advance rates representative of those in the field. Disk floods reflect these velocity gradients.
- Disk floods require shorter experimental times at representative field velocities.

A disk holder is shown in Figure 11. The holder is designed for 6-in.-diameter by about 2-in.-thick disks. Smaller diameter disks can be readily accommodated by using hollow cylindrical inserts. Large-diameter disks are preferred to minimize experimental errors and potential edge effects. The flat surfaces of the disk are sealed by pressurized bladders. Injection and production occur at a $\frac{1}{8}$ -in.-diameter well bore and at the outer lateral area of the disk. A series of taps along a radius allows monitoring of pressure behavior with distance. Produced fluids are collected with a sample fractionator, which allows for incremental fluid analysis throughout the flood. The disk flooding experiment is maintained at the desired reservoir temperature with a constant temperature air bath.

In each disk flood, waterflood performance is measured prior to injection of polymer. This measurement provides a benchmark for each specific disk. Waterflood data are very beneficial in separating results



Figure 11. Disk in holder for radial flooding.

due to rock characteristics from those due to the injected fluid system. In general, with increasing rock heterogeneity, waterflood oil recovery efficiency decreases and oil recovery by polymer flooding increases (7).

Native (uncleaned) disks are flooded in the following sequence: (1) degas under water or oil, depending on wettability; (2) resaturate with crude oil; (3) waterflood; (4) polymer flood; (5) extract by Dean-Stark extraction to obtain residual oil; and (6) clean and dry disk for permeability measurement.

Tertiary Versus Secondary. "Tertiary" polymer floods are conducted in the laboratory to evaluate reservoirs in which waterflood operations have been initiated. In tertiary disk floods, water is first injected (approximately 2 pore volumes) until a low oil cut is reached. Then polymer solution followed by drive water is injected. The produced sample increments allow the measurement of oil cut and recovery versus injection volume (Figure 12). The concentration of produced polymer as a function of injection volume is also obtained. Polymer retention is calculated by material balance. Polymer flooding increases the oil cut, and oil (20 cP) recovery is enhanced over straight waterflooding (Figure 12).

"Secondary" laboratory floods are conducted for reservoirs that have not been subjected to waterflooding. In this case, following the waterflood, the disk is resaturated with crude oil (10 cP) prior to conducting a polymer flood of equal injection volume. An example of a secondary polymer flood is shown in Figure 13. Again, polymer flooding recovers more oil than does waterflooding and requires lower injection volumes.

Mobility Reduction. Polymer does not significantly alter the interfacial tension between oil and water; therefore, polymer flooding theoretically should not recover more oil than can ultimately be recovered by *infinite* waterflooding. However, polymer does increase waterflood oil recovery efficiency (rate) by virtue of reduced water mobility and improved sweep efficiency. Thus, improved vertical and areal conformance by polymer flooding results in additional oil recovery over waterflooding prior to reaching abandonment at an uneconomical oil cut.

As discussed earlier, pressure data are required to study mobility behavior in laboratory disk floods. Total mobility (λ) is equal to the summation of the mobilities of all the phases and for two-phase flow is

$$\lambda = k_o/\mu_o + k_w/\mu_w \quad (2)$$

where k_o and k_w are permeabilities and μ_o and μ_w are viscosities of oil and water, respectively. Mobility for disk floods may be calculated from the Darcy equation for radial flow:

$$\lambda = \frac{q \ln (r_o/r_i)}{h(\Delta P)} \tag{3}$$

which is similar to equation 1 for single-phase flow.

An example of total disk mobility versus average water saturation existing during waterflood and a subsequent polymer flood is shown in Figure 14. Similar data are obtained for a series of concentric rings using the pressure taps along the disk radius. Mobility during waterflood is only dependent upon oil and water permeabilities and viscosities (equation 2). However, oil and water permeabilities are saturation dependent. During the early stages of a waterflood, mobility decreases due to decreasing oil relative permeability and a low water relative permeability (Figure 14). In the later stages of a waterflood, mobility increases as a

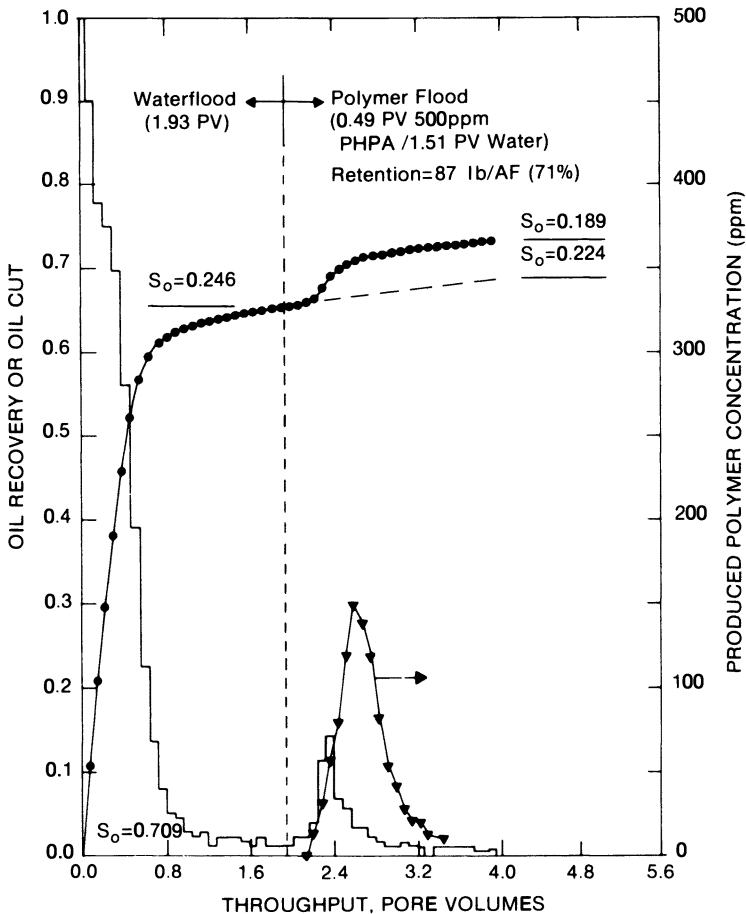


Figure 12. Oil recovery from a 500-millidarcy (500-md) sandstone disk.

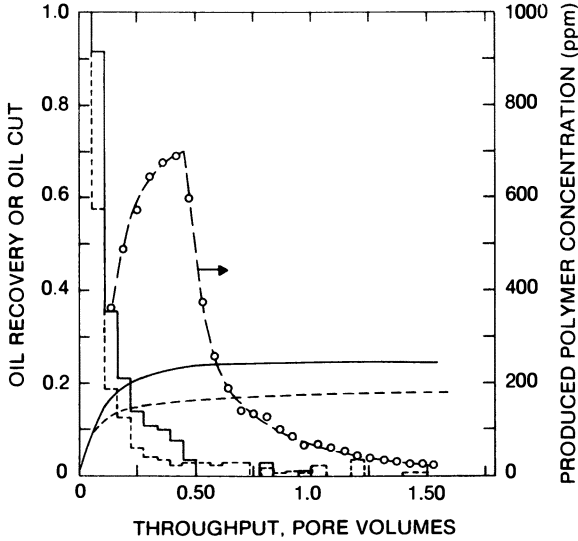


Figure 13. Comparative oil recoveries from a 330-md dolomite disk (7). Key: ---, 1.60-PV waterflood; and —, 0.39 PV of 1000 ppm of PHPA and 1.17 PV of water. Reproduced with permission from reference 7. Copyright 1982 Society of Petroleum Engineers of AIME.

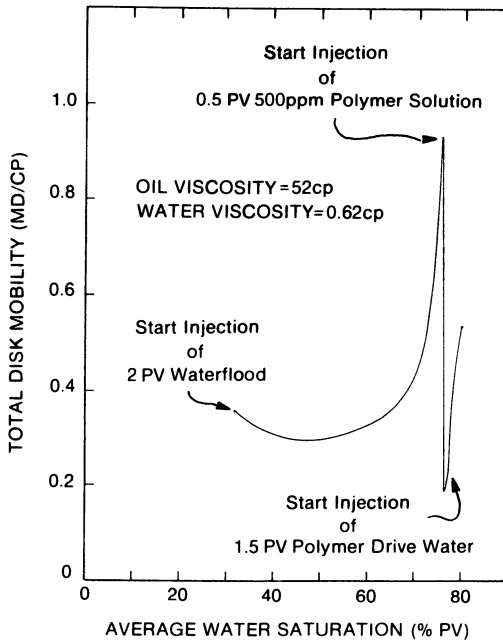


Figure 14. Mobility profile.

result of a low oil relative permeability and an increasing water relative permeability. Upon injection of polymer, a large decrease in mobility is effected. Polymer reduces water mobility through increased viscosity (μ_w) and decreased permeability (k_w). Upon drive-water injection, mobility again increases as the aqueous phase viscosity decreases to that of water. A reduction in mobility remains at the end of polymer drive water as a result of permanent permeability loss caused by entrapped polymer. The mobility reduction by polymer is offset in part by a mobility increase due to a water relative permeability increase accompanying additional oil recovery (increased water saturation).

Reverse Injection. Normally, fluid is injected into the center well bore. However, flow direction can be readily reversed with injection from the outside perimeter resulting in production from the center well bore. Because polymer solution behavior is rate dependent, disk floods are conducted at field rates (a median frontal velocity in the order of 0.25 ft/day). Polymer flood recovery as a function of velocity (injection rate) is shown in Figure 15 for two different types of lithology. Oil recovery increases with flooding velocity, the increase depending on the rock-polymer solution system. Even at 3 ft/day, pressure gradients are not sufficient at any location to reduce oil saturation below true water-flood residual (11, 12). That is, oil is *not* dislodged because of viscous forces exceeding capillary forces. Figure 15 shows that within experimental

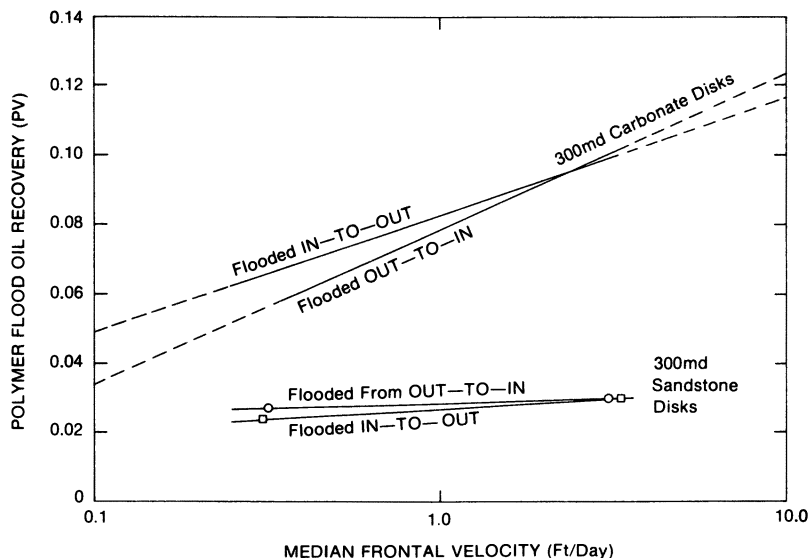


Figure 15. Tertiary polymer flood oil recovery as a function of flood velocity and direction.

error, inward and outward flooding of the disks gave the same oil recovery. This result demonstrates that possible capillary pressure end effects are insignificant.

Injection may be conducted at a constant rate or at constant pressure. From the standpoint of instrumentation, constant-rate experiments are preferred.

Design Parameters. In most field polymer flood applications, only three polymer design variables exist: structure (\bar{M}_r , molecular weight distribution and branching), concentration, and bank size. In some locations, a choice of injection waters is available, which gives a fourth design variable.

In general, performance (oil recovery efficiency) increases with increasing polymer molecular weight. Figure 16 shows higher oil recovery by increasing \bar{M}_r . Both viscosity and permeability reduction are augmented by increasing molecular weight. Polymer retention also increases with molecular weight. The maximum molecular weight suit-

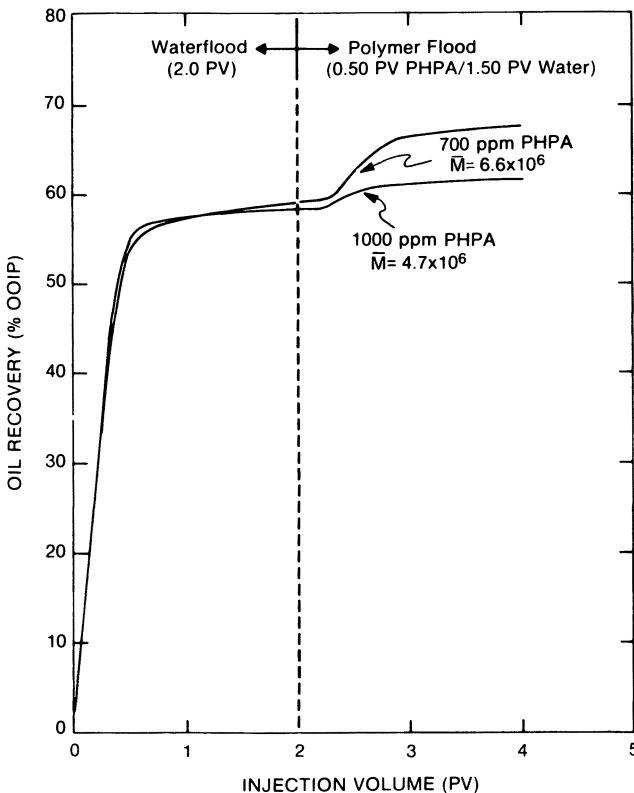


Figure 16. Effect of \bar{M}_r on polymer flood oil recovery efficiency.

able for a particular reservoir is limited by mobility reduction (injectivity loss) and polymer retention considerations.

For any given polymer type, oil recovery increases as the amount of polymer injected (dosage) increases. At the lower polymer dosages, oil recovery increases rapidly. A maximum recovery is approached asymptotically at high polymer dosages. The effect of increasing polymer concentration at a constant polymer bank size is illustrated in Figure 17. A similar polymer dosage versus oil recovery relationship is shown in Figure 18 where the polymer concentration is held constant and the polymer bank size varied. In Figures 17 and 18 relatively large polymer dosages are required to recover significantly more oil than can be obtained by waterflooding alone.

In addition to polymer design variables, the rock properties can affect polymer flood oil recovery. Many oil-bearing reservoirs contain multiple zones in a single formation. In some reservoirs, formations of different lithology (e.g., carbonate and sandstone) are simultaneously flooded from common wells. Reservoirs are not homogeneous over their vertical and areal dimensions. In addition to permeability, rock variation may exist due to localized laminations, cross-bedding, directional permeability, and other heterogeneities. Thus, polymer flood performance must be evaluated by laboratory flooding in all rock types representing significant portions of the reservoir.

In many cases, polymer flooding appears to be more beneficial for

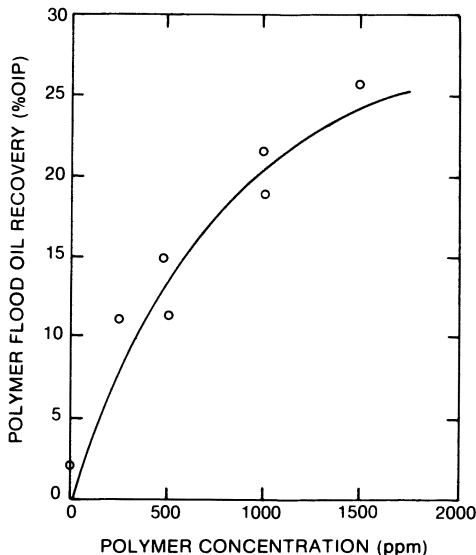


Figure 17. Polymer flood oil recovery as a function of concentration.

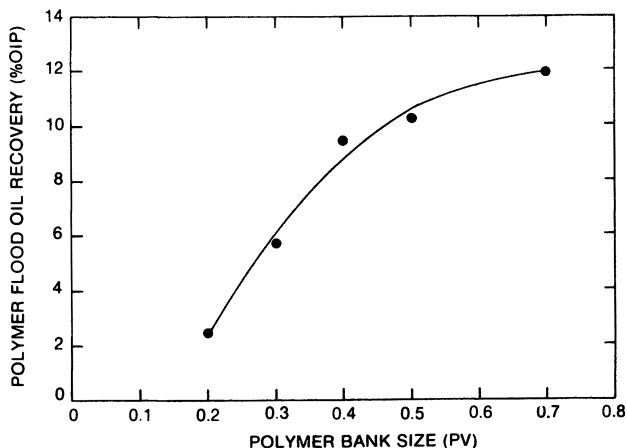


Figure 18. Polymer flood oil recovery as a function of bank size.

incremental oil recovery in dolomite than in sandstone. Figure 19 shows a tertiary polymer flood recovery in a dolomite disk using identical fluids as used in the sandstone disk shown in Figure 12. Typically, waterflood oil recovery is lower in dolomite. Data in Figure 15 using disks from other reservoirs also show a much greater polymer flood oil recovery in the carbonate disks. Surprisingly, polymer retention is generally lower in carbonate disks than in sandstone disks. Polymer retention may be low even in very low permeability (less than 10 md) carbonate disks (Figure 20).

In many reservoirs, polymer flooding may not recover additional oil over waterflooding. Reservoirs that are not good candidates for polymer flooding include (1) those that contain large amounts of clay or have other characteristics that result in extremely high polymer retention, (2) very homogeneous reservoirs, and (3) those having very favorable water-to-oil mobility ratios.

In summary, disk flooding reliably measures the effects of polymer design variables and rock properties on oil recovery by both waterflooding and polymer flooding. A later section discusses how laboratory mobility, oil recovery, and retention data are used to predict field performance.

Field Feasibility Testing

Because prediction of how a particular reservoir will respond to polymer injection is almost impossible, an injectivity field test is normally conducted. In many projects, economics are heavily influenced by injection rates. Because polymer solutions are more viscous than water, wellhead

pressures should increase for comparable flow rates. As pressures approach the maximum injection pressure, injection rates will decrease accordingly. Incremental oil production due to polymer could be delayed considerably by a reduction in field rates.

Data must be generated in all phases of the injectivity test to facilitate the implementation of the subsequent full-field, polymer-augmented waterflood. Therefore, in addition to well pressure data and injection rates, information on mixing, pumping, pipeline frictional pressure losses, mechanical degradation, and polymer solution properties in actual field injection water must be obtained. In cases where polymer is manufactured on site, information on the impact of the field environ-

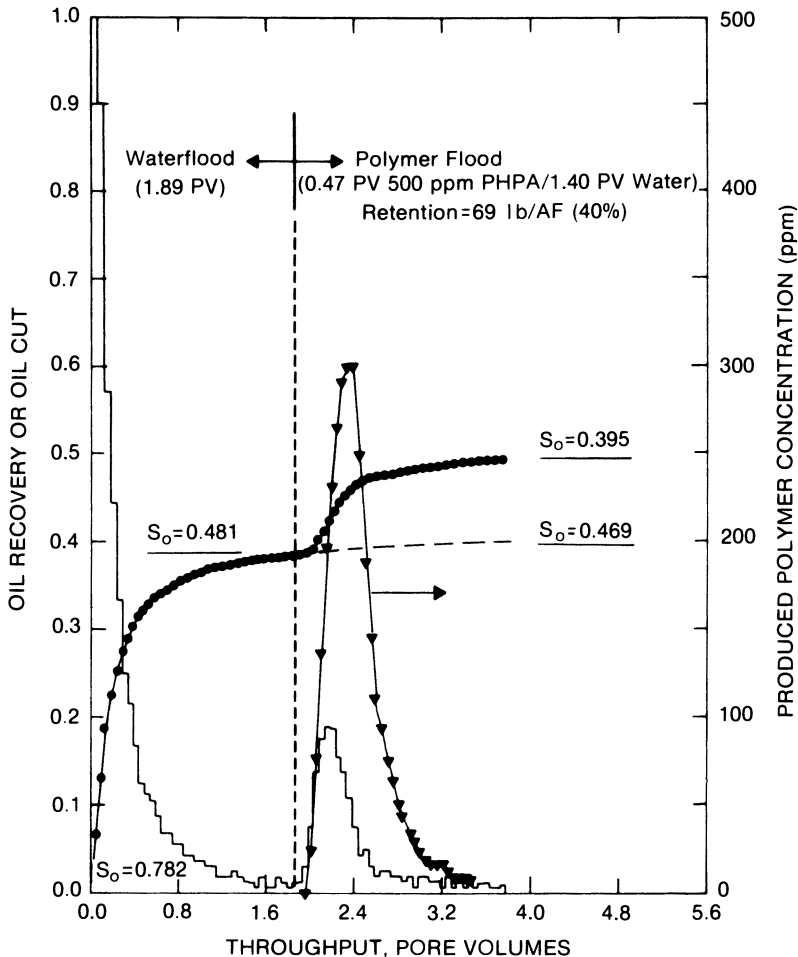


Figure 19. Oil recovery from a 300-md dolomite disk.

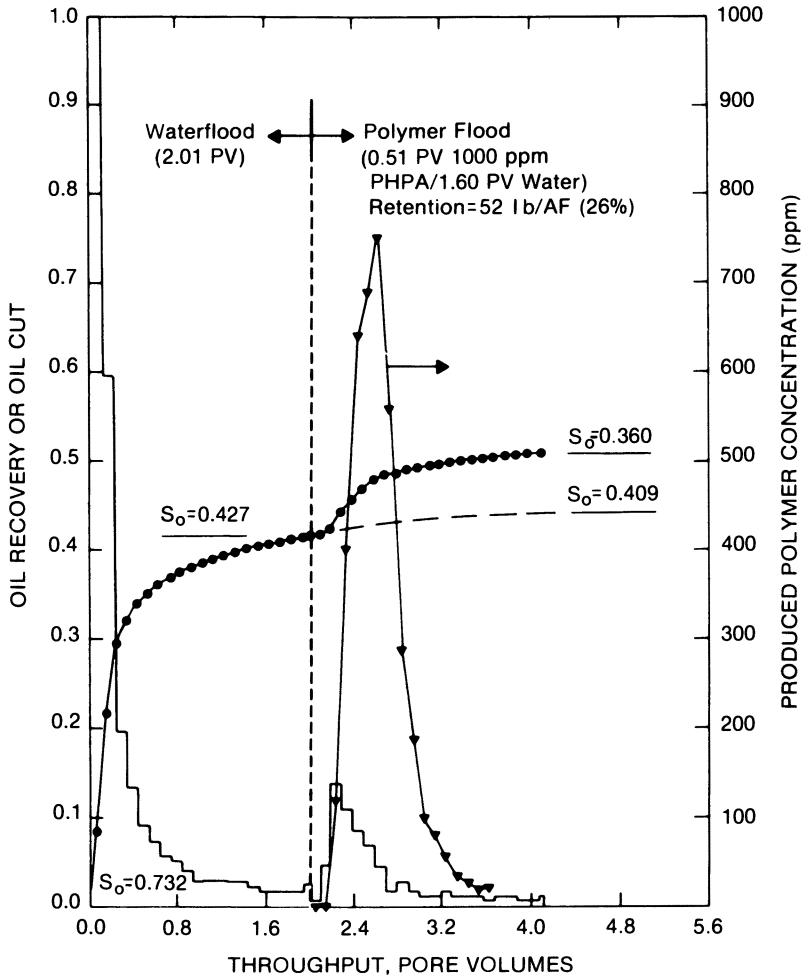


Figure 20. Oil recovery from an 8-md carbonate disk.

ment on the polymerization process is also desired. More importantly, however, a field test gives oil field engineers and operators a chance to work with polymer and polymer systems so that proper handling becomes as routine as other oil field operations. For these reasons, properly designed injectivity tests could more correctly be called feasibility tests because the feasibility of a complete polymer-augmented waterflood is examined, not just injectivity.

Choosing a Well. One of the more important aspects of feasibility testing is injection well selection. Several requirements should be met. The well should be representative of the field average, and a history of

water injection data should be available. In many cases, water injection wells should be stimulated (cleaned) before polymer flooding.

Many different types of well completions exist; some are shown in Figure 21. For polymer flooding, open-hole completions are generally preferred over perforated-hole completions because polymer solutions are exposed to a much greater surface area near the well bore; this factor reduces the amount of shear for a given flow rate. However, open-hole completions are uncommon because of associated mechanical problems. Perforated-hole completions are more predominant and usually must be reperforated to a higher density before polymer injection.

Polymer-Blending Systems. Many different types of polymer-blending systems exist, but basically they can be divided into two categories: dry blending and concentrate blending. In dry blending, polymer is stored as a dry powder and transported to a hopper where it is fed into a mixer consisting of a funnel-shaped device and a tangentially flowing stream of dilution water. A schematic of this type of system is given in Figure 22. Because polymer is difficult to solubilize, filters are

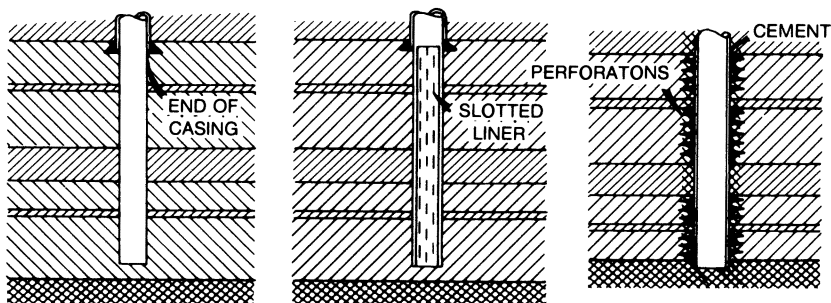


Figure 21. Well completions. Key: left, open-hole completion; middle, open-hole completion with slotted liner; and right, perforated completion.

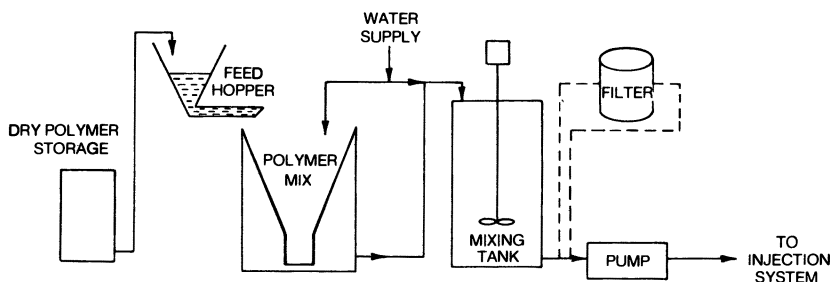


Figure 22. Polymer blending system.

employed to prevent undissolved polymer from entering the injection system and causing formation plugging.

Concentrate blending, on the other hand, requires less equipment and is inherently more dependable because this polymer has never been dried and is already mixed in concentrated form. For small-scale operations, polymer can be purchased, shipped, and stored on site in concentrated form in a suitable polymer holding tank. In large-scale operations, final blending is only one part of an overall semicontinuous manufacturing process. Another form of concentrate blending involves PHPA emulsions wherein the concentrated emulsion is inverted by dilution with water.

Once polymer has been mixed with injection water, oxygen contamination must be prevented because oxygen can induce degradation. This prevention is generally accomplished by blanketing polymer storage tanks with nitrogen. As injection water may contain biocides, scale, and corrosion inhibitors, the polymer concentration must be adjusted to accommodate these chemicals.

Mechanical degradation is also important, particularly when dealing with very high molecular weight polymers. Equipment for handling polymer solutions must be chosen to minimize shearing forces.

Polymer Injection Equipment and Instrumentation. Although final dilution of the polymer concentrate is relatively straightforward, great care must be taken to minimize mechanical degradation. A typical injection system for a polymer feasibility test is given in Figure 23. The positive displacement pump used to deliver concentrated polymer into the injection line must be designed to deliver the proper amount of polymer at the maximum anticipated discharge or wellhead pressure. Although many positive displacement pumps can be used, only a few operate with a minimum of shear. This result will be described more fully under Full-Field Development.

Monitoring flow rates of polymer concentrate also requires special equipment. Because these solutions are usually very viscous and non-Newtonian, only a few types of meters are appropriate—mass flowmeters, magnetic flowmeters, and oval gear meters. Of the three, magnetic flowmeters have been found to be particularly useful in the oil field.

The third important element in the injection system is the static mixer where final dilution is made. Basically, the mixer consists of a series of elements held in place in a straight pipe. Although the concept is relatively simple, designing mixers for polymer and non-Newtonian fluids is largely empirical. The degree of mixing depends on the flow regime (laminar or turbulent), viscosity ratio, flow rate ratio, and composition of the two fluids. The size and number of elements depend on the desired homogeneity, maximum allowable pressure drop across the

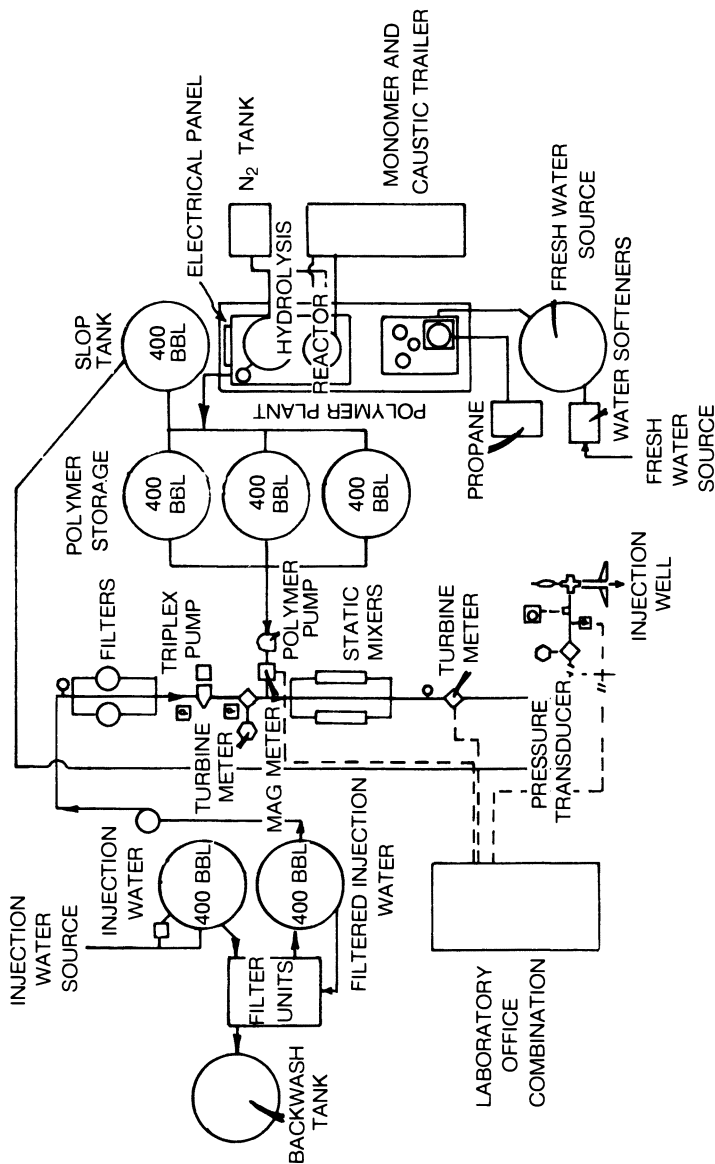


Figure 23. Schematic of polymer feasibility test. Polymer was manufactured on-site.

Publication Date: May 5, 1986 | doi: 10.1021/ba-1986-0213.ch015

mixer, and size restrictions (length or diameter). Pressure drops should be minimized to prevent shear degradation.

In any polymer feasibility test, instrumentation must be relatively rugged to withstand oil field environments. Data acquisition systems are used to monitor all phases of the test. Microprocessor-based ratio controllers can be used to control the pumping rate of concentrated polymer into the water-injection line, particularly when water rates are expected to vary or injection water comes from a common header. A good injectivity test relies on very constant injection rates.

Pressure transducers should be used to continuously record bottom-hole pressure, static mixer pressure drop, wellhead pressure, and any appropriate line pressures. Flowmeters are used to continuously measure water rates, polymer concentrate rate, and diluted polymer flow rate. Bottom-hole and surface injection temperatures should also be measured and recorded.

Water Treatment. Injection water quality is important for polymer feasibility tests. A filtration unit should be installed into the water-injection system. One such unit is shown in Figure 24. This unit provides quality water as well as data for full-field filtration design.

Analytical Data Analysis. Observing polymer properties during the course of a test can indicate potential problems for full-field development. Sampling procedures must be designed to prevent oxygen contamination or shear degradation prior to measurement.

Concentrated polymer should routinely be sampled at both the suction and discharge sides of the polymer pump. A comparison of these two samples indicates the degree of mechanical degradation and also uniformity and consistency of the product.

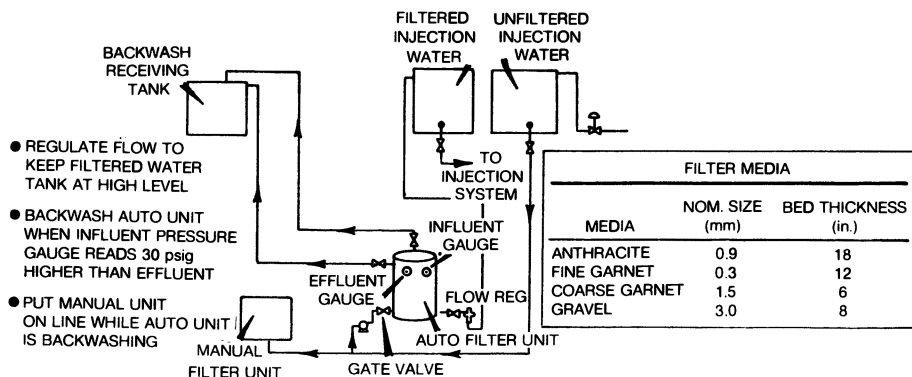


Figure 24. Skid-mounted filtration unit.

Dilute polymer samples should routinely be taken downstream of the static mixer and at the wellhead. Routine measurements of these samples include Brookfield viscosity, screen factor, concentration, and apparent viscosity as a function of shear rate. In this case, some measurements, particularly those of apparent viscosity, should be taken at the measured reservoir bottom-hole temperature.

Figures 25 and 26 give viscosity-shear-rate curves for wellhead samples taken from two different injectivity tests. The large difference in properties is due primarily to the difference in dilution water. Also, the power-law rheological model does not adequately match data over the full range of shear rates. Water-injection samples should also be taken, and a detailed chemical composition should be obtained.

Pressure Data and Analysis. For interpretation of injectivity tests, wellhead and bottom-hole pressures are needed. Many times both should be monitored because wells originally on vacuum will become pressurized after several days of polymer injection.

An example of bottom-hole pressures obtained during the course of a feasibility test is given in Figure 27. Stable readings with water just prior to polymer addition and the subsequent rise thereafter are found. Polymer must be injected over a sufficient time period such that a relatively stabilized pressure is obtained.

Besides stabilized pressure readings, important information can be obtained from transient well-testing analysis performed prior to, during, and after polymer injection. Well-testing analysis is a major field of specialization in petroleum engineering, and many books (13-15) have been written on the subject. Testing with non-Newtonian polymer solutions, however, is not completely understood or defined. If injected polymer solutions are Newtonian and not particularly viscous, conventional methods can be used. But, for very viscous material displaying non-Newtonian characteristics, conventional techniques can give erroneous

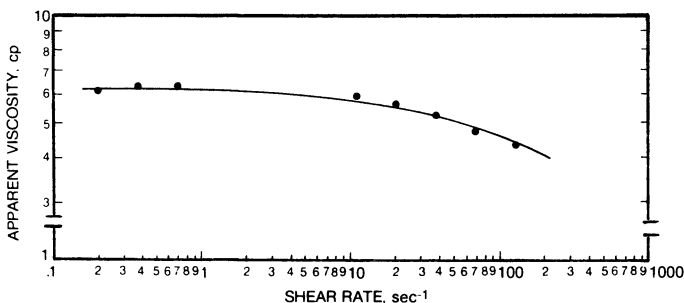


Figure 25. Rheogram of apparent viscosity as a function of shear rate (test A).

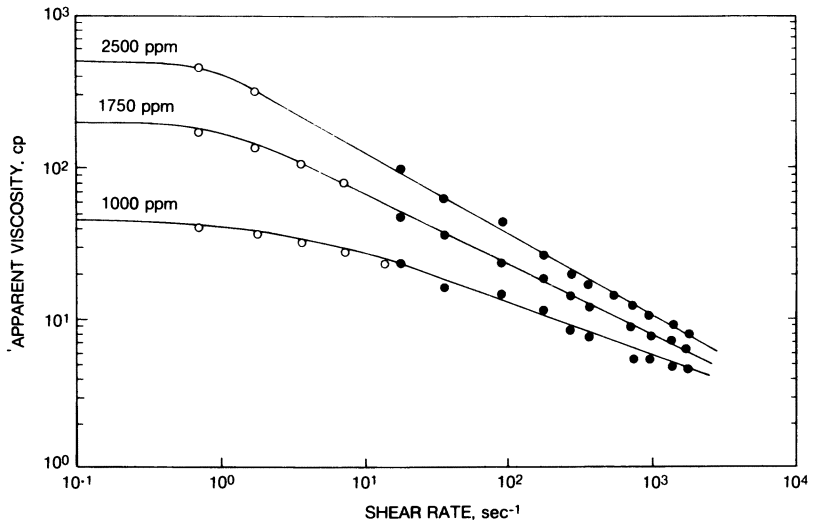


Figure 26. Rheogram of apparent viscosity as a function of shear rate (test B).
Key: ○, Brookfield viscometer; and ●, Ferranti-Shirley viscometer.

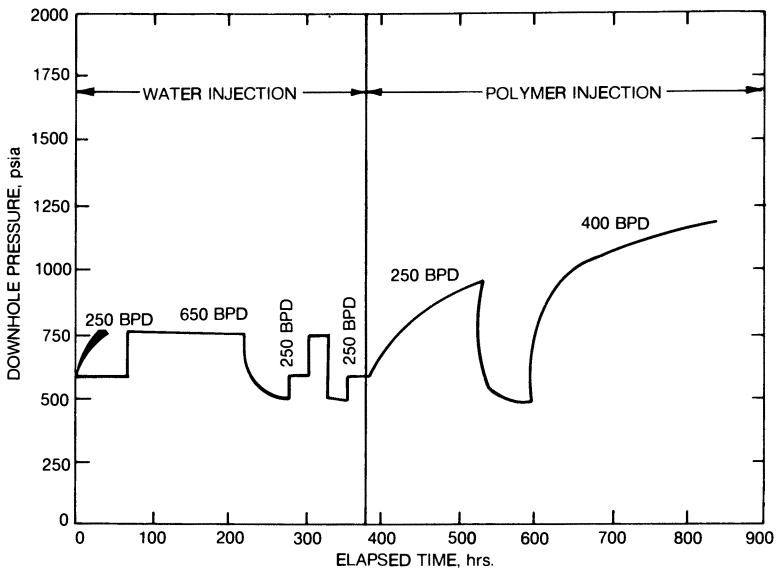


Figure 27. Feasibility test of downhole pressure data as a function of elapsed time.

results, and non-Newtonian analysis (16–18), although still in its infancy, should be applied.

Table I lists several techniques for analyzing injectivity data. Of course, the more tests that are performed, the more confidence in the data. Typical injectivity test results are given in Tables II and III. A difference in mobility before and during polymer injection occurs. If a substantial difference exists, then problems might occur with injectivity. A general criteria for a successful test cannot be given because each reservoir must be treated separately.

Modeling

Mathematical models or simulators are used to help understand polymer feasibility data and to predict injectivity and oil recovery for full-field development. These models use partial differential equations for flow-through porous media and solve them numerically with the aid of a computer. Depending on the complexity of the model, these computations can take anywhere from several minutes to several hours on relatively high-speed computers. Of course, an actual polymer flood is much too complicated to be represented by a series of theoretical equations; as a result, simplifications and various assumptions must be made concerning the mechanisms involved and the reservoir characteristics. Although most of these simplifications seem crude and unrealistic, many modeling attempts have been very successful (19, 20).

The modeling process is iterative in nature. Actual flooding data are matched by choosing appropriate parameters for the model. If theoretical curves obtained from these models do not match experimental data, then these parameters are changed to bring them closer to agreement. As a result, modeling depends quite heavily on experimental data. The more data available, the more a restriction is placed on changing these parameters and, hence, the more confidence exists in using the simulator for predictions.

Two related applications exist where simulators are used: laboratory-curve matching and field-curve matching. First, the polymer simulator is used to match laboratory core flooding data, both waterflood and polymer flood, under reservoir conditions. Water cuts, pressure drops, effluent polymer concentrations, cumulative oil recovery, and some cation concentrations are all matched by a trial-and-error method choosing appropriate computer parameters. These parameters are essentially relative permeabilities (both drainage and imbibition), polymer retention isotherms, inaccessible pore volume, capillary pressure, ion-exchange isotherms, viscosity-velocity relationships, and resistance factors. Several trials are necessary before all experimental curves are matched with one set of parameters. This feature in no way, however, makes the set unique. In fact, several different sets of parameters can

Table I. Well-Testing Techniques for Polymer Flooding

Name	Variables Used	Plotting			Type	Information Obtained	Reference
		Coordinates					
		y	x				
Hall plot	$P_w, Q, \Delta t$, cumulative data	psid	cum. inj.		Cartesian	kh/μ when P_D and s known (useful only if P_D and s constant)	14
Miller-Dyes- Hutchinson	$P_w, \Delta t$	ΔBHP	Δt		semilog	$kh/\mu, s$	14
Horner	$P_w (t_p + \Delta t)/\Delta t$	ΔBHP	$(t_p + \Delta t)/\Delta t$		semilog	$kh/\mu, s$	14
Type curve	$P_w \Delta t$	ΔBHP	Δt		log-log	$kh/\mu, s$	14
Power-law analysis	$P_w \Delta t$	ΔBHP	Δt^m		log-log Cartesian	slope, m , gives n slope gives K and (k/μ) effective (useful only for long injection times, large polymer banks)	16-18

NOTE: Q is flow rate; t is time; cum. inj. is cumulative injection; k is permeability; h is disk thickness; μ is viscosity; K is consistency index; P_w is bottom-hole pressure; t_p is effective production time; P_D is dimensionless pressure; s is skin factor; and Δt^m is delta time where m is equal to $1 - (n/3) - n$ and n is a power-law parameter.

Table II. Fluid Injectivity

Fluid	<i>av</i> Brookfield Viscosity (cP) ^a	Nominal Flow Rate (BPD) ^b	Wellhead Pressure, P _t (psi)	Bottom-Hole Pressure, P _w (psi)		Actual Downhole ΔP ^d (psi)	Injectivity (BPD/psi)	Normalized Injectivity
				Actual	Calcd from Surface ^c			
Injection water before polymer	1.0	250	vacuum	553	—	53	4.72	1.0000
1000 ppm of PHPA in injection water	9.0	250	450	1113	1107	613	0.41	0.0869
Injection water after polymer	1.0	250	300	1013	957	513	0.49	0.1038

^aAt 6 rpm and 72 °F.^bBPD is barrels per day.^cP_w = P_t + 0.433 psi/ft - ΔP_{friction}.^dΔP = P_w - P_t, where P_t = 500 psi.

Table III. Summary of Transient Testing Results

Type of Test	Elapsed Time (h)	Injection Fluid	Semilog Analysis		Type Curve Analysis		
			k/ μ	s	k/ μ	s	μ_e^a
Falloff 1	230-280	water	18.1	-2.0	27.2	-1.4	1.0
Two Rate	280-330	water	29.6	-2.2	—	—	—
Falloff 3	540-610	polymer	6.8	-0.4	7.1	-2.2	2.7

^a μ_e is effective viscosity (cP).

give comparable matches. At this point the modeler uses some subjective judgment and decides which set is reasonable and best to use.

If a reasonable match is not obtained, then rock heterogeneities can be included by increasing the model's complexity such as using permeability variations, layering effects, and fractures. Of course, with more independent parameters to choose, the chances of modeling experimental data increase. Added complexities, however, increase computational times and expenses and, without supporting experimental data, make the simulator less restrictive and predictions more risky.

Figure 28 is an example of output from a simulator used to model a laboratory water and polymer disk flood (21). Considering all the assumptions used in the mathematical equations, a remarkable match can be obtained.

Once laboratory data have been modeled, a field simulator is developed. Polymer parameters obtained from the laboratory match are used

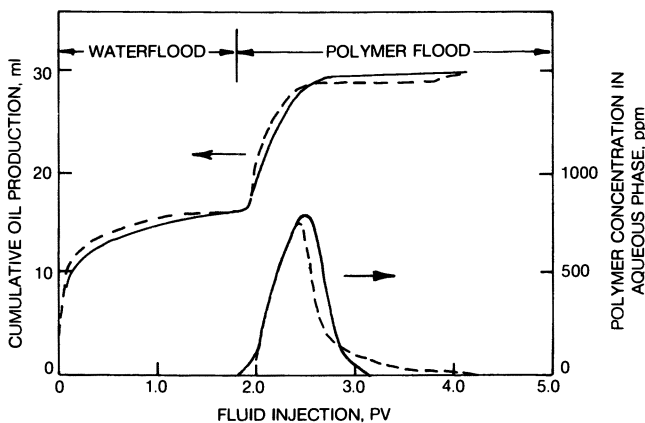


Figure 28. Simulator match of laboratory waterflood and polymer flood. Key: ---, disk flood; and —, simulator. Reproduced with permission from reference 21. Copyright 1983 Society of Petroleum Engineers of AIME.

for the field model. Reservoir parameters, of course, are substituted for disk parameters. The formation can be represented either as a homogeneous system, as a system of layers, as a fractured system, or as other variations, depending on available geologic information, the well-completion technique, and the capability of the model. A single-well model is normally used to match downhole and wellhead pressures, concentrations, and flow rates witnessed during the feasibility test. Well-testing results from falloff and buildup tests are especially important and must be simulated with the model. Once a match is achieved, in situ mobility data can be estimated.

The final step in simulation is to do a conceptual full-field model incorporating all parameters obtained from laboratory and injectivity tests. However, the full-field model should match prior waterflood history, particularly oil production rates and oil cuts from individual producing wells. This modeling is very difficult to do in those cases where the reservoirs are relatively heterogeneous with directional permeabilities and undefined well patterns. Nevertheless, in a conceptual model, general trends can be patterned even though large discrepancies may exist for individual wells. Once a reasonable field match is obtained, the simulator can be used to predict oil recoveries for a continued waterflood and then, with the inclusion of polymer parameters, predict recoveries for a polymer-augmented waterflood. The two recoveries can then be compared and used for economic predictions. Figure 29 gives an example of a field match of a waterflood and predictions of continued waterflood and polymer floods.

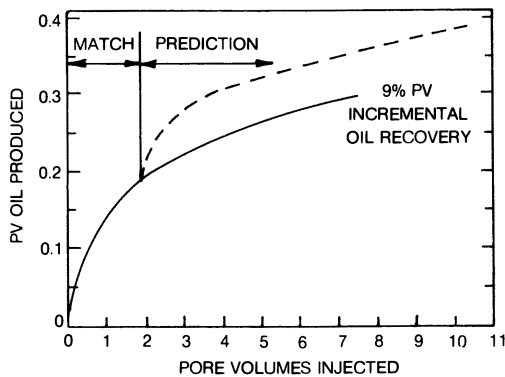


Figure 29. Simulator match of waterflood and prediction of waterflood and polymer flood. Key: —, waterflood; and ---, polymer flood. Reproduced with permission from reference 21. Copyright 1983 Society of Petroleum Engineers of AIME.

Full-Field Development

PHPA Source. PHPA is available in a variety of forms. These forms include dry powders, emulsions, and gels. Each form requires its own unique dissolution technique for field application. Complete solubilization of the polymer is the key to avoiding rapid face plugging in the injection well. Another option is to manufacture the PHPA on site. This approach eliminates the necessity of concentrating the polymer for shipment and redissolving on site. The commercially available PHPAs represent nearly all of the standard acrylamide polymerization techniques—solution, emulsion, redox, and radiation—and appropriate dissolution techniques are applied. The negatively charged carboxylate groups are introduced by either hydrolysis of a preformed poly(acrylamide) or through the copolymerization of acrylamide with an appropriate amount of sodium acrylate.

Pattern. The well patterns used for polymer-augmented waterflooding are very similar to those of straight waterflooding. Most developed fields use some repeated pattern (five spot, nine spot, line drive, etc.) on a consistent spacing (5, 10, or 20 acres, etc.). In fields that have not been fully developed for secondary recovery operations, drilling of new wells, conversion of producing wells to injection wells (or vice versa), recompletion of abandoned wells, or abandonment of old wells may be required to obtain the desired operating pattern.

Much more well work is required in fields that have not been developed for secondary operations. In this case, exhaustive geological and engineering studies must be conducted to select a pattern for the most efficient production of oil reserves.

Injection Well Completion. Polymer molecules subjected to stretch rates in excess of their natural relaxation times may be degraded. That is, very high stresses existing on polymer molecules undergoing elongational deformation in a flow constriction (pore throat of porous media) will cause rupture of the molecule (degradation). Polymer degradation causes main-chain scission (molecular weight reduction) with accompanying loss of solution properties (viscosity and screen factor). Thus, polymer degradation results in a reduction of oil recovery efficiency (Figure 30). In the reservoir, the greatest shear stresses occur in the vicinity of the injection well bore where the flow area is the least and the frontal velocity is the greatest. Therefore, injection wells may require modification to eliminate or minimize polymer shear degradation.

Laboratory floods are used to investigate potential shear degradation. Loss of screen factor and viscosity during flow through a core, a manifestation of degradation, is measured at a number of injection rates. Empirical relationships (Figure 31) are obtained for degradation versus

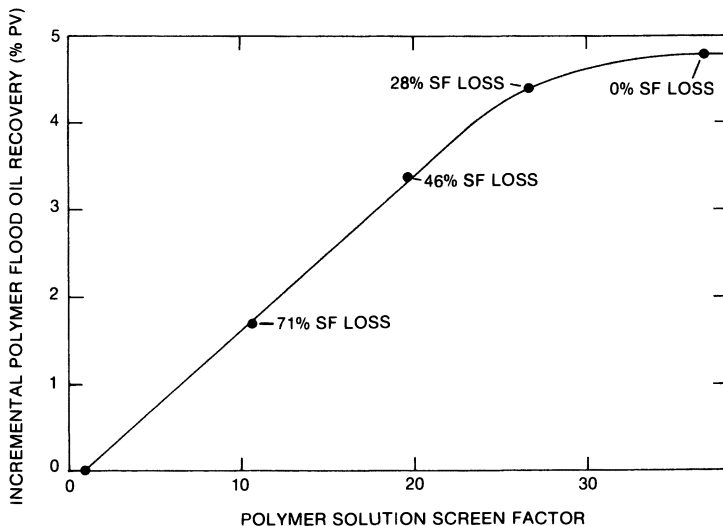


Figure 30. Effect of polymer degradation on recovery.

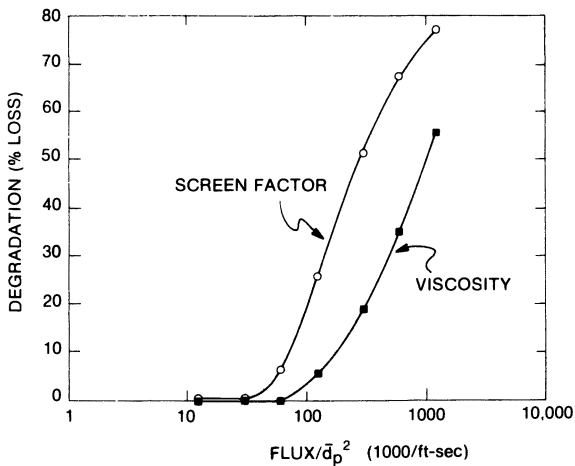


Figure 31. Polymer degradation correlated to flux and average grain diameter for a 600-md sandstone wedge. Key: ○, screen factor; and ■, viscosity.

correlating parameters. Screen factor is thought to be a measure of molecular size and structure (22). Degradation causes a much larger loss of screen factor than viscosity (Figure 31).

Correlation parameters have been developed that contain both flux (velocity) and rock grain diameter terms (23, 24). The interstitial velocity (\bar{v}) term may be calculated from

$$\bar{v} = q/(A\phi S_w) \quad (4)$$

where q is the flow rate, A is the cross-sectional area, ϕ is the porosity fraction, and S_w is the fractional water saturation. The average grain size, \bar{d}_p , is calculated from permeability, k , and porosity, ϕ , by

$$\bar{d}_p = (1 - \phi)/\phi\sqrt{150k/\phi} \quad (5)$$

Maerker (23) has shown that degradation can be correlated to the parameter $\dot{\epsilon}L_D^{1/3}$. In this parameter, $\dot{\epsilon}$ is the stretch rate, or

$$\dot{\epsilon} = 2\bar{v}/\bar{d}_p \quad (6)$$

and L_D is a dimensionless length, or

$$L_D = L/\bar{d}_p \quad (7)$$

where L is the core length.

Sright (24) has reported that both radial and linear degradation data can be correlated to \bar{v}/\bar{d}_p^2 , where the maximum flux existing at the sandface is used.

Predictions of field degradation are based on the actual well completion technique parameters and empirical degradation relationships obtained in laboratory floods. For cased and perforated or open-hole completions, degradation can be predicted on the basis of average field injection rates, sandface area, and reservoir properties (k , ϕ , and S_w).

In many reservoir applications, severe polymer degradation is likely to occur in standard open-hole or perforated well-bore completions. In this case, hydraulic fracturing and propping are generally recommended. Fracturing greatly increases sandface entry area. Thus, the velocity in the reservoir matrix can be greatly reduced to a value where *no* polymer degradation occurs. Although fracturing totally eliminates polymer degradation in the formation matrix, high velocities existing in propped fractures may cause severe degradation. For this reason, linear laboratory sand-pack floods (using actual fracture sand proppant) are conducted to obtain degradation versus the $\dot{\epsilon}L_D^{1/3}$ parameter. This correlation is used to design a propped hydraulic fracture (i.e., sand proppant size, fracture width, and fracture length) that will allow injection at the desired rate with a minimum of polymer degradation.

Distribution and Injection Facilities. In general, polymer can be distributed two ways for a full-field polymer-augmented waterflood project. One method is to dilute concentrated polymer to its final concentration in a central facility and then pump this solution out to injection wells by using a manifold system. Flow resistance at each well determines injection flow rates. In most cases, available header pressure provides considerably more flow than desired; therefore, a flow-control

device is needed at each injection well. The controlling device, however, must not shear-degrade polymer solutions.

A second method to distribute polymer, particularly useful for relatively large oil fields, uses a somewhat different approach. Polymer is transported in concentrated form from a central facility to distribution centers throughout the field. These distribution centers house both polymer-handling facilities and water-injection facilities. Water-rate control is handled as it was during waterflooding, usually with a simple choke valve. Concentrated polymer is added downstream of the valve and mixed with the remaining injection water. No restrictive devices exist downstream of the mixer to shear-degrade the polymer; a very efficient system results. Figure 32 is an example of such a system. Sophisticated instrumentation is used to monitor the amount of concentrated polymer delivered to each well and provides most of the automatic shut-off and control devices.

Distribution centers are designed to control many wells simultaneously and offer the advantage of having centralized information. Computer networking systems can be used to combine information from all distribution centers; an excellent data base from which to monitor a polymer-augmented waterflood results.

Because large capital investments are required for full-field imple-

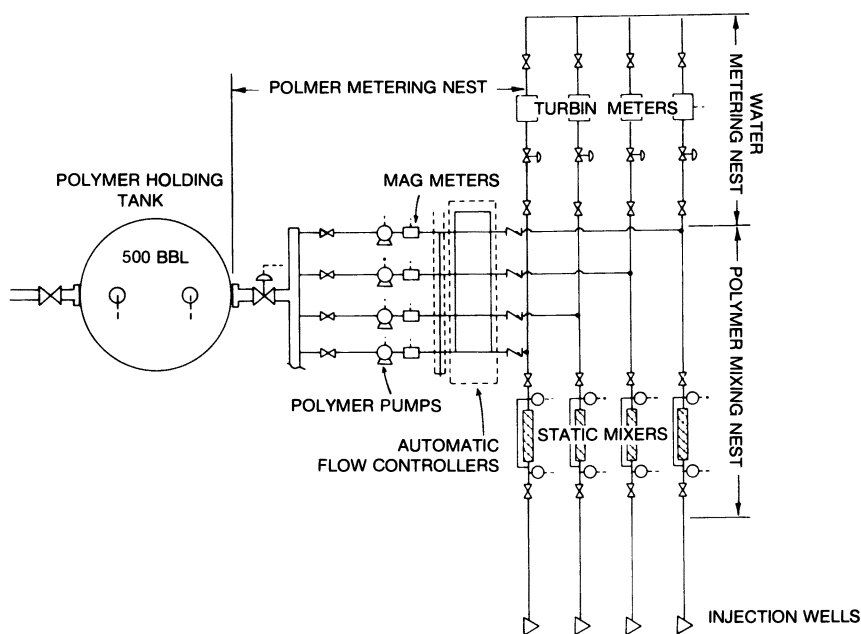


Figure 32. Schematic of the polymer dilution center.

mentation of a polymer flood, additional evaluations of certain major distribution equipment, besides that obtained from feasibility tests, are necessary to minimize cost. Two areas that are relatively unique to polymer flooding and should be studied carefully before designing a field project are pipelining and polymer pumps.

PIPELINING. Transporting concentrated polymer solutions requires knowledge of non-Newtonian fluid flow and measurement of rheological parameters. During the manufacturing process, extremely concentrated PHPA solutions must be transferred from one vessel to another. Although distances are relatively short, the material is so viscous that large frictional pressure drops can occur, requiring large and expensive pumping systems. Fortunately, these polymer solutions have been found to obey the power-law model over a very wide range of shear rates (Figure 33). Thus, pressure drops can be calculated and line sizes designed from conventional power-law relationships (25) as given in equation 8.

$$\Delta P = (8.84 \times 10^{-6})KL \left(\frac{0.787}{D} \right)^{3N+1} \left[\frac{63.13Q}{\pi\rho} \left(\frac{3N+1}{N} \right) \right]^N \quad (8)$$

where ΔP is pressure drop (psi), L is pipe length (ft), D is diameter (inside) (in.), Q is flow rate (gpm), ρ is density (g/cm^3), N is power-law index (unitless), and K is consistency index (cP s^{N-1}). Figure 34 shows a typical set of frictional pressure drop calculations for a high concentration PHPA solution. The power-law index, N , is very close to 0, indicat-

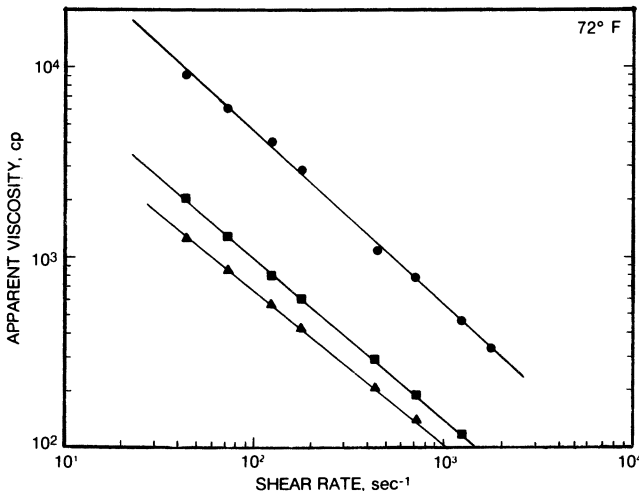


Figure 33. Rheogram of PHPA solution as a function of concentration. Key: ●, 6% PHPA; ■, 2% PHPA; and ▲, 1.5% PHPA.

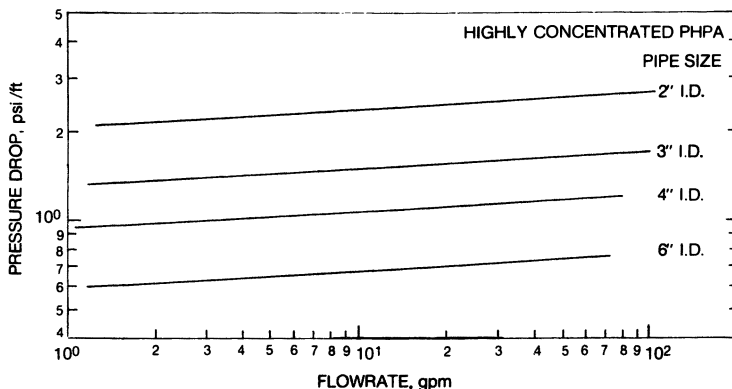


Figure 34. Frictional pressure drops as a function of flow rate for 6% PHPA solution.

ing an extremely non-Newtonian fluid whose frictional losses are almost independent of flow rate. Prediction of other losses, though, such as entrance and exit effects, flow-through fittings and valves, is still largely empirical although conventional techniques using equivalent pipe lengths are usually used. Shear degradation is minimal at these conditions because flow is definitely laminar.

The final stages of dilution produce a polymer solution that is more viscous than water and may be Newtonian. However, frictional pressure losses for these solutions are extremely unusual. Generally, these solutions are classified as drag reducing because frictional pressure losses can be less than that of water at comparable flow rates even though the viscosity is greater. This result, of course, only occurs where the flow of water is in the turbulent region. If injection rates and pipe sizes are such that laminar flow exists, then pressure drops will be greater than that of water with viscous properties dominating.

The last stage of polymer dilution produces a material more highly susceptible to mechanical shear than the 1-6% solution precursors. Some loss of polymer properties can occur with turbulent flow in the pipeline. These losses are usually small but can be great if flow rates are very high, if rough pipes are used, or if numerous fittings and restrictive devices are present before the solution enters the sandface. Figure 35 shows what can happen in coiled tubing (throttling device) and the importance of water composition on shear degradation. Degradation is much greater in the presence of divalent ions.

POLYMER PUMPS. Choosing a pump for a particular polymer application is not an easy task because several different types are available and all have advantages and disadvantages. The basic information needed is (1) available net positive suction head, (2) maximum working

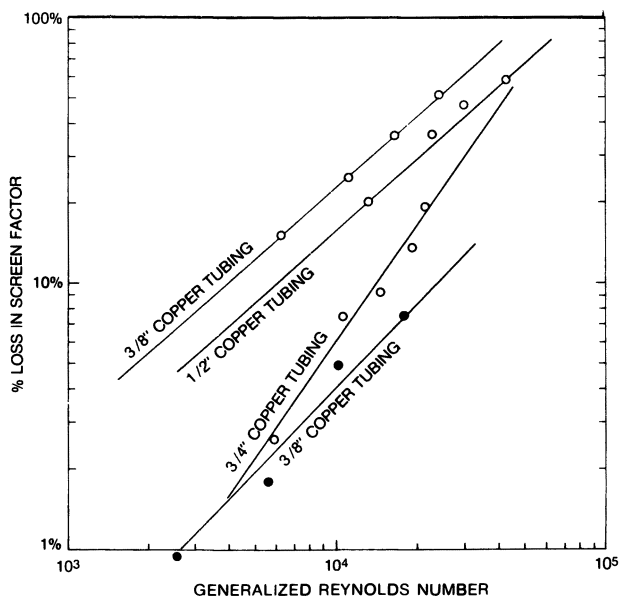


Figure 35. Shear degradation of dilute PHPA flowing through tubing. Key: \circ , 1000 ppm of PHPA, 640 ppm of Ca^{2+} , and 6500 ppm of TDS; and \bullet , 1000 ppm of PHPA, no Ca^{2+} , softened tap H_2O .

temperature and pressure, (3) desired flow rate and pump speed, (4) desired price range, (5) size restrictions, (6) special control requirements, and (7) polymer solution characteristics.

Mechanical degradation is difficult to predict, and often pilot-plant tests are required to obtain this information.

Figures 36 and 37 give results of a typical pilot-plant experiment showing the mechanical degradation in a positive displacement pump—in this case, a screw pump. Polymer was diluted with synthetic reservoir water to approximate field conditions as closely as possible. Pressure, flow rate, and screen factor measurements were taken under varied conditions. Degradation depended on volumetric efficiency and pump speed.

Injection Water and Produced Fluids. Most polymer flood prospects have existing water-treatment facilities on site. For polymer flooding, certain additional features are necessary that were not considered important for waterflooding. Oxygen levels should be kept below 50 ppb, soluble iron should be below 1 ppm and preferably even lower, suspended solids must be minimal, and the oil content should be kept below 100 ppm. In some cases, facilities have to be upgraded or modified to meet these specifications.

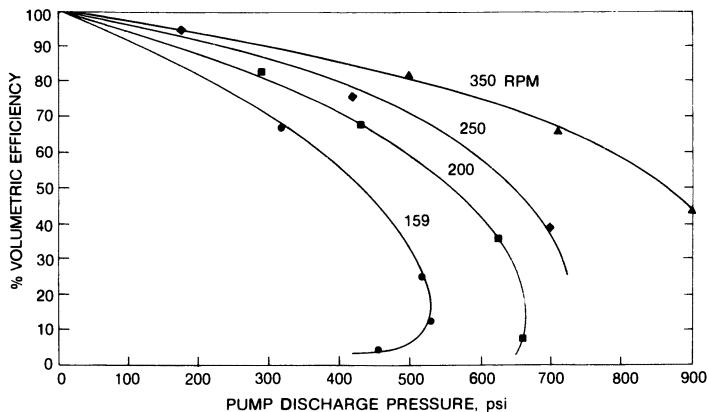


Figure 36. Polymer pump test of volumetric efficiency versus pump discharge pressure.

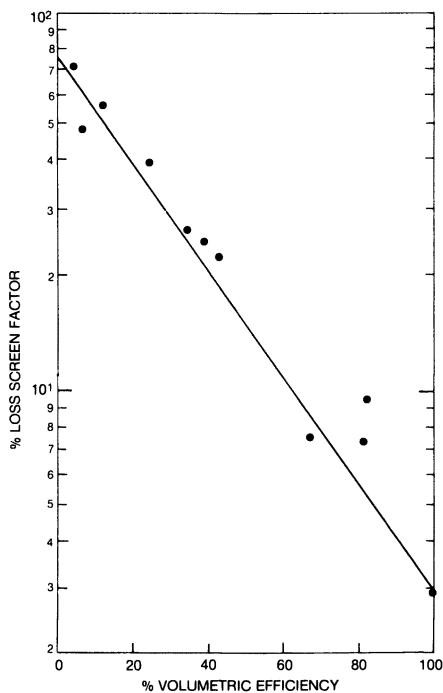


Figure 37. Polymer pump test of shear degradation as a function of volumetric efficiency.

Produced fluid treatment also has to be upgraded for polymer floods. Polymer in produced fluids may interfere with separation facilities, and problems with oil-water separation can begin after polymer breakthrough at the producing wells. An increase in the production of fines may also occur after breakthrough. Treatment of the resulting oil-water suspension is an art, and the experience of established oil field chemical companies helps in solving the problem. Many field tests are often required before a workable solution is obtained.

Environment. PHPA, per se, is a relatively nonhazardous chemical (26). Aqueous solutions of PHPA show very low oral and topical toxicities (27). On the other hand, acrylamide (monomer), a common contaminant in PHPA, is a neurotoxin and should be considered a serious cumulative toxin (26). For this reason, it is essential the level of residual monomer in PHPA must be monitored to avoid potential problems. The high toxicity of acrylamide is somewhat negated by its rapid degradation by soil bacteria.

Literature Cited

1. Shah, D. O.; Schechter, R. S. *Improved Oil Recovery by Surfactant and Polymer Flooding*; Academic Press: New York, 1977.
2. Chang, H. L. *J. Pet. Technol.* **1978**, *30*, 1113.
3. Pye, D. J. *J. Pet. Technol.* **1964**, *16*, 911.
4. Oosawa, F. *Polyelectrolytes*; Marcel Dekker: New York, 1971.
5. McKennon, K. R. U.S. Patent No. 3 039 529, 1962.
6. Herzig, J. P.; LeClerc, D. M.; LeGoff, P. In *Flow Through Porous Media*; Nunge, R. J., Ed.; American Chemical Society: Washington, DC, 1970; p 129.
7. Argabright, P. A.; Rhudy, J. S.; Phillips, B. L. "Partially Hydrolyzed Polyacrylamides with Superior Flooding and Injection Properties"; Presented at the 57th Annual Fall Society of Plastics Engineers Meeting, New Orleans, LA, 1982; Paper SPE 11208.
8. Argabright, P. A.; Phillips, B. L.; Rhudy, J. S.; Bauer, W. R. "Characterization and Performance of Some Partially Hydrolyzed Polyacrylamides"; Presented at the Division of Polymer Chemistry, Inc., National American Chemical Society Meeting in Las Vegas, NV, 1982.
9. Szabo, M. T. *J. Pet. Technol.* **1979**, *31*, 553.
10. Seright, R. S.; Maerker, J. M. "Mechanical Degradation of Polyacrylamides Induced by Flow Through Porous Media"; presented at the Division of Polymer Chemistry, Inc. Symposium on "Polymers in Enhanced Oil Recovery" at the American Chemical Society Meeting in New York, NY, 1981.
11. Chatzis, I.; Morrow, N. R. "Correlation of Capillary Number Relationships for Sandstones"; Presented at 56th Annual Fall Society of Plastics Engineers Meeting, San Antonio, TX, 1981; Paper SPE 10114.
12. Stosur, J. J.; Taber, J. J. *J. Pet. Technol.* **1976**, *28*, 865.
13. Lee, J. *Well Testing*; SPE Textbook Series; Society of Petroleum Engineers of the American Institute of Mining, Metallurgical and Petroleum Engineers, New York, NY, 1982.
14. Earlougher, R. C., Jr. *Advances in Well Test Analysis*; Monograph No. 5; Society of Petroleum Engineers of the American Institute of Mining, Metallurgical and Petroleum Engineers: New York, NY, 1977.

15. Matthews, C. S.; Russell, D. G. *Pressure Buildup and Flow Tests in Wells*; Monograph Series; Society of Petroleum Engineers of the American Institute of Mining, Metallurgical and Petroleum Engineers: Dallas, TX, 1967.
16. Lund, O.; Ikoku, C. U. *Soc. Pet. Eng. J.* **1981**, *21*, 277.
17. Odeh, A. S.; Young, H. T. *Soc. Pet. Eng. J.* **1979**, *19*, 155.
18. Ramey, H. J.; Ikoku, C. U. *Soc. Pet. Eng. J.* **1979**, *19*, 164.
19. Aziz, K. In *Computer Modeling of EOR Processes*; 3rd European Enhanced Oil Recovery Symposium, Developments in Petroleum Science No. 13, Elsevier: New York, NY, 1981; p 367.
20. Camilleri, D.; Fil, A.; Pope, G. A.; Sepehrnoori, K. "Comparison of an Improved Compositional Micellar/Polymer Simulator with Laboratory Core Floods"; Paper SPE 12083 presented at 58th Annual Fall Society of Petroleum Engineers Meeting, San Francisco, CA, 1983.
21. Milton, H. W.; Argabright, P. A. "EOR Prospect Evaluation Using Field Manufactured Polymer"; Presented at the 1983 California Meeting, Ventura, CA, 1983; Paper SPE 11720.
22. Jennings, R. R.; Rogers, J. H.; West, T. J. *J. Pet. Technol.* **1971**, *23*, 391.
23. Maerker, J. M. *Soc. Pet. Eng. J.* **1975**, *15*, 311.
24. Seright, R. S. *Soc. Pet. Eng. J.* **1983**, *23*, 475.
25. Skelland, A. H. P. In *Non-Newtonian Flow and Heat Transfer*; Wiley: New York, NY, 1967; p 109.
26. *Kirk-Othmer Encyclopedia of Chemical Technology*; Wiley: New York, NY, 1978; Vol. 1, p 312.
27. McCollister, D. D.; Hake, C. L.; Sadek, S. E.; Rowe, V. K. *Toxicol. Appl. Pharmacol.* **1965**, *7*, 639.

RECEIVED for review September 9, 1984. ACCEPTED August 8, 1985.

Surface Viscoelasticity and Foam Stability of Waterborne Polymers and Coatings

Richard R. Eley, Richard A. Zander, and Mark E. Koehler

Glidden Coatings and Resins Division, Division of SCM Corporation,
Strongsville, OH 44136

The dilational surface rheology of two series of waterborne, acid-functional, amine-neutralized, model polymer systems and commercial coatings of similar composition was studied. Within each series, the real part of the complex surface dilational modulus (derived from a dynamic surface tension experiment) was found to correlate better to foam stability than the complex modulus itself, the imaginary part (surface dilational viscosity), the bulk fluid shear viscosity, or the equilibrium surface tension. A novel instrument for measuring the dilational surface viscoelastic properties of aqueous polymer systems is also described. Fast Fourier transform analysis was used to remove noise from the data and obtain the amplitude and phase relationships of stress and strain signals.

THE PROPERTIES OF SURFACE VISCOELASTICITY and foam stability of waterborne polymer systems and commercial coatings were studied, and the correlation between them was determined. This chapter also describes a novel instrument that measures the dilational surface viscoelastic properties of aqueous polymer systems (1) and uses fast Fourier transform analysis to obtain relationships of stress and strain.

Static and Dynamic Surface Tension

In any liquid of at least two components, the composition of the liquid-air interface may be different from the bulk, or subphase, composition. That is, a partitioning of the components may occur such that the surface layer is enriched in the minor component for thermodynamic reasons; namely, the free energy of the system is minimized by the partitioning. If the concentration of a component is greater at the interface than in the bulk solution, the component has a positive "surface excess"

0065-2393/86/0213-0315\$06.00/0
© 1986 American Chemical Society

and is said to be surface active. The surface tension (identical with the surface free energy per unit area for a liquid in equilibrium with its vapor) of the mixture will be lowered, relative to that of the pure major component, by the presence of the surface-active component. When the subphase and interphase concentrations of all components are at equilibrium, the static, or equilibrium, surface tension will be measured.

An increase in the surface area of a liquid will create new surface from bulk liquid. The equilibrium concentration of surface-active components (surfactant) is lower in the subphase liquid than in the surface layer, by definition. Therefore, the conversion of bulk liquid to surface will reduce the surface concentration of the surfactant; this reduction raises the surface tension. If the surface is compressed from equilibrium, the surface excess of surfactant will be increased, and the surface tension will drop. The system, displaced from equilibrium, then relaxes at a rate dependent on the relaxation processes available to the system. Mechanisms of relaxation include adsorption-desorption interchange with the subphase and molecular relaxation within the surface layer. The dependence of surface tension on fluctuations in surface area is called the dynamic surface tension.

Dynamic Surface Tension and Coatings

Surface tension is quite universal in its influence on coatings, particularly for water-based systems, and can either drive or inhibit coatings processes. Therefore, whether and to what degree surface tension may vary during a given process are important to know. Although this chapter will be concerned only with dynamic surface tension, coatings performance may also be affected by surface tension gradients that arise from causes other than surface area variation, such as solvent evaporation (2) and surface contamination or inhomogeneities (3).

Bierwagen (3) and also Kornum and Raaschou-Nielsen (4) reviewed the role of both static and dynamic surface tension in controlling coatings defects. Smith (5) recently described the general relationship of dynamic surface tension to coatings application properties and reported on experimental measurements of the dynamic surface tension of coatings-like systems. Surface or interfacial tension is a factor in the dispersion of pigments and the atomization of liquids and a driving force for droplet coalescence and leveling. Cratering, foam stability, substrate wetting, and curtain stability likewise are phenomena that are dependent on static or dynamic surface tension (2-9).

An applied coating will have a high surface-to-volume ratio, by definition. A coating must be converted from a liquid in bulk to a thin liquid film, by means of some application process. Upon application, the surface area will increase by a very large factor, at a high rate. (The

surface area of a cubic decimeter of bulk liquid increases by a factor of about 3,000,000 when converted to 20- μm liquid drops and then decreases by a factor of 750 when deposited as a 1-mil film.) As a consequence, the surface tension may vary dramatically, as a function of both the rate and degree of surface expansion. The properties of the coating will be governed not by the equilibrium surface tension, but by the dependence of the surface tension on the change of surface area of the material. The effectiveness of a surfactant in a coating may not necessarily be in its ability to lower surface tension from the pure-liquid value (equilibrium effects) but rather may be in the degree to which the surface tension deviates from its equilibrium value upon surface deformation (dynamic effects) and its rate of recovery. Therefore, understanding and control of coatings application may require a knowledge of the dynamic effects of application processes on the surface or interfacial tension. Surfactants that produce strong dependence of surface tension on surface area should generally be avoided (5).

Foam Stability

Foam is thermodynamically unstable but can be stabilized in a kinetic sense by the operation of two factors: (a) hydrodynamic factor and (b) film strength factor (10, 11). The hydrodynamic factor influences the rate of drainage of liquid out of the foam-film lamellae from the dual causes of gravity and the capillary suction of fluid into the Plateau borders (Figure 1). The hydrodynamic flow within the lamellae is controlled by the rheology of the bulk fluid and the geometry of the foam and also has consequences for the flow properties of foam in a bulk sense (12), as well as for the microscopic flow involved in film drainage. The film strength factor is determined by the interfacial viscoelastic properties in dilation and imparts to the foam lamella a self-healing ability; this ability makes the foam lamella robust with respect to disturbances.

Film rupture occurs via drainage of intralamellar liquid so that thinning of the lamellae proceeds to a critical thickness (less than 1000 Å), whereupon surface instabilities (waves due to thermal motion), enhanced by van der Waals forces, cause final rupture (13, 14). High viscosity or rigidity of the surface film of the foam lamella significantly retards film drainage and thus influences foam stability via the hydrodynamic factor (14). The presence of a rigid surface film or gel results in very stable foams. An example of foam of this type is beer foam, where a surface gel layer of denatured protein is involved (7, 15).

In the concept of interfacial dilational elasticity (Plateau-Marangoni-Gibbs effect) (16), the surface film elasticity does not arise from any consideration of microscopic network structure or molecular entanglement (i.e., rubberlike elasticity). Elasticity refers instead to a restorative

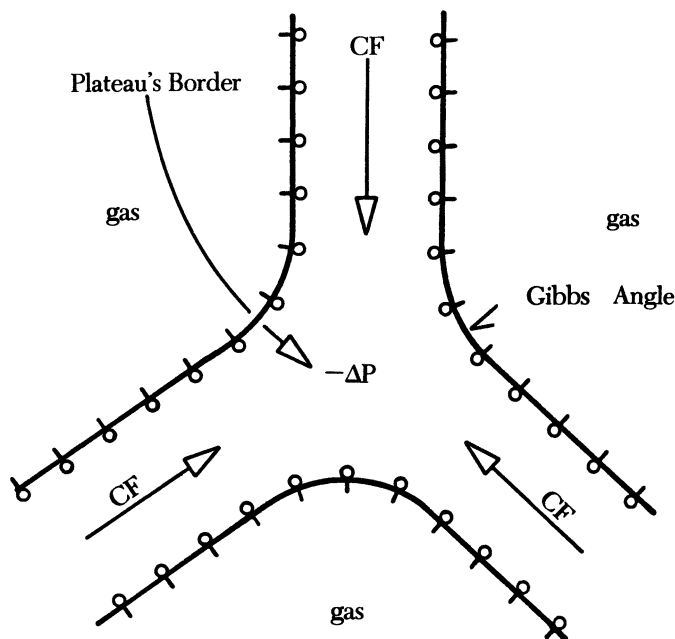


Figure 1. Schematic diagram of the intersection of foam lamellae to form a Plateau border. The fluid flow is indicated by arrows. CF is capillary-driven flow.

flow induced by surface tension gradients arising out of local deformation of films due to spontaneous thinning (6). In fact, a redundancy of effects could occur, because film healing could be achieved by the action of capillary forces alone. Local thinning of a plane film necessarily involves a bending of the surface, and the resulting capillary forces would tend to restore the uniformity of the film (13).

An unequivocal dilational elasticity effect may be described, however (though surface shear viscosity or plasticity may play a dominant role, if present). A mechanism of self-healing is illustrated in Figures 1 and 2 (14, 17). Foam lamellae intersect at angles (Gibbs angle) of 120° at mechanical equilibrium (15). The intersections of foam lamellae are known as Plateau borders (Figure 1). Initially, the foam film is thinned by drainage of liquid into the Plateau borders. This drainage occurs because the pressure within the Plateau borders will be less than in the lamellae due to the curvature of the bounding liquid surface. The sum of surface tension vectors in the curved region produces a net outward thrust or capillary force; this thrust causes the surface to behave as a stretched membrane. Liquid is drawn into the Plateau borders via the resulting pressure gradient. The flow of liquid into the Plateau

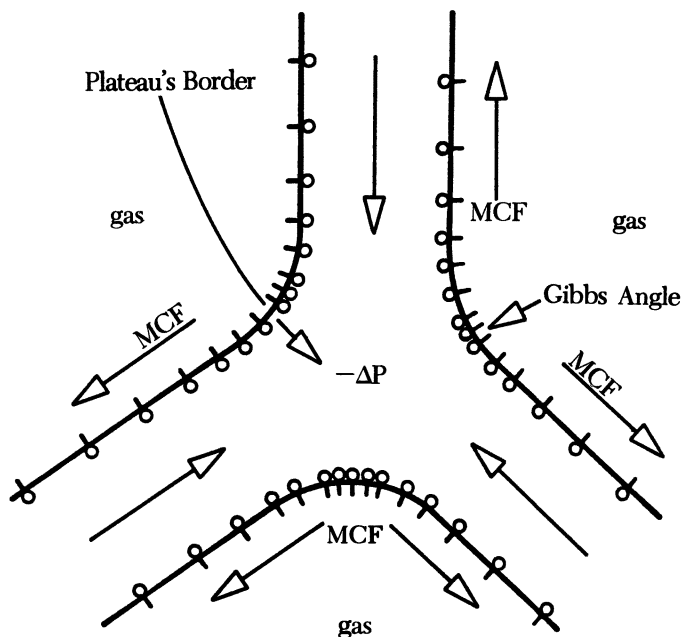


Figure 2. Figure 1 after sweeping of surfactant into Plateau borders by capillary flow. MCF is the surface-tension gradient-driven Marangoni counterflow.

borders also sweeps along surfactant molecules, however. A surface tension gradient is created so that the foam film now acts as a stretched membrane, and a Marangoni counterflow occurs in the surface layer; this counterflow drags subsurface liquid with it and thus restores the thickness of the foam lamella (17) (Figure 2). Thus, high dilational elasticity should correspond to more stable foams.

Experimental Section

Materials. This study consisted of two sample sets representing coatings systems, based on two generically different resin types. Both sets were dispersions of amine-neutralized, acid-functional, polymer resins in a water-glycol ether-alcohol cosolvent blend. Set 1 contained an epoxy-acrylic graft copolymer, and set 2 was based on a commercial acrylic resin having an acid number of 90. Antifoam additives were present in some samples. Set 1 was a visually incompatible but stable dispersion, and set 2 was relatively homogeneous. Composition variations within the sample sets were reasonably broad; these variations roughly approximated the span of practical coatings formulations.

Wilhelmy Plate Method. The surface tension of liquids is ordinarily measured by equilibrium methods, such as the du Nouy ring, capillary rise, or drop volume methods. These methods are generally unsatisfactory for polymer solu-

tions or where surface aging effects may occur (18). The Wilhelmy plate method, however, provides an accurate and convenient method of surface tension measurement for such materials (19).

In the Wilhelmy plate method, a platinum plate or glass slide (roughened to minimize the contact angle) is suspended in a liquid, minimally immersed. Capillary forces due to the curvature of the meniscus act on the plate to produce a net downward force, or apparent increase in weight, proportional to surface tension. The surface tension and weight increase (expressed as a force, F) are related by

$$F = p\gamma \cos \theta \quad (1)$$

where p is the length of the perimeter of the plate in contact with the liquid and θ is the angle made by the liquid in contact with the plate. Assuming the contact angle is zero, the surface tension, γ , is given by

$$\gamma = F/p \quad (2)$$

Instrument Design and Data Analysis. The apparatus most often used for dynamic surface tension measurements by the Wilhelmy plate method is the Langmuir trough (20), in which vertical plane barriers are positioned in the liquid surface and moved in opposition to each other to create the dilation-compression cycle. This design has acknowledged drawbacks primarily leakage of surface around the barriers and surface wave effects. A novel design was selected from the recent literature (1) that circumvents these problems, while allowing higher frequencies and strain rates to be achieved. Instead of the moving barriers, a porous cylinder (of stainless steel mesh) is used that oscillates vertically through the liquid surface, entraining liquid as it does so and thereby creating new surface. Simulation of coatings processes requires large, high-frequency deformations. In this respect, the instrument chosen for this work represents an improvement over the Langmuir trough method; both strain and strain-rate capabilities exceed those of the Langmuir trough method.

The schematic design of the instrument is shown in Figure 3. A variable-speed gear motor drives a cam wheel. The rotating cam drives a crank shaft, which is translated to vertical motion by a slider, to which is attached the 150-mesh stainless steel cylindrical screen. The vertical travel of the cylinder is measured by a "string-pot" position-sensing transducer. The platinum plate is suspended from a microforce transducer. The outputs of both transducers are recorded on a strip-chart recorder and by a microprocessor interfaced with the instrument. The data are later analyzed by a Fortran program.

Operating frequencies for our experiments ranged from 0.15 to 2.2 rad/s. Surface dilation ratios were from 97% to 190%. Stress-strain Lissajous loops generated from the force-displacement outputs were generally quite symmetrical; this result indicates linear viscoelastic behavior, even for these relatively large strains. Strain rates were computed as a two-dimensional average Hencky strain rate, \dot{H} (equation 3), and varied from 0.018 to 0.38 s⁻¹.

$$\dot{H} = \omega/2\pi \ln (1 + \Delta A/A_0) \quad (3)$$

In equation 3, ω is the angular frequency, A_0 is the initial surface area, and ΔA is the area increment. The data were taken at a strain rate of 0.25 s⁻¹.

The data analysis incorporated a fast Fourier transform algorithm (Scientific Subroutine Program Package for the Digital Equipment Corporation PDP

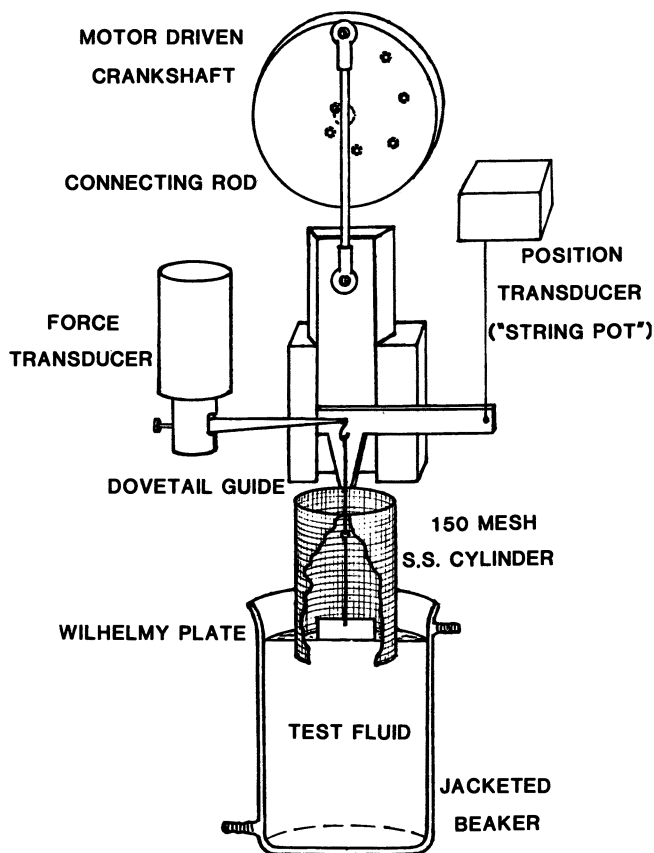


Figure 3. Oscillating cylinder instrument for dynamic surface tension measurement.

11/44). The raw force and displacement data are transformed from the time domain to the frequency domain by the Fourier transform operator. The fundamental (experimental) frequency is then easily chosen by examination of the power spectrum (Figure 4). Noise is edited out by zero-filling all frequencies except the fundamental in both the real and imaginary frequency-domain spectra for the force and displacement.

An inverse Fourier transformation is then performed, to recover the noise-free force and displacement data curves in the time domain. Figure 5 shows a raw force data curve superimposed on noise-free data obtained by Fourier treatment. Figure 6 shows the same for the relatively noiseless displacement data.

Amplitude and phase-shift information are simultaneously obtained for both force and displacement data, by Fourier analysis. The modulus and relative phase shift are calculated, as well as the viscoelastic parameters, from equations 6-10.

Measurement of Foam Stability. Foam stability was evaluated by beating air into a standard volume of liquid with a Brookfield counterrotating mixer. Foam height was followed as a function of time. The area under the foam height-time curve was obtained by numerical integration and was then normalized to the initial foam height, to give an average foam lifetime, according to Bikerman (15). An advantage of this method of treatment is that the entire defoaming curve is taken into account, while the normalization to initial foam volume allows us to take account of foam stability, independent of foaming ability. In the case of set 1, the foams were so unstable that the average foam lifetime could not be computed, so the foam height at 3.5 min was used to correlate the data.

Surface Viscoelasticity. The three-dimensional analogue of the surface dilational modulus is the bulk modulus, K , which describes the change in pres-

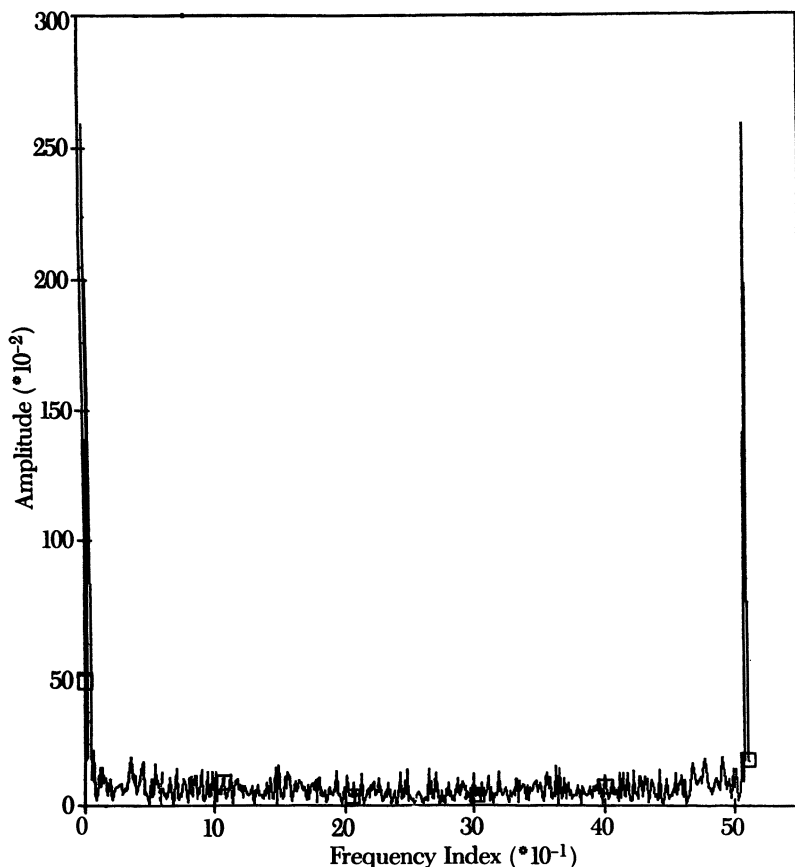


Figure 4. Power spectrum in the frequency domain from forward Fourier transformation.

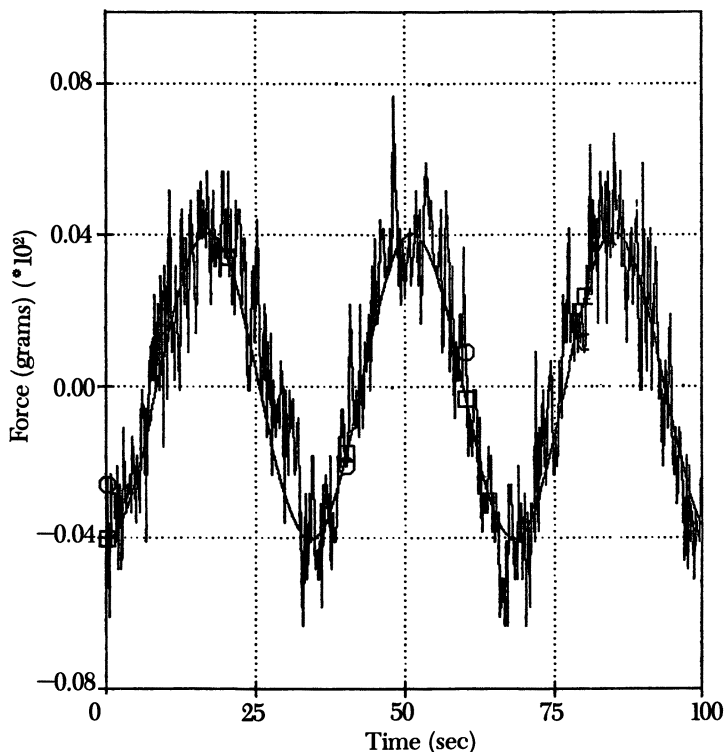


Figure 5. Superimposed raw and noise-free force vs. time data. Key: \square , force vs. time (fast Fourier transformation); \circ , raw data.

sure, P , for a relative change in volume, V , upon isotropic compression of a fluid. K is defined as

$$K = dP/d(\ln V) \quad (4)$$

Polymers often display a time-dependent response to compression; this response indicates that K is a complex modulus, describing a viscoelastic response to isotropic compression-dilation (21)

$$K^* = K' + iK'' \quad (5)$$

where K' and K'' are the compressional storage and loss moduli, respectively (21).

In most dynamic surface tension experiments, variation in surface area is caused mechanically by some means, and the resulting variation in surface tension is measured. The principal quantity derived from the experiment is the surface dilational modulus, ϵ , given by

$$\epsilon = \Delta\gamma/(\Delta A/A) \approx d\gamma/d(\ln A) \quad (6)$$

The analogy to equation 4 (in two dimensions) is obvious. As stated above, dilation or compression of a surface results in a displacement of surface tension from its equilibrium value, followed by a time-dependent relaxation toward equilibrium. Any relaxation process occurring during surface deformation will result in a phase difference between the strain (area change) and the resulting stress (surface tension change). The dilational modulus (equation 6) is actually a complex modulus, therefore, containing both real (energy storage) and imaginary (energy loss) components. Complex moduli are most conveniently defined in the frequency domain, because the magnitude of the measured stress is dependent on both the deformation rate and history (22). Hence, by analogy to equation 5 and linear viscoelasticity (21)

$$\epsilon^*(i\omega) = \epsilon'(\omega) + i\epsilon''(\omega) = |\epsilon^*| \exp(i\delta) \quad (7)$$

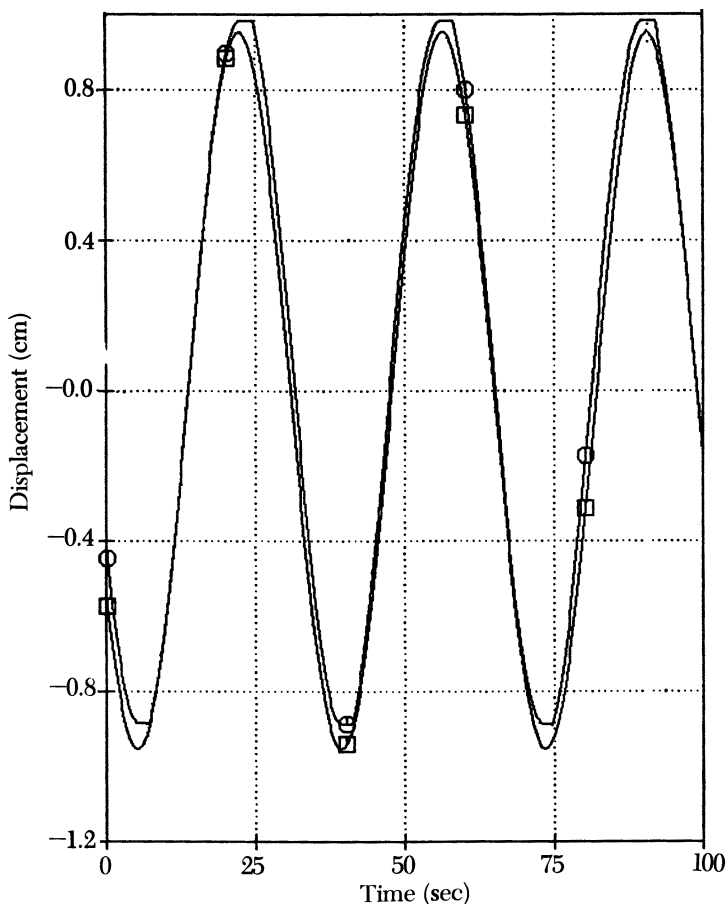


Figure 6. Superimposed raw and noise-free displacement vs. time data. Key: □, displacement vs. time (fast Fourier transformation); ○, raw data.

where δ is the phase angle (viscous loss angle) between the maximum strain (ΔA) and maximum stress ($\Delta\gamma$) and ω is the angular frequency of sinusoidal oscillation of the surface area. Equation 7 can be expanded to

$$\epsilon^* = |\epsilon^*| \cos \delta + i |\epsilon^*| \sin \delta \quad (8)$$

So

$$\epsilon' = |\epsilon^*| \cos \delta \quad \epsilon'' = |\epsilon^*| \sin \delta \quad (9)$$

ϵ' is the dilational storage modulus (modulus of elasticity) (dyn/cm), and ϵ'' is the dilational loss modulus. Again, by analogy to linear viscoelastic relationships, the dynamic surface dilational viscosity, κ' (g/s), is obtained by dividing the loss factor by the angular frequency.

$$\kappa' = (|\epsilon^*| \sin \delta) / \omega \quad (10)$$

Several authors (11, 22–24) have discussed the viscoelastic nature of the surface dilational modulus, but in general, only the complex modulus itself is considered, rather than the separated real and imaginary components. In this work, in view of the fact that the postulated mechanisms of foam stabilization involve primarily surface elastic effects rather than viscous effects, a correlation of foam stability to the real part of the complex dilational modulus was attempted.

Results and Discussion

Plateau–Marangoni–Gibbs elasticity (16) is generally accepted as providing an important mechanism of foam stability, at least in the absence of significant surface shear viscosity or plasticity due to surface gelation (7). Experimental confirmation of this is somewhat meager, however, especially for actual coatings systems. Malysa et al. (25) found a linear relationship between the surface dilational modulus and the frothability, or gas retention of dynamically foamed solutions of 1-octanol and 1-octanoic acid. In this work, the surface dilational viscoelastic properties and foam stability data for two series of coatings systems are reported. Both were based on acid-functional, amine-neutralized, polymer resins dispersed in a water–cosolvent blend. One series was a primarily heterophase system (set 1), and the other was relatively more homogeneous (set 2). The foam stability of these coatings was measured and plotted against the surface rheological parameters.

The foam in the first sample set was of relatively low stability, or evanescent foam, being dissipated in several minutes, for most of the samples. This result implies that for these materials, surface shear viscosity is negligible. Such systems can be a source of difficulty nevertheless if foam is generated rapidly enough in an industrial process. The coatings of set 1 differed compositionally in relatively minor ways, yet some of the coatings showed foaming problems in process and some did not.

Because the postulated mechanisms of Marangoni stabilization of foams involve primarily elastic rather than viscous effects, a correlation of foam stability to the real part of the complex surface dilational modulus, the surface dilational elasticity was attempted. Thus, in this work, the complex surface dilational modulus was resolved into the dilational elasticity and the dilational viscosity and these parameters were plotted, together with the complex modulus, against the measured foam stability. Figures 7, 8, and 9 show the correlation of the complex surface dilational modulus, the surface dilational viscosity, and the surface dilational elasticity, respectively, to foam height at an arbitrary time after agitation for set 1. The dilational modulus of elasticity correlates best with foam stability. The correlation is significant at greater than the 95% confidence level. Furthermore, the trend in bulk shear viscosity of this set was opposite to the foam stability trend (Figure 10); this result indicates that, over the practical composition range studied, the surface elasticity dominates subphase viscosity effects and is the controlling physical property in the foaming of this material.

A study comprising a larger number of samples formulated over a wider composition range, including some with antifoam additives, is represented in set 2. In addition to the three dilational viscoelastic parameters, the equilibrium surface tension and bulk shear viscosity were compared to the foam lifetime (Figures 11 and 12). Comparison of Figures 11-15 show, again, the surface dilational modulus of elasticity is the parameter that best correlates with foam stability, with better than 99.9% confidence. (The data in Figures 11-15 exclude a high-viscosity

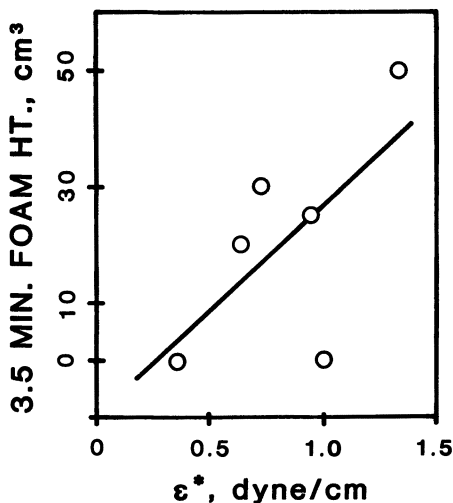


Figure 7. Complex dilational surface modulus vs. foam height after 3.5 min for sample set 1. Correlation coefficient = 0.649.

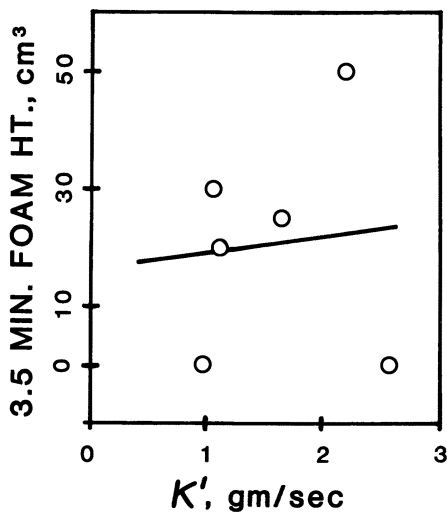


Figure 8. Surface dilational viscosity vs. foam height after 3.5 min for sample set 1. Correlation coefficient = 0.096.

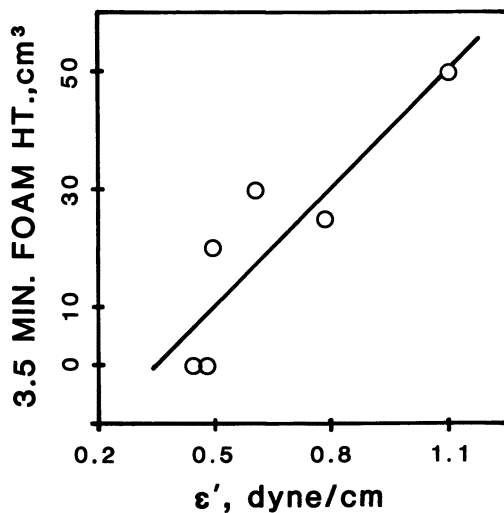


Figure 9. Surface dilational elastic modulus vs. foam height after 3.5 min for sample set 1. Correlation coefficient = 0.884.

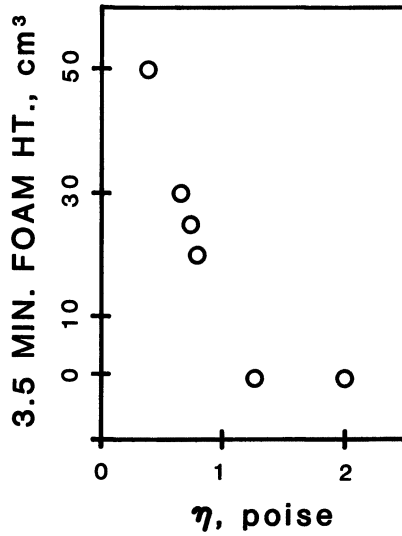


Figure 10. Shear viscosity of bulk fluid (shear rate = 37.5 s^{-1}) vs. foam height after 3.5 min for sample set 1.

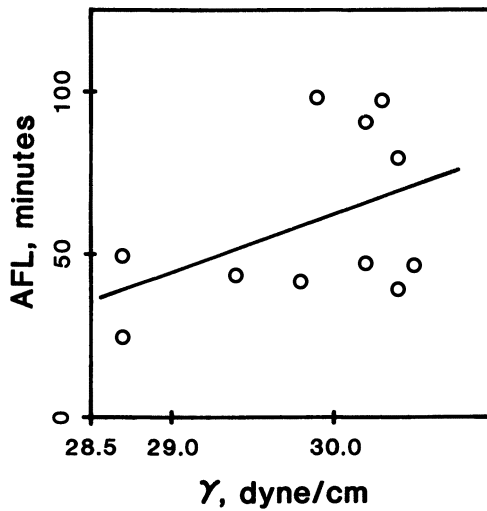


Figure 11. Equilibrium surface tension vs. average foam lifetime for sample set 2. Correlation coefficient = 0.443.

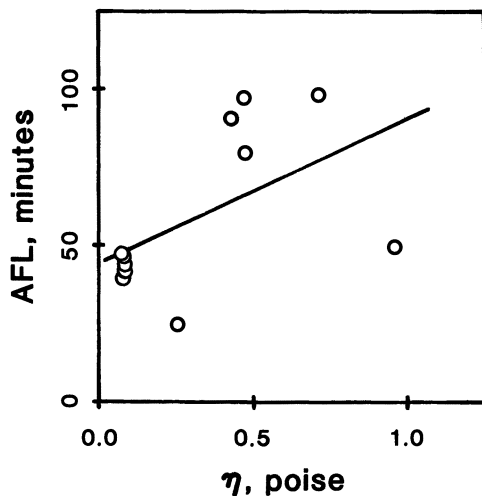


Figure 12. Bulk liquid Newtonian shear viscosity vs. average foam lifetime for sample set 2. Correlation coefficient = 0.533.

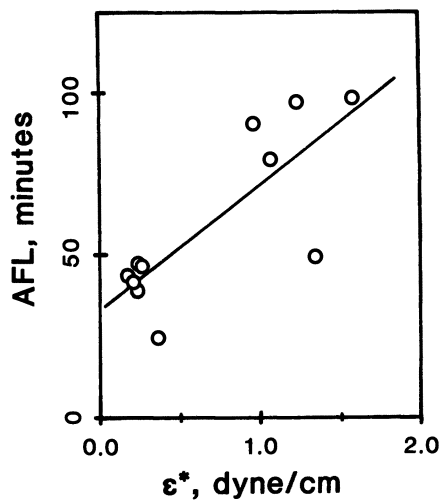


Figure 13. Complex dilational surface modulus vs. average foam lifetime for sample set 2. Correlation coefficient = 0.795.

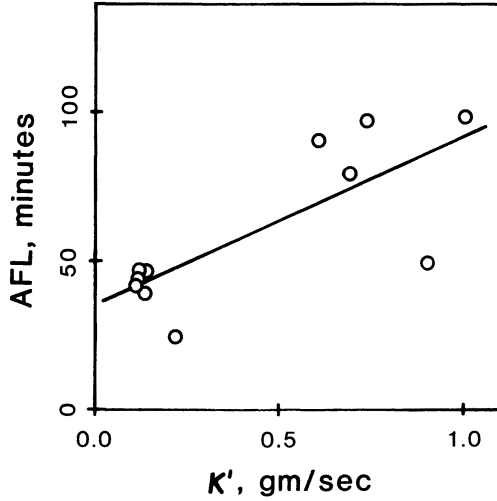


Figure 14. Surface dilational viscosity vs. average foam lifetime for sample set 2. Correlation coefficient = 0.765.

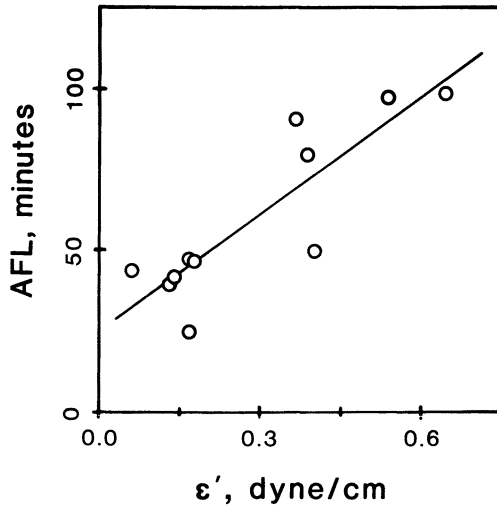


Figure 15. Surface dilational elastic modulus vs. average foam lifetime for sample set 2. Correlation coefficient = 0.866.

sample that was an outlier on all plots. If that point is included, the correlations are indistinguishable.)

For the compatible system (set 2), foam was more persistent; several hours were required for foam collapse, in some cases. Surface shear viscosity was measured for several of these, and none showed any significant non-Newtonian surface character. We speculate that the lower stability of foam in set 1 is due to lower surface shear viscosity, or possibly conjugate defoamer effects in this heterophase system (26).*

Comparison of Figures 14 and 15 (also Figures 8 and 9) reveals that the dilational viscosity is generally significantly greater than the dilational elasticity, for both sample sets studied. Furthermore, the phase angles for many members of sets 1 and 2 ranged frequently higher than 45°, in some cases up to 80°. Such behavior indicates that relaxation via micellar breakdown in the bulk phase is occurring (27). Conceivably, the micelles themselves may be surface active and are playing a role in monolayer relaxation processes.

Conclusions

Over a range of composition corresponding to practical coatings formulations, the dilational surface elastic modulus (storage modulus) correlates better to foam stability than the complex dilational modulus, the dilational surface viscosity, the bulk shear viscosity, or the equilibrium surface tension. The surface rheological parameters as a group showed significantly better correlation to foaming than bulk shear viscosity or equilibrium surface tension. Therefore, for the waterborne coatings systems studied, surface dynamic effects are more important for the stability of foams than equilibrium or bulk effects.

In the study of the influence of surface dilational rheology on foam behavior, the dilational modulus should be treated as a viscoelastic material function. The phase angle should be accurately measured, so that the complex modulus may be resolved into storage and loss moduli, for improved correlations to foam stability. The oscillating cylinder device for dynamic surface tension measurement provides a relatively straightforward and advantageous method for the study of the surface viscoelasticity of waterborne polymer systems.

Acknowledgment

We are grateful to Pamela Kuschnir for the preparation of sample set 2.

Literature Cited

1. Boyle, J.; Mautone, A. J. *Colloid Surf.* **1982**, *4*, 77.
2. Overdiep, W. S., In *Physicochemical Hydrodynamics*; Spalding, D. B., Ed.; Advance Publications: London, 1977; Vol. II.

*P. Kuschnir, R. R. Eley, and F. L. Floyd, unpublished results.

3. Bierwagen, G. P. *Prog. Org. Coat.* **1975**, *3*, 101.
4. Kornum, L. O.; Raaschou-Nielsen, H. K. *Prog. Org. Coat.* **1980**, *8*, 275.
5. Smith, R. E. *Ind. Eng. Chem. Prod. Res. Dev.* **1983**, *22*, 67.
6. Rosen, M. J. *Surfactants and Interfacial Phenomena*; Wiley-Interscience: New York, NY, 1978.
7. Priestmann, K. M. *J. Oil Colour Chem. Assoc.* **1982**, *65*, 21.
8. Hiram, Y.; Nir, A. *J. Colloid Interface Sci.* **1983**, *95*(2), 462.
9. Parfitt, G. D. *Dispersion of Powders in Liquids*; Applied Science: London, 1981; 3rd ed.
10. Gibbs, J. W. *The Scientific Papers of J. Willard Gibbs*; Dover Publications: New York, NY, 1906; Vol. I.
11. Djabbarah, N. F. Ph.D. Thesis, Illinois Institute of Technology, Chicago, 1978.
12. Kraynik, A. M.; Hansen, M. G. *Foam Rheology: "The Role of Viscous and Capillary Forces at Large Strains"* 56th Annual Meeting, Society of Rheology, Feb. 25-27, 1985, Blacksburg, VA.
13. Sheludko, A. *Colloid Chemistry*; Elsevier: New York, 1966.
14. Clunie, J. S.; Goodman, J. F.; Ingram, B. T. In *Surface and Colloid Science*; Matijevic, E., Ed.; Wiley-Interscience: New York, 1971; Vol. 3, p. 204.
15. Bikerman, J. *Foams*; Springer-Verlag: New York, 1973.
16. Scriven, L. E.; Sternling, C. V. *Nature (London)* **1960**, *187*, 186.
17. Ross, S.; Townsend, D. F. private communication, 1984.
18. Jaycock, M. J.; Parfitt, G. D. *Chemistry of Interfaces*; Ellis Horwood: Chichester, 1981.
19. Adamson, A. W. *Physical Chemistry of Surfaces*; Wiley-Interscience: New York, NY, 1982; 4th ed., pp. 24ff.
20. Clements, J. A.; Brown, E. S.; Johnson, R. P. *J. Appl. Physiol.* **1958**, *12*, 262.
21. Ferry, J. D. *Viscoelastic Properties of Polymers*; Wiley-Interscience: New York, 1970; 2nd ed.
22. Loglio, G.; Rillaerts, E.; Joos, P. *Colloid Polym. Sci.* **1981**, *259*, 1221.
23. Lucassen, J.; Giles, D. *J. Chem. Soc. Faraday Trans.* **1975**, *71*, 217.
24. Callaghan, I. C.; Gould, C. M.; Hamilton, R. J.; Neustadter, E. L. *Colloid Surf.* **1983**, *8*, 17.
25. Malysa, K.; Lunkenheimer, K.; Miller, R.; Hartenstein, C. *Colloid Surf.* **1981**, *3*, 329.
26. Ross, S.; Townsend, D. F. *Chem. Eng. Commun.* **1981**, *11*, 347.
27. Lucassen-Reynders, E. H., In *Anionic Surfactants—Physical Chemistry of Surfactant Action*; Surfactant Science Series, Vol. 11; Lucassen-Reynders, E. H., Ed.; Dekker: New York, 1981; Chapter 5.

RECEIVED for review February 8, 1985. ACCEPTED November 22, 1985.

Influence of Cellulose Ethers on Coatings Performance

S. G. Croll and R. L. Kleinlein

Sherwin-Williams Research Center, Chicago, IL 60628

The use of cellulose ethers as thickeners in paint and the consequences of that use for the other aspects of paint performance are reviewed in this chapter. Although cellulose ethers are modified in various ways during production to achieve certain performance, the use of any one cellulosic thickener or combination of thickeners is still a compromise. Their primary function is to thicken water-based paints and provide application characteristics similar to those of oil-based paints. Both the quantity of cellulosic thickener and its molecular weight influence rheological properties of paint. Problems encountered when cellulose ethers are used include roller spatter, imperfect flow and leveling, flocculation of latex or pigment, and water sensitivity of the resultant coating. However, a balanced formulation with the proper thickener choice can reduce these problems.

CELLULOSE ETHERS WERE INTRODUCED after World War II as more efficient alternatives to casein, polysaccharides, and other naturally occurring water-soluble macromolecules that were used to thicken early latex paints. As is the case even now, the requirement was to provide latex paints with the same good rheological properties as oil-based paints (1). Although many other types of thickeners have been developed as potential replacements, cellulose ethers continue to be the most common type of thickener for many latex paints. Despite their imperfect rheological properties, cellulose ethers have many practical advantages for coatings use. Their ability to be used in a broad range of products and their compatibility with a wide range of coatings raw materials make them a common ingredient in many paint formulas.

Quantitative results in this chapter come from work done with a range of (hydroxyethyl)cellulose (HEC) thickeners.

0065-2393/86/0213-0333\$06.00/0
© 1986 American Chemical Society

Composition

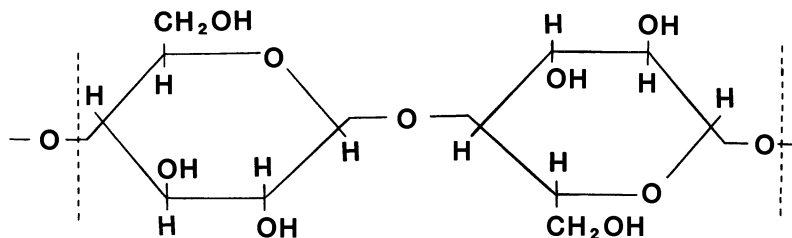
Cellulose ethers are manufactured from naturally formed cellulose (2) containing β -1-4-linked anhydroglucose units (structure I).

Cellulose is the major cell-wall material of all higher and many lower order plants. The cellulose fiber used to produce cellulosic thickeners is generally obtained from either cotton linters or wood pulp. Because wood pulp is the more economical of these two sources, it is the most commonly used. However, cotton linters produce a higher molecular weight cellulose and are often used to make the higher molecular weight grades of thickener. Regardless of how the cellulose is obtained, the next steps are purification and treatment with caustic to eliminate crystallinity. This procedure forms an intermediate alkali cellulose, which is in turn reacted with an etherifying agent to produce the end product of cellulose ether (after neutralization, extraction, drying, and grinding). For better control of the dispersion and hydration time of cellulose ethers, some types are surface-treated.

In the basic anhydroglucose unit structure of cellulose, the ether substituents are typically located at any or all of the three hydroxyl groups. The average number of hydroxyl sites occupied by an ether group is called the degree of substitution (DS). With three available sites, the maximum DS is 3. Because some etherifying groups regenerate additional hydroxyl groups that may also be substituted, an additional term called molar substitution (MS) is also used. MS refers to the moles of substituent group per anhydroglucose unit. Together these two terms describe compositional differences that control the water solubility-gel point of a given thickener, its susceptibility to enzyme attack, and its compatibility with other paint raw materials. For enzyme resistance in particular, higher degrees of substitution (DS values) are desired.

Types of Cellulosic Thickeners Available

Chemistry. The most commonly used cellulose ether at present in the paint industry is HEC, although (carboxymethyl)cellulose (CMC)



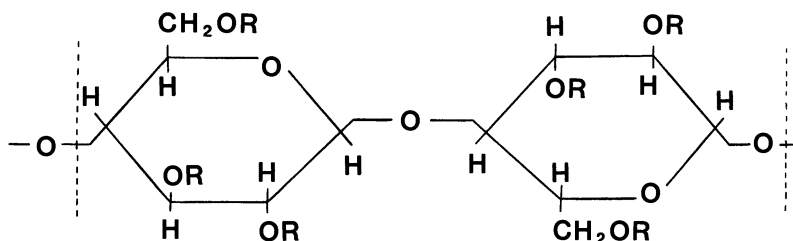
I

and variations of methylcellulose (MC) have found favor in the past and continue to find extensive use. Their general idealized molecular structure is displayed in structure II.

Most of the major cellulose ether types are available in ranges of molecular weight, particle size, surface treatment, and degree of substitution. Differences in molecular weight are readily apparent from aqueous solution viscosities. Viscosities can vary from 5000 cps at 1% solids down to 100–200 cps at 5% solids or higher.

The choices of particle size (fine or granular) and surface treatment (cross-linked or not) are directly related to the ease with which a particular quantity will disperse and solubilize during paint manufacture. Proper dispersion of the thickener particles before they begin to hydrate is extremely important. If proper dispersion is not achieved, gel particles (lumps) will form before the thickener can be adequately dispersed. In turn, these lumps will require extended mixing or other measures (high shear, high temperature, pH adjustment, etc.) before becoming fully solubilized. In addition to the expense and inconvenience, these additional processing requirements are simply not possible for some paint manufacturers. The end result is a waste of thickener, money, and time, because the lumps must be filtered out during the filling process.

Consequently, the choice of particle size and the preference for, or against, surface treatment is usually made on the basis of the addition method being used, the manufacturing equipment available, and the ease of solution required. If manufacturing capabilities are limited, an easier dispersing, slower to solubilize grade will normally be chosen.



R can be H, CH₃ or CH₂CH₂OH

MC: CH₂CHOHCH₃

CMC: CH₂COONa

HEC: CH₂CH₂OCH₂CH₂OH

II

Molecular Weight. Molecular weights referred to in this work are viscosity-average values, M_v . The values were determined by intrinsic viscosity measurements, at 25 °C (± 0.1), according to standard methods. The Mark-Houwink constants were taken as 8.435×10^{-5} and 0.87 (supplied by Hercules, Inc.). Values found for molecular weight ranged from 62,000 to 1,080,000. Viscosity-average molecular weight is usually close to the weight average, although in general it is somewhat lower.

Properties in Paint

Although a number of the performance observations reported here are based on years of direct experience with a variety of different thickeners, the more quantitative results are based on a number of flat and semigloss paints that were made specifically for this study. In this work, different thickener structures (structure II) and wide ranges of molecular weights were studied to identify performance trends.

A general description of the paint formulas used in this study is as follows: (1) Interior flat is made with a vinyl acetate modified acrylic latex [nonvolatile material (NVM) equals 55%; weight per gallon equals 11.72 lb; and pigment volume concentration (PVC) equals 55%]. (2) Interior semigloss was made with an acrylic latex (NVM is 44.5%; weight per gallon is 10.31 lb; and PVC is 19.9%). (3) Exterior semigloss was made with a polyester-modified acrylic latex (NVM is 46.2%; weight per gallon is 10.17 lb; and PVC is 18.7%). Most of the results reported here were obtained with various cellulose ethers in the latex flat formula. The two latex semigloss formulas were prepared in a similar manner to study mainly gloss, adhesion, and flow properties.

Rheology. The fundamental purpose of cellulose ethers in modern paints is that of a thickening agent. As such, cellulose ethers have been the subject of some discussion (3-6). Because HEC is the most widely used type of cellulosic thickener in the paint industry, most of our work was concentrated in this area. Consequently, all subsequent remarks and observations will concern HEC unless otherwise noted.

VISCOSITY AS A FUNCTION OF SHEAR RATE. Viscosity is one of the most important properties of any thickener. Paint properties ranging from in-can storage stability to application characteristics to final film performance and film esthetics are all tied to the choice of thickener and its viscosity characteristics at different shear rates. The relationship between viscosity and shear rate in paints thickened with cellulose ethers, and indeed solutions of cellulose ethers, is shear thinning (and may be thixotropic) (see Figures 1 and 2). Figure 1 shows that in the interior flat formulation the viscosity profiles of paint thickened with low and high molecular weight (62,000 or 715,000) HEC are almost identical with those reported elsewhere (3). The fact that performance differences are known to exist

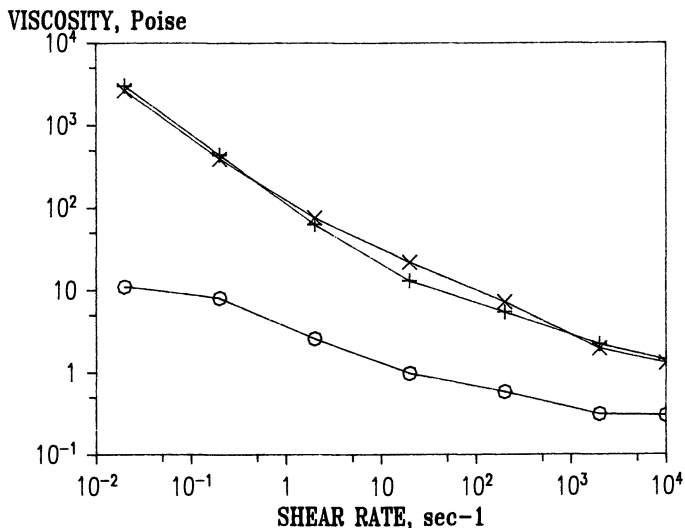


Figure 1. Viscosity profiles of the HEC-thickened paint, including unthickened. Key: ×, M_v 715,000; +, M_v 62,000; and O, unthickened. The equivalent HEC weight in water is 1.2% for M_v 715,000 and 4.1% for M_v 62,000.

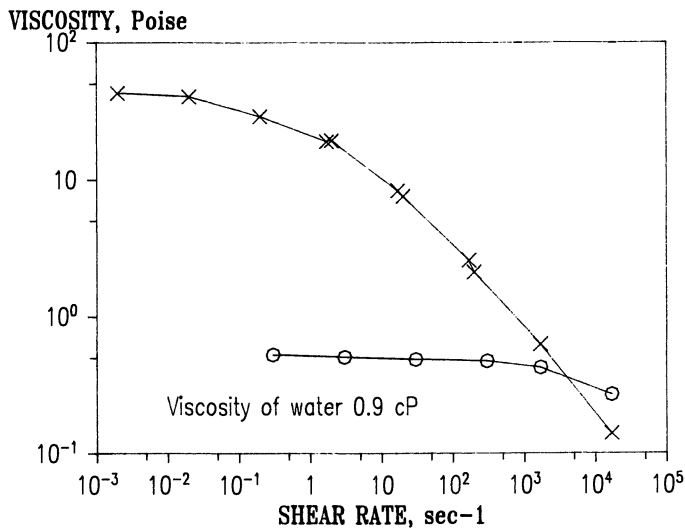


Figure 2. Viscosity profiles of the HEC solutions corresponding to the paints in Figure 3. Key: ×, M_v 715,000; and O, M_v 62,000. The equivalent HEC weight in water is 1.2% for M_v 715,000 and 4.1% for M_v 62,000.

suggests that paint properties are sensitive to small viscosity differences and that properties such as leveling and sag are also influenced by the time-dependent nature of the paint, which this type of graph does not show.

At very low shear rates ($0.01\text{--}0.10\text{ s}^{-1}$), viscosity must be high enough to prevent both in-can settling and sagging after application, yet low enough to provide flow and leveling. At moderately low shear rates ($10\text{--}20\text{ s}^{-1}$), viscosity must be high enough to provide good brush pickup. At high shear rates typical of brushing ($5000\text{--}10,000\text{ s}^{-1}$ or higher), viscosity must be high enough to give good film build, but not so high as to cause excessive brush drag. Generally, paint formulators aim for viscosities of $500\text{--}1000\text{ P}$ at shear rates of $0.06\text{--}0.10\text{ s}^{-1}$, $15\text{--}40\text{ P}$ at shear rates of $10\text{--}20\text{ s}^{-1}$, and $1\text{--}2\text{ P}$ at shear rates of $10,000\text{ s}^{-1}$. The increase in viscosity after brushing has ceased (back to low shear rate values) should also be quick enough to restrict sagging, but slow enough that it permits leveling out of the brush marks. Because many modern paints have very low yield stresses, one often has to rely on this time dependence of viscosity to achieve the proper balance.

THICKENING MECHANISM. The shape of the curves in Figures 1 and 2 shows that the viscosity decreases by several orders of magnitude as the shear rate is increased. That is, some structure in the solution must be broken down by mechanical work. The nature of this structure has been the subject of some study over the years. The high molecular weight thickener (M_r 715,000) produces a greater degree of shear thinning in solution than does the low molecular grade, although paints made with these same thickener concentrations have virtually identical viscosity profiles. Thickener concentrations for both the paints and the aqueous solutions were set by thickening paints to the same Stormer viscosity. Some kind of bridging mechanism for the thickening of latex (or other particulate) systems, wherein adsorptive attachment of a thickener molecule links a number of particles together, with the implication that the linkage is somewhat remote, has been postulated. No direct evidence of this mechanism exists, although the idea seems to be plausible. However, photomicrographs have certainly been published of latex, etc., flocculated in the presence of water-soluble polymers (7). The mechanism of flocculation has been proposed as a volume exclusion effect, which is dealt with in much more detail elsewhere (7, 8). The increase in viscosity in a flocculated system is well-known and arises from the water trapped inside the flocculate not being available to drain into the overall system and provide lubrication. Also, an increase in viscosity results from the shape of the flocculate (9). Nevertheless, no matter what the exact mechanism of this structure building is, undoubtedly flocculation is broken down by mechanical work and reappears naturally when the mechanical input is removed. Another contribution to the

decrease in viscosity at high shear rates may be the tendency for thickener molecules to uncoil and align themselves along the flow field when subject to significant mechanical work.

The high-shear viscosity seems to be proportional to the amount of thickener present and represents the contribution due to the volume fraction of thickener present, even in mixed thickener studies (6). In general, probably molecules of high specific volume are more efficient at high shear rates, although we know of no work directly related to this effect.

If one measures the low-shear viscosity of a polymer in solution as a function of molecular weight, a change in behavior occurs. At a critical value of molecular weight, the slope of a logarithmic plot of viscosity versus molecular weight increases rather quickly. This increase is associated with "entanglements" between the polymer molecules, which increase the viscosity greatly (10, 11). This break in the behavior is generally considered to occur when the polymer length is two to four times the length between entanglements; that is, a few entanglements are needed to produce a significant effect. Generally, in the entangled region the viscosity increases as the molecular weight raised to the power of approximately 3.4. In the low molecular weight end, the slope is unity. These values are typical of monodisperse linear systems. The change from one slope to another is seldom abrupt in practice.

Figure 3 is such a plot gained from a Weissenberg rheogoniometer. The plot shows that HEC, at a concentration of 0.87% (w/w), exhibits this pattern of behavior. The shear rate used was 0.003 s^{-1} . The upper range has a slope of 4.6 (0.3 standard error) and the lower range a slope of 0.8 (± 0.08 standard error). Extrapolation of the two lines produces an intersection at a molecular weight of 266,000 (approximately 985 HEC segments; see Figure 2). Because HEC is not a linear, monodisperse polymer, but a polydisperse branched polymer, this value is in satisfactory agreement with the values of the more ideal systems.

When the high-shear viscosity of the same solutions ($16,890 \text{ s}^{-1}$) is plotted, the molecular weight at which the high-shear and low-shear viscosities coincide (approximately 100,000 at this concentration) can be seen (from Figure 3). This situation is not the same as the molecular weight at the change in slope of the low shear viscosity curve. If one assumes that the two extremes of viscosity coincide when there are no entanglements between molecules in solution, that is, 100,000 is the molecular weight between entanglements, then the factor of 2.7 to arrive at the molecular weight of the break in the low-shear curve is in agreement with theoretical ideas (10, 11). Again, the HEC is not an ideal, monodisperse system. In fact, the slope of the high-shear viscosity on Figure 3 is 0.54 (0.02 standard error), which is not the same as the slope of the low molecular weight, low-shear, logarithmic data.

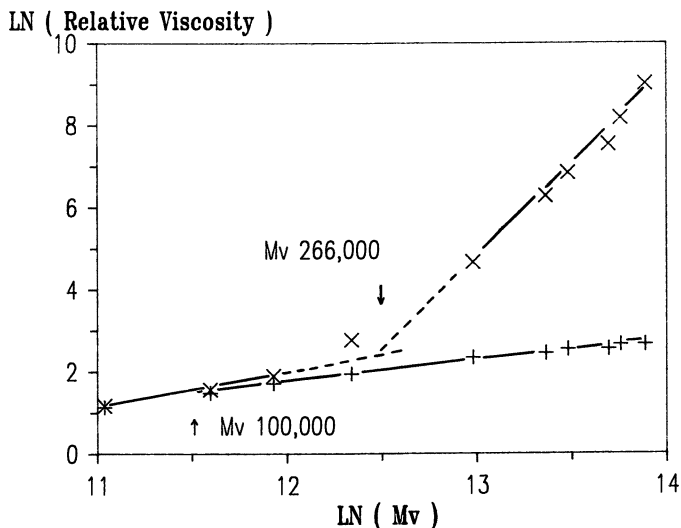


Figure 3. Natural log viscosity vs. natural log M_v at constant concentration. Key: \times , low shear; and $+$, high shear.

The slow increase in high-shear viscosity with molecular weight reinforces the view that in paint, increased high-shear viscosity in formulations using lower molecular weight HEC is due to the quantity of thickener present (*see* Efficiency).

EFFICIENCY. Efficiency is generally measured in terms of the quantity of thickener that must be added to produce a particular viscosity. The fewer pounds per gallon necessary, the more efficient the thickener.

As a rule, an increase in efficiency occurs with increasing molecular weight no matter which cellulosic thickeners are being considered. Unfortunately, as will be discussed later, high molecular weight brings its own problems. In the paint industry, a paint is often formulated to have a predetermined viscosity [generally within a range of 75–100 Kru units (KU)] as measured on a Stormer viscometer. The actual viscosity chosen depends on the purpose and quality of the formulation and the formulator's own experience.

Although the Stormer viscometer is really a constant-stress viscometer, the strain rates that it imposes fall somewhere in the low-middle range. In contrast, the ICI viscometer measures viscosity at a shear rate of $10,000 \text{ s}^{-1}$ and simulates shearing encountered during brushing.

Table I lists results for an interior flat latex paint thickened to 95 KU but with different molecular weight grades of HEC.

The molecular weight decreases as one goes down the columns in Table I. Much less of the high molecular weight material is required to

Table I. Variation in Thickening Efficiency with Molecular Weight of HEC (Interior Flat Formulation)

<i>Thickener</i> M_v	<i>Concn in Paint</i> (wt %)	<i>ICI</i> <i>Viscosity (P)</i>	<i>Stormer</i> <i>Viscosity (KU)</i>
none	0.000	0.30	—
1,080,000	0.384	1.10	95
715,000	0.511	1.10	98
434,000	0.680	1.35	95
109,000	1.517	1.80	95
62,000	1.848	1.80	91

bring the paint base up to the required Stormer viscosity. In conjunction, the increased level of material used results in higher values of the high-shear viscosity even with decreasing molecular weight.

Although this increase in high-shear viscosity is a strong positive feature, unfortunately, a negative flow and leveling trend is also present. (*see* Flow and Leveling/Sag Resistance).

The decrease in thickening efficiency with decreasing molecular weight is well documented. Also, some documentation exists concerning the effect of degree of substitution on efficiency (12). Increasing the degree of substitution tends to increase the low-shear viscosity somewhat in paints thickened to the same Stormer viscosity. This increase in viscosity is not the primary reason for choosing a high degree of substitution, however; the choice is made for solubility, flow and leveling, and enzyme resistance reasons as will be related later.

FLOW AND LEVELING/SAG RESISTANCE. The ability of a paint surface to level itself is most important in brushing applications. Obviously, the brush marks should disappear before the paint dries. This feature is one of the most difficult for latex paints in emulating oil-based paints. If a paint is low enough in viscosity to self-level readily, it may sag, that is, form runs or drips down a vertical surface. A balance must always be maintained between the two requirements.

A quantitative measure of leveling can be obtained by tracing the surface profile of a drawn-down paint film after it has dried. The results listed in Table II were obtained by using a Talysurf (Rank Precision Industries, Ltd., England) profilometer. All the paints listed in Table I were found to have poor flow and leveling and gave a center-line average (CLA) greater than the equipment could measure (maximum is 0.40 mil). Consequently, so that differences could be observed, the paints were diluted and remeasured. Stormer viscosities of diluted paints ranged from 77 to 79 KU (now at the lower end of the formulating spectrum; they started at 95 KU). The results are given in Table II.

A low value of CLA, or the equivalent sine wave amplitude of the brush marks, is obviously a sign of good leveling performance. The improvement with increasing molecular weight seems to be associated more with the decreasing quantity of thickener than any intrinsic flow property of high molecular weight HEC. This feature has been found elsewhere for other water-soluble thickeners (6) and appears to be commonly accepted (4). Some studies maintain that molecular weight has no effect on leveling and formulations made with increasing quantities of lower molecular weights show no reduction in leveling performance (3). This premise runs counter to our own experience. A possible explanation for this discrepancy lies in the marked effect film thickness plays on leveling. Analysis has shown that leveling improves as the cube of film thickness (5). Consequently, paints with significantly better film build when brush-applied will have a distinct advantage in producing the best flow and leveling.

When the flow on drawdowns is rated, film build is essentially constant and flow differences are not due to film thickness differences. Figure 4 shows the differing flow properties of two paints in this series. Both were applied with the same threaded drawdown bar and dried under the same conditions, but paint A, formulated with high molecular weight cellulosic, shows better flow than paint B, formulated with low molecular weight material.

In the extreme case, any tendency for excessive flow (especially at higher film thicknesses) must also be balanced against sag resistance. In principle, a paint that flows well will also sag. This tendency is demonstrated in Figure 5, where two paints with differing amounts of sag are shown. For this test (Leslie sag), paints are drawn down in stepped increments of thickness, each increment separated by a thin notch. Performance is then rated by the thickest coating that has not sagged.

Generally, the concept of a yield stress or slow viscosity recovery is invoked to explain the sag resistance of paints thickened with cellulose

Table II. Leveling of Various Thickened Paints

HEC M _v	Stormer Viscosity (KU)	CLA ^a		Amplitude Equivalent Sine Wave (5)	
		mil	μm	mil	μm
1,080,000	78	0.16	4.1	0.25	6.3
715,000	79	0.14	3.6	0.22	5.6
434,000	77	0.14	3.6	0.22	5.6
109,000	78	0.36	9.1	0.57	14.5
62,000	78	0.32	8.1	0.51	13.0

^aCenter-line average (CLA) is the average value of the surface profile above and below the center line; CLA can be converted to an equivalent sine wave amplitude.

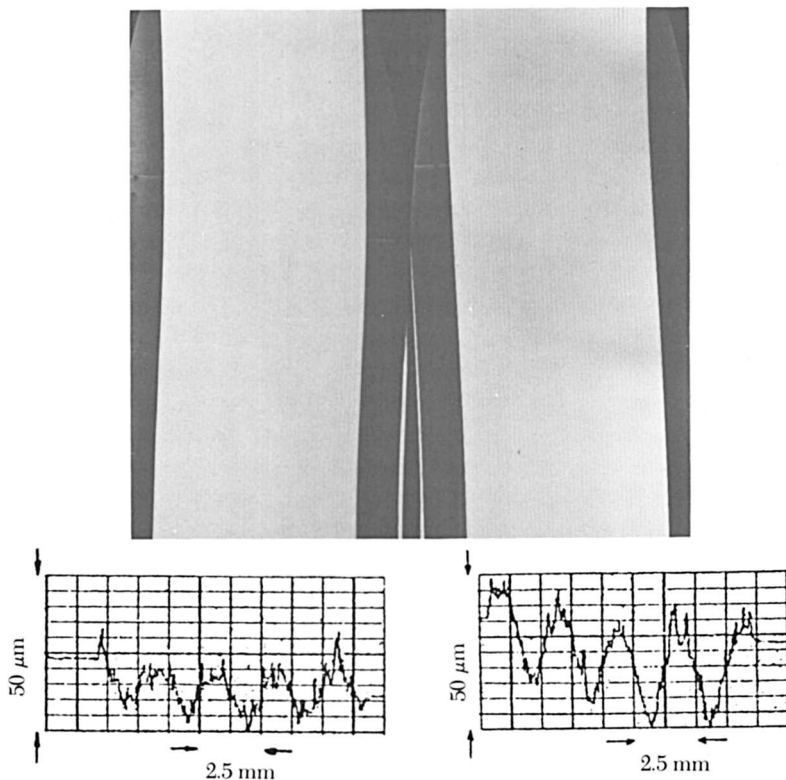


Figure 4. Talysurf leveling charts for two paints. Paint A (left) was formulated with medium-high molecular weight (715,000) cellulosic material. Paint B (right) was formulated with low molecular weight (62,000) material.

ethers. The thickener imparts structure to the latex paint, which requires a certain amount of work done to it for the structure to break down and allow flow. If the yield stress is greater than the shear stress due to gravity, then the paint will not sag. Obviously, if the paint film is too thick and the brush marks are too pronounced, then sag is likely to occur because the "overhanging" weight cannot be supported.

Paint thickened with cellulose ether tends to have good sag resistance at the expense of flow and leveling, although, in practice, a formulator can design a cellulosically thickened paint that has good sag performance and retains respectable flow and leveling properties.

SPATTER. Spatter is the tendency of paints with significant extensional viscosity to form strings that break up into droplets, which are then flung from the roller onto other surfaces. Therefore, the surfaces that are not meant to be painted must be covered for quite a distance around the painting area.

Glass published the definitive work on spatter (13). He found, in studying HEC and other types of thickeners, that the tendency to spatter

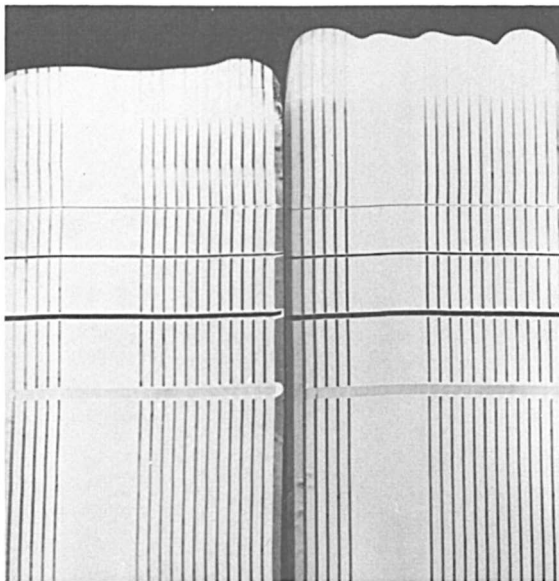


Figure 5. Leslie sag charts for two paints. Paint A (left) was formulated with medium-high molecular weight (715,000) cellulosic material. Paint B (right) was formulated with low molecular weight (62,000) material.

was increased significantly by increased molecular weight, in paints thickened to the same value of Stormer viscosity. This tendency has since been confirmed in (hydroxypropyl)methylcellulose (3). The worst spatter in Glass's study was in paint that was thickened with polyethylene oxide or acrylamide-acrylic acid copolymer. HEC fared very well by comparison. Glass also discussed the relationship between spatter and molecular weight through the extensional viscosity produced by high molecular weight polymers in solution.

Figure 6 shows the spatter results obtained in our laboratory. For this work, each of the paints was roller applied (Rubberset No. 7330 all-purpose 7-in. roller with $\frac{1}{4}$ -in. pile) to a uniform vertical surface located directly above a black plastic panel. A uniform and consistent number of passes was made with each paint.

The panels presented in Figure 6 show our results with varying molecular weight grades of HEC in the interior semigloss formula. As expected, significant differences were observed and are directly related to the molecular weight grade of thickener used. The high molecular weight grade on the left produces significantly more spatter than the lower molecular weight grades to the right. Despite these rather dramatic differences, spattering is a problem with any molecular weight grade commonly used. Not even the seldom-used lowest molecular weight grades are spatter free.

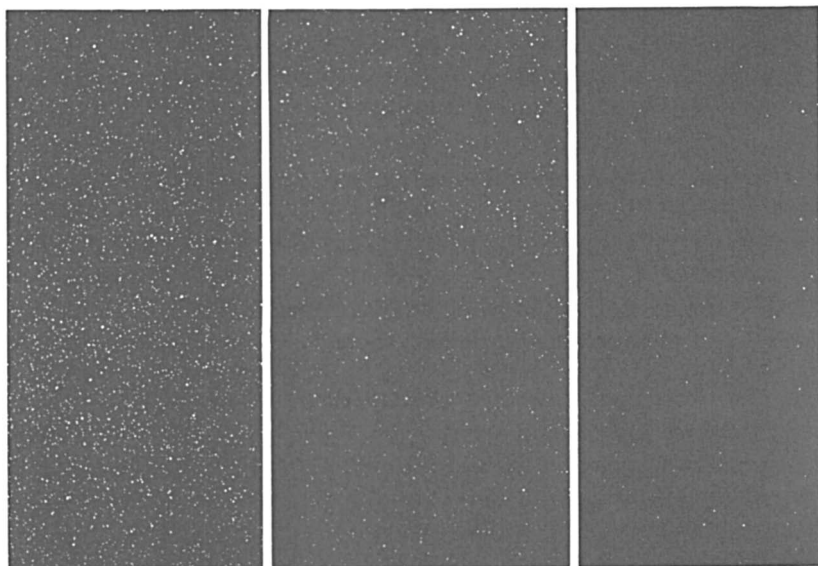


Figure 6. Black spatter panels for three paints. The left panel is paint made with high molecular weight (1,080,000) grade HEC. The center panel is paint made with medium molecular weight (434,000) grade HEC. The right panel is paint made with low molecular weight (109,000) grade HEC.

Table III. Scrub Resistance of Paint as a Function of HEC Molecular Weight

M_v	HEC [% (w/w)]	Scrub Cycles ^a	SD
<i>Flat Interior Paint</i>			
none	0.000	125	±15
1,080,000	0.384	103	±3
715,000	0.558	92	±3
434,000	0.680	97	±3
109,000	1.517	72	±10
62,000	1.848	58	±3
<i>Semigloss Interior Paint</i>			
none	0.000	850	±100
1,080,000	0.246	763	±70
715,000	0.295	682	±35
434,000	0.588	615	±60
109,000	1.361	530	±100

^aScrub cycles are average values.

Water Resistance. SCRUB RESISTANCE. The results presented in Table III were obtained by thickening the same paint base to 95 KU by using HECs of different molecular weights. The scrub resistance test is described in American Society for Testing and Materials (ASTM) D2486-79 (*14a*). It consists of applying a fixed amount of paint to a particular substrate and then scrubbing the coatings in a consistent fashion with a Gardner walability machine until the paint is removed along the path of the scrubbing action.

The first observation from Table III is that the paints containing HEC have lower scrub values than those without thickener. A possible molecular weight trend toward lower scrub resistance is particularly noticeable with low molecular weights. This trend might be expected on the basis of the amount of water-soluble material present. When the higher molecular weight grades commonly used in latex paints are compared, only minimal scrub differences are seen.

One can see the large difference in scrub resistance between the two formulations and also that different formulations may be more or less sensitive to variations in molecular weight of the HEC used to thicken them. Scrub resistance depends not only on the cellulosic thickener but also on the other major and minor constituents of paint.

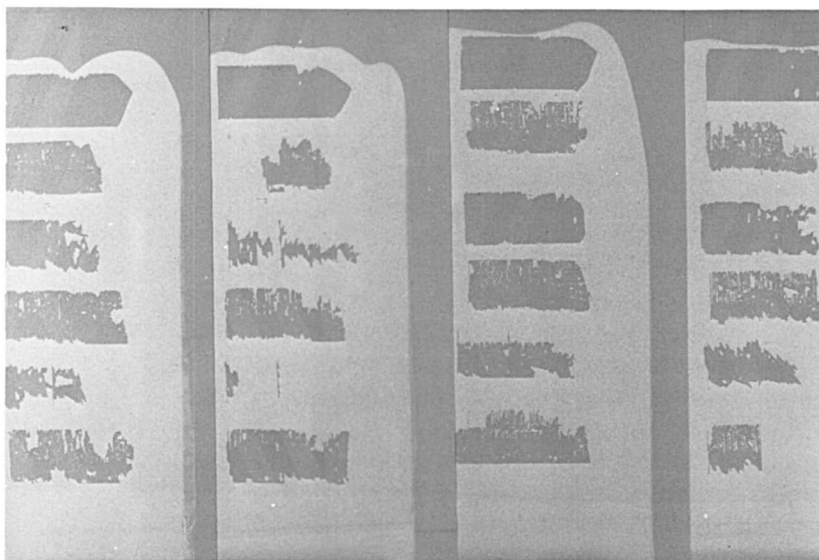


Figure 7. Photos of adhesion panels vs. M_v ; the paints were thickened to the same Kreh unit. The results of the tape adhesion tests of paint applied over an aged alkyd surface are shown for the following HEC-grade paints (left to right): M_v 1,080,000 (high); M_v 715,000 (medium); M_v 434,000 (medium); and M_v 109,000 (low).

WET AND DRY ADHESION. The term "wet adhesion" has been used in the paint industry to cover a great variety of testing methods (14b) and a multitude of "sins". The results shown here in Figure 7 were obtained by tape adhesion tests at various times after the paint was applied over an aged alkyd surface. This alkyd surface was generated by air-drying a standard trade sales semigloss alkyd for a minimum of 1 month at room temperature. Each test paint was then drawn down over this surface and allowed to again air-dry for various periods of time. At each test period, 3M adhesive tape (No. 610) was applied to the test area with uniform pressure and removed (both before and after scribing the test area). Any variation in the amount of paint removed was recorded. As evident from Figure 7 (higher molecular weight grade on the left), no trend related to the molecular weight of the thickener exists. In particular, this type of test seems to be very insensitive to small changes in HEC content and probably reflects the very small proportion of thickener present compared to the latex.

Gloss. Gloss is a measure of the reflectance of a paint and is an important formulating objective. A glossy paint film is not only one that is comparatively rich in polymeric binder (latex) but also one in which the pigments and latex particles are well dispersed. Flocculated particles tend to scatter light diffusely and internally; this scattering reduces gloss. Although changes in the amount of thickener or thickener molecular weight might be expected to have a significant effect on gloss, we did not observe any effect in our study. We saw no gloss differences in any of the various paints containing different thickener structures or molecular weights. Despite their widespread use in semigloss paints, cellulosic thickeners are also occasionally associated with a haze development on dry paint films. Although this haze can normally be wiped off with a damp cloth, it is still of concern to many formulators. Despite looking carefully for any occurrence of this problem in our work, we did not observe any.

Color Acceptance. One of the most crucial characteristics of a tinted paint is its color acceptance. Irrespective of drying conditions or method of application (roller, brush, or spray), a paint should always have an identical and consistent color. This feature is important, not only from can to can but also more importantly where different methods of application have been used side by side, for example, where a rolled surface has been touched up with a brush. Ideally, a pigment should be perfectly dispersed in a paint system; then each batch should be the same, and each method of application will provide the same color independent of the mechanical dispersing power of the method.

Commonly, color acceptance is evaluated by a rub-up method. In this test, a paint is brushed or rolled onto a standard substrate and then

**American Chemical Society
Library**

1155, 16th St., N.W.

In Water-Soluble Polymers, Glass, B.
Washington, D.C. 20036
Advances in Chemistry; American Chemical Society, Washington, DC, 1986.

rubbed in a circular motion at various times of dry with the operator's thumb or finger, although recently less operator-dependent procedures have been tried (3). Roller application is a low-shear application in contrast to the high shear of brushing or the extremely high shear of a finger rub up. Any differences between the rubbed area and the brushed or rolled background are a measure of the increased pigment dispersion caused by the rubbing action. This test is a qualitative assessment of the pigment or latex flocculation in a paint; ideally none should occur.

Figure 8 shows rub ups for a series of paints made with a selection of cellulosic thickeners. Again, the higher molecular weight thickener is on the left. From these typical results, we concluded that all of the color acceptance results in our study were satisfactory and that only minimal differences were attributable to the type and molecular weight grade of thickener used. Although this conclusion is indeed true for the current study, past experience makes us extremely cautious in extending this finding to any other paint or tinting systems. Our tinting study was limited to the one interior flat formula and two different tints (carbon black and red iron oxide). As such, we made no attempt to investigate the many formula, raw material, and tinting system variations that strongly influence this subject.

Freeze-Thaw Stability. Freeze-thaw stability of all paints was also checked, but no compositional trend related to the type or molecular weight grade of cellulose ether was observed. Regardless of the choice of cellulose ether used, all the paints of a given formula performed identically (either all passed or all failed depending on the formula).

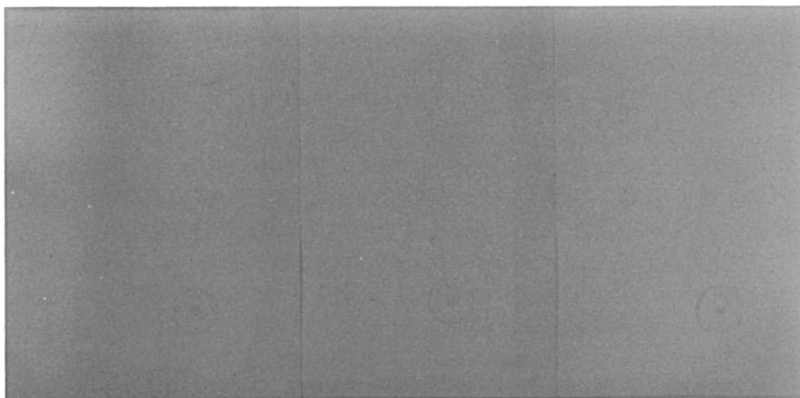


Figure 8. Rub ups for color acceptance of paints made with various HEC-grade paints. The left panel is paint made with high molecular weight (1,080,000) grade HEC. The center panel is paint made with medium molecular weight (434,000) grade HEC. The right panel is paint made with low molecular weight (62,000) grade HEC.

Degradation. Although thickeners have a large effect on the rheological properties of paint, they are present in very small quantities. Consequently, any degradation, whether it be by biological action or otherwise, can have drastic consequences. For example (15), oxidative mechanisms, which seem to be dominant in reducing viscosity, can decrease the Stormer viscosity by as much as 15–30 KU.

Microrganisms feed on cellulosic materials by producing enzymes that break down the cellulose into sugars that the microorganism can metabolize. Although the growth of these microorganisms can possibly be prevented (or they may be killed) by adding a preservative, the best stratagem is to prevent them from getting into the paint in the first place. Once these enzymes are present, the susceptibility of cellulose to attack increases as the number of unsubstituted glucose units increases (16). More evenly spaced substitution along the thickener molecular backbone will restrict the possibility of enzyme attack and minimize the resulting degradation of properties.

Other work (17) has found that the presence of oxidants from latex manufacture, for example, potassium persulfate, promotes the degradation of the thickener and thus the viscosity of the paint. The degradation not only reduces the thickening efficiency but also provides nourishment for microorganisms and thus makes the situation worse.

For the best total resistance to degradation, protection against loss of viscosity should include a combination of good housekeeping, use of an effective preservative, and care to minimize the possible presence of oxidants.

Paint Manufacture. The key to successful paint manufacture with cellulosic thickeners is proper dispersion of the dry thickener. Whether one is making a thickener solution or a thickener slurry or just adding the thickener directly to the paint as a dry powder (or through an eductor), maximum wetting and dispersion of the thickener particles must be achieved before they begin to hydrate. To help in this area, the user needs to be aware of several factors controlling hydration time. These factors include temperature, pH of the material being thickened (within limits increased temperature and pH promote hydration), and choice of the thickener type and grade. As mentioned previously, the type of ether substituent group and the presence or absence of surface treatment greatly influence solubility characteristics.

Acknowledgments

We are grateful to D. E. Slawikowski and L. W. Kisha, who performed most of the experimental work. We thank Hercules, Inc., for the values of the Mark-Houwink constants used to determine the molecular weights.

Literature Cited

1. *Protective and Decorative Coatings*; Mattiello, J. J., Ed.; Wiley: New York, 1943; Vol. III.
2. *Kirk-Othmer Encyclopedia of Chemical Technology*; 3rd ed.; Wiley: New York, 1978; Vol. 5.
3. Blake, D. M. *J. Coat. Technol.* **1983**, *55*, No. 701, 33-42.
4. Massouda, D. F.; Sercel, F. J.; Graybeal, C. J. *Mod. Paint Coat.* **1980**, *70*, 116-118.
5. Dodge, J. S. *J. Coat. Technol.* **1972**, *44*, No. 564, 72-78.
6. Arney, W. C., Jr.; Glass, J. E. *J. Oil Colour Chem. Assoc.* **1976**, *59*, 372-378.
7. Sperry, P. R.; Hopfenberg, H. B.; Thomas, N. L. *J. Colloid Interface Sci.* **1981**, *82*, 62-76.
8. Gast, A. P.; Hall, C. K.; Russel, B. *Faraday Discuss. Chem. Soc.* **1983**, *76*, 189-201.
9. Gillespie, T. *J. Colloid Interface Sci.* **1983**, *94*, 166-173.
10. Doi, M. *J. Polym. Sci., Polym. Lett. Ed.* **1981**, *19*, 265-273.
11. Klein, J. *Macromolecules* **1978**, *11*, 852-858.
12. Glass, J. E. *J. Oil Colour Chem. Assoc.* **1976**, *59*, 86-94.
13. Glass, J. E. *J. Coat. Technol.* **1978**, *50*, No. 641, 56-78.
- 14a. "Scrub Resistance of Interior Latex Flat Wall Paints"; ASTM D2486-79; American Society for Testings and Materials D-1, Philadelphia, PA, 1979.
- 14b. Kambanis, S. M.; Chip, G. *J. Coat. Technol.* **1981**, *53*, 57-64.
15. Winters, H.; Goll, M. *J. Coat. Technol.* **1976**, *48*, 80-85.
16. Klug, E. D.; t'Sas, H. E. *Adv. Org. Sci. Technol. Ser.* **1981**, *1*, 45-54.
17. Irwin, V. L.; Williams, M. M. *J. Coat. Technol.* **1980**, *52*, 71-74.

RECEIVED for review February 8, 1985. ACCEPTED August 14, 1985.

Grafting Reactions of (Hydroxyethyl)-cellulose During Emulsion Polymerization of Vinyl Monomers

D. H. Craig

Research Center, Hercules, Inc., Wilmington, DE 19894

The aqueous phases of vinyl-acrylic and all-acrylic latexes manufactured in the presence of (hydroxyethyl)cellulose (HEC) were analyzed for residual HEC content and HEC molecular weight distribution by using colorimetry and high-performance size-exclusion chromatography, respectively. Vinyl acetate monomer, contrary to traditional thought, grafted very little to HEC, although acrylic monomers grafted extensively under the same emulsion polymerization conditions. In both cases extensive degradation of the HEC molecular weight occurred. A scheme is proposed whereby radicals generated along the HEC backbone, a result of chain transfer from initiator to protective colloid, mediate both the HEC grafting reaction and HEC molecular weight reduction to an extent that depends on the relative reactivities of the monomers used.

THE COMPOUND (HYDROXYETHYL)CELLULOSE (HEC) IS WIDELY EMPLOYED as a protective colloid in the commercial manufacture of vinyl acetate containing homopolymer and copolymer latices destined for use as binders in latex paints (1). The main reasons for this usage are that low levels of HEC impart good mechanical stability and processing characteristics to the latex, particularly under lean surfactant conditions. In commercial paint latices, low levels of surfactants are required to minimize the water sensitivity of the dried film. The small amounts of HEC that are used to replace the correspondingly higher surfactant levels actually improve the film formation and durability of paint latices as well by providing a latex surface that is more compatible with pigments and by controlling the rate of water evaporation; thus, proper coalescence of latex particles is allowed.

The enhanced mechanical stability imparted to vinyl acetate based latexes by inclusion of HEC in the polymerization recipe has tradition-

0065-2393/86/0213-0351\$06.00/0
© 1986 American Chemical Society

ally been explained as arising from the extensive grafting of vinyl acetate onto the HEC backbone; this grafting provides HEC-encapsulated latex particles that are stabilized sterically. This feature has been surmised from the generally high chain-transfer constants of the poly(vinyl acetate) radical determined from bulk, solution, or suspension polymerization measurements, when compared to the chain-transfer constants of other radicals derived from monomers often used in emulsion polymerization, such as methyl methacrylate (2, 3). The known tendency for poly(vinyl acetate) to chain transfer to itself (4) seemed to confirm this viewpoint. However, the traditional theory does not provide an explanation as to how the growing poly(vinyl acetate) radical, which would be located in the growing polymer particles, chain transfers to HEC, which is present in the aqueous phase. Until recently, no definitive studies addressed this issue.

Recently, studies have begun to appear detailing the chemistry of HEC in the presence of persulfate initiators alone (5-8) or under the conditions of vinyl acetate emulsion polymerization (9-14). Donescu et al. (5) suggested that HEC and persulfate form a redox pair at the high temperatures encountered in thermally catalyzed emulsion polymerization and showed that the activation energy for the decomposition of persulfate was lower in the presence of HEC. This result was corroborated by Kislenco et al. (7), who determined the activation energy for persulfate decomposition to be 20.8 and 34.0 kcal/mol in the presence and absence of HEC, respectively. Stepin et al. (11) analyzed the polymer solids of a dibutyl maleate-vinyl acetate copolymer synthesized in the presence of HEC and found HEC-graft copolymers as well as the expected dibutyl maleate-vinyl acetate copolymers. The authors stated that the HEC-graft copolymers are concentrated at the particle interface; this feature ensures colloidal stability. Jakubec and Chocholaty (14) discovered a system to suppress the oxidative degradation of HEC during persulfate-initiated emulsion polymerization of vinyl acetate by employing formate salts; the production of high-viscosity vinyl acetate homopolymer dispersions results.

In contrast to vinyl acetate, persulfate-initiated emulsion polymerization of acrylic monomers or vinyl-acrylic monomer blends of high acrylic content, in the presence of HEC, resulted in extreme thickening and eventual coagulation, especially at relatively high polymer solids (i.e., greater than 30%). Thus, the benefits of HEC stabilization, such as mechanical stability at low surfactant levels, were not realized in all acrylic latices (1). This contrast in behavior relative to that of vinyl acetate had generally been explained as being due to the lack of grafting of acrylic monomers onto HEC; this lack of grafting prevents the formation of the protective layer of HEC at the particle interface, a direct

extrapolation of the chain-transfer constant studies mentioned for vinyl acetate (2, 3).

Nevertheless, the potential improvements in acrylic latex stability resulting from the successful incorporation of HEC fostered research aimed at the development of processes permitting the inclusion of HEC (or related compounds) during the emulsion polymerization of acrylic monomers (15–22). For instance, processes have been patented (15, 16) whereby the protective colloid is gradually added during the course of polymerization, which provide latices of coarse particle size and high viscosity. High-solids HEC-stabilized acrylic latices were produced through the addition of bromotrichloromethane 2–5 min after the formation of “polymer micelles” (17). Alternatively, use of HEC pretreated with peroxidic compounds (18, 19) or use of highly degraded starch (20) as a protective colloid enabled the production of low-viscosity acrylic latices of high stability (18, 19) or latices of increased blocking resistance (20). Two particularly convenient methods produced low-viscosity, shear-stable HEC-containing acrylic polymer dispersions through the simple inclusion of water-soluble “regulators”, such as mercaptoacetic acid or cyclohexylamine (21), or “emulsion stabilizers”, such as allyl alcohol (22), along with the HEC at the beginning of the polymerization reaction.

Only in one instance was any explanation given as to why any of the aforementioned acrylic systems actually worked. Ogata and Wakabayashi (22) suggested that the graft polymerization reaction between acrylic or methacrylic monomer and the protective colloid was moderated by the presence of allyl alcohol and related substances; the coagulation that would ordinarily result from the bridging of the latex particles was prevented. This explanation was contrary to traditional thought (*vide supra*) but nevertheless more readily explained the thickening of HEC-containing acrylic systems before coagulation occurs.

With these arguments in mind, we established a program to help define the chemistry of HEC under the conditions encountered during the production of HEC-stabilized acrylic and vinyl-acrylic copolymer latices. Results from that study are presented here.

Experimental Section

A series of polymerization reactions were carried out according to the procedures outlined in Tables I–III by varying the levels of the components as listed. A number of variations of the recipe in Table I were run including (1) the presence and absence of the water-soluble regulator (*i.e.*, chain-transfer agent) triethanolamine (TEA) (2), an extension of the work detailed in reference 21, which showed that stable, low-viscosity polymer dispersions were produced only in the presence of water-soluble regulators; (2) the substitution of an 85:15

Table I. Acrylic Emulsion Polymerization Recipe

<i>Mixture</i>	<i>Component</i>	<i>Parts by Weight (%)</i>
1	water	45.00–53.00
	Triton X-102 ^a	0.00–2.00
	sodium dodecyl benzenesulfonate	0.00–0.50
	potassium persulfate (5%)	2.00–4.00
	HEC ^b	0.00–1.00
	regulator or stabilizer (TEA) ^c	0.00–1.00
2	monomer	10.00
	potassium persulfate (5%)	0.00–2.00
3	monomer ^d	34.00
	total	100.00

NOTE: The procedure used was as follows: (1) add mixture 1 to kettle under an N₂ blanket and heat to 85 °C; (2) begin addition of mixture 3 via the metering pump; (3) add mixture 2 after 50% of monomer has been added; and (4) maintain at 85 °C for 2 h beyond addition of monomer.

^aTriton X-102 is α -[4-(1,1,3,3-tetramethylbutyl)phenyl]- ω -hydroxypoly(oxy-1,2-ethanediyl).

^bHEC is (hydroxyethyl)cellulose [Natrosol 250 LR HEC (Hercules, Inc.), 5% aqueous Brookfield viscosity = 93 cP and weight-average molecular weight = 80,000].

^cTEA is triethanolamine.

^dThe monomer is composed of butyl acrylate (42.7%), methyl methacrylate (56.8%), and methacrylic acid (0.5%).

Table II. Vinyl Acetate–Acrylic Emulsion Polymerization Recipe

<i>Mixture</i>	<i>Component</i>	<i>Parts by Weight (%)</i>
1	water	43.60
	sodium bicarbonate (5%)	1.44
	Aerosol A-102 ^a	1.40
	Triton X-102	0.70
	HEC ^b	0.50
2	monomer ^c	10.00
3	potassium persulfate (5%)	2.48
4	monomer ^c	38.00
5	Aerosol A-102	0.88
	total	100.00

NOTE: The procedure used was as follows: (1) add mixture 1 to kettle under an N₂ blanket and heat to 85 °C; (2) add mixture 2 and 3 and when refluxing subsides, begin addition of step 4 via the metering pump; (3) add mixture 5 after 50% of monomer addition; and (4) maintain at 85 °C for 2 h after completion of monomer addition.

^aAerosol A-102 is the disodium salt of the sulfosuccinate half-ester of ethoxylated fatty alcohol.

^bHEC is Natrosol 250 MR HEC (Hercules, Inc.) (2% aqueous Brookfield viscosity = 5000 cP and weight-average molecular weight = 650,000) or Natrosol 250 LR HEC (*see* Table I).

^cThe monomer is composed of vinyl acetate (85%) and butyl acrylate (15%).

Table III. Vinyl Acetate Homopolymer Emulsion Polymerization Recipe

<i>Mixture</i>	<i>Component</i>	<i>Parts by Weight (%)</i>
1	water	43.45
	HEC ^a	1.96
	potassium persulfate	0.15
2	vinyl acetate	10.00
3	sodium bicarbonate (5%)	1.44
4	vinyl acetate	43.00
	total	100.00

NOTE: The procedure used was as follows: (1) add mixture 1 to kettle under N₂ blanket and heat to 85 °C; (2) add mixtures 2 and 3 and when refluxing subsides, begin adding mixture 4 via metering pump; and (3) maintain at 85 °C for 2 h beyond final addition of vinyl acetate.

^aSee Table II for a description of HEC.

mixture of vinyl acetate and butyl acrylate for the acrylic monomer mixture listed; (3) the portionwise versus batch addition of the persulfate initiator; and (4) the slow addition of all the monomer feed versus the semibatch method listed.

The resulting latices were characterized for pH, Brookfield viscosity, average particle diameter (Coulter nanosizer), grit content (visual assessment), and mechanical stability (10 min in a Waring blender at the highest setting). The samples subjected to high shear were analyzed for both particle size and viscosity.

For determination of the amount of grafted HEC, the latices were centrifuged at 17,000 rpm to remove the polymer solids, and the supernatant liquid was analyzed by high-performance size-exclusion chromatography (23) for the concentration of residual HEC (estimated by the area under the chromatogram tracing) and HEC molecular weight distribution. The estimates of HEC concentration determined from the chromatograms were refined by colorimetric determination of HEC (24). Controls were run whereby the latex was produced in the absence of HEC and postthickened with HEC after cooling to room temperature. Analysis of these latices proceeded as described. In addition, solvent extraction and fractionation of the centrifuged polymer solids were performed on a number of samples to distinguish between grafted and physically absorbed HEC.

Results and Discussion

To distinguish between grafted HEC and absorbed HEC, we ran a number of experiments, including the synthesis of control latices in the absence of HEC (according to Table I) with subsequent postaddition of HEC. Centrifugation of these latices and analysis of the supernate revealed that 100% of the postadded HEC remained in the aqueous phase with no reduction in molecular weight (*see* Table IV, which pro-

vides some typical analytical data on latices prepared according to Table I). In addition, extensive solvent extractions of selected polymer solids samples obtained from centrifuging demonstrated that only low levels ($\leq 10\%$) of the total grafted HEC were extractable, although 10–20% of the acrylic resin contained insoluble (and therefore cross-linked) material. All of these experiments supported the indication that the latices produced from Table I had little tendency to adsorb HEC and that virtually all of the HEC associated with the latex polymer solids was grafted (i.e., covalently bound). Because most of the HEC was recovered when a vinyl acetate–butyl acrylate monomer mixture was substituted for the acrylic mixture listed in Table I (Table IV, last example), extraction of the polymer solids of these latices was not performed (vide infra).

Figure 1 illustrates the linear increase in the amount of HEC grafted versus the amount present during polymerization for an acrylic latex prepared in the absence of conventional emulsifiers or water-soluble regulators. Interestingly, what little HEC remained in the aqueous phase of the latexes prepared for Figure 1 was extensively degraded, as illustrated in Figure 2, which provides the high-performance size-exclusion

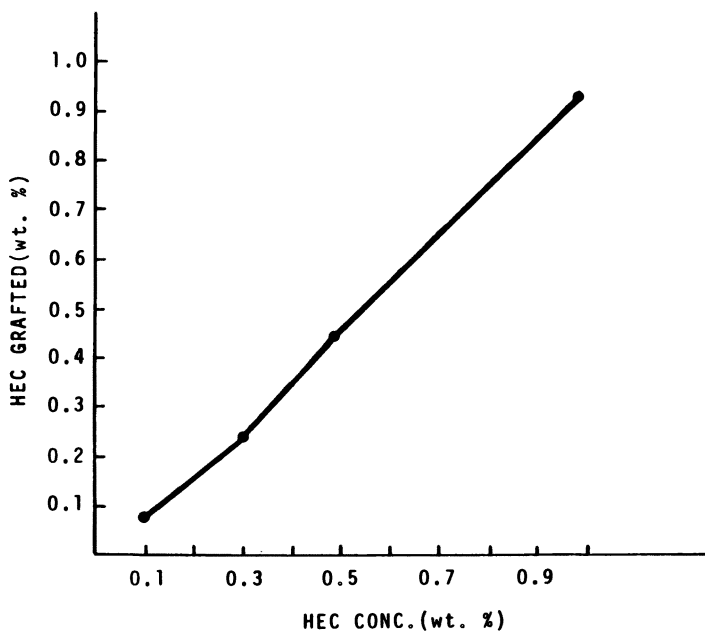


Figure 1. Weight percent grafted HEC vs. initial concentration of HEC. All acrylic latices were produced according to Table I except in the absence of surfactants and TEA. Concentrations are based on the total recipe.

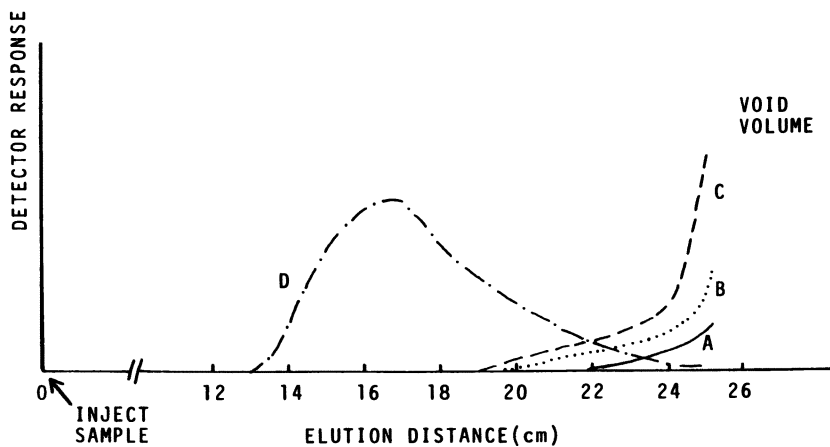


Figure 2. Size exclusion chromatography of residual HEC in the aqueous phase of the latices of Figure 1. Key: A, 0.1% HEC initial; B, 0.3% HEC initial; C, 0.5–1.0% HEC initial; and D, HEC standard.

chromatograms (23) of the residual HEC in the aqueous phase of the latices of Figure 1. Figure 2 shows plots of the detector response versus elution distance, which provides a measurement of molecular weight distribution: the low molecular weight species (for instance, glucose) eluting with the void volume at approximately 26 cm versus the higher molecular weight (i.e., undegraded) HEC standard eluting at 17 cm. At all concentrations, the residual HEC elutes at very low molecular weight between 19 and 22 cm. Comparison to dextran standards has established that this range represents a dextran-equivalent molecular weight of 60,000 (19 cm)–20,000 (22 cm) versus a dextran-equivalent molecular weight of 180,000 at 17 cm. The data in Figures 1 and 2 strongly indicate that both grafting and oxidative degradation of HEC occur extensively during the emulsion polymerization of acrylic monomers.

Figures 3 and 4 provide data on the effect of increasing concentrations of TEA on the same reactions of HEC detailed by Figures 1 and 2, under the same conditions. Obviously, the use of water-soluble regulators (21) suppressed both the grafting and oxidative degradation reactions of HEC; this suppression suggests that a common intermediate exists for both reaction pathways. Because a latex of lower viscosity was produced in the presence of TEA despite the fact that more HEC (of higher molecular weight) remained in the aqueous phase, it is clear that the high viscosity of HEC-stabilized all-acrylic latices manufactured according to traditional recipes is a direct result of the acrylic-HEC grafting reaction and not due to a simple thickening effect of residual water-soluble HEC.

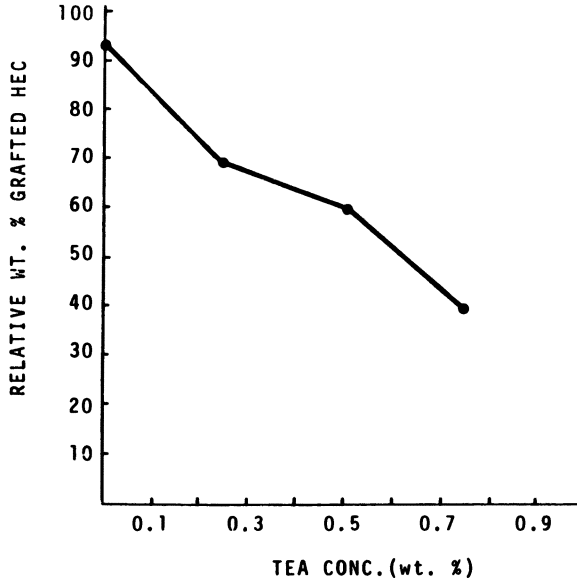


Figure 3. Relative weight percent grafted HEC vs. initial concentration of TEA. All-acrylic latices were produced according to Table I except in the absence of surfactants. Concentrations are based on the total recipe. HEC = 1.0%.

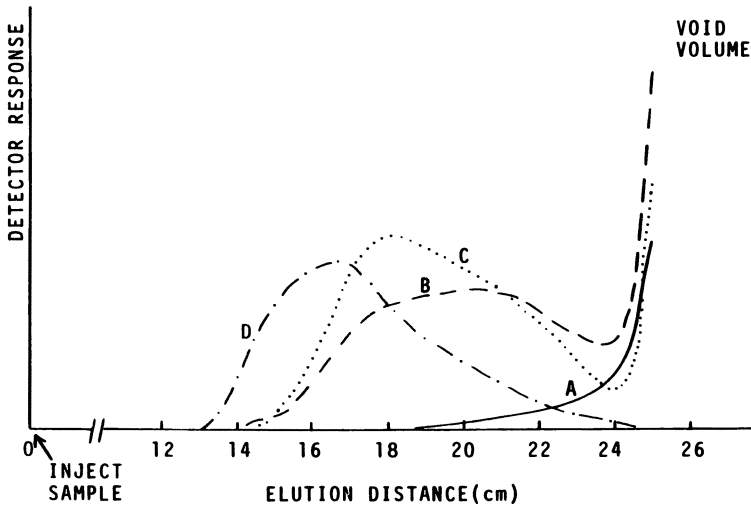


Figure 4. Size-exclusion chromatography of residual HEC in the aqueous phase of the latices of Figure 3. Key: A, 0% TEA; B, 0.25% TEA; C, 0.50% TEA; and D, HEC standard.

The effect of delaying the addition of triethanolamine at suitable time intervals, beginning at the start of the polymerization reaction, is illustrated in Figures 5 and 6. These reactions were run in the presence of surfactants, HEC, and TEA according to Table I. The most dramatic data are provided in Figure 6, which shows that a time delay of 20 min before TEA addition to the reaction vessel (total reaction time approximately 5–6 h) produced a latex whose size-exclusion profile is indistinguishable from that of a latex to which no TEA was ever added (*see* Figure 4, curve A). Data obtained from experiments delaying the addition of HEC, although not as dramatic, exhibit similar trends (Figures 7 and 8). Apparently, most of the grafting and degradation of HEC occurs early in the course of polymerization, perhaps during initiation. This occurrence is reasonable because the concentrations of both the persulfate initiator and HEC are highest at this stage.

Further evidence for early grafting and degradation is provided in Figure 9, which shows that HEC was more extensively grafted and degraded when all of the initiator was added at the beginning of the reaction (curve A) versus a portionwise addition of the initiator (curve B).

The moderating effect of surfactants on the grafting and degradation reactions of HEC is illustrated in Figure 10. Although the moderating effect appears substantial in the presence of TEA, the total reduction in grafting due to the presence of surfactants was relatively small in all

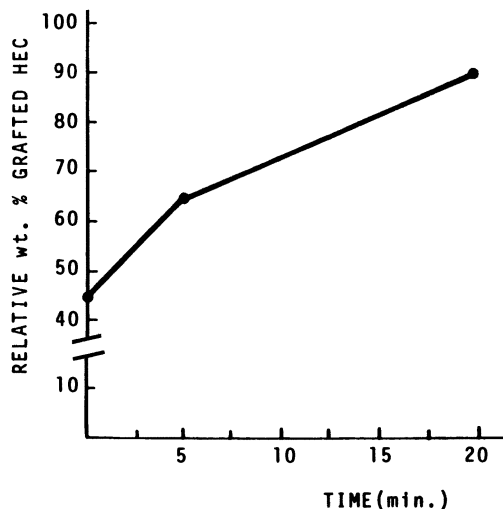


Figure 5. Relative weight percent grafted HEC vs. time of TEA addition. All-acrylic latices were produced according to Table I in the presence of 1.0% Triton X-102, 0.15% SDBS, and 0.5% HEC. Concentrations are based on the total recipe. SDBS = sodium dodecyl benzenesulfonate.

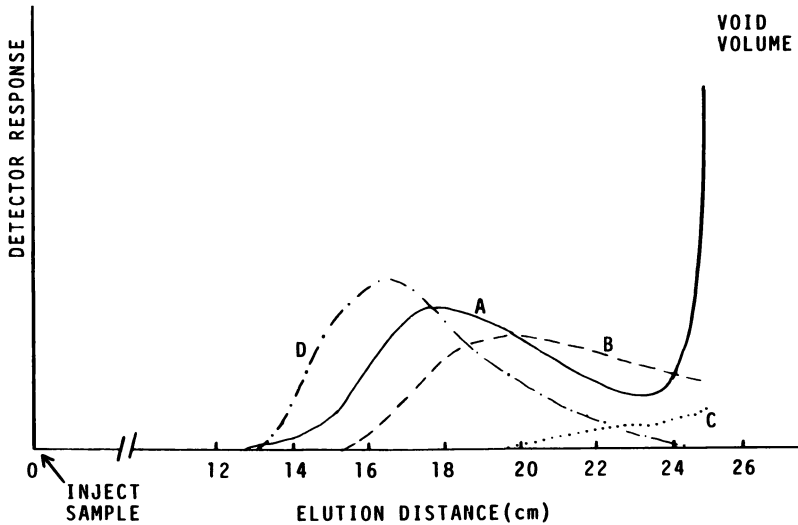


Figure 6. Size-exclusion chromatography of residual HEC in the aqueous phase of the latices of Figure 5. Key: A, time = 0 min; B, time = 5 min; C, time = 20 min; and D, HEC standard.

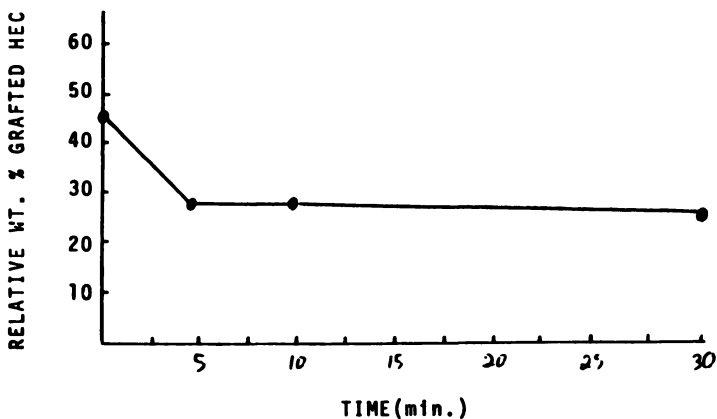


Figure 7. Relative weight percent grafted HEC vs. time of HEC addition. All-acrylic latices were produced according to Table I in the presence of 1.0% Triton X-102, 0.15% SDBS, 0.5% TEA, and 0.5% HEC. Concentrations are based on the total recipe.

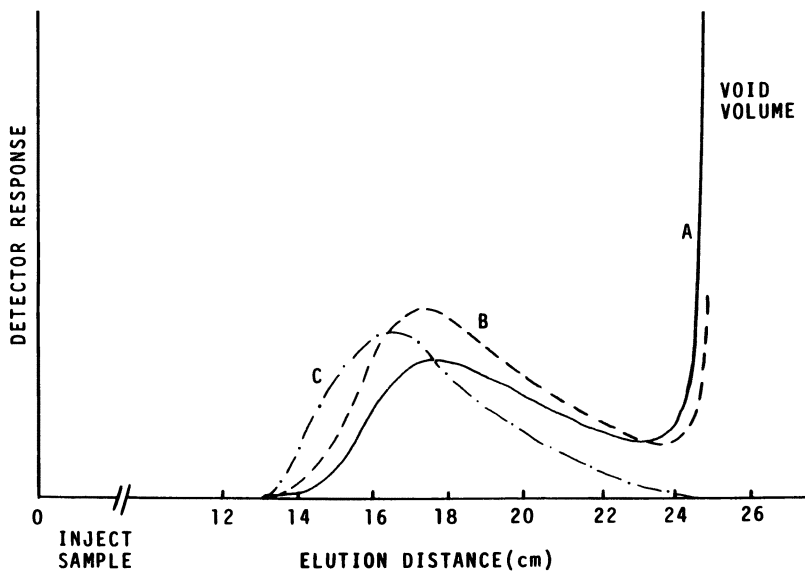


Figure 8. Size-exclusion chromatography of residual HEC in the aqueous phase of the latices of Figure 7. Key: A, time = 0 min; B, time = 5–30 min; and C, HEC standard.

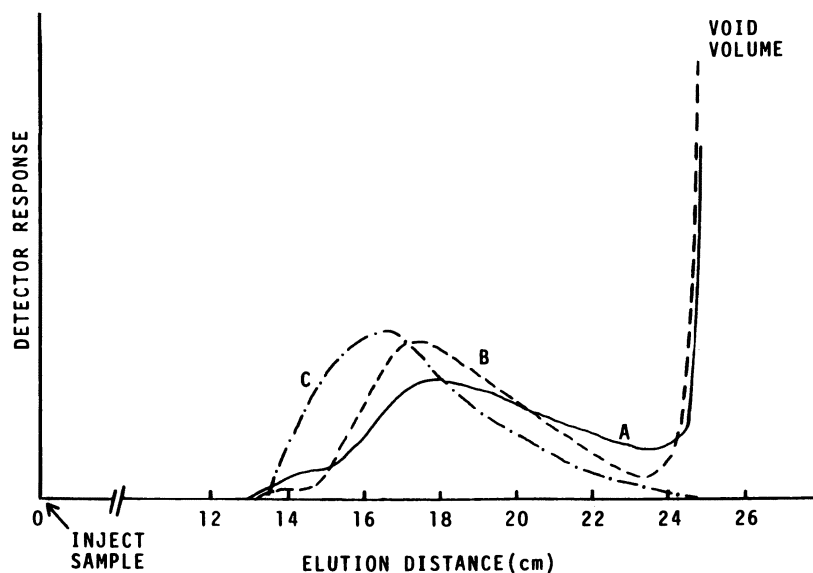


Figure 9. Size-exclusion chromatography of residual HEC in the aqueous phase of the acrylic latices produced according to Table I in the presence of 1.0% Triton X, 0.15% SDBS, 0.5% TEA, and 0.5% HEC: A, all the initiator was present at the beginning; B, half of the initiator was present at the beginning and half was added after 50% monomer addition; and C, HEC standard.

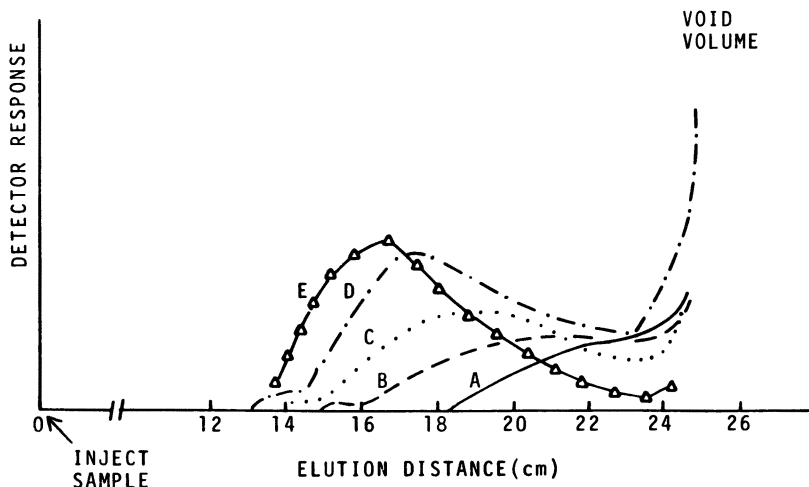


Figure 10. Size-exclusion chromatography of residual HEC in the aqueous phase of the acrylic latices produced according to Table I in the presence and absence of surfactants. Key: A, no surfactant, no TEA, and 0.5% HEC; B, 1.0% Triton X, 0.15% SDBS, 0.5% HEC, and no TEA; C, no surfactant, 0.5% TEA, and 0.5% HEC; D, 1.0% Triton X-102, 0.15% SDBS, 0.5% TEA, and 0.5% HEC; and E, HEC standard.

cases. These data imply that surfactants participate in grafting reactions as well. Although grafting reactions of surfactants are known (25), it appears that surfactants do not compete effectively with compounds such as HEC for the free radicals generated during initiation.

Perhaps more interesting than most of the data presented so far are the size-exclusion chromatograms of Figure 11. Curve A represents the HEC standard, curve B the residual HEC in the latex supernate of an all-acrylic latex prepared in the presence of HEC and surfactants and in the absence of TEA (according to Table I), and curve C the residual HEC profile of the latex supernate generated when the acrylic monomers of curve B have been replaced by an 85:15 mixture of vinyl acetate and butyl acrylate, all other things being equal. One can immediately spot the extensive HEC degradation but distinct lack of HEC grafting that occurs in the vinyl-acrylic system. Contrary to traditional thought, vinyl acetate has much less tendency to graft onto HEC than do acrylic monomers under the conditions encountered in emulsion polymerization.

These observations led to an extensive investigation of the synthesis of HEC-stabilized vinyl acetate homopolymer and copolymer latices (*see* recipes in Tables II and III). Typical data are provided in Table V and Figure 12, although, unlike acrylic systems, a moderate degree of variability was observed in the manufacture of the latices. As expected,

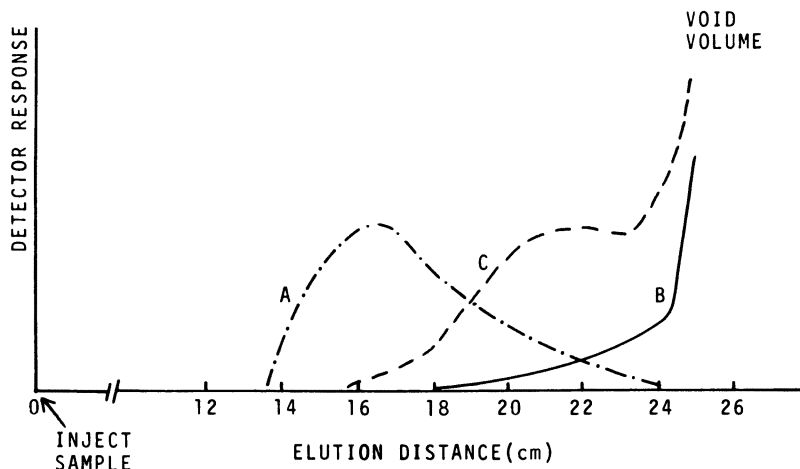


Figure 11. Size-exclusion chromatography of residual HEC in the aqueous phase of the latices produced according to Table I in the presence of 1.0% Triton X-102, 0.15% SDBS, 0.5% HEC, and no TEA. Key: A, HEC standard; B, all-acrylic monomer mixture of Table I; and C, vinyl-acrylic monomer mixture of Table II, in the recipe of Table I.

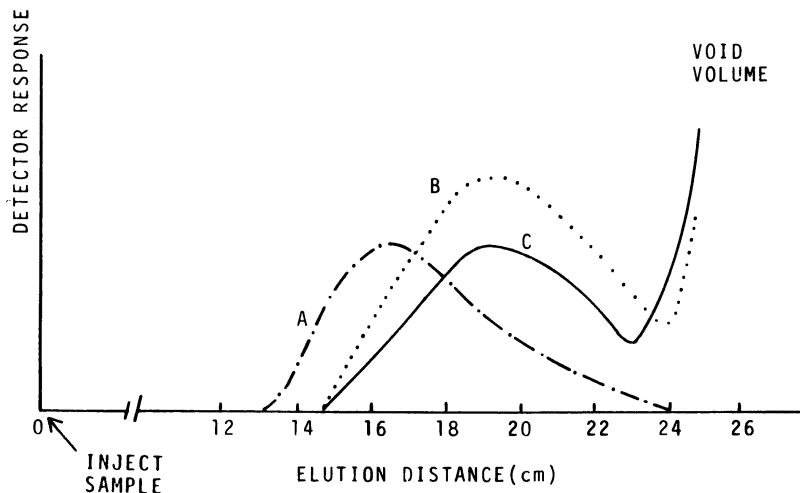


Figure 12. Size-exclusion chromatography of residual HEC in the aqueous phase of the latices produced according to Table II (curve C) and Table III (curve B). Curve A is HEC standard.

Table IV. Acrylic Latices

Monomer	Stabilizer ^a	Concn (wt %)	Viscosity (cP)	Average Particle Diameter (μm)	Shear Stability	% HEC Grafted
BA-MMA-MAA	surfactant	1.15	40	0.1	no	—
BA-MMA-MAA	surfactant-HEC	1.15:0.50	—	>4.0	yes	83
BA-MMA-MAA	surfactant-HEC ^b post add	1.15:0.50	1480	0.1	yes	0
BA-MMA-MAA	surfactant-HEC-TEA	1.15:0.50	670	3.6	yes	45
BA-MMA-MAA	HEC	1.00	>10,000	2.0	yes	93
BA-MMA-MAA	HEC-TEA	1.00:0.50	3200	>4.0	yes	61
VA-BA (85:15)	surfactant-HEC	1.15:0.50	125	0.3	yes	5

NOTE: BA is butyl acrylate, MMA is methyl methacrylate, and MAA is methacrylic acid.

^aThe recipes are listed in Table I.

^bHEC was added after surfactant addition.

Table V. Vinyl Acetate Latices

Monomer	Stabilizer	Concn (wt %)	Viscosity (cps)	Average Particle Diameter (μm)	Shear Stability	% HEC Grafted
VA	HEC (low M_r) ^{a,b}	1.96	750	1.20	yes	0
VA-BA (85:15)	surfactant-HEC (low M_r) ^{b,c}	1.40:0.50	390	0.39	yes	4
VA	HEC (high M_r) ^{a,d}	1.96	1600	1.31	yes	6
VA-BA (85:15)	surfactant-HEC (high M_r) ^{c,d}	1.40:0.50	250	0.63	yes	5

NOTE: VA is vinyl acetate and BA is butyl acrylate.

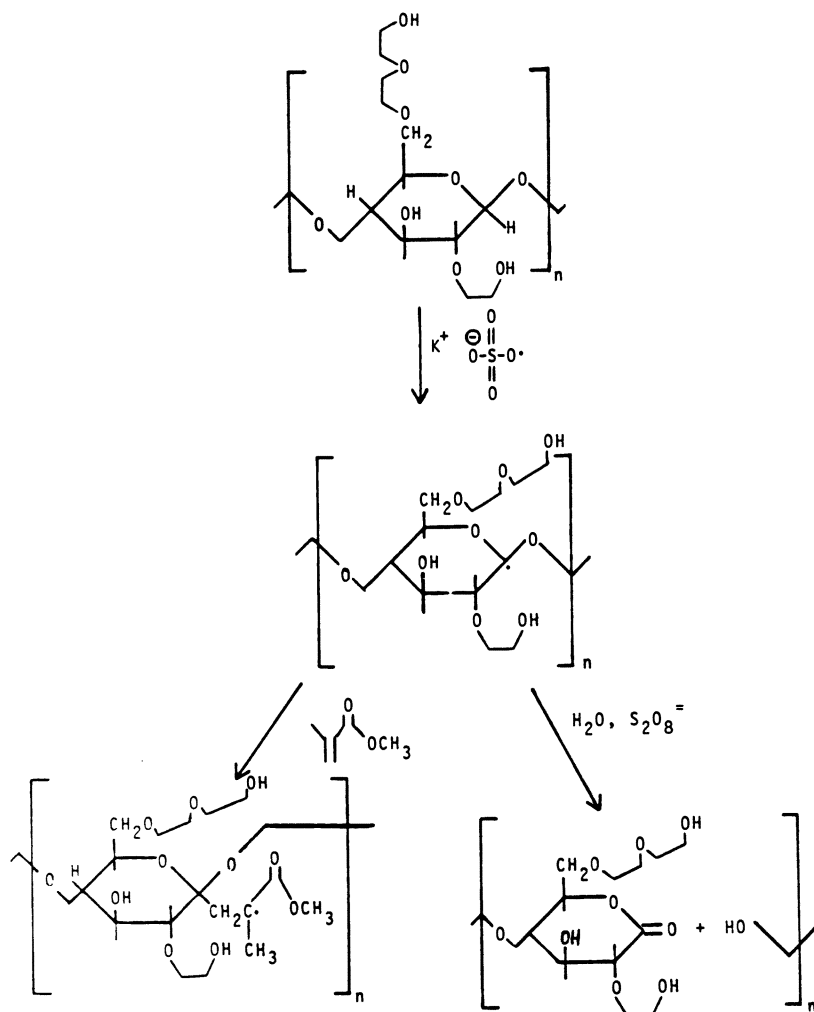
^aThe recipes are listed in Table III.

^bNatrosol 250 LR HEC.

^cThe recipes are listed in Table II.

^dNatrosol 250 MR HEC.

very little grafting of HEC occurred despite the high reactivity of HEC toward degradation in these systems. The chromatograms provided in Figure 12 show that little difference exists in the grafting or degradation reactions of HEC in the presence of vinyl acetate monomer alone versus an 85:15 mixture of vinyl acetate and butyl acrylate or in the presence or absence of surfactants. These experiments confirmed that vinyl acetate has little tendency to graft onto HEC, despite the high reactivity of the poly(vinyl acetate) radical.



Scheme I. Proposed scheme outlining the chemistry of HEC in the presence of persulfate and acrylic monomers under standard emulsion polymerization conditions.

Although the data presented are contrary to established explanations, they are completely consistent with Scheme I. Thus, free radicals generated along the HEC backbone by chain transfer from persulfate anion radicals can act as common intermediates for initiating either grafting or oxidative degradation. In the presence of reactive acrylic monomers, extensive grafting will occur unless artificially controlled via regulators such as TEA, which appear to function by preventing the formation of HEC polymer radicals in the first place. Precedence for this result already exists in the literature (26). In the presence of less reactive monomers such as vinyl acetate, significantly less HEC grafting occurs while persulfate-mediated oxidative degradation predominates. This lack of HEC grafting should not influence the well-known self-branching of poly(vinyl acetate) (4) arising from chain transfer to polymer resin, which occurs in the polymer particles and not in the aqueous phase as does the proposed scheme.

Conclusions

Under similar emulsion polymerization conditions, vinyl acetate monomer has much less of a tendency to graft to HEC relative to acrylic monomers than was previously thought. The extensive grafting of acrylic monomers to HEC produces the characteristic viscosity buildup that occurs prior to coagulation in traditional acrylic-HEC latex systems.

Acknowledgments

The help of H. G. Barth, K. V. Hannon, H. J. Goldy, E. W. Schwarz, F. S. Szczepkowski, and H. C. Tillson is greatly appreciated.

Literature Cited

1. Warson, H. *The Application of Synthetic Resin Emulsions*; Ernest Benn: London, 1972; pp 194-214, 378-415.
2. Bamford, C. H.; Barb, W. G.; Jenkins, A. D.; Onyon, P. F. *The Kinetics of Vinyl Polymerization by Radical Mechanisms*; Academic: New York, 1958; pp 238-243.
3. Fuhrman, N.; Messobian, R. B. *J. Am. Chem. Soc.* **1954**, *76*, 3281.
4. Bevington, J. C.; Guzman, G. M.; Melville, H. W. *Proc. R. Soc.* **1954**, *A221*, 437.
5. Donescu, D.; Gosa, K.; Diaconescu, I.; Carp, N.; Mazare, M. *Colloid Polym. Sci.* **1980**, *258*, 1363.
6. McGinnis, V. D.; Kah, A. F. *J. Coat. Technol.* **1977**, *49(634)*, 61.
7. Chemical Abstracts 93:222083p, Kislenco, V. N.; Berlin, A. A. *Zh. Prikl. Khim. Leningrad* **1980**, *53(9)*, 2069.
8. Chemical Abstracts 99:59529b, Kislenco, V. N.; Domanskaya, T. N.; Berlin, A. A. *Zh. Prikl. Khim. Leningrad* **1983**, *56(5)*, 1093.
9. Harris, G. C. *Am. Paint J.*, **1972** March 13, 14.
10. Chemical Abstracts 80:133908a, Mnatsakanov, S. S.; Rogova, S. G.; Shirinyan, V. T.; Ivanchev, S. S.; Rozenberg, M. E. *Vysokomol Soedin., Ser. B* **1973**, *15(10)*, 723.

11. Chemical Abstracts 85:47287u, Stepin, S. N.; Vagin, Y. L.; Maksimov, V. L.; Talmachev, I. A. *Vysokmol. Soedin., Ser. B* **1976**, *18*(5), 353.
12. Chemical Abstracts 94:4295p, Gosa, K.; Mazare, M.; Gavat, I. *Rev. Roum. Chim.* **1980**, *25*(7), 975.
13. Chemical Abstracts 97:128167e, Donesco, D.; Gosa, K.; Diaconescu, I.; Mazare, M.; Carp, N. *Emulsion Polym. Vinyl Acetate*, [Pap. Symp 1980] **1981**.
14. Chemical Abstracts 98:90530y, Jakubec, I.; Chocholaty, V. *Czech. CS* **1981**, *192*, 215.
15. Pohlemann, H.; Florus, G.; Sliwka, W.; Gellrich, M. British Patent 1 155 275, 1969.
16. Grubert, H.; Druschke, W.; Sliwka, W. U.S. Patent 3 876 596, 1975.
17. Chemical Abstracts 99:123140x, Nakamura, S. *Jpn. Kokai Tokkyo Koho JP* **1983**, *58* 57,402[83 57,402].
18. Chemical Abstracts 94:157929y, Glubish, P. A.; Poznyakevich, A. L.; Baraev, V. L.; Mzenkov, G. M.; Mikhailov, N. M. U.S.S.R. Patent 802 295, 1981.
19. Chemical Abstracts 88:171008e, Hemmings, J.; Geddes, K. R.; Butcher, G. R. British Patent 1 466 064, 1977.
20. Elser, W.; Huebner, K.; Ottofrickenstein, H.; Boessler, H. U.S. Patent 4 171 407, 1979.
21. Mueller-Mall, R.; Wendel, K.; Geelhaar, H. J.; Melan, M. U.S. Patent 4 265 796, 1981.
22. Ogata, S.; Wakabayashi, G. British Patent 1 278 813, 1972.
23. Barth, H. G. Chapter 3 in this book.
24. Dubois, M.; Gilles, K. A.; Hamilton, J. K.; Rebers, P. A.; Smith F. *Anal. Chem.* **1956**, *28*(3), 350.
25. Narders, H.; Hanzes, R. In *Addition and Condensation Polymerization Processes*; Advances in Chemistry Series 91; American Chemical Society: Washington, DC, 1969; pp 188–201.
26. Kolthoff, I. M.; Meehan, E. J.; Carr, E. M. *J. Am. Chem. Soc.* **1953**, *75*, 1439.

RECEIVED for review September 20, 1984. ACCEPTED August 14, 1985.

Advantages and Disadvantages of Associative Thickeners in Coatings Performance

F. G. Schwab

Coatings Research Group, Cleveland, OH 44114

The introduction of new coatings raw materials is usually accompanied by enthusiastic descriptions of their apparent advantages. In critical evaluations, the stated claims may be confirmed or disproved or new advantages may be discovered. Usually some disadvantages are uncovered during the long and demanding process of formulating, manufacturing, and marketing the resulting products. This review examines the effects of associative thickeners on the performance of waterborne latex coatings, from the consumer's viewpoint and from the perspective of the coatings manufacturer.

REPLACING ANY RAW MATERIAL in a coatings formulation requires as the first step the determination of all of the properties on which the raw material has an effect. This statement is obvious but is also a principle that is often ignored. Several examples illustrate this statement: (1) Basic lead silicates were formerly used in exterior latex wood primers to insolubilize wood tannins and prevent them from staining latex topcoats. When use of the lead compounds in consumer products was prohibited by law, they were replaced with various lead-free alternates. Although these substitutes blocked the tannins, sometimes as effectively as the lead materials, some formulators overlooked the fact that the basic lead silicates also contributed to corrosion resistance. As a result, some of the lead-free, stain-blocking primers exhibited severe nailhead rusting. (2) The replacement of asbestos fibers in coatings is another example. Many formulations containing asbestos substitutes fail to duplicate the performance of the asbestos-containing products because the formulators overlooked either the film reinforcement or the control of consistency properties imparted by asbestos. (3) A final example involves the nonionic surfactants of the ethoxylated phenol type. A few years ago, when

0065-2393/86/0213-0369\$06.00/0
© 1986 American Chemical Society

these surfactants were in short supply and replacements were sought, our study (unpublished data) showed that these products affected at least eight paint properties. Location of substitutes that appeared to be good equivalents was relatively easy only to find on critical examination that the substitutes failed to match the controls in one or more of eight properties important in a coating's performance.

Cellulose ethers were the dominant thickeners in latex paints for several decades. Their attributes are discussed in Chapter 17. Recently, hydrophobically modified (HM), water-soluble polymers [a generic structure of the hydrophobically modified, ethoxylated urethane (HEUR) type is given in Chapter 21] were developed that overcome some major deficiencies inherent with cellulose ethers. These new thickeners are referred to as associative thickeners in the coatings industry. Although associative thickeners present an opportunity for improving paint properties, they also have shortcomings in comparison with cellulose ethers. This overview, based on information generated in my laboratory, examines the effects of associative thickeners of the HEUR type on the application performance of latex paints; their advantages are recognized, and the compromises that must be considered in replacing the time-proven cellulose ether thickeners are discussed.

Associative Thickeners: Advantages and Disadvantages

When the various associative thickeners were introduced, the claimed advantages were fairly similar. The advantages and disadvantages observed are summarized in Table I.

Rheology. Paints containing associative thickeners have higher viscosity at the shear rates developed during application. This property keeps the applicator from spreading too little paint over too large an

Table I. Associative Thickeners: HEUR Type

<i>Advantages</i>	<i>Major Disadvantages</i>	<i>Potential Disadvantages</i>
Controlled spreading	phase separation	blocking and softer films
Improved flow, leveling	lifting or roll-up	freeze-thaw instability
Cost savings	sensitivity to variation in	color problems
Less roller spatter	formulation changes	water resistance ^a
Improved compatibility		alkali resistance ^a
Resistance to bacterial attack		wet, chalk adhesion
Convenient liquid form		exterior durability
		open time

^aThese properties are real in hydrophobically modified, alkali-swelling latex (LASHM) thickeners, which have gained acceptance in low-cost interior coatings. If the concern is the scrub resistance of and water-sensitivity of interior coatings, cellulose ethers would be the thickener of choice. In low-cost formulations, if higher viscosities at high shear rates are to be achieved, LASHM-type thickeners are the preferred types.

area with a brush or roller. Considering that the recommended film thickness for one coat of most consumer coatings is about as thick as a sheet of bond paper, the importance of proper film thickness becomes very apparent. Another advantage of associative thickeners is that they impart excellent flow and leveling to latex paints, properties not usually attainable with cellulosics. Production of latex paints with alkyd-like flow and leveling is relatively easy; however, this operation can also cause a problem: the latex paints have an after-flow tendency. The user can apply the paint, observe with satisfaction its excellent leveling, and then, several minutes later, find numerous sags that cannot be corrected because the paint has already set up. This problem can be avoided, but usually with some compromise in other properties. Using associative thickeners plus other additives (cellulosics or clays), the formulator can vary independently the high- and low-shear viscosities of a latex paint over a fairly wide range to obtain the desired rheology over a spectrum of poor- (i.e., low-cost) to excellent-quality paints.

Cost Savings. Although associative thickeners are more expensive than cellulose thickeners, lower paint costs are often obtained with the former thickeners because of their controlled spreading and improved flow properties. Because thicker, smoother films are obtained, the volume solids or the prime pigment (titanium dioxide) content can be lowered without an unfavorable effect on hiding power. This feature results in reduced raw materials costs, illustrated in Table II for commercial paints that are sold for the same end uses. Paint C contains an associative thickener.

Improved Compatibility. Improved compatibility with latices yields higher gloss and less porous films. Improved compatibility with colorants gives better acceptance of tinting colors, reduces the quantity of colorant required, and improves the color stability.

Other Advantages. Anyone who has applied paint with a roller is aware of spatter (discussed in Chapter 17), which is a nuisance that can be reduced or eliminated with associative thickeners. This property is an inherent advantage related to their low molecular weight. Another advantage is their enzymatic stability. Unlike the cellulosics, associative thickeners do not provide food for bacteria. Some associative thickeners are supplied in liquid form, which offers convenient ease of incorporation.

Major Disadvantages: Phase Separation and Picking. Oil-based paints usually show clear liquid separation and pigment settling after aging in the can, and the consumer will accept this. Latex paints are characterized as relatively free of separation and settling. Many compa-

Table II. Commercial Paints Comparison

<i>Property</i>	<i>Paint A</i>	<i>Paint B</i>	<i>Paint C</i>
Pounds of TiO ₂ /100 gallons	336	283	218
High-shear viscosity (P)	0.9	0.8	1.6
Contrast ratio ^a			
Drawdown ^b	0.985	0.969	0.954
Brushout ^b	0.972	0.940	0.969
Spreading rate of brushout (ft ² /gal.)	541	570	404

^a A value of 1 equates to complete hiding.

^b Figures are averages from three operator results. Although all three paints had the same recommended spreading rate (400 ft²/gal.), only paint C applied at that rate on brushing tests. The others were overspread by more than 35%. Paint C, containing 118 lb less of titanium dioxide/100 gal. than paint A, had approximately equal hiding to paint A because of its greater film thickness when applied by brush.

nies would not attempt to market a new latex paint that exhibits phase separation to any significant extent. Paints containing associative thickeners have a much greater tendency to separate than those thickened with a cellulosic. The separation can take several forms. A clear liquid layer can be on top, sometimes up to an inch in depth, and the colorant can also float into this layer. Pigment settling can occur. The phase separation problem is a serious one. Many formulating variables have an effect on it. Remixing is not acceptable to the consumer.

When some latex paints containing associative thickeners are applied by brush or roller over certain undercoats or aged paint layers, the deposited film is picked up on the second pass of the applicator. The newly applied paint is thus stripped away from the base coat. This property has been termed "lifting", "picking", or "roll up". This problem resulted in removal from the market of an associative thickener of the seventies (i.e., SMAT, discussed in Chapter 20). Most formulators now have proprietary techniques for bypassing this problem.

Other potential problems (listed in Table I) must be evaluated. If the two problems discussed can be overcome and the rheology is not negated by certain formulation components (discussed in Chapter 20), possibly whatever other compromises necessary can be endured, until gradual improvements in the secondary problems can be made.

Problems from a Manufacturing Viewpoint

Coatings formulators undertake a major project in trying to replace cellulose with associative thickeners. Useful practices in this process include a careful study of the effects of order of addition of ingredients, film property difference related to testing procedures, and time-dependent changes, particularly in rheological properties. With associative thickeners, a correlation among film properties (i.e., thickness, flow and leveling, gloss, and hiding) obtained from films prepared by stand-

ard industrial tests (i.e., drawdown blade procedures) and films prepared by actual application with brush or roller may not agree because the rate of deformation differences between the two preparation procedures.

When many tens of thousands of gallons of latex paint have been made in a plant over the years using familiar materials and procedures, convincing a production manager that a new method is necessary for effective use of a new raw material is sometimes very difficult. With associative thickeners, new manufacturing procedures are frequently required. Some associative thickeners are viscous materials and are difficult to handle in drums. Frequently, premixes or preneutralizations are required for best results. This step is an extra production operation.

Variations of more than 1 P in high-shear viscosity of a formula containing exactly the same types and amounts of ingredients, but made by different procedures, can occur when associative thickeners are employed. The order of addition is particularly critical with associative thickeners. Ensuring that the specified addition order is carried out in the plant may be difficult. For example, production personnel may not like the odor of a specific product and therefore add the component last, regardless of the specified procedures.

With associative thickeners, the paint viscosity will take longer to stabilize, relative to that for formulations thickened with cellulose ethers. Quality-control problems could result. Also, both low-shear and high-shear viscosities should be monitored for proper quality control. Because small variations in some ingredients (discussed in simple systems on a fundamental basis in Chapter 20) can affect the high-shear-low-shear viscosity relationship, probably new procedures will have to be established to handle factory batch adjustments. Procedures for determining complex interactions as a function of time should be established. The simplest and most sensitive tests are rheological ones.

Some associative thickeners require difficult cleanup procedures (1). For example, one associative thickener requires a mixture of ethoxy-ethanol-methanol-water, and the literature* states that best results are obtained at 80 °C (176 °F), followed by a hot water rinse at 49 °C (120 °F). Many paint plants would find these requirements extremely inconvenient. For this same thickener, the literature recommends that transfer lines be held between 60–79 °C (140–175 °F), which is also not practical in many plants.

The potential advantages to be gained with associative thickeners are very important ones. They justify the very extensive laboratory development work that is required to formulate them into waterborne latex coatings.

RECEIVED for review February 19, 1985. ACCEPTED December 9, 1985.

* Rohm and Haas Bulletin No. 81A40 "Experimental Rheology Modifier QR-708," pages 6 and 7.

Effect of Surfactants and Cosolvents on the Behavior of Associative Thickeners in Latex Systems

J. C. Thibeault, P. R. Sperry, and E. J. Schaller

Research Laboratories, Rohm and Haas Company, Spring House, PA 19477

Adsorption isotherms and viscosity-shear-rate profiles of model anionic and nonionic associative thickeners with acrylic latices are strongly dependent on the latex particle size and system surfactant and cosolvent content. The adsorption data indicate a level of latex-thickener interaction substantially greater than that with the conventional nonassociative thickener (hydroxyethyl)cellulose. Addition of sodium dodecyl sulfate surfactant or butyl Carbitol water-miscible cosolvent results in desorption of the associative thickeners from the latex surface and produces concomitant changes in rheology. These effects provide the coatings formulator with a unique means of independently adjusting the viscosity at both low shear rate (leveling, sagging, and settling) and high shear rate (brushing and film build).

FORMULATING A LATEX PAINT requires careful adjustment of the final rheology. Viscosity at high shear rates must be controlled in a narrow range to give sufficient film build and hiding without extreme brush or roller drag, while low-shear-rate viscosity must be high enough to prevent settling during storage and excessive sagging after application but low enough to allow the flow and leveling necessary for optimum appearance (1). Historically, rheological control in latex coatings has been achieved with high molecular weight water-soluble polymers such as cellulosics and polyacrylates, which thicken both by entrapping water molecules within their highly swollen polymer coils and by chain entanglement (2). Although such thickeners have been used quite successfully over the years, they suffer certain limitations with respect to their viscosity-shear rate profiles, which are inherent in their thickening mechanism (3-5).

Recently, a number of new thickeners have been developed (6) that thicken by an entirely different mechanism and that offer the coatings

0065-2393/86/0213-0375\$06.00/0
© 1986 American Chemical Society

formulator the potential for significant improvements in rheology. These thickeners are related to the traditional thickeners in that they are based on similar water-soluble polymers, although generally of somewhat lower molecular weight. The key difference is that they also contain hydrophobic groups, which allow them to associate with various other hydrophobic components of the coating. A simple illustration of some of the practical differences between conventional thickeners and associative thickeners is shown in Table I where some key rheological parameters are given for three latex paints, which are identical except for the thickener. The first paint listed contains a commercial (hydroxyethyl)-cellulose (HEC) representative of conventional thickeners. The other two contain two recently commercialized associative thickeners based, respectively, on nonionic and anionic water-soluble polymer backbones.

Stormer viscosity is a low-shear viscosity obtained from a paddle viscometer widely used in the paint industry. Shear rate, although not well-defined, is estimated to be about 50–100 s^{-1} . This is the shear-rate region that determines properties such as brush pickup and pourability and is related to what is generally regarded as the consistency of the paint. Although the Stormer viscosity is given in arbitrary Krieb units, the important point with regard to our present purpose is that the paints in Table I have been adjusted to similar low-shear viscosities by varying the thickener use level. Thus, the low-shear thickening efficiencies of our three thickeners are inversely proportional to these use levels. Clearly, associative thickeners can span a wide range of low-shear efficiencies. However, unlike conventional thickeners, this efficiency is not necessarily linked to molecular weight. Thus, the low molecular weight nonionic associative thickener is significantly more efficient at a low shear rate than the substantially higher molecular weight (hydroxyethyl)-cellulose, while the intermediate molecular weight anionic associative thickener is less efficient. We will show later that this difference in efficiency correlates with differences in the degree of associative character built into the polymers.

ICI viscosity is a high-shear-rate viscosity ($10,000 s^{-1}$) that correlates well with performance in applications processes such as brushing, rolling, and spraying. ICI viscosities can be obtained by using associative

Table I. Properties of Thickeners

<i>Thickener Type</i>	<i>M_w</i>	<i>Amt of Thickener (lb/100 gal.)</i>	<i>Stormer Viscosity (KU)</i>	<i>ICI Viscosity (P)</i>	<i>Leveling</i>
(Hydroxyethyl)cellulose	850,000	3.34	81	0.43	2
Nonionic associative	40,000	0.60	82	0.20	8
Anionic associative	400,000	4.75	83	0.90	7

thickeners that are both higher and lower than those obtained by using conventional thickeners (Table I). In a sense, however, the low value obtained with the nonionic associative thickener is misleading. If the ICI data are normalized to the same thickener use level, the nonionic associative thickener is significantly more ICI efficient in terms of poise per pound than either of the other thickeners.

As an aside, this last fact provides the basis for a very useful formulation trick. The degree of association, and therefore the low-shear-rate efficiency, of associative thickeners can be gradually decreased by the careful addition of surfactants or cosolvents. Because this means the thickener use level can be increased, and with it the ICI viscosity, while the same Stormer viscosity is maintained, a method for independently adjusting the high- and low-shear viscosities that can be of substantial practical value to the coatings formulator is obtained.

Leveling, although not a primary rheological parameter, is nevertheless an important one in characterizing the performance of a paint. Leveling is a measure of the ability of a coating to flowout after application so as to obliterate any surface irregularities, such as brush marks, produced by the application process (7). In the present case we have rated leveling subjectively on a scale of 0 to 10 by comparing brushouts of each paint to a series of standards. Because leveling is a very low shear rate process, roughly 10^{-1} s^{-1} or less, the high leveling values obtained for our two associative thickeners relative to that of the HEC imply that they have much lower viscosities at very low shear rates. This result is very general and illustrates one of the primary advantages of associative thickeners over conventional nonassociative thickeners.

The preceding illustrates some of the rheological properties characteristic of associative thickener thickened systems. In what follows, the results of some direct measurements of the degree of latex-thickener association for two model associative thickeners under various conditions are discussed, and an attempt is made to relate these results to rheological behavior. Although latex-thickener association is only one of the many associative interactions that can occur in practical associative thickener systems, under many conditions this association is the dominant interaction in terms of the overall rheological behavior of the system.

Experimental Section

Two model associative thickeners were examined in this study, one a low molecular weight ethylene oxide based urethane copolymer containing a relatively high overall weight fraction of hydrophobe and the other the ammonium salt of an anionic acrylic copolymer of significantly higher molecular weight and lower hydrophobe content. Although not identical with the commercial associative thickeners of Table I, these associative thickeners are very similar and when compared directly show virtually identical behavior. Latices employed are

approximately monodisperse with average diameters of 50, 90, 140, 300, 340, and 600 nm. All are copolymers of butyl acrylate and methyl methacrylate of approximately 0 °C glass temperature and contain about 1% of copolymerized carboxylic acid groups. These copolymers were prepared as described previously (3) with 0.4% ammonium persulfate initiator and 0.05–3.05% sodium dodecyl benzenesulfonate surfactant.

All systems were adjusted to pH 9 with ammonia. Thickener adsorption measurements were carried out by centrifuging the equilibrated thickener–latex mixtures and analyzing the separated serums for free thickener. In the nonionic case, this analysis was conducted by using a modification of a colorimetric method originally developed for nonionic polyethylene oxide surfactants (8). For the anionic case, 0.1% 9-vinylanthracene was included during the thickener synthesis to serve as a fluorescent tag. Viscosity–shear-rate curves shown are a composite of data from several instruments: a Brookfield SynchroLectric viscometer with UL adapter, a Haake Rotovisco RV2 viscometer, and an ICI cone and plate viscometer.

Results and Discussion

Figure 1 shows adsorption isotherms for the two model associative thickeners on a 300-nm-diameter acrylic latex at 25 vol % solids. Data are

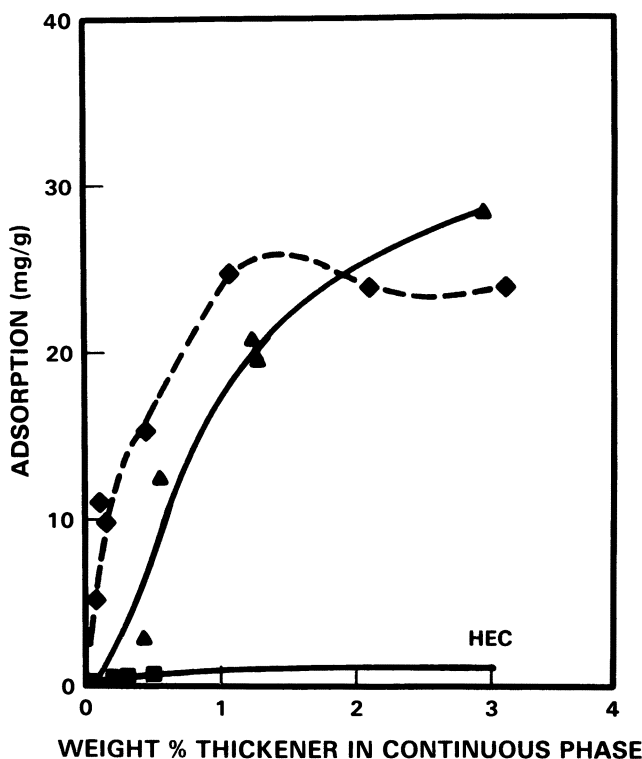


Figure 1. Adsorption isotherms for HEC, nonionic associative, and anionic associative thickeners with a 300-nm latex. Key: \blacktriangle , anionic; \blacklozenge , nonionic; and \blacksquare , HEC.

also shown for a typical nonassociative HEC thickener (Natrosol 250 GR from Hercules, Inc.) (3). The strong adsorption observed for the associative thickeners relative to that for HEC even at very low thickener concentrations is direct evidence for the associative nature of these thickeners.

The shapes of the associative thickener adsorption isotherms in Figure 1 resemble that of the classical Langmuir isotherm, with the strong adsorption observed at very low thickener concentrations gradually leveling off as the thickener level increases and the latex surface becomes saturated. Such behavior is consistent with a simple model in which localized hydrophobic sections of the predominantly hydrophilic thickener attach themselves to hydrophobic binder sites on the latex surface. Because the associative thickener molecules are multifunctional in the sense that each contains two or more hydrophobes, the result is a three-dimensional transient network in which the latex particles serve as the branch points and the thickener molecules act as the cross-links. Similar to a permanently cross-linked polymer network, these cross-links resist the stretching that must occur when the system begins to flow; thus, the cross-links contribute to the apparent viscosity of the system. Of course, the transient nature of the cross-links, that is, the fact they are continually forming, breaking, and re-forming, allows the system to flow rather than just de-form as would be the case in a permanently cross-linked system.

As a final point with reference to Figure 1, the initial slope of the adsorption isotherm is significantly greater for the nonionic associative thickener than for the anionic. Because both thickeners appear to have fairly similar saturation values, this property implies that the former is more strongly associated with the latex surface than the latter. The greater association of the nonionic associative thickener can be attributed to its higher hydrophobe content making it a more highly associative thickener than the anionic associative thickener.

Figure 2 shows viscosity-shear-rate profiles for a 300-nm latex at 25 vol % solids and containing 2% thickener by weight on the continuous phase. The extreme shear thinning behavior observed with HEC (Natrosol 250MR) is typical of thickeners of this type and illustrates their primary limitation with respect to coatings rheology. Clearly, for such a system to maintain both a high enough high-shear-rate viscosity for good film build and hiding and a low enough low-shear-rate viscosity for good leveling is impossible. The two associative thickeners, on the other hand, show a much more Newtonian profile, particularly in the low-shear-rate region, and therefore allow a more equitable balance of high- and low-shear-rate viscosity. Put in slightly different terms, if the thickener levels are adjusted so as to give similar viscosities at some intermediate shear rate (e.g., the Stormer shear rate), the two associative thickeners, because of the flatness of their rheology profiles, must give sub-

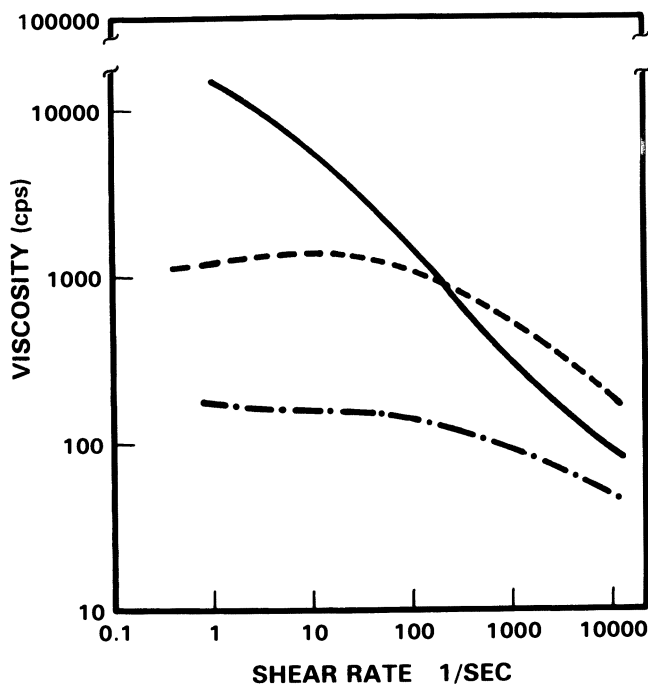


Figure 2. Viscosity-shear-rate profile for HEC, nonionic associative, and anionic associative thickeners with a 300-nm latex. Key: —, HEC; ---, nonionic; and -·-, anionic.

stantially lower viscosities at very low shear rates than HEC. This property, as discussed earlier, translates into markedly better leveling behavior.

The shapes of the latex-associative thickener rheology profiles can be understood in terms of the transient network picture of latex-associative thickener systems if two fairly reasonable assumptions are made: (1) that the viscosity of a particular latex-associative thickener system is directly related to the number of cross-links present at any given time (as is the modulus of a permanently cross-linked polymer network) and (2) that the breaking and re-forming of individual cross-links occur by both thermal and shear-induced processes. At very low shear rates, the thermal processes will clearly dominate and the equilibrium concentration of cross-links will remain approximately constant at the thermal value independent of the shear rate; the result is Newtonian-like viscosity. As the shear rate approaches and then exceeds some critical value, however, shear-induced processes will start to play a bigger and bigger role and the equilibrium concentration of cross-links will decrease rapidly with increasing shear rate, hence the sudden downward turn in

the associative thickener viscosity–shear-rate curves of Figure 2 in the $10\text{--}100\text{-s}^{-1}$ region.

One feature obvious in Figure 2 is the fact that the anionic associative thickener system is significantly less viscous than the nonionic associative thickener system despite the substantially higher molecular weight of the former. The nonionic associative thickener is a much more efficient associative thickener (for latex) than the anionic associative thickener; this feature is totally consistent with the behavior seen earlier in the paint data. Both results, of course, must be related to the conclusion reached previously from the initial slopes of the associative thickener adsorption isotherms, that is, that the nonionic associative thickener associates more strongly with the latex than the anionic associative thickener.

In addition to structural variations in the thickener, variations in the latex are also expected to affect the overall degree of association of the latex–associative thickener system. One simple variation that should have a readily rationalized effect is latex particle size. Figure 3 shows

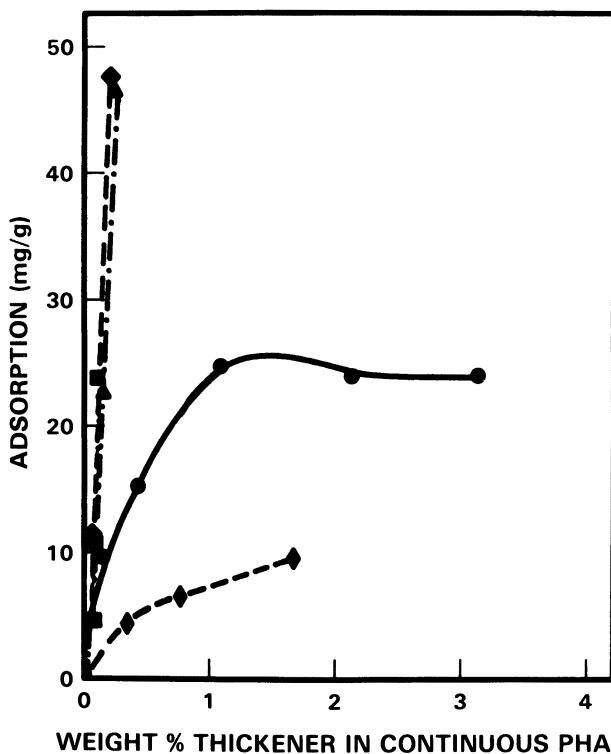


Figure 3. Effect of latex particle size on the adsorption of a nonionic associative thickener. Key: ■, 50 nm; ◆, 90 nm; ▲, 140 nm; ●, 300 nm; and ◇, 600 nm.

adsorption isotherms for our model nonionic associative thickener on five acrylic latices of particle size ranging from 50 to 600 nm. Note that both the saturation value and the initial slope appear to increase as the particle size decreases; this result indicates an increase in the degree of latex-thickener association. Such behavior is clearly due to the inverse relationship between surface area and particle size. Assuming that the average number of hydrophobic binding sites available on the latex surface per unit area depends only on the composition of the latex, one would expect the saturation value also to be inversely related to particle size. A similar result is expected for the initial slope of the isotherm if one adds the additional assumption that the latex-associative thickener binding constant is also only a function of the latex composition.

Very similar results are obtained with the anionic associative thickener as is shown in Figure 4.

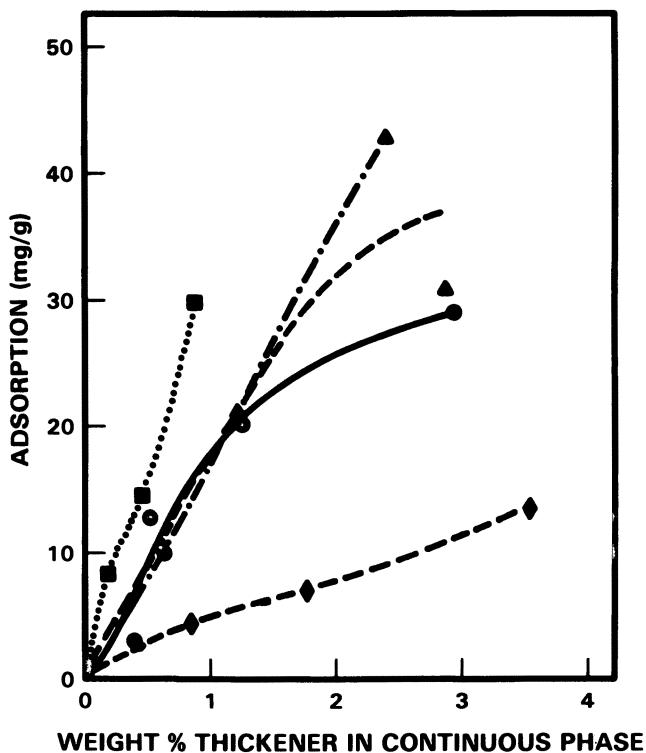


Figure 4. Effect of latex particle size on the adsorption of an anionic associative thickener. Key: ■, 50 nm; ▲, 90 nm; ---, 140 nm; ●, 340 nm; and ◆, 600 nm.

The greater association occurring with the small particle size latices should also translate into higher viscosities in much the same way that the greater association of the nonionic associative thickener yields higher viscosities than the anionic associative thickener. This feature is illustrated by the viscosity-shear-rate profiles for 25 vol % solids 50-, 90-, and 300-nm latices containing 1% nonionic associative thickener shown in Figure 5.

The results presented so far have demonstrated that, because of their totally different thickening mechanisms, the rules governing the thickening characteristics of associative thickener containing latex systems differ greatly from those based on conventional thickeners. The nature of the associative thickening mechanism also gives rise to another important practical difference between associative and nonassociative thickeners. Because hydrophobe-hydrophobe association is a nonspecific type of interaction, other hydrophobic components in the formulated coating

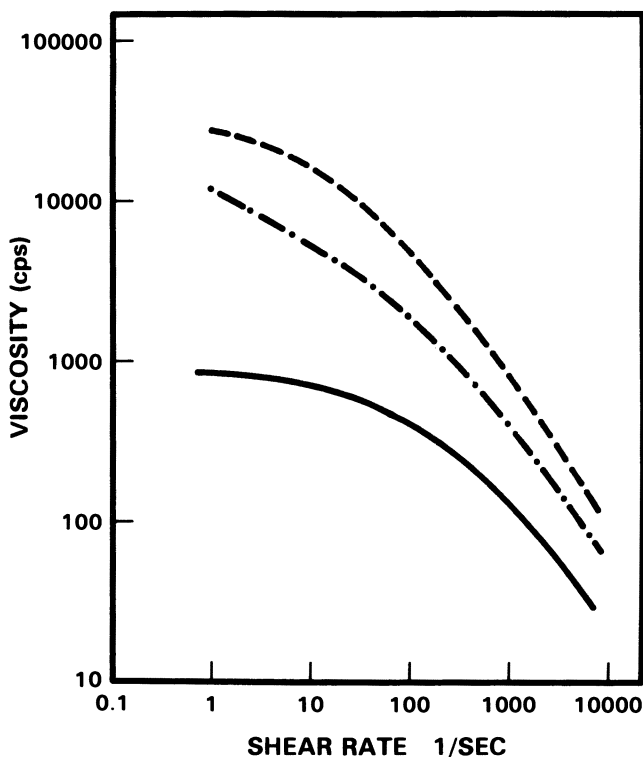


Figure 5. Effect of latex particle size on the viscosity-shear-rate profile of a nonionic associative thickener. Key: ---, 50 nm; -.-, 90 nm; and —, 300 nm.

can have a substantial effect on the final rheology when associative thickeners are present. For example, Figure 6 shows the effect of added sodium dodecyl sulfate (SDS) surfactant on the adsorption of our model associative thickeners on a 300-nm acrylic latex (either 2% anionic or 1% nonionic on continuous phase; 25 vol % solids latex). Because SDS can also bind to the hydrophobic sites on the latex surface, it competes with the associative thickener for these sites; the result is increasing desorption of the associative thickener with increasing surfactant concentration.

Note that in Figure 6 we see once again the effects of the differing associative characters of our two model associative thickeners. Although 0.5% SDS is necessary to completely displace the strongly associative nonionic associative thickener from our 300-nm acrylic latex, the same result is achieved for the weakly associative anionic associative thickener with about a 0.1% SDS. As we will show later, this feature has a profound effect on the practical behavior of these two materials.

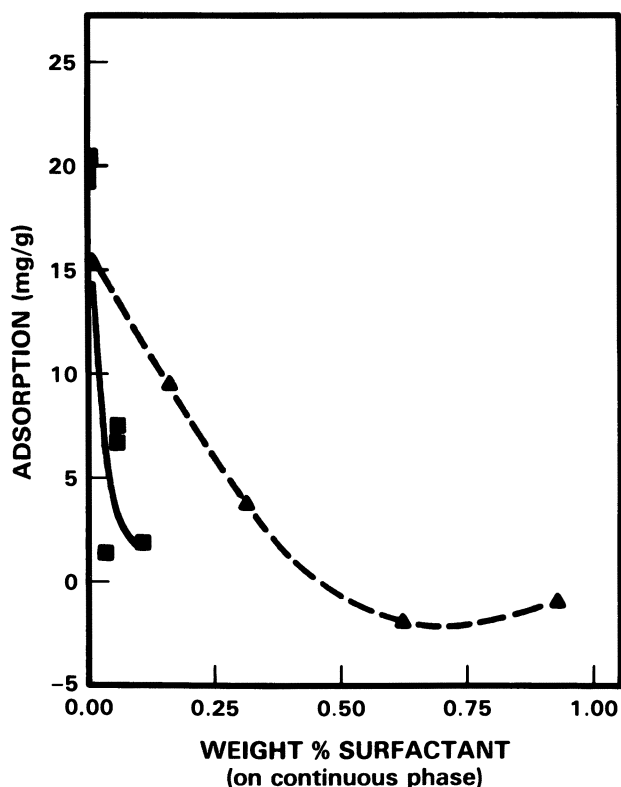


Figure 6. Desorption of nonionic and anionic associative thickeners from a 300-nm latex by sodium dodecyl sulfate. Key: ■, anionic; and ▲, nonionic.

The effect of differing degrees of associative interaction on the ability of a latex-associative thickener system to resist surfactant-induced desorption can also be seen with reference to latex variations. SDS desorption curves for our model nonionic associative thickener as a function of latex particle size are shown in Figure 7 (conditions identical with those of Figure 6). Consistent with the adsorption isotherms, which show a decrease in the magnitude of latex-thickener association with increasing particle size, the amount of SDS needed to completely displace the thickener also decreases with increasing particle size.

Figure 8 shows the effect of the SDS desorption illustrated in Figures 6 and 7 on rheology. The rapid decrease in the low-shear (100-s^{-1}) viscosity of the nonionic associative thickener (AT) with added SDS is clearly a result of the associative thickener desorption process. Note that the viscosity bottoms out at about 0.5% SDS, the same level necessary for complete associative thickener desorption. The somewhat different

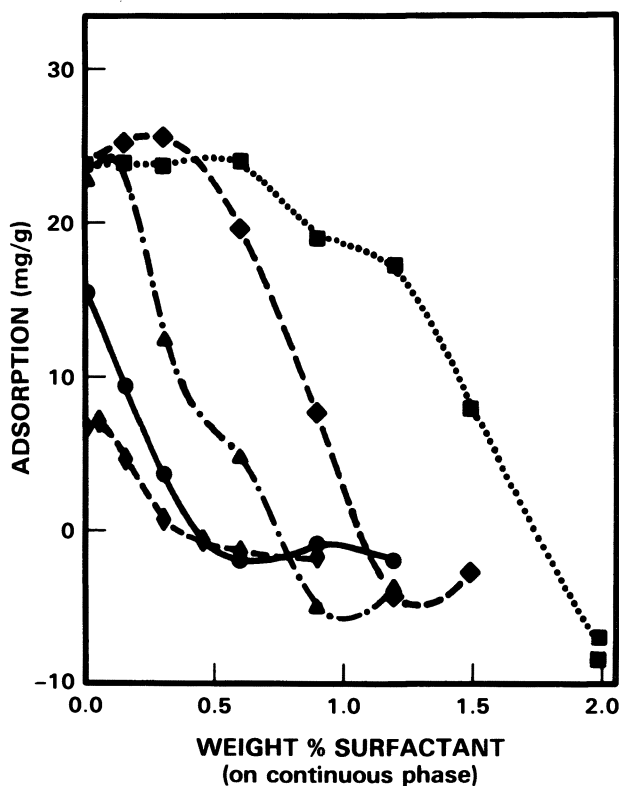


Figure 7. Desorption of a nonionic associative thickener from various particle size latices by sodium dodecyl sulfate. Key: ■, 50 nm; ◆, 90 nm; ▲, 140 nm; ●, 300 nm; and ◆, 600 nm.

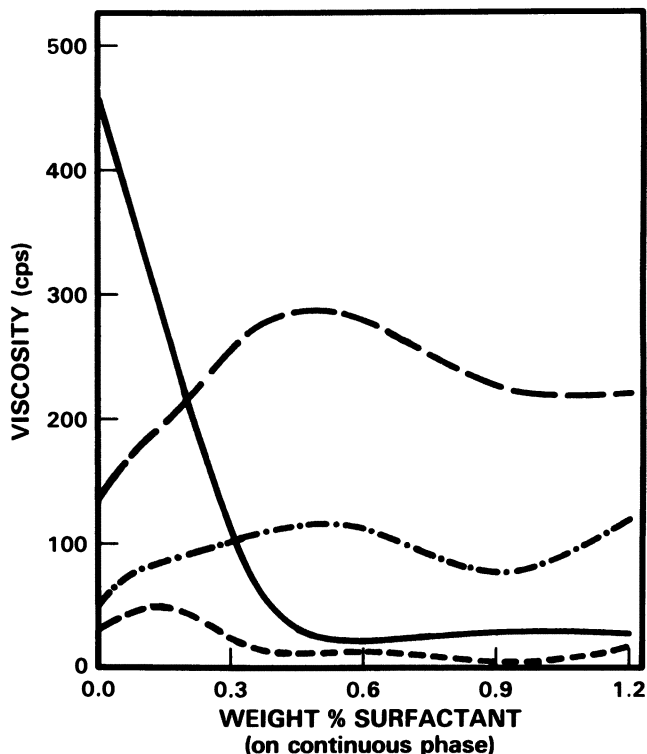


Figure 8. Effect of sodium dodecyl sulfate on the viscosity of a 300-nm latex with associative thickeners. Key: —, nonionic/low shear; ---, anionic/low shear; -·-, anionic/high shear; and ···, nonionic/high shear.

shape of the nonionic-high-shear curve is due to the fact that at very high shear rates ($10,000 \text{ s}^{-1}$) the AT-latex association contributes very little to the overall viscosity of the system. Thus, the principal effect of SDS on high-shear viscosity is not due to AT desorption but rather to other phenomena beyond the scope of the present discussion.

A somewhat similar explanation can be used to rationalize the shape of the anionic-low-shear curve. Because our model anionic associative thickener is both much more weakly associative and of higher molecular weight than our model nonionic associative thickener, it thickens less by the associative thickener-latex association mechanism and more by the traditional hydrodynamic volume mechanism. Thus, even large changes in the level of associative thickener adsorption result in only small changes in the total viscosity, and once again the overall shape of the curve is controlled by other phenomena.

Even though the weak association of our model anionic associative thickener contributes very little to the overall viscosity of the system, this

association is extremely important in determining the shape of the viscosity-shear-rate profile. The significance of this result is illustrated in Figure 9, which shows the effect of added SDS on the Stormer viscosity and leveling behavior of two associative thickener thickened gloss paints. Note that although the paint containing the anionic associative thickener shows a stable Stormer viscosity out to quite high surfactant levels, leveling is impaired substantially at lower surfactant levels. The explanation for this impairment has, of course, to do with the fact that the anionic associative thickener is displaced from the latex surface by the SDS. Once complete displacement has occurred, the associative thickener is in effect no longer an associative thickener and begins to take on the poor leveling characteristics of a high molecular weight water-soluble polymer.

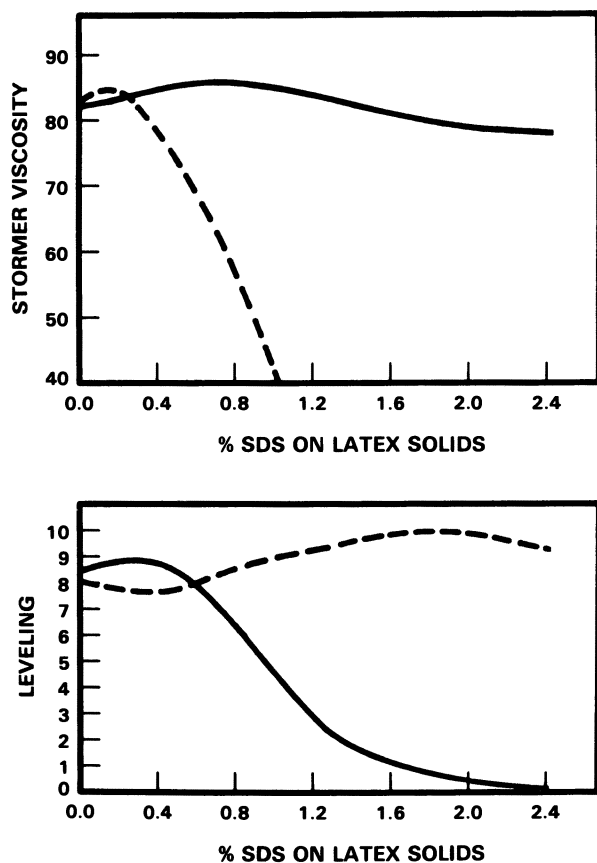


Figure 9. Effect of sodium dodecyl sulfate on the rheology of associative thickener based paints. Key: —, anionic; and ---, nonionic.

Figure 9 also illustrates another interesting point with regard to the practical behavior of associative thickener thickened systems. Note that for the nonionic associative thickener adding surfactant leads to a sharp decrease in viscosity but has little effect on flow, while for the anionic associative thickener the converse is true. This rather profound difference in behavior can be explained by invoking nothing more than the differences in the associative character of the two associative thickeners. Thus, the nonionic associative thickener, which is strongly associative and owes essentially all of its thickening ability to latex-thickener association, loses this ability rapidly as this association is weakened by surfactant. However, because the associative thickener associates so strongly, it is never completely displaced from the latex at any realistic surfactant levels and always manages to retain at least some vestiges of its associative nature and the excellent flow which accompanies it. The anionic associative thickener, on the other hand, is less associative, losing its flow more readily. But, because the associative thickener gains little in the way of thickening power from its association with the latex in the first place, it has little to lose when that association is broken.

Effects similar to those illustrated in Figures 6–9 are also seen when water-miscible cosolvents are added to associative thickener-latex systems. This effect is illustrated in Figure 10 for butyl Carbitol and our

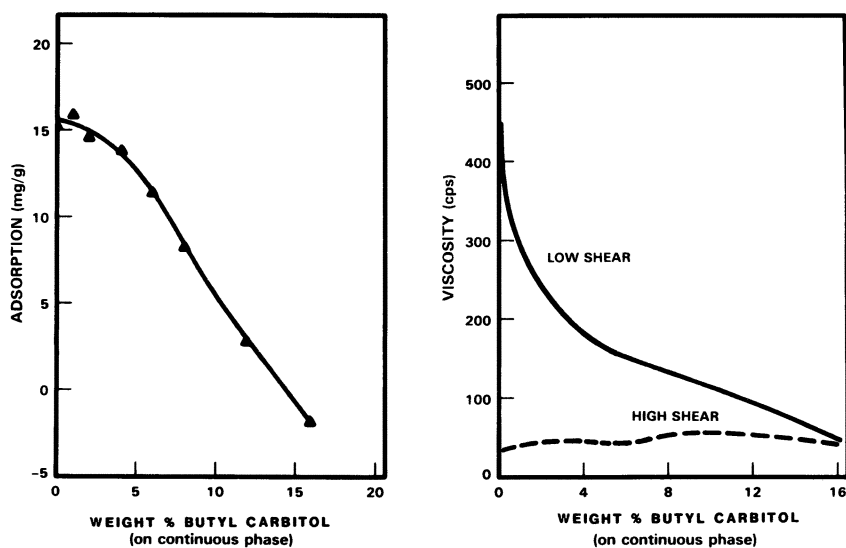


Figure 10. (left) Desorption of a nonionic associative thickener from a 300-nm latex by butyl Carbitol. (right) Effect of butyl Carbitol on the viscosity of a 300-nm latex with a nonionic associative thickener. Key: —, low shear; and ---, high shear.

model nonionic thickener (conditions identical with those of Figure 6). Even though the gross behavior appears similar, the underlying reasons for this behavior may be quite different. Thus, probably, especially in view of the substantial levels of solvent needed to bring about significant associative thickener displacement, the cosolvent effect results from changes in the partitioning of the associative thickener because of changes in the nature of the solvent phase rather than any direct competition between the cosolvent and the associative thickener for latex binding sites as is believed to be the case with surfactants.

Literature Cited

1. Patton, T. C. *Paint Flow and Pigment Dispersion*; Wiley: New York, 1979; p 355.
2. Molyneux, P. In *Chemistry and Technology of Water-Soluble Polymers*; Finch, C. A., Ed.; Plenum: New York, 1983; p 1.
3. Sperry, P. R.; Hopfenberg, H. B.; Thomas, N. L. *J. Colloid Interface Sci.* **1981**, *82*, 62.
4. Blake, D. M. *J. Coatings Technol.* **1983**, *55*, 33.
5. Massouda, D. F.; Sercel, F. J.; Graybeal, C. J. *Modern Paint Coat.* **October 1980**, 116.
6. *The Influence of Associative Thickeners and Rheology on Coatings Performance*; Glass, J. E., Ed.; North Dakota State University: Fargo, ND, 1983.
7. Wu, S. *J. Appl. Polym. Sci.* **1978**, *22*, 2783.
8. Baleux, B. *C. R. Acad. Sci.* **1972**, *Ser. C 274*, 1617.

RECEIVED for review August 15, 1985. ACCEPTED September 28, 1985.

Influence of Water-Soluble Polymers on Rheology of Pigmented Latex Coatings

J. E. Glass

Department of Polymers and Coatings, North Dakota State University,
Fargo, ND 58105

The components of a coating are examined with respect to the mechanism each exhibits in determining the rheological response of the total formulation. In particular, the sensitivities of formulations containing hydrophobically modified, water-soluble polymers are addressed. The sensitivities are examined systematically with variation in the following formulation components: pigment volume concentration, percent nonvolatiles, formulation stabilizers (i.e., dispersant and surfactant levels), latex type and size distribution, and thickener type and molecular weight. A quantitative interpretation of the sensitivities observed across this broad-spectrum investigation cannot be offered because there are too many variables with matrix interactions that are difficult to quantify statistically, but general trends in this new area of technology are discussed.

THE INFLUENCE OF VARIATION IN FORMULATION COMPONENTS on coating rheology and on the sensitivity of formulations containing hydrophobically modified, water-soluble polymers (known in the coatings area as associative thickeners) will be discussed in this chapter. Hydrophobically modified, acid-swellable latex thickeners will not be discussed.

A multiplicity of interactions can influence the associations of a water-soluble polymer (*note* the general discussion in Chapter 5) with the dispersed components of a coatings formulation. In pigmented waterborne latex coatings, this matrix of interactions can potentially interrupt the association between the hydrophobes of the hydrophobically modified, water-soluble polymer and the latex. If higher surface energy pigments, particularly TiO_2 , are not properly stabilized, adsorption will occur on these higher energy surfaces. Low molecular weight copolymers containing carboxylate groups are added to the formulation to ensure pigment dispersion. A formulation surfactant also is added to

0065-2393/86/0213-0391\$07.50/0
© 1986 American Chemical Society

ensure dispersed component stability. The formulation surfactant is generally a nonionic ethoxylate type, whereas the surfactant used in the synthesis of the latex is anionic or an anionic-nonionic combination. As discussed in Chapter 5, nonionic surfactants will generally displace anionics from the surface of latex particles. If the high-energy pigment surfaces are suitably stabilized, association between the hydrophobes of the hydrophobically modified, water-soluble polymer and the latex is favored on a statistical basis. A cohesive interaction between the stabilizing moieties and the hydrophobes of the thickener appears to be important if the desired properties of the coating are to be obtained.

With the multitude of components in a pigmented waterborne latex coating, direct evidence of association is difficult to obtain. Indirect evidence is found in the comparison of rheological profiles (Figure 1) and thickening efficiency data (Table I) in the formulations containing a small (117-nm)-particle latex. Higher high-shear-rate viscosities (HSVs) and lower low-shear-rate viscosities (LSVs) are observed with water-soluble polymers containing hydrophobes at thickener concentrations comparable to those of cellulose ethers required to achieve a given Krieb unit (KU) viscosity (an industrial measurement practice in formulating waterborne coatings). Without hydrophobe modification, low molecular

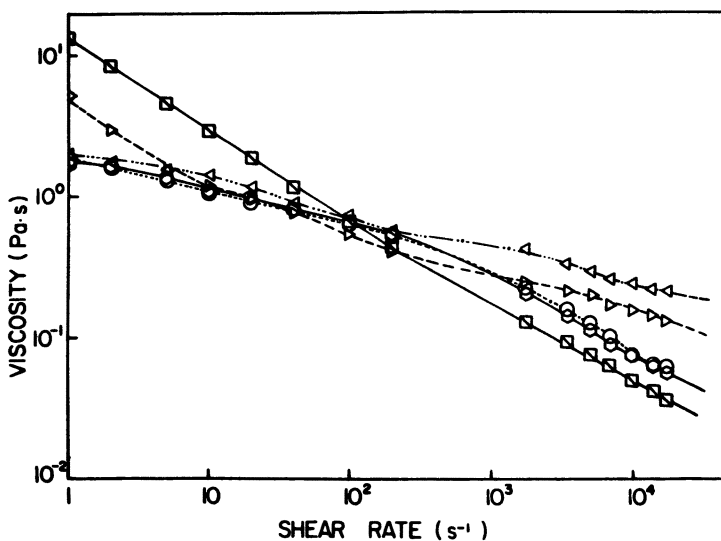


Figure 1. Viscosity (Pa s) dependence on the shear rate (s^{-1}) of an interior coating formulation: 57% PVC, 32% NVV, 90-KU-containing small-particle (100-nm), all-acrylic latex. Water-soluble thickeners: (◻) (Hydroxypropyl)-methylcellulose; (○) SMAT; (◐) HEUR 708; (◁) $M_n 10^4$ poly(oxyethylene); and (▷) $M_n 10^5$ poly(oxyethylene). Reproduced with permission from reference 11. Copyright 1984 Oil and Colour Chemists' Association.

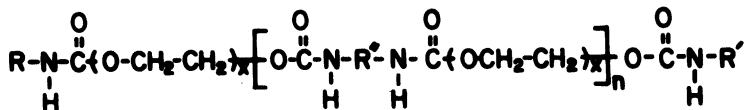
Table I. Thickener Studies for Mechanistic Interpretation

Thickener	Concn (wt %)	24-h Viscosity (KU)
$M_r 1.8 \times 10^4$ poly(oxyethylene)	7.51	92
$M_r 1.0 \times 10^5$ poly(oxyethylene)	3.10	89
HEUR 708	0.40	91
SMAT	0.46	93
HPMC ^a	0.36	93

^aHPMC is (hydroxypropyl)methylcellulose.

weight (18,000) poly(oxyethylene) (POE) provides the lower LSV and higher HSV desired, but the rheology is related to the concentration (7.5 wt %) and molecular weight of the thickener employed, not to an association. The coating thickened with this molecular weight POE imparts rheology approximately equal to those containing hydrophobically modified, water-soluble polymers, but the latter are effective at a 10-fold lower concentration. An increase in POE molecular weight (100,000) decreases the amount required to effect a given Krieb unit viscosity (a viscosity associated with a moderate 25–75-s⁻¹ shear rate), but the LSVs increase and HSVs decrease, a general phenomenon noted in small-particle latex formulations thickened with nonmodified water-soluble polymers. The generic structures of two hydrophobically modified thickeners [an ethoxylated urethane (HEUR 708) and a modified styrene–maleic acid terpolymer (SMAT)] are illustrated in structures I and II. Both hydrophobically modified, water-soluble polymers are effective in promoting the rheological response (Figure 1) of the lower molecular weight POE without large amounts of either hydrophobically modified, water-soluble polymer required to achieve the standard formulation Krieb unit viscosity.

These changes and the sensitivities that arise in coatings with hydrophobe modification of water-soluble polymers are reviewed to



$$\text{R} = \text{C}_{12} - \text{C}_{18}$$

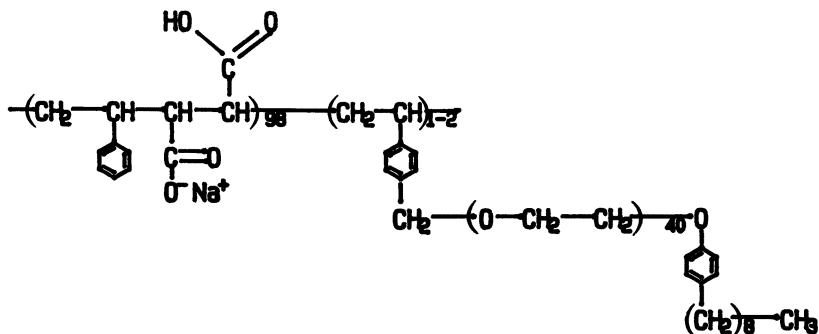
$$\text{R}' = \text{C}_{12} - \text{C}_{18}$$

$$\text{R}^{\circ} = \text{C}_7 - \text{C}_{36} \quad \text{: Structures are all encompassing}$$

$$x = 90 - 455$$

$$n = 1 - 4$$

I



understand the individual contributions and the combined interactions of formulation components on a coating's rheology.

Influence of Thickener-Dispersed Component Interactions on Low-Shear-Rate Viscosities

General. A Weissenberg rheometer has been employed (1, 2) to simulate conditions during application of a coating. The coating is sheared at a comparatively high rate (ca. 3000 s^{-1}); after a constant viscosity response is reached, the deformation is instantaneously changed to a low deformation rate (via an oscillatory mode) and the viscous and elastic responses are observed with time.

HSV's and LSV's are affected by several formulation variables. The influence of the two key components, the thickener and the latex, and their synergies, on the low deformation rate recovery (3) of the applied coating is illustrated in Figure 2. The three thickeners are an acrylic acid-ethyl acrylate copolymer, HEC, and an alkali-swellable latex that has expandable surface acid segments and is not hydrophobically modified. Their influence on the coating's recovery response in the protective colloid stabilized, vinyl-acrylic latex formulation is understandable in terms of the thickener's degree of solvation by water and decreased self-association. A surprisingly strong relationship (3) between the coating's flowout and the proximity of the thickener's solubility parameter to that of water [17-23 (kcal/cm³)] was noted. With the high elastic response of the latex-acid swellable thickener (which is not hydrophobically modified), the influence of latex particle size on the formulation's rheological response is negligible.

The other latex investigated in this study (response illustrated in Figure 2) is that of a small (117-nm) all-acrylic resin. Small-particle latices were preferred in the early 1960s because of their better pigment binding efficiency. The high elastic response of the small-particle latex

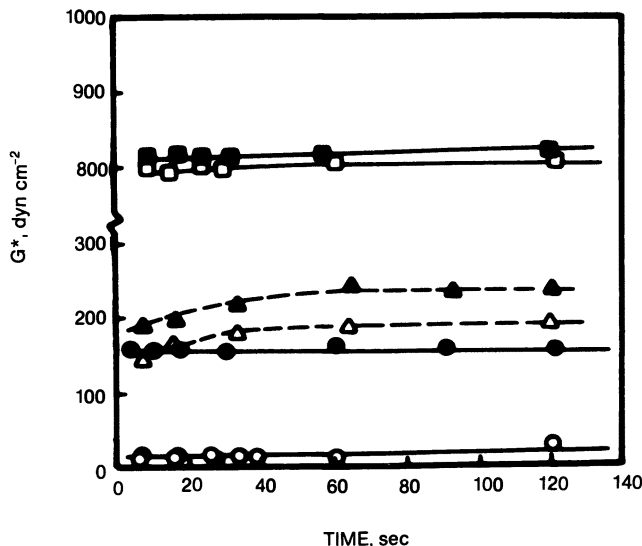


Figure 2. Time dependence of G^* recovery: I 1212 paints; 90 $\bar{K}U$. Strain amplitude is 28 μm . Open symbols, 347-nm vinyl acetate-butyl acrylate (BMD) latex with HEC-stabilizing segments chemically attached to the surface; closed symbols, 117-nm all-acrylic (SMD) latex. Thickener: (\circ , \bullet) acrylic acid-ethyl acrylate copolymer (PAAC), (Δ , \blacktriangle) HEC; and (\square , \blacksquare) alkali-swellaible latex thickener (MAP). Reproduced with permission from reference 14. Copyright 1978 Federation of Societies for Coatings Technology.

even with the most hydrophilic thickener is the consequence of flocculation of the small-particle latex, which results in poorer flowout, and a film integrity dependent on the thinnest sections of the film.

Parameters influencing the flowout time of a coating that could be controlled by formulation components are shown in equation 1 (4):

$$t_{1/2} = \eta / \sigma X^3 \quad (1)$$

where $t_{1/2}$ is the half-life (s) for an amplitude decrease in surface irregularity; η is the non-Newtonian viscosity (Pa s) (the influence of the elastic component on the response was not recognized); σ is the surface tension at the coating-air interface; and X is the film thickness of the applied coating. The film thickness is primarily influenced by the coating's HSV, which can be affected by the median particle size (5) of the latex. Thus, the better pigment binding efficiency of small-particle latices sought by coatings chemists of the 1960s is offset by their poor flowout produced by unfavorable viscosities at both high and low shear rates (5) (Figure 3).

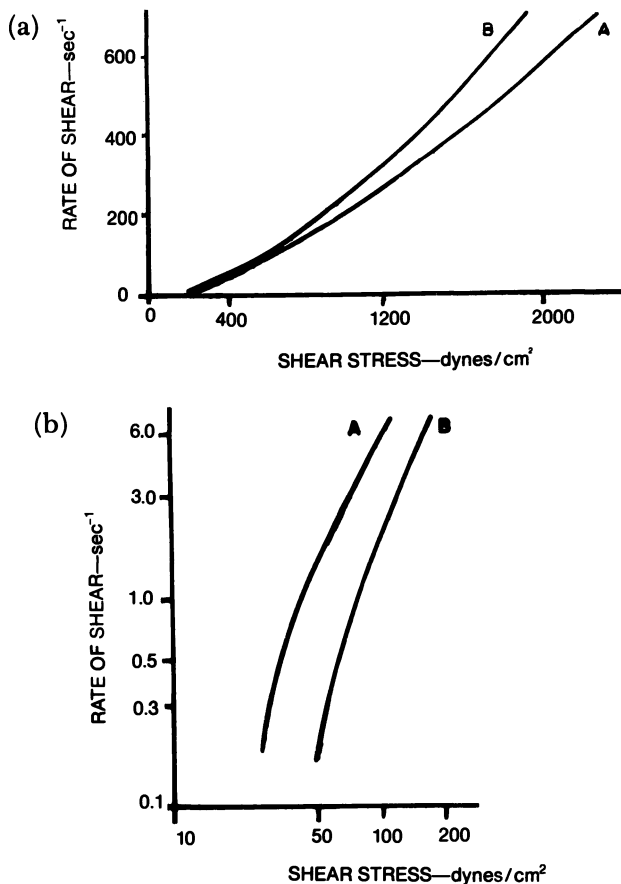


Figure 3. Viscosity dependence on particle-size distribution: (a) high shear rate and (b) low shear rate. Curve A is paint with 0.63- μ m latex. Curve B is paint with 70% 0.63- μ m latex and 30% 0.103- μ m latex.

As waterborne latex coatings improved to gradually dominate all segments of the trade-sales market, the inability to achieve good flowout with small particle size latices was mechanistically interpreted as an interbridging phenomenon (6-9). In the early 1970s, one of the manufacturers of cellulose ethers introduced (10) SMAT. The termonomer was a hydrophobe-modified styrene moiety obtained from the reaction of a nonylphenol ethoxylate (40 mol average) oxyanion with vinylbenzyl chloride. During the same approximate time period, HEUR, another hydrophobe-modified water-soluble polymer, was introduced to the European coatings industry.

The influence of both types of hydrophobe-modified water-soluble polymers on the rheology of a small particle size latex is illustrated in

Figure 4; the viscosities at low shear rates are lower and viscosities at high shear rates are higher than observed in formulations prepared from the same grind but thickened with a cellulose ether. The molecular weight, molecular weight distribution, and surface tension of aqueous hydrophobe-modified, water-soluble polymers are given (11) in Table II.

Mechanistic Interpretation of LSV Response. The lower LSVs produced by the hydrophobically modified, water-soluble polymers can be interpreted in terms of an elastic response (as reflected in first normal stress differences, N_1) of the coating formulation. In dispersions containing only a water-soluble polymer and an HEC-stabilized latex, the slope approaches a value of 2 at low shear rates (Figure 5). This relationship is defined (12, 13) in equation 2

$$N_1 = \Psi \dot{\gamma}_{21}^2 \quad (2)$$

where N_1 is the first normal stress difference (Pa), Ψ is its coefficient, and $\dot{\gamma}_{21}$ is the shear rate (s^{-1}). In a series of commercial paints (14), such a relationship was not observed (Figure 6) and the N_1 behavior was interpreted in terms of yield stress characteristics. In studies comparing hydrophobically modified, water-soluble polymer and cellulose ether

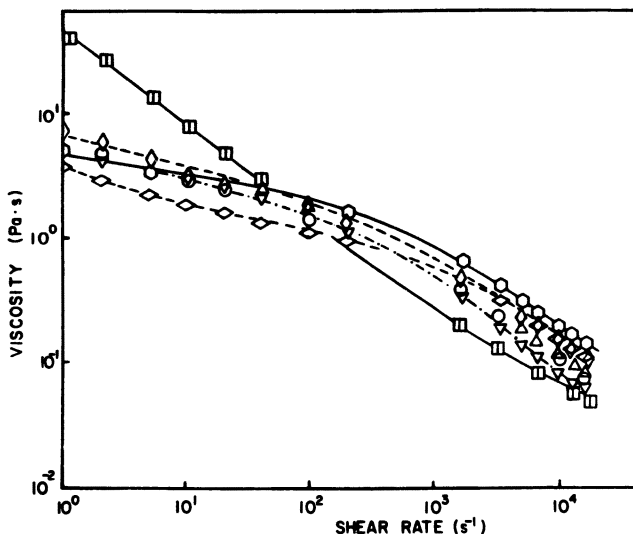


Figure 4. Viscosity (Pa s) dependence on the shear rate (s^{-1}) of an interior formulation: 57% PVC, 32% NVV, 120-KU-containing small-particle (117-nm), all-acrylic latex. Water-soluble thickeners: (□) HEC-MHR; (○) SMAT; (◐) HEUR 708; (◇) HEUR 200; (◇) HEUR 100; (△) HEUR L 75; and (▽) HEUR LR 8500. Reproduced with permission from reference 11. Copyright 1984 Oil and Colour Chemists' Association.

Table II. Molecular Weight and Surface Tension Data of Aqueous Solutions (0.1 wt %) of Synthetic Thickeners

<i>Thickener</i>	M_w	M_n	<i>Polydispersity</i> (M_w/M_n)	<i>Surface Tension</i> (mN/m)
HEUR 100	10,848	8,679	1.3	49
HEUR 200	93,992	46,638	2.0	56
HEUR 708	37,051	23,216	1.6	54
SMAT	32,331	6,395	5.1	58

thickened formulations, the predicted slope is approached in the hydrophobically modified, water-soluble polymer thickened coatings (Figure 7); thus, these thickeners are effective in inhibiting flocculation of the dispersed components and thereby yield stress behavior. The elasticity reflected in the complex modulus recovery data (Figure 4) is also reflected in $N_1-\dot{\gamma}$ (Figure 8) analysis of the same coatings (i.e., the slope approaches 2 in the protective colloid stabilized, vinyl acetate-acrylate latex formulation when the thickener is the well-solvated acrylic acid-ethyl acrylate copolymer) paralleling the low G^* recovery.

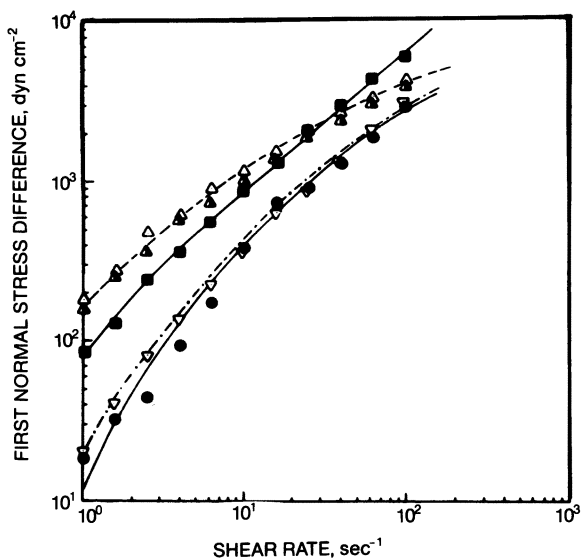


Figure 5. First normal stress difference dependence on the shear rate of aqueous water-soluble polymer solutions thickened to ~ 127 KU. The aqueous solutions also contained a vinyl-acrylic latex in amounts equivalent to that used in formulation I 1212. For latex and thickener identification, see the legend to Figure 2. Reproduced with permission from reference 14. Copyright 1978 Federation of Societies for Coatings Technology.

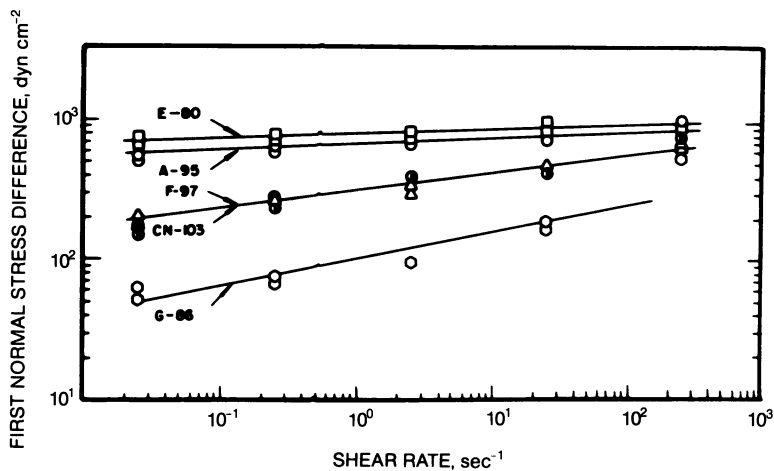


Figure 6. Shear-rate dependence of the first normal stress difference (commercial trade-sale paints). Key: \square , E-80; \circ , A-95; \triangle , F-97; \bullet , CN-103; and \circ , G-86. Reproduced with permission from reference 14. Copyright 1978 Federation of Societies for Coatings Technology.

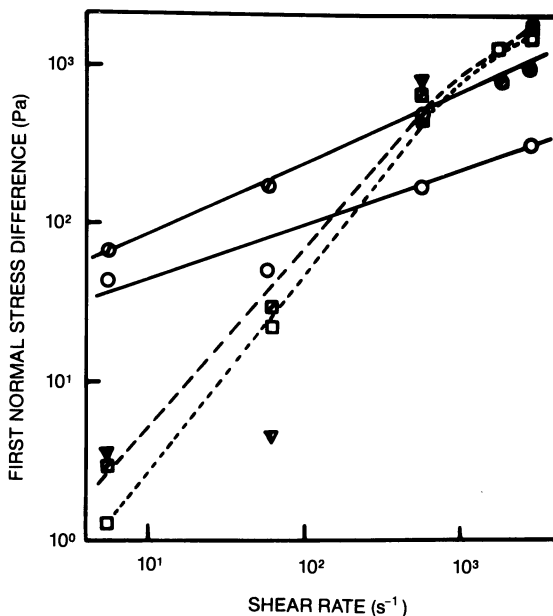


Figure 7. Shear-rate dependence of first normal stress difference of interior formulations containing small-particle (117-nm), all-acrylic latex. Water-soluble thickeners: (\circ , \circ) HEC; (∇ , ∇) SMAT; and (\square , \square) HEUR 708. Open symbols, 90 KU; hatched symbols, 105 KU.

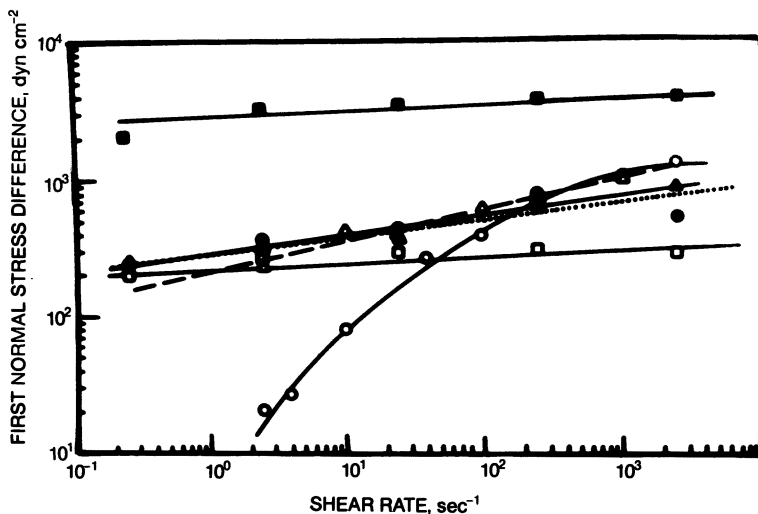


Figure 8. Shear-rate dependence of the first normal stress difference of an interior formulation (90 KU). For latex and thickener identification, see the legend to Figure 2. Reproduced with permission from reference 14. Copyright 1978 Federation of Societies for Coatings Technology.

An alternative explanation to the interparticle bridging phenomenon commonly cited by coatings chemists for the poor flowout of small particle size latices and a viable explanation of these data can be found by the integration of several individual research studies. In the late 1950s theoretical (15) arguments based on entropy concepts predicted phase separation of high molecular weight polymer solutions containing latex. Experiments in simple unpigmented systems (16-18) have supported the concept; recent additional refinements (19, 20) have been reported.

With either the SMAT- or HEUR-type thickeners, the hydrophobe moieties are capable of exchanging or interacting with the stabilizing surfactant, particularly if the stabilizer is an anionic surfactant, commonly used in the synthesis of small-particle latices. Cohesive interactions with the surfactant(s) stabilizing the latex would anchor that part of the hydrophobe-modified, water-soluble polymer to the surface, particularly at low shear rates. With an increasing number of hydrophobes attached to a given hydrophobically modified, water-soluble polymer, greater stability of the association would be realized, and this feature, combined with a greater number of contiguous, solvated oxyethylene chains peripherally blanketing the dispersed components, could be expected to provide greater stability to the small-particle latex to flocculation. Flocculation of the dispersed components would have increased their effective volume fraction by inclusion (and thereby removal) of the

continuous aqueous phase, increasing viscosities at low deformation rates (21, 22). If the hydrophobically modified thickeners associate with the dispersed components of the formulation and provide osmotic stabilization (discussed in Chapter 5) to inhibit flocculation, the LSVs would remain low, with better flowout of the applied coating.

Thickener Influence on HSV. The thickener's influence on the coating's HSV is important. A higher HSV inhibits overspreading during application, and via a thicker film, HSV also influences the flowout of the applied coating (equation 1).

With conventional water-soluble polymers, the HSV is determined by the amount used to thicken the formulation to a given *Kreb* unit; this amount is controlled by the molecular weight and conformational flexibility of the macromolecule. With lower molecular weight thickeners, greater quantities can be added and higher HSVs achieved (2) (Figure 9). Combinations of molecular weights and chemical types can therefore be used to balance the economics of achieving HSVs and influencing the flowout of the applied coating. The relationship delineated in Figure 9 is valid across a broad spectrum of water-soluble polymers. The commonality is that the thickener must be a true polymer (i.e., >30,000 in molecular weight) and devoid of pendant hydrophobe units.

The incorporation of pendant surfactant hydrophobes in a water-soluble polymer removes the HSV limitation. This removal is illustrated clearly if formulations [at a 35% pigment volume concentration (PVC)] are prepared at four *Kreb* unit levels (80, 90, 105, and 120) and their HSVs presented as a function of the amount of thickener required (11) to achieve each *Kreb* unit viscosity (Figure 10). If the thickener remains associated with the dispersed components at high shear rates, their effective hydrodynamic radii will be larger than the totally dispersed components, and higher HSVs will be realized.

Sensitivity of Hydrophobically Modified, Water-Soluble Polymer Thickened Formulations

Formulations thickened with hydrophobically modified, water-soluble polymers are sensitive to component changes. The sensitivity includes variation in rheological and applied film properties to changes in PVC (11, 23), latex type and particle-size characteristics (24), dispersant and formulation surfactant types and levels (22), percent nonvolatiles (25), the cosolvent employed when adding colorants, etc. Examples are given in the following sections for the first four variables.

Pigment Volume Concentration. Although most of the hydrophobically modified, water-soluble polymer thickened formulations provide a

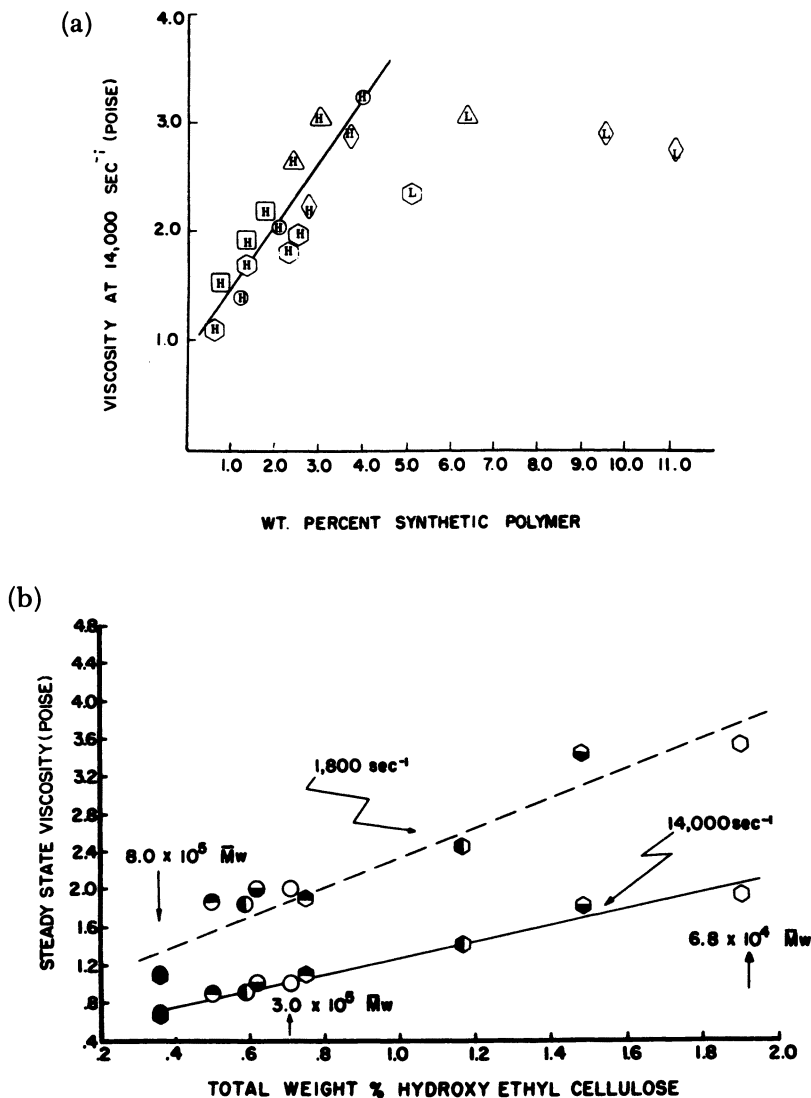


Figure 9. High shear viscosity dependence on the chemical structure of synthetic water-soluble polymers and molecular weights. (a) Synthetic polymers: (○) polyoxyethylene (POE); (△) 89% vinyl alcohol-vinyl acetate (11% copolymer (PVAI); (□) 99% PVAI; (◇) PVP; and (⊙) SMA-Na₂⁺. Mean molecular weight of synthetic water-soluble polymers: H = greater than 0.4×10^5 ; and L = less than 0.4×10^5 ; (b) Blends of different molecular weight HECs. Reproduced with permission from reference 2. Copyright 1975 Oil and Colour Chemists' Association.

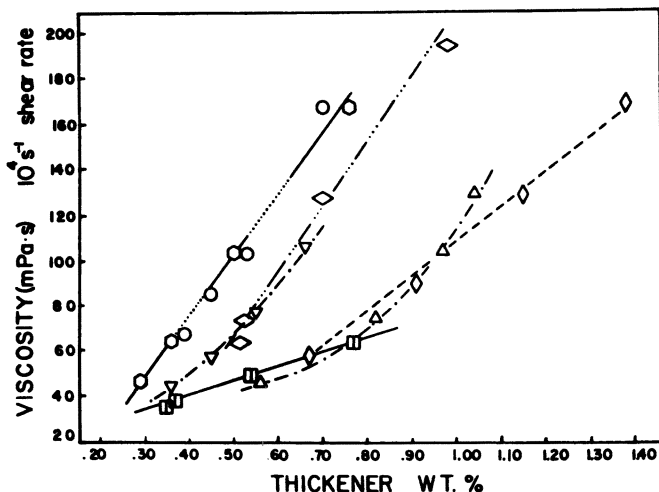


Figure 10. Viscosity (Pa s) at 10^4 s^{-1} shear-rate dependence on the weight percent thickener required to attain Stormer viscosities of 80, 90, 105, and 120 KU in a 35% PVC interior formulation. Component symbols are given in the legend to Figure 4. Reproduced with permission from reference 11. Copyright 1984 Oil and Colour Chemists' Association.

HSV-weight percent relationship comparable or superior to that of a cellulose ether thickened formulation, a sensitivity to variations in PVC exists (compare Figures 10, 11, and 12) in most hydrophobically modified, water-soluble polymer thickened coatings. Only SMAT and one of the HEUR types maintain a general HSV-weight percent insensitivity to variation in PVC.

The sensitivity to PVC variation cannot be understood in terms of thickener molecular weight or surface tension data (Table II). A limited interpretation can be made by returning to the viscosity-shear-rate profiles and by examining the yield stress peculiarities of some hydrophobically modified, water-soluble polymer thickened coatings. In the 35% PVC formulations, variations among hydrophobically modified, water-soluble polymers in the LSV area [80- and 120-KU formulations (Figures 13 and 14)] are evident, particularly in the HEUR 200 formulations. As the PVC is decreased (11) (the 120-KU formulation results in Figure 14 should be compared with the data in Figure 4), the LSVs of the HEUR 200 coating increase. With only the thickener level increasing in both comparisons, the distinctly higher LSVs, not observed in the other hydrophobically modified, water-soluble polymer formulations, appear to denote thickener-thickener associations in the HEUR 200 coatings (11). If hydrophobically modified, water-soluble polymer associations exist at the expense of thickener-dispersed component interactions, flocc-

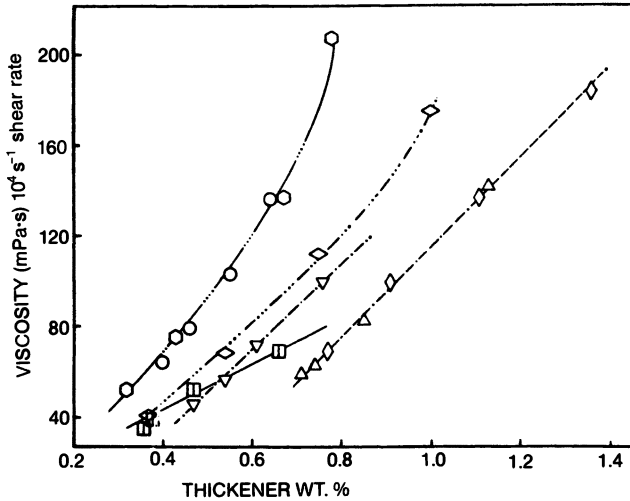


Figure 11. Viscosity (Pa s) at 10^4-s^{-1} shear-rate dependence on the weight percent thickener required to attain Stormer viscosities of 80, 90, 105, and 120 KU in a 45% PVC interior formulation. Component symbols are given in the legend to Figure 4. Reproduced with permission from reference 11. Copyright 1984 Oil and Colour Chemists' Association.

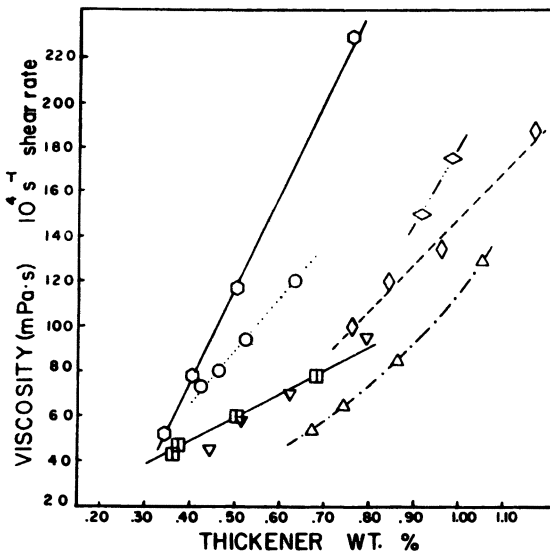


Figure 12. Viscosity (Pa s) at 10^4-s^{-1} shear-rate dependence on the weight percent thickener required to attain Stormer viscosities of 80, 90, 105, and 120 KU in a 57% PVC interior formulation. Component symbols are given in the legend to Figure 4. Reproduced with permission from reference 11. Copyright 1984 Oil and Colour Chemists' Association.

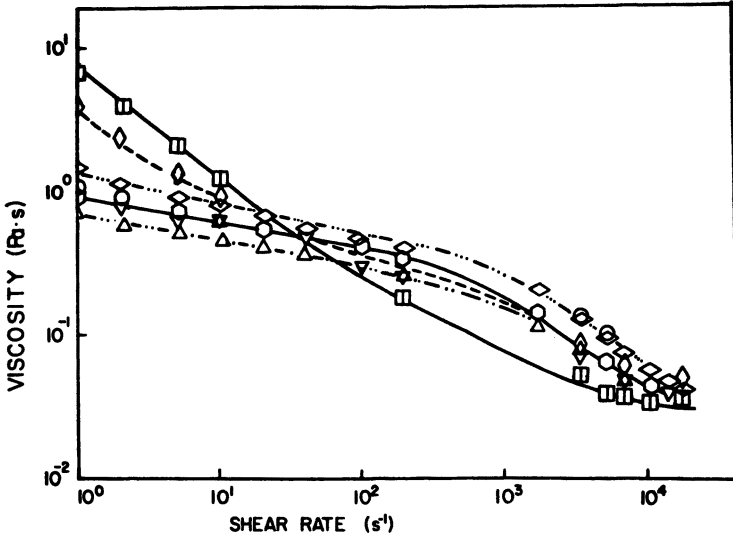


Figure 13. Viscosity (Pa s) dependence on the shear rate (s^{-1}) of an interior formulation: 35% PVC; 32% NVV; and 80 KU. Thickener symbols are given in the legend to Figure 4. Reproduced with permission from reference 11. Copyright 1984 Oil and Colour Chemists' Association.

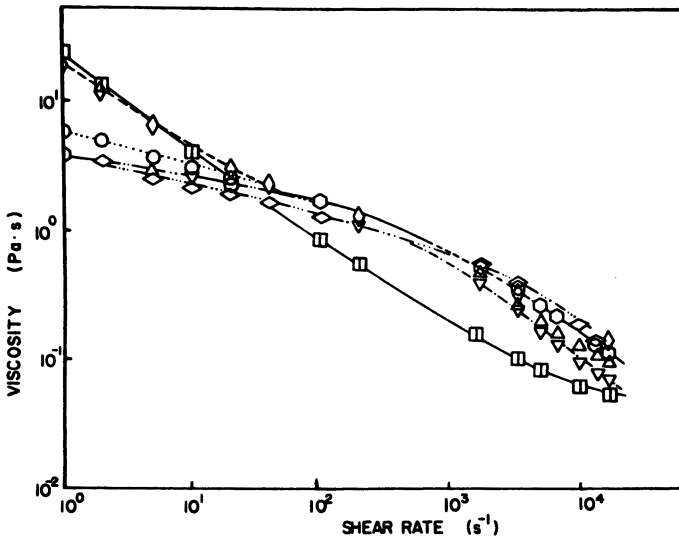


Figure 14. Viscosity (Pa s) dependence on the shear rate (s^{-1}) of an interior formulation: 35% PVC; 32% NVV; and 120 KU. Thickener symbols are given in the legend to Figure 4. Reproduced with permission from reference 11. Copyright 1984 Oil and Colour Chemists' Association.

ulation of the dispersed components would be expected; higher LSVs and lower gloss in the dry film result. A lower gloss equivalent to the cellulose ether thickened formulation is observed (11) in HEUR 200 coatings.

This interpretation of the performance is supported by the yield stress behavior as a function of PVC. Yield stress behavior was assessed by the conventional method used by coatings chemists, the Casson equation (26, 27) (equation 3):

$$\eta^{0.5} = \eta_{\infty}^{0.5} + \tau_0^{0.5}/\dot{\gamma}^{0.5} \quad (3)$$

where η is the viscosity (Pa s) at a given shear rate $\dot{\gamma}$ (s^{-1}), η_{∞} is the viscosity at a higher, limiting shear rate, and τ_0 is the yield stress.

The yield stress (reflected in the slope of the line; Figure 15) undergoes a transition between 35% and 45% PVC, with a dramatic decrease in the aggregation index at lower PVCs in the cellulose ether thickened formulation. The data follow a trend previously observed (28). Most of the hydrophobically modified, water-soluble polymer thickened formulation changes in yield stress with variation in PVC are small and within experimental error. The notable exception is the HEUR 200 formulations where the yield stress values increase with decreasing PVC, an unusual occurrence in waterborne latex formulations. The yield stress values and

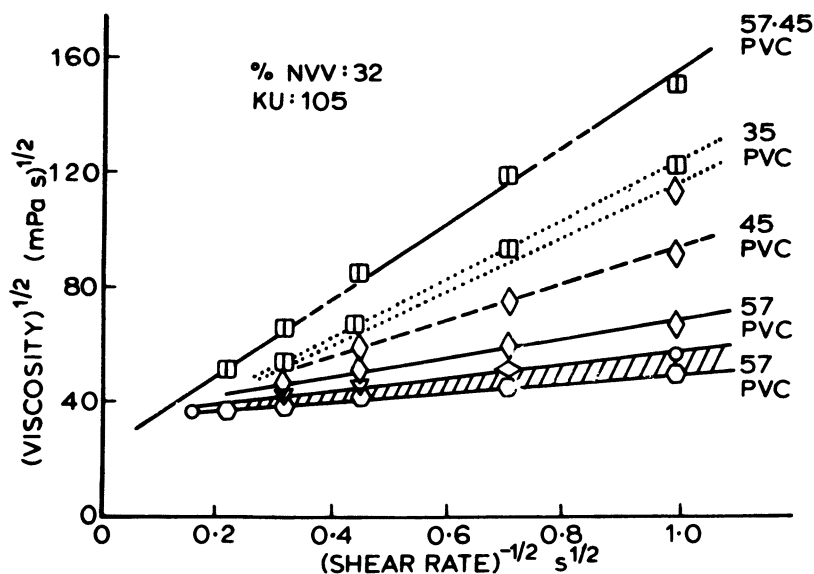


Figure 15. Casson plot: the slope of the lines reflects (equation 3) the yield stress value of the formulation. Thickener symbols are given in the legend to Figure 4: 32% NVV; and 105 KU. Reproduced with permission from reference 11. Copyright 1984 Oil and Colour Chemists' Association.

LSVs remain low at all PVC levels with the other hydrophobically modified, water-soluble polymers; these polymers associate to variable extents with the dispersed components and, through the osmotic stabilization mechanism, prevent dispersed component flocculation.

Latex. A second example of the sensitivity of hydrophobically modified, water-soluble polymers to changes in formulation ingredients is observed with variation in the latex. In hydrophobic latices of similar compositions, a marked particle size effect occurs; HSVs decrease with increasing median size up to approximately 350 nm. This phenomenon can be offset by changes in surface composition. For example, when a small, all-acrylic latex (Figure 12) is replaced with an approximately equal-sized styrene-acrylic binder (Figure 16) or with a larger, multimodal particle size vinyl acetate-acrylate latex (Figure 17), dramatic variations in HSV-weight percent relationships among most of the hydrophobically modified, water-soluble polymer thickened formulations occur. In the small particle size comparison, the latices are of similar surface energies (discussed in Chapter 5). The smaller styrene latex contains a highly carboxylated surface, which is difficult to achieve (29) and must involve a core-shell synthesis. The surface of the all-acrylic latex is lightly carboxylated; this surface is produced by a semicontinuous process. A dramatic difference in surface structure occurs; the large vinyl-acrylic binder is stabilized with chemically attached HEC fragments (discussed in Chapter 18) and a nonionic (e.g., ethoxylated nonylphenol) surfactant.

The most notable difference in the small particle latex formulation comparison (Figures 12 and 16) is the relative improvement in performance (25) of HEUR 200 in the styrene-acrylic latex formulation. The

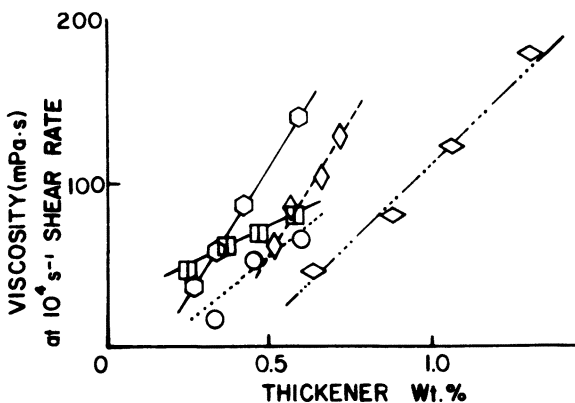


Figure 16. Viscosity (Pa s) dependence on the shear rate (s^{-1}) of an interior formulation: 57% PVC; 32% NVV; and 80 KU. Thickener symbols are given in the legend to Figure 4. The latex in this formulation is a 160-nm styrene-acrylic latex.

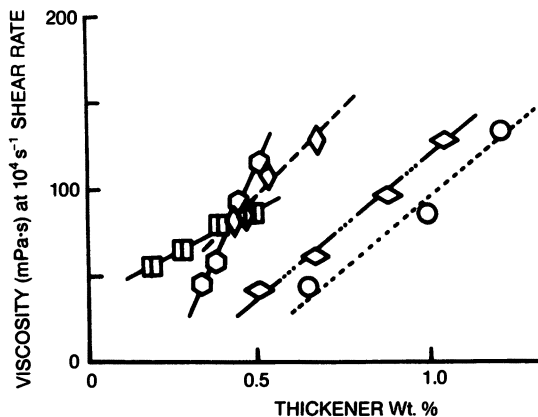


Figure 17. Viscosity (Pa s) dependence on the shear rate (s^{-1}) of an interior formulation: 57% PVC; 32% NVV; and 80 KU. Thickener symbols are given in the legend to Figure 4. The latex in this formulation is a multimodal 347-nm vinyl acetate-butyl acrylate latex with HEC-stabilizing segments chemically attached to the surface. Reproduced with permission from reference 23. Copyright 1984 Oil and Colour Chemists' Association.

decreases in HSVs for a given weight percent thickener in HEUR 100 thickened and SMAT-thickened coatings containing the vinyl-acrylic latex are also dramatic.

Although a significant difference exists in particle-size characteristics and the interfacial moieties stabilizing the latices compared in Figures 16 and 17, fewer variations in hydrophobically modified, water-soluble polymer influences on HSV between the vinyl-acrylic latex and styrene-acrylic latex formulations were noted than between the latter and the all-acrylic latex formulation at 57% PVC. These differences must be related to the hydrophilicities of the latex's surface (discussed in Chapter 5), complemented by the hydrophilicity and structural features of the stabilizing moieties.

Percent Nonvolatiles by Volume. The studies described above were conducted at a variety of PVC levels, but at a constant NVV concentration of 32%. Variation in the percent nonvolatiles level provides additional insight in the performance of the different thickeners and their mechanism of thickening. Levels of 22% and 42% NVV were achieved by varying the amount of water in the formulation; the variations were made concomitant with variations in the PVC of the formulation. When the percent NVV level was varied, less thickener was required to achieve a given Krieb unit viscosity in formulations containing greater solids levels. For comparison of performance differences in variable percent NVV formulations, a weight percent of thickener was

selected from arbitrary values of 100 mPa s for HSVs and 10 Pa s for LSVs and then normalized with respect to the amount of water present (25), to obtain high (e_h) and low (e_l) efficiency factors.

As noted earlier, LSVs (via elastic contributions) are increased by self-association of the thickener or flocculation of components. Flocculation also increases the viscosity by inclusion of the continuous phase. Examination of the viscosifying efficiency at low shear rates as a function of both variation in the PVC and percent NVV reveals two distinctive features regardless of the thickener: (1) e_l is significantly more sensitive to increases in the percent NVV level of the formulation than to changes in PVC and (2) in 42% NVV formulations, e_l increases with decreasing PVC. These features are evident in formulations thickened with HEC and HEUR 708 (Figures 18 and 19, respectively). The pre-stabilization of pigments via enthalpic interactions with a dispersant stabilizer provides greater stability to these "hard" TiO₂ spheres than that provided by adsorbed anionic or anionic-nonionic surfactants to the "soft" latex. As the percent NVV level is increased, a marked increase in e_l (Figure 18) in HEC-thickened formulations occurs. The increase in e_l

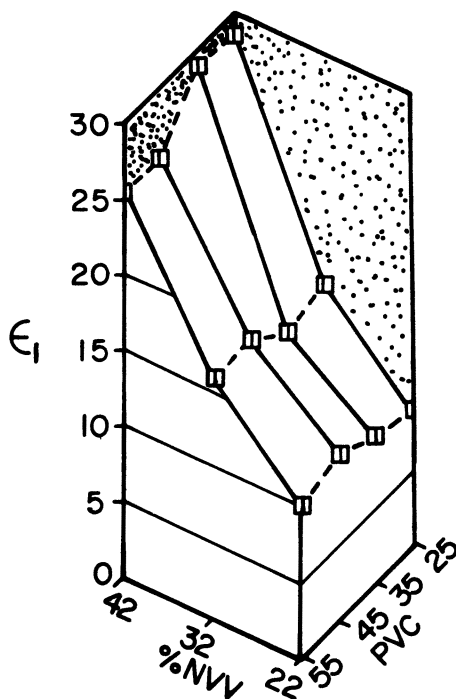


Figure 18. LSV efficiency factor (e_l) dependence on percent NVV and PVC in small-particle, all-acrylic latex formulations thickened with HEC-MHR.

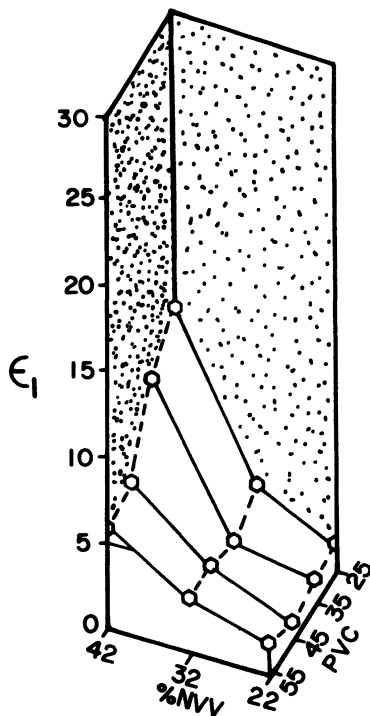


Figure 19. LSV efficiency factor (e_1) dependence on percent NVV and PVC in small-particle, all-acrylic latex formulations thickened with HEUR 708.

can be mechanistically related to volume restricted flocculation, primarily, of the all-acrylic latex component. Relatively little change in HEUR 708 formulations at 22% and 32% NVV coatings occurs; this feature can be interpreted in terms of osmotic stabilization of the dispersed components by association of hydrophobically modified, water-soluble polymers. Only in the crowded 42% NVV formulation does the osmotic stability provided by the association fail, and this failure is most notable when the ratio of latex to pigment is highest.

The e_h dependence on PVC and percent NVV variations is similar to that observed in e_1 studies except that the increase in the e_h plane is greatest with HEUR 708 (Figure 20). This increase would be expected if association resulted in an increase in the hydrodynamic volume of the latex and any flocculant structures were disrupted at high deformation rates. The increases in e_h with an increase in percent NVV in HEUR 200 and HEC formulations are relatively small.

Dispersant and Formulation Surfactant Effects. In the formulation studies described, a nonionic surfactant, having an average hydrophobe

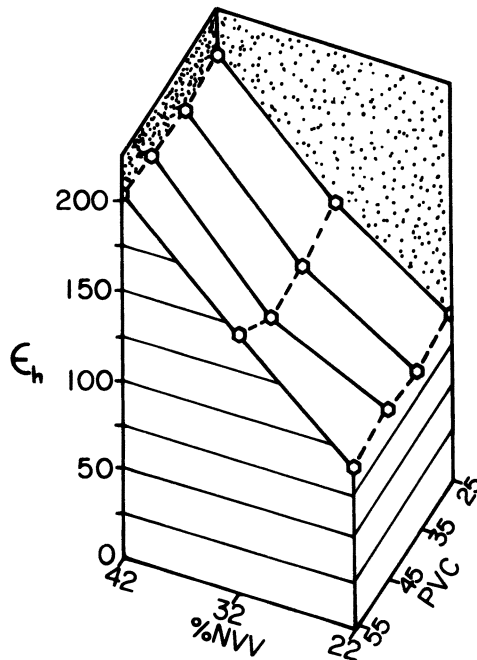


Figure 20. HSV efficiency factor (e_h) dependence on percent NVV and PVC in small-particle, all-acrylic latex formulations thickened with HEUR 708.

length of 15 carbon atoms and an average ethoxylate chain length of nine, was added to ensure dispersion stability. A nonionic formulation surfactant is normally selected over an anionic poststabilizer to achieve adequate freeze-thaw stability, less water sensitivity, and greater color development in the applied film. In parallel with the adsorption studies discussed in Chapter 5, nonionic nonylphenol surfactants (with average ethoxylate chain lengths of 4 and 40) were employed as formulation stabilizers. The short ethoxylate chain length surfactant is dispersible but not water soluble. The surfactant exhibited a remarkable ability to equalize the HSVs (compare Figures 21 and 22) of hydrophobically modified, water-soluble polymer thickened coatings.

Statistical analysis of the HSV data in the variable formulation surfactant studies revealed that the equivalency affected by the hydrophobic, low ethoxylate nonylphenol dispersant resulted from a dramatic decrease in the efficiency of all hydrophobically modified, water-soluble polymers, except HEUR 200. In the HEUR 200 thickened formulations, a moderate increase in HSV was observed. Part of the data from this statistical study is presented in Figure 23 for a 35% PVC formulation containing the small all-acrylic latex.

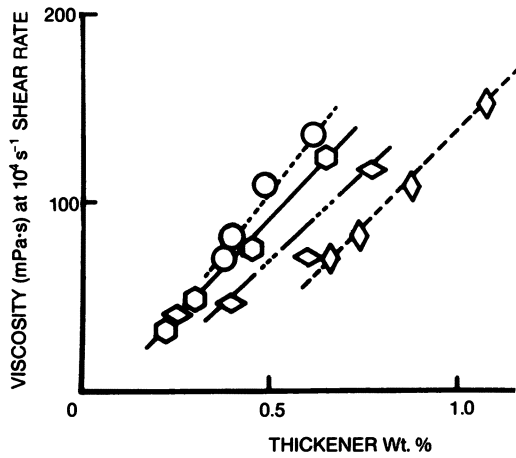


Figure 21. HSV dependence on the weight percent of thickener required to attain Stormer viscosities of 80, 90, 105, and 120 KU in a 35% PVC, 32% NVV formulation containing a small-particle (100-nm), all-acrylic latex and nonylphenol surfactant with four ethoxylate units. Component symbols are given in the legend to Figure 4.

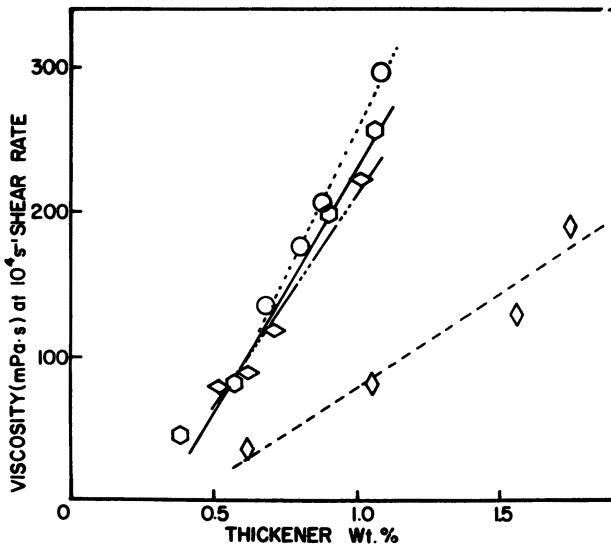


Figure 22. HSV dependence on the weight percent of thickener required to attain Stormer viscosities of 80, 90, 105, and 120 KU in a 35% PVC, 32% NVV formulation containing a small-particle (100-nm), all-acrylic latex and nonylphenol surfactant with 40 ethoxylate units. Component symbols are given in the legend to Figure 4.

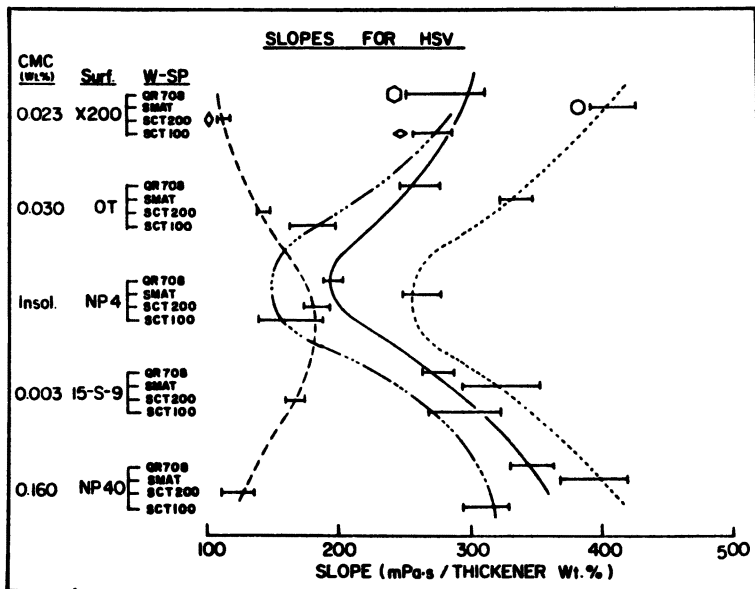


Figure 23. HSV efficiency in terms of slopes (mPa s/thickener wt %) of thickeners in a 35% PVC, 32% NVV formulation containing small-particle (100-nm), all-acrylic latex: dependence on the formulation surfactant. Component symbols are given in the legend to Figure 4.

LSV sensitivities to variation in the concentration of the standard 9 mol ethoxylate stabilizer are observed. A decrease below a certain plateau level in surfactant concentration results in an increase in the LSVs (denoting flocculation). Again, a notable exception in this study was observed in formulations containing HEUR 200; an extreme sensitivity to surfactant concentration was observed with no obvious viscosity plateau, even with this standard formulation surfactant at high concentrations.

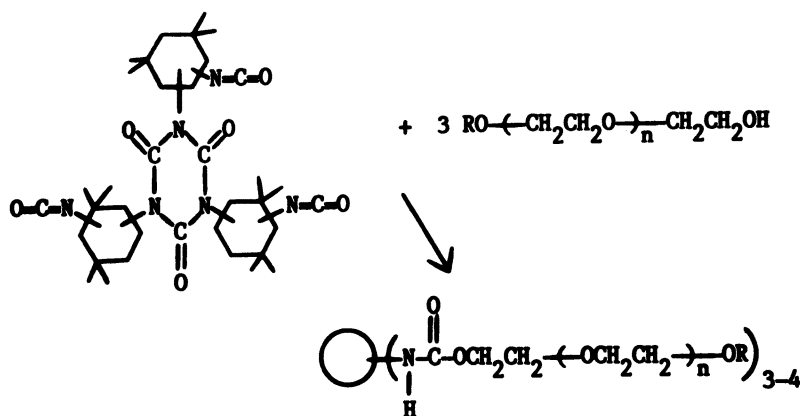
Variations in LSVs were evident when the concentration of a pigment dispersant (i.e., a low molecular weight copolymer containing carboxylate groups) was varied in hydrophobically modified, water-soluble thickened formulations. An increase in LSVs would be expected only at low dispersant concentrations, and this increase was observed in formulations thickened with hydrophobically modified, water-soluble polymers containing the HEC-stabilized, vinyl-acrylic latex.

Adsorption and Hydrophobically Modified, Water-Soluble Polymer Structural Effects

The combined data in Figure 1 and Table I, complemented by the influence of formulation component changes on the coating's rheology, indi-

cate the importance of association of the hydrophobically modified, water-soluble polymer with the latex. Additional data delineating the importance of hydrophobes, chemically attached to the water-soluble polymer, are provided in star-shaped polymers synthesized from the isophorone-diisocyanate trimer (Scheme I) by using both nonylphenol-capped and methoxyl-capped oxyethylene chains with greater than 40 ether linkages (31). The small-particle, all-acrylic latex formulations are the most demanding of the formulations studied. The HSVs (Figure 24) of coatings containing the all-acrylic latex are dependent on both the molecular weight and the presence of attached hydrophobe structures.

The remaining question pertains to the performance differences among commercial HEUR types; this question cannot be answered on the basis of their slight differences in surface tension behavior or in their more considerable variation in molecular weights (Table II). The differences probably are related to variations in the frequency of hydrophobe sequences and to the chemical structure of the hydrophobe unit. Multiple hydrophobes could promote a greater degree of association stability at higher shear rates and therefore higher viscosities. The frequency and proximity of placement could maintain polymer-polymer associations at low shear rates and promote particle flocculation (as proposed for the HEUR 200-all-acrylic latex formulation). Such interactions would depend on the nature of the cohesive interactions among the hydrophobe attached to the thickener, the structure of the latex-stabilizing moieties, and the cohesive interactions between these two structural units. In addition, the other dispersed components—all of higher surface energy than the latex (discussed in Chapter 5)—must be properly stabilized or the thickener will preferentially adsorb on or interact with these higher



Scheme I. Reaction diagram for the synthesis of an associative thickener from an isophorone-diisocyanate trimer.

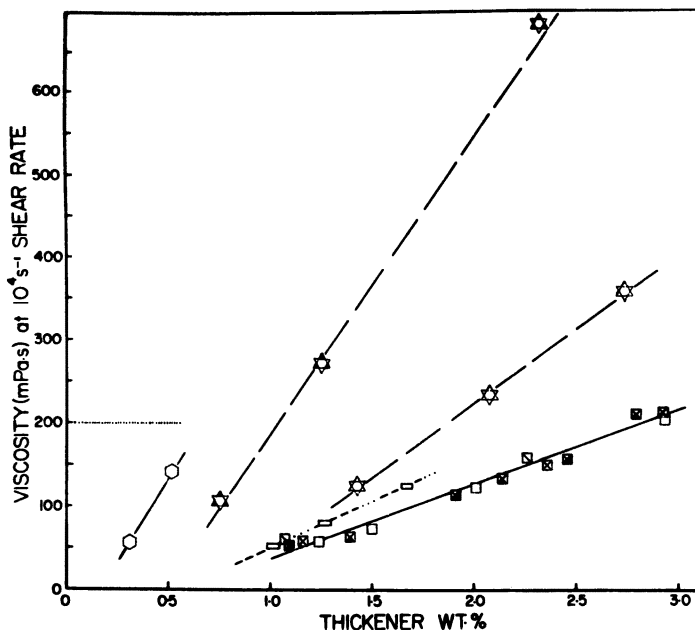


Figure 24. HSV (Pa s) dependence on thickener concentration (wt %): (\star) star NP 5000; (\star) star MPEG 5000; (\circ) HEUR 708; and (\square , \boxtimes , \boxminus) HEC of variable molecular weights.

energy surfaces. With small particle latices, where the use of hydrophobically modified, water-soluble polymers offer unique coatings rheology, the geometry of the water-soluble polymer appears to be less important than the moieties stabilizing the latex. For example, SMAT is as effective as the best HEUR thickener in formulations containing the lightly carboxylated all-acrylic latex, but SMAT is very ineffective in formulations containing HEC fragments attached to the latex's surface.

Conclusions

The importance of cohesive interactions among surfactant moieties to the stability of emulsions was highlighted more than 30 years ago. The structures stabilizing latices are, however, more complex, and the influence of such groups on cohesive interactions with the hydrophobes of hydrophobically modified, water-soluble polymers has not been assessed. Furthermore, the geometry of the water-soluble polymer that has been hydrophobically modified is not specific, in that the desired coating rheology can be affected by both star- and comb-type architecture in the most demanding formulation (i.e., wherein the latex is a small-particle, all-acrylic resin). From the investigations to date, apparently the architecture, molecular weight, and hydrophobe structures require

coordination if optimum coating rheology is to be realized. This fine tuning of variables in the performance of hydrophobically modified, water-soluble polymers will be the object of numerous future investigations and will include applications outside the coatings area.

Literature Cited

1. Dodge, J. S. *J. Paint Technol.* **1972**, *44*, 73.
2. Glass, J. E. *J. Oil Colour Chem. Assoc.* **1975**, *58*, 169.
3. Glass, J. E. *J. Oil Colour Chem. Assoc.* **1976**, *59*, 86.
4. Smith, N. D. P.; Orchard, S. E.; Rheud-Tutt, A. J. *J. Oil Colour Chem. Assoc.* **1961**, *44*, 618.
5. Bowell, S. T. In *Applied Polymer Science*; Craver, J. K.; Tess, K. W., Eds.; American Chemical Society: Washington, DC, 1975. Chapter 41.
6. Saunders, F. L.; Sanders, J. W. *Colloid Sci.* **1956**, *11*, 260.
7. Kreider, R. W. *Fed. Soc. Paint. Technol. Off. Dig.* **1964**, *36*, 1244.
8. Saunders, F. L. *J. Colloid Interface Sci.* **1967**, *23*, 230.
9. Kreider, R. W. *J. Polym. Sci.* **1969**, *C-27*, 275.
10. Evani, S. R.; Lalk, R. H.; Fiero, T. H. *Am. Chem. Soc., Div. Org. Coat. Plast. Chem. Prepr. Pap.* **1974**, *34(2)*, 142.
11. Glass, J. E.; Fernando, R. H.; Jongewaard, S. K. E.; Brown, R. G. *J. Oil Colour Chem.* **1984**, *67*, 256.
12. Ferry, J. D. *Viscoelastic Properties of Polymers*; Wiley: New York, 1970.
13. Bird, R. B.; Hassager, O.; Armstrong, R. C.; Curtiss, C. F. *Dynamics of Polymeric Liquids*; Wiley: New York, 1977; Vol. I.
14. Glass, J. E. *J. Coat. Technol.* **1978**, *50*, 53.
15. Asakura, S.; Oosawa, F. *J. Polym. Sci.* **1958**, *33*, 183.
16. Sieglaff, C. L.; *J. Polym. Sci.* **1959**, *41*, 319.
17. De Hek, H.; Vrij, A. *J. Colloid Interface Sci.* **1979**, *70*, 3; **1982**, *88*, 1.
18. Sperry, P. R.; Hopfenberg, H. B.; Thomas, N. L. *J. Colloid Interface Sci.* **1981**, *82*, 1.
19. Sperry, P. R. *J. Colloid Interface Sci.* **1982**, *87*, 2; **1984**, *99*, 97.
20. Gast, A. P.; Hall, C. K.; Russel, W. B. *J. Colloid Interface Sci.* **1983**, *96*, 251.
21. Gillespie, T. *J. Colloid Interface Sci.* **1983**, *94*, 166, 377.
22. Bergh, J. S. M.S. Thesis, North Dakota State University, Fargo, North Dakota, in preparation.
23. Fernando, R. H.; Glass, J. E. *J. Oil Colour Chem. Assoc.* **1984**, *67*, 279.
24. Murakami, T. M.S. Thesis, North Dakota State University, Fargo, North Dakota, 1985.
25. Fernando, R. H. Ph.D. Thesis, North Dakota State University, Fargo, North Dakota, 1986.
26. Asbeck, W. K. *Fed. Soc. Paint Techn., Off. Dig.* **1960**, *32*, 668.
27. Asbeck, W. K. *Fed. Soc. Paint Techn., Off. Dig.* **1961**, *33*, 65.
28. Los Angeles Paint Society *Fed. Soc. Paint Tech., Off. Dig.* **1953**, *25*, 205.
29. Hoy, K. L. *J. Coat. Technol.* **1979**, *51*, 27.
30. Jongewaard, S. K. E. M.S. Thesis, North Dakota State University, Fargo, North Dakota, 1985.
31. Brown, R. G. Ph.D. Thesis, North Dakota State University, Fargo, North Dakota, in preparation.

RECEIVED for review March 5, 1985. ACCEPTED August 29, 1985.

Rheology: A Unique Synthesis and Characterization of Water-Reducible Epoxy-Acrylic Graft Copolymers

James T. K. Woo and Richard R. Eley

Glidden Coatings and Resins Division, Division of SCM Corporation, Strongsville, OH 44136

High molecular weight epoxy resins were grafted with styrene-methacrylic monomers; the epoxy-g(styrene-methacrylic acid) copolymer was water reducible when neutralized with a base. Grafting was achieved by using a very high level of free-radical initiator. The level of free-radical initiator used to prepare these epoxy-g-acrylic copolymers plays an important role in the properties and performance of the material. A higher level of free-radical initiator favors a higher level of grafting and increased blister resistance on spraying. Casson viscosity and measured high-shear-rate viscosity both decrease with increasing initiator level. The correlation of the two effects is discussed mechanistically.

THE STRUCTURE AND PROPERTIES OF MULTICOMPONENT POLYMERS have attracted a great deal of interest recently. For most polymers (1), the formation of homogeneous mixtures with each other is often thermodynamically unfavorable. The key is to produce microheterogeneous polymeric systems so that each component polymer can still retain most of its individual properties while contributing in a synergistic way to provide new microscopic properties for the material as a whole. One way to produce such a compatible system is by graft copolymerization.

Epoxy resins are used extensively in the coating industry. In papers 1-4 of this series, synthesis and characterization of epoxy-g(styrene-methacrylic acid) copolymers were described. In this chapter, we present the results of rheological studies by two different methods of a series of graft copolymers synthesized with different free-radical initiator

NOTE: This paper is part 5 in a series.

0065-2393/86/0213-0417\$06.00/0
© 1986 American Chemical Society

levels. The application performance of the coatings is interpreted in terms of the rheological properties.

Experimental Section

Synthesis of the epoxy-*g*-(styrene-methacrylic acid) copolymer was reported (2-8). The structure of the graft polymer on the average contained two graft chains per epoxy molecule. The molecular weight of the epoxy is 9000, and the molecular weight of the acrylic graft chain is 830. From a starting composition of 80 parts of epoxy, 7 parts of styrene, and 13 parts of methacrylic acid, the final product consists of the following: (1) 47% of the epoxy is ungrafted, (2) 61% of the styrene-methacrylic acid is ungrafted, and (3) 39% of the styrene-methacrylic acid is grafted onto 53% of the epoxy.

Flow curves (shear rate-shear stress profiles) were obtained on the materials by using the Ferranti-Shirley cone and plate viscometer (9) to a 7000-s^{-1} maximum shear rate. The Casson viscosity (high-shear viscosity) was obtained by extrapolation of a Casson plot to infinite shear rate (10). The high-shear-rate rheological properties were measured directly by means of a high-pressure capillary rheometer (11).

Results and Discussion

Grafting of epoxy resins by reaction of carboxyl-epoxide functionalities has been known for many years (12). The carboxyl-bearing molecules can be fatty acids or acrylic copolymers containing carboxyl functionalities. The reaction is normally catalyzed by the presence of a base. Grafting of epoxy by carbon-carbon bond formation was first reported by Ceresa (13) in which methyl methacrylate was grafted onto the epoxy resin with a free-radical initiator. In this work, carboxyl-containing monomers were grafted onto high molecular weight epoxy resins via carbon to carbon bonds, giving a hydrolysis-resistant polymer. Graft copolymers of epoxy resin made by an ester synthesis route lack this property due to the hydrolytic instability of the ester linkage.

All emulsions are thermodynamically unstable (14) because their interfacial area is orders of magnitude greater than the interfacial area of the corresponding coagulated systems. A so-called "stable emulsion" is in reality a metastable system. The input of a certain activation energy is necessary for coagulation to occur, and the higher this activation energy, the higher the metastability of the emulsion.

The mechanism of stabilization of polymeric oil-in-oil emulsions consists of the following: (1) incompatibility of polymers causes the phenomenon of phase separation of polymers in solution; (2) this phase separation causes the force that drives the graft copolymer into the interface of polymeric oil-in-oil emulsions and the graft copolymer in essence behaves like a mediator between two incompatible polymers, as most graft copolymers behave as emulsifiers; and (3) this behavior causes the formation of coalescence barriers. Without the phenomenon of phase separation, due to a repulsion of dissimilar polymer chains, a graft

copolymer would have no reason to accumulate in the interface of an immiscible polymer solution. For stabilization of a polymeric oil-in-oil emulsion, a graft copolymer must accumulate in the interface of the emulsion and form a protective coating around the emulsion droplets, a so-called coalescence barrier (14).

In the case of the epoxy-acrylic graft copolymer, the epoxy is not soluble in the acrylic monomer mixture at even as low as 10% solution. However, 1-*n*-butoxyethanol is a solvent for both the epoxy resin and the styrene-methacrylic acid polymer. 1-*n*-Butoxyethanol can, therefore, pass freely between the free epoxy resin and free styrene-methacrylic acid copolymer phases. The interface is comparable to a semipermeable membrane in osmosis. However, 1-butanol, which is the other cosolvent, cannot pass freely between the two polymer phases because 1-butanol is a solvent for the styrene-methacrylic acid copolymer but a nonsolvent for the epoxy resin. Free epoxy resin and free styrene-methacrylic acid copolymer cannot pass freely through this interface. The purpose of the grafted epoxy-styrene-methacrylic acid copolymer is to lower the barrier at the interface so that a stable oil-in-oil emulsion is first obtained and then, upon neutralization with a tertiary amine (dimethylethanolamine), a stable emulsion in water is obtained.

The application (15) of these graft copolymers made with different free-radical initiator levels is listed in Table I.

Table I shows the effect of the increasing initiator level as the test dispersion series is traversed from 1% to 10% initiators. Two critical parameters in the application of coatings to cans are coverage and blister resistance. Coverage refers to the property of obtaining a thin coating that is blemish and pinhole free. The minimum weight of dry polymer in the can that can be obtained while still maintaining blemish-free coatings

Table I. Effect of Increasing Initiator Level as Dispersion Series Moves from 1% to 10% Initiator

Expt No.	Free-Radical Initiator Based on Total Monomers (%)	Dispersion (%)		Coverage (mg/can)	Blister (mg)
		NV ^a	AN ^b		
1	1	22.8	85.9	120	120
2	2	22.5	85.7	120	130
3	3	23.1	90.5	120	130
4	5	22.4	88.1	110	215
5	7	21.5	90.6	130	230
6	10	22.6	93.0	120	250

NOTE: All values are averaged from several observations.

^aNV is nonvolatiles.

^bAN is acid number (NV).

is determined by an electrical test. The resistance to blistering, or solvent popping, on the other hand, refers to the ability of the coating to produce a thick film without blistering during the bake process. Table I gives values of these parameters for several coatings. Clearly, coatings such as 1-3 would find limited utility on a commercial line because of a narrow application window (inability to obtain high film weight without blistering). On the other hand, coatings made from dispersions 4-6 represent systems of greater commercial utility in that coatings of different film weights can be obtained from the same system for use in packaging different kinds of beverage.

From previous (4, 6-8) work, the amount of grafting appears to be a direct function of free-radical initiator concentration.

The molecular weight data of these epoxy graft copolymers made with different levels of free-radical initiator (2) are shown in Table II. The molecular weight is determined by gel permeation chromatography (GPC).

The molecular weight does not seem to be a factor except in the copolymer made with 1% free-radical initiator. These molecular weight data are for the graft copolymer mixture that includes the free epoxy resin, free acrylic copolymer, and the graft copolymer. The level of free-radical initiator should have the same effect on the molecular weight of the graft side chain.

A search in the literature revealed that the length of the graft side chain affects the rheology of the system. For example, short branch type graft copolymers of dextran-*g*-[poly(acrylamide)-*co*-sodium acrylate] show less viscosity drop due to a temperature increase than polymer with fewer but long branches (16). Short, more frequent, graft chains (R. R. Eley, unpublished data) are known to be in a more folded conformation, resulting in a reduction in viscosity, while less frequent, long, graft chains are known to give high viscosity due to aggregation.

Table II. GPC Data of Grafted Copolymers Made with Different Levels of Free-Radical Initiator

<i>Expt No.</i>	<i>Free-Radical Initiator (%)</i>	M_n^a	M_w^b	M_z^c
1	1	8,480	26,680	64,800
2	2	4,440	12,960	32,120
3	3	4,000	12,880	35,080
4	5	4,200	13,240	35,160
5	7	3,904	13,000	40,400
6	10	4,120	14,120	42,400
7	15	4,920	17,720	72,400

^a M_n is number-average molecular weight.

^b M_w is weight-average molecular weight.

^c M_z is z-average molecular weight.

In polyethylene-*g*-polyacrylonitrile graft copolymer (17), for the same acrylonitrile (15%) content the copolymer with short, frequent grafts ($M_n = 1200$) has a lower crystallinity than those with longer, less frequent grafts ($M_n = 2500$).

The particle size of the emulsion from the epoxy-*g*-(styrene-methacrylic acid) graft copolymers made with different levels of free-radical initiators was reported (6). The particle size of the emulsion formed is inversely related to the free-radical initiator concentration. The reason for this correlation is believed to be the increased amount of graft copolymer (emulsifier) formed with an increased level of free-radical initiator.

The Casson viscosity data of these epoxy-*g*-(styrene-methacrylic acid) graft copolymers made with different levels of free-radical initiators is summarized in Figure 1. A correlation between Casson viscosity and the level of free-radical initiator used in preparing the graft copolymers seems to occur. The copolymers with low levels of free-radical initiators have high Casson viscosities, and the copolymers with high levels of free-radical initiators have low Casson viscosities.

Rheology and Sprayability. Sprayability is defined as adequate coverage of the substrate, which is assumed to be related to adequate atomization, plus acceptable blister (solvent popping) resistance. The

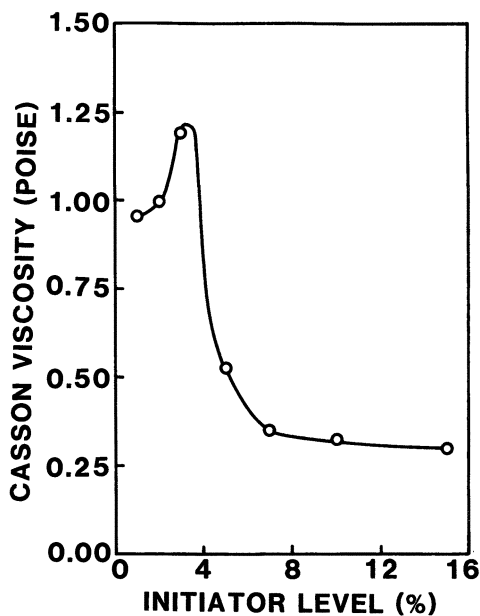


Figure 1. Dependence of Casson viscosity on initiator.

breakup of a liquid jet in airless spray is mainly due to air resistance encountered by the jet leaving the nozzle and is also promoted by turbulence within the liquid itself at that point (18). Other factors influencing the breakup and atomization process are the explicit rheological properties or material functions: the shear viscosity, extensional viscosity, and bulk and surface viscoelasticity. Easiest to measure is the shear viscosity-shear rate profile, or flow curve, which may be analyzed according to the Casson model (10). The Casson viscosity (infinite shear viscosity) was taken as an indicator of viscosity under high-shear-rate conditions, such as those involved in the application of coatings by airless spray. The Casson viscosity, however, is at best an approximation to the viscosity at some unspecified high shear rate, higher than the maximum shear rate of the test run. In this laboratory, it was observed that the value of the Casson viscosity does in fact depend on the maximum experimental shear rate used (19).

The coating materials were tested by using a high-shear-rate pneumatic capillary rheometer to obtain a more reliable indicator of the viscosity appropriate to the application process (22). For non-Newtonian fluids, such as coatings, the shear rate experienced during a given application process depends on the functional relationship of the viscosity and shear stress. The samples were forced through a precision-bore glass capillary at high, constant pressure. In this way, the samples experienced a constant average shear stress but varying shear rates, exactly as in the actual spraying process. Experimental shear rates were in the range 30,000–350,000 s⁻¹.

The predictions of the Casson equation and the actual high-shear viscosities were compared and are plotted in Figure 2. The Casson viscosity correlates to the high-shear viscosity (at constant shear stress) for these materials. The regression line was forced through the origin; a correlation coefficient of 0.98 was obtained. A plot of the high-shear-rate viscosities versus initiator level is similar in appearance to Figure 1 (*see* Figure 3).

We believe that blistering is related to the stability of the emulsion toward the very high shear rates encountered in airless spray. That is, postspray viscosity loss, allowing excessive sag, may be the key to this problem. The greater resistance to blistering with increasing initiator level may be due to the presence of a more effective interfacial coalescence barrier resulting from relatively more grafting, as described previously. Another factor could be improved atomization of the higher initiator level materials, due to the lower viscosity. Also, at the lower viscosity, the velocity of the liquid stream is higher, at constant shear stress. Smaller atomized droplet size is favored both by higher jet velocity and by lower liquid viscosity. The mass transfer rate (loss of volatiles) during spray is increased both by greater atomization and by the

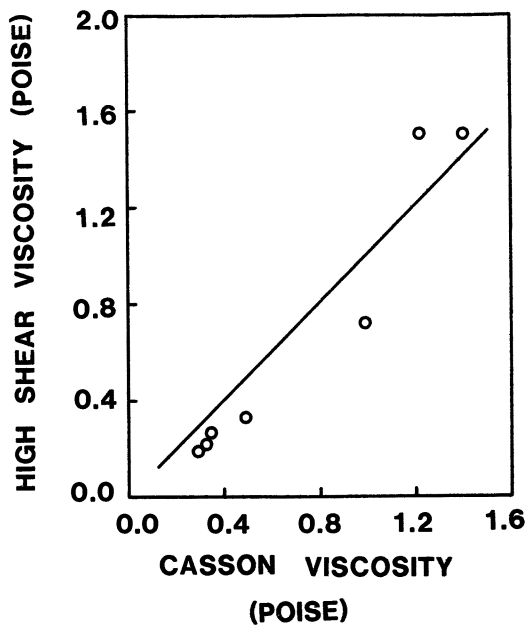


Figure 2. High-shear-rate viscosity vs. Casson viscosity. $R = 0.98$ (forced through origin).

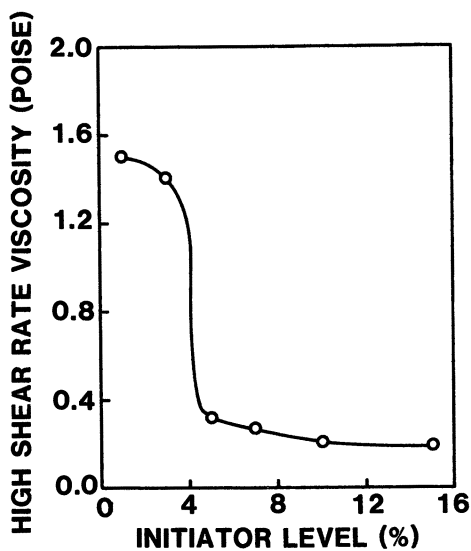


Figure 3. High-shear-rate viscosity vs. initiator level.

higher particle velocity; a higher postspray viscosity and greater sag resistance result.

Acknowledgments

We thank Glidden Coatings and Resins, Division of SCM Corporation, for permission to publish this work. We also thank C. Y. Kuo for the GPC analysis and R. A. Zander for his assistance in obtaining the capillary rheometer data.

Literature Cited

1. Shen, M.; Kawai, H. *Am. Inst. Chem. Eng. J.* **1978**, *24*, 1.
2. Woo, J. T. K. In *Prepr. Org. Coat. Plast. Div. Am. Chem. Soc.* **1980**, *43*, 142.
3. Woo, J. T. K. In *Prepr. Org. Coat. Plast. Div. Am. Chem. Soc.* **1981**, *45*, 516.
4. *Ibid.*, 527.
5. *Ibid.*, 534.
6. Woo, J. T. K.; Ting, V.; Evans, J.; Marcinko, R.; Carlson, G.; Ortiz, C. J. *Coat. Technol.* **1982**, *54*(689), 41.
7. Woo, J. T. K. In *Proc. IUPAC I.U.P.A.C. Macromol. Symp. 28th, 1982*, Amherst, MA, 1982, p 191.
8. Woo, J. T. K. In *Proc. 7th Int. Conf. Org. Coat. Sci. Technol.*, Athens, Greece, 1981.
9. Kah, A. F.; Koehler, M. E.; Niemann, T. F.; Provder, T.; Eley, R. R. In *Computer Applicators in Applied Polymer Science*; Provder, T., Ed.; ACS Symposium Series 197; American Chemical Society: Washington, DC, 1982; pp 223-241.
10. Casson, N. In "Rheology of Disperse Systems"; Mill, C. C., Ed.; Pergamon Press: London, 1959.
11. Krieger, I. M.; Dodge, J. S. *Soc. Pet. Eng. J.* **1967**, 259.
12. Walus, A. N. U.S. Patent 3 707 516, 1972; Wu, S., U.S. Patent 3 943 187, 1976; Wu, S. U.S. Patent 3 997 694, 1976; Wu, S. U.S. Patent 4 021 396, 1977.
13. Ceresa, R. J. *The Chemistry of Polymerization Process*, ACS Monograph Series 20; American Chemical Society: Washington, DC, 1966; pp 249-260.
14. Molau, G. *J. Polym. Sci., Pt. A* **1964**, *3*, 4235.
15. Robinson, P. V. *J. Coat. Technol.* **1981**, *53*(674), 23-30.
16. McCormick, C. L.; Park, L. S. *Am. Chem. Soc. Polym. Prepr.* **1982**, *23*, 122.
17. Shalabi, S. E.; Nazarina, L. A.; Rogovina, L. Z.; Gabrielyan G. A. *Polym. Sci. USSR* **1979**, *21*, 1266-1274.
18. Buniyat-Zade, A. A.; Kakhranov, N. T.; Shcharinskii, Ye. A. *Polym. Sci. USSR* **1981**, *23*, 1132.
19. Grant, R. P.; Middleman, S. *Am. Inst. Chem. Eng. J.* **1966**, *12*(4), 669.

RECEIVED for review January 7, 1985. ACCEPTED November 22, 1985.

Poly(2-ethyl-2-oxazoline): A New Water- and Organic-Soluble Adhesive

Thomas T. Chiu, Bruce P. Thill, and William J. Fairchok

The Dow Chemical Company, Midland, MI 48674

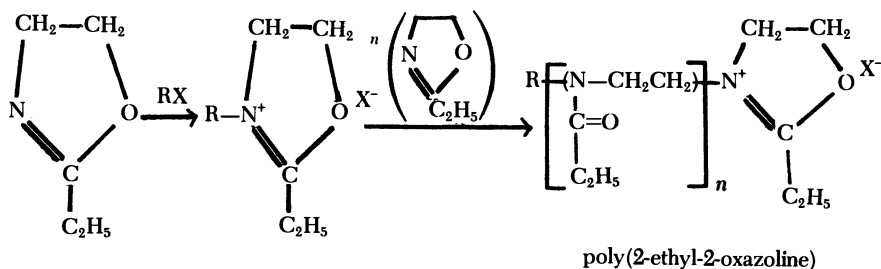
Poly(2-ethyl-2-oxazoline) is prepared by the ring-opening polymerization of 2-ethyl-2-oxazoline with a cationic initiator. Many of the polymer's characteristics stem from its molecular structure, which has a backbone of alternating two carbon atoms and one nitrogen with a pendent propionyl group off the nitrogen. Rheologically, the behavior of poly(2-ethyl-2-oxazoline) is more Newtonian and relatively shear stable compared to that of common thermoplastics. The polymer's broad solubility, ranging from water and acetonitrile to methylene chloride, leads to applications of miscible polymeric systems. Single glass transition temperatures have been observed in a number of blends with poly(2-ethyl-2-oxazoline). The unique property of poly(2-ethyl-2-oxazoline), being water soluble and hot meltable, suggests utilities such as heat sealing of disposable products, water remoistenable hot-melt adhesives, and other adhesion-enhancement applications.

THE BEHAVIOR AND PROPERTIES OF POLY(2-ETHYL-2-OXAZOLINE) (PEOX, a trademark of Dow Chemical), a novel tertiary amide polymer, are described in this chapter. This polymer is prepared by a cationic ring-opening polymerization of 2-ethyl-2-oxazoline (1-5). Many applications (6-11) of poly(2-ethyl-2-oxazoline) were reported. This chapter presents the physical property background of poly(2-ethyl-2-oxazoline); the physical factors suggest its utility as an adhesive or as a compatibilizing agent.

Experimental Section

2-Ethyl-2-oxazoline. 2-Ethyl-2-oxazoline is both a reactive intermediate for aminoethylation and a unique monomer. The synthesis of oxazolines has been extensively reviewed (3). One method of preparation for 2-ethyl-2-oxazoline is via alumina-catalyzed dehydration in the vapor phase to cyclize *N*-(2-hydroxyethyl)propionamide (4). 2-Ethyl-2-oxazoline is a clear, colorless liquid with a musky amine-like odor. Its boiling point and freezing point are 128 and -62 °C, respectively. 2-Ethyl-2-oxazoline is very soluble in most solvents, including acetone, methylene chloride, diethyl ether, toluene, and hexane.

0065-2393/86/0213-0425\$06.00/0
© 1986 American Chemical Society



2-ethyl-2-oxazoline

Polymerization. The 2-ethyl-2-oxazoline used is available from Dow Chemical. This compound was dried prior to polymerization by passage through a column containing 4-Å molecular sieves that had been activated by drying at 170 °C/25 torr for 24 h. The dried 2-ethyl-2-oxazoline was protected from contact with moist air. The water content of 2-ethyl-2-oxazoline was determined by Karl Fischer titration. Water levels below 20 ppm were considered acceptable.

Methyl tosylate (Aldrich Chemical) was used as received as the initiator throughout this study.

Polymerizations were performed in sealed ampules. Ten grams (0.101 mol) of dried 2-ethyl-2-oxazoline was delivered to a carefully dried ampule, and the appropriate amount of 0.538 M methyl tosylate in dry ethyl acetate was added.

Monomer-to-initiator ratios of 200–2000 were employed. The ampule was cooled in methylene chloride–dry ice, evacuated to approximately 5 torr, and sealed. After being warmed to room temperature, the ampules were placed in a 150 °C oil bath for 15 h. The ampules were removed, cooled, and opened, and the conversion was determined by percent nonvolatiles after 15 min at 225 °C/25 torr. Conversions were typically greater than 99%.

Molecular Weight Determination. Poly(2-ethyl-2-oxazoline) molecular weights were determined by size-exclusion chromatography (SEC) on TSK-G6000PW and G5000PW columns. A sample of polymer at a concentration of 0.25% by weight in 0.1 M sodium phosphate buffer at pH 7.0 was eluted with the same solvent at 1.0 mL/min. Detection was by UV at 214 nm. The columns were calibrated with a sample of poly(2-ethyl-2-oxazoline) polymer of broad molecular weight distribution standard that was characterized by a coupled SEC–low-angle laser light scattering (LALLS) technique. Data acquisition and reduction were computer-assisted. Number-average molecular weight (\bar{M}_n), weight-average molecular weight (\bar{M}_w), z-average molecular weight (\bar{M}_z), the ratio of \bar{M}_w to \bar{M}_n ($\bar{M}_w:\bar{M}_n$), and integral and differential molecular weight distribution curves were obtained from the SEC analyses.

Density. A value of 1.14 g/cm³ was obtained by using a density gradient column according to ASTM D-1505-79.

Refractive Index (n_D^{25}). A flat disk of poly(2-ethyl-2-oxazoline) was prepared by using a heated Pasadena Hydraulics, Inc., platen press and 1-in. disk mold. A portion of the disk was cut out and mounted on the prism of a Bausch & Lomb Abbe refractometer. A liquid of higher refractive index was placed between the prism and disk. The sample temperature was maintained at 25 °C.

Vicat Softening Temperature. The Vicat softening temperature was obtained according to American Society for Testing and Materials (ASTM) D-1525-82.

Glass Transition Temperature (T_g). T_g was obtained by using a Du Pont 1090B thermal analyzer and 910 differential scanning calorimeter and following ASTM D-3418-82.

Thermogravimetric Analysis (TGA). An analysis was made by using a Du Pont 1090B thermal analyzer and a 951 thermogravimetric analyzer.

Melt Blending. Poly(2-ethyl-2-oxazoline) was melt blended with other polymers at 190 °C for 10 min in an oil-heated Brabender mixer. The polymer blends were ground in a Wiley mill with a 16-mesh screen and stored in glass bottles.

Results and Discussion

Physical Properties. Poly(2-ethyl-2-oxazoline) is amorphous. It has a T_g of 55 °C when measured on a quenched sample. With an unquenched specimen, the T_g ranges from 69 to 71 °C.

The polymer has a Vicat temperature of 70 °C. Depending on its molecular weight, poly(2-ethyl-2-oxazoline) exhibits a softening range of 110 to 120 °C. The thermal stability of the polymer is exceptionally good. Figure 1 shows a TGA of a \bar{M}_w 500,000 polymer. No substantial

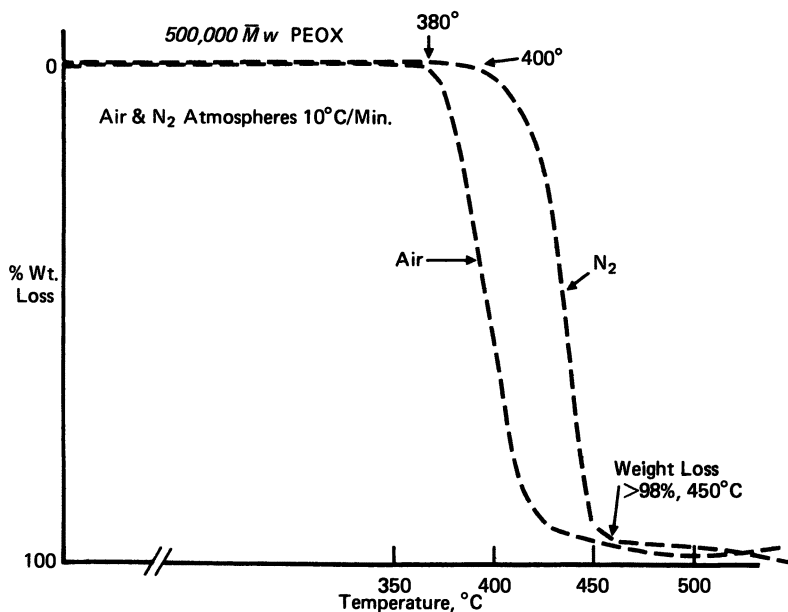


Figure 1. Thermal gravimetric analysis of a \bar{M}_w 500,000 poly(2-ethyl-2-oxazoline). The air and nitrogen atmospheres changed at a rate of 10 °C/min.

degradation occurs until 380 °C (716 °F) in air and 400 °C in a nitrogen atmosphere.

The polymer's refractive index of 1.520 ± 0.001 coincidentally matches that of glass. This fact may suggest utilities where a close match of refractive indexes is preferred in certain glass-polymer systems.

Rheology. As an amorphous linear polymer, poly(2-ethyl-2-oxazoline) exhibits a rather unexpected rheological behavior. Figure 2 shows the viscosity of molten polymer plotted against varying shear rates at 170 °C. A polystyrene ($\bar{M}_w = 275,000$) curve was included for reference of a well-known pseudoplastic material. The lower the molecular weight of the polymer, the more the behavior of the polymer approaches Newtonian behavior. Under the high-shear conditions of a Vickers vane pump, a formulated aqueous solution of \bar{M}_w 200,000 poly(2-ethyl-2-oxazoline) retained three-quarters of its initial viscosity after 260 h of test operation. This behavior is generally manifested in the excellent melt flow and relative shear stability of the polymer in handling and processing.

The solution properties of poly(2-ethyl-2-oxazoline) were studied. Intrinsic viscosities were determined for four samples of the polymer with molecular weights of 50,000, 100,000, 200,000, and 500,000 in aqueous solutions (12). Figure 3 plots $\log [\eta]$ versus $\log M$. The Mark-Houwink equation deduced is

$$[\eta] = (6.5 \times 10^{-4})M^{0.56}$$

The value of the exponent of M being 0.56 indicates that water is nearly a θ solvent for the polymer. Consequently, high concentrations of the polymer in aqueous solution can be handled without excessive thickening. A comparison of viscosity versus percent concentration in water for the polymer and four other water-soluble polymers is shown in Figure 4.

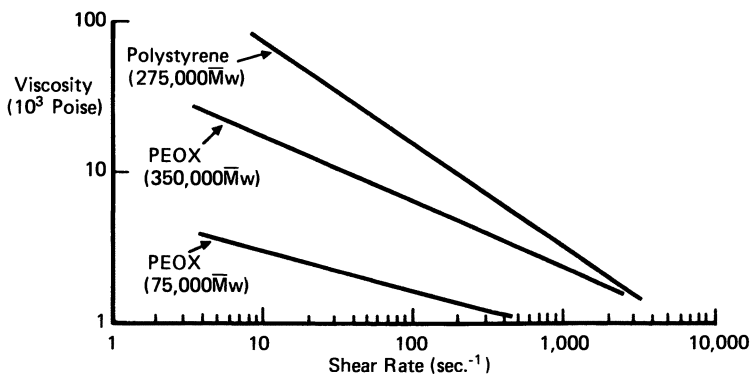


Figure 2. Viscosity of poly(2-ethyl-2-oxazoline) vs. shear rate at 170 °C.

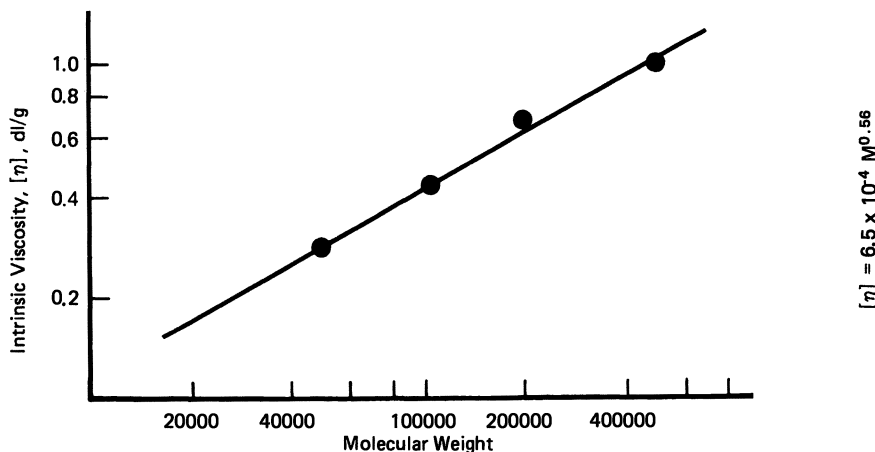


Figure 3. Intrinsic viscosity vs. the molecular weight of an aqueous solution of poly(2-ethyl-2-oxazoline) at 25 °C. $[\eta] = 6.5 \times 10^{-4} M^{0.56}$.

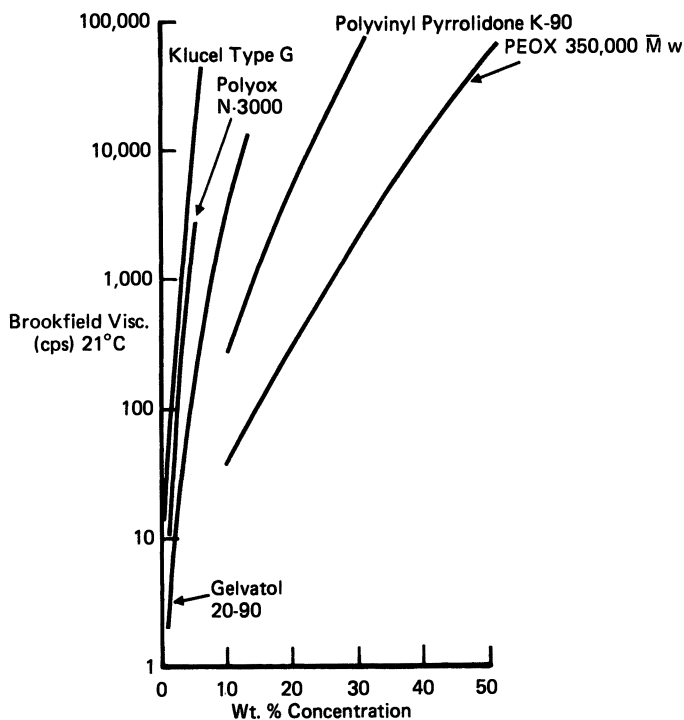


Figure 4. Aqueous solution viscosity vs. the concentration of poly(2-ethyl-2-oxazoline) compared to that of other water-soluble polymers. The weight-average molecular weight was 300,000 for Klucel Type G; 400,000 for Polyox N-3000; 125,000 for Gelvitol 20-90; and 350,000 for poly(2-ethyl-2-oxazoline). The number-average molecular weight was 360,000 for poly(vinylpyrrolidone).

At comparable concentrations, solutions of poly(2-ethyl-2-oxazoline) appear to be several orders of magnitude less viscous than (hydroxypropyl)cellulose (Klucel), poly(ethylene oxide) (Polyox), poly(vinyl alcohol) (Gelvatol), and poly(vinylpyrrolidone).

Solubility and Cloud Point. Table I highlights the solubility of poly(2-ethyl-2-oxazoline) in various solvents arranged according to their solubility parameter, δ . The polymer has an unusually broad solubility in solvents ranging from chloroform, methyl acetate, methylene chloride, acetonitrile, ethanol, and water. Water has been noted to be a room-temperature θ solvent for the polymer. At elevated temperatures, the polymer tends to drop out of the solution and exhibits a cloud point as shown in Figure 5. For a higher weight-average molecular weight polymer of 350,000, the cloud point is 62.0 °C; a lower weight-average molecular weight polymer of 70,000 has a cloud point of about 64.5 °C. The cloud point of an aqueous solution of the polymer can be raised by the addition of a surfactant or a better solvent, such as a glycol, which is miscible with water.

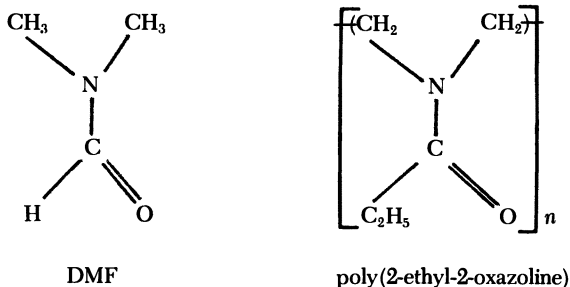
Polymer Blends. Oxazoline polymers may be considered as polymeric analogues of *N,N*-dimethylformamide (DMF) (13):

Table I. Solubility of Poly(2-ethyl-2-oxazoline)

δ	<i>Solvent</i>	<i>Solubility</i>
7.0	<i>n</i> -pentane	P ^a
7.4	diethyl ether	P
7.8	diisobutyl ketone	P
8.5	<i>n</i> -butyl acetate	P
8.9	toluene	P
9.3	perchloroethylene	P
9.3	dibutyl phthalate	P
9.3	chloroform	S ^b
9.3	methyl ethyl ketone	S
9.5	ethylhexanol	S
9.6	methyl acetate	S
9.7	methylene chloride	S
9.9	acetone	S
10.0	dioxane	S
11.9	acetonitrile	S
12.7	nitromethane	S
12.7	ethanol	S
13.3	propylene carbonate	S
14.5	methanol	S
23.4	water	S

^aP is less than 2% by weight.

^bS is greater than 25% by weight.



This suggests that poly(2-ethyl-2-oxazoline) could be a broadly compatible polymeric solvent. This suggestion was verified by the observation that a number of blends (14) with the polymer exhibit miscibility such that single T_g values resulted for the systems. Some of the polymers found to be miscible with poly(2-ethyl-2-oxazoline) polymer are styrene-acrylonitrile copolymer, acrylonitrile-butadiene-styrene copolymer, and phenoxy resin. Partial miscibility was observed with vinylidene chloride-vinyl chloride copolymer.

Applications. Many of the novel utilities of poly(2-ethyl-2-oxazoline) stem from its polymeric-solvent nature. Compounding with poly(2-ethyl-2-oxazoline) enhances the adhesion of some polymer sys-

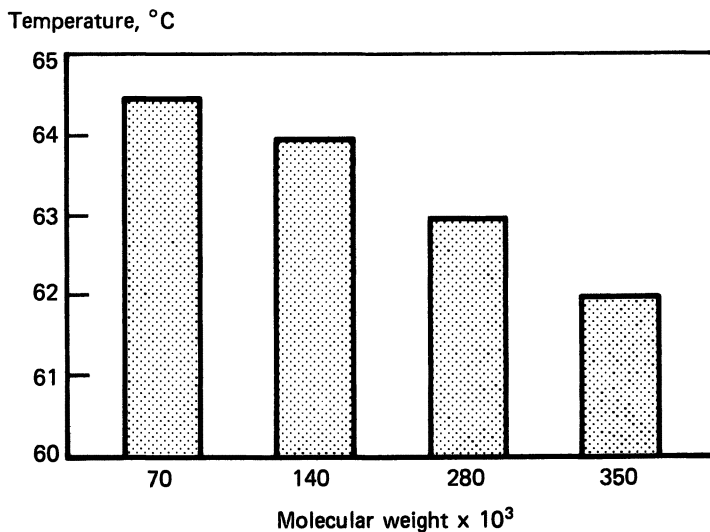


Figure 5. Cloud point of poly(2-ethyl-2-oxazoline) of four different molecular weights. The concentration of poly(2-ethyl-2-oxazoline) was 1.0% in water.

tems to polar substrates. In some blends, the addition of poly(2-ethyl-2-oxazoline) modifies the fluid permeability. An example of this modification would be the improved moisture transmission through a blend of plasticized poly(vinyl chloride) and poly(2-ethyl-2-oxazoline). In other instances, controlled release of specific ingredients may be achieved via formulations with poly(2-ethyl-2-oxazoline) into a carrier matrix.

The rheological and thermal properties of poly(2-ethyl-2-oxazoline) allow it to be applied either from solution or by the hot-melt technique. Such an adhesive coating can be employed directly and used in a moisture-activatable system or in a heat-sealable construction.

Poly(2-ethyl-2-oxazoline) applied from aqueous solutions adheres to aluminum foil, cellophane, nylon, poly(vinyl alcohol), poly(methyl methacrylate), and poly(ethylene terephthalate). Poly(2-ethyl-2-oxazoline)'s adhesion compares very favorably with that of poly(vinylpyrrolidone) or poly(vinyl alcohol) as shown in Table II. In a composite system, chopped fiberglass sized with a formulation containing PEOX-brand polymer has been used to reinforce a styrene-acrylonitrile copolymer. Outstanding tensile strength and Izod impact have been noted.

Summary

Poly(2-ethyl-2-oxazoline) is unique because of the combination of its properties:

- nonionic;
- soluble in water and polar organic solvents;
- low viscosity;
- polymer compatibility;
- thermoplastic;
- high thermal stability;
- adhesion enhancement; and
- low hazard.

Table II. Adhesion of Poly(2-ethyl-2-oxazoline), Poly(vinylpyrrolidone) and Poly(vinyl alcohol) to Plastic-Metal Films

<i>Substrate</i>	<i>Poly(2-ethyl-2-oxazoline), M_w 500,000</i>	<i>Poly(vinylpyrrolidone), M_n 360,000</i>	<i>Poly(vinyl alcohol), M_w 125,000</i>
Aluminum foil	pass	pass	fail
Cellophane	pass	fail	pass
Nylon	pass	fail	fail
Poly(vinyl alcohol)	pass	fail	—
Poly(methyl methacrylate)	pass	fail	fail
Poly(ethylene terephthalate)	pass	fail	fail

NOTE: The Scotch Tape test (Scotchbrand 600 tape) was used.

The physical properties of the polymer allow it to be utilized in both hot-melt and solution adhesives for dissimilar materials. The adhesion properties of the polymer may be activated by heat or moisture. Because it is water soluble, adhesives formulated with the polymer provide recyclability. Many innovative applications of the polymer are suggested by its combination of properties.

Literature Cited

1. Tomalia, D. A.; Sheetz, D. P. *J. Polym. Sci.* **1966**, A-1, 4, 2253.
2. Bassiri, T. G.; Levy, A.; Litt, M. *Polym. Lett.* **1967**, 5, 187.
3. Frump, J. A. *Chem. Rev.* **1971**, 71(10), 483.
4. Seeliger, W. et. al. *Angew. Chem., Int. Ed. Engl.* **1966**, 5(10), 875.
5. Kem, K. M. *J. Polym. Sci., Polym. Chem. Ed.* **1979**, 17, 1977.
6. Chamberlin, T. A.; Madison, N. L. U.S. Patent 4 001 160, 1977.
7. Kelyman, J. S. U.S. Patent 4 087 413, 1978.
8. Tomalia, D. A. et al. U.S. Patent 4 112 067, 1978.
9. Miller, S. L.; Dickert, Y. J. U.S. Patent 4 113 674, 1978.
10. Dickert, Y. J.; DeRoo, A. M. U.S. Patent 4 132 831, 1979.
11. Chamberlin, T. A.; Bangs, S. W. U.S. Patent 4 144 211, 1979.
12. Buchholz, F. L. The Dow Chemical Company, private communication.
13. Miyamoto, M. et. al. *Eur. Polym. J.* **1983**, 19(10/11), 955.
14. Keskkula, H.; Paul, D. R. *Proc. Div. PMSE ACS Meeting, St. Louis, MO* **1984**, p 11.

RECEIVED for review September 28, 1984. ACCEPTED October 10, 1985.

AUTHOR INDEX

- Argabright, P. A., 269
Barth, Howard G., 31, 101
Chauveteau, G., 227
Chen, Robert Gow-Sheng, 197
Chiu, Thomas T., 425
Clark, R. K., 171
Craig, D. H., 351
Croll, S. G., 315
Eley, Richard R., 315, 417
Estes, Jack, 155
Fairchok, William J., 425
Fishman, Marshall L., 57
Gelman, Robert A., 101
Glass, J. E., 3, 85, 183, 391
Heimle, S. A., 183
Hughes, Kathleen, 145
Kleinle, R. L., 333
Koehler, Mark E., 315
Menjivar, Juan A., 209
Patel, Arvind D., 197
Pepper, Leonard, 57
Pfeffer, Philip E., 57
Rey, P. A., 113
Rhudy, J. S., 269
Rudin, Alfred, 71
Schaller, E. J., 375
Schwab, F. G., 369
Shah, S., 183
Sperry, P. R., 375
Swift, Graham, 145
Tchir, Morris F., 71
Thibeault, J. C., 375
Thill, Bruce P., 425
Trujillo, E. M., 269
Varsanik, R. G., 113
Woo, James T. K., 417
Zander, Richard A., 315

SUBJECT INDEX

A

- Absolute molecular weight detectors for size-exclusion chromatography
low-angle laser light-scattering photometry, 46–48
viscometry, 46, 48–49
Absorbed polymers, generalized conformation, 88, 89f
Acrylamide polymers
applications, ¹³C-NMR analyses, 80–81
effects of hydrolysis, 81
Acrylic latices, percent (hydroxyethyl)cellulose grafted, 363, 364t
Activated sludge process, description, 134
Adsorption
conformation of adsorbed polymer, 88, 89f
effect on coatings applications, 93–96
vs. degree of substitution, 190, 191f
effect on petroleum applications, 96, 97f, 98
enthalpic contributions, 86–87, 88–90f
entropic contributions, 86, 87f
general characteristics, 87, 88f
Adsorption—Continued
general concepts, 85–86
K_D vs. ionic strength, 36, 37f
K_D vs. temperature, 37–38
mobile-phase selection for aqueous size-exclusion chromatography, 36
vs. molecular weight, 193f
variation of surface pressure and concentration with time, 88, 89–90f
Aerobic digestion, classifications, 134
Agarose, structure and properties, 25
Alginate acid
egg-crate complex formation, 22–23
properties, 18
structure, 17–19
Amylopectin, structure, 15
Amylose
derivatization, 13
structure, 7
Anaerobic digestion, description, 234
Analytical data analysis for polymer feasibility tests
sampling procedures, 294–295
viscosity vs. shear rate, 295–296f
Anionic and nonionic polymers
effect of pH on charge, 117, 120f
use as flocculents, 117

AUTHOR INDEX

- Argabright, P. A., 269
Barth, Howard G., 31, 101
Chauveteau, G., 227
Chen, Robert Gow-Sheng, 197
Chiu, Thomas T., 425
Clark, R. K., 171
Craig, D. H., 351
Croll, S. G., 315
Eley, Richard R., 315, 417
Estes, Jack, 155
Fairchok, William J., 425
Fishman, Marshall L., 57
Gelman, Robert A., 101
Glass, J. E., 3, 85, 183, 391
Heimle, S. A., 183
Hughes, Kathleen, 145
Kleinle, R. L., 333
Koehler, Mark E., 315
Menjivar, Juan A., 209
Patel, Arvind D., 197
Pepper, Leonard, 57
Pfeffer, Philip E., 57
Rey, P. A., 113
Rhudy, J. S., 269
Rudin, Alfred, 71
Schaller, E. J., 375
Schwab, F. G., 369
Shah, S., 183
Sperry, P. R., 375
Swift, Graham, 145
Tchir, Morris F., 71
Thibeault, J. C., 375
Thill, Bruce P., 425
Trujillo, E. M., 269
Varsanik, R. G., 113
Woo, James T. K., 417
Zander, Richard A., 315

SUBJECT INDEX

A

- Absolute molecular weight detectors for size-exclusion chromatography
low-angle laser light-scattering photometry, 46–48
viscometry, 46, 48–49
Absorbed polymers, generalized conformation, 88, 89f
Acrylamide polymers
applications, ¹³C-NMR analyses, 80–81
effects of hydrolysis, 81
Acrylic latices, percent (hydroxyethyl)cellulose grafted, 363, 364t
Activated sludge process, description, 134
Adsorption
conformation of adsorbed polymer, 88, 89f
effect on coatings applications, 93–96
vs. degree of substitution, 190, 191f
effect on petroleum applications, 96, 97f, 98
enthalpic contributions, 86–87, 88–90f
entropic contributions, 86, 87f
general characteristics, 87, 88f
Adsorption—Continued
general concepts, 85–86
K_D vs. ionic strength, 36, 37f
K_D vs. temperature, 37–38
mobile-phase selection for aqueous size-exclusion chromatography, 36
vs. molecular weight, 193f
variation of surface pressure and concentration with time, 88, 89–90f
Aerobic digestion, classifications, 134
Agarose, structure and properties, 25
Alginate acid
egg-crate complex formation, 22–23
properties, 18
structure, 17–19
Amylopectin, structure, 15
Amylose
derivatization, 13
structure, 7
Anaerobic digestion, description, 234
Analytical data analysis for polymer feasibility tests
sampling procedures, 294–295
viscosity vs. shear rate, 295–296f
Anionic and nonionic polymers
effect of pH on charge, 117, 120f
use as flocculents, 117

- Applications
 coatings, 93-96
 petroleum, 96-98
- Applications of ^{13}C NMR
 acrylamide polymers, 80-81
 cellulosics, 79-80
 future trends, 82
 poly(vinyl alcohol), 81-82
- Aqueous drilling fluids
 filtrate loss, 200*t*
 performance, 203-206
 preparation, 199
 rheological measurements, 199
- Associative thickeners
 adsorption isotherms, 378-379
 advantages, 370*t*, 371
 cleanup procedures, 373
 cost savings, 371, 372*t*
 degree of association, 376
 difference from conventional thickeners, 376*t*, 377
 disadvantages, 370*t*
 effect of hydrophobic components, 383, 384-386*f*
 effect of latex particle size on adsorption, 381-382*f*
 effect of latex particle size on viscosity-shear-rate profile, 383*f*
 effect of sodium dodecyl sulfate on rheology, 387*f*
 effect of water-miscible cosolvents, 388*f*, 389
 efficiency of nonionic vs. anionic, 381, 384, 388
 improved compatibility, 371
 leveling, 377
 phase separation, 371-372
 picking, 372
 problems from a manufacturing viewpoint, 372-373
 quality-control problems, 373
 rheology, 370-371
 stormer viscosity, 376*t*
 synthesis, 414
 use of new manufacturing procedures, 373
 viscosity, 376*t*, 377
 viscosity-shear-rate profiles, 379-380*f*
- Axial, definition, 6
- Axial ratios, heated vs. unheated pectins, 66, 67*t*

B

- Belt press, use in sludge dewatering, 137, 140*f*
- Bentonite
 beneficiation, 158
 clay preparation, 184-185
 filtration control of muds, 183-195
 polymer extenders, 163-167
 thickener agent for drilling, 183
- Bentonite slurry, rheological profiles, 187, 188*f*
- Biopolymers, definition, 31

- Bit design, effect on drilling rate, 157
- Blistering
 definition, 420
 influencing factors, 422, 424
 values for coatings, 419*t*, 420
- Branching, effect on water solubility, 14-17
- Brookfield viscosities, effect of hydrophobically modified (hydroxyethyl)cellulose concentration, 103, 104*t*

C

- ^{13}C NMR
 applications, 79-82
 qualitative analyses, 76-77
 quantitative analyses, 77-79
- ^{13}C -NMR analytical techniques
 advantage over ^1H NMR, 72
 background, 72
 factors affecting choice of spectrometer, 73
 future trends, 79
 instrumentation, 72-74
 sample preparation and resolution, 74-76
 spectrum, 76-79
- Carbohydrate polymers
 chemistry, 3-4
 structural features that affect water solubility, 14-25
- Carboxylate anions, properties, 19
- Carboxylate groups, characteristics, 17
- Carrageenans, structure and properties, 24-25
- Cassion viscosity data, epoxy-g-(styrene-methacrylic acid) graft copolymers, 421
- Cationic polymers
 copolymer composition, 120-121
 improvements in molecular weight, 120
 use as flocculents, 117, 120-121
- Caustic concentration, effect on reactivity, 9-11
- Cellobiose, structure, 6
- Cellulose
 basic anhydroglucose unit, 334
 description, 334
 effect of caustic concentration, 10
 reactivities of the hydroxyl groups, 80
 solubilization through derivatization, 9
- Cellulose acetate, water solubility, 80
- Cellulose ethers
 advantages for coatings use, 333
 color acceptance, 347, 348*f*
 composition and structure, 334
 degradation, 348-349
 efficiency, 340, 341*t*
 flow and leveling-sag resistance, 341, 342*t*, 343*f*, 344
 freeze-thaw stability, 348
 gloss, 347
 paint manufacture, 349
 replacement by hydrophobically modified water-soluble polymers, 370

Cellulose ethers—*Continued*
 spatter, 344, 345f
 thickening mechanism, 338–339, 340f
 water resistance, 344–347

Cellulose sulfate ester
 stability, 22
 synthesis, 19

Cellulosic thickeners, 334–335

Cellulosics, ¹³C-NMR analyses, 79–80

Centrifuges, use in sludge dewatering, 137

Chair form, definition, 5–6

Characterization of macromolecules in solution
 chemical structure, 228–230
 concentration regimen, 232
 dynamic properties, 231–232
 macromolecular dimensions, 230–231
 macromolecular near an interface, 233
 molecular weight distribution, 233–236
 salt sensitivity, 233

Charge density
 effect of sodium maleate, 202
 effect of carboxylate units, 201–202
 sodium tetrahydrophthalate, 202

Chemical heterogeneity, 49–52

Clay minerals
 composition, 173
 response to water, 173

Coatings, effect of surface tension, 316–317

Coatings applications
 effect of flocculation, 95
 effect of preadded stabilizers, 95–96
 effect of stabilizers, 95
 interfacial energies, 93, 94f

Coatings performance, influence of cellulose ethers, 333–349

Color acceptance for paint
 effect of molecular weight, 348f
 evaluation by a rub-up method, 347, 348f

Column calibration for size-exclusion chromatography
 average molecular weight determination, 44–45
 broad molecular weight distribution approach, 45
 curve construction, 44
 Mark–Houwink approach, 45
 universal calibration procedure, 45–46

Commercial partially hydrolyzed poly(acrylamide), mobility behavior, 274, 275f, 276

Commercial trade-sale paints, shear-rate dependence of the first normal stress difference, 397, 399f

Composition of solids, dewatering rate vs. composition, 115, 116f

Concentration regimen of macromolecules, 232

Coring
 coring fluid, 278
 laboratory flooding of core, 279
 purpose, 278–279
 size of core, 279

Coring geologic description of core, 279, 280f

Counterion binding, heated vs. unheated pectins, 66, 67t, 68f

Coverage
 definition, 419
 values for coatings, 419t

Critical polymer concentration
 effect
 of elastic properties, 219, 220f
 of polymer molecular weight, 218, 219t
 on rheological properties of polymer solutions and gels, 219, 220–221f
 experimental determination, 216–219
 low-shear specific
 viscosity-concentration profiles, 217f, 218
 solution behavior transition, 217f, 218

Custom-manufactured partially hydrolyzed poly(acrylamide), mobility behavior, 273, 274f, 275

D

Data analysis, surface tension measurements, 320–321, 322–324f

Degradation of cellulosic thickeners, effect of microorganisms, 348–349

Degree of polymerization, weight average, determination, 109–110

Degree of substitution, definition, 334

Design parameters for field polymer flood applications
 bank size, 287, 288f
 concentration, 287f
 rock properties, 287–288, 289–290f
 structure, 286f, 287

Dextran, description, 20

Disk flooding
 design parameters, 286–290f
 mobility reduction, 282–285
 purpose, 279
 reverse injection, 285f, 286
 schematic, 281
 technique, 280–282
 tertiary vs. secondary floods, 282, 283–284f

Dissolved air flotation, description, 135, 137f

Drilling fluid–shale interactions, effect of water phase on shale properties, 174

Drilling fluids
 description, 171–172
 vs. drilling rates, 185t, 186–187f
 method to assess additive performance as shale stabilizers, 175–176

Drilling rates
 vs. clay-solids contents, 160, 161f, 162–163
 vs. drilling fluid, 185t
 effect
 of bit design, 157
 of elasticity of a fluid, 186f–187f
 of polymer extenders, 161–163
 of sloughing shale, 156–157
 effect of solids content, 157f, 158

Dry polymers, automatic feed system, 126, 127f

- Dynamic properties of macromolecules, calculation, 231
- Dynamic surface tension
 - definition, 316
 - influence on coatings, 316-317
- Dynamic testing methods of shale-fluid interactions, description, 176

E

- Efficiency
 - effect of degree of substitution, 341
 - measurement, 340
 - variation with molecular weight, 340,341*t*
- Elasticity, definition, 317,318
- Electroviscosity, description, 39,40*f*
- Elongational strain rate
 - cause, 43
 - effect on polymer shear degradation during size-exclusion chromatography, 42-43
- Elution volume of a polymer, definition, 32-33
- Emulsion polymerization
 - acrylic recipe, 353, 354*t*, 355
 - grafted (hydroxyethyl)cellulose determination, 355
 - latex characterization, 355
 - vinyl acetate homopolymer, 353, 355*t*
 - vinyl acetate-acrylic recipe, 353, 354*t*, 355
- Emulsion polymers
 - advantages in wastewater treatment, 127-128
 - feed system, 128*f*
- Emulsions, thermodynamic stability, 418
- Enthalpic contributions to adsorption
 - coatings applications, 93, 94*t*,*f*, 95-96
 - interactions, 86-87
 - polymer-substrate interactions, 92*t*
 - polymer-water interactions, 90,91*f*,92
 - substrate-water affinity, 92,93*f*
- Entropic contributions to adsorption, temperature dependence, 86, 87*f*
- Epoxy resins, grafting by reaction of carboxyl-epoxide functionalities, 418
- Epoxy-*g*-(styrene-methacrylic acid) copolymer
 - properties, 418
 - structure, 418
 - synthesis, 418
- Equatorial bonds, definition, 6
- Ethylene oxide
 - addition to caustic, 10
 - reactivity, 10
 - selective of addition, 10
 - slurry process, 11
- 2-Ethyl-2-oxazoline
 - polymerization, 426
 - properties, 425
- Eugenol
 - molecular weight control, 201
 - structure, 201-202

- Eugenol-maleic anhydride-*n*-vinyl-*n*-methylacetamide terpolymer
 - IR measurement, 199
 - IR spectroscopy, 202, 203*f*
 - membrane osmometry, 199
 - preparation, 199
 - sulfomethylation, 199, 202
 - viscosity-temperature relationship, 204, 206*f*
- Exterior semigloss paint, definition, 336
- Extracellular polysaccharides
 - fermentation synthesis, 8-9
 - solution properties, 9

F

- Face plugging, definition, 272
- Fenton oxidations, mechanism, 146
- Field feasibility testing
 - advantages, 288-290
 - injection well selection, 290, 291*f*
 - polymer injection equipment and instrumentation, 292, 293*f*, 294
 - polymer-blending systems, 291*f*, 292
 - pressure data and analysis, 295-300
 - water testing, 294*f*
- Field-curve matching in feasibility description, 300-301
 - example of simulator output, 301*f*
- Film strength factor, description, 317
- Filtration control of bentonite slurries
 - adsorption vs. degree of substitution, 190, 191*f*
 - adsorption-bridging-flocculation mechanism, 194-195
 - fluid loss dependence on polymer concentration, 189, 190*f*, 192*f*
 - montmorillonite flocculation mechanism, 195
 - preferential adsorption of anionic polymer mechanism, 195
 - vs. type of water-soluble polymer, 190
- Fisheyes, definition, 126
- Flocculation, mechanism, 338-339
- Flocculation mechanisms, polymer bridging of particles, 122-123
- Flow behavior of macromolecules in porous media
 - flow through nonadsorbent pores, 248-254
 - flow through porous media having large pores, 246-248
 - flow through small adsorbent pores, 254-257
 - pore-size dependence of thickening behavior and of mechanical degradation, 257-258
- Flow through capillaries, relative viscosity measurements, 241,242*f*
- Flow through nonadsorbent small pores
 - effects of polymer concentration, 251, 252, 253-255*f*
 - Newtonian regimen, 249*f*, 250*f*
 - problems with microgels, 248-249
 - shear-thinning regime, 250, 251-252*f*

- Flow through small adsorbent pores
 effect of polymer concentration, 256, 257f
 thickness of adsorbed layer, 254-255, 256f
- Flowout, phase separation, 400-401
- Flowout time of a coating, influencing parameters, 395, 396f
- Foam, properties, 317
- Foam stability
 bulk liquid Newtonian shear viscosity vs. average foam lifetime, 326, 329f, 331
 complex dilational surface modulus vs. average foam lifetime, 326, 329f, 331
 vs. foam height, 326f
 equilibrium surface tension vs. average foam lifetime, 326, 328f, 331
 film strength factor, 317
 hydrodynamic factor, 317, 318f
 interfacial dilational elasticity, 317, 318-319f
 measurement, 322
 Plateau-Marangoni-Gibbs elasticity, 325-331
 shear viscosity vs. foam height, 326, 328f
 surface dilational elastic modulus vs. average foam lifetime, 326, 330f, 331
 vs. foam height, 326, 327f
 surface dilational viscosity vs. average foam lifetime, 326, 330f, 331
 vs. foam height, 326, 327f
- Fracturing gels
 effect of metal type on thermal stability, 223, 224f
 stability at high temperatures, 223
 performance in hydraulic fracturing treatments, 210
 polysaccharides used in fluids, 211
- Freeze-thaw stability of paint, effect of thickener, 348
- Full-field development for polymer-augmented waterflooding
 distribution and injection facilities, 304-309
 environmental hazards, 310
 injection water and produced fluids, 308, 310
 injection well completion, 302
 partially hydrolyzed poly(acrylamide) source, 302
 well patterns, 302

G

- Galactomannans, derivatization, 14
- Gel polymers, advantages in wastewater treatment, 128
- Gel strength of aqueous drilling fluids, 200t, 203
- Gelation
 mechanism, 212-214
 theory, 214-216

- Gelation theory
 liquid-gel phase diagram, 215, 216f
 model, 214-216
 use of pressure rheometer, 216
- Geometric factors, effects on thickening behavior, 242, 243f
- Gloss
 definition, 347
 effect of thickener or thickner molecular weight, 347
- $\alpha(1-4)$ -Glucopyranose, effect of branching on water solubility, 15-16
- $\beta(1-3)$ -Glucopyranose, effect of branching on water solubility, 16-17
- Glyceraldehyde, structure, 3-4
- Glycogen, structure, 15
- Graft copolymers, preparation, 198-199
- Grafted epoxy-strene-methacrylic acid copolymer
 application with various free radical initiator levels, 419t
 Casson viscosity data, 421f
 effect of free-radical initiator on particle size, 421
 effect of molecular weight, 420t, 421
 purpose, 419
- Grafted (hydroxyethyl)cellulose
 amount, 355-356
 amount vs. initial concentration during acrylic latex polymerization, 356f
 degradation, 356, 357f
 effect of increasing concentration of triethanolamine, 357, 358f
 effect of surfactant, 359, 362f
 effect of time
 of (hydroxyethyl)cellulose addition, 359, 360-361f
 of initiator addition, 359, 361f
 of triethanolamine addition, 359-360f
 grafting of acrylic monomer vs. vinyl-acrylic system, 362, 363f
 molecular weight distribution, 356, 357f
- Grafting
 Casson viscosity, 421t
 effect of free-radical initiator on particle size, 421
 effect of molecular weight, 420t, 421
 function of free-radical initiator concentration, 419t, 420
- Gravity thickening, description, 135
- Guaran, derivatization, 13

H

- Heated pectins
 axial ratios vs. unheated pectins, 66, 67t
 counterion binding vs. unheated pectins, 66, 67t, 68f
 degree of polymerization vs. unheated pectins, 64, 65f, t, 66-67
 dissociation, 62, 63t, 63-64f
 heated vs. unheated pectins, 64, 65f, t, 66, 67t
- Hexoses, structure, 4

- High-shear-rate viscosities
 vs. amount of thickener required, 401, 403f
 dependence on chemical structure, 401, 402f
 effect of formulation variables, 394, 395f
 thickener influence, 401
- High-shear-rate viscosity
 effect of latex size, 407–408f
 effect of percent nonvolatiles, 410, 411f
- Huggins constant
 definition, 105, 107
 for sodium oleate solutions, 107, 109f
 vs. solvent composition, 107, 108f
- Hydraulic fracturing
 additives to improve performance, 210
 description, 209, 210f
 role of polymer thickening agent, 210
- Hydrodynamic chromatography
 description, 233–234
 influence of polymer concentration on chromatographic fractionation, 234, 235f
 influence of shear rate on chromatographic fraction, 234f
- Hydrodynamic factor, description, 317, 318f
- Hydrolyzed poly(acrylamides)
 characteristics, 236f
 chemical structure, 229–230
 molecular weight distribution, 234, 236f
 salt sensitivity, 233
 use in enhanced oil recovery processes, 228
- Hydrophobically modified (hydroxyethyl)cellulose
 Brookfield viscosity measurements, 102
 enhanced solution viscosity, 101–102
- Hydrophobically modified thickeners, structures, 393–394
- Hydrophobically modified, water-soluble polymer thickened formulations, 401–413
- Hydrophobically modified, water-soluble polymers, molecular weight and surface tension data, 397, 398f
- (Hydroxyethyl)cellulose
 adsorption isotherms, 378f, 379
¹³C-NMR analyses, 80
 chemistry in the presence of persulfate and acrylic monomers, 365
 grafting of vinyl acetate, 351
 production of acrylic and vinyl-acrylic copolymer latices, 353
 thickening mechanism, 338–339, 340f
 use as protective colloid, 351
 viscosity vs. shear, 336, 337f, 338
 viscosity-shear-rate profiles, 379, 380f
 viscosity studies, 101–110
- I**
- Injection water and produced fluids, treatment for polymer-augmented waterflooding, 308, 310
- Injection well selection
 requirements, 290–291
 well completion types, 291f
- Instrument design, surface tension measurements, 320–321f
- Instrumentation for ¹³C NMR
 field lock system, 73–74
 number designation of spectrometer, 72
 pulsed Fourier transform spectrometers, 72
 resolution factors, 73
- Interfacial dilational elasticity
 description, 317, 318–319f
 mechanism of self-handling, 318–319f
- Interior flat paint, definition, 336
- Interior semigloss paint, definition, 336
- Interunit positional bonding
 description, 19–23
 effect on water solubility, 14
- Intramolecular electrostatic effects
 electroviscosity, 39, 40f
 K_D vs. ionic strength, 38, 39f
- Intrinsic viscosity, description, 159
- Intrinsic viscosity measurements
 Huggins constant, 105, 107, 108f
 vs. methanol composition, 107, 108f
 vs. solvent composition, 105t, f, 106f, 107
- Ion exchange interactions, mobile-phase selection for aqueous size-exclusion chromatography, 34–35
- Ion exclusion interactions, mobile-phase selection for aqueous size-exclusion chromatography, 35
- Ion inclusion interactions, mobile-phase selection for aqueous size-exclusion chromatography, 35–36
- Ionizing groups
 effect of branching on water solubility, 16–17
 effect on water solubility, 14
- L**
- Laboratory-curve matching in feasibility tests
 description, 297–298
 example of simulator output, 300
- Laboratory testing of shale-fluid interactions, static methods, 175
- Latex-associative thickener association
 adsorption isotherms, 378f
 effect of hydrophobic components, 383, 384–386f
 effect of latex particle size
 on adsorption, 381–382f
 on viscosity-shear-rate profile, 383f
 effect of water-miscible cosolvents, 388f, 389
 experimental procedures, 377–378
 viscosity-shear-rate profiles, 379, 380f
- Latex paint, 375–376
- Latex variation
 effect of size, 407–408f

- Latex variation—*Continued*
 sensitivity, of hydrophobically modified, water-soluble polymer thickened formulations, 407
- Leveling, definition, 377
- Leveling of paint
 center-line average, 341, 342t
 effect of molecular weight, 342t
 flow properties for two paints, 342, 343f
 quantitative measurement, 341
 sag charts for two paints, 342, 343f
- Lignosulfonates, effectiveness as a dispersant, 198
- Line width
 definition, 74
 effect of high viscosity, 75
 effect of relaxation times, 75
 resolution, 74–75
- Linear hydrocarbons, ring formation, 5–6
- Low-angle laser light scattering
 advantages, 47
 limitations, 47–48
 principles, 46–48
 Rayleigh factor, 47
- Low molecular weight water-soluble polymers, metal-activated redox initiation, 145–151
- Low-shear-rate viscosity
 dependence on thickener concentration, 414, 415f
 dispersant and formulation surfactant effects, 413
 effect of formulation variables, 394, 395f
 effect of percent nonvolatiles, 409–410f
 influence of thickener-dispersed component interactions, 394–401

M

- Macromolecular dimensions, calculation, 230–231
- Macromolecules near an interface, effect on properties, 233
- Macromolecules in porous media, flow behavior, 246–258
- Macromolecules in solution
 characterization, 228–236
 rheological properties, 236–246
- Maltose, structure, 6
- $\beta(1-4)$ -Mannopyranose
 effect of branching on water solubility, 16–17
 structure, 16
- Mechanical degradation, pore-size dependence, 257, 258f
- Mechanical degradation in elongational flows, results, 246
- Mechanism, of polymer-augmented waterflooding, 271
- Membrane osmometry
 experimental procedures for pectin, 59–60
 theory, 58–59

- Metal-activated redox initiation processes for poly(acrylic acid) synthesis
 effect of amine level, 149, 150t
 effect of copper to hydrogen peroxide molar ratio variations, 147, 148t
 effect of hydrogen peroxide as an initiator, 146, 147t
 effect of hydrogen peroxide level variation, 148, 149t,f
 effect of temperature, 150t
 proposed mechanisms, 150–151
- Metal cross-linked polymer gels, characterization, 209–225
- Metal cross-linked polymer hydrogels, effect of temperature on elastic properties, 222–225
- Metal cross-linked polysaccharide gels
 gelation mechanism, 212–214
 gelation theory, 214–216
 metals used in fracturing fluids, 211 vs. un-cross-linked gels, 211
- Methylene blue test procedure, estimation of submicron particles in drilling mud, 162–163
- Mobile-phase selection for aqueous size-exclusion chromatography
 adsorption, 36–38
 ion exchange, 34–35
 ion exclusion, 35
 ion inclusion, 35–36
- Mobility behavior
 for commercial partially hydrolyzed poly(acrylamide), 274, 275f, 276
 for custom-manufactured partially hydrolyzed poly(acrylamide), 272, 274–275f
 influence of salt, 276, 277f
 reduction by polymer, 282–283, 284f, 285
- Mobility of displacement water in oil well drilling, viscosity vs. partially hydrolyzed poly(acrylamide)
 concentration, 271, 272f
- Modeling of polymer feasibility tests
 field-curve matching, 300, 301f
 full-field model, 301
 iterative process, 297
 laboratory curve matching, 297, 300f
- Molar substitution, definition, 334
- Molecular weight, role in performance of partially hydrolyzed poly(acrylamide), 276, 277–278f
- Molecular weight distribution, hydrodynamic chromatographic technique, 233–234
- Molecular weight of cellulose esters, 336
- Molecular weight of flocculents, 121, 122f

N

- Newtonian regimen, effective viscosity in nuclepore membranes, 249–250f
- Nigeran, structure, 24
- Non-size-exclusion effects, viscosity effects, 39, 40f

- Nonuniformity in repeating structure
 - advantage, 23-24
 - effect on water solubility, 23
- Number-average degree of polymerization
 - heated vs. unheated pectins, 64, 65*f*,*t*, 66, 67*t*
 - unheated pectins, 60, 61*t*
- Number-average molecular weight for pectin
 - end-group titration procedures, 60
 - membrane osmometry procedures, 59-60

O

- Oil well drilling
 - primary production, 269-270
 - secondary recovery, 270
- Oil well drilling muds
 - background investigations, 155-156
 - problems, 156-160
- Operation factors of flocculation
 - physical form of polymers and their application, 124-128
 - polymer application, 123-124*f*

P

- Packings, high performance for aqueous size-exclusion chromatography
 - polymeric based, 41-42
 - silica based, 40-42
- Paint formulas, 336
- Paint manufacture, proper dispersion of the dry thickener, 349
- Partially hydrolyzed poly(acrylamide)
 - application in polymer-augmented waterflooding, 270-310
 - factors affecting performance, 276, 277-278*f*
 - mobility behavior, 273, 274-275*f*, 276
 - structure, 270
- Particle charge, effect on colloidal stability, 114, 115*f*
- Particle size, effect on settling and dewatering, 114
- Pectin
 - aggregation, 57
 - concentration-dependent dissociation, 66, 68, 69*f*
 - dilute solution properties, 57-69
 - function, 57
 - membrane osmometry, 57-69
 - number-average molecular weight, 57
- Pectinic acid
 - egg-crate complex formation, 22-23
 - product types, 18
 - structure, 17-18
- Pentoses, structure, 4
- Peptized montmorillonite surfaces,
 - adsorption, 185
- Percent nonvolatiles by volume, effect on thickener performance, 408-410
- Performance of aqueous drilling fluids
 - gel strength, 200*t*, 203
 - viscosity-temperature relationships, 204-206*f*
 - yield point and plastic viscosity, 204
- Petroleum applications
 - filtration control, 98
 - fluid loss control, 96, 97*f*
 - removal of drill solids, 96
- Physical forms of polymers, advantages and disadvantages, 124, 125*t*, 126-128
- Pigment volume concentration
 - sensitivity of hydrophobically modified, water-soluble polymer thickened formulations, 401, 403
 - viscosity vs. shear rate, 403, 405*f*
 - viscosity vs. weight percent thickener, 403, 404*f*
 - vs. yield stress behavior, 406*f*, 407
- Pigmented latex coatings, influence of water-soluble polymers on rheology, 391-415
- Pipelining
 - frictional pressure drops vs. flow rate, 306, 307*f*
 - power-law model, 306*f*
 - shear degradation, 307, 308*f*
- Poly(acrylic acid) polymers
 - characterization, 146
 - synthesis, 146
- Poly(acrylic acid) synthesis
 - effect of amine level, 149, 150*t*
 - effect of copper to hydrogen peroxide molar ratio variation, 147, 148*t*
 - effect of hydrogen peroxide level variation, 148, 149*t*
 - effect of temperature, 150*t*
 - efficiency of hydrogen peroxide as an initiator, 146, 147*t*
 - proposed mechanism, 150-151
- Poly(2-ethyl-2-oxazoline)
 - adhesion, 423*t*
 - applications, 431-432
 - cloud point, 430, 431*f*
 - density, 425
 - glass transition temperature, 427
 - melt blending, 427
 - molecular weight determination, 426
 - physical properties, 427-428
 - polymer blends, 427
 - preparation, 425-426
 - refractive index, 426
 - rheology, 428
 - solubility, 430*t*
 - solution profiles, 428, 429*f*, 430
 - thermal gravimetric analysis, 427*f*, 428
 - thermogravimetric analysis, 425
 - Vicat softening temperature, 427
 - viscosity vs. shear rate, 427
- Poly- β (1-3)-glucopyranose, 21
- Poly[α -(1-6)-D-maltotriose], description, 20-21
- Polymer applications in wastewater treatment
 - description of stages, 129, 131*t*
 - preliminary treatment, 129
 - primary clarification, 129, 132*t*

- Polymer applications in wastewater treatment—*Continued*
 secondary treatment, 133f, 134
 sludge dewatering, 135–138
 sludge thickening, 134–135
 summary, 138–139f, 140
- Polymer-augmented waterflooding
 anatomy, 269–310
 coring, 278–279, 280f
 description, 270
 environmental hazards, 310
 field feasibility tests, 288–297
 full-field development, 302–310
 modeling, 297, 300–301
 oil recovery, 279–288
 partially hydrolyzed poly(acrylamide), 271–278
 stepwise procedure, 270
- Polymer-blending systems
 concentrate blending, 292
 dry blending, 291f, 292
- Polymer concentration, effect on thickening behavior, 243, 244f
- Polymer concentration effects on flow behavior
 bulk and pore relative viscosities vs. relative molecular and pore size, 252, 253–255f
 diagram of profiles in cylindrical pores, 251, 252f
- Polymer conformation, effect on thickening behavior, 244, 245f, 246
- Polymer design
 charge density, 201–202
 molecular weight control, 200–201
- Polymer distribution for a polymer-augmented waterflood project
 dilution center schematic, 305f
 methods, 304, 305f
 pipelining, 306–308f
 polymer pumps, 307–308, 309f
- Polymer enhanced oil recovery
 fundamental criteria, 261–262
 selection, 261–264
- Polymer extenders
 apparent viscosity vs. extender concentration, 164f, 165–166, 167f
 effect on drilling rate, 161–162
 yield for bentonite, 163–167
- Polymer flocculent performance, effect of sludge conditioning, 123
- Polymer injection equipment and instrumentation
 instrumentation, 294
 monitoring flow rates of polymer concentrate, 292
 positive displacement pumps, 292
 static mixer, 292, 294
 typical system for a feasibility test, 292, 293f
- Polymer-modified bentonite slurries
 preparation, 184
 rheological profiles, 189f
- Polymer-related parameters of flocculation
 molecular weight and associated mechanisms of flocculation, 121–123
- Polymer-related parameters of flocculation—*Continued*
 sign and magnitude of charge, 117
 typical synthetic polymeric structures, 116–117, 118–119f
- Polymer properties
 effect of pressure, 160
 intrinsic viscosity, 159–160
- Polymer pumps
 mechanical degradation vs. volumetric efficiency and pump speed, 308, 309f
 selection criteria, 307–308
- Polymer shear degradation
 elimination by injection well modification, 302, 303f
 investigation by laboratory floods, 302, 303f, 304
 predictions of field degradation, 304
- Polymer shear degradation during size-exclusion chromatography, influencing parameters, 42–43
- Polymer slugs in porous media, propagation, 258–261
- Polymer-substrate interactions
 effect of cation, 92
 effect of cellulose ethers, 92f
- Polymer-water interactions
 temperature dependence, 90, 91f, 92
 time dependence, 90, 91f
- Polymeric-based high-performance packings for aqueous size-exclusion chromatography
 advantages and disadvantages, 41
 characterization, 41, 42–43f
- Polymeric flocculent performance, influencing factors, 114–128
- Polymeric flocculents, application and function in wastewater treatment, 113–140
- Polymeric surfactants, background, 101
- Polymerization systems, adsorption and kinetic characteristics, 93, 94f
- Polymers, use as shale stabilizers, 174–175
- Polymers in drilling, future, 168–169
- Polymers as shale stabilizers
 effective polymers, 178f, 179
 ineffective polymers, 178, 179f
 laboratory performance test results, 176, 177–178f
- Polysaccharide gels, 211
- Polysaccharides, classification by natural function, 6–9
- Poly(vinyl alcohol), ¹³C-NMR analyses, 81–82
- Preliminary wastewater treatment, purpose, 129
- Pressure data analysis for polymer feasibility tests
 example of bottom-hole pressures, 295, 296f
 injectivity test results, 297, 299–300f
 techniques, 295, 297, 298f
- Pressure filters and filter presses, use in sludge dewatering, 140

- Primary sedimentation-clarification in wastewater treatment, effect of chemical treatment, 129, 132*t*
- Propagation of polymer slugs in porous media
 - concentration dependence of polymer spreading out at the trailing edge of the slug, 261*f*
 - effects of pore-wall exclusion on polymer velocity, 259, 260*f*
 - flow-rate dependence of polymer spreading out at the trailing edge of the slug, 261, 262*f*
 - influence of inaccessible pore volume, 258–259
 - spreading out of slug during propagation, 259, 260*f*, 261

Q

- Qualitative analysis of ¹³C NMR
 - assignment of peaks, 76–77
 - standard conditions, 76
- Quantitative analyses for ¹³C NMR
 - disadvantages, 79
 - inverse gated decoupling, 77–78
 - recovery of magnetization, 78
 - size of computer memory, 78
 - temperature effect on resolution, 78

R

- Radial disk flooding
 - description, 272–273
 - disk configuration, 272, 273*f*
- Radius of gyration, definition, 230
- Raw material in a coatings formulation, effect of replacement, 369–370
- Rayleigh factor, definition, 47
- Resolution for ¹³C NMR
 - definition in terms of line width, 74
 - influencing factors, 74–75
- Reverse injection, description, 285*f*, 286
- Rheological measurements of aqueous drilling fluid, 199, 200*t*
- Rheological properties of macromolecules in solution
 - mechanical degradation in elongational flows, 246
 - viscosity in partly elongational flows, 241–246
 - viscosity in shear flows, 237–241
- Rheological properties of polymer solutions and gels, effect of polymer molecular weight, 219, 220–221*f*
- Rub-up method for testing color acceptance in paint, description, 347, 348*f*

S

- Saccharides, structure, 4
- Sag resistance of paint, charts for two paints, 341–342, 343*f*

- Salinity effect
 - on adsorption, 193, 194*f*
 - on filtration control for water-soluble polymers, 194
 - in polymer-augmented waterflooding, 276–277*f*
- Salt sensitivity of macromolecules, 233
- Sample preparation for ¹³C NMR
 - filtration, 75–76
 - reference to an internal standard, 76
- Sclerotium glaucanum* polysaccharide, description, 21–22
- Scrub resistance of paint
 - effect of constituents, 346
 - effect of molecular weight, 344, 345*t*, 346
- Secondary polymer floods
 - description, 282
 - oil recovery, 282, 284*f*
- Secondary wastewater treatment
 - effect of a cationic polyelectrolyte on secondary sedimentation basin performance, 133*f*, 134
 - purpose, 133
 - unit processes, 133–134
- Selection of partially hydrolyzed poly(acrylamide)
 - comparative behavior, 272–276
 - mechanism, 271
 - molecular weight, 276–278
 - salinity, 276
- Selection of polymers for enhanced oil recovery
 - fundamental criteria, 261–262
 - influence of microgels on behavior in porous media, 264–265*f*
 - procedure for testing filterability, 262, 263*f*
- Selectivity of ethylene oxide addition
 - effect of caustic level, 10–11
 - effect of water, 11, 12*f*
- Selectivity of propylene oxide, reactivity profiles, 11, 13*f*
- Sensitivity of hydrophobically modified, water-soluble polymer thickened formulations
 - dispersant and formulation surfactant effects, 410–413
 - latex variation, 407–408
 - percent monovolatiles by volume, 408–410
 - pigment volume concentration, 401, 403–406*f*, 407
 - viscosity vs. shear rate, 403–405*f*
- Shale formations, sloughing into the well bore, 156–157
- Shale stability, polymers, 174–175
- Shale stabilization, laboratory test methods, 175–176
- Shale stabilizers, laboratory performance of polymers, 176
- Shale stabilizing mechanisms, 179–180
- Shales
 - characterization, 173–174
 - composition, 173
 - drilling fluid interaction, 174
 - polymers for stability, 174–175
 - response to water, 173

- Shear degradation
 vs. molecular weight, 160
 vs. structure, 160
- Shear-thinning regimen
 effective viscosity in glass bead packs, 250, 251*f*
 effective viscosity in sandstones, 250, 251*f*
 pore throat diameter determination, 250–251, 252*f*
- Silica-based high-performance packings for aqueous size-exclusion chromatography
 characterization, 41, 42–43*t*
 composition, 40–41
- Size-exclusion chromatographic distribution coefficient, definition, 33
- Size-exclusion chromatography
 absolute molecular weight detectors, 46–49
 calibration curve, 32, 33*f*
 chemical heterogeneity, 49–52
 column calibration, 43–46
 high-performance packings, 40
 mobile-phase selection, 34–38
 non-size-exclusion effects, 38–40
 polymer shear degradation, 42–43
 separation mechanism, 32–34
- Sludge dewatering
 description, 135
 unit processes, 136–137, 140
- Sludge digestion, description, 134
- Sludge thickening, unit processing, 134–135
- Slurry process
 reaction profiles, 11, 12*f*
 use in maintaining viscosity control, 11
- Small particle size latex, influence of hydrophobically modified, water-soluble polymers, 396–397*f*
- Sodium lignosulfonate
 molecular weight control, 201
 structure, 201
- Sodium oleate solutions
 Huggins constant, 107, 109*t*
 intrinsic viscosity, 107, 109*t*,*f*
 weight-average degree of polymerization, 109*f*, 110
- Solids concentration, effect on particle interaction, 114
- Solids content, effect on drilling rate, 157–158, 160–163
- Solution polymers
 feed system, 124, 126*f*
 products, 124, 126
- Solution salinity, effect on thickening behavior, 243–244, 245*f*
- Spatter
 definition, 344
 effect of molecular weight, 344, 345*f*
- Sprayability
 definition, 421
 influencing factors, 422
- Stabilization of polymeric oil, mechanism, 418–419
- Stabilizing polymers, field applications, 180–181
- Starch, 14
- Static surface tension, definition, 315–316
- Static testing methods of shale–fluid interactions, description, 175
- Storage polysaccharides, 6–7
- Stormer viscometer, measurement of viscosity, 340
- Stormer viscosity, definition, 376
- Structural polysaccharides, 7–8
- Substrate-water affinity, effect of interfacial energy, 92, 93*f*
- Sugars, 4
- Surface tension measurements
 data analysis, 319
 instrument design, 320–322
 materials, 319
 measurement of foam stability, 322
 surface viscoelasticity, 322–325
 Wilhelmy plate method, 319–320
- Surface viscoelasticity, surface dilational modulus, 323–325
- Surfactant effects
 high-shear-rate viscosity, 410, 411–413*f*
 low-shear-rate viscosity, 413
- Suspension polymerization of vinyl chloride and styrene, 98–99
- Synthesis of low molecular weight poly(acrylic acids), methods, 145
- Synthetic water-soluble polymers, definition, 31
- System variables of flocculation
 composition of solids, 115–116
 solids concentration, 114

T

- Tertiary polymer floods, oil recovery, 282, 283*f*, 285*f*
- Tetrahydrophthalic salts acid
 molecular weight control, 200–201
 structure, 200–201
- Thermal breakdown temperature
 characterization cross-linking bond strength, 223*f*
 definition, 223
- Thermal stability, metal cross-linked polymer hydrogels, 222–223*f*
- Thickeners
 influence on high-shear-rate viscosities, 401
 properties, 376*t*
- Thickening behavior
 effect of solution salinity, 243–244, 245*f*
 effects of geometric factors, 242, 243*f*
 effects of polymer concentration, 243, 244*f*
 effects of polymer conformation, 244, 245*f*, 246
 in glass-bead pack vs. model including successive constrictions, 247, 248*f*
 in two different glass-bead arrangements, 246, 247*f*
 pore-size dependence, 257, 258*f*
- Thickening mechanism of paints
 effect of entanglements, 339, 340*f*

American Chemical Society
 Library

1155 16th St. N.W.

Advances in Chemical Physics, Vol. 10, Wiley-Interscience, Inc., New York, 1966.
 Washington, D.C. 20036
 Society: Washington, DC, 1986.

Thickening mechanism of paints—
Continued
 high-shear viscosity vs. amount of thickener present, 339
 high-shear vs. low-shear viscosity, 339, 340f
 mechanism of flocculation, 338
 Titanium cross-linked polysaccharide gels
 acid addition, 213–214
 competing reactions, 212–213
 cross-linking characteristics, 212
 hydrolysis of metals, 213, 214f
 mechanism gelation, 212–214
 Trickling filters, description, 134
 Types of cellulosic thickeners, 334–336

U

Unheated pectins
 axial ratios vs. heated pectins, 66, 67t
 counterion binding vs. heated pectins, 66, 67t, 68f
 degree of polymerization vs. heated pectins, 64, 65f, t, 66, 67t
 number-average degree of polymerization, 60, 61t
 van't Hoff plots, 60, 61–62f

V

Vacuum filtration, use in sludge dewatering, 137
 Vinyl acetate, grafting to (hydroxyethyl)cellulose, 351–366
 Vinyl acetate latices, percent (hydroxyethyl)cellulose grafted, 362, 364t, 365
 Viscometry
 limitations, 49
 principle of operation, 48
 Viscosity
 high shear rate vs. Casson, 422–423
 high shear rate vs. initiator level, 422, 423f
 of cellulose thickener, 336, 337f, 338
 viscosity as a function of shear rate, 336, 337f, 338
 Viscosity effects
 macromolecular crowding, 39–40
 viscous fingering, 39–40
 Viscosity in partly elongational flows
 effects of geometric factors on thickening behavior, 242, 243f
 effects of polymer concentration and solution salinity, 243, 244–245f
 effects of polymer conformation, 244, 245f, 246
 flow through capillaries, 241, 242f
 Viscosity in shear flows
 influence of polymer conformation, 240f, 241
 intrinsic viscosity and macromolecular dimensions, 238f

Viscosity in shear flows—*Continued*
 shear-rate dependence
 of concentration regimen, 239–240f
 of intrinsic viscosity, 239f
 viscosity vs. shear rate and polymer concentration, 237f, 238
 Viscosity studies of hydrophobically modified (hydroxyethyl)cellulose
 experimental procedures, 102
 in aqueous solutions, 102, 103t
 using methanol, 103–107
 using sodium oleate solutions, 107–110

W

Wastewater treatment
 application of polymeric flocculents, 113–140
 flow diagram, 129, 130f
 Water mobility, control by high molecular weight water-soluble polymers, 227–264
 Water resistance of paint, wet and dry adhesion, 346f, 347
 Water solubility, effects of structural features, 14–25
 Water-soluble cellulose ethers
 commercial importance, 9
 degree of substitution, 9
 molar substitution, 9
 production, 9
 reaction profiles, 11, 12–13f
 relative reactivities of addices, 9–10
 Water-soluble polymer–latex coating interactions
 first normal stress difference on shear rate, 397, 398f
 influencing factors, 391–392
 rheological profiles, 392f, 393
 thickening efficiency data, 392, 393t
 Water-soluble polymer–latex interactions
 importance of hydroprobes, 414, 415f
 performance differences, 414–415
 Water-soluble polymers
 adsorption, 85–99
 applications in oil and gas well drilling fluids, 171
 characterization, 71–82
 definition, 31–32
 dissolution, 184
 drilling fluid additives, 197–206
 effect of filtration control in modified bentonite slurries, 192–193
 effect of salinity on filtration control, 194
 role in oil well drilling muds, 155–169
 Water-soluble thickeners, shear-rate dependence of first normal stress differences, 398, 399–400f
 Water treatment for polymer feasibility tests, filtration unit, 294f
 Waterborne latex coatings, flowout problems, 396
 Waterborne polymers and coatings
 foam stability, 315–331
 surface viscoelasticity, 315–331

Weight-average degree of polymerization,
determination, 109-110
Wet and dry adhesion of paint, effect of
molecular weight, 346*f*, 347
Wilhelmy plate method, description,
319-320

X

Xanthan gums
characteristics, 236*t*
chemical structure, 228-229

Xanthan gums—*Continued*
molecular weight distribution, 234, 235*f*
salt sensitivity, 233
use in enhanced oil recovery processes,
228
Xanthomonas campestris polysaccharide,
description, 22

Y

Yield stress of paint, effect on sag
resistance, 344